

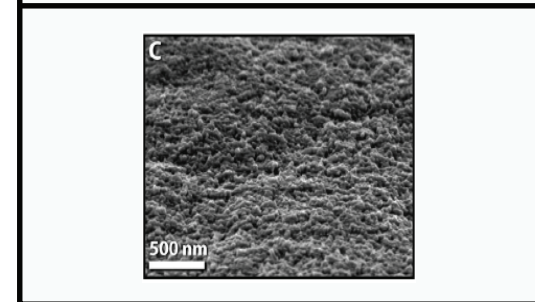
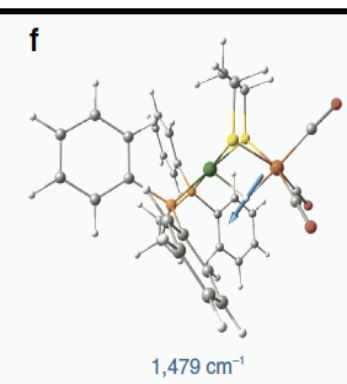
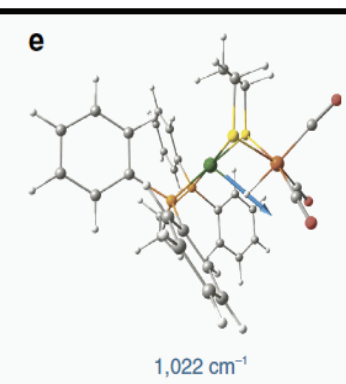
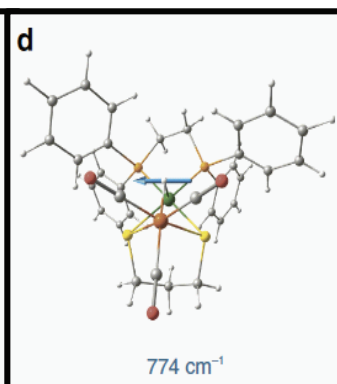
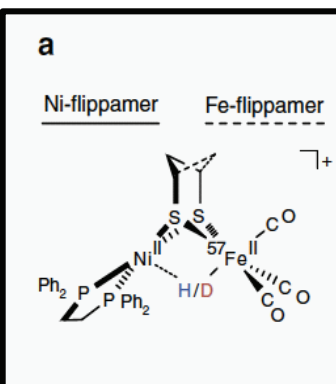
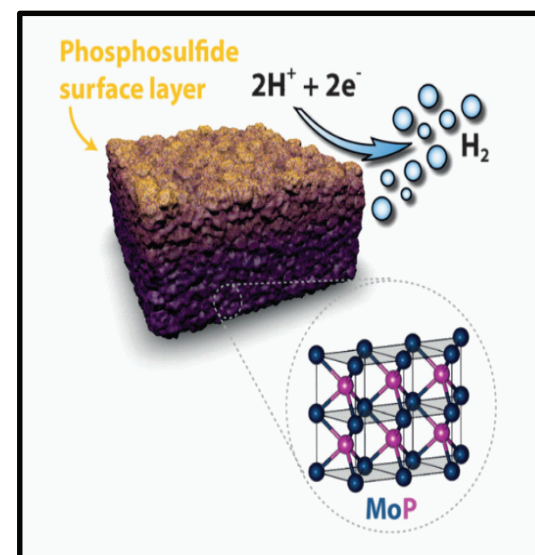
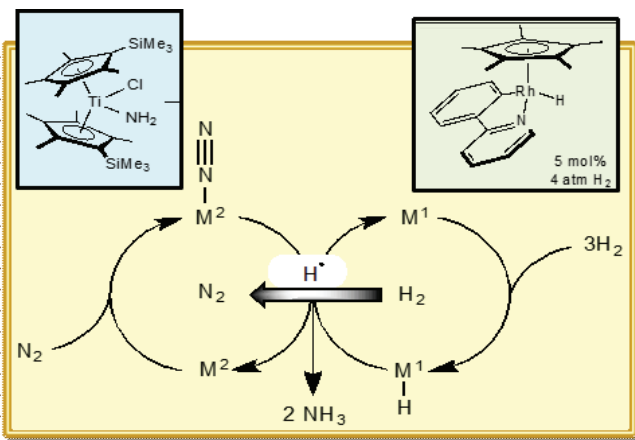
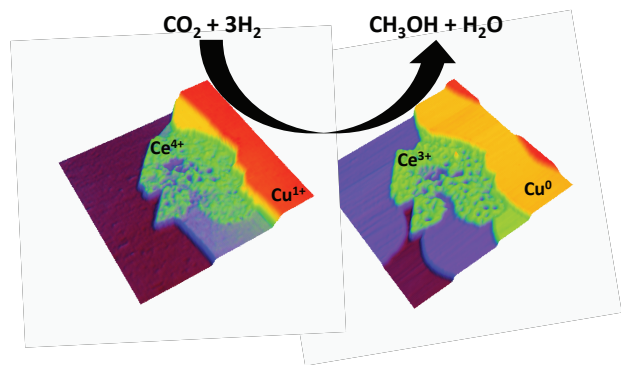
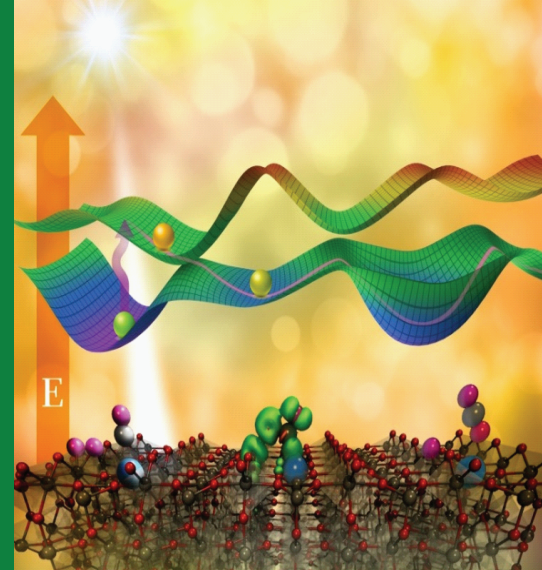
2016 Catalysis Science PI Meeting

Science of Catalytic Reaction Mechanisms

Gaithersburg Marriott Washingtonian Center

Gaithersburg, MD

June 22-24, 2016



Program and Abstracts for the

2016 BES/Catalysis Science Research PI Meeting: *"Science of Catalytic Reaction Mechanisms"*



U.S. DEPARTMENT OF
ENERGY

Office of
Science

Gaithersburg Marriott Washingtonian Center
Gaithersburg, Maryland
June 21-24, 2016

The research grants and contracts described in this document are supported by the U.S. Department of Energy, Office of Science/Basic Energy Sciences, as part of the Catalysis Science Program within the Chemical Sciences, Geosciences and Biosciences Division.

FOREWORD

The 2016 Catalysis Science Program Meeting is sponsored by the Division of Chemical Sciences, Geosciences and Biosciences, Office of Basic Energy Sciences (BES), U.S. Department of Energy. It is being held on June 21–24, 2016, at the Marriott Washingtonian Hotel, Gaithersburg, Maryland. The purposes of this meeting are to discuss the recent advances in the chemical, physical, and biological bases of catalysis science, to foster exchange of ideas and cooperation among participants, and to discuss the new challenges and opportunities recently emerging in energy technologies.

Catalysis activities within BES emphasize fundamental research aimed at understanding mechanisms and ultimately controlling the chemical conversion of natural and artificial feedstocks. The long-term goal of this research is to discover fundamental principles and produce insightful approaches to predict structure-reactivity behavior. Such knowledge, integrated with advances in chemical and materials synthesis, *in situ* and *operando* analytical instrumentation, and chemical kinetics and computational chemistry methods, will allow the control of chemical reactions along desired pathways. This new knowledge will impact the efficiency of conversion of natural resources into fuels, chemicals, materials, or other forms of energy, while minimizing the impact to the environment.

This year's meeting pursues the continuing goal of highlighting the potential advances in catalysis science to be made via studies of the mechanisms of important catalytic reactions, with the theme of the "*Science of Catalytic Reaction Mechanisms*". Such studies go to the heart of the essential fundamental information needed to understand catalyst materials, and the chemical reactions that are enabled by catalysts. In addition to a plenary address by Professor Alan Goldman, Rutgers University ("*Hydrocarbon Conversions Catalyzed by Iridium Complexes: High and Low Oxidation States*"), the meeting consists of 17 oral and 52 poster presentations by BES/Catalysis Science PIs. Two special sessions are also being held to discuss progress, challenges and opportunities related to the meeting theme, with a particular focus on the elementary processes of C-H, C-O, H-H and N-N bond making and breaking.

Special thanks go to the program investigators and their students, postdocs, and collaborators for their dedication to the continuous success and visibility of the BES Catalysis Science Program, and to the breakout session moderators for their invaluable help. We also thank Diane Marceau³, Josh Haines³ and the Oak Ridge Institute for Science and Education staff for the logistical and web support of the meeting. Finally very special thanks go to Raul Miranda³ for his longstanding and continuing contributions to the BES Catalysis Science Program, now from his role as Team Lead for Chemical Transformations in the BES Chemical Sciences, Geosciences and Biosciences Division.

Tom Rauchfuss¹, Peter Stair², Viviane Schwartz³ and Chuck Peden³

¹University of Illinois, Champaign-Urbana

²Northwestern University and Argonne National Laboratory

³Office of Basic Energy Sciences - U.S. Department of Energy

**2016 Catalysis Science PI Meeting
Science of Catalytic Reaction Mechanisms**

June 21-24, 2016

Marriott Washingtonian, Gaithersburg, MD

Program chairs: Tom Rauchfuss and Peter Stair

Tuesday Afternoon, June 21

2:00 – 5:00 p.m. **Registration**

Wednesday Morning, June 22

7:00-8:30 a.m. **Breakfast**

OPENING SESSION

Session Chairs: **Tom Rauchfuss and Peter Stair**

8:30-9:00 a.m. Welcoming remarks
Viviane Schwartz and Chuck Peden, DOE/BES/Catalysis Science Program

9:00-9:10 a.m. PI Meeting Theme – “*Science of Catalytic Reaction Mechanisms*”
Peter Stair, Northwestern Univ., **Tom Rauchfuss**, University of Illinois,
Champaign-Urbana

9:10-9:30 a.m. BES Update
Gail Mclean, DOE/BES/Chemical Sciences, Geosciences and Biosciences Division

GENERAL SESSION I

Session Chair: **Peter Stair**, Northwestern University

9:30-10:10 a.m. Understanding and Controlling C-H Bond Transformations and Partial Oxidation
of Light Alkanes with Less and Less Oxygen
Eric McFarland, University of California, Santa Barbara

10:10-10:30 a.m. **Coffee Break**

GENERAL SESSION II

Session Chair: **Dan Mindiola**, University of Pennsylvania

10:30-11:10 a.m. Catalytic Approaches to Complex Molecules from Carbohydrate Biomass
Michel Gagne, University of North Carolina, Chapel Hill

- 11:10-11:40 a.m. Discovering Emergent Phenomena in Catalysis through Large Scale Ab Initio Molecular Dynamics Simulations
Roger Rousseau, Pacific Northwest National Laboratory
- 11:40 am-12:10 p.m. Oxidation Reactions on PdO(101)
Jason Weaver, University of Florida
- 12:10-1:30 p.m. **Working Lunch**

Wednesday Afternoon, June 22

GENERAL SESSION III

Session Chair: **Fabio Ribeiro**, Purdue University

- 1:30-2:10 p.m. Synthetic and Mechanistic Studies Pertaining to Homogeneous Catalytic Transformations of Small Molecules by Metal Centers
Ged Parkin, Columbia University
- 2:10-2:40 p.m. Analysis of the Mechanisms of Electrochemical Oxygen Reduction and Development of Ag-alloy and Pt-alloy Electro-catalysis for Low Temperature Fuel Cells
Suljo Linic, University of Michigan
- 2:40-3:10 p.m. Reaction Mechanisms of Oxygenates over Oxide Catalysts: Role of Surface Structure and Composition
Zili Wu, Oak Ridge National Laboratory
- 3:10-3:30 p.m. **Coffee Break**
- 3:30-5:00 p.m. **BREAKOUT SESSION I**
- 5:00-7:00 p.m. **Dinner (on your own)**

Wednesday Evening, June 22

- 7:00-9:00 p.m. **Posters (Odd numbers)**

Thursday Morning, June 23

7:00-8:00 a.m. **Breakfast**

GENERAL SESSION IV

Session Chair: **Peter Stair**, Northwestern University

8:00-8:50 a.m. **Breakout session I recap** (10 minutes each) – Breakout Session Chairs

8:50-9:30 a.m. Reaction Mechanisms: Interplay of Thermodynamics and Kinetics
Talat Rahman, University of Central Florida

9:30-10:00 a.m. Catalysis by Design: Heterogeneous Single Atom Catalysts
Maria Flytzani-Stephanopoulos, Tufts University

10:00-10:20 a.m. **Coffee Break**

GENERAL SESSION V

Session Chair: **Lars Grabow**, University of Houston

10:20-11:00 a.m. Towards More Accurate Descriptors of Reactivity in Acid and Oxidation
Catalysis on Metal Oxides
Enrique Iglesia, University of California, Berkeley

11:00-11:30 a.m. Electrocatalysis of Reactions for Direct Energy Conversion: Changing the
Reaction Mechanism for Increased Kinetics
Radoslav Adzic, Brookhaven National Laboratory

11:30-12:00pm Highly Active Metal-Oxide Catalysts for Water Splitting
Aleksandra Vojvodic, SUNCAT/SLAC National Accelerator Laboratory

12:00-1:30 p.m. **Working Lunch**

Thursday Afternoon, June 23

1:30-3:00 p.m. **BREAKOUT SESSION II**

3:00-3:20 p.m. **Coffee Break**

PLENARY SESSION

Session Chair: **Tom Rauchfuss**, University of Illinois, Champaign-Urbana

- 3:20-4:20 p.m. Hydrocarbon Conversions Catalyzed by Iridium Complexes: High and Low Oxidation States
Invited lecture – Alan Goldman, Rutgers University
- 4:20-4:50 p.m. Mechanistic Studies of Bioinspired Oxidative Organometallic Reactions
Liviu Mirica, Washington University
- 4:50-7:00 p.m. **Dinner (on your own)**

Thursday Evening, June 23

- 7:00-9:00 p.m. **Posters (Even numbers)**

Friday Morning, June 24

- 7:00-8:00 a.m. **Breakfast**

GENERAL SESSION VI

Session Chair: **Bill Jones**, University of Rochester

- 8:00-8:40 a.m. The Interconversion of Ammonia with Its Elements
Paul Chirik, Princeton University
- 8:40-9:10 a.m. Molecular-Level Design of Heterogeneous Chiral Catalysts
Eddy Tysoe, University of Wisconsin, Milwaukee
- 9:10-9:40 a.m. Organometallic Chemistry for Alkane Dehydrogenation
Adam Hock, Illinois Institute of Technology and Argonne National Lab
- 9:40-10:20 a.m. Stereospecific ROMP of Cyclic Olefins with Mo and W Initiators
Richard Schrock, Massachusetts Institute of Technology
- 10:20-10:40 a.m. **Coffee Break**

CLOSING SESSION

Session Chair: **Tom Rauchfuss**, University of Illinois, Champaign-Urbana

- 10:40-11:40 a.m. **Breakout session II recap** (15 minutes each) – Breakout Session Chairs
- 11:40-12:00 p.m. Closing Remarks
Rauchfuss, Stair, Schwartz, Peden
- 12:00 p.m. **Adjourn**

TABLE OF CONTENTS

TITLE PAGE	i
FOREWORD.....	ii
AGENDA	iii
TABLE OF CONTENTS	vii
ABSTRACTS	1
<u>Plenary Speaker Abstract</u>	
<i>Probing Ion Solvation and Charge Transfer at Electrochemical Interfaces Using Nonlinear Soft X Ray Spectroscopy</i>	
Alan Goldman (Rutgers University)	3
<u>Principal Investigator Abstracts</u>	
<u>Oral Sessions</u>	
<i>Understanding and Controlling C-H Bond Transformations and Partial Oxidation of Light Alkanes with Less and Less Oxygen</i>	
Eric McFarland (University of California, Santa Barbara)	5
<i>Catalytic Approaches to Complex Molecules from Carbohydrate Biomass</i>	
Mike Gagne (University of North Carolina, Chapel Hill)	11
<i>Discovering Emergent Phenomena in Catalysis through Large Scale Ab Initio Molecular Dynamics Simulations</i>	
Roger Rousseau (Pacific Northwest National Laboratory)	17
<i>Oxidation Reactions on PdO(101)</i>	
Jason Weaver (University of Florida)	18
<i>Synthetic and Mechanistic Studies Pertaining to Homogeneous Catalytic Transformations of Small Molecules by Metal Centers</i>	
Ged Parkin (Columbia University).....	22
<i>Analysis of the Mechanisms of Electrochemical Oxygen Reduction and Development of Ag-alloy and Pt-alloy Electro-catalysis for Low Temperature Fuel Cells</i>	
Suljo Linc (University of Michigan).....	26
<i>Reaction Mechanisms of Oxygenates over Oxide Catalysts: Role of Surface Structure and Composition</i>	
Zili Wu (Oak Ridge National Laboratory)	30
<i>Reaction Mechanisms: Interplay of Thermodynamics and Kinetics</i>	
Talat Rahman (University of Central Florida)	42
<i>Catalysis by Design: Heterogeneous Single Atom Catalysts</i>	
Maria Flytzani-Stephanopoulos (Tufts University)	49

<i>Towards More Accurate Descriptors of Reactivity in Acid and Oxidation Catalysis on Metal Oxides</i> Enrique Iglesia (University of California, Berkeley)	56
<i>Structure and Function in Electrocatalysis of Reactions for Direct Energy Conversion</i> Radoslav Adzic (Brookhaven National Laboratory)	58
<i>Highly Active Metal-Oxide Catalysts for Water Splitting</i> Aleksandra Vojvodic (SUNCAT/SLAC National Accelerator Laboratory)	66
<i>Mechanistic Studies of Bioinspired Oxidative Organometallic Reactions</i> Liviu Mirica (Washington University).....	67
<i>The Interconversion of Ammonia with Its Elements</i> Paul Chirik (Princeton University).....	73
<i>Molecular-Level Design of Heterogeneous Chiral Catalysts</i> Eddy Tysoe (University of Wisconsin, Milwaukee)	75
<i>Organometallic Chemistry for Alkane Dehydrogenation</i> Adam Hock (Illinois Institute of Technology and Argonne National Laboratory).....	82
<i>Stereospecific ROMP of Cyclic Olefins with Mo and W Initiators</i> Richard Schrock (Massachusetts Institute of Technology).....	83
<u>Poster Session Abstracts</u>	
<i>Heterogeneous Catalysis - Predictions from Bond-order Conservation Principles</i> Frank Abild-Pedersen (SUNCAT/SLAC National Accelerator Laboratory)	85
<i>Applying Surface Science Approaches to Modeling Zeolite Catalysts</i> Eric Altman (Yale University)	93
<i>Designing Catalysts Using an Energy-Based Approach: Molecular Catalysis for CO₂ Reduction</i> Aaron Appel (Pacific Northwest National Laboratory).....	98
<i>Evolution of the Catalyst Composition and Structure During Reaction</i> Perla Balbuena (Texas A&M University).....	99
<i>Multiscale Imaging and Characterization of the Interaction of Thiols with Single-Layer MoS₂</i> Ludwig Bartels (University of California, Riverside).....	104
<i>Transition Metal Catalysts for Syngas Conversion to Higher Oxygenates</i> Stacey Bent (Stanford University, SUNCAT/SLAC National Accelerator Laboratory).....	105
<i>Hybrid Bioinorganic Approach to Solar-to-Chemical Conversion</i> Michelle Chang (Lawrence Berkeley National Laboratory and UC Berkeley).....	108
<i>Sub Nanometer Sized Clusters for Heterogeneous Catalysis</i> Abhaya Datye (University of New Mexico).....	109
<i>On the Reactivity of Hydroxyapatite</i> Bob Davis (University of Virginia)	115

<i>Supported Alkyl-Aluminum Catalysts for Olefin Hydrogenation</i> Massimiliano Delferro (Argonne National Laboratory)	119
<i>Benchmarking Computational Approaches for Catalytic Reactions of TMO Nanoclusters</i> Dave Dixon (University of Alabama)	126
<i>Control of Reactivity in Nanoporous Metal/Ionic Liquid Composite Catalysts</i> Jonah Erlebacher (Johns Hopkins University)	127
<i>Fabrication of nano-Structured Catalyst Supports by ALD</i> Ray Gorte (University of Pennsylvania)	131
<i>Dual Site Requirement for Efficient Hydrodeoxygenation of Model Biomass Compounds</i> Lars Grabow (University of Houston)	135
<i>Characterization of Tungsten and Zirconium Decorated Multi-Walled Carbon Nanotube Catalysts by XAS and NO_x TPD</i> Gary Haller (Yale University)	139
<i>Theoretical Investigation of Heterogeneous Catalysis at the Solid-Liquid Interface for the Conversion of Lignocellulosic Biomass Model Molecules</i> Andreas Heyden (University of South Carolina)	143
<i>Engineering Surfaces and Nanomaterials for H₂ and O₂ Electrocatalysis</i> Thomas Jaramillo (Stanford University, SUNCAT/SLAC National Accelerator Laboratory)	146
<i>Determination of Rhodium-Alkoxide Bond Strengths in Tp³Rh(PMe₃)(OR)H</i> Bill Jones (University of Rochester)	155
<i>Multifunctional Catalysts for CO₂ Reduction</i> Abhi Karkamkar (Pacific Northwest National Laboratory)	160
<i>Control of Supported Catalysis with Metallocalixarene Surface Complexes</i> Alex Katz (University of California, Berkeley)	161
<i>Morphological Role of Binary Metal Oxides on Organic Catalytic Transformations</i> Michelle Kidder (Oak Ridge National Laboratory)	166
<i>Supported Tetrahedral Oxo-Sn Catalyst: Single-Site, Two Modes of Catalysis</i> Harold Kung (Northwestern University)	167
<i>Understanding Catalysis of Lignin to Fuels on a Molecular Level</i> Johannes Lercher (Pacific Northwest National Laboratory)	168
<i>Toward Modeling Practical Catalytic Environments from First Principles</i> Ping Liu (Brookhaven National Laboratory)	192
<i>Dehydration and Dehydrogenation of Isopropanol on Metal Oxide Catalysts</i> Daniel Lutterman (Oak Ridge National Laboratory)	193
<i>Elucidating the Function of Each Metal in Pd/Fe Bimetallic Catalysts for Hydrodeoxygenation Reactions</i> Jean-Sabin McEwen (Washington State University)	194

<i>Tuning the Dehydration Activity of Alcohols using Phosphonic Acid Self-Assembled Monolayers</i> Will Medlin (University of Colorado)	198
<i>Chemistry of the Metal Catalyzed C-O Bond Cleavage of Lignin in the Condensed Phase</i> Donghai Mei (Pacific Northwest National Laboratory)	201
<i>Molecular Titanium Nitrides: Nucleophiles Unleashed</i> Dan Mindiola (University of Pennsylvania).....	202
<i>Adsorption and Reaction of Methanol and Ethanol on La_{0.7}Sr_{0.3}MnO₃(100) Perovskite by Ambient Pressure XPS</i> Dave Mullins (Oak Ridge National Laboratory)	206
<i>Dually functionalized MOF-NP Catalysts: Understanding and Controlling Oxidant generation-Epoxidation Catalysis in Solution Phase</i> SonBinh Nguyen (Northwestern University and Argonne National Laboratory)	207
<i>Dynamic Restructuring of Working Catalysts Revealed by Correlating Multiple (Optical, X-ray and Electron) Probes and First Principle Simulations</i> Ralph Nuzzo (University of Illinois, Urbana-Champaign).....	208
<i>Support and Artificial SMSI Effects on Selective Hydrogenation by Noble Metal Nanoparticles</i> Ken Poeppelmeier (Northwestern University)	216
<i>Characterization of Catalytic Materials by DNP-Enhanced Solid-State NMR</i> Marek Pruski (AMES Laboratory).....	217
<i>Thermodynamics of Methanol Decomposition on Graphene-Pt₁₃ Nanocomposites</i> Ashwin Ramasubramaniam (University of Massachusetts, Amherst).....	219
<i>Redox Reactions of Redox-Innocent Imine Ligands on Fe</i> Tom Rauchfuss (University of Illinois at Urbana-Champaign)	223
<i>Fundamental Studies of Oxidation Reactions on Model Catalysts Gradient Check a Tool to Check Heat and Mass Transfer Gradients in a Catalyst</i> Fabio Ribeiro (Purdue University).....	226
<i>Structure-Performance Relationships in Zeolite Catalysis: Impact of Crystal Size and Morphology in MTH</i> Jeff Rimer (University of Houston).....	228
<i>Mechanistic Studies on the Water-Gas Shift and CO₂ Hydrogenation: Importance of the Metal-Oxide Interface</i> Jose Rodriguez (Brookhaven National Laboratory)	231
<i>Interfacial catalysts for reactions of oxygenates: characterization, catalytic activity and reaction mechanisms</i> Aaron Sadow (Ames Laboratory).....	239
<i>The CleanCat Core Facility – a Facilitator and Educator in Catalysis Research</i> Neil Schweitzer (Northwestern University)	249
<i>Unraveling Reforming Reactions over Ni-CeOx Catalysts: Importance of Metal-Oxide Interactions in Chemical Conversion</i> Sanjaya Senanayake (Brookhaven National Laboratory).....	250

<i>Achieving Enzyme-Like Behavior with Amino Acids and Peptides in the Outer Coordination Sphere of Hydrogenase Mimics</i> Wendy Shaw (Pacific Northwest National Laboratory)	251
<i>Understanding and Controlling the Effects of Surface Species on Catalytic Processes within Mesoporous Silica Supports</i> Igor Slowing (Ames Laboratory).....	255
<i>Highly Dispersed SiO_x/Al₂O₃ Materials Illuminate the Reactivity of Isolated Silanol Sites</i> Peter Stair (Northwestern University)	256
<i>Graphite-Conjugated Catalysis</i> Yogesh Surendranath (Massachusetts Institute of Technology)	269
<i>Fundamental Understanding the Correlation of Transition Metal Oxide Surfaces and Selectivity in Production of Ethylene through Oxidative Dehydrogenation of Ethane</i> Franklin (Feng) Tao (University of Kansas)	271
<i>Multimetallic Centers in Oxidation Chemistry: Mechanism for Oxygen Evolution and Development of Mixed Manganese-Cobalt Oxido Cubanes</i> Don Tilley (Lawrence Berkeley National Laboratory)	276
<i>New Fluoroalkylation Methods Employing Earth Abundant Metals</i> David Vacic (Lehigh University).....	277
<i>Molecular Level Foundation for Olefin Metathesis by Heterogeneous Supported Molybdena Catalysts</i> Israel Wachs (Lehigh University).....	282
<i>Fundamentals of Acid/base and Redox Reactions on Metal Oxide Catalysts</i> Yong Wang (Washington State University and Pacific Northwest National Laboratory).....	285
<i>Mechanistic Studies of Oxidation Reactions on Supported Vanadia Catalysts</i> Eric Weitz (Northwestern University).....	286
LIST OF PARTICIPANTS	287
BREAKOUT SESSION DISCUSSIONS	292
<i>H-H Bond Activation</i> Fabio Ribeiro (Purdue University) and Wendy Shaw (Pacific Northwest National Laboratory)	293
<i>C-H Bond Activation</i> Bill Jones (University of Rochester) and Matt Neurock (University of Minnesota).....	299
<i>C-O Bond Activation</i> Aaron Appel (Pacific Northwest National Laboratory) and Lars Grabow (University of Houston)	312
<i>N-N Bond Activation</i> Tom Jaramillo (Stanford University and SUNCAT/SLAC) and Dan Mindiola (University of Pennsylvania).....	323

ABSTRACTS

Plenary Session Speaker

**Hydrocarbon Conversions Catalyzed by Iridium Complexes:
High and Low Oxidation States**

Alan S. Goldman,¹ Maurice Brookhart,² Karen I. Goldberg,³ William D. Jones,⁴ and Karsten Krogh-Jespersen¹

¹Rutgers University

²University of North Carolina

³University of Washington

⁴University of Rochester

Presentation Abstract

Iridium has played a leading role in the organometallic chemistry of alkanes and unreactive C-H bonds since the inception of the field 30 years ago. We have found that “PCP”-pincer-ligated iridium complexes are particularly effective for the dehydrogenation of alkanes and have incorporated this reaction into tandem systems for catalytic transformations based on dehydrogenation. The selectivity for dehydrogenation at the terminal position of *n*-alkanes displayed by some (PCP)Ir derivatives is of particular interest; the factors that determine such selectivity (or the lack thereof) have been elucidated. More recently we have turned attention to iridium Phebox complexes. Although the (PCP)Ir and (Phebox)Ir units are formally isoelectronic, the former effects dehydrogenation via C-H activation by Ir(I) while the latter operates via Ir(III) (as an acetate complex) and possibly Ir(V) intermediates. Such a high-oxidation-state catalytic cycle offers many potential advantages. In addition to dehydrogenation-based conversions, we have found that (PCP)Ir can catalyze other conversions based on C-H bond activation, including, most recently, dehydrogenative C-H bond coupling. In this reaction, preliminary results indicate that (PCP)Ir appears to operate via a high-oxidation-state catalytic cycle.

Wednesday Oral Presentations

Eric McFarland

**Understanding and Controlling C-H Bond Transformations
and Partial Oxidation of Light Alkanes with Less and Less Oxygen**

Mike Gordon, Horia Metiu, and Eric McFarland
University of California, Santa Barbara
Departments of Chemical Engineering and Chemistry

Presentation Abstract

Natural gas will provide a low cost source of light alkanes for several decades. Cost-effective C-H bond activation and selective partial oxidation of alkanes to make olefins, without producing carbon dioxide, is presently not possible and would be beneficial to the United States. It is not possible, using molecular oxygen as an oxidant, to achieve high single pass yields of olefins, alcohols, or aromatic hydrocarbons from light alkanes. The activity of metal oxide catalysts for C-X bond transformations is shown to be controllable by electronic modification of host oxides through doping. Density functional theory combined with experiments is used to develop a predictive framework for design of catalysts. Reducible metal oxides result in high selectivity to desired products and low selectivity to carbon oxides, and exploration of these alternative oxidants suggests more optimal partial oxidation pathways with intriguing potentials for significant changes in yields and efficiencies of light alkane conversion. Many interesting fundamental questions exist related to these alternative pathways for which we have little present understanding.

DE-FG02-89ER14048 Investigations of C-H Bond Activation and Doped Metal Oxide Catalysts

Postdoc(s): Henrik H. Kristoffersen

Student(s): David Chester Upham

RECENT PROGRESS

The surface chemistry of oxides and modified oxides

1. *The coadsorption of Lewis acid with Lewis bases.* In previous work, we postulated, based on computations on a variety of oxides and adsorbates, that if two adsorbates are amphoteric (each could be acid or base, depending on partner), they will adsorb so that one is a base and the other is an acid. We found that this is the case in dissociative adsorption of hydrogen⁴ or methane²⁰ on oxides, where H binds to surface oxygen, and donates electrons to CH₃, which binds to cations even though both CH₃ and H bind to oxygen if they are alone on the surface. Dissociative binding of methane is heterolytic, while previous work assumed homolytic dissociation.

2. *The water-oxide interface.* We have performed *ab initio* molecular dynamics²³ to investigate adsorption of molecules at the water-TiO₂ interface. We studied catechol and HCl as examples of weak and strong electrolytes, respectively, and showed that the structure of the first two water layers next to the surface is very different from the bulk. The binding energy of the two molecules at the water-oxide interface is dramatically different from that in vacuum; for example, HCl binds strongly to the oxide in vacuum, but it is equally happy at the water-solid interface, or in the water film. These studies are an important step towards understanding electrocatalysis.

3. *The energy of oxygen vacancy formation.* The formation of oxygen vacancies is invoked by the Mars-van Krevelen mechanism, which is widely accepted for alkane activation. It is very difficult to measure the energy of vacancy formation, and for this reason, it has been calculated for many oxides. It was generally assumed that the energy of vacancy formation depends on concentration, which is no doubt correct. However, we have shown⁵ that vacancy formation strongly depends on how they are distributed on the surface, i.e., two systems with the same vacancy concentration, but different surface arrangement, will have very different formation energy.

4. *Two-dimensional oxides.* Some oxides have a layered structure and we became interested in the possibility of exfoliating them to create two-dimensional, one-atom-thin ribbons.¹⁰ We decided to examine V₂O₅ and MoO₃ and showed that their ability to break the C-H bond is very different from that of powders or supported submonolayers. Our calculations show that they will react with water to form bilayers with very unexpected structures⁶ and protons in the surrounding water. These gels are potential Brønsted acid catalysts.

5. *Vanadium oxide clusters supported on metals.* Vanadium oxide submonolayers, supported on an oxide, are popular systems in catalysis. We used DFT calculations¹⁵ to show that such clusters supported on Ag or Au are active for methane dissociation.

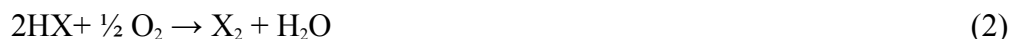
Halogen-assisted alkane dehydrogenation in gas phase

In two publications^{12,13} we have shown that one can use Br₂ as an “oxidant” to convert propane to propylene. A surprising result of this work was that the addition of I₂ to the feed increased substantially the propylene yield and selectivity. I₂ acts as a gas-phase catalyst. The use of two halogens is not additive: they cooperate in propylene production. We have argued for the following mechanism for this cooperation: the iodine dissociates more readily than Br₂, the I atoms react with Br₂ to produce IBr and Br; the latter is more aggressive in removing hydrogen from propane. We believe that this procedure will work for the dehydrogenation of other alkanes.

Halogen-mediated oxidative dehydrogenation of alkanes

1. *Halogen-mediated oxidative dehydrogenation: the mechanism.* We have performed experiments⁷ that demonstrate that iodine is a gas-phase catalyst for propane *oxidative dehydrogenation* with higher yields than those reported in the literature or in industry. The reaction can be described formally by





where X is a halogen. This reaction scheme is formal: it is used only to keep track of net stoichiometry.

2. *The mechanism of iodine-mediated oxidative dehydrogenation.* We have found that propylene production in our system proceeds through a radical mechanism initiated by iodine dissociation. We have studied every step individually and the mechanism is well documented. The most important question for us was why almost no CO_x is produced even though the feed contained propane, I_2 and O_2 ? The answer is simple: the reaction of O_2 with HI is extremely fast, much faster than hydrocarbon oxidation; as such, HI, which is formed when propane reacts with I_2 , “protects” the hydrocarbon from oxidation. In addition, the fast reaction of HI with oxygen shifts $\text{C}_3\text{H}_7\text{I}$ disproportionation towards higher yield. This suggests a very important improvement in the reactor: introduce oxygen gradually along the reactor so that the amount of oxygen at any place in the reactor matches the amount of HI produced by the reaction.

3. *Halogen-mediated oxidative dehydrogenation: which halogen?* Based on discoveries made in previous work^{12,13}, we investigated using a mixture of I_2 and Br_2 with propane and oxygen. This system produces the same yield as using I_2 alone, but propylene formation is three times faster than when using I_2 alone). We now know the reaction mechanism and we believe that using mixed halogens is very promising, and we plan to study this system in detail and optimize reaction conditions.

4. *The source of halogen.* We have run halogen-mediated oxidative dehydrogenation in two ways: (a) gaseous feed of propane, oxygen, and halogens and (b) generation of halogen *in situ* by reacting propane and oxygen with molten Li halide. To generate a mixture of bromine and iodine, we used a molten mixture of LiI and LiBr. Using molten salts is beneficial because: (a) the melt has high heat capacity and conductivity, allowing better heat management, and (b) the small amount of coke formed by the reaction floats to the surface of the melt and can be easily removed, whereas in industrial processes, decoking is frequent and expensive. We performed *ab initio*, constant-temperature molecular dynamics calculations to explore the reactivity of LiI⁸, and concluded that the melt is not a catalyst, but a source of I_2 . Our simulations are the first *ab initio* studies of the structure and chemistry of molten salts.

5. *Performance.* (a) We have found that the single-pass propylene yield is 65%, which is better than existing industrial processes or the published academic studies of oxidative dehydrogenation in the absence of a halogen. (b) The yield we quoted was obtained at 500 °C, while industry works at 650 °C. (c) Our system produces very small amounts of coke, while coking is a severe problem in the industrial process. (d) The net reaction, in our case, is exothermic, while the industrial process is endothermic and consumes a large amount of energy.

6. *Should we use other iodides or bromides?* We have no reason to believe that LiI and LiBr are the best possible halogen sources. To be used in our scheme, a halide must react with oxygen to form halogen and an oxide (or a hydroxide when water is present), and the oxide (or the hydroxide) must react with HX to form the halide and water. We have performed thermodynamic calculations and found 12 iodides and 18 bromides that satisfy these conditions. We plan to explore these systems in search of better performance for

halogen-mediated oxidative dehydrogenation of propane. From the point of view of pure science, it is interesting to learn how the charge of the cation in the halide influences the ease with which the halogen is formed when the halide reacts with oxygen. This is also a fertile field for *ab initio* molecular dynamics simulations since, except for our work, nothing is known about the chemistry of structure of these melts.

7. *Problems with HBr.* The use of I_2 alone has the advantage that the HI produced is rapidly and completely oxidized to regenerate I_2 *in situ*. While using a combination of I_2 and Br_2 increases the rate of propylene formation, the fact that HBr is contained in the effluent is a drawback. The problem is that HBr is oxidized very slowly at the temperatures we studied. We have performed preliminary experiments with a system consisting of a slurry of NiO in molten LiBr-KBr, and found that NiO reacts with HBr to form $NiBr_2$ which is *soluble in the melt*. This is very beneficial since past work using solid-to-solid transformations failed because of particle fracture. The $NiBr_2$ produced was converted back to NiO using O_2 , and the nickel oxide-bromide pair could be cycled back and forth 50 times using O_2 and HBr.

Other work

1. We have performed DFT calculations² to compare the acidity of Al-containing zeolites to that of Al-containing silica, both of which have hydroxyls on their surfaces. We concluded that some of the hydroxyls in Al-containing silica are as acid as those present in Al-containing zeolites. The main difference between the two is that the zeolites have higher “area” and have shape selectivity.

2. We performed experiments that show that the effective activation energy for methane oxidation by lanthana doped with Cu, Zn, Mg, Fe, Nb, Ti, Zr, or Ta follows the rules predicted by DFT: the activation energy is a linear function of the calculated energy of vacancy formation. Moreover the lower-valence dopants and the higher-valence ones generate different lines indicating a different mechanism as predicted by calculations.

3. We have performed several studies^{14,18} aimed at determining why hydrogen oxidation does not take place on a sulfide electrode with a HBr electrolyte. This system was studied because of its potential use for energy storage. We found that the reaction $H_2 + D_2 = 2DH$ proceeds very rapidly when the sulfide electrode is exposed to a mixture of gaseous H_2 and D_2 . We concluded that H_2 adsorption and dissociation is not the reason for the high overvoltage.

4. As part of our work to understand the role of dopants in catalysis by oxides, we studied dry reforming of methane catalyzed by Ru-doped ceria. We found that the catalyst is the reduced oxide, by pulsing oxygen in the system during reaction and showing that this shuts off dry reforming. The role of Ru dopant is to facilitate the reduction of ceria. We suggested that this behavior is general for all oxides doped with lower valence cations.

Publications Acknowledging this Grant in 2013-2016

(I) Exclusively funded by this grant

1. Ding, K. L.; Metiu, H.; Stucky, G. D. Interplay between bromine and iodine in oxidative dehydrogenation. *ChemCatChem* **2013**, *5*, 1906-1910.
2. Agarwal, V.; Metiu, H. Hydrogen abstraction energies and ammonia binding to BEA, ZSM-5, and α -quartz, doped with Al, Sc, B, or Ga. *J. Phys. Chem. C* **2015**, *119*, 16106-16114.
3. Upham, D. C.; Derk, A. R.; Sharma, S.; Metiu, H.; McFarland, E. W. CO₂ methanation by Ru-doped ceria: The role of the oxidation state of the surface. *Catal. Sci. Tech.* **2015**, *5*, 1783-1791.
4. Chretien, S.; Metiu, H. Hydrogen dissociative adsorption on lanthana: Polaron formation and the role of acid–base interactions. *J. Phys. Chem. C* **2015**, *119*, 19876-19882.
5. Agarwal, V.; Metiu, H. Energy of oxygen-vacancy formation on oxide surfaces: Role of the spatial distribution. *J. Phys. Chem. C* **2016**, *120*, 2320-2323.
6. Kristoffersen, H. H.; Metiu, H. Structure of V₂O₅.nH₂O xerogels. *J. Phys. Chem. C* **2016**, *120*, 3986-3992.
7. Upham, D. C.; Gordon, M. J.; Metiu, H.; McFarland, E. W. Halogen-mediated oxidative dehydrogenation of propane using iodine or molten lithium iodide. *Catal. Lett.* **2016**, *146*, 744-754.
8. Huang, C.; Kristoffersen, H. H.; Gong, X.-Q.; Metiu, H. Reactions of molten LiI with I₂, H₂O, and O₂ relevant to halogen-mediated oxidative dehydrogenation of alkanes. *J. Phys. Chem. C* **2016**, *120*, 4931-4936.
9. Pradhan, S.; Upham, D. C.; Metiu, H.; McFarland, E. W. Partial oxidation of propane with CO₂ on Ru-doped catalysts. *Catalysis Science & Technology* **2016**, 10.1039/C6CY00011H.
10. Kristoffersen, H. H.; Metiu, H. Structure and oxidizing power of single layer α -V₂O₅. *Top. Catal.* **2016**, *59*, 809-816.

(II) Jointly funded by this grant and other grants with leading intellectual contribution from this grant

11. McFarland, E. W.; Metiu, H. Catalysis by doped oxides *Chem. Rev.* **2013**, *113*, 4391-4427.
12. Ding, K.; Metiu, H.; Stucky, G. D. The selective high-yield conversion of methane using iodine-catalyzed methane bromination. *ACS Catalysis* **2013**, *3*, 474-477
13. Derk, A. R.; Li, B.; Sharma, S.; Moore, G. M.; McFarland, E. W.; Metiu, H. Methane oxidation by lanthanum oxide doped with Cu, Zn, Mg, Fe, Nb, Ti, Zr, or Ta: The connection between the activation energy and the energy of oxygen-vacancy formation. *Catal. Lett.* **2013**, *143*, 406-410.
14. Singh, N.; Upham, D. C.; Metiu, H.; McFarland, E. W. Gas-phase chemistry to understand electrochemical hydrogen evolution and oxidation on doped transition metal sulfides. *J. Electrochemical Society* **2013**, *160*, A1902-A1906.
15. Yu, J.; Scheffler, M.; Metiu, H. Oxidative dehydrogenation of methane by isolated vanadium oxide clusters supported on Au (111) and Ag (111) surfaces. *J. Phys. Chem. C* **2013**, *117*, 18475-18483.

16. Sun, X.; Li, B.; Metiu, H. Ethane activation by Nb-doped NiO. *J. Phys. Chem. C* **2013**, *117*, 23597-23608.
17. Derk, A. R.; Moore, G. M.; Sharma, S.; McFarland, E. W.; Metiu, H. Catalytic dry reforming of methane on ruthenium-doped ceria and ruthenium supported on ceria. *Top. Catal.* **2014**, *57*, 118-124.
18. Singh, N.; Upham, D. C.; Liu, R.-F.; Burk, J. J.; Economou, N. J.; Buratto, S. K.; Metiu, H.; McFarland, E. W. Investigation of the active sites of rhodium sulfide for hydrogen evolution/oxidation using carbon monoxide as a probe. *Langmuir* **2014**, *30*, 5662-5668.
19. Chretien, S.; Metiu, H. Oxygen adsorption on irreducible oxides doped with higher-valence ions: O₂ binding to the dopant. *J. Phys. Chem. C* **2014**, *118*, 23070-23082.
20. Chretien, S.; Metiu, H. Acid-base interaction and its role in alkane dissociative chemisorption on oxide surfaces. *J. Phys. Chem. C* **2014**, *118*, 27336-27342.
21. Kristoffersen, H. H.; Metiu, H. Molten LiCl layer supported on MgO: Its possible role in enhancing the oxidative dehydrogenation of ethane. *J. Phys. Chem. C* **2015**, *119*, 8681-8691.
22. Kristoffersen, H. H.; Metiu, H. Reconstruction of low-index α -V₂O₅ surfaces. *J. Phys. Chem. C* **2015**, *119*, 10500-10506.
23. Kristoffersen, H. H.; Shea, J.-E.; Metiu, H. Catechol and HCl adsorption on TiO₂(110) in vacuum and at the water-TiO₂ interface. *J. Phys. Chem. Lett.* **2015**, *6*, 2277-2281.

Michel R. Gagné

**Catalytic Approaches to Complex Molecules from
Carbohydrate Biomass**

Michel R. Gagné, Trandon Bender, Laura Adduci, Phillipa Payne
University of North Carolina at Chapel Hill

Presentation Abstract

There are a number of interesting known catalysts for the heterolytic activation of silanes, including those based on Ir and B complexes. This presentation will present the state-of-the-art in utilizing these catalysts to activate the C–O bonds of carbohydrates, with a special emphasis on their selective reduction (to C–H bonds). In contrast to traditional methods for the deoxygenation of overly functionalized poly-saccharides, which are eliminative in nature, these catalysts promote stereoselective and stereospecific mechanisms that provide products that maintain a high sp^3 content (and are hence chiral with multiple stereocenters), are functionalized and readily functionalizable, and may thus provide routes to high-value materials from bio-renewables. From a recent study on the readily available C6O6 and C5O5 starting materials (sorbitol, etc) our ability to control the catalytic reactions have enabled the synthesis (in 1 or 2 steps usually) of a number of new C6On and C5On compounds not previously reported in the literature. Given how long synthetic chemists have been making derivatives of glucose and the like, it is noteworthy that one can find derivatives that have not yet been synthesized.

In addition to describing the reaction chemistry, the influence of silane, catalyst, and the substrate will be examined to paint a picture of the underlying mechanisms that control reactivity and selectivity. Key intermediates that have been observed and/or proposed include sila-oxonium ions (R_2O-Si^+), sila-oxocarbenium ions ($C=O-Si^+$), and less exotic Lewis adducts. Several methods have been uncovered to modulate the speciation of the catalysts under reaction conditions and these will be also discussed.

DE-FG02-05ER15630: Methods for the Selective Deoxygenation of Carbohydrates

PI: Michel R. Gagné

Postdoc(s): Phillipa Payne

Student(s): Trandon Bender, Laura Adduci

Affiliations(s): UNC Chapel Hill

RECENT PROGRESS

Chem. Sci. under review (abridged)

B(C₆F₅)₃-Catalyzed Reductive Cyclopentane and Cyclopropane Formation

A powerful but difficult to realize disconnection for the synthesis of complex molecules are the carbon-carbon (C-C) bonds of their carbocycles. These elements are ubiquitous in natural products, drug candidates, and agrochemicals (e.g. Figure 1), with cyclopentane and cyclopropane rings being common motifs. Cyclopropane installation is a well-established strategy for imparting beneficial properties in active pharmaceuticals, and more recently cyclopentane cores have provided intriguing activities differentiated from other carbocyclic cores. Cyclopentane synthesis strategies are varied, but often are mediated by metal catalysis. It is often the case that conformational biasing via a tetra-substituted carbon in the chain (Thorpe-Ingold) is required for high efficiency and selectivity. Post ring-forming diversification consequently puts a premium on methods that install functional groups capable of being modified to installing stereochemical complexity. Less explored are methods for the ring closure of highly pre-functionalized compounds as these groups can interfere with the catalyst.

We recently demonstrated that B(C₆F₅)₃ exhibits high chemo- and diastereoselectivity for C-O bond

reduction, functioning by a mechanism first proposed by Piers (Scheme 1A). The key feature is the activation of the silane rather than the carbonyl (as with BF₃•OEt₂). Silane activation by B(C₆F₅)₃ in combination with a Lewis base (e.g. carbonyl) transiently generates a reactive ion pair, H-B(C₆F₅)₃⁻ and L-SiR₃⁺. Rapid C-O reduction by H-B(C₆F₅)₃⁻ ensues unless a good neighbouring group can trap the activated species prior to reduction (e.g. Scheme 1B).

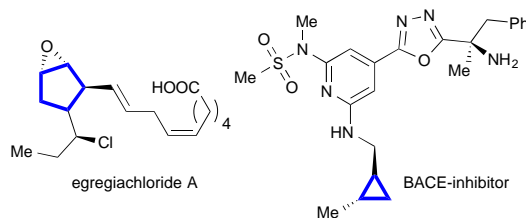
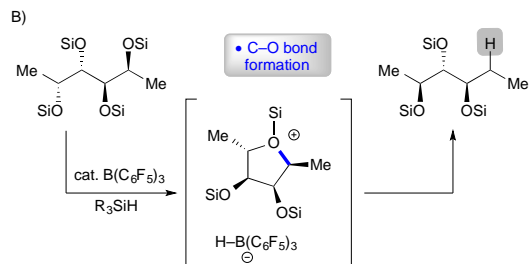
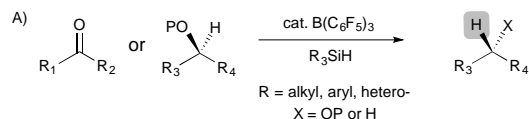


Figure 1. Examples of complex bioactive materials built upon carbocyclic frameworks.

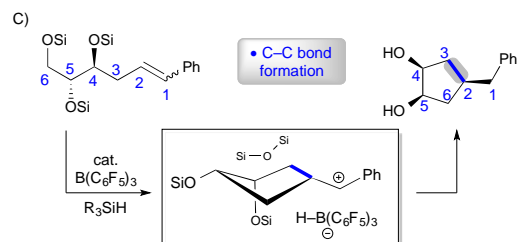
Knowing that intramolecular additions prior to reduction are feasible, we examined the propensity of alkenes to behave similarly and provide interesting carbocycles. This notion has been successfully realized to reveal mild, catalytic C-C bond forming reactions that *efficiently transform linear carbohydrate-derived molecules into complex carbocyclic cores* while

preserving much of the imbedded stereochemistry.

previous work:



this work:

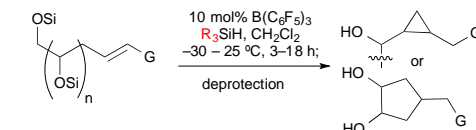


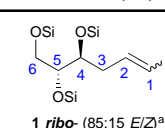
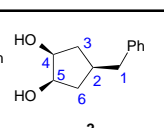
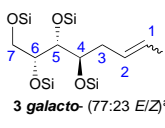
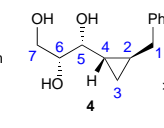
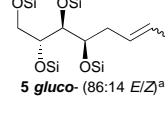
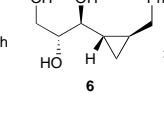
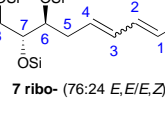
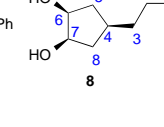
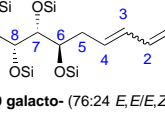
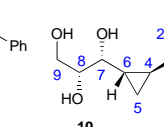
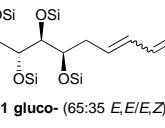
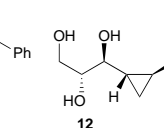
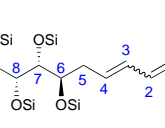
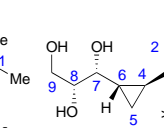
Scheme 1. B(C₆F₅)₃ mediated hydrosilylative transformations.

We began with a series of alkenyl-sugars that establish a 1,3 (homoallylic) and 1,5 relationship between an olefin and the alcohol targeted for activation (Scheme 1c). Testing began with **1**, made from 2-deoxyribose in a single step. **1** cleanly provides **2** as a 9:1 mixture of diastereomers (60%, Table 1, Entry 1). It results from preferential activation (by silylium) of the single 1° C–O bond (to form the C6–OSi⁺), followed by alkenyl attack and carbocation reduction by H–B(C₆F₅)₃[–]. Mechanistic data suggests a variant of this mechanism may also be operative (*vide infra*).

We reasoned that a substrate lacking the 1,5-relationship between the nucleophilic end of the olefin and the 1° C–O bond might favour an alternate ring size. For **4** (Entry 2), this cleanly provides a single diastereomer of cyclopropane **4** (95%),

Table 1. Formation of cyclopentane and cyclopropane rings.



Entry	R	Substrate (E/Z)	Product	Yield (%)
1	Me ₂ Et	 1 ribo- (85:15 E/Z) ^a	 2	60 90:10 dr ^b
2	Ph ₃	 3 galacto- (77:23 E/Z) ^a	 4	95 >98:2 dr ^{c,d}
3	Et ₃	 5 gluco- (86:14 E/Z) ^a	 6	82 >98:2 dr ^e
4	Me ₂ Et	 7 ribo- (76:24 E,E,E,Z) ^f	 8	71 92:8 dr ^b
5	Me ₂ Et	 9 galacto- (76:24 E,E,E,Z) ^f	 10	71 >98:2 dr ^c
6	Me ₂ Et	 11 gluco- (65:35 E,E,E,Z) ^f	 12	82 >98:2 dr ^c
7	Ph ₃ Si	 13 galacto- (68:32 E,E,E,Z) ^a	 14	78 >98:2 dr ^{d,g}

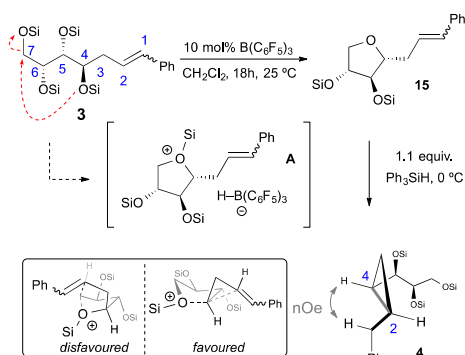
^a per-Me₃Si-protected. ^b By analogy to (**23**). ^c assigned by NOE. ^d 25 °C. ^e 0 °C. ^f per-Me₂EtSiH-protected. ^g from NOE.

a result of preferential homoallylic C–O activation. The *gluco*-derived **5** generated the diastereomeric cyclopropane **6**, with high efficiency and selectivity (Entry 3). The existing stereochemistry does not influence the

efficiency or selectivity of the reaction. Dienes are also viable and are readily functionalizable (Entries 4-7). High diastereoselectivity is noted in all cases.

Control experiments with $B(C_6F_5)_3$ alone converted **3** to furan **15** on a slower timescale (18 h) than catalysis. It results from the dehydrative cyclization of the C_3 -OSi onto the primary C_7 position. Reduction of **15** with Ph_3SiH yields **4** suggesting that **A** may reside on the reaction path (Scheme 2). If correct this suggests that: 1) the enhanced basicity of the ethereal oxygen (relative to silyl ether) acts to sequester the silylium ion and direct C–C bond formation to between the C_2 and C_4 positions (Scheme 2); and 2) catalytically generated silylium ion is more active than BCF for cyclodehydration.

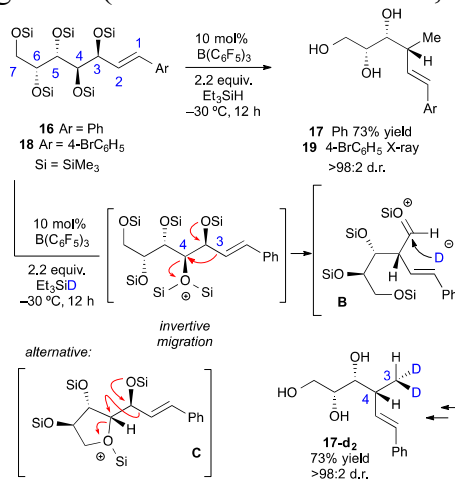
The cyclopropanative ring opening of **A** provides a model for the preferred alkene addition onto C_4 over C_7 (Scheme 2).



Scheme 2. Model for cyclopropane formation and selectivity.

Njarderson has shown that allylic C–O bond reductions with $B(C_6F_5)_3$ and R_3SiH are facile. Can intramolecular trapping compete? Studies with the *galacto*-derived alkenyl sugar **16** yields a single diastereomer of methyl pentene, **17**. Deuteration studies with Et_3SiD indicate the intermediacy of silyloxycarbenium ion **B** (Scheme 3),

which is doubly reduced to **20**. X-ray diffraction of **19** verified an invertive vinyl shift at C_4 . An alternative mechanism invokes a precyclization to **C**, which is analogous to **A** except that it additionally contains an allylic silyl ether at C_3 and thus stabilizes the intermediate resulting from vinyl migration (sila-oxo-carbenium ion, **B**).



Scheme 3. Proposed mechanism for the conversion of **16** to **17**.

As illustrated in Scheme 4, reduction of **21** with $B(C_6F_5)_3$ and Me_2EtSiH led to a single diastereomer of **22**, a product with 4 contiguous stereocenters (83%). **22** could be obtained in a single step from **16**, and is thus available from galactose in three steps (Wittig, TMS-protection, cyclization/reduction). Altering the stereochemistry of the poly-ol portion had little effect on the efficiency and selectivity. The *manno*- and *gluco*-substrates converge on to **25** (86:14 dr, Entries 3-4, Table 2).

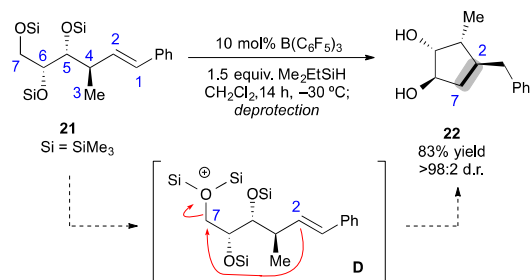
The combination of $B(C_6F_5)_3$ and a tertiary silane enables the selective deoxygenation of alkene containing carbohydrates. C–C bond forming ring closure is efficient and follows the trend of 5 (1°) > 3 (2°) > 6 (1°), where the substitution of the activated C–O

leaving group is indicated. Transiently formed heterocycles may alter this inherent kinetic profile. The reactions are operationally robust, selective, and efficient at converting alkene containing biomass-derived feedstock materials into stereochemically complex materials. Our experiments establish the role of neighbouring group participation in guiding the reductions, while also revealing a set of reactivity principles that enable the predictive synthesis of new synthons from renewable feedstocks.

Table 2. Tetra-substituted cyclopentane formation.

Entry	Substrate (<i>E/Z</i>)	Product	Yield (%)
1	 <i>galacto-</i> (>98% <i>E</i>) ^a 16 Ar = Ph		82 >98:2 dr
2	18 Ar = 4-Br-C ₆ H ₄ (63:27 <i>E/Z</i>)		71 >98:2 dr ^b X-ray
3	24 <i>manno-</i> (33:67 <i>E/Z</i>) ^a		79 86:14 dr ^c
4	26 <i>gluco-</i> (67:33 <i>E/Z</i>) ^a		

^{a.} per-Me₃Si-protected. ^{b.} assigned by X-ray. ^{c.} by analogy to **23**.



Scheme 4. 1-step synthesis of tetrasubstituted cyclopentanes.

Acknowledgements

We gratefully acknowledge the Department of Energy (Basic Energy Sciences, DE-FG02-05ER15630) for financial support.

Publications Acknowledging this Grant in 2013-2016

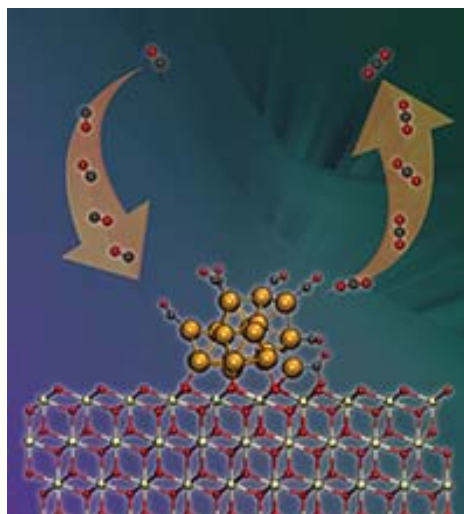
- Bender, T. A.; Dabrowski, J. A.; Zhong, H.; Gagné, M. R. “Alkene Directed Defunctionalization of Biomass-Derived Materials” *Chem. Sci.* **2016**, *Submitted*. This new development is provided in an abridged form above.
- Adduci, L. A.; Bender, T. A.; Dabrowski, J. A.; Gagné, M. R. “Chemoselective conversion of biologically sourced polyols into chiral synthons” *Synform* **2015**, *12*, A169-A171.
- Adduci, L. A.; Bender, T. A.; Dabrowski, J. A.; Gagné, M. R. “Chemoselective conversion of biologically sourced polyols into chiral synthons” *Nature: Chemistry* **2015**, *7*, 576-581.
- Adduci, L. L.; McLaughlin, M. P.; Bender, T. A.; Becker, J. J.; Gagné, M. R. “Metal-free Deoxygenation of Carbohydrates” *Angew. Chem. Int. Ed.* **2014**, *53*, 1646-1649.
- McLaughlin, M. P.; Adduci, L. A.; Adduci, L. A.; Becker, J. J.; Gagné, M. R. “Iridium-catalyzed hydrosilylative reduction of glucose to hexane(s)” *J. Am. Chem. Soc.* **2013**, *135*, 1225-1227.

Discovering Emergent Phenomena in Catalysis Through Large Scale Ab Initio Molecular Dynamics Simulations

Roger Rousseau, Vassiliki-Alexandra Glezakou, Mal-Soon Lee, Wang-Gang Wang,
David C. Cantu, Manh-Thuong Nguyen.

Institute for Integrated Catalysis, Pacific Northwest National Laboratory, Richland WA 99354

The current state of the art of electronic structure methods allows us to tackle model systems on the order of 100s to 1000s of atoms with suitable speed and efficiency to perform statistical mechanical sampling on millions of configurations. This has opened the door to using theoretical tools such as ab initio molecular dynamics (combined with enhanced sampling techniques) to discover novel emergent phenomena that result from chemical complexity. Nowhere is this more needed than in catalysis where models need to include support materials, the catalysts, the reactants and products all at elevated temperature and pressures. In this context, both global and local anharmonicities on the potential energy surface can lead to unexpected phenomena that can be discovered through large scale simulation yet are often not accounted for in our current models. This will be illustrated with examples drawn from the chemistry of metal particles on reducible supports [1-2], Brønsted acid chemistry in confined spaces [3] and reactivity at solid-liquid interfaces [4,5]. Our perspective is that modern simulations tools, when directly compared with concurrent experimental measurements for validation and verification, can be used to craft the next generation of concepts that better account for emergent behavior and complexity than our current models.



References

1. Wang Y.-G., Mei, D., V.-A. Glezakou, Li, J., Rousseau R Nature Comm. **6**, 651 (2015)..
2. Wang, Y.-G., Yoon, Y., Glezakou, V.-A., Li, J. and Rousseau, R. *J. Am. Chem. Soc.* **135**, 10673-10683 (2013).
3. Alexopoulos, K., Lee, M.-S., Liu, Y., Zhi, Y., Liu, Y., Reyniers, M.-F., Marin, G. B., Glezakou, V.-A. Rousseau, R., Lercher J. A.. *J. Phys. Chem. C* **2016**, 120, 7172-7182.
4. Yoon, Y., Rousseau, R., Weber, R. S., Mei, D., Lercher, J. A.. *J. Am. Chem. Soc.* **2014**, 136 10287-10298.
5. Lee, M.-S.; McGrail, B. P.; Rousseau, R. & Glezakou, V.-A. *Scientific reports* **2015**, 5 14857.

Oxidation Reactions on PdO(101)

Jason F. Weaver,¹⁾ Aravind Asthagiri,²⁾ Feng Zhang,¹⁾ Li Pan,²⁾ Juhee Choi,¹⁾ Vikram Mehar¹⁾

¹⁾ Department of Chemical Engineering, University of Florida, Gainesville, FL 32611

²⁾ Department of Chemical and Biomolecular Engineering, The Ohio State University,
Columbus, OH 43210

Presentation Abstract

Interest in the surface chemistry of late transition-metal oxides has been stimulated by observations that the formation of metal oxide layers tends to dramatically alter the catalytic performance of transition metals in applications of oxidation catalysis. As an example, the formation of palladium oxide (PdO) is thought to be responsible for the exceptional activity of supported Pd catalysts toward the complete oxidation of alkanes under oxygen-rich conditions. In this talk, I will discuss our investigations of the surface chemical properties of a PdO(101) thin film that is grown in ultrahigh vacuum using plasma-generated oxygen atom beams, and will focus particularly on our studies of the adsorption and activation of alkanes as well as the oxidation of CO. We find that *n*-alkanes adsorb strongly on the PdO(101) surface by forming σ -complexes along rows of coordinatively-unsaturated Pd atoms, and that this adsorbed state acts as the precursor for initial C-H bond cleavage. I will discuss characteristics of the binding and selective activation of alkane σ -complexes on PdO(101) as determined from both experiment and density functional theory (DFT) calculations. I will also discuss elementary processes involved in the oxidation of CO on PdO(101) and clarify the role that oxygen vacancies play in mediating this chemistry.

DE-FG02-03ER15478: Oxidation Chemistry on Pd and Pd-Pt Oxide Surfaces

Student(s): F. Zhang, L. Pan, J. Choi, M. Kim, V. Mehar

RECENT PROGRESS

Selective coordination and activation of primary C-H bonds of propane σ -complexes on PdO(101)

We reported results that clarify the molecular-level origin for an exceptionally strong preference for propane to dissociate on the crystalline PdO(101) surface via primary C-H bond cleavage. Using reflection absorption infrared spectroscopy (RAIRS) and DFT calculations, we find that the Pd-coordinated C-H bonds of propane σ -complexes on PdO(101) exhibit stretch frequencies that are redshifted from the gas-phase values by up to 400 cm^{-1} , demonstrating that dative

bonding with Pd_{cus} atoms significantly softens alkane C-H bonds. By performing experiments with partially-deuterated propane compounds, we further show that the adsorbed propane complexes undergo a configurational change as a function of the coverage, wherein the molecules preferentially coordinate through the CH₃ groups at low coverage but through the CH₂ groups at high coverage. Our results demonstrate that adsorbed propane σ -complexes preferentially adopt geometries on PdO(101) in which only primary C-H bonds datively interact with the surface Pd atoms at low propane coverages and are thus activated under typical catalytic reaction conditions. We show that a propane molecule achieves maximum stability on PdO(101) at low coverage by adopting a bidentate geometry in which a H-Pd dative bond forms at each CH₃ group. Our results demonstrate that structural registry between the molecule and surface can strongly influence the selectivity of a metal oxide surface in activating alkane C-H bonds.

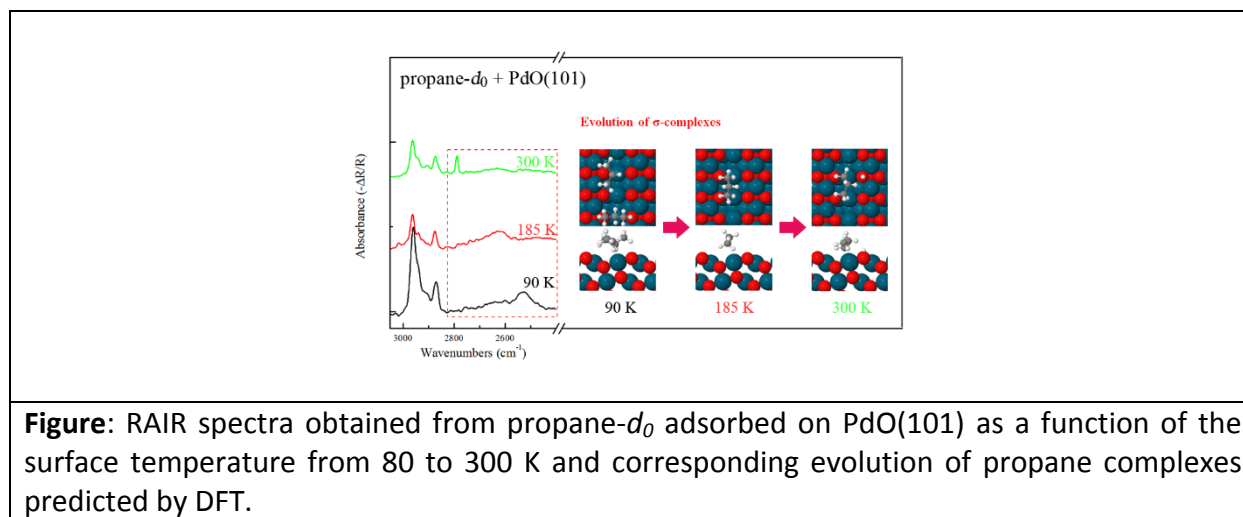


Figure: RAIR spectra obtained from propane- d_0 adsorbed on PdO(101) as a function of the surface temperature from 80 to 300 K and corresponding evolution of propane complexes predicted by DFT.

Promotion of CO oxidation on PdO(101) by adsorbed water

We investigated the influence of adsorbed H₂O on the oxidation of CO on PdO(101) using temperature programmed reaction spectroscopy (TPRS), RAIRS and DFT calculations. In the presence of adsorbed H₂O, the oxidation of CO on PdO(101) produces a CO₂ TPRS peak that is centered at a temperature ~50 K lower than the main CO₂ TPRS peak arising from CO oxidation on clean PdO(101) (~330 vs. 380 K). RAIRS shows that CO continues to adsorb on atop-Pd sites of PdO(101) when H₂O is co-adsorbed, and provides no evidence of other reactive intermediates. According to DFT, hydrogen bonding interactions with adsorbed H₂O species stabilize the carboxyl-like transition structure and intermediate that result from the initial recombination of CO and O on the PdO(101) surface. This stabilization lowers the energy barrier for CO oxidation on PdO(101) by ~10 kJ/mol, in good agreement with our experimental estimate.

Tuning the reactivity of ultra-thin oxides: NO adsorption on monolayer FeO(111)

In collaboration with research groups in Sweden, we reported a study last year showing that monolayer FeO(111) films supported on metal surfaces show large differences in reactivity

depending on the metal substrate, potentially enabling tunability of these materials' catalytic properties. Using TPD and RAIRS, we show that nitric oxide (NO) adsorption is facile on silver-supported FeO(111) monolayers, whereas a similar film grown on platinum is inert to NO under similar conditions. Ab initio calculations link this substrate-dependent behavior to steric hindrance caused by substrate-induced rumpling of the FeO layer, which is stronger for the platinum-supported film. The calculations show that the size of the activation barrier to adsorption caused by the rumpling is dictated by the strength of the metal-oxide interaction, offering a straightforward way to tailor the adsorption properties of ultrathin films.

Publications Acknowledging this Grant in 2013-2016

1) Exclusively funded by this grant;

- 1) "Promotion of CO oxidation on PdO(101) by adsorbed H₂O", J. Choi, L. Pan, V. Mehar, F. Zhang, A. Asthagiri and J.F. Weaver, *Surf. Sci.* 650 (2016) 203-209.
- 2) "Catalytic chemistry of oxide nanostructures", A. Asthagiri, D. Dixon, Z. Dohnálek, B. Kay, R. Rousseau, J. Rodriguez, D. Stacchiola, and J. F. Weaver in *Oxide materials at the two-dimensional limit*, Springer Series in Materials Science, Vol. 234 (2016). Editors: F. Netzer and A. Fortunelli.
- 3) "Propane σ -complexes on PdO(101): Spectroscopic evidence of the selective coordination and activation of primary C-H bonds", F. Zhang, L. Pan, J. Choi, V. Mehar, J.T. Diulus, A. Asthagiri and J.F. Weaver, *Angew. Chem. Int. Ed.*, 54 (2015) 13907-13911.
- 4) "Vacancy-mediated processes in the oxidation of CO on PdO(101)", J.F. Weaver, F. Zhang, T. Li, L. Pan and A. Asthagiri, *Acc. Chem. Res.* 48 (2015) 1515–1523.
- 5) "Molecular adsorption of NO on PdO(101)", J. Choi, L. Pan, F. Zhang, J. Diulus, A. Asthagiri and J.F. Weaver, *Surf. Sci.* 640 (2015) 150-158.
- 6) "CO oxidation on PdO(101) during temperature programmed reaction spectroscopy: Role of oxygen vacancies", F. Zhang, L. Pan, T. Li, J. Diulus, A. Asthagiri and J.F. Weaver, *J. Phys. Chem. C* 118 (2014) 28647–28661.
- 7) "Intrinsic ligand effect governing the catalytic activity of Pd oxide thin films", N.M. Martin, M. Van den Bossche, A. Hellman, H. Grönbeck, C. Hakanoglu, J. Gustafson, S. Blomberg, N. Johanson, Z. Liu, S. Axnanda, J.F. Weaver, and E. Lundgren, *ACS Catal.* 4 (2014) 3330-3334.
- 8) "CO oxidation on single and multilayer Pd oxides on Pd(111): Mechanistic insights from RAIRS", F. Zhang, T. Li, L. Pan, A. Asthagiri and J.F. Weaver, *Catal. Sci. Technol.* 4 (2014) **3826-3834**.
- 9) "Effects of non-local exchange on core-level shifts for gas-phase and adsorbed molecules", M. Van den Bossche, N.M. Martin, C. Hakanoglu, J. Gustafson, J.F. Weaver, E. Lundgren and H. Grönbeck, *J. Chem. Phys.* 141 (2014) 034706.
- 10) "Alkane activation on crystalline metal oxide surfaces", J.F. Weaver, C. Hakanoglu, A. Antony and A. Asthagiri, *Chem. Soc. Rev.* 43 (2014) **7536-7547**.

- 11) "CO adsorption on clean and oxidized Pd(111)", N.M. Martin, M. Van den Bossche, H. Grönbeck, C. Hakanoglu, F. Zhang, T. Li, J. Gustafson, J.F. Weaver and E. Lundgren, *J. Phys. Chem. C* 118 (2014) 1118–1128.
 - 12) "Pathways and kinetics for methane and ethane C-H bond cleavage on PdO(101)", A. Antony, A. Asthagiri and J.F. Weaver, *J. Chem. Phys.* 139 (2013) 104702: 1-12.
 - 13) "Inhibition of methane adsorption on PdO(101) by water and molecular oxygen", F. Zhang, C. Hakanoglu, J. Hinojosa, Jr. and J.F. Weaver, *Surf. Sci.* 617 (2013) 249-255.
 - 14) "Dissociative adsorption of hydrogen on PdO(101) studied by HRCLS and DFT", N.M. Martin, M. Van den Bossche, H. Grönbeck, C. Hakanoglu, J. Gustafson, S. Blomberg, M.A. Arman, A. Antony, R. Rai, A. Asthagiri, J.F. Weaver and E. Lundgren, *J. Phys. Chem. C* 117 (2013) 13510–13519.
 - 15) "Selectivity in the initial C-H bond cleavage of n-butane on PdO(101)", C. Hakanoglu, F. Zhang, A. Antony, A. Asthagiri and J.F. Weaver, *Phys. Chem. Chem. Phys.* 15 (29) (2013) 12075 - 12087.
 - 16) "Surface chemistry of late transition metal oxides", J.F. Weaver, *Chem. Rev.* 113 (2013) 4164-4215.
 - 17) "Surface reactivity of oxide phases on Pd(111) generated during the growth vs reduction of PdO(101) films", C. Hakanoglu and J.F. Weaver, *Surf. Sci.* 611 (2013) 40-48.
- II) *Jointly funded by this grant and other grants with leading intellectual contribution from this grant;*
- 1) "Tuning the chemical properties of ultrathin oxides: NO adsorption on monolayer FeO(111)", L. Merte, C.J. Heard, F. Zhang, J. Choi, M. Shipilin, J.F. Weaver, H. Grönbeck and E. Lundgren, *Angew. Chem. Int. Ed.*, (2016) in press.
 - 2) "Adsorption of NO on FeO_x films grown on Ag(111)", V. Mehar, L. Merte, J. Choi, M. Shipilin, E. Lundgren and J.F. Weaver, *J. Phys. Chem. C* 120 (2016) 9282-9291.

Synthetic and Mechanistic Studies Pertaining to Homogeneous Catalytic Transformations of Small Molecules by Metal Centers

Wesley Sattler, Michelle C. Neary, Serge Ruccolo, Mahnaz Rostami Chaijan, Tawfiq Nasr Allah, and Gerard Parkin
Columbia University, Department of Chemistry

Presentation Abstract

Transformations involving small molecules such as carbon dioxide and formic acid are of much current interest. For example, formic acid has received considerable attention with respect to its potential as a chemical storage medium for hydrogen fuel *via* its catalytic release of H₂, while the conversion of CO₂ into valuable chemicals provides a beneficial use of this greenhouse gas. In addition to achieving these transformations, it is also important to perform them with non-precious metal catalysts. Thus, with respect to the release of H₂ from formic acid, we have demonstrated that this transformation may be achieved by cyclopentadienyl molybdenum complexes, namely CpMo(CO)_x(PMe₃)_{3-x}H (*x* = 1, 2, 3). Furthermore, these complexes are also capable of effecting the disproportionation of formic acid into CO₂ and methanol, which is of relevance to a potential methanol economy. The disproportionation of formic acid is a manifestation of a transfer hydrogenation reaction, which has also been applied to the reduction of aldehydes and ketones. With respect to the conversion of CO₂ into useful chemicals, the zinc hydride complex, [*tris*(2-pyridylthio)methyl]zinc hydride ([Tptm]ZnH), is effective for the catalytic hydrosilylation of CO₂. Specifically, [Tptm]ZnH catalyzes the addition of (EtO)₃SiH to CO₂ to give (EtO)₃SiO₂CH₃, which may subsequently be converted into useful chemicals, such as *N,N*-dimethylformamide. [Tptm]ZnH is also an effective catalyst for other transformations, such as the multiple insertions of carbonyl groups into the Si–H bonds of silanes, and dehydrocoupling of silanes with alcohols. Related reactivity of other metal complexes will also be discussed.

DE-FG02-93ER14339: Fundamental Studies of Metal Centered Transformations Relevant to Catalysis

Students: Michelle Neary, Serge Ruccolo

RECENT PROGRESS

1. Hydrosilylation of Aldehydes and Ketones Catalyzed by a Terminal Zinc Hydride Complex, [Tptm]ZnH

Catalytic hydrosilylation of carbonyl compounds to afford alkoxy silanes provides a method to achieve the overall reduction to the alcohol *via* subsequent hydrolysis of the alkoxy silane.

Furthermore, alkoxy silanes have applications in organic synthesis and materials chemistry. In addition to obtaining improved catalysts for this transformation, it is important to develop effective catalysts that are based on abundant non-precious metals. Zinc is one such metal, and we have demonstrated that the [*tris*(2-pyridylthio)methyl]zinc hydride complex, [Tptm]ZnH, is capable of achieving multiple insertion of carbonyl compounds into the Si–H bonds of PhSiH₃ and Ph₂SiH₂.

A large variety of aldehydes and ketones undergo [Tptm]ZnH catalyzed insertion into the Si–H bonds of PhSiH₃, some examples of which include RCHO (R = Me, Ph) and R₂CO (R = Me, Et, Ph). In each case, treatment of a 1:3.3 mixture of PhSiH₃ and RC(O)R' with 3.3 mol % of catalyst (relative to PhSiH₃) results in the quantitative formation of the triple insertion product, PhSi[OCH(R)R']₃. Aldehydes are the most active, and the reactions proceed to completion in less than 20 minutes, with turnover frequencies (TOFs) > 200 h⁻¹ over this period. Dialkyl ketones are the slowest but proceed smoothly to completion over a period of one day. In contrast to dialkyl ketones, however, the diaryl ketone Ph₂CO is very reactive and the reaction proceeds to completion in less than 10 minutes at room temperature. The reactions can also be performed in the absence of solvent. Thus, addition of PhC(O)Me (3.3 equivalents) to PhSiH₃ in the presence of [Tptm]ZnH (3.3 mol %) results in the rapid formation of PhSi[OCH(Me)Ph]₃.

While selective triple insertion is observed upon treatment of PhSiH₃ with three equivalents of RC(O)R', a mixture of single, double and triple insertion products, PhSiH₂[OCH(R)R'], PhSiH[OCH(R)R']₂ and PhSi[OCH(R)R']₃, is observed upon treatment of PhSiH₃ with fewer equivalents of RC(O)R'. For example, a 1:1 mixture of PhC(O)Me and PhSiH₃ gives a mixture that contains predominantly PhSiH[OCH(Me)Ph]₂, together with a small amount of PhSiH₂[OCH(Me)Ph] (3 %) and unreacted PhSiH₃, while a 2:1 mixture of PhC(O)Me and PhSiH₃ gives a mixture that contains PhSi[OCH(Me)Ph]₃ and PhSiH[OCH(Me)Ph]₂. The observation that both 1:1 and 2:1 mixtures of PhC(O)Me and PhSiH₃ give primarily the double insertion product indicates that, whereas incorporation of one alkoxy group significantly promotes the insertion into the remaining Si–H bonds, the effect is less pronounced upon incorporation of a second alkoxy substituent.

A noteworthy feature of the reactions of prochiral ketones is that the triple insertion products, PhSi[OCH(R)R']₃, exist as two diastereomers by virtue of the fact that the molecule contains three chiral centers. Thus, PhSi[OCH(Me)Ph]₃ consists of two diastereomers, each of which exists as an enantiomeric pair, *i.e.* *RRR/SSS* and *RRS/SSR*. Evidence for this assignment is provided by the synthesis of enantiopure (*R,R,R*)-PhSi[OCH(Me)Ph]₃ and (*S,S,S*)-PhSi[OCH(Me)Ph]₃ by the [Tptm]ZnH catalyzed alcoholysis of PhSiH₃ with (*R*)-(+)-1-phenylethanol and (*S*)-(–)-1-phenylethanol, respectively.

Ph₂SiH₂ is also a commonly used reagent for the hydrosilylation of aldehydes and ketones, although it often exhibits reduced reactivity compared to PhSiH₃. Therefore, it is significant that [Tptm]ZnH is also an effective catalyst for room temperature hydrosilylation reactions employing Ph₂SiH₂, affording products derived from both single and double insertion. The ability of [Tptm]ZnH to achieve double insertion of ketones into Ph₂SiH₂ is of note since only the monoinsertion product is typically observed.

A large variety of mechanisms for hydrosilylation of carbonyl compounds has been discussed in the literature but, in view of the presence of the hydride ligand, a reasonable mechanism for the [Tptm]ZnH catalyzed hydrosilylation of carbonyl compounds consists of two principal steps, namely: (*i*) insertion of the carbonyl group into the Zn–H bond of [Tptm]ZnH to form an alkoxide, [Tptm]ZnOCH(R)R', and (*ii*) metathesis of the Zn–O and H–Si bonds to

regenerate $[\text{Tptm}]\text{ZnH}$ and release the alkoxysilane, $\text{PhSiH}_2[\text{OCH}(\text{R})\text{R}']$. Additional cycles allow for the subsequent formation of the double and triple insertion products, $\text{PhSiH}[\text{OCH}(\text{R})\text{R}']_2$ and $\text{PhSi}[\text{OCH}(\text{R})\text{R}']_3$.

Several pieces of evidence indicate that the hydride ligand of $[\text{Tptm}]\text{ZnH}$ plays a critical role in the mechanism. For example, ^1H NMR spectroscopy demonstrates that insertion of the carbonyl group into the Zn-H bond of $[\text{Tptm}]\text{ZnH}$ to form an alkoxide, $[\text{Tptm}]\text{ZnOCH}(\text{R})\text{R}'$, is facile, and that subsequent treatment with PhSiH_3 regenerates $[\text{Tptm}]\text{ZnH}$ and liberates an alkoxysilane.

2. Nickel-catalyzed Release of H_2 from Formic Acid

The growing demand for energy has prompted much effort in the utilization of fuels that are more sustainable than those based on fossil feedstocks. For example, hydrogen, which can be generated by renewable means, is a promising alternative because it can be used in either a fuel cell or a combustion engine. A problem with the use of hydrogen as a fuel, however, is that current storage and transportation techniques are inadequate. Therefore, much attention has been directed towards discovering both physical and chemical methods to provide hydrogen on demand. Formic acid, in particular, has garnered interest as a chemical medium for storing H_2 because it is a liquid at room temperature and, as a consequence, is easy to handle and transport. The utilization of formic acid as a storage medium for H_2 , however, requires effective catalysts to release H_2 on demand and there is much interest in the discovery of catalysts that utilize earth abundant non-precious metals. Therefore, we have investigated the ability of a nickel compound, and specifically $\text{Ni}(\text{PMe}_3)_4$, to serve as a catalyst for the release of H_2 from formic acid.

Significantly, $\text{Ni}(\text{PMe}_3)_4$ does indeed catalyze this transformation. The ability of $\text{Ni}(\text{PMe}_3)_4$ to achieve this transformation is noteworthy in view of the fact that there is only one other example of a nickel compound, namely $[\kappa^3\text{-C}_6\text{H}_3(\text{CH}_2\text{P}^t\text{Bu}_2)_2]\text{NiH}$, that has recently been reported to release H_2 from formic acid. Also of note, $\text{Ni}(\text{PMe}_3)_4$ can achieve the catalytic conversion in absence of a base, whereas $[\kappa^3\text{-C}_6\text{H}_3(\text{CH}_2\text{P}^t\text{Bu}_2)_2]\text{NiH}$ requires the presence of an amine (either Et_3N or OctNH_2) to achieve catalysis.

The essential features of the mechanism of the catalytic cycle are proposed to involve (i) formation of a nickel formate species, (ii) decarboxylation of the nickel formate to afford a nickel hydride intermediate, and (iii) release of H_2 . For example, one possible sequence involves oxidative addition of formic acid to give a five-coordinate formate-hydride, namely $\text{Ni}(\text{PMe}_3)_3(\text{O}_2\text{CH})\text{H}$, which exists in equilibrium with four-coordinate $\text{Ni}(\text{PMe}_3)_2(\text{O}_2\text{CH})\text{H}$. Subsequent elimination of CO_2 forms a dihydride intermediate, $\text{Ni}(\text{PMe}_3)_2\text{H}_2$, which releases H_2 by either reductive elimination or by reaction with formic acid.

In view of the proposal that the catalytic mechanism for the release of H_2 from formic acid involves decarboxylation of a formate intermediate, we sought to examine the ability of PMe_3 to induce the transformation in a well-defined nickel formate complex. Significantly, we observed that addition of PMe_3 to the pyridine complex, $\text{Ni}(\text{py})_4(\text{O}_2\text{CH})_2$, results in the release of CO_2 and H_2 at room temperature, with the accompanying formation of $\text{Ni}(\text{PMe}_3)_4$. Furthermore, PMe_3 also reacts with a suspension of $\text{Ni}(\text{O}_2\text{CH})_2 \cdot 2\text{H}_2\text{O}$ in benzene to release CO_2 and H_2 at 60 °C and form $\text{Ni}(\text{PMe}_3)_4$.

The ability of PMe_3 to induce the room temperature decarboxylation of a nickel formate species is of considerable significance in view of the fact that the reverse reaction, *i.e.* the insertion of CO_2 into a M-H bond, is more commonly observed. With respect to the mechanism of the PMe_3 induced decarboxylation, a plausible sequence involves the initial coordination of

PMe₃ to afford a four-coordinate adduct, Ni(PMe₃)₂(O₂CH)₂. Two decarboxylation events would sequentially form Ni(PMe₃)₂(O₂CH)H and Ni(PMe₃)₂H₂, of which the latter would be expected to release H₂ in the presence of PMe₃ to form Ni(PMe₃)₄. Finally, in addition to the PMe₃ induced decarboxylation of formate being of mechanistic interest, it is also of synthetic relevance since it provides a very useful method for obtaining Ni(PMe₃)₄.

Publications (2013 – 2016)

(I) Exclusively funded by this grant

1. Wesley Sattler, W.; Parkin, G. Reduction of Bicarbonate and Carbonate to Formate in Molecular Zinc Complexes. *Catal. Sci. Tech.* **2014**, *4*, 1578–1584.
2. Zuzek, A. A.; Parkin, G. Si–H and Si–C Bond Cleavage Reactions of Silane and Phenylsilanes with Mo(PMe₃)₆: Silyl, Hypervalent Silyl, Silane, and Disilane Complexes. *J. Am. Chem. Soc.* **2014**, *136*, 8177–8180.
3. Sattler, A.; Zuzek, A. A.; Parkin, G. Molecular Structure of W(PMe₃)₃H₆ in the Solid State and in Solution. *Inorg. Chim. Acta* **2014**, *422*, 102-108.
4. Sattler, A.; Parkin, G. Trinuclear, Tetranuclear and Octanuclear Chalcogenido Clusters of Molybdenum and Tungsten Supported by Trimethylphosphine Ligands. *Polyhedron* **2014**, *84*, 74-86.
5. Shin, J. H.; Churchill, D. G.; Parkin, G. Bis(η⁵-pentamethylcyclopentadienyl) Complexes of Molybdenum. *Inorganic Syntheses* **2014**, *36*, 58-62.
6. Zuzek, A. A.; Parkin, G. Oxidative Addition of SiH₄ and GeH₄ to Ir(PPh₃)₂(CO)Cl: Structural and Spectroscopic Evidence for the Formation of Products Derived from *Cis* Oxidative Addition. *Dalton Trans.* **2015**, *44*, 2801-2808.
7. Sattler, W.; Ruccolo, S.; Rostami Chaijan, M.; Nasr Allah, T.; Parkin, G. Hydrosilylation of Aldehydes and Ketones Catalyzed by a Terminal Zinc Hydride Complex, [κ³-Tptm]ZnH. *Organometallics* **2015**, *34*, 4717-4731.
8. Green, M. L. H.; Parkin, G. The Covalent Bond Classification Method and its Application to Compounds that Feature Three-Center Two-Electron Bonds. *Struct. Bond.* DOI: 10.1007/430_2015_206.

(II) Jointly funded by this grant and other grants with leading intellectual contribution from this grant

9. Zuzek, A. A.; Neary, M. C.; Parkin, G. σ-Silane, Disilanyl, and [W(μ-H)Si(μ-H)W] Bridging Silylene Complexes via the Reactions of W(PMe₃)₄(η²-CH₂PMe₂)H with Phenylsilanes. *J. Am. Chem. Soc.* **2014**, *136*, 17934-17937.
10. Neary, M. C.; Parkin, G. Dehydrogenation, Disproportionation and Transfer Hydrogenation Reactions of Formic Acid Catalyzed by Molybdenum Hydride Compounds. *Chem. Sci.* **2015**, *6*, 1859-1865.
11. Neary, M. C.; Parkin, G. Nickel-catalyzed Release of H₂ from Formic Acid and a New Method for the Synthesis of Zerovalent Ni(PMe₃)₄. *Dalton Trans.* DOI: 10.1039/c6dt01499b.
12. Neary, M. C.; Parkin, G. Structural Characterization of the Nickel(II) Formate Complex, Ni(py)₄(O₂CH)₂•2py, and Re-evaluation of the Nitrate Counterpart, Ni(py)₄(ONO₂)₂•2py: Evidence for Non-Linear Nitrate Coordination. *Polyhedron* DOI: 10.1016/j.poly.2016.04.033.

Analysis of the Mechanisms of Electrochemical Oxygen Reduction and Development of Ag-alloy and Pt-alloy Electro-catalysis for Low Temperature Fuel Cells

(University of Michigan, Department of Chemical Engineering)

Presentation Abstract

Electrochemical oxygen reduction reaction (ORR) is the major source of overpotential loss in low-temperature fuel cells. Expensive, Pt-based materials have been found to be the most effective catalysts. Exploration of alternatives has been hampered by stability constraints at the typical operating conditions of low pH and high potential.

I will discuss our studies of elementary mechanism of ORR on various metal electrodes using kinetic analysis of reaction pathways and quantum chemical calculations. These studies allowed us to identify the elementary steps and molecular descriptors that govern the rate of ORR. Using these performance descriptors we have been able to identify families of Pt and Ag-based alloys that exhibit superior ORR performance in acid and base respectively.

We have synthesized these alloys to demonstrate the superior ORR activity with rotating disk electrode experiments. We have also performed thorough structural characterization of the bulk and surface properties with a combination of cyclic voltammetry, x-ray diffraction, and electron microscopy with spatially resolved energy-dispersive x-ray spectroscopy and electron energy loss spectroscopy

Grant or FWP Number: DE-FG02-05ER15686

Development of physically transparent, predictive structure-performance relationships for rational design of multi-component catalytic materials

Postdoc(s): Adam Holewinski (currently Assistant Professor at University of Colorado)

Student(s): Hongliang Xin (currently Assistant Professor at Virginia Tech), Adam Halowinski (currently Assistant Professor at University of Colorado), Tim Van Cleve, Saman Moniri

RECENT PROGRESS

Objectives

The broad objective of our research efforts is to employ combined experimental/theoretical approaches to study the impact of small perturbations in the structure of solid catalysts (for example promotion by alkali promoters, poisoning, or alloying) on the outcome of chemical and catalytic surface reactions. Ultimately, we are interested in developing predictive theories that would guide us in the design of new or improved solid catalysts and electro-catalysts.^{1,2}

Accomplishments

So far we have focused on four central themes: (a) development of a general, physically transparent framework designed to shed light on underlying mechanisms associated with the impact of the perturbation of a metal surface on the chemical transformation on the surface, (b) the analysis of the impact of alkali promoters on chemical transformation on metals and, (c) the study of the effect of the perturbation in the chemical composition of active metal sites by formation of an alloy on the chemical activity of the site, and (d) applying the predictive models

to identify promising alloy catalysts in a number of probe reactions, including electrochemical oxygen reduction reaction (ORR). Concrete accomplishments include:

1. We have developed a general and physically transparent model, based on DFT methodology, which allows us to identify underlying physical mechanisms that govern the changes in the chemical activity of a metal surface site as the local chemical environment of the site is perturbed. This framework allows us to de-convolute and quantify various mechanisms by which the perturbation of a metal surface changes its chemical activity. These mechanisms induce: (i) local electronic effect, (ii) electrostatic, and (iii) polarization effect. This framework can be used to study various perturbations, including chemical promotion, poisoning and alloying. The work has been accepted for publication in The Journal of Chemical Physics.³
2. This model was utilized in a case study of the effect of Cs adsorbates (promoters) on the O₂ dissociation reaction on Ag(111). These studies revealed that the main mode by which Cs affects the dissociation of O₂ on Ag(111) is a long-range electrostatic/polarization interaction between Cs and relevant reaction intermediates. These interactions stabilize the transition state involved in the dissociation of O₂, therefore lowering the activation barrier. We demonstrated that these findings are fairly universal for metal surfaces promoted with alkali promoters.³
3. We have also studied how a working state of an alkali promoter changes as a function of external conditions, i.e., pressure and temperature of reactants. In this context, we have examined possible formation of Cs-oxide complexes as a function of the chemical potential of gas-phase O₂ (pressure and temperature). We employed ab-initio statistical mechanics to account for the effect of finite temperature and pressure of reactants. We have investigated whether and how the underlying mechanism of promotion depends on the nature of the alkali complex.
4. We have also employed the model, referenced under Accomplishment 1, to analyze mechanisms associated with the changes in the chemical activity of metal surfaces in response to the formation of alloys. In this context, we developed a predictive framework that can relate the geometric structure of an active center in a metal alloy material to its chemical activity.³⁻⁵ The model allows us to relate readily accessible physical properties of the metals that form the active site in the alloy (electronegativity and the geometric extend of d-orbitals) to various descriptors of catalytic activity (e.g., the adsorption energy of critical adsorbates). We performed a number of experimental studies verifying and validating the predictive capacity of the proposed framework.³⁻⁵
5. We have used this predictive model to screen through large libraries of alloy materials identifying the most optimal active sites for electrochemical oxygen reduction reaction (ORR) in acid and base.^{1,5,6}
6. The screening process has led us to the discovery of a number of Ag-based alloys for ORR in base that could meet techno-economic targets.⁷ We have synthesized and tested one of these alloys in the form of Ag-Co nanoparticles. Rigorous measurements demonstrated the superior activity and stability of this material in electrochemical ORR compared to pure Ag nanoparticles of equal size. In base, this material reaches approximately 50 % the rate of commercial Pt electro-catalysts which meets the techno-economic target.^{7,8}
7. More recently, we have expanded our studies to the development of a new family of Pt-based ORR electro-catalysts for ORR in acid. This has led to the development of novel Pt-alloy compositions which include layered structures of Au-Co core, covered by layers of Au and

one layer of Pt. Testing of these alloy materials showed that the materials are ~ 4 times more active than the commercial Pt standards for this reaction.⁹

References:

- (1) Holewinski, A.; Xin, H.; Nikolla, E.; Linic, S. Identifying Optimal Active Sites for Heterogeneous Catalysis by Metal Alloys Based on Molecular Descriptors and Electronic Structure Engineering. *Curr. Opin. Chem. Eng.* **2013**, *2* (3), 312–319.
- (2) Linic, S.; Christopher, P.; Xin, H.; Marimuthu, A. Catalytic and Photocatalytic Transformations on Metal Nanoparticles with Targeted Geometric and Plasmonic Properties. *Acc. Chem. Res.* **2013**, *46* (8), 1890–1899.
- (3) Xin, H.; Linic, S. Analyzing Relationships between Surface Perturbations and Local Chemical Reactivity of Metal Sites: Alkali Promotion of O₂ Dissociation on Ag(111). *J. Chem. Phys.* Accepted for publication.
- (4) Xin, H.; Holewinski, A.; Schweitzer, N.; Nikolla, E.; Linic, S. Electronic Structure Engineering in Heterogeneous Catalysis: Identifying Novel Alloy Catalysts Based on Rapid Screening for Materials with Desired Electronic Properties. *Top. Catal.* **2012**, *55* (5-6), 376–390.
- (5) Xin, H.; Holewinski, A.; Linic, S. Predictive Structure–Reactivity Models for Rapid Screening of Pt-Based Multimetallic Electrocatalysts for the Oxygen Reduction Reaction. *ACS Catal.* **2012**, *2* (1), 12–16.
- (6) Holewinski, A.; Xin, H.; Nikolla, E.; Linic, S. Identifying Optimal Active Sites for Heterogeneous Catalysis by Metal Alloys Based on Molecular Descriptors and Electronic Structure Engineering. *Curr. Opin. Chem. Eng.* **2013**.
- (7) Holewinski, A.; Idrobo, J.-C.; Linic, S. High-Performance Ag–Co Alloy Catalysts for Electrochemical Oxygen Reduction. *Nat. Chem.* **2014**, *6* (9), 828–834.
- (8) Van Cleve, T.; Gibara, E.; Linic, S. Electrochemical Oxygen Reduction Reaction on Ag Nanoparticles of Different Shapes. *ChemCatChem* **2016**, *8* (1), 256–261.
- (9) Van Cleve, T.; Moniri, S.; Linic, S. Atomistic Engineering of Efficient Oxygen Reduction Electro-Catalysts by Tailoring Local Chemical Environment of Pt Surface Sites. *Rev.*

Recent Publications Acknowledging this Grant

Funded exclusively by this grant (i)

1. Van Cleve, T.; Moniri, S.; Linic, S. Atomistic Engineering of Efficient Oxygen Reduction Electro-Catalysts by Tailoring Local Chemical Environment of Pt Surface Sites. *Under review*.
2. Xin, H.; Linic, S. Analyzing Relationships between Surface Perturbations and Local Chemical Reactivity of Metal Sites: Alkali Promotion of O₂ Dissociation on Ag(111). *J. Chem. Phys.* Accepted for publication.
3. Van Cleve, T.; Gibara, E.; Linic, S. Electrochemical Oxygen Reduction Reaction on Ag Nanoparticles of Different Shapes. *ChemCatChem* **2016**, *8* (1), 256–261.
4. Farrell, B. & Linic, S. Direct electrochemical oxidation of ethanol on SOFCs: Improved carbon tolerance of Ni anode by alloying. *Appl. Catal. B Environ.* **183**, 386–393 (2016).
5. Holewinski, A., Idrobo, J.-C. & Linic, S. High-performance Ag–Co alloy catalysts for electrochemical oxygen reduction. *Nature Chemistry*, **6**, 828–834 (2014).
6. Holewinski, A., Xin, H., Nikolla, E. & Linic, S. Identifying optimal active sites for heterogeneous catalysis by metal alloys based on molecular descriptors and electronic structure engineering. *Curr. Opin. Chem. Eng.* **2**, 312–319 (2013).

- Xin, H., Holewinski, A., Schweitzer, N., Nikolla, E. & Linic, S. Electronic Structure Engineering in Heterogeneous Catalysis: Identifying Novel Alloy Catalysts Based on Rapid Screening for Materials with Desired Electronic Properties. *Topics in Catalysis*, **55**, 376–390 (2012).

Jointly funded by this grant and other grants with leading intellectual contribution from this grant (ii);

- Linic, S., Christopher, P., Xin, H. & Marimuthu, A. Catalytic and Photocatalytic Transformations on Metal Nanoparticles with Targeted Geometric and Plasmonic Properties. *Acc. Chem. Res.* **46**, 1890–1899 (2013).
- Linic, S., Aslam, U., Boerigter, C. & Morabito, M. Photochemical transformations on plasmonic metal nanoparticles. *Nat. Mater.* **14**, 567–576 (2015).
- Marimuthu, A., Zhang, J. & Linic, S. Tuning Selectivity in Propylene Epoxidation by Plasmon Mediated Photo-Switching of Cu Oxidation State. *Science* **339**, 1590–1593 (2013).
- Christopher, P., Xin, H., Marimuthu, A. & Linic, S. Singular characteristics and unique chemical bond activation mechanisms of photocatalytic reactions on plasmonic nanostructures. *Nat. Mater.* **11**, 1044–1050 (2012).
- Marimuthu, A., Christopher, P. & Linic, S. Design of Plasmonic Platforms for Selective Molecular Sensing Based on Surface-Enhanced Raman Spectroscopy. *J. Phys. Chem. C* **116**, 9824–9829 (2012).

Jointly funded by this grant and other grants with minor intellectual contribution from this grant (iii);

- Boerigter, C., Campana, R., Morabito, M. & Linic, S. Evidence and implications of direct charge excitation as the dominant mechanism in plasmon-mediated photocatalysis. *Nat. Commun.* **7**, 10545 (2016).
- Farrell, B. L. & Linic, S. Oxidative coupling of methane over mixed oxide catalysts designed for solid oxide membrane reactors. *Catal. Sci. Technol.* (2016). doi:10.1039/C5CY01622C

**Reaction Mechanisms of Oxygenates over Oxide Catalysts:
Role of Surface Structure and Composition**

Zili Wu, Amanda Mann, Guo Shiou Foo, Felipe Polo Garzon, David Mullins, Ariana Beste,
Daniel A. Lutterman, Michelle K. Kidder, Sheng Dai and Steven H. Overbury
Chemical Science Division, Oak Ridge National Laboratory

Presentation Abstract

Metal oxides have shown interesting catalytic behaviors in the transformations of oxygenated molecules including dehydrogenation, dehydration, ketonization, condensation and coupling reactions. Although it has been accepted that the composition of oxide catalysts plays an important role in determining the catalysis, it remains largely unexplored how the surface structure of the oxide catalysts impacts the activity and selectivity. In this talk, I will discuss our recent work on understanding the role of surface structure and composition of oxide catalysts in the conversion of C₁-C₃ model oxygenates. To understand the surface structure effect, we utilized both UHV oriented surfaces (single crystal/thin films) and shaped nanocrystals of ceria to vary the surface site geometry, redox and acid base properties. The surface dependent reactions of methanol, ethanol and acetaldehyde were explored over the two different types of ceria surfaces to bridge material and pressure gaps. In extension to understand how composition affects the reactions of oxygenates, we compared the conversion of model oxygenates over mono-oxides and binary oxides including ceria, titania and perovskites. One common theme among the two research areas is to reveal how the interplay between the acid-base sites and the redox sites in oxide catalysts determines the reactivity and selectivity in the oxygenate reactions. The implication for tuning the reaction pathways of oxygenates over oxide catalysts will be discussed.

FWP ERKCC96: Fundamentals of Catalysis and Chemical Transformations

PIs: Zili Wu, Ariana Beste, Sheng Dai, Michelle K. Kidder, Daniel A. Lutterman, David R. Mullins, Aditya (Ashi) Savara, Steven H. Overbury

Postdoc(s): Amanda K.P. Mann, Zhenan Qiao, Chengcheng Tian, Guo Shiou Foo, Felipe Polo Garzon, Yafen Zhang

Student(s): Andrew Binder, Michelle Lukosi

Affiliations(s): Oak Ridge National Laboratory

RECENT PROGRESS

The overarching goal of this project is to understand how to control reaction selectivity through tuning cooperativity in multi-functional catalysts. The vision of our research is that by fundamentally understanding the composition and structure of catalytic sites and the mechanistic pathways, we will be enabled to precisely assemble closely interacting components into a catalyst to achieve the desired level of selectivity and activity. Specifically, we aim to elucidate the role of site geometry, surface and bulk composition, acid-base and redox sites, confinement,

and metal-support interactions in controlling selectivity in reactions catalyzed by oxides surfaces and supported metal particles. Our approach has been based on model catalysts with increasing complexity and model reactions with multistep pathways. The model catalysts range from thin films and single crystal in UHV surface science study to oxide nanocrystals with controlled surface facets and compositions, and supported metals with defined architectures. This allows us to bridge the materials and pressure gaps between UHV and reactor based methods. Over the last two years, the focus of this research has shifted from ceria-central to studying the transformation of model oxygenates and hydrocarbons over binary oxides such as perovskites. The surface chemistry, reaction kinetics and catalytic properties are studied by a collection of state-of-the-art *operando* and *in situ* methods including the neutron scattering methods at ORNL. The experimental work combines computational methods to aid interpretation of the experimental measurements and to create detailed models of reaction pathways.

Surface composition effect of oxide catalysts

Adsorption and reaction of oxygenates and hydrocarbons can be controlled not only by the surface structure of oxides such as CeO₂ with different facets (mentioned below), but also by the surface composition of oxides such as binary oxides including perovskites and mixed oxides. We choose perovskites as the initial model binary oxides because of the wide tunability of the A and B cations in ABO₃ perovskites and thus great opportunity in tuning not only the redox property but also the acid-base property of oxides to control catalytic reactions.

Alcohol reactions over perovskite particles. We aim to understand how the coupling of the acid-base and redox properties of perovskites is controlling the reactivity and selectivity in alcohol conversion. In an on-going effort, we have studied ABO₃ where A = Ba, Sr, Zn, La, Ce and B = Ti, Zr, Mn, Co for alcohol conversion because these perovskites differ in reducibility and acid-base properties. The dehydration vs dehydrogenation of isopropanol was used as a model reaction to understand the acid-base catalysis while methanol oxidation was tested to probe the interplay between the redox and acid-base sites. *In situ* IR, inelastic neutron scattering (INS) and microcalorimetry were used to characterize both qualitatively and quantitatively the surface acid-base, redox sites and reaction chemistry of alcohols. The type, strength and amount of acid-base sites were found to vary with the A and B cations in the perovskites. Reactivity tests are currently underway to correlate the acid-base and redox properties to the reaction activity and selectivity.

Ambient pressure XPS of alcohol on perovskite thin film. It is worth noting that there is little work reported on the surface chemistry of any perovskite surfaces in surface science study. Our goal is to use model perovskite surfaces to understand the interplay of the A and B cations in controlling the surface reactivity, selectivity and reaction mechanism of oxygenates. One of our aims is to correlate the surface science results to the catalysis observed on powder counterparts through bridging the “pressure gap” using ambient pressure x-ray photoelectron spectroscopy (APXPS). We are taking advantage of the BES material science programs at ORNL which provides us well-characterized perovskite thin films. We started with a thin film of doped La_{0.7}Sr_{0.3}MnO₃ (001) for methanol and ethanol oxidation. In order to investigate the “pressure gap” that may occur between reactions studied under vacuum conditions and at pressure approaching atmospheric pressure, experiments were conducted at nominally 10⁻⁵ torr and at 0.1 torr between 250 °C and 350 °C in the APXPS. Results using methanol or ethanol as the reactant are generally the same (see **Figure 1**), i.e., only methoxy/ethoxy on the surface at lower

pressures, a mixture of methoxy/ethoxy and formate/acetate at higher pressure in the absence of O_2 , and exclusively formate/acetate on the surface when O_2 was present. The only significant difference between methanol and ethanol was a greater tendency for ethanol to form the carboxylate in the absence of O_2 . At higher pressures, the Mn 2p spectra indicated that the alcohol partially reduced Mn^{3+} to Mn^{2+} and there was also an indication in the O 1s spectra that O was removed from the surface. These observations indicated that methanol was being oxidized through reaction with the surface.

Hydrocarbon oxidation over mixed oxides. Catalytic synergy often occurs when two oxides are intimately mixed such as in a solid solution. We aim to probe how this synergism may be tuned to control reaction pathways.

We synthesized a $Mn_{0.5}Ce_{0.5}O_x$ solid solution that shows exceptional catalytic performance in the low temperature, heterogeneous oxidation of cyclohexane (100 °C, conversion: 17.7%, selectivity for KA oils (K: cyclohexanone, A: cyclohexanol): 81%) with

molecular oxygen as the oxidant. It is significantly superior to the best current technology (140–160 °C, conversion: 3–5%). Detailed investigation indicates several unique characteristics of the $Mn_{0.5}Ce_{0.5}O_x$ solid solution: (1) A high proportion (44.1%) of active oxygen species on the surface to promote O–O/C–H bond activation; (2) the introduction of 50 mol% Mn^{4+} ions into ceria matrix for the formation of maximum solid solution phases that can lower the energy for oxygen vacancy formation and benefit the rapid migration of oxygen vacancies from the bulk to the surface, thus continuing the activation of gas oxygen molecules; (3) a mesoporous structure for fast mass transfer/diffusion, and rich porosity to expose any more active sites ready for interaction with cyclohexane/ O_2 . We expect that the $Mn_{0.5}Ce_{0.5}O_x$ solid solution will provide a strategy for oxidation of cyclohexane and other hydrocarbons under mild conditions.

Surface structure effect of oxide catalysts

This goal of this effort is to understand the role that atomic surface structure plays in controlling selectivity in catalysis at oxide surfaces. In the past, we have focused on CeO_2 as a catalytic oxide because of its versatile reducibility and acid-base properties. We are

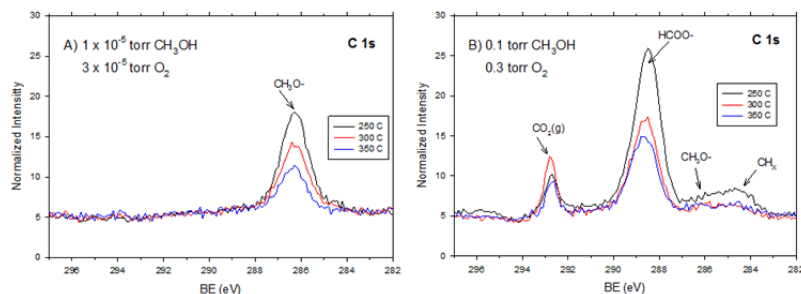


Figure 1. Comparison of AP-XPS spectra for methanol + O_2 reaction on $La_{0.7}Sr_{0.3}MnO_3(001)$ at different pressures.

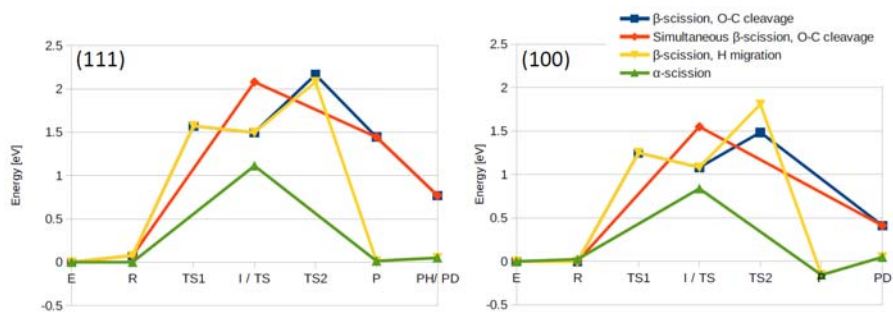


Figure 2. Reaction profiles for ethylene and acetaldehyde formation on the (111) and (100) ceria surface; E - ethoxy, R - rotated/tilted ethoxy, TS1, TS, TS2 - transition states, I - intermediate, P - product, PH - product with migrated H (ethylene product), PD - desorbed product.

currently expanding this effort to binary oxides including nanoshaped perovskite particles and oriented perovskite thin films and single crystals.

DFT studies of ethanol reactions on ceria. In our experimental efforts, we have observed many cases where molecules react differently on CeO₂(111) and CeO₂(100). In general, the CeO₂(100) surface has been more reactive than CeO₂(111) as indicated by a stronger adsorption energy for molecules such as water, CO₂, alcohols and aldehydes. To further understand our experimental observations, we used computational methods to gain insights into chemical conversion on ceria surfaces at the atomic level. Specifically, we employed density functional theory, where the surfaces were modeled as semi-infinite, two-dimensional slabs applying periodic boundary conditions. We studied ethanol reactions on the (111) and (100) ceria surfaces starting from ethoxy, the experimentally determined dominant surface species. Reaction pathways leading to ethylene and acetaldehyde are shown in **Figure 2**. Ethylene and acetaldehyde can be produced in a single step through simultaneous β -scission and oxygen-carbon bond cleavage and α -scission, respectively. Alternatively, ethylene and acetaldehyde can be formed through a common radical intermediate formed from the β -scission reaction. The kinetically and thermodynamically preferred pathway on both surfaces, however, is the single step acetaldehyde formation via α -scission. We observed that intermediate and transition state structures are stabilized on the (100) surface compared to the (111) surface. To assess pathway contributions, we computed transition state rate constants and carried out kinetic analysis. Our results are consistent with temperature programmed surface reaction and steady-state experiments, where acetaldehyde was found as the main product and evidence was presented that ethylene formation at higher temperature originates from changes in adsorbate and surface structure.

SO₂ adsorption on ceria. It is our goal to understand how SO₂ interaction with ceria is dependent upon the surface structure of the oxide. It has shown that CeO₂ has a high affinity for the adsorption of SO₂, which can be detrimental as in the poisoning of automotive exhaust catalysts but could also possibly be exploited by utilizing ceria to trap SO₂ in effluent streams. Previous studies have shown that SO₂ adsorbs on fully oxidized CeO₂(111) as sulfite, SO₃²⁻. This species is non-reactive and eventually desorbs as SO₂ at elevated temperatures. On partially reduced CeO_{2-x}(111), the SO₂ adsorbs as sulfite at low temperatures but decomposes into O²⁻ and S²⁻ creating a sulfide and re-oxidizing Ce³⁺ to Ce⁴⁺.

We hypothesized that the increased reactivity of CeO₂(100) might result in sulfate (SO₄²⁻) following SO₂ exposure and possibly different decomposition paths with S⁰ as a product. Surprisingly, considering the differences observed for other molecules on CeO₂(111) and CeO₂(100), the adsorption of SO₂ on these two surfaces was virtually identical in terms of the species formed on the surfaces and their stabilities. SO₃²⁻ was the only species observed on the fully oxidized surfaces. The sulfite decomposed into sulfide on the reduced surfaces.

Supported Metal nanoparticles

Catalysis of oxides can be drastically tuned or changed when metal nanoparticles are attached on the surface. Additional complexity arises from the introduced metal – support interaction where the perimeter sites between metal and oxide seem to be important for catalysis. We have explored ways how to tune the interface structure to tune the catalysis of supported metal nanoparticles.

Interface engineering via surface structure of oxides. The strong support effect is known for metal catalysis, especially for gold catalysis. Instead of the changing the composition of the support, we investigated how the surface structure of an oxide (CeO_2) can affect the catalysis of gold nanoparticles. The different CeO_2 nanostructures (i.e., nanorods vs. nanocubes) can impact the size, morphology, and interface structures of Au catalysts through the metal-support interaction. Yet a detailed and atomistic view of the interface in Au- CeO_2 catalytic system is still missing. Recently, we have performed aberration-corrected high angle annular dark field (HAADF) scanning transmission electron microscopy (STEM) imaging on Au- CeO_2 nanostructures with well-defined shapes. With atoms clearly resolved, the size, morphology, and atomic interface structures of the Au- CeO_2 catalysts before and after the water-gas shift (WGS) reaction were systematically analyzed. It was found that the oxidation state of the ceria substrate plays a major role for both Au- CeO_2 systems, with larger adhesion for Au under oxidative condition. Under oxidative condition, Au particles with SK layers are present on the Au- CeO_2 nanocubes (see **Figure 3**). The SK layers vanish and there is a morphological change of the Au particles after the WGS reaction, which is attributed to reduction of the Au- CeO_2 (100) interface. In contrast, the Au- CeO_2 nanorods contain regular Au particles and some rafts under oxidative conditions. After the WGS reaction, the Au atoms in the rafts migrate to the particles. The Au particles on the CeO_2 nanorods are almost unchanged before and after the WGS reaction. The loss of strong adhesion of Au to the support CeO_2 (the SK layer and the rafts) is partly responsible for the decrease of the activities in the WGS reaction.

Construction of hierarchical metal-oxide interfaces. Decreasing the size of metal nanoparticles is a general approach to enhance the catalytic activity. But it comes with the price of instability of small metal particles. One dimensional (1D) metal nanowires, small in diameter and with a high percentage of exposed active sites, are more stable than the nanoparticle counterparts. Further increase of their activity can involve the engineering of the interfaces. We demonstrated in constructing catalytic active hierarchical interfaces in 1D nanostructure as exemplified by the synthesis of TiO_2 -supported PtFe-FeOx nanowires (NWs). The hierarchical interface, constituting atomic level interactions between PtFe and FeOx within each NW and the interactions between NWs and support (TiO_2), enables CO oxidation with 100% conversion at room temperature. We identify the role of the two interfaces by probing the CO oxidation reaction with isotopic labeling experiments. Both the oxygen atoms (Os) in FeOx and TiO_2 participate in the initial CO oxidation, facilitating the reaction through a redox pathway. Moreover, the intact 1D structure leads to the high stability of the catalyst. After 30 h in the reaction stream, the PtFe-FeOx/ TiO_2 catalyst exhibits no activity decay. Our results provide a general approach and new insights into the construction of hierarchical interfaces for advanced

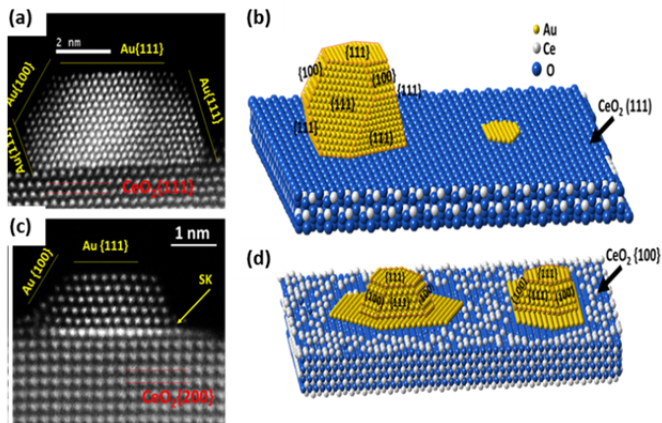


Figure 3. The morphology and atomic structures of Au- CeO_2 nanostructures before the WGS reaction: atomic resolution HAADF image of an Au nanoparticle on CeO_2 nanorods (a) and on CeO_2 nanocubes (c); Schematic view of an Au particle and raft supported by the CeO_2 (111) nanorods (b) and by the CeO_2 (100) nanocubes.

catalysis. Current on-going effort includes the tuning of the support thickness by using BN thin sheets to control the electronic property and consequently the catalysis of supported Pt nanoparticles.

Kinetic Modeling. One of our goals is to use kinetic modeling to connect fundamental surface science studies with liquid or gas phase reactor studies. This is showcased by our work on benzylic alcohol oxidation over supported palladium nanoparticles. In the first of two studies, we used surface science knowledge and kinetic studies to elucidate the mechanism for benzylic alcohol oxidation over palladium nanoparticles. We found that the six different products were produced by a mechanism that included two main branches (an alkoxy pathway, and a carbonyloxyl pathway). In the second study, we used that mechanism for micro-kinetic modeling of the transient kinetics under various conditions, including applying the concept of a sticking coefficient in solution. The kinetic simulations were able to reproduce the 18 trends observed in the responses of the six products when varying the alcohol concentration, oxygen pressure, and temperature. The six products were benzaldehyde, toluene, benzyl ether, benzene, benzoic acid, and benzyl benzoate. Along similar line, we are currently planning on obtaining molecular beam steady state methanol oxidation reaction data over perovskite surfaces in UHV to use in conjunction with atmospheric pressure reactor studies of the same reaction.

Publications Acknowledging this Grant in 2013-2016

(I) *Exclusively funded by this grant:*

1. Albrecht, P. M.; Mullins, D. R., Adsorption and Reaction of Methanol over CeO_x(100) Thin Films, *Langmuir* **2013**, *29*, 4559–4567.
2. Bauer, J. C.; Mullins, D. R.; Oyola, Y.; Overbury, S. H.; Dai, S., Structure Activity Relationships of Silica Supported AuCu and AuCuPd Alloy Catalysts for the Oxidation of CO, *Catalysis Letters* **2013**, *143*(9), 926-935.
3. Beste, A.; Buchanan, A. C., III, Computational Investigation of the Pyrolysis Product Selectivity for alpha-Hydroxy Phenethyl Phenyl Ether and Phenethyl Phenyl Ether: Analysis of Substituent Effects and Reactant Conformer Selection, *J. Phys. Chem. A* **2013**, *117*, 3235–3242.
4. Binder, A. J.; Qiao, Z. A.; Veith, G. M.; Dai, S., Deposition-Precipitation and Stabilization of a Silica-Supported Au Catalyst by Surface Modification with Carbon Nitride, *Catalysis Letters* **2013**, *143*(12), 1339-1345.
5. Jiang, D.-e.; Overbury, S. H.; Dai, S., On the Structure of Au₁₅(SR)₁₃ and its Implication on the Origin of the Nucleus in Thiolated Gold Nanoclusters *Journal of the American Chemical Society* **2013**, *135*, 8786–8789.
6. Li, M.; Wu, Z.; Overbury, S. H., Surface structure dependence of selective oxidation of ethanol on faceted CeO₂ nanocrystals, *Journal of Catalysis* **2013**, *306*, 164-176.
7. Liu, Z. G.; Chai, S. H.; Binder, A.; Li, Y. Y.; Ji, L. T.; Dai, S., Influence of calcination temperature on the structure and catalytic performance of CuO_x-CoO_y-CeO₂ ternary mixed oxide for CO oxidation, *Applied Catalysis a-General* **2013**, *451*, 282-288.
8. Mullins, D. R.; Albrecht, P. M.; Calaza, F. C., Variations in Reactivity on Different Crystallographic Orientations of Cerium Oxide, *Topics in Catalysis* **2013**, *56*, 1345-1362.
9. Mullins, D. R.; Albrecht, P. M., Acetaldehyde Adsorption and Reaction on CeO₂(100) Thin Films, *Journal of Physical Chemistry C* **2013**, *117*(28), 14692-14700.
10. Qiao, Z. A.; Wu, Z. L.; Dai, S., Shape-Controlled Ceria-based Nanostructures for Catalysis Applications, *ChemSusChem* **2013**, *6*(10), 1821-1833.
11. Ren, Y.; Ma, Z.; Morris, R. E.; Liu, Z.; Jiao, F.; Dai, S.; Bruce, P. G., A solid with a hierarchical tetramodal micro-meso-macro pore size distribution, *Nature Communications* **2013**, *4*.

12. Tian, C.; Chai, S.-H.; Mullins, D. R.; Zhu, X.; Binder, A.; Guo, Y.; Dai, S., Heterostructured BaSO₄-SiO₂ mesoporous materials as new supports for gold nanoparticles in low-temperature CO oxidation, *Chemical Communications* **2013**, *49*, 3464-3466.
13. Tian, C. C.; Bao, C. H.; Binder, A.; Zhu, Z. Q.; Hu, B.; Guo, Y. L.; Zhao, B.; Dai, S., An efficient and reusable "hairy" particle acid catalyst for the synthesis of 5-hydroxymethylfurfural from dehydration of fructose in water, *Chem. Commun.* **2013**, *49*, 8668-8670.
14. Tian, C. C.; Oyola, Y.; Nelson, K. M.; Chai, S. H.; Zhu, X.; Bauer, J. C.; Janke, C. J.; Brown, S.; Guo, Y. L.; Dai, S., A renewable HSO₃/H₂PO₃-grafted polyethylene fiber catalyst: an efficient heterogeneous catalyst for the synthesis of 5-hydroxymethylfurfural from fructose in water, *RSC Adv* **2013**, *3*, 21242-21246.
15. Albrecht, P. M.; Jiang, D.-e.; Mullins, D. R., CO₂ Adsorption As a Flat-Lying, Tridentate Carbonate on CeO₂(100), *J. Phys. Chem. C* **2014**, *118*, 9042-9050.
16. Kandziolka, M. V.; Kidder, M. K.; Gill, L.; Wu, Z.; Savara, A., Aromatic-Hydroxyl Interaction of an aryl ether Lignin Model-Compound on SBA-15 Present at Pyrolysis Temperatures, *PCCP* **2014**, *16*, 24188--24193.
17. Li, L.; Chai, S.-H.; Binder, A.; Brown, S.; Veith, G. M.; Dai, S., Catalytic CO Oxidation Over Gold Nanoparticles: Support Modification by Monolayer- and Submonolayer-Dispersed Sb₂O₃, *Catal. s Lett.* **2014**, *144*, 912.
18. Li, L.; Tian, C. C.; Chai, S. H.; Binder, A.; Brown, S.; Veith, G. M.; Dai, S., Gold nanocatalysts supported on heterostructured PbSO₄-MCF mesoporous materials for CO oxidation, *Catalysis Communications* **2014**, *46*, 234-237.
19. Liu, Z.; Wu, Z.; Peng, X.; Binder, A.; Chai, S.; Dai, S., The Origin of Active Oxygen in a Ternary CuOx/Co₃O₄-CeO₂ Catalyst for CO Oxidation, *J. Phys. Chem C* **2014**, *118*, 27870-27877
20. Mann, A. K. P.; Wu, Z.; Calaza, F. C.; Overbury, S. H., Adsorption and Reaction of Acetaldehyde on Shape-Controlled CeO₂ Nanocrystals: Elucidation of Structure-function Relationships, *ACS Catalysis* **2014**, *4*, 2437-2448.
21. Qiao, Z.-A.; Zhang, P.; Chai, S.-H.; Chi, M.; Veith, G.; Gallego, N.; Kidder, M.; Dai, S., Lab-in-a-Shell: Encapsulating Metal Clusters for Size Sieving Catalysis, *J. Am. Chem. Soc.* **2014**, *136* (32), 11260-11263.
22. Ren, Y.; Ma, Z.; Dai, S., Nanosize Control on Porous beta-MnO₂ and Their Catalytic Activity in CO Oxidation and N₂O Decomposition. *Materials* **2014**, *7*, 3547.
23. Savara, A., Vibrational spectra of CO adsorbed on oxide thin films: A tool to probe the surface defects and phase changes of oxide thin films, *J. Vacuum Science & Technology A* **2014**, *32*(2).
24. Savara, A.; Chan-Thaw, C. E.; Rossetti, I.; Villa, A.; Prati, L., Benzyl Alcohol Oxidation on Carbon Supported Pd Nanoparticles: Elucidating the Reaction Mechanism, *ChemCatChem* **2014**, *6*, 3464-3473.
25. Savara, A.; Weitz, E., Elucidation of Intermediates and Mechanisms in Heterogeneous Catalysis Using Infrared Spectroscopy, *Annual Review of Physical Chemistry, Vol 65* **2014**, *65*, 249-273.
26. Tian, C. C.; Zhu, X.; Chai, S. H.; Wu, Z. L.; Binder, A.; Brown, S.; Li, L.; Luo, H. M.; Guo, Y. L.; Dai, S., Three-Phase Catalytic System of H₂O, Ionic Liquid, and VOPO₄-SiO₂ Solid Acid for Conversion of Fructose to 5-Hydroxymethylfurfural. , *ChemSuschem* **2014**, *7*, 1703-1709.
27. Wu, Z.; Jiang, D.-e.; Mann, A. K. P.; Mullins, D. R.; Qiao, Z.-A.; Allard, L. F.; Zeng, C.; Jin, R.; Overbury, S. H., Thiolate Ligands as a Double-Edged Sword for CO Oxidation on CeO₂ Supported Au₂₅(SCH₂CH₂Ph)₁₈ Nanoclusters, *J. Amer. Chem. Soc.* **2014**, *136*(16), 6111-6122.
28. Wu, Z. L.; Overbury, S. H. (2014c). Infrared Spectroscopic insights into the role of supports in heterogeneous Au catalysis. *Heterogeneous Gold Catalysts and Catalysis*. Z. Ma and D. S. RSC: 512-532, **2014**.
29. Beste, A.; Overbury, S. H., Pathways for Ethanol Dehydrogenation and Dehydration Catalyzed by Ceria (111) and (100) Surfaces, *J. Phys. Chem C* **2015**, *119*, 2447-2455.
30. Calaza, F. C.; Chen, T.-L.; Mullins, D. R.; Xu, Y.; Overbury, S. H., Reactivity and reaction intermediates for acetic acid adsorbed on CeO₂(111), *Catalysis Today* **2015**, *253*, 65-76.

31. Mann, A. K. P.; Wu, Z. L.; Overbury, S. H. (2015). The Characterization and Structure-dependent Catalysis of Ceria with Well-defined Facets in Catalysis by Materials with Well-Defined Structures (edition 1). Z. Wu and S. H. Overbury, Elsevier.
32. Mullins, D. R., The Surface Chemistry of Cerium Oxide, *Surface Science Reports* **2015**, *70*, 42 - 85.
33. Wu, Z.; Mann, A. K. P.; Li, M.; Overbury, S. H., Spectroscopic Investigation of Surface-Dependent Acid-Base Property of Ceria Nanoshapes, *Journal of Physical Chemistry C* **2015**, *119*(13), 7340-7350.
34. Wu, Z. L.; Overbury, S. H., Catalysis by Materials with Well-defined Structures, Book Eds., Elsevier, **2015**.
35. Beste, A.; Overbury, S. H., Dehydrogenation of Methanol to Formaldehyde Catalyzed by Pristine and Defective Ceria Surfaces, *PCCP* **2016**, *18*, 9990.
36. Lukosi, M.; Zhu, H.; Dai, S., Recent advances in gold-metal oxide core-shell nanoparticles: Synthesis, characterization, and their application for heterogeneous catalysis. *Frontiers of Chemical Science and Engineering* **2016**, *10* (1), 39-56.
37. Savara, A.; Rossetti, I.; Chan-Thaw, C.E.; Prati, L.; Villa, A. "Microkinetic Modeling of Benzyl Alcohol Oxidation on Carbon Supported Pd Nanoparticles" *ChemCatChem*, **2016**, DOI: 10.1002/cctc.201600368.
38. Yue, Y.; Zhang, L.; Chen, J.; Hensley, D. K.; Dai, S.; Overbury, S. H., Mesoporous xEr₂O₃-CoTiO₃ composite oxide catalysts for low temperature dehydrogenation of ethylbenzene to styrene using CO₂ as a soft oxidant. *RSC Advances* **2016**, *6* (39), 32989-32993.

(II) *Jointly funded by this grant and other grants with leading intellectual contribution from this grant:*

39. Bravo Suarez, J.; Kidder, M. K.; Schwartz, V. Eds, *Novel Materials for Catalysis and Fuels Processing*; ACS Symposium Series 1132; American Chemical Society: Washington, DC, **2013**.
40. Moses-DeBusk, M.; Yoon, M.; Allard, L. F.; Mullins, D. R.; Wu, Z. L.; Yang, X. F.; Veith, G.; Stocks, G. M.; Narula, C. K., CO Oxidation on Supported Single Pt Atoms: Experimental and ab Initio Density Functional Studies of CO Interaction with Pt Atom on Al₂O₃(010) Surface, *Journal of the American Chemical Society* **2013**, *135*(34), 12634-12645.
41. Binder, A. J.; Toops, T.; Parks, J.; Dai, S., CuO-Co₃O₄-CeO₂ ternary mixed oxide outperforms PGM catalysts in CO oxidation with high resistance to inhibition by propene, *Science Communications* **2014**.
42. Bauer, J. C.; Toops, T. J.; Oyola, Y.; Parks, J. E.; Dai, S.; Overbury, S. H., Catalytic activity and thermal stability of Au-CuO/SiO₂ catalysts for the low temperature oxidation of CO in the presence of propylene and NO, *Catalysis Today* **2014**, *231*, 15-21.
43. Li, G.; Jiang, D.-e.; Kumar, S.; Chen, Y.; Jin, R., Size Dependence of Atomically Precise Gold Nanoclusters in Chemoselective Hydrogenation and Active Site Structure, *ACS Catalysis* **2014**, 2463-2469.
44. Lin, Y. Y.; Wu, Z. L.; Wen, J. G.; Poepelmeier, K. R.; Marks, L. D., Imaging the Atomic Surface Structures of CeO₂ Nanoparticles, *Nano Letters* **2014**, *14*(1), 191-196.
45. Luo, Z.; Nachammai, V.; Zhang, B.; Yan, N.; Leong, D. T.; Jiang, D.-e.; Xie, J., Toward Understanding the Growth Mechanism: Tracing All Stable Intermediate Species from Reduction of Au(I)-Thiolate Complexes to Evolution of Au₂₅ Nanoclusters, *Journal of the American Chemical Society* **2014**, *136*(30), 10577-10580.
46. Ma, Z.; Dai, S., Stabilizing Gold Nanoparticles by Solid Supports in Heterogeneous Gold Catalysts and Catalysis, Ma, Z.; Dai, S Eds., RSC, **2014**.
47. Ma, Z.; Dai, S., Heterogeneous Gold Catalysts and Catalysis, Book Eds., RSC, **2014**.
48. Yu, Y.; Luo, Z.; Chevrier, D. M.; Leong, D. T.; Zhang, P.; Jiang, D.-e.; Xie, J., Identification of a Highly Luminescent Au₂₂(SG)₁₈ Nanocluster, *Journal of the American Chemical Society* **2014**, *136*, 1246-1249.

49. Wu, Z. L., Multi-wavelength Raman spectroscopy study of supported vanadia catalysts: Structure identification and quantification., *Chinese Journal of Catalysis* **2014b**, *35*, 1591-1608.
50. Binder, A. J.; Toops, T. J.; Unocic, R. R.; Parks, J. E.; Dai, S., Low-Temperature CO Oxidation over a Ternary Oxide Catalyst with High Resistance to Hydrocarbon Inhibition. *Angewandte Chemie International Edition* **2015**, *54* (45), 13263-13267.
51. Feyngenson, M.; Bauer, J. C.; Gai, Z.; Marques, C.; Aronson, M. C.; Teng, X.; Su, D.; Stanic, V.; Urban, V. S.; Beyer, K. A.; Dai, S., Exchange bias effect Au-Fe₃O₄ dumbbell nanoparticles induced by the charge transfer from gold. *Physical Review B* **2015**, *92* (5), 054416.
52. Hu, J.; Yang, Q.; Yang, L.; Zhang, Z.; Su, B.; Bao, Z.; Ren, Q.; Xing, H.; Dai, S., Confining Noble Metal (Pd, Au, Pt) Nanoparticles in Surfactant Ionic Liquids: Active Non-Mercury Catalysts for Hydrochlorination of Acetylene. *ACS Catalysis* **2015**, *5* (11), 6724-6731.
53. Li, L.; Chai, S.-H.; Binder, A.; Brown, S.; Yang, S.-Z.; Dai, S., Synthesis of MCF-supported AuCo nanoparticle catalysts and the catalytic performance for the CO oxidation reaction. *RSC Advances* **2015**, *5* (121), 100212-100222.
54. Lu, H.; Zhang, P.; Qiao, Z.-A.; Zhang, J.; Zhu, H.; Chen, J.; Chen, Y.; Dai, S., Ionic liquid-mediated synthesis of meso-scale porous lanthanum-transition-metal perovskites with high CO oxidation performance, *Chem. Communications* **2015**, *51*, 5910--5913.
55. Lin, Y.; Wu, Z.; Wen, J.; Ding, K.; Yang, X.; Poeppelmeier, K. R.; Marks, L. D., Adhesion and Atomic Structures of Gold on Ceria Nanostructures: The Role of Surface Structure and Oxidation State of Ceria Supports, *Nano Letters* **2015**, *15*(8).
56. Wu, P.; Zhu, W.; Wei, A.; Dai, B.; Chao, Y.; Li, C.; Li, H.; Dai, S., Controllable Fabrication of Tungsten Oxide Nanoparticles Confined in Graphene-Analogous Boron Nitride as an Efficient Desulfurization Catalyst. *Chemistry – A European Journal* **2015**, *21* (43), 15421-15427.
57. Zhang, P.; Li, H.; Veith, G. M.; Dai, S., Soluble Porous Coordination Polymers by Mechanochemistry: From Metal-Containing Films/Membranes to Active Catalysts for Aerobic Oxidation. *Advanced Materials* **2015**, *27* (2), 234-239.
58. Zhang, P.; Lu, H.; Zhou, Y.; Zhang, L.; Wu, Z.; Yang, S.; Shi, H.; Zhu, Q.; Chen, Y.; Dai, S., Mesoporous MnCeO_x solid solutions for low temperature and selective oxidation of hydrocarbons, *Nature Communications* **2015**, *6*, 8446.
59. Zhang, P.; Qiao, Z.-A.; Jiang, X.; Veith, G. M.; Dai, S., Nanoporous ionic organic networks: stabilizing and supporting gold nanoparticles for catalysis, *Nano Letters* **2015**, *15*(2), 823-828.
60. Zhang, P.; Zhu, H.; Dai, S., Porous Carbon Supports: Recent Advances with Various Morphologies and Compositions. *ChemCatChem* **2015**, *7* (18), 2788-2805.
61. Zhu, H.; Wu, Z.; Su, D.; Veith, G. M.; Lu, H.; Zhang, P.; Chai, S.-H.; Dai, S., Constructing Hierarchical Interfaces: TiO₂-Supported PtFe-FeO_x Nanowires for Room Temperature CO Oxidation. *Journal of the American Chemical Society* **2015**, *137* (32), 10156-10159.
62. Zhu, H.; Zhang, P.; Dai, S., Recent Advances of Lanthanum-Based Perovskite Oxides for Catalysis, *ACS Catalysis* **2015**, *5*, 6370–6385.
63. Li, H.; Meng, B.; Chai, S.-H.; Liu, H.; Dai, S., Hyper-crosslinked [small beta]-cyclodextrin porous polymer: an adsorption-facilitated molecular catalyst support for transformation of water-soluble aromatic molecules. *Chemical Science* **2016**, *7* (2), 905-909.
64. Wu, P.; Zhu, W.; Chao, Y.; Zhang, J.; Zhang, P.; Zhu, H.; Li, C.; Chen, Z.; Li, H.; Dai, S., A template-free solvent-mediated synthesis of high surface area boron nitride nanosheets for aerobic oxidative desulfurization. *Chemical Communications* **2016**, *52* (1), 144-147.

(III) *Jointly funded by this grant and other grants with relatively minor intellectual contribution from this grant:*

65. Galhenage, R. P.; Yan, H.; Tenney, S. A.; Park, N.; Henkelman, G.; Albrecht, P. M.; Mullins, D. R.; Chen, D. A., Understanding the Nucleation and Growth of Metals on TiO₂: Co compared to Au, Ni and Pt, *Journal of Physical Chemistry C* **2013**, *117*, 7191-7201.

66. Ghidui, M. J.; Pistner, A. J.; Yap, G. P. A.; Lutterman, D. A.; Rosenthal, J., Thermal versus Photochemical Reductive Elimination of Aryl Chlorides from NHC-Gold Complexes, *Organometallics* **2013**, 32(18), 5026-5029.
67. Pistner, A. J.; Lutterman, D. A.; Ghidui, M. J.; Ma, Y.-Z.; Rosenthal, J., Synthesis, Electrochemistry, and Photophysics of a Family of Phlorin Macrocycles That Display Cooperative Fluoride Binding. , *J. Am. Chem. Soc* **2013**, 135,, 6601-6607.
68. Pollock, J. B.; Cook, T. R.; Schneider, G. L.; Lutterman, D. A.; Davies, A. S.; Stang, P. J., Photophysical Properties of Endohedral Amine-Functionalized Bis(phosphine) Pt(II) Complexes as Models for Emissive Metallacycles, *Inorg. Chem* **2013**, 52(16), 9254-9265.
69. Veith, G. M.; Lupini, A. R.; Baggetto, L.; Browning, J. F.; Keum, J. K.; Villa, A.; Prati, L.; Papandrew, A. B.; Goenaga, G. A.; Mullins, D. R.; Bullock, S. E.; Dudney, N. J., Evidence for the Formation of Nitrogen-Rich Platinum and Palladium Nitride Nanoparticles, *Chemistry of Materials* **2013**, 25(24), 4936-4945.
70. Baggetto, L.; Carroll, K. J.; Hah, H.-Y.; Johnson, C. E.; Mullins, D. R.; Unocic, R. R.; Johnson, J. A.; Meng, Y. S.; Veith, G. M., Probing the Mechanism of Sodium Ion Insertion into Copper Antimony Cu₂Sb Anodes, *J. Phys. Chem. C* **2014**, 118 7856.
71. Baggetto, L.; Bridges, C. A.; Jumas, J. C.; Mullins, D. R.; Carroll, K. J.; Meisner, R. A.; Crumlin, E. J.; Liu, X. S.; Yang, W. L.; Veith, G. M., The local atomic structure and chemical bonding in sodium tin phases. *J Mater Chem A* **2014**, 2 (44), 18959-18973.
72. Graham, D. E.; Gresback, R. G.; Ivanov, I. N.; Jang, G. G.; Kidder, M. K;
73. Meyer, H. M. III; Phelps, T. J.; Moon, J. W. Invention Disclosure 201403337, DOES-124,957, Microbially-Mediated Method for Nanoparticle Formation and Films Thereby, May, 2014.
74. Pistner, A. J.; Lutterman, D. A.; Ghidui, M. J.; Walker, E.; Yap, G. P. A.; Rosenthal, J., Factors Controlling the Spectroscopic Properties and Supramolecular Chemistry of an Electron Deficient 5,5-Dimethylphlorin Architecture. , *J. Phys. Chem. C* **2014**, 118, 14124-14132.
75. Pistner, A. J.; Pupillo, R. C.; Yap, G. P. A.; Lutterman, D. A.; Ma, Y. Z.; Rosenthal, J., Electrochemical, Spectroscopic, and O-1(2) Sensitization Characteristics of 10,10-Dimethylbiladiene Complexes of Zinc and Copper, , *J. Phys. Chem. A* **2014**, 118,, 10639-10648.
76. Dong, Y.; Brooks, J. D.; Chen, T.-L.; Mullins, D. R.; Cox, D. F., Methylene migration and coupling on a non-reducible metal oxide: The reaction of dichloromethane on stoichiometric α -Cr₂O₃(0001), *Surface Science* **2015**, 632, 28-38.
77. Dong, Y. J.; Brooks, J. D.; Chen, T. L.; Mullins, D. R.; Cox, D. F., Reactions of methyl groups on a non-reducible metal oxide: The reaction of iodomethane on stoichiometric α -Cr₂O₃(0001). *Surf Sci* **2015**, 641, 148-153.
78. Jang, G. G.; Jacobs, C. B.; Ivanov, I. N.; Joshi, P. C.; III, H. M. M.; Kidder, M.; Armstrong, B. L.; Datskos, P. G.; Graham, D. E.; Moon, J.-W., In situ capping for size control of monochalcogenide (ZnS, CdS and SnS) nanocrystals produced by anaerobic metal reducing bacteria, *Nanotechnology* **2015**, 26, 325602.
79. Jang, G. G.; Jacobs, C. B.; Gresback, G. R.; Ivanov, I. N.; Meyer, H. M.; Kidder, M. K.; Joshi, P. C.; Jellison, J. E.; Phelps, T. J.; Graham, D. E.; Moon, J., Size tunable elemental copper nanoparticles: extracellular synthesis by thermoanaerobic bacteria and capping molecules. *J. Materials Chem. C.*, **2015**, 3, 644-650.
80. Mathis, J. E.; Lieffers, J. J; Mitra, C.; Reboredo, F. A.; Bi, Z.; Bridges, C. A.; Kidder, M. K.; Paranthaman, M. P. Increased Photocatalytic Activity of TiO₂ Mesoporous Microspheres from Co-doping with Transition Metals and Nitrogen. *Ceramics International*, **2016**, 42, 3556-3562.
81. Moon, J.-W., Phelps, T.J., Oremland, R., Graham, D.E., Joshi, P.C., Kidder, M., Jang, G.G., Ivanov, I.N., Jacobs, C.B. ORNL Invention Disclosure IDN 201503497, DOE SN S-138,128 (2015) "Improved properties of nanomaterials using complementary Nano Fermentation technique" (3/13/2015).

82. Villa, A.; Schiavoni, M.; Chan-Thaw, C. E.; Fulvio, P. F.; Mayes, R. T.; Dai, S.; More, K. L.; Veith, G. M.; Prati, L., Acid-Functionalized Mesoporous Carbon: An Efficient Support for Ruthenium-Catalyzed γ -Valerolactone Production. *ChemSusChem* **2015**, 8 (15), 2520-2528.
83. Moon, J.; Phelps, T. J.; Fitzgerald, C. L.; Lind, R. F.; Elkins, J. G.; Jang, G. G.; Joshi, P. C.; Kidder, M. K.; Armstrong, B. L.; Watkins, T. R.; Graham, D. E., Manufacturing demonstration of microbially mediated zinc sulfide nanoparticles in pilot-plant scale reactors. , *Applied Microbiology and Biotechnology* **2016**, DOI 10.1007/s00253-016-7556-y.

Thursday Oral Presentations

Reaction mechanisms: interplay of thermodynamics and kinetics

Talat S. Rahman*
University of Central Florida

Presentation Abstract

Density functional theory (DFT) has become the work horse for determination of reaction pathways and activation energy barriers. It has also been used extensively to determine reaction mechanisms, site selectivity and reactivity. Yet it is clear that in addition to thermodynamics, kinetics plays a major role in predicting reaction selectivity and turn over frequencies. In this talk I will present some examples which illustrate the crucial role played by kinetics, particularly when reactions are carried out under ambient conditions. One case in point is that of ammonia oxidation on RuO₂(110) for which Wang et al [1] found high selectivity for NO formation around 530 K, under UHV conditions. Related DFT based kinetic Monte Carlo (KMC) simulations [2] provided further support for this selectivity. On the other hand, Perez et al [3], showed N₂ to be the dominant product in experiments at ambient pressure on polycrystalline RuO₂ samples. To address possible pressure and/or material gap in the products, we extended our DFT-based KMC calculations to include reactions rates for a large set of reaction intermediates that may be found under ambient conditions [4]. We also carried out simulations using databases proposed by Perez et al [3] and others. Interestingly, all databases show NO to be the dominant species under UHV conditions at or above the peak NO desorption temperature. On the other hand, we find that N₂ is the dominant product under ambient conditions. The rationale for the pressure gap is the activation of secondary reaction of NO i.e. active formation and decomposition of N₂O to N₂, an intermediate not found under UHV. I will also include results from our recent work on methanol synthesis on defect-laden MoS₂, which again points to the importance of inclusion of kinetics in making predictions of product selectivity.

- [1] Y. Wang, K. Jacobi, W. -D Schone, G. Ertl, *J. Phys. Chem.B* 109, 7883 (2005)
- [2] S. Hong, A. Karim, T.S. Rahman, K. Jacobi, and G. Ertl, *J. Catal.*, 276, 371 (2010).
- [3] J. Perez-Ramirez, N. Lopez, and E. V. Kondratenko, *J. Phys. Chem. C* 114, 16660 (2010).
- [4] S.I. Shah, S. Hong, and T.S. Rahman, *J. Phys. Chem. C* **118**, 5226-5238 (2014).

*Work done in collaboration with L. Bartels, P. Dowben, S. Hong, S. I. Shah, D. Le, T. Rawal

Funded by DE-FG02-07ER15842: Controlling Structural, Electronic, and Energy Flow Dynamics of Catalytic Processes through Tailored Nanostructures

Towards alcohol synthesis via functionalized MoS₂-based nanocatalyst

Talat S. Rahman¹, Ludwig Bartels², and Peter Dowben³

¹University of Central Florida, ²University of California, Riverside, ³University of Nebraska, Lincoln

Presentation Abstract

The objective of our joint theoretical and experimental project is to enable the design of MoS₂-based catalysts for (higher) alcohol formation from syngas (CO + H₂) through a microscopic understanding of the factors that determine site activity and selectivity. Initial efforts have focused on extracting the role of vacancy structures, of a metal substrate, and of adsorbed metallic nanoparticles on the chemical properties of single - layer MoS₂. Of these three, our density functional theory (DFT) based calculations of reaction pathways and kinetic Monte Carlo simulations of reaction rates find vacancy-laden single-layer MoS₂ grown on Cu(111) to provide the environment most facile for methanol formation. We trace this to the charge transfer from the metal substrate to the Mo and S layers which in turn causes the frontier orbitals of the system to appear at the Fermi level. Preliminary experimental data on the activation energy barriers for methoxy adsorption on MoS₂ show good agreement with our calculated values. At the same time, calculations of the energy pathways for water gas shift reaction show the process to be unfavorable on defect laden MoS₂. To further validate the choice of frontier orbitals as descriptors of chemical reactivity, in our quest for earth abundant materials with promising catalytic properties, we have obtained preliminary results for single and multilayered WS₂ and WSe₂, synthesized via chemical vapor deposition (CVD) and characterized via angle resolved photo emission (ARPES) and DFT.

Additional work in this project addressed multiscale imaging and characterization of the interaction of thiols with locally (via CVD) synthesized single-layer MoS₂ is being presented as separate poster.

DE-FG02-07ER15842: Controlling Structural, Electronic, and Energy Flow Dynamics of Catalytic Processes through Tailored Nanostructures

PI: Talat S. Rahman, Ludwig Bartels, Peter Dowben

Postdocs: Duy Le, Sampyo Hong, Hae-Kyung Jeong

Students: Wenhao Lu, Koichi Yamaguchi, Chen Wang, Quan Ma, Miguel Isarraraz, Michael Gomez, Cindy Merida, Emily Li, Ariana Nguyen, Gretel von Son, Joseph Martinez, Iori Tanabe, Prescott Evens, Sahar Naghibi, Takat B. Rawal, Ghazal Shafai

RECENT PROGRESS

We have focused on understanding ways to functionalize both single layer MoS₂ and MoS₂(1000) so as to convert its inert basal plane into one that can sustain catalytic activity. Based on our computational findings that the presence of vacancies is essential for such reactivity [11], and some preliminary experimental results shown in Fig. 1, we have created sulfur vacancies through controlled ion bombardment [2] and carried out experimental and computational investigations of their impact on material characteristics. We are particularly interested in designing MoS₂-based structures capable of converting syngas (CO, H₂) to (higher) alcohol, the formation of which is an

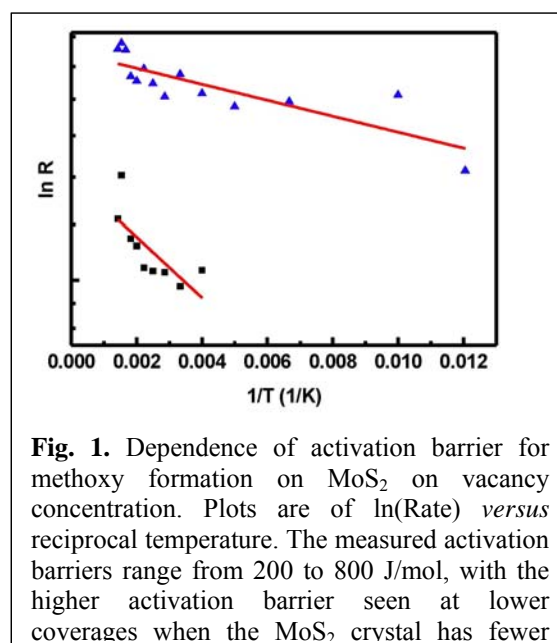


Fig. 1. Dependence of activation barrier for methoxy formation on MoS₂ on vacancy concentration. Plots are of ln(Rate) versus reciprocal temperature. The measured activation barriers range from 200 to 800 J/mol, with the higher activation barrier seen at lower coverages when the MoS₂ crystal has fewer

important part of an economy based on renewable fuels. At a first step, we focus on methanol synthesis from syngas that consists of the following main steps:

- (i) CO (g) adsorption to form CO*
- (ii) H₂ dissociative adsorption to form H*
- (iii) CO* + H* → CHO*
- (iv) CHO* + H* → CH₂O*
- (v) CH₂O* + H* → CH₃O*

(* denotes adsorbed and (g) gas-phase species) which are summarized in Fig. 2.

For the above reactions on vacancy-laden MoS₂, we have considered the role of the following:

- Vacancy cluster shape
- Adsorbed transition metal nanoparticles
- Cu(111) as support

We have grown single layer MoS₂ on several substrates [7] including

Cu(111). Also ARPES measurements and DFT calculations [14-16] have allowed tracking of frontier orbitals and traced their shifts with respect to the Fermi level to charge transfer and geometric and electronic-structural changes in the local environment of the Mo atoms, whose d-orbitals are essential for initiating the reactions of interest. In this theory-led effort in discovering novel earth-abundant catalysts for technologically important reactions, we are guided by the schematics presented in Fig. 3 which point to desirable shifts in the frontier orbitals as indicators of chemical reactivity of the particular catalyst local environment.

Below we present some of our recent highlights.

Reaction pathways for methanol synthesis on defect-laden single-layer MoS₂ supported on Cu(111):

Despite being the preferred structure in single layer MoS₂, the sulfur vacancy row is not very facile alcohol synthesis from syngas because its narrow size limits adsorption, diffusion, and formation of possible intermediates [11]. On the other hand, if MoS₂ is grown on Cu(111), strong interactions with the substrate may reduce the corrugations caused by sulfur vacancy rows (see Fig. 3), resulting in a greater exposure of the vacancies to adsorbates. This, in turn, could enhance the catalytic activity of the row towards alcohol synthesis from syngas. Our DFT calculations using PBE functional together with DFT-D3 correction for accounting the vdW interactions, indeed show this to be the case. We show that: (1) there is significant charge transfer from the Cu(111) surface to MoS₂ (Fig. 4) enhancing its catalytic properties, (2) the binding energies of CO and dissociated H₂ increase by 0.3 eV in comparison to that on unsupported MoS₂, indicating stronger interactions, and (3) the barriers for forming intermediate species in the alcohol synthesis process reduce significantly in comparison to that on unsupported MoS₂. On the basis of these energetics, we

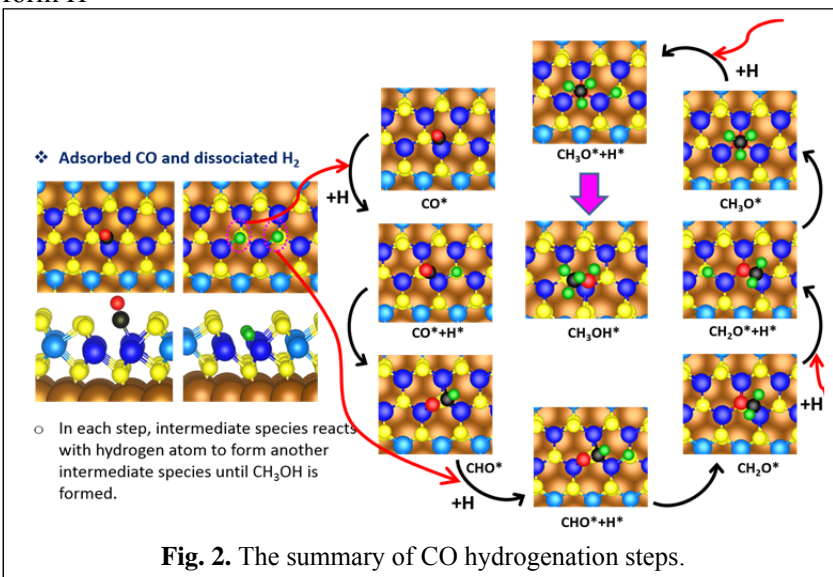


Fig. 2. The summary of CO hydrogenation steps.

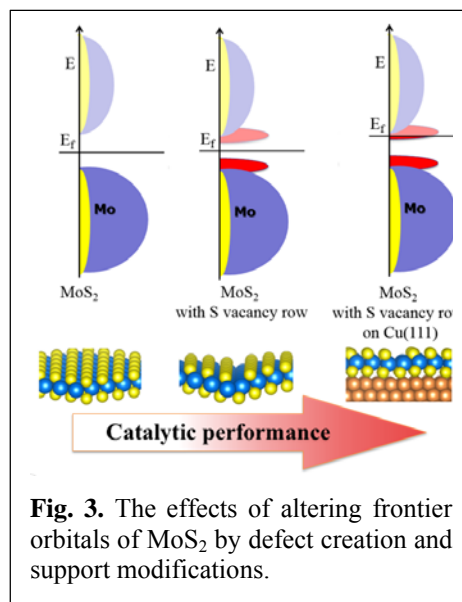


Fig. 3. The effects of altering frontier orbitals of MoS₂ by defect creation and support modifications.

conclude the Cu(111) substrate promotes methanol synthesis from syngas on single-layer MoS₂ with a vacancy row (Fig. 5). In addition, our preliminary results for water gas shift reaction indicate that H₂O may dissociate at a sulfur vacancy row of MoS₂ on Cu(111) and that CO₂ also dissociates here forming CO and atomic oxygen which adsorbed on the MoS₂/Cu(111) system. The influence of the substrate on the MoS₂ adlayer is also seen to be significant as is evident from our experimental studies of MoS₂ on SiO₂ compared with MoS₂ on LiNbO₃. Both the charge displacement and the placement of the MoS₂ chemical potential can vary widely as a result of substrate interactions.

Reaction pathways on gold nanoparticles supported on defect-laden single-layer MoS₂

We have investigated the geometry, electronic structure, and catalytic properties of gold nanoparticles on defect-laden single-layer MoS₂ using DFT based calculations with semi-empirical van der Waals interaction (DFT-D3). Our results (Fig. 6) show that the two-dimensional planar structure, the most favorable one for unsupported Au₁₃ nanoparticle, transforms into a distorted three-dimensional (3D) structure when supported on single-layer MoS₂ with single S-vacancy. This 3D structure is

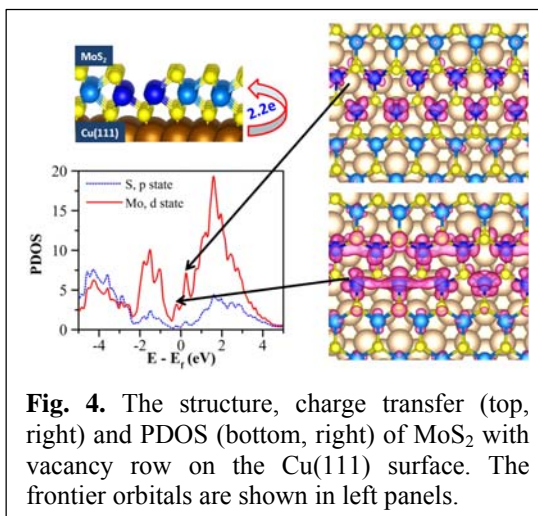


Fig. 4. The structure, charge transfer (top, right) and PDOS (bottom, right) of MoS₂ with vacancy row on the Cu(111) surface. The frontier orbitals are shown in left panels.

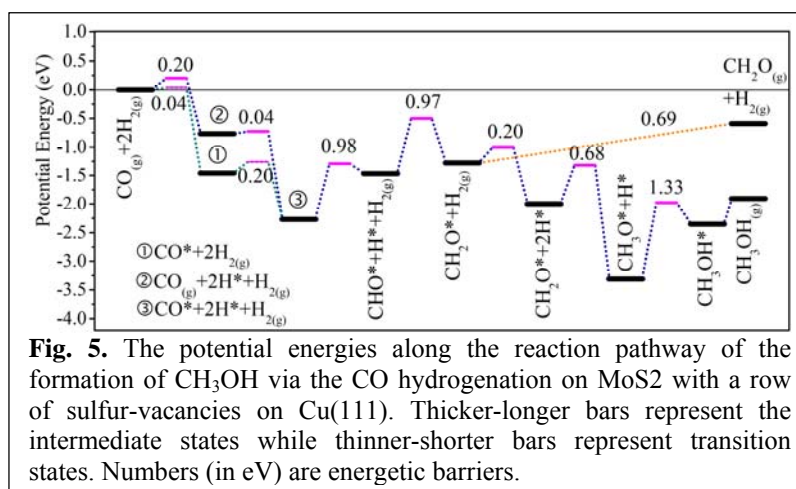


Fig. 5. The potential energies along the reaction pathway of the formation of CH₃OH via the CO hydrogenation on MoS₂ with a row of sulfur-vacancies on Cu(111). Thicker-longer bars represent the intermediate states while thinner-shorter bars represent transition states. Numbers (in eV) are energetic barriers.

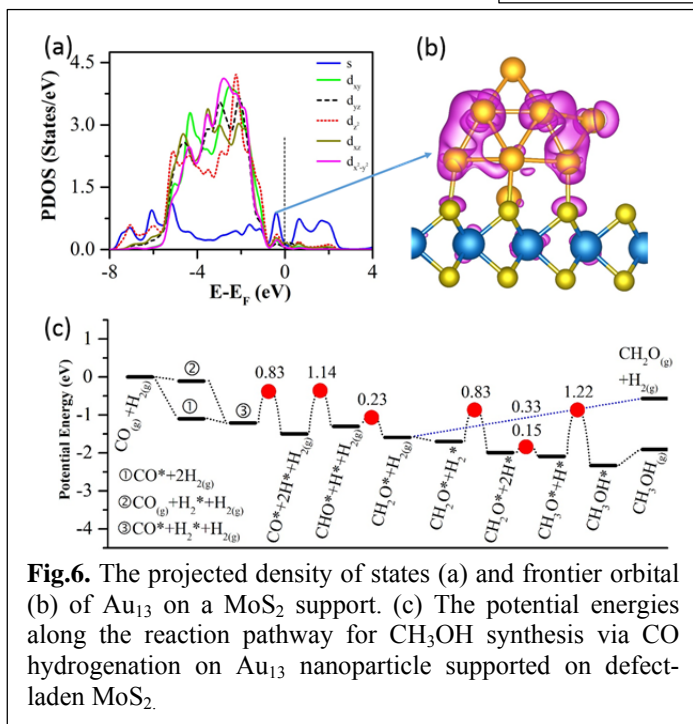


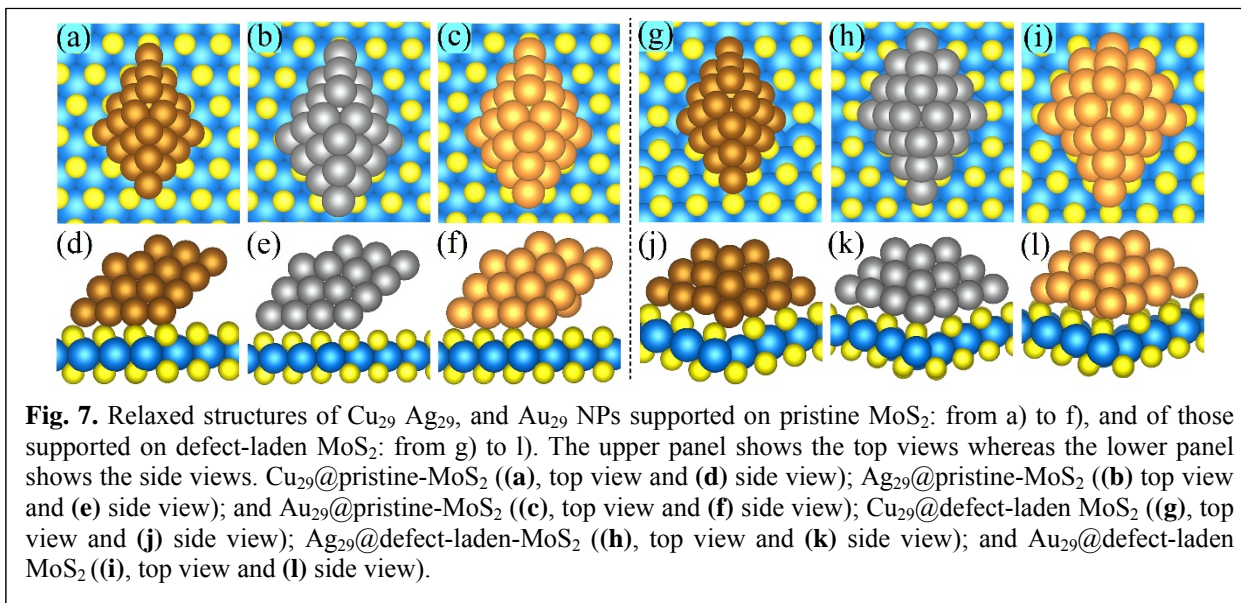
Fig.6. The projected density of states (a) and frontier orbital (b) of Au₁₃ on a MoS₂ support. (c) The potential energies along the reaction pathway for CH₃OH synthesis via CO hydrogenation on Au₁₃ nanoparticle supported on defect-laden MoS₂.

favored over the icosahedral, decahedron and cuboctahedron forms. The MoS₂ support substantially alters the electronic structure of Au₁₃ nanoparticle near the Fermi level, owing to the strong interaction of MoS₂ support with Au₁₃ in the presence of a S-vacancy. This modified electronic structure remarkably affects the catalytic activity of the system as seen by the low activation energy barriers in Fig. 6. We thus predict that an Au nanoparticle will have enhanced activity towards methanol synthesis via CO hydrogenation reaction – a contrast from that of a titania-supported Au₁₃ nanoparticle [6], which promotes methanol decomposition.

Functionalizing single layer MoS₂ via transition metal nanoparticle deposition

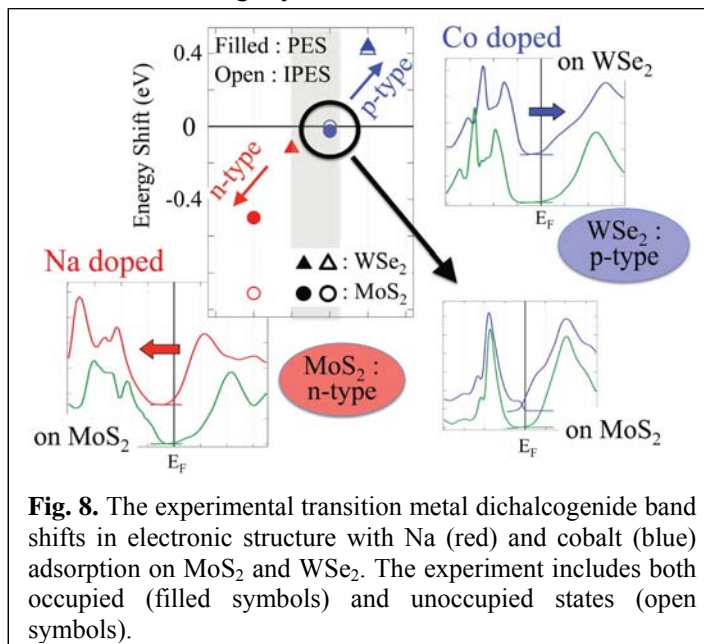
We have also investigated the adsorption of sub-nanometer-sized transition metal nanoparticles

(Cu₂₉, Ag₂₉, and Au₂₉) on both pristine and defect-laden single-layer MoS₂ using DFT with dispersion forces (optB88-vdW functional), as illustrated in Fig. 7. Although these nanoparticles bind reasonably well (-7.14 eV, -6.91 eV and -5.96 eV) to the defect sites of MoS₂, the interface does not appear to provide the active sites for adsorption (and dissociation) of molecules such as O₂, CO, and H₂, unlike similar interfaces on metal-oxide surfaces. Preliminary results for the adsorption of CH₃OH, CO & dissociation of H₂ on these MoS₂ supported transition metal nanoparticles suggests their possible application in methanol synthesis. We will continue further investigations of these nanocatalysts experimentally and theoretically in the next funding period.



The influence of catalytic promoters on MoS₂ electronic structure

Both cobalt and alkali metals are known to promote the catalytic activity of MoS₂. We have found the MoS₂ electronic structure to be significantly influenced with adsorption of Na and Co, and the effect to be profoundly different from that on WSe₂. The electronic structure is rigidly shifted with small amounts of Na or Co adsorption. In case of MoS₂, the electronic structure shifts remain electron donor (n-type) for Na adsorption, and little band structure shift, rather band gap reduction with Co, as illustrated from the combined photoemission and inverse photoemission studies summarized in Figure 8. Yet for Co on WSe₂ the band structure shifts very significantly, as an electron acceptor (p-type). We find that MoS₂ and WSe₂ are, themselves, n-type and p-type, respectively. The lesson to be learned is that we can make the n-type transition metal dichalcogenide more n-type and the p-type transition metal dichalcogenide more p-type, but the reverse is difficult. So the influence of the various catalytic promoters is not simply the effect of adding a metal to the surface and likely different catalytic promoters promote catalytic activity through different mechanisms.



Publications Acknowledging this Grant in 2013-2016¹⁻²⁰

1. K.F. Mak, K. He, C. Lee, G.H. Lee, J. Hone, T.F. Heinz, and J. Shan, "Tightly bound trions in monolayer MoS₂," *Nature Materials* **12**, 207-11 (2013).
2. D. Le and T.S. Rahman, "Joined edges in MoS₂: metallic and half-metallic wires," *Journal of Physics: Condensed Matter* **25**, 312201 (2013).
3. Q. Ma, P.M. Odenthal, J. Mann, D. Le, C.S. Wang, Y. Zhu, T. Chen, D. Sun, K. Yamaguchi, T. Tran, M. Wurch, J.L. McKinley, J. Wyrick, K. Magnone, T.F. Heinz, T.S. Rahman, R. Kawakami, and L. Bartels, "Controlled Argon Beam-Induced Desulfurization of Monolayer Molybdenum Disulfide," *Journal of Physics: Condensed Matter* **25**, 252201 (2013).
4. S. Hong, D. Le, and T. Rahman, "Deactivation of Cu₂O(100) by CO Poisoning," *Topics in Catalysis* **56**, 1082-1087 (2013).
5. D. Le, D. Sun, W. Lu, M. Aminpour, C. Wang, Q. Ma, T.S. Rahman, and L. Bartels, "Growth of aligned Mo₆S₆ nanowires on Cu(111)," *Surface Science* **611**, 1-4 (2013).
6. S. Hong and T.S. Rahman, "Rationale for the higher reactivity of interfacial sites in methanol decomposition on Au₁₃/TiO₂(110)," *Journal of the American Chemical Society* **135**, 7629-35 (2013).
7. J. Mann, D.Z. Sun, Q. Ma, J.R. Chen, E. Preciado, T. Ohta, B. Diaconescu, K. Yamaguchi, T. Tran, M. Wurch, K. Magnone, T.F. Heinz, G.L. Kellogg, R. Kawakami, and L. Bartels, "Facile growth of monolayer MoS₂ film areas on SiO₂," *European Physical Journal B* **86**, 2261-4 (2013).
8. E.A. Lewis, D. Le, A.D. Jewell, C.J. Murphy, T.S. Rahman, and E.C.H. Sykes, "Visualization of Compression and Spillover in a Coadsorbed System: Syngas on Cobalt Nanoparticles," *ACS Nano* **7**, 4384-4392 (2013).
9. S.I. Shah, S. Hong, and T.S. Rahman, "Combined Density Functional Theory and Kinetic Monte Carlo Study of Selective Oxidation of NH₃ on Rutile RuO₂(110) at Ambient Pressures," *The Journal of Physical Chemistry C* **118**, 5226-5238 (2014).
10. J. Mann, Q. Ma, P.M. Odenthal, M. Isarraraz, D. Le, E. Preciado, D. Barroso, K. Yamaguchi, G. von Son Palacio, A. Nguyen, T. Tran, M. Wurch, A. Nguyen, V. Klee, S. Bobek, D. Sun, T.F. Heinz, T.S. Rahman, R. Kawakami, and L. Bartels, "2-Dimensional Transition Metal Dichalcogenides with Tunable Direct Band Gaps: MoS_{2(1-x)}Se_{2x} Monolayers," *Advanced Materials* **26**, 1399-404 (2014).
11. D. Le, T.B. Rawal, and T.S. Rahman, "Single-Layer MoS₂ with Sulfur Vacancies: Structure and Catalytic Application," *The Journal of Physical Chemistry C* **118**, 5346-5351 (2014).
12. Q. Ma, M. Isarraraz, C.S. Wang, E. Preciado, V. Klee, S. Bobek, K. Yamaguchi, E. Li, P.M. Odenthal, A. Nguyen, D. Barroso, D. Sun, G. von Son Palacio, M. Gomez, A. Nguyen, D. Le, G. Pawin, J. Mann, T.F. Heinz, T.S. Rahman, and L. Bartels, "Post-Growth Tuning of the Bandgap of Single-Layer Molybdenum Disulfide Films by Sulfur/Selenium Exchange," *ACS Nano* **8**, 4672-7 (2014).
13. E.A. Lewis, D. Le, A.D. Jewell, C.J. Murphy, T.S. Rahman, and E.C.H. Sykes, "Segregation of Fischer-Tropsch reactants on cobalt nanoparticle surfaces," *Chemical Communications* **50**, 6537-9 (2014).
14. T. Komesu, D. Le, Q. Ma, E.F. Schwier, Y. Kojima, M. Zheng, H. Iwasawa, K. Shimada, M. Taniguchi, L. Bartels, T.S. Rahman, and P.A. Dowben, "Symmetry Resolved Surface-Derived Electronic Structure of MoS₂(0001)," *Journal of Physics: Condensed Matter* **26**, 455501 (2014).
15. T. Komesu, D. Le, X. Zhang, Q. Ma, E.F. Schwier, Y. Kojima, M. Zheng, H. Iwasawa, K. Shimada, M. Taniguchi, L. Bartels, T.S. Rahman, and P.A. Dowben, "Occupied and unoccupied electronic structure of Na doped MoS₂(0001)," *Applied Physics Letters* **105**, 241602 (2014).
16. D. Le, A. Barinov, E. Preciado, M. Isarraraz, I. Tanabe, T. Komesu, C. Troha, L. Bartels, T.S. Rahman, and P.A. Dowben, "Spin-Orbit Coupling in the Band Structure of Monolayer WSe₂," *Journal of Physics: Condensed Matter* **27**, 182201 (2015).

17. D.T. Restrepo, K.E. Giesler, R.A. Penabe, M. Aminpour, D. Le, T.S. Rahman, and R.G. Blair, "Heterogeneous Metal-Free Hydrogenation Over Defect Hexagonal Boron Nitride," Submitted (2015).
18. P. Patoka, G. Ulrich, A.E. Nguyen, L. Bartels, P.A. Dowben, V. Turkowski, T.S. Rahman, P. Hermann, B. Kastner, A. Hoehl, G. Ulm, and E. Ruhl, "Nanoscale plasmonic phenomena in CVD-grown MoS₂ monolayer revealed by ultra-broadband synchrotron radiation based nano-FTIR spectroscopy and near-field microscopy," *Optics Express* **24**, 1154-1164 (2016).
19. I. Tanabe, T. Komesu, D. Le, T.B. Rawal, E.F. Schwier, M. Zheng, Y. Kojima, H. Iwasawa, K. Shimada, T.S. Rahman, and P.A. Dowben, "The symmetry-resolved electronic structure of 2H-WSe₂(0001)," *Journal of Physics: Condensed Matter* **In Press** (2016).
20. I. Tanabe, M. Gomez, W.C. Coley, D. Le, E.M. Echeverria, G. Stecklein, V. Kandyba, S.K. Balijepalli, V. Klee, A.E. Nguyen, E. Preciado, I.-H. Lu, S. Bobek, D. Barroso, D. Martinez-Ta, A. Barinov, T.S. Rahman, P.A. Dowben, P. Crowell, and L. Bartels, "Chemical Vapor Deposited WS₂ Brillouin Zone-Edge and -Center Band Structure Characteristics," submitted to *Applied Physics Letters* (2016).

Catalysis by Design: Heterogeneous Single Atom Catalysts

Maria Flytzani-Stephanopoulos,¹ Charles Sykes,² Jilei Liu,¹ Chongyang Wang,¹ Ming Yang,¹ Sufeng Cao,¹ Felicia Lucci,² Andrew Therrien²

¹Department of Chemical and Biological Engineering, ²Department of Chemistry
Tufts University, Medford, MA

Presentation Abstract

A comprehensive approach is followed in this project to elucidate catalytic activity at the single atom limit. Atomically dispersed supported metals and single atom alloy (SAA) catalysts are investigated in the project by surface science and catalysis methods. The reactions of interest include (i) methanol and ethanol reactions (dehydrogenation, partial oxidation, steam reforming) on atomically dispersed gold. For the methanol reactions, experimental and computational work on single-site Au-O_x-Na_y(OH)_z clusters has demonstrated the self-coupling of methanol to methyl formate and hydrogen as the reaction mechanism, similar to what has been previously reported for other gold catalyst configurations. (ii) selective hydrogenation and dehydrogenation reactions on model single-crystal SAA catalysts and their nanoparticle analogs at ambient pressures. The Pt₁Cu SAA catalyst was evaluated for selective hydrogenation (butadiene to butene, acetylene to ethylene) and dehydrogenation (methanol to formaldehyde) reactions, and for its tolerance to carbon monoxide. We found that carbon monoxide binds more weakly to single platinum atoms than to platinum clusters, so that the SAA design leaves more CO-free active platinum sites available for catalysis. These surfaces exhibit minimal poisoning in both model and realistic catalysts for reactions such as acetylene hydrogenation. The SAA approach could be used with other metal combinations in order to improve catalysts for industrially important processes that are prone to carbon monoxide poisoning.

DE-FG02-05ER15730: Atomically dispersed supported metal species as catalysts for alcohol conversion, and hydrogen and chemicals production

Collaborators: Manos Mavrikakis (U. Wisconsin), Sungsik Lee (ANL), Lawrence F. Allard (ORNL); Guido Busca (U. Genoa)

RECENT PROGRESS

During the past year, work with single-atom heterogeneous catalysts was continued with (i) gold atoms stabilized either with -O-M- ligands on certain oxide supports or with O-Na- ligands on any oxide support; and (ii) single atom alloy catalysts in which the metal atom (Pt, Pd) is stabilized in the majority metal (e.g. Cu) surface. The desired outcome is a good mechanistic understanding of the chemistries under investigation and the reaction-

induced evolution of key catalyst structures, in order to propose general catalyst design guidelines for the reactions of interest. The main project findings are summarized below.

Novel one-pot synthesis of supported single atom gold catalysts at high loadings

A new facile, one-pot route to prepare stable single-gold atom catalytic sites at high loadings was developed, using alkaline aqueous solutions of $\text{Au}(\text{OH})_3$ and NaOH with a $\sim 10/1$ Na/Au atomic ratio. Incipient wetness impregnation of titania with these solutions was used to prepare 1wt.% gold, exclusively as single-atom sites. This green synthesis method involves no extra reagents or wastes, no organometallics, and requires no after-treatment for catalytic activation. We demonstrated activity for the low-temperature water-gas shift, the steam reforming of methanol, and the methanol dehydrogenation reaction to methyl formate and hydrogen as examples of reactions for which these single-site clusters may be used in heterogeneous catalysis. Fig. 1a shows the same TOF (s^{-1}) of the methanol steam reforming reaction over the $\text{Au}-\text{O}_x-\text{Na}_y(\text{OH})_z$ clusters on anatase and other single-atom gold catalysts like the leached Au/ZnZrO_x mixed oxide catalysts previously investigated in the project.^{1,2} Fig. 1b shows the single gold atoms on titania.

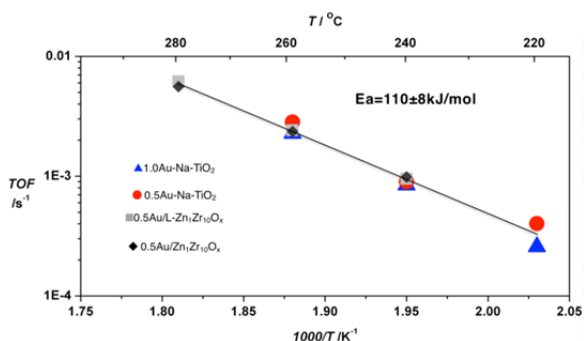


Fig. 1a. Methanol steam reforming

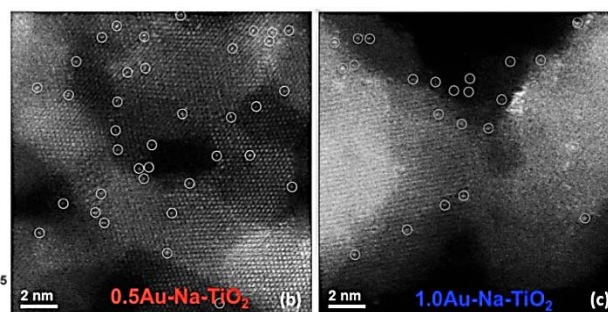


Fig. 1b. $\text{Na}-\text{O}_x$ stabilized gold atoms on TiO_2

Pt₁Cu Single Atom Alloys

Water co-catalyzed selective dehydrogenation of methanol to formaldehyde and hydrogen

The non oxidative dehydrogenation of methanol to formaldehyde is considered a good method to produce formaldehyde and clean hydrogen gas. Although Cu-based catalysts have excellent catalytic activity in the oxidative dehydrogenation of methanol, metallic Cu is commonly believed to be unreactive for the dehydrogenation of methanol in the absence of oxygen adatoms or oxidized copper. In this work we showed that metallic Cu can catalyze the dehydrogenation of methanol in the absence of oxygen adatoms by using water as a co-catalyst both under realistic reaction conditions using silica-supported PtCu nanoparticles in a flow reactor system at temperatures below 250 °C, and in ultra-high vacuum using model PtCu(111) catalysts.³ Adding small amounts of isolated Pt atoms into the Cu surface to form Pt₁Cu single atom alloys (SAAs) enhances the dehydrogenation activity of Cu. The promotional effect of water is attributed to the stabilization of H atoms by water clusters that facilitate the dehydrogenation of methanol

to methoxy, which can be further dehydrogenated to formaldehyde. The selectivities to formaldehyde on PtCu SAA nanoparticle catalysts and on PtCu(111) SAA model catalysts are both nearly 100%. PtCu SAA catalysts also exhibit very good stability in the high-pressure flow reactor tests and under UHV conditions.

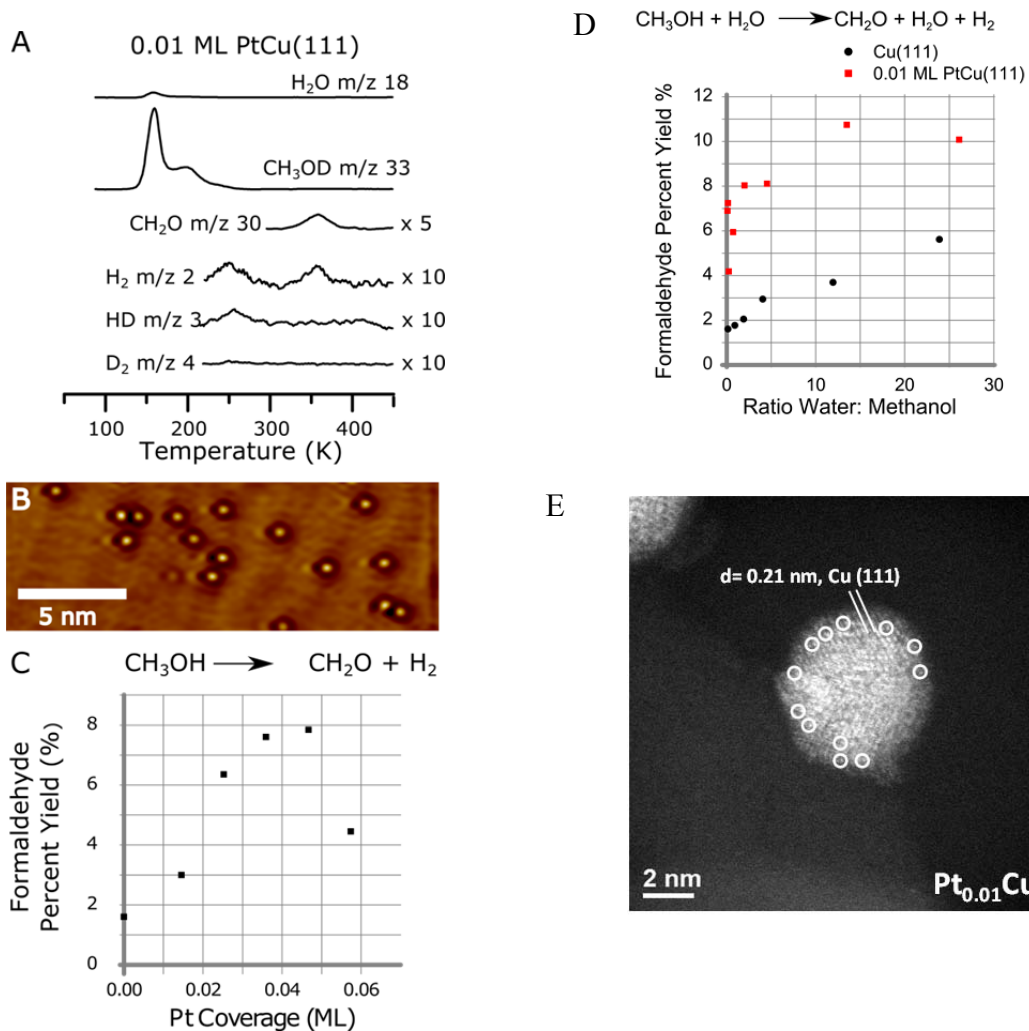


Fig.2 (A) TPD/R traces of methanol on a PtCu SAA. 0.6 ML methanol-D was adsorbed on 0.01 ML PtCu(111) surface (water : methanol = 0.2:1); (B) STM image of PtCu(111) SAA surface where the bright features are Pt atoms substituted into the Cu(111) surface; (C) Formaldehyde percent yield versus Pt concentration for adsorption of 0.6 ML methanol onto varying surface coverages of Pt (water : methanol = 0.2:1); (D) Formaldehyde yield as a function of water to methanol ratio for Cu(111) and PtCu(111) SAA surfaces. Methanol was adsorbed prior to water and the methanol surface coverage was 0.6 ML for each trial; (E) ac-HAADF-STEM image of a typical region of the Pt_{0.01}Cu/SiO₂ nanoparticles. The sample was pre-reduced in H₂ at 350 °C. Some of the isolated Pt atoms are highlighted by white circles.

Selective hydrogenation of butadiene on Pt/Cu alloys at the single atom limit

In this work, surface science and atomic resolution microscopy studies of the selective hydrogenation of butadiene to butenes on model Pt/Cu(111) alloy surfaces have shown that individual, isolated Pt atoms in the Cu(111) surface are all that is required to ensure stable activity and 100% selectivity.⁴ We have extended these findings to realistic

pressures (1 bar) by synthesizing and testing Pt/Cu SAA nanoparticle catalysts. At low loadings, Pt exists as individual, isolated atoms substituted into the Cu(111) surface, see Fig. 2(E). These single Pt atoms activate the dissociation of H₂ and spillover of H to Cu. The weak binding of butadiene to Cu allows for the highly selective hydrogenation to butenes. No decomposition or poisoning of these alloys was observed which can be attributed to the lack of extended Pt surface sites. At higher Pt content in Pt/Cu alloy surfaces, we directly visualized extended Pt ensembles responsible for the reduced selectivity. This combined model system/NP catalyst strategy is a powerful approach to the design of new alloy catalysts. This approach is especially useful for highly diluted single-site systems in which identification of the active sites and elucidation of the surface chemistry is very challenging.

Tackling CO Poisoning with Single Atom Alloy Catalysts

The fundamentals of CO adsorption on PtCu alloys were investigated using a variety of surface science and catalysis techniques. We found that CO binds weaker to single Pt atoms in Cu compared to larger Pt ensembles or monometallic Pt.⁵ Thus, when CO is present in the gas phase, more CO-free Pt sites are available on the SAA than the monometallic Pt, yielding higher H₂ activation reactivity as shown by H₂-D₂ exchange experiments at ambient pressure in a flow reactor setup, Fig. 3.⁵ The CO tolerance of the Pt₁Cu was also shown under realistic conditions in the selective hydrogenation of acetylene to ethylene, Fig. 4.⁵

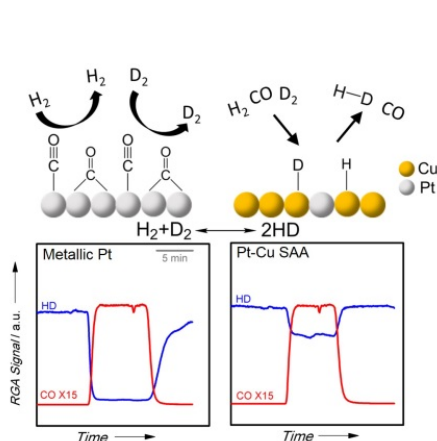


Fig.3

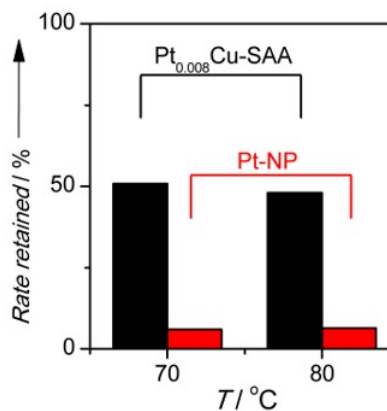


Fig.4. C₂H₂ hydrogenation rate retained in the presence of CO in 20% H₂, 2.2% C₂H₂, 200 ppm CO, 10% Ar, bal. He.⁵

References

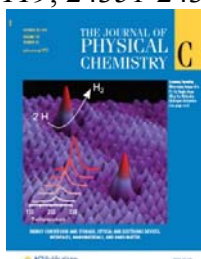
1. Wang, C.; Garbarino, G.; Allard L.F.; Wilson, F.; Busca, G.; Flytzani-Stephanopoulos, M. Low-temperature dehydrogenation of ethanol on atomically dispersed gold supported on ZnZrO_x, *ACS Catalysis* **2015**, DOI: 10.1021/acscatal.5b01593.
2. Wang, C.; Yang, M.; Flytzani-Stephanopoulos, M. Single gold atoms stabilized on nanoscale metal oxide supports are catalytic active centers for various reactions, *AIChE J.* **2015**, DOI: 10.1002/aic.15134.
3. Shan, J.; Lucci, F.; Liu, J., *et al.* Water co-catalyzed selective dehydrogenation of methanol to formaldehyde and hydrogen, *Surface Science* **2016**, DOI: 10.1016/j.susc.2016.02.010.
4. Lucci, F.; Liu, J.; Marcinkowski, M.; Yang, M.; Flytzani-Stephanopoulos, M.; Sykes, E.C.H. Selective hydrogenation of butadiene on platinum copper alloys at the single atom limit, *Nat. Commun.* **2015**, *6*, 8550.
5. Liu, J.; Lucci, F.; Yang, M.; *et al.* Tackling CO Poisoning with Single-Atom Alloy Catalysts, *J. Am. Chem. Soc.* **2016**, DOI: 10.1021/jacs.6b03339.

Publications Acknowledging this Grant in 2013-2016

(I) Exclusively funded by this grant

1. Yi, N.; Saltsburg, H.; Flytzani-Stephanopoulos, M. Hydrogen Production by Dehydrogenation of Formic Acid on Atomically Dispersed Gold on Ceria, *ChemSusChem* **2013**, *6*, 816-819.
2. Yang, M.; Allard, L. F.; Flytzani-Stephanopoulos, M. Atomically Dispersed Au-(OH)_x Species Bound on Titania Catalyze the Low-Temperature Water-Gas Shift Reaction, *J. Am. Chem. Soc.* **2013**, *135*, 3768-3771.
3. Boucher, M. B., Zugic, B., Cladaras, G., Kammert, J., Marcinkowski, M. D., Lawton, T. J., Sykes, E. C. H., Flytzani-Stephanopoulos, M. Single atom alloy surface analogs in Pd_{0.18}Cu_{1.5} nanoparticles for selective hydrogenation reactions, *PCCP* **2013**, *15*, 12187-12196.
4. Boucher, M. B., Marcinkowski, M. D., Liriano, M. L., Murphy, C. J., Lewis, E. A., Jewell, A. D., Mattera, M. F. G., Kyriakou, G., Flytzani-Stephanopoulos, M., Sykes, E. C. H. "Molecular-Scale Perspective of Water-Catalyzed Methanol Dehydrogenation to Formaldehyde", *ACS Nano* **2013**, *7*, 6181-6187.
5. Flytzani-Stephanopoulos M, "Gold atoms stabilized on various supports catalyze the water-gas shift reaction", *Acc. Chem. Res.* **2013**, DOI: 10.1021/ar4001845.
6. Wang C, Boucher MB, Ming Y, Saltsburg H, Flytzani-Stephanopoulos M, "ZnO-Modified Zirconia as Gold Catalyst Support for the Low-Temperature Methanol Steam Reforming Reaction", *Appl. Catal. B: Environmental*, **2014**, [154–155](#), 142–152 ; doi.org/10.1016/j.apcatb.2014.02.008
7. Yang, M.; Sha, L.; Wang Y.; Allard, L.F.; Herron, J.; Xu, Y.; Lee, S.; Huang, J.; Mavrikakis, M.; Flytzani-Stephanopoulos, M. [Catalytically active Au-O\(OH\)_x- species stabilized by alkali ions on zeolites and mesoporous oxides](#), *Science* **2014**, *346*, 1498-1501.
8. Flytzani-Stephanopoulos, M. [Gold Atoms Stabilized on Various Supports Catalyze the Water–Gas Shift Reaction](#), *Acc. Chem. Res.*, **2014**, *47* (3), 783–792
9. Garbarino G, Wang C, Valdamakis I, [Chitsazan](#) S, Riani P, Finocchio E, Flytzani-Stephanopoulos M, Busca G. A study of Ni/Al₂O₃ and Ni–La/Al₂O₃ catalysts for the steam reforming of ethanol and phenol, *Applied Catalysis B: Envir.* **2015**, 174-175, 21–34.
10. Yang, M., Liu J, Lee S, Zugic B, Huang J, Allard LF, Flytzani-Stephanopoulos M. [A Common Single-Site Pt\(II\)–O\(OH\)_x– Species Stabilized by Sodium on 'Active' and 'Inert' Supports Catalyzes the Water-Gas Shift Reaction](#), *J. Am. Chem. Soc.* **2015**, *137* (10), 3470–3473

11. Lucci, F. R.; Marcinkowski, M. D.; Lawton, T. J.; Sykes, E. C. H. H₂ Activation and Spillover on Catalytically Relevant Pt-Cu Single Atom Alloys. *J. Phys. Chem. C* **2015**, *119*, 24351-24357

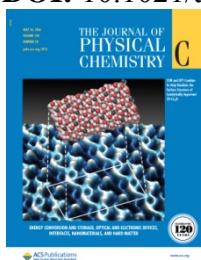


12. Yi, N., Flytzani-Stephanopoulos, M. Gold-Ceria: the making of a robust catalyst for fuel processing and hydrogen production, **2015**, Chapter 5 in *Catalysis by Materials with Well-Defined Structures* (Edited by Wu and Overbury). Elsevier Science, ISBN: 9780128012178

13. Wang, C.; Garbarino, G.; Allard L.F.; Wilson, F.; Busca, G.; Flytzani-Stephanopoulos, M. Low-temperature dehydrogenation of ethanol on atomically dispersed gold supported on ZnZrO_x, *ACS Catalysis* **2015**, DOI: 10.1021/acscatal.5b01593

14. Wang, C.; Yang, M.; Flytzani-Stephanopoulos, M. Single gold atoms stabilized on nanoscale metal oxide supports are catalytic active centers for various reactions, *AIChE J.* **2015**, DOI: 10.1002/aic.15134.

15. Therrien, A. J.; Zhang, R.; Lucci, F. R.; Marcinkowski, M. D.; Hensley, A. J. R.; McEwen, J. S.; Sykes, E. C. H. Structurally Accurate Model for the “29”-Structure of Cu_xO/Cu(111): A DFT and STM Study. *J. Phys. Chem. C*. 2016, DOI: 10.1021/acs.jpcc.6b01284



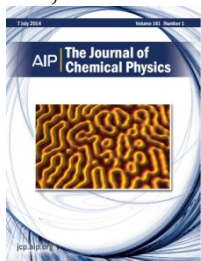
(II) Jointly funded by this grant and other grants with leading intellectual contribution from this grant;

16. Lawton, T. J.; Kyriakou, G.; Baber, A. E.; Sykes, E. C. H. An Atomic Scale View of Methanol Reactivity at the Cu(111)/CuO_x Interface. *ChemCatChem*. **2013**, *5*, 2684-2690

17. Zugic, B.; Bell, D. C.; Flytzani-Stephanopoulos, M. Activation of carbon-supported platinum catalysts by sodium for the low-temperature water-gas shift reaction. *Applied Catalysis B: Environmental* **2014**, *144*, 243-251
18. Lucci, F. R.; Lawton, T. J.; Pronschinske, A.; Sykes, E. C. H. Atomic Scale Surface Structure of Pt/Cu(111) Surface Alloys. *J. Phys. Chem. C* **2014**, *118*, 3015-3022
19. Zugic, B.; Zhang, S.; Bell, D.C.; Tao, F.; Flytzani-Stephanopoulos, M. [Probing the Low-Temperature Water Gas Shift Activity of Alkali-Promoted Platinum Catalysts Stabilized on Carbon Supports](#). *J. Am. Chem. Soc.* **2014**, *136* (8), 3238–3245.
20. Lucci, F.; Liu, J.; Marcinkowski, M. D.; Yang, M.; Flytzani-Stephanopoulos, M.; Sykes, E.C.H. Selective hydrogenation of butadiene on platinum copper alloys at the single atom limit, *Nat. Commun.* **2015**, *6*, 8550.
21. Liu, J.; Lucci, F.; Yang, M.; Lee, S.; Therrien, A.; Marcinkowski, M.D.; Williams, C.; Sykes, E.C.H.; Flytzani-Stephanopoulos, M. Tackling CO Poisoning with Single-Atom Alloy Catalysts *J. Am. Chem. Soc.* **2016**, DOI: 10.1021/jacs.6b03339.

(III) Jointly funded by this grant and other grants with relatively minor intellectual contribution from this grant;

22. Murphy, C. J.; Carrasco, J.; Lawton, T. J.; Liriano, M. L.; Baber, A. E.; Lewis, E. A.; Michaelides, A.; Sykes, E. C. H. Structure and Energetics of Hydrogen-Bonded Networks of Methanol on Close Packed Transition Metal Surfaces. *J. Chem. Phys.* **2014**, *141*, 014701



23. Li, Z.; Potapenko, D.V.; Rim, K.T.; Flytzani-Stephanopoulos, M.; Flynn, G.W.; Osgood, R.M.; Wen, X-D; Batista, E.R. Reactions of Deuterated Methanol (CD₃OD) on Fe₃O₄(111). *J. Phys. Chem. C*, **2015**, *119* (2), 1113–1120.
24. Shan, J.; Lucci, F; Liu, J., El-Soda, M.; Marcinkowski, M.D.; Allard, L.F.; Sykes, E.C.H.; Flytzani-Stephanopoulos, M. Water co-catalyzed selective dehydrogenation of methanol to formaldehyde and hydrogen, *Surface Science* **2016**, DOI: 10.1016/j.susc.2016.02.010.

**Towards More Accurate Descriptors of Reactivity in Acid and Oxidation
Catalysis on Metal Oxides**

Prashant Deshlahra, William Knaeble, Enrique Iglesia
Department of Chemical and Biomolecular Engineering
University of California at Berkeley

The catalytic function of oxides in acid and redox catalysis is examined here by a combination of kinetic and isotopic probes, structural and surface characterization, and theoretical assessments of elementary steps and binding sites based on density functional theory (DFT). These strategies exploit oxide clusters of known structure and diverse compositions and crystalline microporous solids with well-defined confining voids in order to identify rigorous descriptors of reactivity and selectivity. DFT-derived deprotonation energies (DPE) and the proton affinity of gaseous analogs of transition states determine reactivity for a broad range of acid-catalyzed reactions. DPE values rigorously reflect the acid strength of oxides, but represent an incomplete descriptor of their catalytic properties, because interactions between organic moieties (e.g. intermediates, transition states) and the conjugate anion in solid acids depend on the ability of molecules and oxide surfaces to reorganize charge. This requires that we dissect DPE values into their covalent and ionic components and that we describe transition states for families of reactions various reactions in terms of their ability to recover a fraction of each component of DPE upon formation of ion-pair transition states. The redox cycles that mediate catalytic oxidations, with few exceptions, are limited by C-H activation elementary steps that reduce metal centers in oxide catalysts. These steps involve late transition states containing nearly formed O-H bonds, making H-addition energies (HAE) a relevant, but incomplete, descriptor of reactivity. The stability of transition states also depends on di-radical interactions that are influenced by how the organic moieties delocalize the unpaired electron. In acid and oxidation catalysis, reactivity descriptors solely based on molecular and catalyst properties become accurate and more complete only when we consider how molecules and solids “adapt” as they interact at ion-pair and di-radical transition states. The reciprocal benchmarking of theoretical methods against mechanistic inferences from experiment requires the use of solids that preserve known structures during catalysis, the interpretation of chemical reactivity in terms of elementary steps, and the reporting of intrinsic rates, rigorously normalized by the number of active sites.

FWP 47319: Low Temperature Catalytic Routes for Energy Carriers via Spatial and Chemical Organization

Publications Acknowledging this Grant in 2013-2016

Deshlahra, P.; Iglesia, E. Methanol Oxidative Dehydrogenation on Oxide Catalysts: Molecular and Dissociative Routes and Hydrogen Addition Energies as Descriptors of Reactivity. *J. Phys. Chem. C* **2014**, *118*, 26115-26129. (I)

Deshlahra, P.; Carr, R.; Iglesia, E. Ionic and Covalent Stabilization of Intermediates and Transition States in Catalysis by Solid Acids. *J. Amer. Chem. Soc.* **2014**, *136*, 15229-15247. (I)

Jones, A.; Carr, R.; Zones, S.; Iglesia, E. Acid Strength and Solvation in Catalysis by MFI Zeolites and Effects of the Identity, Concentration and Location of Framework Heteroatoms. *J. Catal.* **2014**, *312*, 58-68. (II)

Knaeble, W.; Carr, R.; Iglesia, E., Mechanistic Interpretation of the Effects of Acid Strength on Alkane Isomerization Turnover Rates and Selectivity. *J. Catal.* **2014**, *319*, 283-296. (I)

Deshlahra, P.; Carr, R.; Chai, S.-H.; Iglesia, E. Mechanistic Details and Reactivity Descriptors in Oxidation and Acid Catalysis of Methanol. *ACS Catal.* **2015**, *5*, 666-682. (I)

Knaeble, W.; Iglesia, E. Kinetic and Theoretical Insights into the Mechanism of Alkanol Dehydration on Solid Brønsted Acid Catalysts. *J. Phys. Chem. C* **2016**, *120*, 3371-3389. (I)

Deshlahra, P.; Iglesia, E., Reactivity and Selectivity Descriptors for the Activation of C-H Bonds in Hydrocarbons and Oxygenates on Metal Oxides. *J. Phys. Chem. C* (submitted) (I)

Deshlahra, P.; Iglesia, E., Towards More Complete Descriptors of Reactivity in Catalysis by Solid Acids. *ACS Catal.* (submitted) (I)

Knaeble, W.; Iglesia, E., Acid Strength and Metal-Acid Proximity Effects on Methylcyclohexane Ring Contraction Turnover Rates and Selectivities. *J. Catal.* (submitted) (I)

Structure and Function in Electrocatalysis of Reactions for Direct Energy Conversion

Radoslav R. Adzic¹, Jia Wang¹, Kotaro Sasaki¹, Miomir Vukmirovic¹, Meng Li¹, Kurian A. Kuttiyiel¹, Ping Liu¹, Dong Su², Lijun Wu³,

¹Chemistry Department, ²Center for Functional Nanomaterials, ³Department of Condensed Matter Physics and Materials Science, Brookhaven National Laboratory

Abstract

We conduct studies of Pt monolayer electrocatalysts, and related core-shell catalysts for reactions of direct energy conversion including the O₂ reduction (ORR) and O₂ evolution reactions (OER), oxidation of ethanol and methanol, H₂ oxidation and evolution and CO₂ reduction. We aim at increasing our understanding of their kinetics and synthesizing ultimately low Pt content electrocatalysts with high activity and good stability. We demonstrated the extension of the core-shell nanoparticle catalysts to metal oxides by developing the RuO₂@IrO₂ core-shell catalyst for the oxygen evolution reaction (OER) and determined the mechanism of that OER using a two-step kinetic equation for a sequential water dissociation pathway with adsorbed O as the main OER intermediate: (1) $\frac{1}{2} \text{H}_2\text{O} = \frac{1}{2} \text{O}_{\text{ad}} + \text{H}^+ + \text{e}^-$ and (2) $\frac{1}{2} \text{H}_2\text{O} + \frac{1}{2} \text{O}_{\text{ad}} = \frac{1}{2} \text{O}_2 + \text{H}^+ + \text{e}^-$.

Hydrogen oxidation and evolution reactions (HOR-HER) on Pt in acid are facile processes, while in alkaline electrolytes they are two-orders-of-magnitude slower. Kinetic analyses of polarization curves over a wide range of potential indicate that from acid to base, the activation free energies increase the most for the Volmer reaction, resulting in a switch of the rate-determining step from the Tafel- to the Volmer-reaction, and a shift to a weaker optimal hydrogen-binding energy.

We demonstrated that the Pt monolayer under tensile strain on Au substrates has a highly enhanced activity for methanol and ethanol oxidation. The C-C bond splitting in ethanol, and a lack of CO formation in methanol oxidation, on Pt monolayer under tensile strain cause major changes in the reaction mechanism and increased the reaction kinetics.

Grant Number: 2016-BNL-MA510MAEA-Budg

Grant Title: Structure and Function in Electrocatalysis of Reactions for Direct Energy Conversion

Postdoc(s): Kurian Kuttiyiel, Meng Li

Student(s): Yu Zhang, Zhixiu Liang, Zhong Ma

BNL – FWP : B&R No. KC03020

RECENT PROGRESS

Oxygen evolution reaction mechanism and enhanced activity of the RuO₂@IrO₂ core-shell nanocatalysts

We demonstrated the extension of the core-shell nanoparticle catalysts to metal oxides by developing the RuO₂@IrO₂ core-shell catalyst for the oxygen evolution reaction (OER), and determined the OER mechanism by quantitative kinetic analysis and detailed DFT calculations. Both accomplishments may have a significant impact on future research for advancing water electrolyzers in clean energy applications. Iridium dioxide, IrO₂, is an active, highly durable catalyst for the OER. However, Ir is one of the rarest elements on earth. To maximize the mass-normalized IrO₂ surface area, and to enhance its area-normalized specific activity, we developed a facile synthesis to prepare RuO₂ and RuO₂@IrO₂ core-shell nanocatalysts. Ru nanoparticles on a carbon support (Ru/C) were used as the precursor of RuO₂, and H₂IrCl₆ as the precursor of IrO₂ shell. The carbon support in Ru/C acted as a template to disperse Ru nanoparticles. During calcinations at temperatures between 350 and 450 °C in air, the carbon support was burnt off, yielding RuO₂ nanoparticles or RuO₂@IrO₂ core-shell nanoparticles when H₂IrCl₆ was mixed with Ru/C. At 1.48 V, the specific activity on RuO₂@IrO₂ is threefold of that on IrO₂, but remains lower than that on RuO₂ as shown in Fig. 1a. The origin of this enhancement and the OER mechanism seem particularly interesting.

Early OER mechanistic studies proposed the pathways having the O-O bond forming from two adsorbed oxygen species. In the 2000s, DFT studies suggested that the activation barrier is lower with sequential addition of a second O to an adsorbed one via water dissociative adsorption on the O-adsorbed site. However, the rate-determining steps remain elusive on the most active RuO₂ and IrO₂ catalysts. This study confirmed the sequential water dissociation pathway by reproducing the polarization curves measured over a wide potential range with a two-step kinetic equation, found the rate-determining-step on IrO₂ and RuO₂, and provided guidance for finding more suitable core oxide to further enhanced the OER activity on the IrO₂ shell.

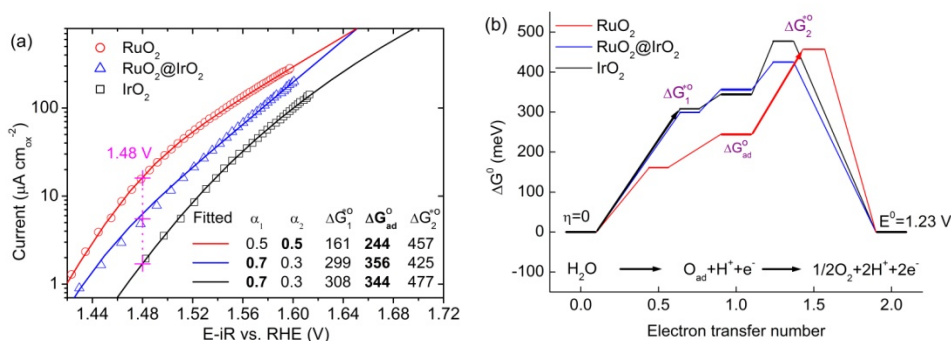


Fig. 1 (a) Surface-area-normalized polarization curves (symbols) and the best fits (lines) using the sequential OER kinetic equation. (b) The OER free energy diagrams at 1.23 V constructed using the fitted standard free energies as given in (a).

We analyzed the OER polarization curves using a two-step kinetic equation for a sequential water dissociation pathway with adsorbed O as the main OER intermediate:

(1) $\frac{1}{2} \text{H}_2\text{O} = \frac{1}{2} \text{O}_{\text{ad}} + \text{H}^+ + \text{e}^-$ and (2) $\frac{1}{2} \text{H}_2\text{O} + \frac{1}{2} \text{O}_{\text{ad}} = \frac{1}{2} \text{O}_2 + \text{H}^+ + \text{e}^-$. The lines in Fig. 1a show that the best fits well reproduced the measured polarization curves. From the fitted parameters, we constructed the free energy diagrams in Fig. 1b. The arrows for the highest barriers show that the rate-limiting step is the step 2 for the RuO_2 , and the step 1 for the IrO_2 and $\text{RuO}_2@\text{IrO}_2$. We further found that the experimentally derived free energy of adsorption of O linearly correlate with the DFT-calculated values (Fig. 2 (left top panel)). The order of weakened O adsorbed phase explains the O intermediate coverage rises at lowest potential on RuO_2 and slowest on the $\text{RuO}_2@\text{IrO}_2$. The peak potentials in the voltammetry curves also follow the same order. (Fig. 2c). Combining experimentally determined activation barriers for the rate-limiting step with DFT calculated reaction free energies, we summarize in Fig. 2 (Left, bottom) that the O the rate-determining step on IrO_2 is the formation of O adsorbed phase, while the OOH formation limits the reaction rate on RuO_2 . A core oxide that can shift the O adsorption free energy to the middle is likely to be the best for enhancing the OER activity.

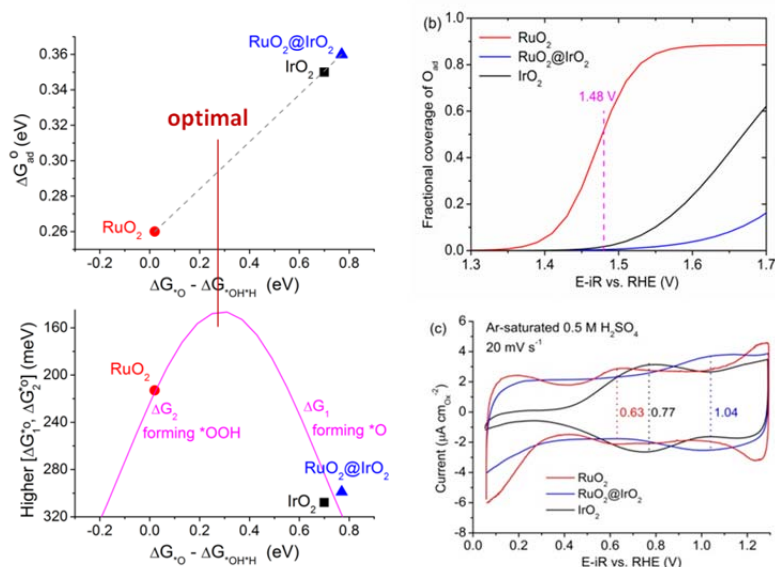


Fig. 2 (Top, left) Correlation between fitted and DFT-calculated adsorption free energies. (bottom, left) Volcano plot and suggested optimal O adsorption free energy. (b) Adsorption isotherm derived from kinetic analysis. (c) voltammetry curves for RuO_2 , $\text{RuO}_2@\text{IrO}_2$ and IrO_2 .

Elucidating Hydrogen Oxidation/Evolution Kinetics in Alkaline and Acid Solutions

Hydrogen oxidation and evolution reactions (HOR-HER) on Pt in acid are facile processes, while in alkaline electrolytes they are two-orders-of-magnitude slower. This behavior is not understood. Thus, increasing the understanding of different kinetics and developing catalysts that are more active than Pt for these two reactions is important for advancing the performance of anion-exchange-membrane fuel cells and water electrolyzers. We found a four-fold enhancement in Pt mass activity for single crystalline $\text{Ru}@Pt$ core-shell nanoparticles with two-monolayer-thick Pt shells, which doubles the activity on Pt-Ru alloy nanocatalysts. For Pt specific activity, the 2- and 1-monolayer-thick Pt shells, respectively, exhibited an enhancement factor of 3.1 and 2.3 compared to

the Pt nanocatalysts in base, differing considerably from the values of 1 and 0.4 in acid. To explain such behavior and the orders-of-magnitude difference in activity in acid and base, we performed kinetic analyses of polarization curves over a wide range of potential, from -250 to 250 mV using the dual-pathway kinetic equation. From acid to base, the activation free energies increase the most for the Volmer reaction, resulting in a switch of the rate-determining step from the Tafel- to the Volmer-reaction, and a shift to a weaker optimal hydrogen-binding energy. The much higher activation barrier for the Volmer reaction in base than in acid is ascribed to one or both of the two catalyst-insensitive factors – slower transport of OH^- than H^+ , and a stronger O-H bond in water molecules (HO-H) than in hydrated protons ($\text{H}_2\text{O}-\text{H}^+$).

Enhancing oxidation kinetics of methanol and ethanol by changing the reaction mechanism induced by tensile strain

We demonstrated that the Pt monolayer under tensile strain on Au(111) and Au nanoparticle substrates has a highly enhanced activity for methanol and ethanol oxidation. The C-C bond splitting in ethanol on Pt monolayer under tensile strain causes a major change in the reaction mechanism facilitating the oxidation to CO_2 . In methanol oxidation, the formation of CO, the blocking intermediate, is precluded, which facilitates a sevenfold increase of the reaction rate [2].

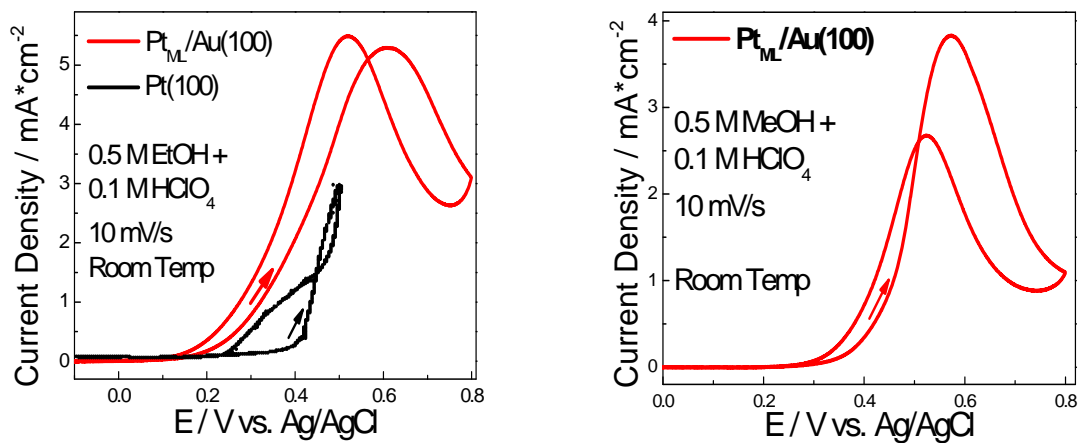


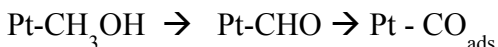
Fig. 3 Oxidation of ethanol (left) and methanol (right) on Pt monolayer under tensile strain on Au(100).

Another demonstration of the effectiveness of expansive strain in increasing the rate of alcohol oxidation is obtained with a Pt monolayer on Au(100) showing significantly enhanced EOR activity and ~ 200 mV shift of onset potential relative to Pt(100) (Fig. 3).

Changing the mechanisms of CH₃OH and C₂H₅OH oxidation for increased kinetics

Formation of CO the blocking intermediate is the main problem of ethanol electrocatalysis. It is an obstacle that does not allow a broad application of direct methanol fuel cells. For Pt ML on Au under tensile strain *in situ* infrared spectroscopy studies with single-crystal- and nanoparticle-based catalysts showed no adsorbed CO band ($\sim 2090\text{ cm}^{-1}$) in methanol oxidation, which proceeded to CO₂. This observation was in agreement with theoretical prediction by DFT calculation.

New route that does not involve CO formation is likely to avoid the reaction established for Pt:



In it, the reactive intermediate CHO forms CO, which blocks Pt sites for CH₃OH adsorption.

Instead, the reaction on Pt/Au:



accomplishes the oxidation of CHO to CO₂. The reactive strained Pt surface forms PtOH at more negative potentials than Pt. The reactive intermediate, CHO, reacts with Pt-OH formed at strained Pt producing CO₂ rather than CO adsorbed. This change in mechanism increases the reaction rate by sevenfold.

During ethanol oxidation on Pt_{ML}/Au(111), the absence of both the CO_{ads} and CO₂ bands suggested that ethanol dissociative adsorption did not occur and that the reaction followed partial oxidation pathway without cleavage of the C–C bond. However, the splitting of C-C bond was observed on nanoparticles Pt_{ML}/Au/C and RhSO₂/Pt_{ML}/Au/C catalysts, as evidenced by the CO₂ band.

The instability of SnO₂ as a co-catalyst causes performance decay. Successful replacement of SnO₂ by oxide materials with higher chemical stability has been achieved. Preliminary data exemplified by use of CeO₂ are shown in Fig. 4.

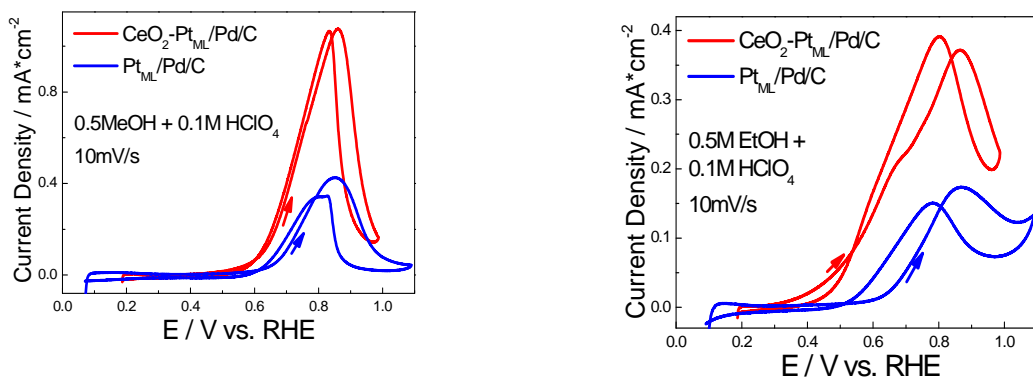


Fig. 4 Oxidation of methanol (left) and ethanol (right) on Pt monolayer modified by CeO₂.

Publications Acknowledging this Grant in 2013-2016

Exclusive funds this grant:

1. Bliznakov S.; Vukmirovic M.; Adzic R. Electrochemical Atomic-Level Controlled Syntheses of Electrocatalysts for the Oxygen Reduction Reaction, In *Atomically-Precise Methods for Synthesis of Solid Catalysts*, Hermans S., de Bocarme T. V., Eds., RSC Catalysis Series, The Royal Society of Chemistry, 2015; No. 22, p 144-166.
2. Scofield M. E.; Koenigsmann C.; Bobb-Semple D.; Tao J.; Tong X.; Wang L.; Lewis C, S.; Vukmirovic M. B.; Zhu Y.; Adzic R. R.; Wong S. S. Correlating the chemical composition and size of various metal oxide substrates with the catalytic activity and stability of as-deposited Pt nanoparticles for the methanol oxidation reaction, *Catal. Sci. Technol.* **2016**, *6*, 2435-2450.
3. Elbert, K.; Hu, J.; Ma, Z.; Zhang, Y.; Chen, G.; An, W.; Liu, P.; Isaacs, H. S.; Adzic, R. R.; Wang, J. X. Elucidating Hydrogen Oxidation/Evolution Kinetics in Alkaline and Acid Solutions via Optimizing Pt-Shell Thickness on Ru Core. *ACS Catal.* **2015**, *5*, 6764–6772.
4. Kuttiyiel, K. A.; Sasaki, K.; Su, D.; Wu, L. J.; Zhu, Y. M.; Adzic, R. R., Gold-promoted structurally ordered intermetallic PdCo nanoparticles for the oxygen reduction reaction. *Nature Communications* 2014, *5*.
5. Kuttiyiel, K. A.; Sasaki, K.; Chen, W. F.; Su, D.; Adzic, R. R., Core-shell, hollow-structured iridium-nickel nitride nanoparticles for the hydrogen evolution reaction. *J. Materials Chemistry A* 2014, *2* (3), 591-594.
6. Gong, K. P.; Park, J.; Su, D.; Adzic, R. R., Metalizing carbon nanotubes with Pd-Pt core-shell nanowires enhances electrocatalytic activity and stability in the oxygen reduction reaction. *Journal of Solid State Electrochemistry* 2014, *18* (5), 1171-1179.
7. Li, M.; Zhou, W. P.; Marinkovic, N. S.; Sasaki, K.; Adzic, R. R., The role of rhodium and tin oxide in the platinum-based electrocatalysts for ethanol oxidation to CO₂. *Electrochimica Acta* 2013, *104*, 454-461.
8. Li, M.; Cullen, D. A.; Sasaki, K.; Marinkovic, N. S.; More, K.; Adzic, R. R., Ternary Electrocatalysts for Oxidizing Ethanol to Carbon Dioxide: Making Ir Capable of Splitting C-C Bond. *J Am Chem Soc* 2013, *135* (1), 132-141.
9. Sasaki, K.; Marinkovic, N.; Isaacs, H. S.; Adzic, R. R. “Synchrotron-Based *In Situ* Characterization of Carbon-Supported Platinum and Platinum Monolayer Electrocatalysts”, *ACS Catal.* **2016**, *6*, 69
10. Chen, G.; Li, M.; Kuttiyiel, K. A.; Sasaki, K.; Kong, F.; Du, C.; Gao, Y.; Yin, G.; Adzic, R. R. “Evaluation of Oxygen Reduction Activity by the Thin-Film Rotating Disk Electrode Methodology: The Effects of Potentiodynamic Parameters”, *Electrocatalysis*, accepted.

Jointly funded leading contribution this grant

1. Kuttiyiel, K. A.; Choi, Y. M.; Sasaki, K.; Su, D.; Hwang, S.-M.; Yim, S.-D.; Yang, T.-H.; Park, G.-G.; Adzic, R. R. “Tuning Electrocatalytic Activity of Pt Monolayer Shell by Bimetallic Ir-M (M = Fe, Co, Ni or Cu) Cores for the Oxygen Reduction Reaction”, *Nano Energ.*, accepted.
2. Marinkovic, N.; Sasaki, K.; Adzic, R. R. “Evaluation of Particle Size of Nanoparticle Catalysts by EXAFS Analysis”, *Zastita Materijala* **2016**, *57*, 101.
3. Kuttiyiel, K. A.; Choi, Y.; Hwang, S.-M.; Park, G.-G.; Yang, T.-H.; Su, D.; Sasaki, K.; Liu, P.; Adzic, R. R., Enhancement of the oxygen reduction on nitride stabilized Pt-M (M=Fe, Co, and Ni) core-shell nanoparticle electrocatalysts. *Nano Energy* 2015, *13*, 442–449.

4. Zhang, Y.; Hsieh, Y. C.; Volkov, V.; Su, D.; An, W.; Si, R.; Zhu, Y. M.; Liu, P.; Wang, J. X.; Adzic, R. R., High Performance Pt Mono layer Catalysts Produced via Core-Catalyzed Coating in Ethanol. *Acs Catalysis* 2014, 4 (3), 738-742.
5. Zhang, Y.; Ma, C.; Zhu, Y. M.; Si, R.; Cai, Y.; Wang, J. X.; Adzic, R. R., Hollow core supported Pt monolayer catalysts for oxygen reduction. *Catal. Today* 2013, 202, 50-54.
6. Yang, L. J.; Vukmirovic, M. B.; Su, D.; Sasaki, K.; Herron, J. A.; Mavrikakis, M.; Liao, S. J.; Adzic, R. R., Tuning the Catalytic Activity of Ru@Pt Core-Shell Nanoparticles for the Oxygen Reduction Reaction by Varying the Shell Thickness. *J. Phys. Chem. C* 2013, 117 (4), 1748-1753.
7. Vukmirovic, M. B.; Zhang, Y.; Wang, J. X.; Buceta, D.; Wu, L. J.; Adzic, R. R., Pt monolayer shell on hollow Pd core electrocatalysts: scale up synthesis, structure, and activity for the oxygen reduction reaction. *Journal of the Serbian Chemical Society* 2013, 78 (12), 1983-1992.
8. Kuttiyiel, K. A.; Sasaki, K.; Su, D.; Vukmirovic, M. B.; Marinkovic, N. S.; Adzic, R. R., Pt monolayer on Au-stabilized PdNi core-shell nanoparticles for oxygen reduction reaction. *Electrochimica Acta* 2013, 110, 267-272.
9. Hsieh, Y. C.; Zhang, Y.; Su, D.; Volkov, V.; Si, R.; Wu, L. J.; Zhu, Y. M.; An, W.; Liu, P.; He, P.; Ye, S. Y.; Adzic, R. R.; Wang, J. X., Ordered bilayer ruthenium-platinum core-shell nanoparticles as carbon monoxide-tolerant fuel cell catalysts. *Nature Communications* 2013, 4.

Jointly funded leading contribution other grants

1. Buceta David.; Tojo C.; Vukmirovic M. B.; Deepak F. L.; López-Quintela M. A. Controlling Bimetallic Nanostructures by the Microemulsion Method with Subnanometer Resolution Using a Prediction Model, *Langmuir* **2015**, 31, 7435-7439.
2. Scofield M. E.; Zhou Y.; Yue S.; Wang L.; Su D.; Tong X.; Vukmirovic M. B.; Adzic R. R.; Wong S. S. Role of Chemical Composition in the Enhanced Catalytic Activity of Pt-Based Alloyed Ultrathin Nanowires for the Hydrogen Oxidation Reaction under Alkaline Conditions, *ACS Catal.* **2016**, 6, 3895-3908.
3. Wang, J. X.; He, P.; Zhang, Y.; Ye, S., Can CO-tolerant Anodes be Economically Viable for PEMFC Applications with Reformates?, *ECS Trans*, 64 (2014) 121-127.
4. Wang, J. X.; Zhang, Y.; Capuano, C. B.; Ayers, K. E. Ultralow Charge-Transfer Resistance with Ultralow Pt Loading for Hydrogen Evolution and Oxidation Using Ru@Pt Core-Shell Nanocatalysts. *Sci. Rep.* **2015**, 5, 12220.
5. Ayers, K. E.; Renner, J. N.; Danilovic, N.; Wang, J. X.; Zhang, Y.; Maric, R.; Yu, H. Pathways to Ultra-Low Platinum Group Metal Catalyst Loading in Proton Exchange Membrane Electrolyzers. *Catal. Today* **2016**, 262 (262), 121-132.
6. Hwang, S.-M.; Choi, Y. M.; Kim, M. G.; Young, J.; Cheon, J. Y.; Joo, S. H.; Yim, S.-D.; Kuttiyiel, K. A.; Sasaki, K.; Adzic, R. R.; Park, G.-G. "Enhancement of Oxygen Reduction Activities by Pt Nanoclusters Decorated on Ordered Mesoporous Porphyrinic Carbons", *J. Mater. Chem. A* **2016**, 4, 5869
7. Scofield, M. E.; Koenigsmann, C.; Bobb-Semple, D.; Tao, J.; Tong, X.; Wang, L.; Lewis, C. S.; Vukmirovic, M. B.; Zhu, Y.; Adzic, R. R.; Wong, S. S. "Correlating the Chemical Composition and Size of Various Metal Oxide Substrates with the Catalytic Activity and Stability of As-Deposited Pt Nanoparticles for the Methanol Oxidation Reaction", *Catal. Sci. Technol.* **2016**, 6, 2435.
8. Tian, X.; Luo, J.; Nan, H.; Zou, H.; Chen, R.; Shu, T.; Li, X.; Li, Y.; Song, H.; Liao, S.; Adzic, R. R. "Transition Metal Nitride Coated with Atomic Layers of Pt as a Low-Cost, Highly Stable Electrocatalyst for the Oxygen Reduction Reaction", *J. Am. Chem. Soc.* **2016**, 138, 1575.
9. Tsai, H. C.; Hsieh, Y. C.; Yu, T. H.; Lee, Y. J.; Wu, Y. H.; Merinov, B. V.; Wu, P. W.; Chen, S. Y.; Adzic, R. R.; Goddard, W. A., DFT Study of Oxygen Reduction Reaction on Os/Pt Core-Shell Catalysts Validated by Electrochemical Experiment. *ACS Catalysis* 2015, 5 (3), 1568-1580.
10. Cao, B. F.; Neufeind, J. C.; Adzic, R. R.; Khalifah, P. G., Molybdenum Nitrides as Oxygen Reduction Reaction Catalysts: Structural and Electrochemical Studies. *Inorganic Chemistry* 2015, 54 (5), 2128-2136.

11. Roller, J.; Yu, H.; Vukmirovic, M. S.; Bliznakov, S.; Kotula, P. G.; Carter, C. B.; Adzic, R. R.; Maric, R., Flame-Based Synthesis of Core-Shell Structures Using Pd-Ru and Pd Cores. *Electrochim. Acta* 2014, 138, 341-352.
12. Liu, H. Q.; Koenigsmann, C.; Adzic, R. R.; Wong, S. S., Probing Ultrathin One-Dimensional Pd-Ni Nanostructures As Oxygen Reduction Reaction Catalysts. *ACS Catalysis* 2014, 4 (8), 2544-2555.
13. Kang, Y. J.; Ye, X. C.; Chen, J.; Cai, Y.; Diaz, R. E.; Adzic, R. R.; Stach, E. A.; Murray, C. B., Design of Pt-Pd Binary Superlattices Exploiting Shape Effects and Synergistic Effects for Oxygen Reduction Reactions. *J Am Chem Soc* 2013, 135 (1), 42-45.
14. Kang, Y.; Li, M.; Cai, Y.; Cargnello, M.; Diaz, R. E.; Gordon, T. R.; Wieder, N. L.; Adzic, R. R.; Gorte, R. J.; Stach, E. A.; Murray, C. B., Heterogeneous Catalysts Need Not Be so "Heterogeneous": Monodisperse Pt Nanocrystals by Combining Shape-Controlled Synthesis and Purification by Colloidal Recrystallization. *J Am Chem Soc* 2013, 135 (7), 2741-2747.
15. Choi, Y. M.; Kuttiyiel, K. A.; Labis, J. P.; Sasaki, K.; Park, G. G.; Yang, T. H.; Adzic, R. R., Enhanced Oxygen Reduction Activity of IrCu Core Platinum Monolayer Shell Nanoelectrocatalysts. *Topics in Catalysis* 2013, 56 (12), 1059-1064.
16. Cheon, J. Y.; Kim, T.; Choi, Y.; Jeong, H. Y.; Kim, M. G.; Sa, Y. J.; Kim, J.; Lee, Z.; Yang, T. H.; Kwon, K.; Terasaki, O.; Park, G. G.; Adzic, R. R.; Joo, S. H., Ordered mesoporous porphyrinic carbons with very high electrocatalytic activity for the oxygen reduction reaction. *Scientific Reports* 2013, 3.
17. Chen, W. F.; Wang, C. H.; Sasaki, K.; Marinkovic, N.; Xu, W.; Muckerman, J. T.; Zhu, Y.; Adzic, R. R., Highly active and durable nanostructured molybdenum carbide electrocatalysts for hydrogen production. *Energy & Environmental Science* 2013, 6 (3), 943-951.
18. Cao, B. F.; Veith, G. M.; Neuefeind, J. C.; Adzic, R. R.; Khalifah, P. G., Mixed Close-Packed Cobalt Molybdenum Nitrides as Non-noble Metal Electrocatalysts for the Hydrogen Evolution Reaction. *J Am Chem Soc* 2013, 135 (51), 19186-19192.
19. Cao, B. F.; Veith, G. M.; Diaz, R. E.; Liu, J.; Stach, E. A.; Adzic, R. R.; Khalifah, P. G., Cobalt Molybdenum Oxynitrides: Synthesis, Structural Characterization, and Catalytic Activity for the Oxygen Reduction Reaction. *Angewandte Chemie-International Edition* 2013, 52 (41), 10753-10757.

Highly active metal-oxide catalysts for water splitting

Aleksandra Vojvodic

In this talk I will present our recent findings on water splitting with the focus on the oxygen evolution reaction.¹⁻⁸ We have computationally identified new highly active transition-metal oxide OER catalysts that have been experimentally synthesized, characterized and tested.¹⁻³ I will discuss the dependence of OER activity on the geometry of the catalyst material³⁻⁵ and different OER reaction mechanisms.⁷⁻⁸

1. B. Zhang, X. Zheng, O. Voznyy, R. Comin, M. Bajdich, M. García-Melchor, J. Xu, M. Liu, F. P. García de Arquer, C. T. Dinh, F. Fan, M. Yuan, E. Yassitepe, A. Janmohamed, N. Chen, T. Regier, L. Han, H. L. Xin, L. Zheng, H. Yang, A. Vojvodic, and Edward H. Sargent, "Homogeneously-Dispersed Multi-Metal Oxygen-Evolving Catalysts", *Science* **352**, 333-337 (2016).
2. J. W. D. Ng, M. García-Melchor, M. Bajdich, C. Kirk, P. Chakthranont, A. Vojvodic, and T. F. Jaramillo, "Gold-Supported Cerium-Doped NiO_x Catalysts for Water Oxidation", *Nature Energy* **1**, 16053 (2016).
3. L. C. Seitz, C. Dickens, K. Nishio, Y. Hikita, J. Montoya, A. Doyle, C. Kirk, A. Vojvodic, H. Y. Hwang, J. K. Nørskov, and T. F. Jaramillo, "A Highly Active and Stable SrIrO₃/IrO_x Catalyst for the Oxygen Evolution Reaction", Submitted (2016).
4. A. S. Walton, J. Fester, et al, A. Vojvodic, and J. V. Lauritsen, "Interface Controlled Oxidation States in Layered Cobalt Oxide Nano-Islands on Gold", *ACS Nano* **9**, 2445-2453 (2015).
5. J. Fester, M. García-Melchor, A. S. Walton, M. Bajdich, Z. Li, L. Lammich, A. Vojvodic, and J. V. Lauritsen, "Edge Reactivity and Water-Assisted Dissociation on Cobalt Oxide Nanoislands", *Submitted* (2016).
6. A. Vojvodic and J. K. Nørskov, "New Design Paradigm for Heterogeneous Catalysts", *National Science Review* **2**, 140-143 (2015).
7. A. D. Doyle, J. H. Montoya, and A. Vojvodic, "Improving Oxygen Electrochemistry Through Nanoscopic Confinement", *ChemCatChem* **7**, 738-742 (2015).
8. M. García-Melchor, L. Vilella, N. López, and A. Vojvodic, "Computationally Probing the Performance of Hybrid, Heterogeneous and Homogeneous Ir-based Catalysts for Water Oxidation", *ChemCatChem*, **8**, 1792-1798 (2016).

Liviu M. Mirica

Mechanistic Studies of Bioinspired Oxidative Organometallic Reactions

Liviu M. Mirica, Nicholas Ruhs, Andrew J. Wessel, and Wen Zhou
Department of Chemistry, Washington University in St. Louis

Presentation Abstract

The long term goal of this project is to develop novel transition metal catalysts that exhibit reactivity profiles resembling both organometallic and bioinorganic systems. Given the importance of Pd systems in chemical catalysis transformations we have been investigating the electronic properties and organometallic reactivity of uncommon Pd^{III} and Pd^I complexes to better understand various redox reactions involving palladium. Our approach employs flexible multidentate ligands that can accommodate different metal coordination geometries corresponding to various oxidation states, and thus promote facile redox reactions. Of particular interest are bioinspired aerobic oxidative reactions that lead to formation of new C-C and C-heteroatom bonds. Detailed mechanistic studies of these oxidative reactions will be discussed, as well as recent novel organometallic reactions employing Pd^{III} and/or Pd^I species. Overall, the development of novel transition metal-catalyzed aerobic oxidative reactions should have a significant impact in organometallic catalysis applied energy-related transformations.

DE-FG02-11ER16254: Novel Redox Catalysts for Greenhouse Gases Utilization

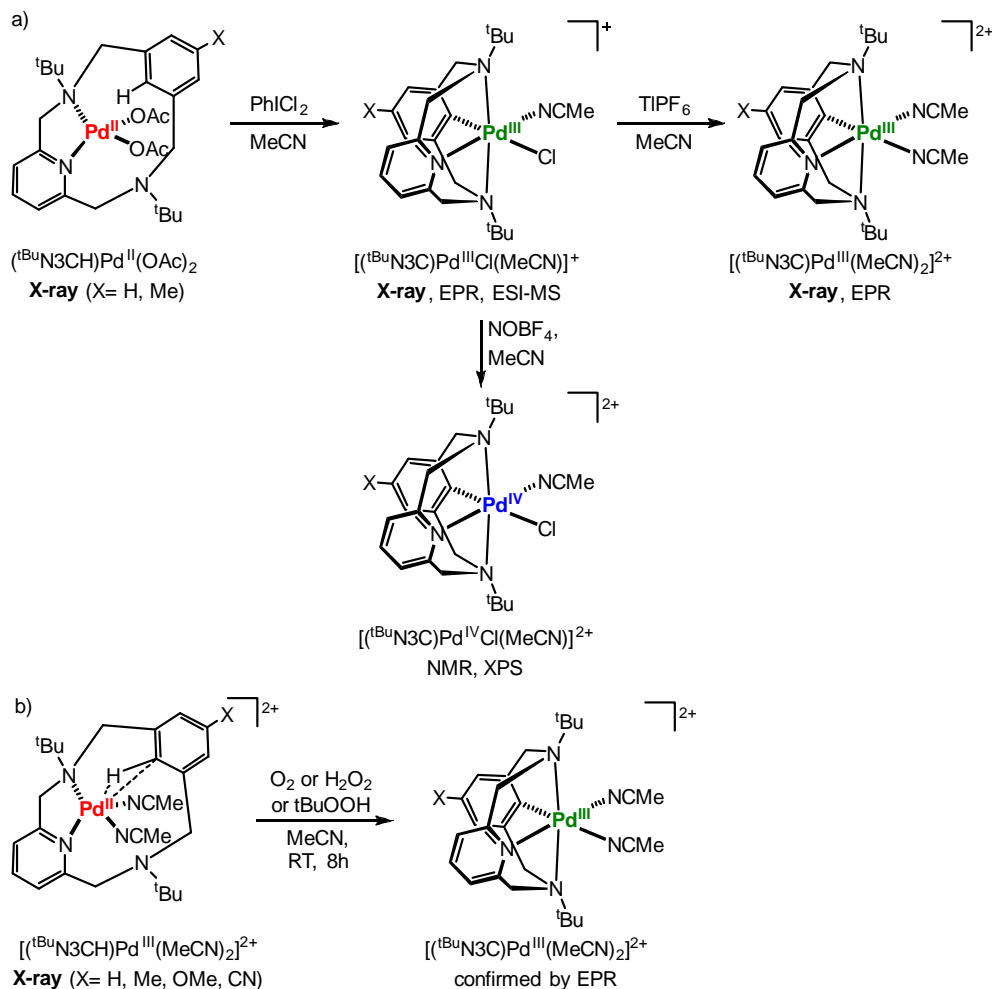
Postdoc(s): Wen Zhou

Student(s): Nicholas Ruhs, Andrew J. Wessel, Kei Fuchigami, Jia Luo, Fengrui Qu, Fengzhi Tang

RECENT PROGRESS

During this reporting period, we have employed a pyridinophane-type C-donor ligand in which one of the one pyridine ring was replaced with a phenyl ring (e.g., ^tBuN3CH, Scheme 1a) that was proposed to be more electron rich and thus further stabilize high-valent Pd species. Importantly, the ^RN3CH ligand allows us to perform C-H activation studies at high-valent Pd centers. Recent results show that (^RN3CH)Pd^{II} complexes exhibit oxidation reactivity that is dependent on the counteranion employed. For example, the (^tBuN3CH)Pd^{II}(OAc)₂ complex – in which the *ipso*-C-H bond of ^tBuN3CH has not been cleaved, can be oxidized with oxidants such as PhICl₂ to generate a Pd^{III} complex [(^tBuN3C)Pd^{III}Cl(MeCN)]⁺ that contains a Pd-C bond (Scheme 1a). This result suggests that the C-H activation has likely occurred at a Pd^{III} (or Pd^{IV}) center.

Interestingly, only one anionic exogenous ligand, a chloride ion, is bound to the Pd^{III} center, the other coordination site being occupied by a solvent MeCN molecule, most likely due to the strong *trans* influence of the phenyl ligand. Moreover, the chloride anion can be removed by TlPF₆ to generate an uncommon dicationic Pd^{III}-disolvento complex with two available coordination sites that was structurally characterized (Scheme 1a). Finally, the [(^tBuN3C)Pd^{III}Cl(MeCN)]⁺ complex can be further oxidized to the Pd^{IV} analog that can be characterized by NMR and XPS to support the Pd^{IV} oxidation state assignment (Scheme 1a). All these complexes are essential precursors that will be employed in our future organometallic reactivity studies.

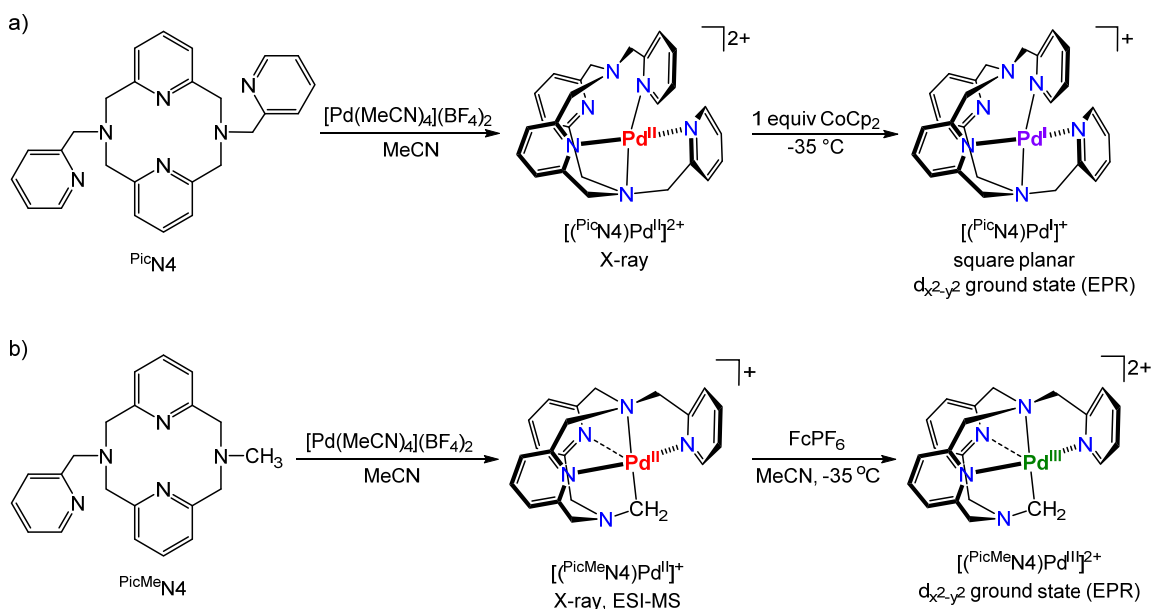


Scheme 1. a) Generation of organometallic Pd^{III}- and Pd^{IV}-solvento complexes of the ^tBuN3CH ligand, and b) unprecedented aerobically-induced oxidation and C-H bond activation at a dicationic Pd^{III} complex.

Interestingly, use [Pd(MeCN)₄](BF₄)₂ salt generated the [(^tBuN3CH)Pd^{II}(MeCN)₂]²⁺ complex that exhibits an agostic interaction between the Pd center and the *ipso* C-H bond (Scheme 1b). Moreover, this complex is surprisingly oxidized under ambient conditions by mild oxidants such as O₂, H₂O₂ and tBuOOH to generate a Pd^{III} species, as observed by EPR and UV-vis and assigned to the [(^tBuN3C)Pd^{III}(MeCN)₂]²⁺ complex (Scheme 1b).

These are very exciting results, showing an unprecedented aerobic oxidation of a dicationic Pd^{II} complex, which is also undergoing a C-H bond activation process during the oxidation. This system can thus be employed toward the development of aerobically-induced C-H functionalization reactions.

Another goal of our research project is the synthesis and detailed characterization of low-valent Pd complexes that could lead to the development of novel catalysts for reductive transformations. In this context, in the previous reporting period we have begun employing multidentate ligands that limit the number of open coordination sites and thus preclude dimerization of Pd^I species. For example, the hexadentate ligand ^{Pic}N4 (an N4 derivative with two picolyl N-substituents) can support a Pd^I species whose EPR spectrum is suggestive of a d_{x²-y²} ground state (Scheme 2a), however this species showed limited reactivity toward exogenous substrates. To increase the reactivity of the corresponding Pd complexes, during this reporting period we have synthesized a pentadentate pyridinophane ligand with one picolyl arm, ^{PicMe}N4 (Scheme 2b). Interestingly, when ^{PicMe}N4 was reacted with [Pd(MeCN)₄](BF₄)₂, the ligand undergoes C-H bond activation of the N-methyl group under ambient conditions, as observed by X-ray crystallography and NMR (Scheme 2b). This result strongly supports that the (^{PicMe}N4)Pd complexes should exhibit enhanced reactivity, including uncommon aliphatic C-H bond activation. Overall, these ligand systems are very promising, since having a system that can stabilize both Pd^{III} and Pd^I species is essential for our proposed reactivity studies aimed toward catalyst development for reduction processes.



Scheme 2. A) Use of a hexadentate ^{Pic}N4 ligand to generate a Pd^I species, and b) Aliphatic C-H bond activation at a Pd^{II} center supported by a pentadentate ^{PicMe}N4 ligand, and generation of a Pd^{III} species.

Future plans

For our proposed oxidative C-H activation and functionalization studies, the generated organometallic Pd^{III}-solvento complexes that were obtained through oxidatively-induced C-H bond activation are essential species that will allow us to investigate their reactivity toward the formation of new C-C or C-heteroatom bonds, in the context of development of novel catalysts for C-H functionalization reactions. During the next reporting period we plan to react these complexes with various exogenous organic substrates and investigate their transmetalation, C-H activation, and reductive elimination reactions. We will also compare the organometallic reactivity of analogous Pd^{III} and Pd^{IV} complexes, and establish the requirements for efficient C-C and C-heteroatom bond formation reactions. In addition, we are currently performing detailed mechanistic studies of the observed aerobically-induced C-H activation the dicationic [(^tBuN₃CH)Pd^{II}(MeCN)₂]²⁺ species in order to determine whether the C-H activation step occurs before, after, or in concert with the oxidation of the metal center to yield the Pd^{III} product.

For our proposed development of reductive catalytic systems involving both low-valent and high-valent Pd intermediate, we will employ our recently developed multidentate ^{Pic}N₄ and ^{PicMe}N₄ ligands to stabilize various Pd^I and Pd^{III} species. Then we will investigate the reactivity of any detectable Pd^I intermediates toward exogenous substrates such as small molecules (CO₂, H₂O) as well as organic electrophiles that could be employed in reductive transformations.

Publications Acknowledging this Grant in 2013-2016

(IV) Publications exclusively funded by this grant

1. Fuchigami, K.; Rath, N. P.; Mirica, L. M. "Mononuclear Rhodium(II) and Iridium(II) Complexes Supported by Tetradentate Pyridinophane Ligands", *submitted*.
2. Tang, F.; Park, S.; Rath, N. P.; Mirica, L. M. "Electronic Versus Steric Effects of Pyridinophane Ligands that Stabilize Pd(III) Complexes", *submitted*.
3. Luo, J.; Rath, N. P.; Mirica, L. M. "Spectroscopic and Stability studies of Transient (N₂S₂)Pd^I Complexes", *submitted*.
4. Khusnutdinova, J. R.; Rath, N. P.; Mirica, L. M. "The Conformational Flexibility of the Tetradentate Ligand ^tBuN₄ is Essential for the Stabilization of (^tBuN₄)Pd^{III} Complexes", *Inorg. Chem.*, **2014**, 53, 13112-13129, DOI: 10.1021/ic5023054.
5. Qu, F.; Khusnutdinova, J. R.; Rath, N. P.; Mirica, L. M. "Dioxygen Activation by an Organometallic Pd(II) Precursor: Formation of a Pd(IV)-OH Complex and Its C-O Bond Formation Reactivity", *Chem. Comm.*, **2014**, 50, 3036-3039; DOI: 10.1039/c3cc49387c.

6. Khusnutdinova, J. R.; Mirica, L. M.* “Organometallic Pd(III) Complexes in C-C and C-Heteroatom Bond Formation Reactions”, book chapter in *C-H Activation and Functionalization, Transition Metal Mediation*, Royal Society of Chemistry, **2013**.
7. Luo, J.; Rath, N. P.; Mirica, L. M. “Oxidative Reactivity of (N₂S₂)PdRX Complexes (R = Me, Cl; X = Me, Cl, Br): Involvement of Palladium(III) and Palladium(IV) Intermediate”, *Organometallics*, **2013**, 32, 3343-3353; DOI: 10.1021/om400286j.
8. Khusnutdinova, J. R.; Luo, J.; Rath, N. P.; Mirica, L. M. “Late First Row Transition Metal Complexes of a Tetradentate Pyridinophane Ligand: Electronic Properties and Reactivity Implications”, *Inorg. Chem.*, **2013**, 52, 3920-3932, DOI: 10.1021/ic400260z.
- (V) *Jointly funded by this grant and other grants with leading intellectual contribution from this grant*
9. Mirica, L. M.; Khusnutdinova, J. R., “Structure and Electronic Properties of Pd(III) Complexes”, *Coord. Chem. Rev.*, **2013**, 257, 299-314. DOI: 10.1016/j.ccr.2012.04.030.
- (VI) *Jointly funded by this grant and other grants with relatively minor intellectual contribution from this grant*
10. Pedrick, E. A.; Schultz, J. W.; Wu, G.; Mirica, L. M.; Hayton, T. W. “Perturbation of the O–U–O Angle in Uranyl by Coordination to a 12-Membered Macrocycle”, *Inorg. Chem.*, **2016**, 55; DOI: 10.1021/acs.inorgchem.6b00799.

Friday Oral Presentations

The Interconversion of Ammonia with Its Elements

Iraklis Pappas, Máté J. Bezdek, Paul J. Chirik*
Department of Chemistry, Princeton University, Princeton, New Jersey, 08544

Presentation Abstract

The synthesis of ammonia from its elements, N_2 and H_2 , and the reverse reaction, the oxidation of NH_3 to dinitrogen and dihydrogen are chemical transformations that are key for carbon neutrality. Our research group is exploring proton coupled electron transfer (PCET) methods as a pathway for N-H bond formation and scission. Measurement of N-H bond dissociation free energies (BDFEs) of coordinated nitrogen ligands (amides, imides, hydrazides, and ammonia) are at the core our approach and guides rational design of transition metal complexes and optimization of ligands to attenuate redox potentials and N-H acidity. Determination of the N-H BDFEs of bis(cyclopentadienyl) titanium and zirconium amides and applying PCET from Cr and Rh hydrides to the metal amides has provided a new route to breaking strong M-NH₂ bonds and liberating ammonia. The thermodynamic viability of PCET can be predicted and attenuated through an understanding of both the hydrogen atom donor and the nitrogen acceptor using thermochemical square schemes. Notably, the Cr and Rh hydrides are regenerated under an atmosphere of hydrogen enabling the catalytic hydrogenolysis of metal amides, imides, and hydrazides using PCET. Metal-ligand cooperativity effects in molybdenum complexes supported by redox-active terpyridine ligands, which are less prone to chemical modification, are also under investigation. Ligand-mediated N-N bond cleavage of dinitrogen to form a Mo nitride has been observed. Key steps in the oxidation of ammonia such as preparation of molybdenum amides from NH_3 with loss of H_2 have been demonstrated. Ligand design principles and mechanisms of these transformations will be the focus of my lecture.

DE-SC0006498: New Approaches to Nitrogen Fixation

Student(s): Iraklis Pappas, Máté Bezdek, Grant Margulieux

Publications Acknowledging this Grant in 2013-2016

(I) *Exclusively funded by this grant:*

Bezdek, M. J.; Guo, S.; Chirik, P. J. "Terpyridine molybdenum dinitrogen chemistry: Synthesis of dinitrogen complexes that vary by five oxidation states." *Inorg. Chem.* **2016**, *55*, 3117-3127.

Pappas, I.; Chirik, P. J. "Ammonia synthesis by hydrogenolysis of titanium-nitrogen bonds using proton coupled electron transfer." *J. Am. Chem. Soc.* **2015**, *137*, 3498-3501. (Selected for *JACS Spotlight*).

Pappas, I.; Chirik, P. J. "Alkyne cycloaddition to a titanocene oxide as a route to cyclopentadienyl modification." *Angew. Chem. Int. Ed.* **2014**, *53*, 6241-6244.

Semproni, S. P.; Chirik, P. J. "N-H and N-C bond formation with an N₂-derived dihafnium μ -nitrido complex." *Organometallics* **2014**, *33*, 3727-3737.

Pappas, I.; Chirik, P. J. "Synthesis and carbonylation of oxotitanacyclobutanes derived from allene cycloaddition to a monomeric titanocene oxide." *Polyhedron* **2014**, *84*, 67-73.

Semproni, S. P.; Chirik, P. J. "Synthesis of a Base-Free Hafnium Nitride from N₂ Cleavage: A Versatile Platform for Dinitrogen Functionalization." *J. Am. Chem. Soc.* **2013**, *135*, 11373-11383.

Semproni, S. P.; Chirik, P. J. "Activation of N₂-Derived Hafnium Nitrides for Nucleophilic N-C Bond Formation with a Terminal Isocyanate." *Angew. Chem. Int. Ed. Engl.* **2013**, *52*, 12965-12969.

Semproni, S. P.; Chirik, "Dinitrogen Borylation with group 4 Metallocene Complexes." *Eur. J. Inorg. Chem.* **2013**, 3907-3915.

(II) Jointly funded by this grant and other grants with leading intellectual contribution from this grant:

Milsmann, C.; Semproni, S. P.; Chirik, P. J. "N-N bond cleavage of 1,2-diarylhydrazines and N-H bond formation via H-atom transfer in vanadium complexes supported by a redox-active ligand." *J. Am. Chem. Soc.* **2014**, *136*, 12099-12107.

Margulieux, G. W.; Semproni, S. P.; Chirik, P. J. "Photochemically-induced reductive elimination as a route to a zirconocene complex with a strongly activated N₂ ligand." *Angew. Chem. Int. Ed.* **2014**, *53*, 9189-9192.

Semproni, S. P.; Knobloch, D. J.; Milsmann, C.; Chirik, P. J. "Redox-Induced Hapticity Switching in Zirconocene Dinitrogen Complexes." *Angew. Chem. Int. Ed.* **2013**, *52*, 5372-5376.

Wilfred T. Tysoe

Molecular-Level Design of Heterogeneous Chiral Catalysts

Wilfred T. Tysoe, Andrew Gellman, Charles Sykes and Francisco Zaera
Department of Chemistry and Biochemistry, University of Wisconsin-Milwaukee
Department of Chemical Engineering, Carnegie Mellon University
Department of Chemistry, Tufts University
Department of Chemistry, University of California-Riverside

Presentation Abstract

The fact that two enantiomers of a chiral compound can have completely different physiological effects means that chiral pharmaceuticals must be synthesized in their enantiomerically pure forms creating the enormous market for chiral compounds. Currently, pharmaceuticals are synthesized by *homogeneous*-phase catalysts, many of which are achiral and produce racemic products requiring separation of the catalyst and enantioseparation of the product, issues that are addressed by the use of *heterogeneous*-phase chiral catalysts. Unfortunately, the empirical development of such heterogeneous catalysts has met with limited success, in part because of the existence of unmodified sites on the extended surface that lead to the formation of racemic products. The goal of the Chiral Catalysis Group is to obtain a fundamental mechanistic understanding of the interactions that control enantioselectivity and to develop the concepts necessary to design novel, heterogeneous catalytic materials. The Group is organized conceptually around three types of enantiospecific interactions with chiral catalytic surfaces: interactions with *naturally chiral* surfaces (those that are intrinsically chiral); interactions with modified surfaces categorized as *chirally templated* surfaces (with modifiers that act cooperatively to create a chiral reaction or adsorption site); and *one-to-one* interactions of prochiral molecules with chiral surface modifiers. Recent results are discussed within the context of the three categories.

Grant Number: DE-SC008703:

Molecular-Level Design of Heterogeneous Chiral Catalysts

Postdoc(s): Michael Garvey, Sunil Devarajan, Ilkeun Lee, Alexander Gordon, Stavros Karakalos, Yongju Yu, Mausumi Mahapatra

Student(s): Junghyun Hong, Charles Janini, John Kestell, Nathan Khosla, Chen Lin, Mausumi Mahapatra, Bharat Mhatre, Nathaniel Ondeck, Alex Petti, Aaron Reinkicker, Xin Xing, Yongju Yu, Jerry Praeger, Yufei Ni, Gardenia Rodriguez, Matt Payne, Felicia Lucci, Matthew Michels.

RECENT PROGRESS

Naturally Chiral Surfaces

Work has focused on understanding enantioselectivity on naturally chiral metal surfaces, specifically on the explosive decomposition of tartaric (TA) and aspartic acid (Asp) on Cu surfaces that leads to super-enantiospecific decomposition kinetics. A key feature of this work is that mixtures of D-Asp and ^{13}C -L-Asp can be used for mass spectrometric enantiodifferentiation of the species adsorbing, desorbing and reacting on the surface. These experiments have provided new insights into the enantiospecific surface chemistry of chiral compounds.

Gas phase mixtures of D- and *L-amino acids on the naturally chiral $\text{Cu}\{3,1,17\}^{\text{R\&S}}$ surfaces have been studied by both experiment and density functional theory (DFT)-based modeling. Measurements of equilibrium adsorption of racemic D*L-Asp on the $\text{Cu}\{3,1,17\}^{\text{R\&S}}$ surfaces demonstrated enantiospecific separation on a naturally chiral metal surface (Fig. 1A) and quantitative determination of enantiospecific adsorption equilibrium constants $K_{D/R}/K_{*L/R} = K_{*L/S}/K_{D/S} = 2.2 \pm 0.2$. Similar measurements have been made on the $\text{Cu}\{3,1,17\}^{\text{R\&S}}$ surfaces using mixtures of D/*L-alanine (Ala), D/*L-serine, and D/*L-phenylalanine, and using D/*L-Asp mixtures on both $\text{Cu}\{653\}^{\text{R\&S}}$ and $\text{Cu}\{111\}$.

An important feature of the isotope labeling methodology is that it allows determination of enantiomeric excesses in both the adsorbed phase, ee_s , and the gas phase, ee_g , and thus quantitative determination of $ee_s(ee_g)$ (Fig. 1B). Ala adsorption on $\text{Cu}\{3,1,17\}^{\text{R\&S}}$ is non-enantiospecific with $ee_s = ee_g$. As mentioned, $\text{Asp/Cu}\{3,1,17\}^{\text{R\&S}}$ is enantio-specific with $ee_s(0) \neq 0$. Surprisingly, $\text{Asp/Cu}\{111\}$ exhibits auto-amplification, $|ee_s| > |ee_g|$, in spite of the fact that $\text{Cu}\{111\}$ is achiral. This arises from homochiral enantiomer disproportionation, the formation of homochiral adsorbate clusters. Finally, $\text{Asp/Cu}\{653\}^{\text{S}}$ is dominated by homochiral enantiomer disproportionation, in spite of the fact that the surface is chiral.

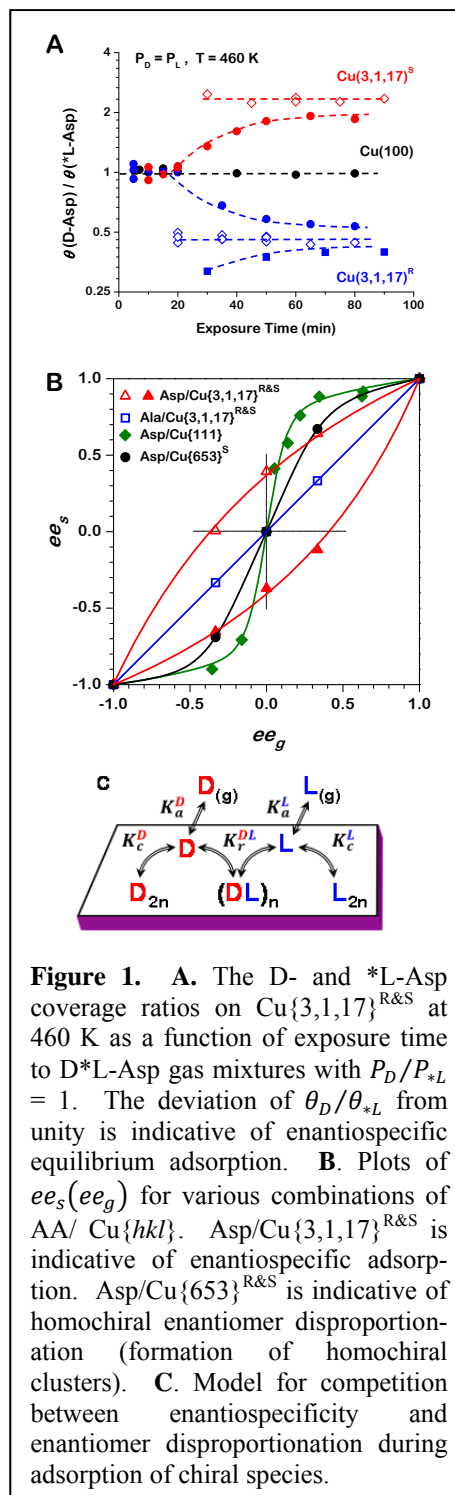


Figure 1. **A.** The D- and *L-Asp coverage ratios on $\text{Cu}\{3,1,17\}^{\text{R\&S}}$ at 460 K as a function of exposure time to D*L-Asp gas mixtures with $P_D/P_{*L} = 1$. The deviation of θ_D/θ_{*L} from unity is indicative of enantiospecific equilibrium adsorption. **B.** Plots of $ee_s(ee_g)$ for various combinations of AA/Cu{hkl}. $\text{Asp/Cu}\{3,1,17\}^{\text{R\&S}}$ is indicative of enantiospecific adsorption. $\text{Asp/Cu}\{653\}^{\text{R\&S}}$ is indicative of homochiral enantiomer disproportionation (formation of homochiral clusters). **C.** Model for competition between enantiospecificity and enantiomer disproportionation during adsorption of chiral species.

A general model for the adsorption of chiral mixtures is illustrated in Figure 1C and describes adsorption (which is enantiospecific on chiral surfaces) coupled with enantiomer disproportionation (homochiral or heterochiral clustering). The mathematical formulation of a Langmuir-like adsorption isotherm based on this model yields the fits to the various types of behavior observed in Fig. 1B. It generally predicts the complex behaviors observed for all of the systems studied in Fig. 1B.

We have demonstrated that the decomposition of D- and *L-Asp can be performed catalytically and in steady state during continuous exposure of the Cu(111) surface to gas phase Asp. The decomposition mechanism for aspartic acid on Cu(111) is:

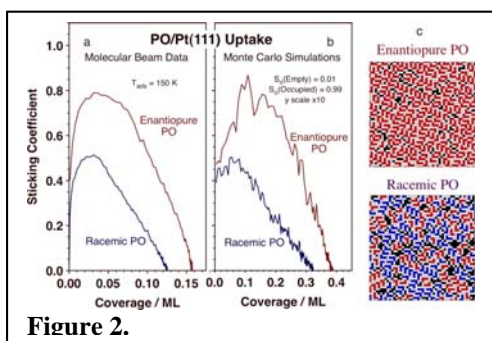
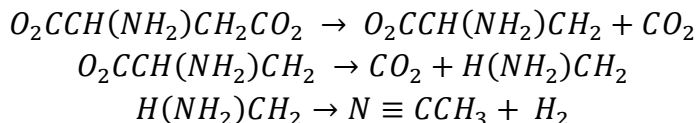


Figure 2.

The reaction has been performed to ~50 turnovers at 600 K without signs of deactivating the Cu(111) surface. These results open the door to study of enantioselective catalysis on naturally chiral Cu(*hkl*) single crystal surfaces.

We are now collecting data on TA decomposition on Structure Spread Single Crystal Surfaces (S⁴Cs). These are spherical sections of Cu single crystals that expose a continuous distribution of crystal planes spanning the stereographic projection. From

these measurements we will obtain reaction rate constants, $k_d(hkl)$, for TA decomposition on surfaces with all possible Miller indices.

Templated Chiral Surfaces

Work on chiral templates has focused on our ability to correlate surface structures with the enantioselective adsorption of a chiral probe on modified surfaces, using propylene oxide and glycidol as the probe molecules. Work has focused on two areas. In the first area, fundamentals of auto-enantioselective effects is being explored using propylene oxide as a modifier for itself. The idea underlying this approach is that different packing structures may be available for chiral and racemic mixtures of propylene oxide that modify their maximum attainable saturation coverages. These are phenomena are similar in nature to the auto-amplification demonstrated above using isotopic labeling of Asp on Cu(111). In the second area, the formation of local chiral templates from amino acids on Pd(111) has been studied and their enantioselectivity measured using chiral probes

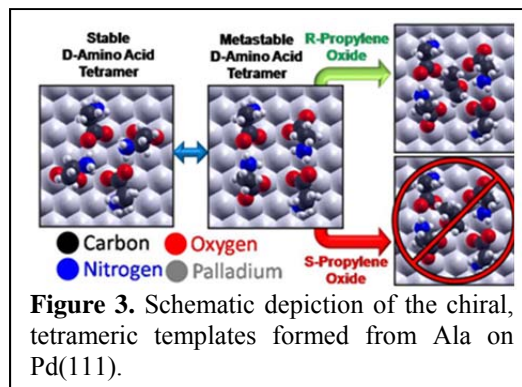


Figure 3. Schematic depiction of the chiral, tetrameric templates formed from Ala on Pd(111).

A unique behavior was found in the uptake of propylene oxide (PO) on Pt(111), that was ascribed to a kinetic effect. Temperature-programmed desorption (TPD) data showed that the density of the saturated monolayers

of propylene oxide (PO) adsorbed on a Pt(111) single-crystal surface changes monotonically with enantiomeric composition, decreasing by approximately 20% when going from enantiopure to racemic layers. Curiously, no such effect was found on Pd(111). Data from isothermal molecular-beam measurements indicated that the sticking

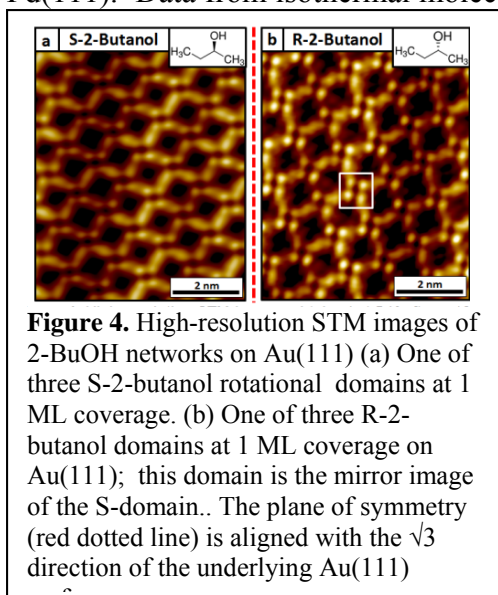


Figure 4. High-resolution STM images of 2-BuOH networks on Au(111) (a) One of three S-2-butanol rotational domains at 1 ML coverage. (b) One of three R-2-butanol domains at 1 ML coverage on Au(111); this domain is the mirror image of the S-domain. The plane of symmetry (red dotted line) is aligned with the $\sqrt{3}$ direction of the underlying Au(111)

probabilities of PO increase with coverage in the early stages of the uptake, reflecting an adsorption process aided by the presence of other adsorbates on the surface. Kinetic Monte Carlo simulations qualitatively reproduce the experimental measurements and highlight the kinetic driving force for the differences observed (Fig. 2). Strikingly, this effect reverses itself at saturation, and in equilibrium the preference is toward racemic mixtures.

Tetrameric assemblies have been identified following the adsorption on alanine and some other aminoacids on a Pd(111) surface, where enantioselectivity is found when using propylene oxide and glycidol as chiral probes only for those aminoacids that form tetramers. Surface analyses showed that the aminoacids

exist in both the zwitterionic and anionic forms. DFT calculations revealed that amino acids dimerize by an interaction between an anionic and zwitterionic form of the amino acid that, in some cases, further assemble to form tetramers. It was found that only those amino acids that formed tetramers were enantioselective, indicating that they formed (local) chiral templates as illustrated in Figure 3.

However, such local templates still leave unmodified regions of the surface. In order to address this issue we are attempting to grow extended template arrays. We have shown that aspartic acid on Pd(111) adsorbs in a similar fashion to other amino acids, through the acetate and amine groups, but aggregate into networks that expose chiral pockets. In an alternative approach, 2-butanol also forms extended two-dimensional chiral arrays as illustrated in Figure 4.

One-to-One Interactions

One-to-one modifiers operate through a direct interaction between the prochiral reactant and the chiral modifier, as proposed to occur for the Orito reaction in which cinchona alkaloids serve as a modifier for the enantioselective hydrogenation of methyl pyruvate (MP) to methyl lactate (ML). We have investigated the molecular details of this promotion by using MP on 1-(1-naphthyl) ethylamine (NEA, a cinchonidine analog)-modified Pd(111). TPD experiments reveal that co-adsorbed NEA accelerates the rate of MP hydrogenation on Pd(111) (Figure 5). Docking complexes are analyzed by imaging

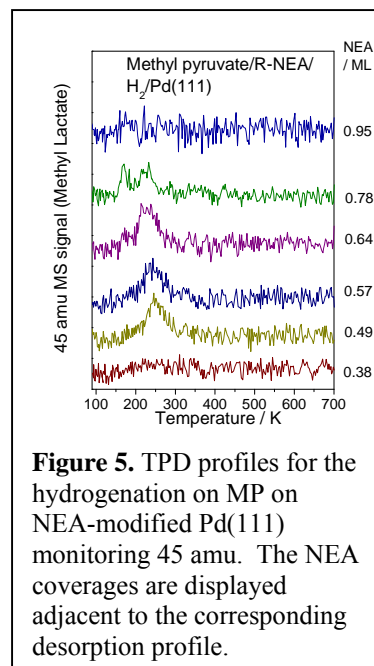
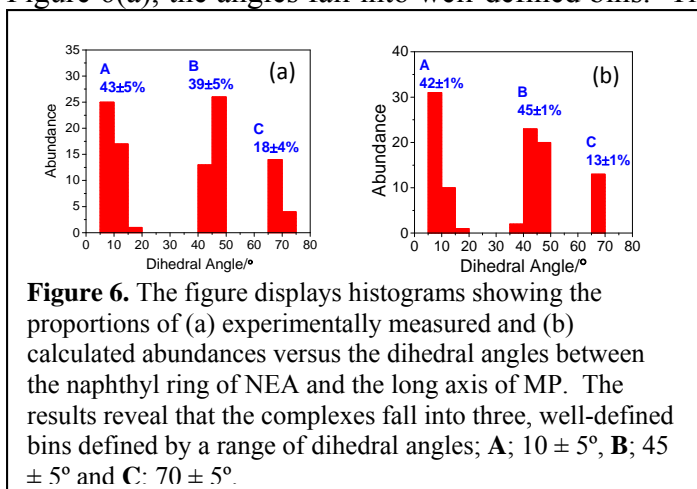


Figure 5. TPD profiles for the hydrogenation on MP on NEA-modified Pd(111) monitoring 45 amu. The NEA coverages are displayed adjacent to the corresponding desorption profile.

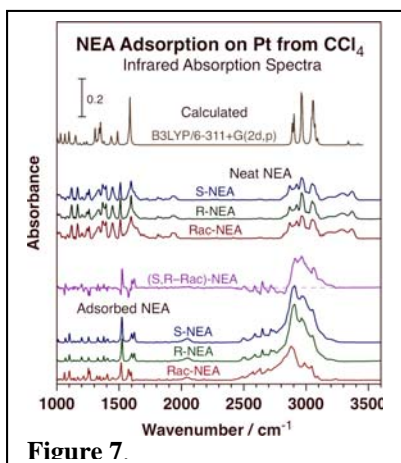
MP hydrogenation on Pd(111) (Figure 5). Docking complexes are analyzed by imaging

co-adsorbed NEA and MP by scanning tunneling microscopy (STM) and the structures characterized by measuring the angle subtended between the long axes of the docked MP and the naphthyl ring of MP in the images of the docking complexes. As shown in Figure 6(a), the angles fall into well-defined bins. The docking structures were analyzed



by extensive DFT calculations of the interactions between combinations of *exo* and *endo* NEA with the *keto* and *enol* tautomers of MP located proximate to the chiral center on NEA using Van der Waals' corrections. The equilibrium proportions of each docking complex were calculated from a Boltzmann distribution using the interaction energies from DFT at the experimental imaging temperature of ~120 K. The angles between the MP and naphthyl ring of the simulated images were then calculated for the most stable docking complexes. The resulting distribution, displayed in Figure 6(b), shows that the measured angles for the calculated structures fall into the same ranges as for the experiment, with similar distributions.

Analysis of the calculated structures reveal that stable docking complexes form predominantly between the *enol* tautomer of MP with both the *exo* and *endo* rotamers of NEA. The formation of the complexes is primarily dictated by the surface ensemble requirements of binding the carbon-carbon double bond to the surface while simultaneously optimizing C=O...H₂N hydrogen-bonding interactions that predominantly stabilizes the *enol* tautomer in pro-*R* configurations on an *R*-NEA-modified surface. The stabilization of the *enol* tautomer results in enhanced hydrogenation of MP to methyl lactate due to the presence of a more easily hydrogenated C=C double bond. The combination of chiral-NEA driven diastereomeric docking with a tautomeric preference causes an enhancement of hydrogenation activity that leads to an increase in enantiomeric excesses in the catalytic reaction for chirally modified surface, as found experimentally.



However, the story may be more complex under real conditions that include the presence of a solvent. The nature of the adsorption of saturated monolayers obtained by uptake of NEA from CCl₄ solutions were characterized *in situ* by reflection-absorption infrared spectroscopy (RAIRS). It was found that racemic mixtures behave differently than enantiopure layers, yielding different IR spectra. This is shown in Figure 7, where new peaks are seen for the adsorbed (but not neat) racemic mixture, especially in the 1500 - 1700 cm⁻¹ region. This behavior was interpreted as the

result of the formation of racemate pairs *via* hydrogen bonding at the amine moiety also responsible for bonding to the surface. NEA adsorption under these conditions is reversible and can be modified by subsequent exposures to solutions of different chiral compositions, but that appears to take place only *via* changes in the relative fractions of enantiopure *versus* racemic domains on the surface; no other enantiomeric ratios are apparent at any stage of the uptake or adsorbate exchange process in the IR data.

Publications Acknowledging this Grant in 2013-2016

(I) Exclusively funded by this grant

1. Garvey, M.; Bai, Y.; Boscoboinik, J.A.; Burkholder, L.; Sorensen, T.E.; Tysoe, W.T. Identifying Molecular Species on Surfaces by Scanning Tunneling Microscopy: Methyl Pyruvate on Pd(111), *J. Phys. Chem. C*, **2013**, *117*, 4505-4514.
2. Yun, Y.; Gellman, A.J.; Enantioselective separation of DL-aspartic acid on naturally chiral Cu(3,1,17)^{R&S} surfaces. *Angewandte Chemie International Edition*, **52**, (2013), 3394-3397.
3. Gellman, A.J.; Huang, Y.; Xu, F.; Pushkarev, V.V.; Holsclaw, B.; Mhatre, B. Super-enantioselective chiral surface explosions. *J. Am. Chem. Soc.* **2013**, *135*, 19208-19214
4. Gordon, A.D.; Zaera, F. Adsorption of 1-(1-Naphthyl)ethylamine from Solution onto Pt Surfaces: Implications for the Chiral Modification of Heterogeneous Catalysts, *Angew. Chem., Int. Ed.*, **2013**, *52*, 3453-3456.
5. Mahapatra, M.; Burkholder, L.; Bai, Y.; Garvey, M.; Boscoboinik, J.A.; Hirschmugl, C.; Tysoe, W.T. Formation of Chiral Self-Assembled Structures of Amino Acids on Transition-Metal Surfaces: Alanine on Pd(111), *J. Phys. Chem. C*, 2014, *118*, 6856-6865.
6. Structure and Decomposition Pathways of D-(-)-Tartaric Acid on Pd(111), Mausumi Mahapatra and Wilfred T. Tysoe, *Surf. Sci.* **2014**, *629*, 132-138.
7. Shukla, N.; Ondeck, N.; Gellman, A.J. Quantitation of Enantiospecific Adsorption on Chiral Nanoparticles from Optical Rotation. *Surf. Sci.* **2014**, *629*, 15-19.
8. Gordon, A.D.; Karakalos, S.; Zaera, F. Dependence of the Adsorption of Chiral Compounds on their Enantiomeric Composition, *Surf. Sci.*, **2014**, *629*, 3-10
9. Mahapatra, M.; Tysoe, W.T. Adsorption and Reaction Pathways of a Chiral Probe Molecule, S-glycidol on a Pd(111) Surface, *Catal. Sci. Technol.* **2015**, *5*, 738-742.
10. Mahapatra, M.; Tysoe, W.T. Chemisorptive Enantioselectivity of Chiral Epoxides on Tartaric-Acid Modified Pd(111): Three-Point Bonding, *Phys. Chem. Chem. Phys.* **2015**, *17*, 5450-5458.
11. Gellman, A.J.; Tysoe, W.T.; Zaera, F. Surface Chemistry for Enantioselective Catalysis, *Catal. Lett.* **2015**, *145*, 220-232.
12. Yun Y., Gellman A.J., Auto-amplification of enantiomeric excess on an achiral surface *Nature Chem.* **2015**, *7*, 520 - 525
13. Shukla N., Ondeck N., Khosla N., Klara S., Petti A., Gellman A.J., Polarimetric detection of enantioselective adsorption by chiral Au nanoparticles: Effects of temperature, wavelength and size *Nanomater. Nanotechno.* **2015**, *5*, 1-8

14. Yun Y., Gellman A.J., Enantiospecificity of amino acids on naturally chiral Cu{3,1,17}^{R&S} surfaces: alanine, aspartic acid, lysine, phenylalanine, serine *Langmuir* **2015**, *31*, 6055–6063
15. Burkholder, L.; Mahapatra, M.; Devarajan, S.; Boscoboinik J.A.; Garvey, M.; Bai, Y.; Tysoe, W.T. Formation of Induced Fit Chiral Templates by Amino Acid Functionalized Pd(111) Surfaces, *J. Phys. Chem. C*, **2015**, *119*, 3556-3563.
16. Karakalos, S.; Zaera, F. Amplification of Enantioselectivity on Solid Surfaces using Non-Chiral Adsorbates, *J. Phys. Chem. C*, **2015**, *119*(24), 13785-13790.
17. Mahapatra, M.; Tysoe, W.T. Local and Extended Structures of D-(-)-Tartaric Acid on Pd(111), *J. Phys. Chem. C*, **2016**, *120*, 2309-2319
18. Hong, J.; Karakalos, S.; Zaera, F. Changes in the Enantiomeric Composition of Chiral Mixtures Upon Adsorption on a Non-Chiral Surface, *Angew. Chem., Int. Ed.*, **2016**, DOI: 10.1002/anie.201601549 and 10.1002/ange.201601549.
19. Shukla N., Yang D., Gellman A.J., Enantiomeric Separations of Chiral Pharmaceuticals using Chirally Modified Tetrahedral Au Nanoparticles *Surf. Sci.* **2016**, *648*, 29-34
20. Liriano M. L., Carrasco J., Lewis E. A., Murphy C. J., Lawton T. J., Marcinkowski M. D., Therrien A. J. Michaelides A., and Sykes E. C. H., The Interplay of Covalency, Hydrogen Bonding and Dispersion Leads to a Long Range Chiral Network: The Example of 2-Butanol *J. Chem. Phys.* **2016**, *144*, 094703

(II) Jointly funded by this grant and other grants with leading intellectual contribution from this grant;

1. Karakalos, S.; Lawton, T.J.; Lucci, F.R.; Sykes, E.C.H, Zaera, F. Enantiospecific Kinetics in Surface Adsorption: Propylene Oxide on Pt(111) Surfaces, *J. Phys. Chem. C*, **2013**, *117*, 18588-18594
2. Zaera, F. Shape-Controlled Nanostructures in Heterogeneous Catalysis, *ChemSusChem*, **2013**, *6*, 1797-1820.
3. Zaera, F. New Advances in Infrared Absorption Spectroscopy for the Characterization of Heterogeneous Catalytic Reactions, *Chem. Soc. Rev.*, **2014**, *43*(22), 7624 - 7663.
4. Yun Y., Wei D., Sholl D.S., Gellman A.J., Equilibrium adsorption of D- and L-alanine mixtures on naturally chiral Cu{3,1,17}^{R&S} surfaces, *J. Phys.Chem. C* **2014** *118*, 14957-14966
5. Hong, J.; Lee, I.; Zaera, F. Correlated Bifunctionality in Heterogeneous Catalysts: Selective Tethering of Cinchonidine Next to Supported Pt Nanoparticles, *Catal. Sci. Technol.*, **2015**, *5*, 680-689.
6. Gellman A.J., Baker L.D., Holsclaw B.S., Xe Adsorption Site Distributions on Pt(111), Pt(221) and Pt(531) *Surf. Sci.* **2016**, *646*, 83-89

Organometallic Chemistry for Alkane Dehydrogenation

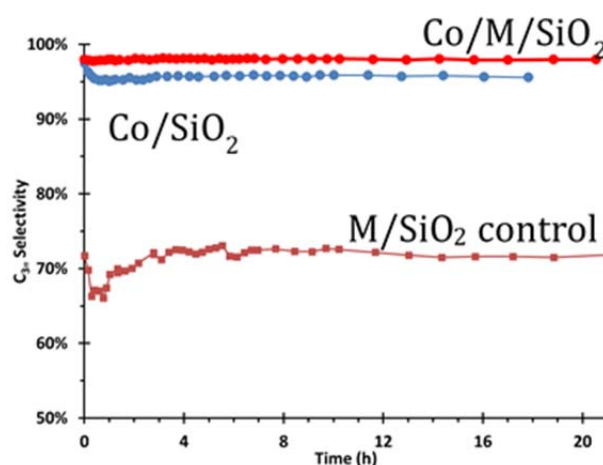
Adam S. Hock,^{1,2} Bo Hu,² Yiqing Zhao,² Andrew ‘Bean’ Getsoian,¹ Jeffrey Camacho-Bunquin,¹ Magali Ferrandon,¹ Ujjal Das,¹ Fulya Dogan,¹ Theodore R. Krause,¹ Emilio A. Bunel,¹ Larry A. Curtiss,¹ Jeffrey T. Miller,^{1,3} SonBinh T. Nguyen,^{1,4} Christopher L. Marshall,¹ Peter C. Stair,^{1,4} and Massimiliano Delferro¹

¹Chemical Sciences and Engineering Division, Argonne National Laboratory, ²Department of Chemistry, Illinois Institute of Technology, ³Department of Chemical Engineering, Purdue University, ⁴Department of Chemistry, Northwestern University

hock@anl.gov

Our isolated metal catalysts Zn^{2+} , Co^{2+} , Fe^{2+} , and Ga^{3+} on SiO_2 are highly selective for nonoxidative propane dehydrogenation. While these are Lewis acid centers, the key step for effective catalysis is not purely based upon the Lewis acidity of the catalytic metal, but also the catalyst-oxygen bond strength. This conclusion is the result of computational modeling, spectroscopic, and mechanistic study of our M/SiO_2 catalysts. Key insight was obtained from highly Lewis acidic Y^{3+} and Sc^{3+} materials that are not catalytic for dehydrogenation but do catalyze the low temperature hydrogenation reaction. We have also directly prepared zinc alkyl precatalysts and compared their catalytic function to the previously reported Zn^{2+}/SiO_2 system prepared via aqueous synthesis. The need for multiple characterization methods, including kinetic studies, X-ray absorption, resonance Raman, and infrared spectroscopies will be highlighted by our preparation of model compounds and use of computational methods to validate structural and functional models of catalytic sites of Ga, Zn, and new, predicted catalysts.

To test the hypothesis that the catalyst-oxygen-support (M-O-M') bond strength is a valid descriptor of catalytic performance in our systems, we have synthesized new catalysts where we have used an electrophilic metal (e.g. Zr^{4+}) to modify the ‘ligand’ properties of the SiO_2 surface in terms of catalyst-oxygen bond strength. This was accomplished using conventional aqueous, organometallic, or atomic layer deposition (ALD) chemistries. The resulting materials were found to be superior catalysts to our previously reported Co/SiO_2 in terms of both catalyst *activity* and *selectivity*. The implications for future catalyst design will also be discussed.



Stereospecific ROMP of Cyclic Olefins with Mo and W Initiators

Richard R. Schrock

Massachusetts Institute of Technology

Department of Chemistry 6-331

77 Massachusetts Avenue 02139

617 253-1596

rrs@mit.edu

Approximately twenty years ago well-defined ROMP catalysts based on molybdenum imido alkylidene complexes that contain a biphenolate or binaphtholate ligand (Mo(NR)(CHR')(Biphen) catalysts) were shown to yield *cis, isotactic* poly(2,3-dicarbomethoxynorbornadiene) and related polymers from other monomers. In the last five years Mo and W MAP (MonoAryloxiide Pyrrolide) imido alkylidene initiators, M(NR)(CHR')(Pyrrolide)(OR'''), and analogous tungsten oxo initiators, have been found to produce *cis, syndiotactic* polynorbornenes and substituted norbornadienes through what has been called stereogenic metal control. A syndiotactic structure is formed because the approach of the monomer to the metal is regulated by the chirality at the metal, and that chirality switches with addition of each monomer unit. The mode of forming *cis, syndiotactic* polynorbornenes has allowed the formation of a third regular structure, syndiotactic polymers prepared from *racemic* monomers that contain alternating enantiomers within the main chain, so-called "*cis, syndiotactic, alt*" structures where *alt* refers to the alternating incorporation of enantiomers. Recently we have found that two chemically different monomers with similar reactivities but "opposite" chiralities can be copolymerized to give *cis, syndiotactic, alt* structures through "stereogenic metal control" of the polymerization. Unusual *trans*-poly(**A-alt-B**) polymers can be prepared stereoselectively from a 1:1 mixture of **A** and **B** where **A** is a cyclic olefin such as cyclooctene (**A**₁) or cycloheptene (**A**₂) and **B** is a large norbornadiene or norbornene derivative such as 2,3-dicarbomethoxy-7-isopropylidenenorbornadiene (**B**₁) or dimethylspirobicyclo[2.2.1]hepta-2,5-diene-2,3-dicarboxylate-7,1'-cyclopropane (**B**₂) with initiators Mo(N-2,6-Me₂C₆H₃)(CHCMe₂Ph)[OCMe(CF₃)₂]₂ or Mo(N-2,6-*i*-Pr₂C₆H₃)(CHCMe₂Ph)[OCMe(CF₃)₂]₂. The proposed mechanism involves the sequential formation of *syn-MB* (where **B** was last inserted into a Mo=C bond) and *anti-MA* intermediates (where **A** was last inserted into a Mo=C bond), where *syn* and *anti* are isomeric forms of an alkylidene.

Poster Session Abstracts

Frank Abild-Pedersen

**Heterogeneous Catalysis -
Predictions from Bond-order Conservation Principles**

Frank Abild-Pedersen¹, Philipp N. Plessow^{1,2}, and Liang Yu^{1,2}

¹SUNCAT Center for Interface Science and Catalysis, SLAC National Accelerator Laboratory, 2575 Sand Hill Road, Menlo Park, California 94025, United States

²SUNCAT Center for Interface Science and Catalysis, Department of Chemical Engineering, Stanford University, 443 Via Ortega, Stanford, California 94305, United States

Presentation Abstract

The primary purpose of this presentation is to outline our developments in understanding heterogeneous catalysis to the point that a set of catalyst design principles is revealed. The cornerstone of our approach and the focus of this presentation is the combination of knowledge from computational investigations and modeling tools to develop a comprehensive theory of heterogeneous catalysis. The theory we aim for is a set of concepts that allow us to identify the catalyst properties that are most important in determining the catalytic activity. This involves studying the energetics (reaction energies as well as activation energies) and properties related to catalyst deactivation such as sintering and strong metal support interactions. We make extensive use of computational chemistry methods and we rely on the development of models that allows us to study trends in surface chemistry. The final test of our efforts is the ability to design new catalysts based on insight, something that is not possible without the combination of theory and experiment.

Grant or FWP Number: 10049

PI: Frank Abild-Pedersen

Postdoc(s): Philipp N. Plessow, Liang Yu

RECENT PROGRESS

The focus in this presentation is to expand our understanding of correlation between the electronic structure and the energetics of adsorbate-surface interactions with specific focus on activation energy scaling relations.

The d-band model has shown significant predictive power in correlating simple transition metal surface properties directly to the bond-strength between the adsorbate and the adsorbent. Many studies have shown that the model is more than adequate to describe observed results.

The d-band model provides general guidelines on what to require from a surface in order to promote certain reactions but it is not very convenient when it comes to catalyst screening.

The introduction of linear scaling relations for energies has proven extremely useful in the quest to identify, understand and predict reactivity trends of solid catalysts and we have shown several cases of this applicability over the years. Their ability to relate complex properties such as the energies of adsorbates or transition states to simple descriptors provide all the ingredients required to calculate trends in rates, equilibria and turn-over-frequencies of complex reaction networks. We have devoted a major part of our efforts expanding these scaling relations to enhance our understanding of the relations and test their applicability to new and more complex systems.

Scaling - beyond simple relations

The concept of scaling can in a simple way be extended to adsorbate systems that have been perturbed from their equilibrium structure.

If we have a di-atomic molecule $(A - B)_{eq}$ in its equilibrium structure in vacuum, then for each $(A - B)_d$, where the index d describes a perturbation from the equilibrium structure, we shall assume that there is a well-defined scaling term per surface bonded fragment such that:

$$\Delta E^{A-Bd} = \gamma_s^A \Delta E^A + \gamma_s^B \Delta E^B + \xi^{A-Bd} \quad (1)$$

where γ_s^A and γ_s^B are scaling parameters for each element and ξ^{A-Bd} is the intercept at the zero interaction limit, i.e. $\Delta E^A = \Delta E^B = 0$. Without loss of generalization, the same arguments can be used where A and B are molecular fragments instead of single atoms.

The data in Figure 1 clearly justifies this assumption showing the adsorption energy of molecular nitrogen, N_2 , as a function of the N adsorption energy on a number of stepped transition metal surfaces for a number of different $N - N$ bond distances.

Equation (1) above can be generalized to an n -dimensional energy space (descriptors) for any fixed structure r , such that:

$$\begin{aligned} \Delta E(r, \{\Delta E^1, \dots, \Delta E^n\}) &= \sum_{i=1}^n \gamma_s^i(r) \Delta E^i + \xi(r, \{\Delta E^1, \dots, \Delta E^n\}) \\ &= \bar{\gamma}_s \bar{\varepsilon} + \xi(r, \bar{\varepsilon}) \end{aligned} \quad (2)$$

where $\bar{\gamma}_s$ and $\bar{\varepsilon}$ are n -dimensional scaling- and energy-vectors, respectively.

We note, that BEP relations, or any linear scaling between transition state energies and reaction dependent energies one may choose, are scaling relations that explicitly assumes that the structure of the transition state is fixed and that its structure is independent of the surface interaction.

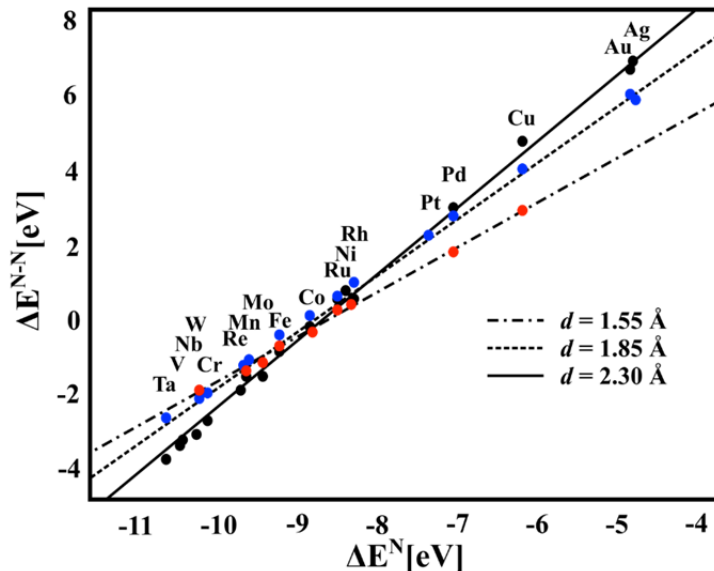


Figure 1. $N - N$ binding energies calculated for three fixed structures $d = 1.55\text{\AA}, 1.85\text{\AA}, 2.30\text{\AA}$ as a function of the N binding energy on stepped metal surfaces. Lines show fits to the points.

It is a fact, that the geometry of the transition state can vary quite significantly between different transition metals and hence Eq. (2) has to be an approximation to the real correlation between transition state energies and the descriptors of surface reactivity. Under the assumption that scaling holds throughout an elementary step reaction, we immediately deduce from Eq. (2) that for the transition state energy binding energy. The dashed lines represent the maximum and minimum slope that the transition state can have and hence defines the limits of $E^{ts}(\bar{\epsilon})$. The dot-dashed line shows the curvature variation of $E^{ts}(\bar{\epsilon})$.

$$\frac{dE^{ts}(\bar{\epsilon})}{d\varepsilon_i} = \gamma_s^i(\bar{\epsilon}) + \left(\bar{\epsilon} \frac{\partial \gamma_s^i(\bar{\epsilon})}{\partial \varepsilon_i} + \frac{\partial \xi(\bar{\epsilon})}{\partial \varepsilon_i} \right) \quad (3)$$

with the requirement that the last term in parenthesis vanish in the transition state. This is a consequence of Eq. (2) and it allows us to interpret how the scaling parameters γ and ξ are correlated. Clearly, to first order in the i^{th} energy ε_i , the induced perturbation of the system and the effective change $\partial \xi$ is compensated by the change in reactivity $\partial \gamma$. This is equivalent to bond order conservation.

We also find, that the curvature, given by the second derivative of $E^{ts}(\bar{\epsilon})$ with respect to ε_i , varies so little that one with some confidence can use a linear approximation to fit the transition state energies as seen in Figure 2. This justifies the use of BEP and related correlations in the literature when interpreting kinetics of chemical reactions.

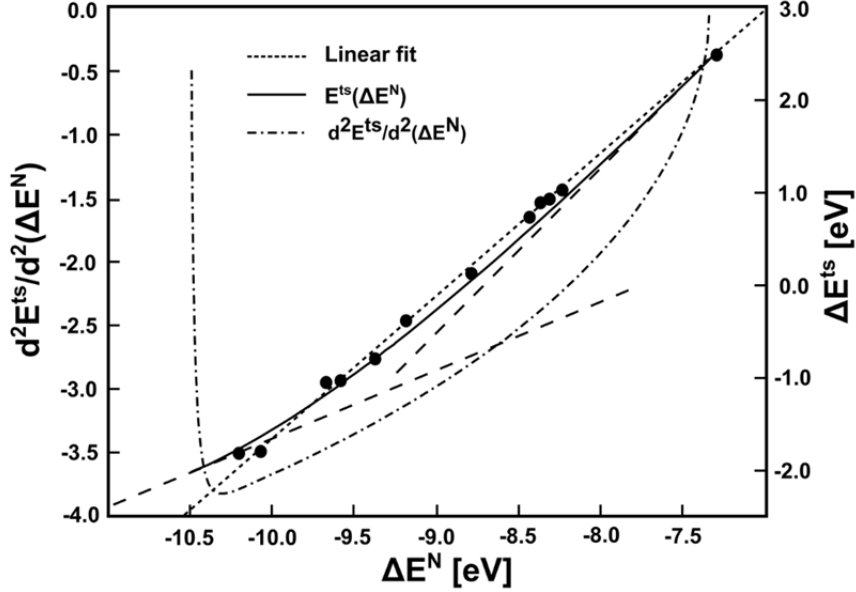


Figure 2. Calculated transition state energies for N_2 splitting on stepped transition metal surfaces (solid points), best linear fit to all the points (dotted line), and from Eq. (5) derived functional form for the transition state (solid line) as a function of the nitrogen.

The approach introduced provides a way to develop a scheme in which the actual functional form of $E^{ts}(\bar{\epsilon})$ can be derived.

If one rewrites the complex total energy in Eq. (2) such that:

$$\Delta E(r) = \Delta E^{hyb}(r) + \Delta E^{strain}(r) \quad (4)$$

where ΔE^{hyb} is the contribution from the hybridization between the surface and the adsorbate in structure r and ΔE^{strain} is the energy needed to perturb the adsorbate from its equilibrium structure to the structure defined by r in the gas phase.

This rewriting divides the total energy into two much simpler terms, a surface and a gas phase dependent part as seen in Figure 3. The end points on the total energy curve $\Delta E(r)$ are given by the adsorption energy scaling relations as obtained from Eq. (2). For simple molecules, $\Delta E^{strain}(r)$ is easily obtained by calculating the gas phase value of the molecule for a range of fixed structures defined by r . To obtain accurate enough values for the scaling parameters γ and ξ as a function of the reaction coordinate r we only need a few points along the potential energy surface and then to utilize that the function $\Delta E^{hyb}(r)$ is monotonous. Knowing $\gamma_s^i(r)$ and $\xi(r)$ for all r , we can then calculate $\Delta E(r, \bar{\epsilon})$ through Eq. (2) for any value of the vector $\bar{\epsilon}$ and extract $E^{ts}(\bar{\epsilon})$ as:

$$E^{ts}(\bar{\epsilon}) = \max[\Delta E(r, \bar{\epsilon})] \quad (5)$$

Similar to the adsorption energies, where we only needed one calculation to establish the scaling relations we have now introduced a simple scheme where transition state energies can be obtained knowing (a) $\Delta E^{strain}(r)$ from simple gas phase calculations, (b) the scaling relations for the initial and final state in the reaction, and (c) at least one fixed structure calculation in the transition state region on as many surfaces as there are

independent scaling parameters. In Figure 2 the functional form obtained for N_2 dissociation is shown as a solid curve and it is in remarkably good agreement with calculations considering that it is based on very few adsorbate/surface calculations.

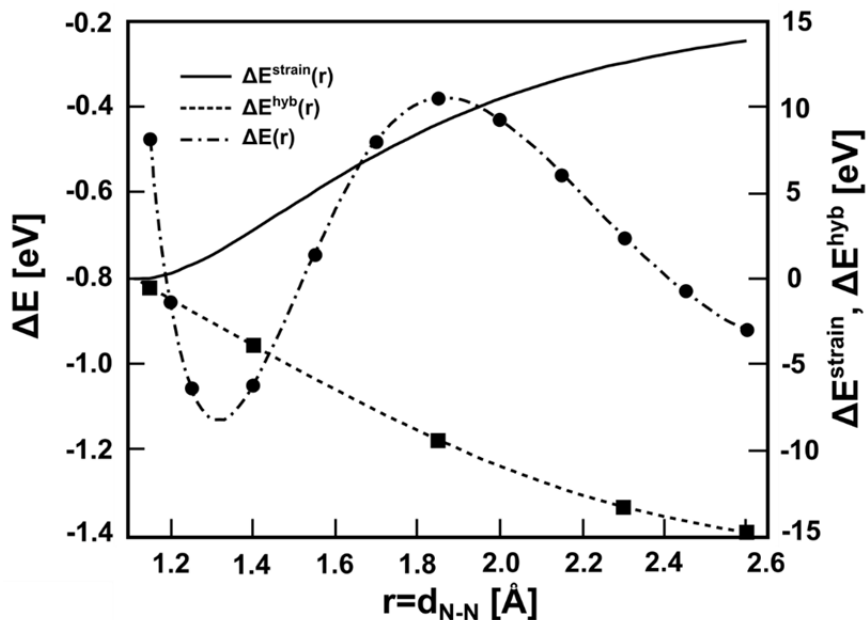


Figure 3. The three terms in Eq. (4); (solid line) the energy needed to strain N_2 from its equilibrium structure, $\Delta E^{strain}(r)$, (dotted line) the energy of the strained structure due to interaction with the surface, $\Delta E^{hyb}(r)$, (dot-dashed line) the total energy, $\Delta E(r)$. $\Delta E^{strain}(r)$ has been obtained from calculations, $\Delta E^{hyb}(r)$ has been fitted and $\Delta E(r)$ is given through Eq. (4). The solid black squares are the calculations used to fit $\Delta E^{hyb}(r)$ and the solid circles are full DFT calculations along the reaction path.

Analytically, we have found general constraints on the functional form of scaling relations, $E^{ts}(\bar{\epsilon})$.

To first order in the descriptor, ϵ , effects on the transition state energy resulting from change of the transition state geometry cancel.

This can be interpreted as bond-order conservation where loss of intramolecular bonding is compensated by adsorbate-surface bonding.

In general, the curvature of $E^{ts}(\bar{\epsilon})$ is positive and is expected to be small in the intermediate ϵ -range that is neither very close to being completely up- or downhill.

This region is where, according to the Sabatier principle, we expect the best catalysts.

This is illustrated in a simple activity volcano for ammonia formation (Figure 4), where we assume competition between rate-limiting N_2 -dissociation and formation of ammonia from adsorbed N atoms. Under this assumption the two avenues provide very similar results but compared to the BEP approach our new scheme introduces a significant reduction in computational time since transition state energies are among the most difficult numbers to obtain from DFT calculations.

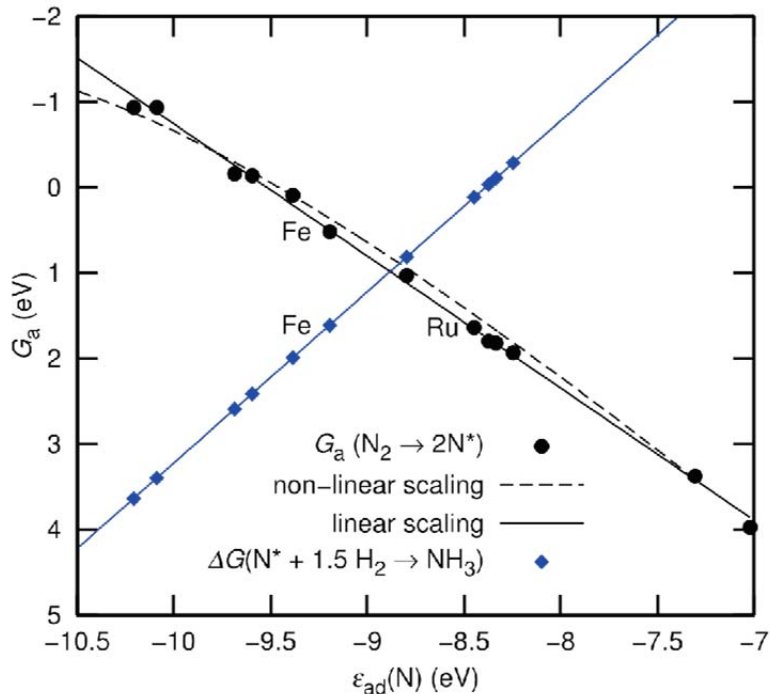


Figure 4. Plot of (negative) free activation barrier for N_2 dissociation and free energy of ammonia relative to adsorbed atomic nitrogen at $p = 200$ bar and $T = 700$ K.

Publications Acknowledging this Grant in 2013-2016

(I) Exclusively funded by this grant;

1. Reinecke, B. N.; Kuhl, K. P.; Ogasawara, H.; Li, L.; Voss, J.; Abild-Pedersen, F.; Nilsson, A.; Jaramillo, T. F. *Surf. Sci.* **2016**, *650*, 24–33.
2. Plessow, P. N.; Bajdich, M.; Greene, J.; Vojvodic, A.; Abild-Pedersen, F. *J. Phys. Chem. C* **2016**, acs.jpcc.6b01404.
3. Plessow, P. N.; Sánchez-Carrera, R. S.; Li, L.; Rieger, M.; Sauer, S.; Schaefer, A.; Abild-Pedersen, F. *J. Phys. Chem. C* **2016**, acs.jpcc.6b01403.
4. Li, H.; Tsai, C.; Koh, A. L.; Cai, L.; Contryman, A. W.; Fragapane, A. H.; Zhao, J.; Han, H. S.; Manoharan, H. C.; Abild-Pedersen, F.; Nørskov, J. K.; Zheng, X. *Nature Materials* **2016**, *15* (1), 48–53.
5. Lee, S. C.; Benck, J. D.; Tsai, C.; Park, J.; Koh, A. L.; Abild-Pedersen, F.; Jaramillo, T. F.; Sinclair, R. *ACS Nano* **2015**, *10* (1), 624–632.
6. Kibsgaard, J.; Tsai, C.; Chan, K.; Benck, J. D.; Nørskov, J. K.; Abild-Pedersen, F.; Jaramillo, T. F. *Energy Environ. Sci.* **2015**, *8* (10), 3022–3029.
7. Abild-Pedersen, F. *Catal. Today* **2015**.
8. Li, L.; Abild-Pedersen, F.; Greeley, J.; Nørskov, J. K. *J. Phys. Chem. Lett.* **2015**, *6* (19), 3797–3801.

9. Tsai, C.; Chan, K.; Nørskov, J. K.; Abild-Pedersen, F. *Surf. Sci.* **2015**, *640*, 133–140.
10. Tsai, C.; Latimer, A. A.; Yoo, J. S.; Studt, F.; Abild-Pedersen, F. *J. Phys. Chem. Lett.* **2015**, *6* (18), 3670–3674.
11. Kunkes, E. L.; Studt, F.; Abild-Pedersen, F.; Schlögl, R.; Behrens, M. *J. Catal.* **2015**, *328*, 43–48.
12. Medford, A. J.; Vojvodic, A.; Hummelshoj, J. S.; Voss, J.; Abild-Pedersen, F.; Studt, F.; Bligaard, T.; Nilsson, A.; Nørskov, J. K. *J. Catal.* **2015**, *328*, 36–42.
13. Singh, V.; Cassidy, C.; Abild-Pedersen, F.; Kim, J.-H.; Aranishi, K.; Kumar, S.; Lal, C.; Gspan, C.; Grogger, W.; Sowwan, M. *Nanoscale* **2015**, *7* (32), 13387–13392.
14. Santos, E. J. G.; Nørskov, J. K.; Harutyunyan, A. R.; Abild-Pedersen, F. *J. Phys. Chem. Lett.* **2015**, *6* (12), 2232–2237.
15. Ng, M. L.; Abild-Pedersen, F.; Kaya, S.; Mbuga, F.; Ogasawara, H.; Nilsson, A. *Phys. Rev. Lett.* **2015**, *114* (24), 246101.
16. Plessow, P. N.; Abild-Pedersen, F. *J. Phys. Chem. C* **2015**, *119* (19), 10448–10453.
17. Xin, H.; LaRue, J.; Öberg, H.; Beye, M.; Dell'Angela, M.; Turner, J. J.; Gladh, J.; Ng, M. L.; Sellberg, J. A.; Kaya, S.; Mercurio, G.; Hieke, F.; Nordlund, D.; Schlotter, W. F.; Dakovski, G. L.; Minitti, M. P.; Föhlisch, A.; Wolf, M.; Wurth, W.; Ogasawara, H.; Nørskov, J. K.; Öström, H.; Pettersson, L. G. M.; Nilsson, A.; Abild-Pedersen, F. *Phys. Rev. Lett.* **2015**, *114* (15), 156101.
18. Studt, F.; Behrens, M.; Kunkes, E. L.; Thomas, N.; Zander, S.; Tarasov, A.; Schumann, J.; Frei, E.; Varley, J. B.; Abild-Pedersen, F.; Nørskov, J. K.; Schlögl, R. *ChemCatChem* **2015**, *7* (7), 1105–1111.
19. Öström, H.; Öberg, H.; Xin, H.; LaRue, J.; Beye, M.; Dell'Angela, M.; Gladh, J.; Ng, M. L.; Sellberg, J. A.; Kaya, S.; Mercurio, G.; Nordlund, D.; Hantschmann, M.; Hieke, F.; Kuhn, D.; Schlotter, W. F.; Dakovski, G. L.; Turner, J. J.; Minitti, M. P.; Mitra, A.; Moeller, S. P.; Föhlisch, A.; Wolf, M.; Wurth, W.; Persson, M.; Nørskov, J. K.; Abild-Pedersen, F.; Ogasawara, H.; Pettersson, L. G. M.; Nilsson, A. *Science* **2015**, *347* (6225), 978–982.
20. Wang, H.; Tsai, C.; Kong, D.; Chan, K.; Abild-Pedersen, F.; Nørskov, J. K.; Cui, Y. *Nano Res.* **2015**, *8* (2), 566–575.
21. Yoo, J. S.; Khan, T. S.; Abild-Pedersen, F.; Nørskov, J. K.; Studt, F. *Chem. Commun.* **2015**, *51* (13), 2621–2624.
22. Tsai, C.; Chan, K.; Nørskov, J. K.; Abild-Pedersen, F. *Catal. Sci. Technol.* **2015**, *5* (1), 246–253.
23. Casalongue, H. G. S.; Benck, J. D.; Tsai, C.; Karlsson, R. K. B.; Kaya, S.; Ng, M. L.; Pettersson, L. G. M.; Abild-Pedersen, F.; Nørskov, J. K.; Ogasawara, H.; Jaramillo, T. F.; Nilsson, A. *J. Phys. Chem. C* **2014**, *118* (50), 29252–29259.
24. Tsai, C.; Chan, K.; Nørskov, J. K.; Abild-Pedersen, F. *J. Phys. Chem. Lett.* **2014**, *5* (21), 3884–3889.
25. Studt, F.; Behrens, M.; Abild-Pedersen, F. *Catal. Lett.* **2014**, *144* (11), 1973–1977.
26. Rao, R.; Sharma, R.; Abild-Pedersen, F.; Nørskov, J. K.; Harutyunyan, A. R. *Sci. Rep.* **2014**, *4*, 6510.

27. Voss, J.; Vojvodic, A.; Chou, S. H.; Howe, R. T.; Abild-Pedersen, F. *Phys. Rev. Applied* **2014**, *2* (2), 024004.
28. Medford, A. J.; Wellendorff, J.; Vojvodic, A.; Studt, F.; Abild-Pedersen, F.; Jacobsen, K. W.; Bligaard, T.; Nørskov, J. K. *Science* **2014**, *345* (6193), 197–200.
29. Chou, S. H.; Voss, J.; Vojvodic, A.; Howe, R. T.; Abild-Pedersen, F. *J. Phys. Chem. C* **2014**, *118* (21), 11303–11309.
30. Tsai, C.; Chan, K.; Abild-Pedersen, F.; Nørskov, J. K. *Phys. Chem. Chem. Phys.* **2014**, *16* (26), 13156.
31. Yoo, J. S.; Abild-Pedersen, F.; Nørskov, J. K.; Studt, F. *ACS Catal.* **2014**, *4* (4), 1226–1233.
32. Vojvodic, A.; Medford, A. J.; Studt, F.; Abild-Pedersen, F.; Khan, T. S.; Bligaard, T.; Nørskov, J. K. *Chem. Phys. Lett.* **2014**, *598*, 108–112.
33. Xin, H.; Vojvodic, A.; Voss, J.; Nørskov, J. K.; Abild-Pedersen, F. *Phys. Rev. B* **2014**, *89* (11), 115114.
34. Tsai, C.; Abild-Pedersen, F.; Nørskov, J. K. *Nano Lett.* **2014**, *14* (3), 1381–1387.
35. Studt, F.; Sharafutdinov, I.; Abild-Pedersen, F.; Elkjær, C. F.; Hummelshøj, J. S.; Dahl, S.; Chorkendorff, I.; Nørskov, J. K. *Nature Chemistry* **2014**, *6* (4), 320–324.
36. Vojvodic, A.; Nørskov, J. K.; Abild-Pedersen, F. *Top. Catal.* **2014**, *57* (1-4), 25–32.
37. Xu, Y.; Lausche, A. C.; Wang, S.; Khan, T. S.; Abild-Pedersen, F.; Studt, F.; Nørskov, J. K.; Bligaard, T. *New J. Phys.* **2013**, *15* (12), 125021.
38. Lausche, A. C.; Medford, A. J.; Khan, T. S.; Xu, Y.; Bligaard, T.; Abild-Pedersen, F.; Nørskov, J. K.; Studt, F. *J. Catal.* **2013**, *307*, 275–282.
39. Medford, A. J.; Lausche, A. C.; Abild-Pedersen, F.; Temel, B.; Schjødt, N. C.; Nørskov, J. K.; Studt, F. *Top. Catal.* **2013**, *57* (1-4), 135–142.
40. Öberg, H.; Anniyev, T.; Vojvodic, A.; Kaya, S.; Ogasawara, H.; Friebel, D.; Miller, D. J.; Nordlund, D.; Bergmann, U.; Ljungberg, M. P.; Abild-Pedersen, F.; Nilsson, A.; Pettersson, L. G. M. *J. Phys. Chem. C* **2013**, *117* (32), 16371–16380.
41. Rajasekaran, S.; Abild-Pedersen, F.; Ogasawara, H.; Nilsson, A.; Kaya, S. *Phys. Rev. Lett.* **2013**, *111* (8), 085503.
42. Lausche, A. C.; Abild-Pedersen, F.; Madix, R. J.; Nørskov, J. K.; Studt, F. *Surf. Sci.* **2013**, *613*, 58–62.
43. Voss, J.; Vojvodic, A.; Chou, S. H.; Howe, R. T.; Bargatin, I.; Abild-Pedersen, F. *J. Chem. Phys.* **2013**, *138* (20), 204701.
44. Abild-Pedersen, F.; Nilsson, A.; Nørskov, J. K. *J. Phys. Chem. C* **2013**, *117* (13), 6914–6915.
45. Viñes, F.; Vojvodic, A.; Abild-Pedersen, F.; Illas, F. *J. Phys. Chem. C* **2013**, *117* (8), 4168–4171.
46. García Mota, M.; Vojvodic, A.; Abild-Pedersen, F.; Nørskov, J. K. *J. Phys. Chem. C* **2013**, *117* (1), 460–465.
47. Studt, F.; Abild-Pedersen, F.; Varley, J. B.; Nørskov, J. K. *Catal. Lett.* **2013**, *143* (1), 71–73.

Eric I. Altman

Applying Surface Science Approaches to Modeling Zeolite Catalysis

J.-H. Jhang¹, G. Hutchings¹, C. Zhou², A. Malashevich³, U.D. Schwarz^{1,2}, S. Ismail-Beigi^{2,3} and E.I. Altman¹

¹Department of Chemical & Environmental Engineering

²Department of Mechanical Engineering & Materials Science

³Department of Applied Physics

Yale University

New Haven, CT 06520

Presentation Abstract

The development of 2D silicate bilayers has opened up the possibility of using surface science methods to elucidate structure-reactivity relationships for zeolitic materials. Similar to the catalytically relevant internal surfaces of zeolites, SiO₂ bilayers lack dangling bonds and only become reactive when Si is replaced by another element. Substituting trivalent Al for Si creates cation exchange sites that provide acid functionality when the cation is a proton or redox activity when the cation is a transition metal; the focus of this project is on Co cations that make zeolites active for NO reduction by hydrocarbons and their interaction with acid sites. Density functional theory (DFT), has been used to investigate the effect of Al and the accompanying cations on the stability of competing structural moieties in 2D SiO₂. The results reveal that Al by itself does not shift the energetics away from six-membered rings of corner-sharing Si(Al)O₄ tetrahedra; however, the inability to fit larger cations (e.g., Cs) within the six-membered rings can induce a shift to combinations of eight- and four-membered rings. Meanwhile, smaller transition metal and divalent cations comfortably fit in the six-membered rings occupying a site very similar to that seen in the zeolite chabazite. Results indicate that Cu⁺ in both the 2D and 3D materials chemisorbs NO but cannot dissociate it. Further computational work is addressing differences in acid functionality between the 2D and 3D materials. On the experimental side, 2D silicates have been grown and characterized on Pd(111), chosen for its inability to dissociate NO. In contrast to Ru(0001) and Pd(100) where strained epitaxial crystalline layers form and Pt(111) where only amorphous 2D SiO₂ is seen, on Pd(111) unstrained incommensurate crystalline 2D SiO₂ forms with two preferred orientations. Comparison of the growth on the different metal surfaces reveals the maximum strain that can be imparted as well as differences in the ability to accommodate uniaxial versus biaxial strain. The incommensurate crystalline nature of the layers also makes Pd(111) a good choice for adsorption and reaction studies as it signals a weak interaction with the metal, avoids the need to consider strain, and reduces the ability of reactants to reach the metal substrate.

Grant or FWP Number: DE-SC0014414

Grant Title: Applying Surface Science Approaches to Modeling Zeolite Catalysis

PI: Eric I. Altman **Postdoc(s):** Jin-Hao Jhang

RECENT PROGRESS

Structure of Reactive Sites on 2D Aluminosilicate Surfaces

Two-dimensional SiO_2 favors a hexagonal structure with the corner-sharing SiO_4 tetrahedra arranged in six-membered rings;^{1,2} in addition an amorphous phase with four- through nine-membered rings is also seen.^{1,3} Therefore, key questions have been: does adding Al alter the stability of the different size rings?; if the structure includes different size rings where does the Al prefer to sit?; is the stability of the different size rings affected by the charge balancing cation?; where do the charge balancing cations prefer to sit? DFT calculations on a broad range of 2D aluminosilicate structures with a number of different charge balancing cations were performed. The results indicate that adding Al to 2D SiO_2 does not appreciably alter the energetics of the different ring sizes; however, the size of the charge balancing cation plays a decisive role. The energy to convert six-membered rings to a combination of four- and eight-membered rings is plotted as a function of cation size in Fig. 1a. Only for the largest Cs cation are the energetics shifted away from the six-membered ring structure. The peaked shape of the curve is due to distortion of the eight-membered ring to bring the oxygen atoms close to the intermediate sized cations, while the smaller cations form more local bonds and the larger fit in the center of the ring. The smaller divalent and late transition metal cations, e.g. Co^{2+} and Cu^+ , fall on the left side of the curve and thus favor six-membered ring structures. Starting with Ca as a prototypical divalent cation, it was found that the divalent cation strongly prefers to sit in a six-membered ring with two Al atoms (Fig. 1b); at low Al concentrations the calculations suggest that a clustering of the Al to allow this motif would be favored. A very similar site has been suggested in the literature for Co^{2+} in chabazite. Overall, it was found that the energetics of Al substitution and the siting of the cations in the 2D aluminosilicate were very similar to chabazite which includes a double six-membered ring structural motif analogous to that in 2D silica.

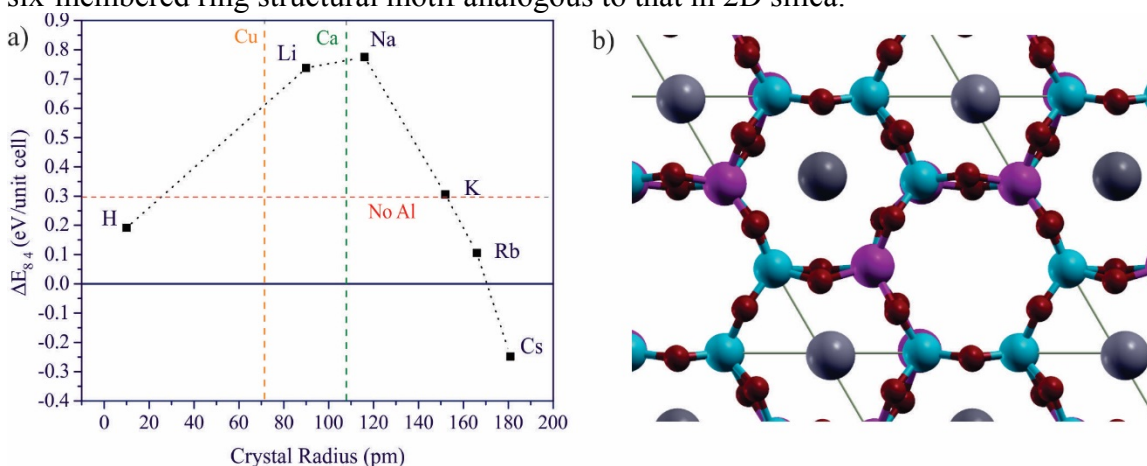


Fig. 1. a) Plot of the calculated energy to convert 2D $\text{AlSi}_3\text{O}_8\text{X}$ from a six-membered ring structure to a structure containing eight- and four-membered rings as a function of the size of the charge balancing alkali cation 'X.' The dashed horizontal red line indicates the value for pure SiO_2 and the vertical dashed lines the sizes of Cu^+ (orange) and Ca^{2+} (green). **b)** Ball and stick model of the lowest energy structure of Al-doped 2D SiO_2 with Ca^{2+} as the charge balancing cation. Cyan represents Si, red O, magenta Al, dark gray Ca, and light gray K (on the backside).

Comparison of the Reactivity of 2D and 3D Aluminosilicates

A theoretical investigation of adsorption on the 2D aluminosilicate surfaces was begun. Water adsorption on $\text{Si}_2\text{AlO}_6\text{Ca}$ was investigated to determine if water splitting due to the divalent cation could create acidic protons as has been suggested in the literature. It was found that dissociated water was unstable on this surface; however, molecular water adsorbed 777 meV stronger to the $\text{Si}_2\text{AlO}_6\text{Ca}$ surface than to the pure silica bilayer, which could be associated with stronger hydrogen bonding to oxygens adjacent to Al. Therefore, it was concluded that acid sites do not necessarily accompany divalent cations. For NO adsorption, Cu^+ was initially considered as the transition metal cation because Cu zeolites are important NO reduction catalysts for diesel emissions⁴ and because electron correlations are less significant in Cu^+ compounds than in Co-containing oxides making the calculations more tractable and applicable to experiment without requiring correction factors for electron correlations. It was found that NO dissociation on a single Cu site was unstable but that molecular adsorption was quite strong with an adsorption energy of -1.51 eV. Interestingly, it was found that NO adsorption relaxes much of the distortion induced by incorporating the small Cu^+ ion into the six-membered ring. The results were compared to chabazite with the same Al content and a significantly lower -1.05 eV adsorption energy was obtained. It is suggested that relief of the ring strain afforded by NO adsorption on the 2D aluminosilicate is in part responsible for the stronger adsorption. The results show that the transition metal cation behaves qualitatively similar in the two environments (molecular adsorption) and that the strain in fitting the small Cu^+ into the 2D structure can make the 2D material more reactive than a conventional zeolite. Building on this result, calculations on adsorption energies on a series of bases with the protonated form of the 2D aluminosilicate and chabazite were initiated to get a measure of how the acidity of the 2D material compares to conventional zeolites. It was found that adsorption energies do not correlate with the proton affinity of the base but rather non-acid-base interactions with the framework play a decisive role. Therefore, continuing effort is directed towards understanding differences in the ability of the materials to promote chemical transformations with alcohol dehydration as a model reaction.

Growth and Characterization of 2D Aluminosilicates

Experimental work has focused on preparing and characterizing 2D aluminosilicate surfaces. Late transition metals stable to high temperatures are required substrates for 2D aluminosilicate growth. For this work, Pd(111) was an appealing substrate since it only molecularly adsorbs NO in a well-defined way and so its contribution to NO adsorption and reaction measurements could easily be taken into account. Thus far, 2D SiO_2 has been grown and characterized on the Pd(111) surface. Electron diffraction data (Fig. 2a) reveals two preferred orientations of a crystalline hexagonal film: one aligned with the substrate close-packed directions and the other rotated 30°. Additional spots close to the primary spots can be attributed to the lattice mismatch between the 2D material and the substrate. The wider range STM image in Fig. 2c, shows periodic features that are much too large to be due to atomic features. Zooming further in, Fig. 2c, shows a hexagonal arrangement of holes superimposed on the larger corrugation; the spacing between these features corresponds to the unit cell of the bilayer. The larger range corrugation can then be assigned to a moiré pattern due to the lattice mismatch between the 2D material and

the substrate. As illustrated in Figs. 2d,e, a model with a relaxed bilayer rotated 4° with respect to Pd[011] can reproduce both the moiré pattern in the STM image and the LEED pattern. Therefore, it is concluded that the 2D material relaxes to its favored lattice constant and is not stretched to match the substrate as occurs with growth on Pd(100) and Ru(0001).^{1,2} This can be attributed to the larger mismatch compared to Ru(0001) and the biaxial strain required to match the hexagonal Pd(111) surface compared to Pd(100) where uniaxial strain would suffice. Curiously, Pt(111) with an even larger mismatch than Pd(111) only supports the growth of an amorphous 2D silica phase.⁵

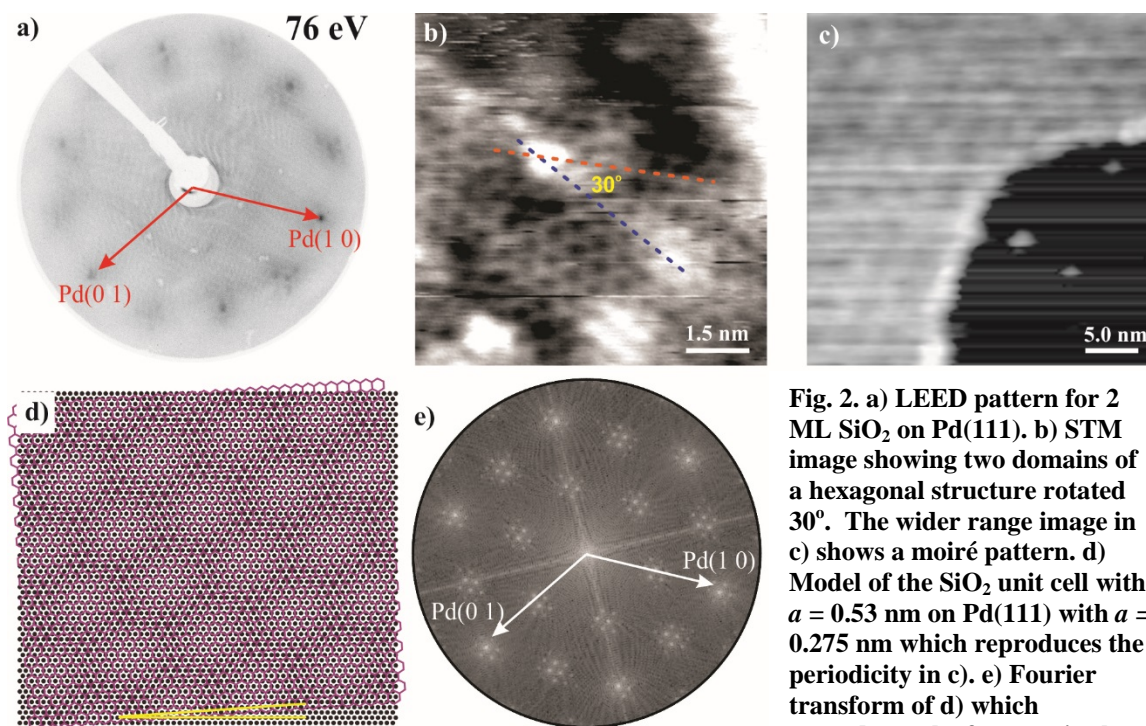


Fig. 2. a) LEED pattern for 2 ML SiO₂ on Pd(111). b) STM image showing two domains of a hexagonal structure rotated 30°. The wider range image in c) shows a moiré pattern. d) Model of the SiO₂ unit cell with $a = 0.53$ nm on Pd(111) with $a = 0.275$ nm which reproduces the periodicity in c). e) Fourier transform of d) which reproduces the features in the LEED pattern in a).

Publications Acknowledging this Grant in 2013-2016

Grant started in 8/2015 – publications in progress:

(II) *Jointly funded by this grant and other grants with leading intellectual contribution from this grant;*

J.-H. Jhang, C. Zhou, G. Hutchings, U.D. Schwarz and E.I. Altman, “Growth of Incommensurate Crystalline Two-Dimensional Silicates on Pd(111),” in preparation

(III) *Jointly funded by this grant and other grants with relatively minor intellectual contribution from this grant;*

A. Malashevich, S. Ismail-Beigi and E.I. Altman, “Evaluating Approaches to Directing the Structure of Two-Dimensional Silica and Silicates,” ACS Nano, to be submitted.

References

- ¹M. Heyde, S. Shaikhutdinov, and H. J. Freund. *Two-dimensional Silica: Crystalline and Vitreous*. Chemical Physics Letters **550**, 1 (2012).
- ²E. I. Altman, J. Götzen, N. Samudrala, and U. D. Schwarz. *Growth and Characterization of Crystalline Silica Films on Pd(100)*. Journal of Physical Chemistry C **117**, 26144 (2013).
- ³E. I. Altman and U. D. Schwarz. *Structural and Electronic Heterogeneity of Two Dimensional Amorphous Silica Layers*. Advanced Materials Interfaces **1**, 1400108 (2014).
- ⁴F. Gao, J. H. Kwak, J. Szanyi, and C. H. F. Peden. *Current Understanding of Cu-Exchanged Chabazite Molecular Sieves for Use as Commercial Diesel Engine DeNOx Catalysts*. Topics in Catalysis **56**, 1441 (2013).
- ⁵Y. Xin, Y. Bing, J. Anibal Boscoboinik, S. Shaikhutdinov, and H. J. Freund. *Support Effects on the Atomic Structure of Ultrathin Silica Films on Metals*. Applied Physics Letters **100**, 151608 (2012).

Aaron M. Appel

**Designing Catalysts Using an Energy-Based Approach:
Molecular Catalysis for CO₂ Reduction**

Aaron Appel, John Linehan, Eric Wiedner,
Kit Zall, Samantha Connelly, Samantha Burgess
Institute for Integrated Catalysis, Pacific Northwest National Laboratory

Presentation Abstract

The intermittent and distributed nature of carbon-neutral energy production necessitates efficient energy storage with a high capacity. The storage of energy in the form of chemical fuels can meet this need, but these transformations require catalysts. The reduction of CO₂ has a particular advantage over production of H₂, in that liquid fuels can be produced for use in transportation. We seek to develop an understanding of how to rationally design catalysts for the reduction of CO₂. Our approach involves studying each of the reduction steps in the overall transformation.

One of the first steps in the reduction of CO₂ is the formation of the initial C-H bond by hydride transfer. For the hydrogenation of CO₂ to formate using first row transition metal complexes, we are focused on using the free energy of transferring a hydride to CO₂ to design catalyst systems. Nickel hydride complexes are typically unable to hydrogenate CO₂ due to inadequate hydricities, however, we have used a change in solvent to bias the relative stabilities of the catalytic intermediates. Copper hydride complexes have been shown to be active for stoichiometric CO₂ reduction, but typically do not turnover using H₂ as the reductant. Thermodynamic and catalytic studies of copper complexes for the hydrogenation of CO₂ will be presented and demonstrate that the active metal hydride can be regenerated with H₂.

**FWP-47319: Low-Temperature Catalytic Routes for Energy Carriers via Spatial
and Chemical Organization**

PI: Johannes Lercher

Evolution of the Catalyst Composition and Structure during Reaction

Perla B. Balbuena¹, Jose L. Gomez-Ballesteros¹ and Juan C. Burgos;¹ Pin Ann Lin^{2,3} and Renu Sharma²

¹Department of Chemical Engineering, Texas A& M University, College Station, TX 77843; ²Center for Nanoscale Science and Technology, National Institute of Standards and Technology, Gaithersburg, MD 20899-6203³; University of Maryland – IREAP, College Park, MD 20742

Presentation Abstract

A combined theoretical and experimental approach is used to elucidate the changes in composition and structure occurring in Co nanoparticles supported on MgO during decomposition of acetylene forming single-walled carbon nanotubes. High resolution environmental transmission electron microscopy (ETEM) measurements identify the presence of carbide and metallic phases inside the nanoparticle. Reactive molecular dynamics simulations follow the trajectories of carbon atoms in a nanoparticle with a Co₂C composition during reaction and recognize changes in the composition of the nanocatalyst while the nanotube starts nucleating and growing over the nanoparticle. A carbon mass balance in the nanocatalyst is formulated on the carbide nanoparticle including rates of dissolution, carbide formation and decomposition, and nanotube growth. Each of the terms is characterized via molecular simulations coupled with ETEM images.

Grant Number: DE-FG02-06ER15836 Grant Title: Modeling Catalyzed Growth of Single-Walled Carbon Nanotubes

PI: Perla B. Balbuena

Postdoc(s): Juan C. Burgos

Student(s): Jose L. Gomez-Ballesteros, Behnaz Rahmani Didar

RECENT PROGRESS

Dynamics and stability of a carburized nanocatalyst

The dynamics and stability of a carburized nanocatalyst at the single-walled carbon nanotubes (SWCNTs) synthesis temperature (1000K), its local composition, shape, electronic structure, and interactions with nascent nanotube caps were investigated using density functional theory (DFT) and ab initio molecular dynamics simulations (AIMD).

Although the dynamic evolution of the catalyst and the nanotube was studied by us and others in the past using reactive classical molecular dynamics (RMD) providing a step-by-step picture of the catalytic process, diffusion in the nanoparticle, and incorporation into the growing nanotube of the precursor carbon, we have gained further insights into the effects of electronic distribution without the bias imposed by effective force fields. We used AIMD to study the dynamics of a carburized Ni nanoparticle under typical CVD synthesis conditions and the same nanoparticle in contact with model nanotube caps resembling the early stages of nanotube growth. Because the extension of the simulated timeframe is limited and phenomena such as the incorporation of C atoms to the nanotube rim were not included, this study resembled growth in the limit of low pressure of precursor gas. Comparisons between the pure metallic particle and the carburized particle helped us to elucidate the interactions of these catalysts with the growing carbon nanotube.

Carbon dissolution and stability of the carburized metal nanoparticle were observed throughout the simulation. Structural changes in the nanocatalyst structure were monitored through the extension of the simulation showing that in the absence of a substrate, the nanocatalyst fails to maintain a defined faceted structure. However, in the presence of a nascent nanotube cap, the floating catalyst accommodates to the shape of the nanotube in accordance with what is known as an “inverse template effect”. We found lack of association of carbon atoms inside the nanoparticle and evidence of short-range ordering from distance- and radial distribution function analyses, which may be indicators of the stability and potential for evolution of the nanoparticle system into a more thermodynamically stable phase such as that of a carbide phase. Moreover, the lack of incorporation of C atoms from the nanoparticle into the nanotube rim supports the idea that a state of saturation or supersaturation of the nanoparticle is needed for the precipitation of C from the stable Ni–C core to the surface, and incorporation into the nanotube rim to occur, leaving the most of the catalytic growth to the surface-diffusing C species as reported in previous studies.

Analyses of the electronic structure of the nanoparticle during growth revealed that a charge transfer process occurs from the surface Ni atoms and rim C atoms to the interfacial region between the growing nanotube and the nanoparticle. This process leaves an interfacial region rich in electron density, where incorporation of precursor C may continue the growth process, and electron depleted regions in the vicinity of the nanotube rim that may allow rearrangement of the C atoms near the rim and healing of defects (Figure 1).

A comparison between the charge transfer in a carburized nanoparticle and a pure metal nanoparticle reveals that the process occurs similarly in both systems, but in the case of the carburized nanoparticle the interfacial region is larger and almost continuous along the nanotube rim, whereas the metal nanoparticle displays a smaller and more localized accumulation region. Surface Ni atoms that are not in direct contact with the cap are also affected: a neutral charge characterizes surface Ni atoms in the pure nanoparticle, and positively charged Ni atoms are found at the carburized nanoparticle surface. These observations suggest that the carburized nanoparticle may be able to offer a more reactive environment for nanotube growth than the metallic one. These results were reported in a peer-reviewed publication (*Phys. Chem. Chem. Phys.*, 2015, 17, 15056-15064)

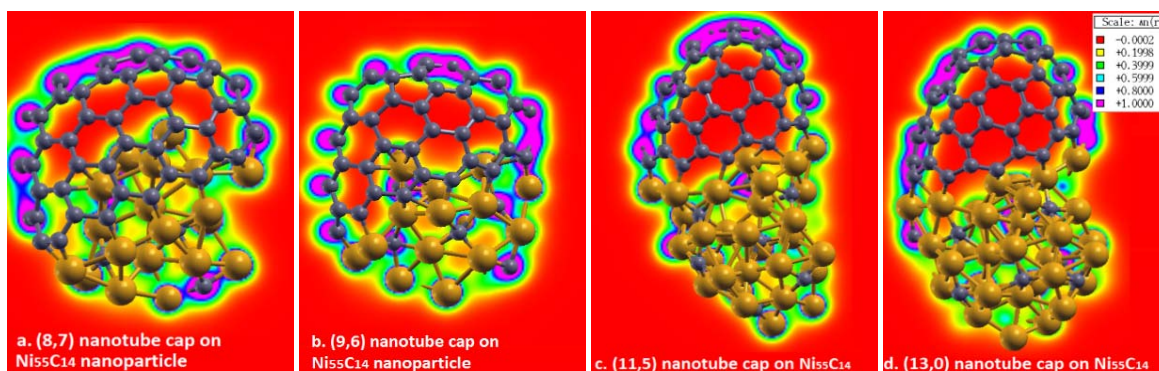


Figure 1. Electron density maps for the carburized nanoparticle with a cap of chiral indexes a. (8,7), b. (9,6), c. (11,5), and d. (13,0). The color images were obtained using the software XCrySDen.

Nanocatalyst shape and composition during nucleation of SWCNTs

In collaborative work with the group of Dr. Renu Sharma at NIST, we studied the evolution of the structure of the catalyst nanoparticle during the early stages of carbon dissolution and nucleation of SWCNTs. Variations in shape, atomic ordering, and carbon concentration profile were investigated by a combination of RMD and AIMD simulations coupled to analyses of real-time atomic-resolution videos taken in an environmental transmission electron microscope (ETEM) carried out at NIST. We looked closely at the interactions of the nanoparticle with the substrate and the nucleating nanotube cap, and their effect on the nanoparticle structural parameters. Changes in the nanocatalyst shape and composition are examined throughout the nucleation process beginning with carbon dissolution, diffusion and formation of carbon chains on the surface until a cap is fully formed and the nanotube structure defined (Figure 2).

The amount of carbon dissolved in the carbide-like nanoparticle decreases as C atoms precipitate at the surface. Once nucleation of the surface C atoms begins, a steady state global C concentration is reached. Changes in the nanoparticle shape occur linked with changes in the dynamics of C atoms according to experiments and RMD simulations: a decrease of the nanoparticle height and spreading over the substrate is observed while the C composition is stabilized, no changes occur as the cap is being formed, and subsequent elongation and shape recovery take place due to interactions with the cap as it lifts off. The main two factors influencing nanoparticle shape and C distribution can thus be summarized as: interactions with the substrate and interactions with the nascent nanotube. The nanoparticle evolution in relation to its interaction with the substrate from AIMD studies reveals that the nanoparticle–substrate interface is dominated by interactions between Co atoms located atop O atoms in the substrate. Strong nanoparticle–substrate interactions are characterized by electron transfer and re-arrangement of Co atoms at the interface stemming from a given Co_2C surface termination (i.e. (020) and (210)). The interactions of the nanocatalyst with the cap are responsible for the C gradient observed along the direction perpendicular to the substrate

in both simulations and experiments. This suggests that the catalyst topmost layer is a primary source of C atoms for the formation of the nanotube cap. Overall we concluded that the combination of atomistic simulations and in situ observation of SWCNT growth provides insights into the fundamental phenomena driving the observed changes in the nanoparticle and allows the identification of key aspects for the formulation of models and mechanisms to better understand and control the catalytic process. These results were published in *RSC Adv.*, 2015, 5, 106377–106386.

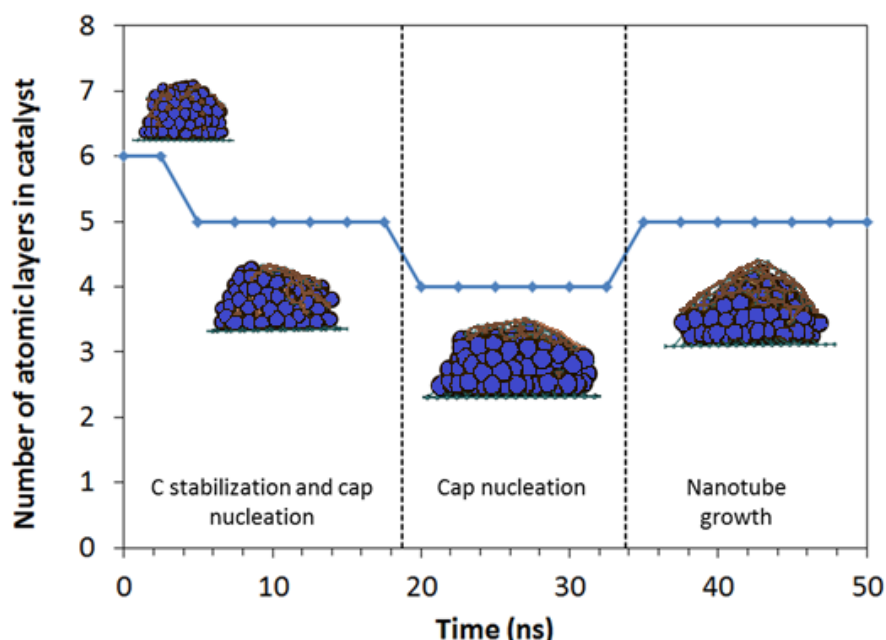


Figure 2. Shape evolution of the catalyst nanoparticle during the various nucleation and growth stages. RMD simulations illustrate that during carbon stabilization, the metal layer in contact with the substrate tends to wet the substrate (first ≈ 15 ns). Carbon nucleation starts before carbon stabilization is reached and leads to further reduction in the number of layers of the nanocatalyst particle. The slight vertical elongation of the nanocatalyst particle coincides with the beginning of the growth stage.

Currently we are finishing another report in collaboration with the NIST group that deals with the identification of changes in the catalytic composition and structure during the catalytic reaction and the connection of those changes to the rate of the reaction. Highlights of this work will be discussed in the poster presentation.

Publications Acknowledging this Grant in 2013-2016

(1) *Exclusively funded by this grant*

1. D. A. Gómez-Gualdrón and P. B. Balbuena, “Characterization of Carbon Atomistic Pathways during Single-Walled Carbon Nanotube Growth on Supported Metal Nanoparticles”, *Carbon*, **2013**, 57, 298-309.

2. D. A. Gómez-Gualdrón, J. M. Beetge, J. C. Burgos, and P. B. Balbuena, "Effects of precursor type on the CVD growth of single-walled carbon nanotubes," *J. Phys. Chem. C*, **2013**, *117*, 10397-10409.
3. D. A. Gómez-Gualdrón, J. M. Beetge, and P. B. Balbuena, "Characterization of metal nanocatalyst state and morphology during simulated single-walled carbon nanotube growth," *J. Phys. Chem. C*, **2013**, *117*, 12061-12070.
4. J. C. Burgos and P. B. Balbuena, "Preferential Adsorption of Zigzag Single-Walled Carbon Nanotubes on the ST-cut of Quartz," *J. Phys. Chem. C*, **2013**, *117*, 4639-4646.
5. J. C. Burgos, E. Jones, and P. B. Balbuena, "Dynamics of Topological Defects in Single-Walled Carbon Nanotubes during Catalytic Growth," *J. Phys. Chem. C*, **2014**, *118*, 4808-4817.
6. J. C. Burgos and P. B. Balbuena, "Engineering Preferential Adsorption of Single-Walled Carbon Nanotubes on Functionalized ST-cut Surfaces of Quartz," *ACS Appl. Mater. Inter.*, **2014**, *6*, 12665-12673.
7. M. Picher, P. A. Linn, J. L. Gómez-Ballesteros, P. B. Balbuena, and R. Sharma, "Nucleation of Graphene and its Conversion to Single-Walled Carbon Nanotubes," *Nano Lett.*, **2014**, *14*, 6104-6108.
8. Jose L. Gomez-Ballesteros and Perla B. Balbuena, "Structure and Dynamics of Metallic and Carburized Catalytic Ni Nanoparticles: Effects on Growth of Single-Walled Carbon Nanotubes," *Phys. Chem. Chem. Phys.*, **2015**, *17*, 15056-15064.
9. Jose L. Gomez-Ballesteros, Juan C. Burgos, Pin Ann Lin, Renu Sharma, and Perla B. Balbuena, "Nanocatalyst shape and composition during nucleation of single-walled carbon nanotubes," *RSC Advances*, **2015**, *5*, 106377-106386.

(2) Jointly funded by this grant and other grants with leading intellectual contribution from this grant

J. L. Gómez-Ballesteros, A. Callejas-Tovar, L. A. F. Coelho, and P. B. Balbuena, "Molecular dynamics studies of graphene exfoliation using supercritical CO₂," in J. M. Seminario (Editor) "Design and applications of nanomaterials for devices and sensors," V. **2014**, *16*, p. 171-183.

Ludwig Bartels

Multiscale Imaging and Characterization of the Interaction of Thiols with Single-Layer MoS₂

Ludwig Bartels, Talat S. Rahman^{*}, Peter Dowben⁺, Koichi Yamaguchi, Duy Le,^{*} Takat B. Rawal,^{*} Miguel Isarraraz, Joseph Martinez, Michael Valentin, Alison Guan, Ariana Nguyen, Emily Li, KatieMarie Magnone, Sampyo Hong^{*}
University of California at Riverside
(*=University of Central Florida; +=University of Nebraska)

Presentation Abstract

We present experimental and theoretical investigations of the chemical interaction of single-layer films/islands of MoS₂ with thiol-containing adsorbates. MoS₂ is a versatile catalyst with industrial application in hydro-desulfurization (HDS) and emerging applications in electrochemical water splitting and alcohol formation. Interaction with sulfur-containing species is important for HDS as well as MoS₂ catalyst regeneration in any other application. Our multipronged effort involves scanning tunneling microscopy imaging, density functional theory simulation, photoluminescence imaging and thermally programmed desorption. The latter two approaches are based on the setup of dedicated instrumentation; they offer a complementary approach to the properties of this catalyst material that permits probing from ultra-high vacuum to ambient pressures and above.

Additional work in this project addresses the formation and decomposition of alcohols on MoS₂ surfaces, which is described in a separate poster.

Stacey F. Bent

Transition Metal Catalysts for Syngas Conversion to Higher Oxygenates

Nuoya Yang, Joseph Singh, and Stacey F. Bent
Department of Chemical Engineering
443 Via Ortega, Shriram Building
Stanford University
Stanford, CA 94305-5025
Phone: (650) 723-0385
E-mail: sbent@stanford.edu

Presentation Abstract

Synthesis gas ($\text{CO} + \text{H}_2$) conversion is a promising route for converting coal, natural gas, or biomass into synthetic liquid fuels. Currently, however, no catalyst meets the selectivity and activity requirements for industrial-scale production of ethanol. This effort within the FWP focuses on developing a basic understanding of catalytic activity and selectivity toward syngas conversion into higher oxygenates, and identifies heterogeneous catalysts, active sites, and structures favorable for this reaction. We will report on both single elemental Rh catalysts as well as metal alloys. The intrinsic selectivity of Rh is investigated by combining experiments and theoretical calculation. A microkinetic model based upon density functional theory (DFT) calculations shows that the intrinsic selectivity of Rh is highly structure sensitive. Rh/SiO₂ catalysts are synthesized using different silica pretreatment, Rh precursors and choice of silica supports. From experimental reaction testing, a strong inverse correlation between catalytic activity and C₂₊ oxygenate selectivity is observed, consistent with the structure-sensitivity predicted from theory. Beyond elemental metals, metal alloys are a potential class of catalysts for syngas conversion. Alloy screening studies based on DFT point to a narrow list of candidates for the selective hydrogenation of carbon monoxide to higher alcohols. One of these candidates, Pt-Co, was synthesized using traditional wet synthesis and atomic layer deposition. The prepared catalysts demonstrate increased selectivity towards methanol and higher alcohols. *In situ* infrared spectroscopy studies point to the importance of a balance between bridging and linear CO motifs in obtaining higher alcohol selectivity in this reaction.

FWP SLAC-10049: SUNCAT Center for Interface Science and Catalysis

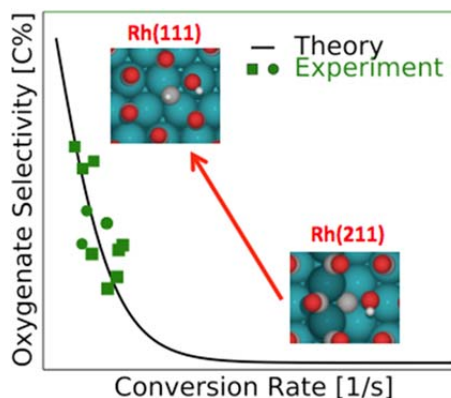
PI: Jens Norskov

Student(s): Nuoya Yang, Joseph Singh, A.J. Medford

RECENT PROGRESS

Structure Sensitivity of Rhodium Catalysts for C₂₊ Oxygenate Production

Rhodium has long been studied as a catalyst for synthesis gas (CO + H₂) conversion as it is the only elemental catalyst that has demonstrated selectivity to ethanol and other C₂₊ oxygenates. However, the fundamentals of syngas conversion over rhodium are still debated. To improve atomic-scale understanding of the active sites for higher alcohol synthesis, we investigated the intrinsic selectivity of Rh by combining experiments and theoretical calculation. We developed a microkinetic model for conversion of CO and H₂ into methane, ethanol, and acetaldehyde on the Rh (211) and (111) surfaces, chosen to describe steps and close-packed facets on catalyst particles. The model was based on DFT calculations using the BEEF-vdW functional. The mean-field kinetic model included lateral adsorbate-adsorbate interactions, and the BEEF-vdW error estimation ensemble was used to propagate error from the DFT calculations to the predicted rates. The model showed the Rh(211) surface to be ~6 orders of magnitude more active than (111) surface, but highly selective towards methane, while the Rh(111) surface is intrinsically selective toward acetaldehyde. A variety of Rh/SiO₂ catalysts were synthesized, tested for catalytic oxygenate production, and characterized using TEM. The experimental results indicated that the Rh(111) surface is intrinsically selective towards acetaldehyde, and a strong inverse correlation between catalytic activity and oxygenate selectivity was observed. The experimental observations are consistent with the structure-sensitivity predicted from theory. This work provided an improved atomic-scale understanding and new insight into the mechanism, active site, and intrinsic selectivity of syngas conversion over rhodium catalysts and may also guide rational design of alloy catalysts made from more abundant elements.



Correlation between activity and selectivity toward total C₂₊ oxygenates: comparison of theory and experiment

Understanding Active Sites in Ethanol Synthesis on PtCo Catalysts Prepared using Atomic Layer Deposition

Currently, no catalyst meets the selectivity and activity requirements for industrial-scale production of ethanol from syngas. Using atomic layer deposition (ALD), we have synthesized transition metal catalysts for this reaction by introducing metalorganic precursors in the gas phase. Through controlled deposition of metal layers, we created model alloy catalysts to gain insights into the mechanism of syngas conversions to ethanol and other oxygenates. In particular, platinum cobalt alloys have been reported as a potential catalyst candidate. We created PtCo catalysts using ALD and compared their catalytic performance and structure to catalysts prepared using traditional methodologies.

The addition of Pt using ALD to Co catalysts resulted in increased selectivity towards methanol and higher alcohols and decreased selectivity towards longer chain hydrocarbon products. Using *in situ* diffuse reflectance infrared Fourier transform spectroscopy, we demonstrated that the interplay of bridging and linear CO species is important in carrying out oxygenate synthesis on PtCo catalysts.

Publications Acknowledging this Grant in 2013-2016

(1) *Exclusively funded by this grant;*

N. Yang, A. J. Medford, X. Liu, F. Studt, T. Bligaard, S. F. Bent, and J. K. Nørskov, On the Intrinsic Selectivity and Structure Sensitivity of Rhodium Catalysts for C₂₊ Oxygenate Production, *J. Am. Chem. Soc.*, **2016**, *138*, 3705–3714.

The abstract/progress represents work on heterogeneous catalysis for syngas conversion supervised by Stacey Bent within the FWP.

Michelle C. Chang

Hybrid Bioinorganic Approach to Solar-to-Chemical Conversion

Michelle C. Chang, Christopher J. Chang, and Peidong Yang
Lawrence Berkeley National Laboratory and UC Berkeley

Presentation Abstract

Our collaborative work between our group and the C. Chang and Yang groups seeks to develop approaches to integrate chemical and biology catalysis for solar-to-fuel conversion consisting of light-harvesting nanowires functionalized with hydrogen-producing catalysts and living microbes as an autotrophic chassis for the production of value-added fuels and other chemicals from CO₂ and photogenic H₂. Using this approach, we have been able to produce acetate and methane from CO₂ and light energy. Interfacing biocompatible solid-state nanodevices with living systems provides a starting point for developing a programmable system of chemical synthesis entirely powered by sunlight.

Grant or FWP Number: CH030201

Grant Title: Catalysis Research Program

PI: John F. Hartwig

Student(s): Joseph J. Gallagher and Eva M. Nichols

RECENT PROGRESS

Genetic engineering of methanogens

We have been able to culture and make genetic modifications to *Methanococcus maripaludis*, a non-model methanogen. We have overexpressed genes to make ethanol from fixed CO₂ and generated knockout strains to deregulate nitrogen fixation. We are in the process of analyzing these strains for their metabolic physiology.

Publications Acknowledging this Grant in 2013-2016

Liu, C.; Gallagher, J. J.; Sakimoto, K. K.; Nichols, E. M.; Chang, C. J.; Chang, M. C. Y.; Yang, P. Nanowire-Bacteria Hybrids for Unassisted Solar Carbon Dioxide Fixation to Value-Added Chemicals. *Nano Lett.* **2015**, *15*, 3634-3639. (II)

Nichols, E. M.; Gallagher, J. J.; Liu, C.; Su, Y.; Rasasco, J.; Yu, Y.; Sun, Y.; Yang, P.; M. C. Y.; Chang, C. J. Hybrid Bioinorganic Approach to Solar-to-Chemical Conversion. *PNAS* **2015**, *112*, 11461-11466. (II)

Abhaya K. Datye and Yong Wang

Sub Nanometer Sized Clusters for Heterogeneous Catalysis

Abhaya Datye¹ and Yong Wang²

¹University of New Mexico and ²Washington State University

Presentation Abstract

The focus of this project is the synthesis, characterization and reactivity of transition metal moieties ranging from single atoms to clusters of about 1 nm in diameter that are present on high surface area supports. A major barrier in the utilization of sub-nm clusters is that they are subject to Ostwald ripening, leading to growth in size to form nanoparticles. Previous work suggests that trapping single atoms on the support could help to slow the rates of ripening. Hence, one of the goals of this project is the understanding of anchoring sites on high surface area catalyst supports. Conventional (non-reducible) oxide supports provide only limited number of sites to anchor ionic species. Reducible oxides provide many more sites for anchoring due to the presence of defects, such as vacancies. But reducible oxides are often not available in high surface area form, and they may not be as robust (can react to form carbonates, for example, or sinter easily) compared to the commonly-used high surface area supports such as silica, alumina, or carbon. Increasing atomic trapping sites on conventional catalyst supports is therefore important for improving the stability of sub-nm metal clusters on a supported catalyst. Another goal of this project is to expand the applicability of single atom catalysts to a broader class of catalyzed reactions. Transition metals in ionic form are perfectly situated for further manipulation of their catalytic activity by use of ligands, as in homogeneous catalysis. Understanding the principles that help in the design of robust single atom catalysts is one of the research challenges that is addressed in this project.

DOE grant # DE-FG02-05ER15712

Sub Nanometer Sized Clusters for Heterogeneous Catalysis

Post-docs: Andrew DeLaRiva and Eric Petersen (UNM)

Graduate Students: Angelica Benavidez, Monique Curley, Chris Riley (UNM), Xavier Isidro Pereira Hernández, Jianghao Zhang, Nick Jaeger (WSU)

RECENT PROGRESS

Thermally Stable Single Atom Catalysis via Atom Trapping

Single atom catalysts have attracted attention due to enhanced reactivity, selectivity and the benefit of efficient utilization of scarce precious metals. However, single atoms on catalyst supports can be mobile and aggregate into nanoparticles when heated at elevated temperatures. Heating these catalysts to high temperatures is detrimental to performance, unless, as we show here, these mobile species can be trapped. We used ceria powders having similar surface areas, but different exposed surface facets. When mixed with a Pt/Al₂O₃ catalyst and aged in air at 800 °C, the Pt transferred to the ceria. Polyhedral ceria and nanorods were more effective than ceria cubes at anchoring the Pt. The benefit of the high temperature synthesis is that only the most stable binding sites are occupied, creating a sinter-resistant, atomically dispersed catalyst.

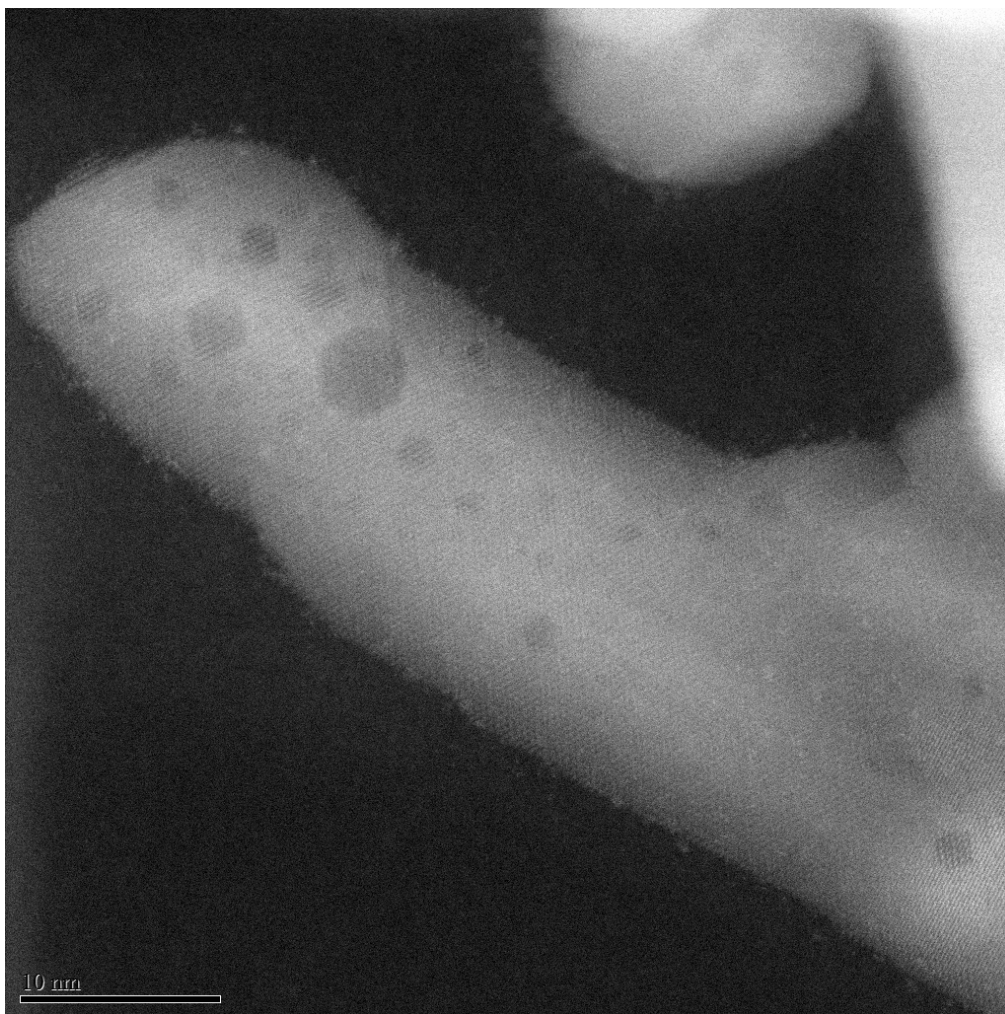


Figure 1. AC-STEM image of Pt/CeO₂ nano rods after aging in air for 800 °C in flowing air. Single atom Pt species are trapped on the surface of ceria.

Role of Sn in the regeneration of Pt-Sn/alumina catalysts for propane dehydrogenation

Alumina-supported Pt is one of the major industrial catalysts for light alkane dehydrogenation. This catalyst loses activity during reaction, with coke formation often considered as the reason for deactivation. As we recently demonstrated, the amount and nature of carbon deposits do not directly correlate with the loss of activity. Rather, it is the transformation of sub-nanometer Pt species into larger Pt nanoparticles that appears to be responsible for the loss of catalytic activity. Surprisingly, a portion of the Sn remains atomically dispersed on the alumina surface in the spent catalyst and helps in the redispersion of the Pt. In the absence of Sn on the alumina support, the larger Pt nanoparticles formed during reaction are not redispersed during oxidative regeneration. It is known that Sn is added as a promoter in the industrial catalyst to help in achieving high propene selectivity and to minimize coke formation. We have shown that an important role of Sn is to help in the regeneration of Pt, by providing nucleation sites on the alumina surface. Aberration-corrected scanning transmission electron microscopy helps to provide unique insights into the operating characteristics of an industrially important catalyst by demonstrating the role of promoter elements, such as Sn, in the oxidative regeneration of Pt on γ -Al₂O₃.

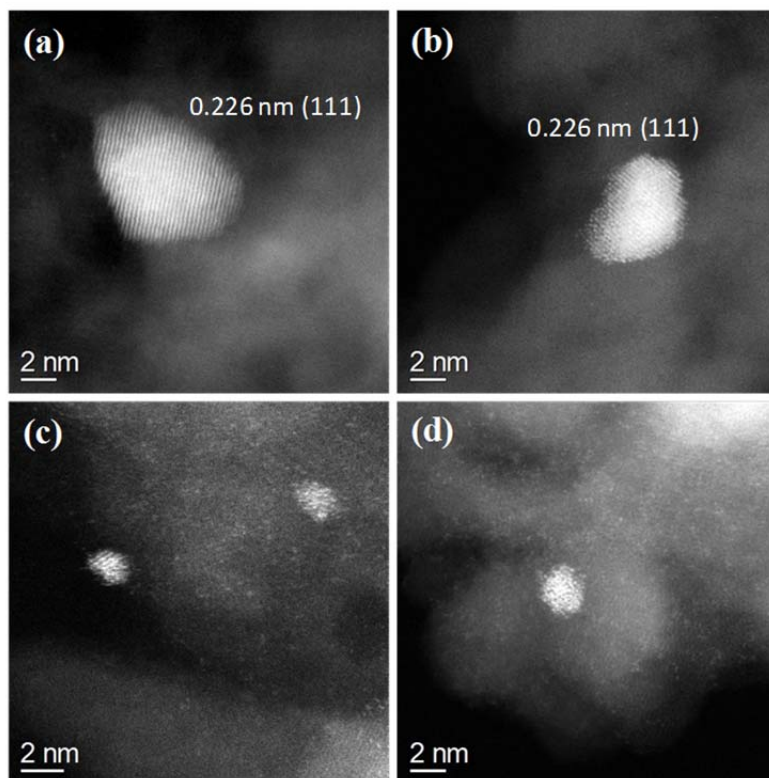


Figure 2. AC-STEM images of the Pt/ γ -Al₂O₃ (a, b) and Pt-Sn/ γ -Al₂O₃ (c, d) catalysts after 10 propane dehydrogenation cycles. No single atoms are present in Pt/ γ -Al₂O₃, but isolated single atoms are abundant on the bimetallic catalyst. These single atoms are needed to regenerate the catalyst by re-dispersion of Pt, as is seen to occur in the case of Pt-Sn/ γ -Al₂O₃.

Pd modified Fe₂O₃ catalysts

Hydrodeoxygenation (HDO) of phenolic compounds is an important model reaction in understanding the fundamental and application of catalysis in lignin based biofuel production. Recently, Fe has emerged as a promising catalyst for HDO of phenolics, due to its low cost and high selectivity in C-O bond cleavage. However, the low HDO activity of Fe and poor stability under HDO conditions has limited its application. We have recently developed an efficient approach to promote the activity and stability of Fe without altering its unique selectivity in HDO of phenolics, by doping noble metals such as Pd onto the Fe catalyst surface. A series of noble metal doped Fe catalysts were tested in HDO of m-cresol. Noble metals remarkably promoted the activity and stability of Fe, while maintaining the high C-O bond cleavage selectivity of Fe. The Pd-on-Fe nanostructure with sub-nm Pd clusters on reduced Fe surface in Pd-Fe catalyst was evidenced by high resolution STEM and pseudo in situ XPS. A direct C-O bond cleavage mechanism, in which m-cresol decomposes on Fe surface into C₇H₇* and OH* species and the formed species further reacts with H atoms to form toluene and water, respectively, was proposed based on DFT calculation and kinetic modeling. Kinetic modeling and in situ AP-XPS results suggested that the Fe catalyst surface is dominated by OH* species, which ultimately lead to a deactivation of Fe catalyst. Addition of Pd to Fe significantly changes its kinetics by creating new sites for H₂ activation and new reaction pathways via reaction between H activated on Pd sites and C₇H₇* and OH* on Fe sites, as suggested by kinetic modeling. As a result, the surface of Pd-Fe is no longer dominated by OH* and catalyst deactivation by water induced oxidation is thus avoided.

Publications acknowledging this grant (2013-2016)

1. H.N. Pham, J.J.H.B. Sattler, B.M. Weckhuysen, and A.K. Datye, *Role of Sn in the Regeneration of Pt/ γ -Al₂O₃ Light Alkane Dehydrogenation Catalysts*. ACS Catalysis, 2016: p. 2257-2264.
2. H. Xiong, A. DeLaRiva, Y. Wang, and A.K. Datye, *Low-temperature aqueous-phase reforming of ethanol on bimetallic PdZn catalysts*. Catalysis Science & Technology, 2015. **5**(1): p. 254-263.
3. H. Xiong, A. DeLaRiva, Y. Wang, and A.K. Datye, *Low-temperature aqueous-phase reforming of ethanol on bimetallic PdZn catalysts*. Catalysis Science & Technology, 2015. **5**(1): p. 254-263.
4. Z. Wei, A.M. Karim, Y. Li, D.L. King, and Y. Wang, *Elucidation of the roles of Re in steam reforming of glycerol over Pt-Re/C catalysts*. Journal of Catalysis, 2015. **322**: p. 49-59.
5. J. Sun, A.M. Karim, D. Mei, M. Engelhard, X. Bao, and Y. Wang, *New insights into reaction mechanisms of ethanol steam reforming on Co-ZrO₂*. Applied Catalysis B-Environmental, 2015. **162**: p. 141-148.

6. A.M. Karim, N. Al Hasan, S. Ivanov, S. Siefert, R.T. Kelly, N.G. Hallfors, A. Benavidez, L. Kovarik, A. Jenkins, R.E. Winans, and A.K. Datye, *Synthesis of 1 nm Pd Nanoparticles in a Microfluidic Reactor: Insights from in Situ X-ray Absorption Fine Structure Spectroscopy and Small-Angle X-ray Scattering*. *Journal of Physical Chemistry C*, 2015. **119**(23): p. 13257-13267.
7. H. Zhang, J. Sun, V.L. Dagle, B. Halevi, A.K. Datye, and Y. Wang, *Influence of ZnO Facets on Pd/ZnO Catalysts for Methanol Steam Reforming*. *ACS Catalysis*, 2014. **4**(7): p. 2379-2386.
8. J. Sun and Y. Wang, *Recent Advances in Catalytic Conversion of Ethanol to Chemicals*. *ACS Catalysis*, 2014. **4**(4): p. 1078-1090.
9. E.J. Peterson, A.T. Delariva, S. Lin, R.S. Johnson, H. Guo, J.T. Miller, J.H. Kwak, C.H.F. Peden, B. Kiefer, L.F. Allard, F.H. Ribeiro, and A.K. Datye, *Low-temperature carbon monoxide oxidation catalysed by regenerable atomically dispersed palladium on alumina*. *Nature Communications*, 2014. **5**.
10. J. Paiz, J. Fitch, E. Peterson, T. Hough, W. Barnard, and A. Datye, *Synthesis of PdO-ZnO mixed oxide precursors for PdZn intermetallic catalysts*. *Crystal Research and Technology*, 2014. **49**(9): p. 699-707.
11. C. Liu, H. Wang, A.M. Karim, J. Sun, and Y. Wang, *Catalytic fast pyrolysis of lignocellulosic biomass*. *Chemical Society Reviews*, 2014. **43**(22): p. 7594-7623.
12. J.H. Kwak, R. Dagle, G.C. Tustin, J.R. Zoeller, L.F. Allard, and Y. Wang, *Molecular Active Sites in Heterogeneous Ir-La/C-Catalyzed Carbonylation of Methanol to Acetates*. *Journal of Physical Chemistry Letters*, 2014. **5**(3): p. 566-572.
13. Y. Hong, H. Zhang, J. Sun, K.M. Ayman, A.J.R. Hensley, M. Gu, M.H. Engelhard, J.-S. McEwen, and Y. Wang, *Synergistic Catalysis between Pd and Fe in Gas Phase Hydrodeoxygenation of m-Cresol*. *ACS Catalysis*, 2014. **4**(10): p. 3335-3345.
14. A.J.R. Hensley, Y. Wang, and J.-S. McEwen, *Adsorption of phenol on Fe (110) and Pd (111) from first principles*. *Surface Science*, 2014. **630**: p. 244-253.
15. A.J.R. Hensley, Y. Hong, R. Zhang, H. Zhang, J. Sun, Y. Wang, and J.-S. McEwen, *Enhanced Fe₂O₃ Reducibility via Surface Modification with Pd: Characterizing the Synergy within Pd/Fe Catalysts for Hydrodeoxygenation Reactions*. *ACS Catalysis*, 2014. **4**(10): p. 3381-3392.
16. S.D. Davidson, H. Zhang, J. Sun, and Y. Wang, *Supported metal catalysts for alcohol/sugar alcohol steam reforming*. *Dalton Transactions*, 2014. **43**(31): p. 11782-11802.
17. S.D. Davidson, J. Sun, Y. Hong, A.M. Karim, A.K. Datye, and Y. Wang, *The effect of ZnO addition on Co/C catalyst for vapor and aqueous phase reforming of ethanol*. *Catalysis Today*, 2014. **233**: p. 38-45.
18. A.D. Benavidez, P.D. Burton, J.L. Nogales, A.R. Jenkins, S.A. Ivanov, J.T. Miller, A.M. Karim, and A.K. Datye, *Improved selectivity of carbon-supported palladium catalysts for the hydrogenation of acetylene in excess ethylene*. *Applied Catalysis a-General*, 2014. **482**: p. 108-115.
19. J. Sun, D. Mei, A.M. Karim, A.K. Datye, and Y. Wang, *Minimizing the Formation of Coke and Methane on Co Nanoparticles in Steam Reforming of Biomass-Derived Oxygenates*. *Chemcatchem*, 2013. **5**(6): p. 1299-1303.

20. J. Sun, A.M. Karim, H. Zhang, L. Kovarik, X.S. Li, A.J. Hensley, J.-S. McEwen, and Y. Wang, *Carbon-supported bimetallic Pd-Fe catalysts for vapor-phase hydrodeoxygenation of guaiacol*. *Journal of Catalysis*, 2013. **306**: p. 47-57.
21. C. Liu, J. Sun, C. Smith, and Y. Wang, *A study of Zn_xZr_yO_z mixed oxides for direct conversion of ethanol to isobutene*. *Applied Catalysis a-General*, 2013. **467**: p. 91-97.
22. R.S. Johnson, A. DeLaRiva, V. Ashbacher, B. Halevi, C.J. Villanueva, G.K. Smith, S. Lin, A.K. Datye, and H. Guo, *The CO oxidation mechanism and reactivity on PdZn alloys*. *Physical Chemistry Chemical Physics*, 2013. **15**(20): p. 7768-7776.
23. A.J.R. Hensley, R.Q. Zhang, Y. Wang, and J.S. McEwen, *Tailoring the Adsorption of Benzene on PdFe Surfaces: A Density Functional Theory Study*. *Journal of Physical Chemistry C*, 2013. **117**(46): p. 24317-24328.
24. B. Halevi, S. Lin, A. Roy, H. Zhang, E. Jeroro, J. Vohs, Y. Wang, H. Guo, and A.K. Datye, *High CO₂ Selectivity of ZnO Powder Catalysts for Methanol Steam Reforming*. *Journal of Physical Chemistry C*, 2013. **117**(13): p. 6493-6503.
25. J.R. Gaudet, A. de la Riva, E.J. Peterson, T. Bolin, and A.K. Datye, *Improved Low-Temperature CO Oxidation Performance of Pd Supported on La-Stabilized Alumina*. *Acs Catalysis*, 2013. **3**(5): p. 846-855.
26. A.T. DeLaRiva, T.W. Hansen, S.R. Challa, and A.K. Datye, *In situ Transmission Electron Microscopy of catalyst sintering*. *Journal of Catalysis*, 2013. **308**: p. 291-305.
27. S. Davidson, J. Sun, and Y. Wang, *Ethanol Steam Reforming on Co/CeO₂: The Effect of ZnO Promoter*. *Topics in Catalysis*, 2013. **56**(18-20): p. 1651-1659.
28. A. Datye, *Imaging of Heterogeneous Catalysts*, in *Comprehensive Inorganic Chemistry II (Second Edition)*, J. Reedijk and K. Poeppelmeier, Editors. 2013, Elsevier: Amsterdam. p. p.103-129.

Robert J. Davis

On the Reactivity of Hydroxyapatite Catalysts for C-C Coupling Reactions

Robert J. Davis, Sabra Hanspal, and Zachary Young
Department of Chemical Engineering, University of Virginia,
Charlottesville, VA 22904

Presentation Abstract

The kinetics of aldol condensation of acetaldehyde were studied over anatase titania (TiO_2), hydroxyapatite (HAP) and magnesia (MgO). Reactions were carried out in a fixed bed reactor with a total system pressure of 220 kPa at temperatures between 533 and 633 K and acetaldehyde partial pressures between 0.05 and 50 kPa. Crotonaldehyde was the only product observed over all three catalysts and severe catalyst deactivation occurred at acetaldehyde partial pressures of 5 kPa or greater. The aldol condensation reaction over all three catalysts was first order at low acetaldehyde partial pressure and approached zero order at high acetaldehyde partial pressure. No kinetic isotope effect (KIE) was observed with fully deuterated acetaldehyde reacting over TiO_2 or HAP implying C-H bond activation is not kinetically relevant. These measurements are consistent with a mechanism in which adsorption and desorption steps are kinetically significant during the reaction. Characterization of the catalysts by adsorption microcalorimetry of acetaldehyde and ethanol and diffuse reflectance Fourier transformed infrared spectroscopy of adsorbed acetaldehyde, crotonaldehyde and acetic acid revealed a very high reactivity of these catalysts, even at low temperatures.

DE-FG02-95ER14549: Structure and Function of Supported Base Catalysts

RECENT PROGRESS

Solid bases are heterogeneous catalysts that have not been broadly exploited compared to solid acids. Thus, we have focused our efforts for many years on understanding how a variety of solid bases, including metal oxides, mixed metal oxides and zeolites, function in catalytic transformations. A major objective of our recent activities in this area was to initiate a new research direction that explores acid/base bifunctional surfaces as catalysts for C-C bond forming reactions. The coupling of two ethanol molecules to form butanol is desirable because butanol has a higher energy density than ethanol and is not as soluble in water as ethanol, thus making it a potentially more attractive oxygenated additive to transportation fuels. The so-called Guerbet reaction (alcohol coupling reaction) has been the focus of our recent work.

Multiproduct steady-state isotopic transient kinetic analysis (SSITKA) of the ethanol coupling reaction was used over a stoichiometric calcium hydroxyapatite (HAP) catalyst and compared to the results obtained with magnesia (MgO), a standard solid base catalyst, in an attempt to evaluate important intrinsic kinetic parameters and benchmark the reaction. Results from surface characterization, reactivity testing, and isotopic transient studies were used to propose key structural and compositional properties that facilitate the Guerbet coupling reaction. The isotopic transient results revealed the surface coverage of reactive intermediates leading to butanol (N_{BuOH}) relative to that leading to acetaldehyde (N_{AcH}) was very high on HAP ($N_{\text{BuOH}} \gg N_{\text{AcH}}$) whereas on MgO the opposite trend was observed ($N_{\text{AcH}} > N_{\text{BuOH}}$). These results were the subject of our presentation at last year's Contractor's meeting.

Over the past year, we have explored the aldol condensation of acetaldehyde over acid-base bifunctional materials to elucidate the role of this C-C bond forming reaction in the Guerbet reaction network. The condensation reaction was studied over three catalysts, anatase TiO_2 , HAP and MgO. Both HAP and MgO are common Guerbet coupling catalysts whereas TiO_2 is a commonly-studied catalyst for aldol condensation. Diffuse reflectance infrared Fourier transform spectroscopy (DRIFTS) and adsorption microcalorimetry of various probe molecules were used to probe the affinity of catalyst surfaces for species relevant to the condensation reaction.

Titania and HAP were active at 553 K for acetaldehyde condensation while MgO had comparable areal rates at 633 K. In all three cases, significant deactivation was observed over the first 6 hours on stream with acetaldehyde partial pressures of 5 kPa or greater. We observed very little deactivation over HAP and TiO_2 at acetaldehyde pressures below 0.4 kPa. Initial rate measurements were therefore used to examine the influence of acetaldehyde pressure and reaction temperature on the kinetics and to rank the activity of the catalysts. Results revealed an activity ranking per surface area of $\text{TiO}_2 > \text{HAP} \gg \text{MgO}$. Aldol condensation using fully deuterated acetaldehyde showed no kinetic isotope effect indicating that C-H bond activation is not kinetically relevant. A plausible mechanism of aldol condensation over these materials consists of kinetically relevant reactant adsorption and product desorption steps. At the conditions used here, the presence of ethanol had no effect on the rate of aldol condensation over HAP or MgO, but inhibited the rate of aldol condensation over TiO_2 .

Adsorption microcalorimetry and DRIFTS were used to investigate the affinity of the catalysts for acetaldehyde at 303 K and to estimate an upper bound on the total number of active sites on each catalyst. A high heat of adsorption as well as a high acetaldehyde uptake were observed on both HAP and MgO. We suspect that a surface reaction occurred during the adsorption microcalorimetry experiment, resulting in higher heats of adsorption and perhaps higher surface coverages than would be expected from simple chemisorption. On TiO_2 , the $-\Delta H_{\text{ads}}$ of acetaldehyde was much lower compared to that on HAP and MgO. The performance of the materials in aldol condensation can be related to the relative affinity of the surface for aldehydes, and other intermediate species with TiO_2 having the lowest affinity (greatest reaction rate) and MgO having the greatest affinity (lowest reaction rate). The weak affinity of TiO_2 for the reacting species

accounts for the inhibiting effect of ethanol on the aldol condensation rate because of the competitive adsorption.

We then explored the performance of the catalysts in the Guerbet coupling reaction. Table 1 summarizes the rate and selectivity associated with ethanol conversion over TiO₂, HAP and MgO.

Table 1. Ethanol Reaction (~8 kPa) over TiO₂, HAP and MgO

Catalyst	T (K)	Conversion (Carbon %)	Rate (mol m ⁻² s ⁻¹)	Selectivity (C%)				
				Ethene	Ethane	AcH ^(a)	Butanol	Diethyl Ether
TiO ₂	613	1.9	1.3 x 10 ⁻⁸	0	7	51	0	42
HAP	613	4.3	4.4 x 10 ⁻⁸	1	0	32	67	0
MgO	653	4.5	1.4 x 10 ⁻⁸	12	0	67	21	0

(a) AcH represents acetaldehyde

Although TiO₂ is the most active catalyst for aldol condensation at lower temperature, it is unable to convert ethanol to butanol at 613 K, instead favoring diethyl ether formation. Since the production of diethyl ether is typically associated with an acidic catalyst, the TiO₂ surface is apparently too acidic to convert ethanol to butanol at elevated temperatures. The HAP sample is the most active of the three catalysts for Guerbet coupling with a selectivity to butanol of 67% at a temperature 40 K lower than used for MgO. Magnesia is the least active catalyst, requiring a temperature 40 K higher than HAP and TiO₂ to achieve a similar rate of conversion. Hydroxyapatite has a higher selectivity to butanol while MgO has a higher selectivity to acetaldehyde. The high selectivity towards butanol over HAP is likely due to a large number of appropriate strength acid-base pairs on the surface.

Current work is exploring other acid-base bifunctional materials for C-C bond forming reactions in an effort to elucidate structure-reactivity and composition-reactivity relationships for these catalysts.

Publications Acknowledging this Grant in 2013-2016

(I) *Exclusively funded by this grant*

1. Young, Z.D.; Hanspal, S.; Davis, R.J. "Aldol Condensation of Acetaldehyde over Titania, Hydroxyapatite and Magnesia," *ACS Catal.*, **2016**, *6*, 3193-3202.
2. Hill, I.M.; Hanspal, S.; Young, Z.D.; Davis, R.J. "DRIFTS of Probe Molecules Adsorbed on Magnesia, Zirconia and Hydroxyapatite Catalysts" *J. Phys. Chem. C*, **2015**, *119*, 9186-9197.
3. Hanspal, S.; Young, Z.D.; Shou, H.; Davis, R.J. "Multi-product steady-state isotopic transient kinetic analysis of the ethanol coupling reaction over hydroxyapatite and magnesia," *ACS Catal.* **2015**, *5*, 1737-1746.

4. Birky, T.W.; Kozlowski, J.T.; Davis, R.J. "Isotopic Transient Analysis of the Ethanol Coupling Reaction over Magnesia," *J. Catal.* **2013**, 298, 130-137.
5. Kozlowski, J.T.; Davis, R.J.; "Sodium Modification of Zirconia Catalysts for Ethanol Coupling to 1-Butanol," *J. Energy Chem.* **2013**, 22, 58-64.
6. Kozlowski, J.T.; Davis, R.J. "Heterogeneous Catalysts for the Guerbet Coupling of Alcohols," *ACS Catal.* **2013**, 3, 1588-1600.

(II) Jointly funded by this grant and other grants with leading intellectual contribution from this grant;

1. Kozlowski, J.T.; Behrens, M.; Schlögl, R.; Davis, R.J. "Influence of Precipitation Method on Acid-Base-Catalyzed Reactions over Mg-Zr Mixed Oxides," *ChemCatChem* **2013**, 5, 1989-1997.

Supported Alkyl-Aluminum Catalysts for Olefin Hydrogenation

Massimiliano Delferro,¹ Jeffrey Camacho-Bunquin,¹ Magali Ferrandon,¹ Ujjal Das,¹ Fulya Dogan,¹ Cong Liu,¹ Casey Larsen,¹ Theodore R. Krause,¹ Emilio A. Bunel,¹ Larry A. Curtiss,¹ Adam S. Hock,^{1,2} Jeffrey T. Miller,^{1,3} SonBinh T. Nguyen,^{1,4} Christopher L. Marshall,¹ and Peter C. Stair^{1,4}

¹Chemical Sciences and Engineering Division, Argonne National Laboratory, ²Department of Chemistry, Illinois Institute of Technology, ³Department of Chemical Engineering, Purdue University, ⁴Department of Chemistry, Northwestern University

delferro@anl.gov

Low-coordinate alkylaluminum sites supported on a catechol-containing porous organic polymer (CatPOP) were developed for the isomerization/hydrogenation of a range of aliphatic and aromatic alkenes and alkynes. Infrared spectroscopy (FT-IR), solid-state ¹H and ²⁷Al NMR spectroscopy, and elemental analysis of precatalysts were employed to elucidate the aluminum coordination (Figure 1A). Active alkylaluminum sites catalytically

hydrogenate and isomerize a range of mono- and di-substituted alkenes and alkynes under mild conditions (80 °C, 5 bar H₂). Results of experimental mechanistic studies and DFT calculations are consistent with a heterolytic hydrogenation mechanism proceeding in two steps: (1) hydroalumination of a carbon-carbon double bond, followed by (2) protonation of the Al-C_{alkyl} bond by an adjacent catechol hydroxyl group (Figure

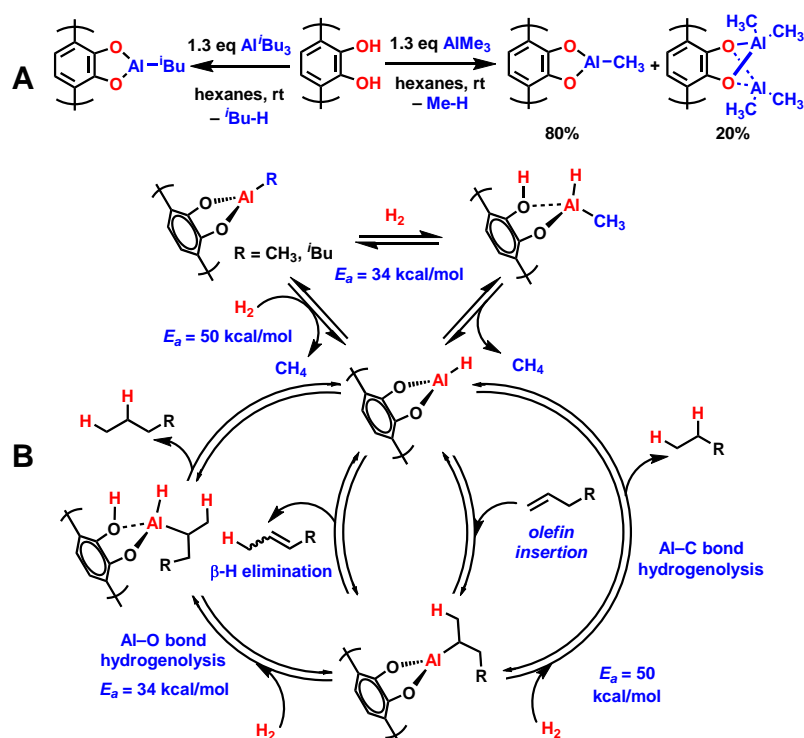


Figure 1. A) Synthesis of supported alkyl-aluminum catalysts on CatPOP. B) Proposed scenario for alkenes hydrogenation/isomerization.

1B). In addition, DFT calculations revealed that heterolytic activation of hydrogen over an Al–O bond ($E_a = 34$ kcal/mol) is more favored than direct hydrogenolysis of the Al–C_{alkyl} functionality ($E_a = 50$ kcal/mol).

FWP50966: Tunable Single-Site Catalysts for Selective Functionalization of Alkanes

PI: Massimiliano Delferro,¹ Larry A. Curtiss,¹ Adam S. Hock,^{1,2} SonBinh T. Nguyen,^{1,3} Peter C. Stair.^{1,3}

Postdoc(s): Jeffrey Camacho-Bunquin, Theodore Helgert, Rachel C. Klet, Cong Liu, Casey Larsen (former), Ujjal Das (former), Kristine Tanabe (former), Andrew Getsoian (former), Debabrata Mukherjee (former).

Student(s): Yiqing Zhao,² Bo Hu² (former).

Affiliations(s): ¹Chemical Sciences and Engineering, Argonne National Laboratory, ²Department of Chemistry, Illinois Institute of Technology, ³Department of Chemistry, Northwestern University.

RECENT PROGRESS

Goals

Of interest to our group is the development of single-site, supported catalysts for kinetically limited transformations (e.g., alkane C–H activation and functionalization) and the mechanisms by which these occur. The energy input required to drive such reactions *could* compromise the selectivity of traditional heterogeneous catalysts, resulting in a distribution of reaction products, or compromise the stability of homogeneous active sites, leading to catalyst deactivation. Our group's recent successes in the synthesis of isolated, single-site catalysts on both traditional hard supports like SiO₂ or Al₂O₃ as well as a new class of tailorable porous organic polymers (CatPOPs), employing the tools of surface organometallic chemistry and atomic layer deposition (ALD) over the nature of active site support platforms provided efficient routes to isolated, single-site surface species that exhibit catalytic activity, selectivity and stability, notably under reaction conditions where their molecular analogs are largely unstable and unreactive. These isolated, “homogeneous-in-function” catalysts are amenable to kinetic and spectroscopic characterization techniques, thereby providing opportunities for systematic investigation of the roles of the metal and the supporting ligand in the catalytic cycle.

DOE Interest

A Grand Challenge in Basic Energy Science research is to design and perfect atom- and energy-efficient synthesis of new forms of materials with tailored properties. In the field of catalysis, advances in single-site heterogeneous catalysis and surface organometallic chemistry have become key enabling tools to achieve molecular-level control over catalyst synthesis, providing the ability to tune catalyst structure-function relationships with unprecedented precision. These strategies enable construction of novel, robust, single-site supported materials which combine the critical elements of activity and selectivity of homogeneous catalysts with the stability of heterogeneous systems, while

providing for homogeneous-level understanding of active site structures and control of catalytic mechanisms.

Single-site Catalysts on Metal Oxides: Recently we have reported a variety of isolated metal catalysts on silica for propane dehydrogenation. Through combined spectroscopic, mechanistic, and computational investigations we determined that the reaction proceeds without metal-based redox, with the key step being heterolytic cleavage of the alkane C-H bond. Lewis acidity is readily correlated to catalyst activity for Fe^{2+} , Zn^{2+} , Ga^{3+} , and Co^{2+} . However, the rate-determining step for the reaction varies. First, beta hydride elimination has been calculated to be the rate-determining step for Zn and Ga alkyls during alkane dehydrogenation. Conversely, the less Lewis acidic Fe and Co are believed to have heterolytic cleavage C-H cleavage across the metal-oxygen bond as the rate-determining step. Y and Sc are far more Lewis acidic than transition metals and thus might be expected to be faster catalysts if they proceed via a similar mechanism. However, given homogeneous and supported organometallic studies it is also possible that they might proceed via a sigma bond metathesis type mechanism. As such, we prepared single-site Y and Sc alkyls on SiO_2 by grafting $\text{Sc}(\text{CH}_2\text{Si}(\text{CH}_3)_3)_3(\text{THF})_2$ and $\text{Y}(\text{CH}_2\text{Si}(\text{CH}_3)_3)_3(\text{THF})_2$, respectively. The resulting materials are catalytic for olefin hydrogenation at low temperatures ($<100^\circ\text{C}$). However, they are thermally unstable at higher temperatures necessary for alkane dehydrogenation. We concluded that this is likely due to the very high M-O-Si bond strengths, which must be broken through heterolytic dissociation of C-H bonds during alkane activation for either alkane dehydrogenation or olefin hydrogenation reactions. As a comparison to the more Lewis acidic Y and Sc materials, we also prepared catalysts that were designed to test the hypothesis that the catalyst-oxygen-support (M-O-M') bond strength is a valid descriptor of catalytic performance in our systems. We used organometallic and atomic layer deposition (ALD) chemistries to prepare modified silica with electrophilic, non-catalytic metals. The resulting materials have higher catalytic activity and selectivity for nonoxidative propane dehydrogenation than the unmodified catalysts. The origin of effect of such 'promoters' on these isolated metal catalysts is the subject of ongoing analysis.

Supported Organometallic on Porous Organic Polymers: Recently we reported a variety of catechol-supported metal complexes that are active catalysts for selective alkyne semi-

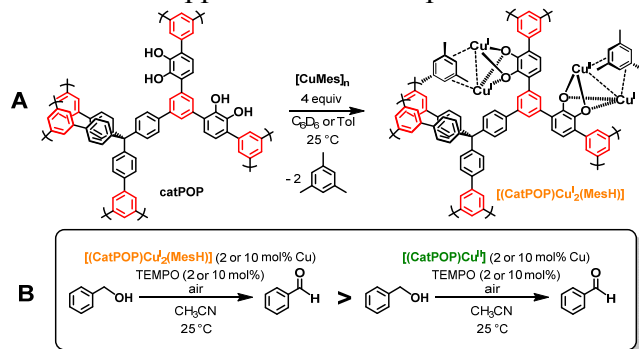
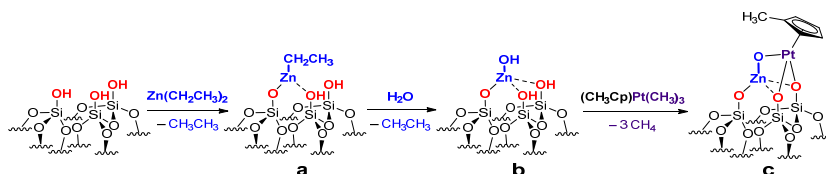


Figure 1. A) Synthesis of supported bimetallic Cu^{I} catalyst on CatPOP. B) Catalytic oxidation of benzylic alcohol in presence of TEMPO with air as an oxidant.

hydrogenation. Since the reactive catecholate coordination sites are already integrated into the polymer backbone, the CatPOP architecture allows for nucleation of isolated low-coordinate, monomeric species that are typically unstable in solution. In contrast to inorganic oxide supports, the bidentate catecholate site on CatPOP provides a uniform and specific ligand coordination environment

that can impart unique and unprecedented reactivity to low-coordinate organometallic species. Dicopper(I) centers have been stabilized within close proximity (~ 2.7 Å) on a catechol-containing porous organic polymer CatPOP (Figure 1). The $[(\text{CatPOP})\text{Cu}_2^{\text{I}}(\text{MesH})]$ has been characterized by ATR-IR, DR-UV-vis, ^{13}C SS NMR, XAS, EPR, ICP-OES, and elemental analyses. These data suggest the presence of two Cu^{I} centers stabilized by a dianionic catechol backbone with an η^2 -coordinated mesitylene ligand bound to each Cu^{I} center. Ligand-displacement experiments of $[(\text{CatPOP})\text{Cu}_2^{\text{I}}(\text{MesH})]$ were performed with pyridine, CH_3CN , THF, and thioanisole. Of all the ligands tested, only pyridine was observed to displace all the mesitylene. $[(\text{CatPOP})\text{Cu}_2^{\text{I}}(\text{MesH})]$ was catalytically oxidizes benzyl alcohol to benzaldehyde in the presence of TEMPO with air as an oxidant. Under identical conditions, $[(\text{CatPOP})\text{Cu}_2^{\text{I}}(\text{MesH})]$ oxidizes benzyl alcohol 3 to 10 times faster than the previously reported $[(\text{CatPOP})\text{Cu}^{\text{II}}]$.

High Throughput Atomic Layer Deposition (HT-ALD): Atomic layer deposition (ALD) has recently gained interest as a method for the synthesis of heterogeneous catalysts with precise, Ångstrom-level control over the resulting surface structures. ALD relies on a stoichiometric and thus self-limiting reaction of chemical precursors with substrate surface functionalities to provide (1) uniform active site dispersion, (2) high conformity to surface features, and (3) high level of reproducibility. The Integrated Atomic Layer Deposition-Catalysis (I-ALD-CAT) testing tool available at Argonne is capable of ALD synthesis and *in situ* (without exposure to air) catalyst performance evaluation under plug-flow conditions. Using this powerful tool, we recently reported the systematic study of the intrinsic reactivity of different isolated Zn^{II} active sites and the transformations they undergo at the atomic-scale/submonolayer level during catalytic reactions (Scheme 1). Ethyl-zinc (**a**) and zinc oxide (**b**) sites were synthesized via one-cycle ALD experiments with diethylzinc (DEZ) on silica. Note that, the



Scheme 1. ALD synthesis of Zn/SiO_2 and multimetallic catalysts for alkane dehydrogenation

open-shell 16-electron, tri-coordinate ethyl zinc-silica sites (**a**) exhibit higher activity in propane dehydrogenation-propylene hydrogenation compared to 18- electron, tetra-coordinate zinc oxide-type centers (**b**). The I-ALD-CAT approach provided key insights into the reactivity and stability of different Zn sites as a function of dispersion at the sub-monolayer level. Silica surface saturation with $\text{Zn}(\text{II})$ sites ($\sim 75\%$ of a monolayer) results in facile zinc agglomeration and catalyst deactivation under reaction conditions. Sub-saturation DEZ dosing and substrate pretreatment (e.g., dehydration under vacuum) resulted in increased Zn dispersion and produced catalysts with improved activity and stability under propylene hydrogenation (200 °C) and propane dehydrogenation (550 °C) conditions. Additionally, the use of ethyl(C_2) groups in the precatalyst (**b**) enabled the unambiguous monitoring of alkyl-zinc activation pathways under propylene (C_3) hydrogenation conditions. DFT calculations revealed that protonation of Zn -ethyl fragments ($E_a = 35.9$ kcal/mol) is more favored than direct Zn -ethyl hydrogenolysis ($E_a = 57.5$ kcal/mol), giving ethane (major C_2 species observed) and an active $\text{Zn}(\text{II})$ species.

On the other hand, Zn-ethyl group activation via β -H elimination ($E_a = 50.9$ kcal/mol) is less favored as indicated by the low concentration of ethylene in the product feed.

The I-ALD-CAT system was also used to discover a series of multimetallic active sites (c) on high-surface-area silica for selective non-oxidative propane dehydrogenation to produce propylene. The catalysts are multimetallic in nature, composed of platinum sites on transition metal oxide or main group element oxide layer(s) on silica support (e.g., Pt/ZnO/SiO₂ and Pt/Al₂O₃/SiO₂). X-ray absorption spectroscopic studies of the precatalyst prepared from one-cycle ZnO ALD followed by one-cycle Pt deposition (Scheme 1) confirmed monodispersity of the Zn(II) and Pt(IV) sites. Deposition of a submonolayer of oxide promoters on SiO₂ prior to platinum ALD resulted in significantly increased catalytic performance (Figure 2). Dehydrogenation of propane (5 mol% in Ar) at 550 °C with a series of ZnO-promoted Pt catalysts showed higher propane conversions (40-70% vs 10% with Pt/SiO₂). High propylene selectivity (99%) and slow catalyst deactivation (>7 days without regeneration) were also observed in the presence of ZnO promoters. Additionally, investigation of the effects of synthesis methods on the catalytic activity revealed a possible advantage of ALD synthesis over solution-phase techniques. These high-reactivity, high-selectivity propane dehydrogenation catalysts are being evaluated and optimized for selective dehydrogenation of longer chain alkanes to produce value-added chemicals (e.g., *n*-butane to 1,3-butadiene).

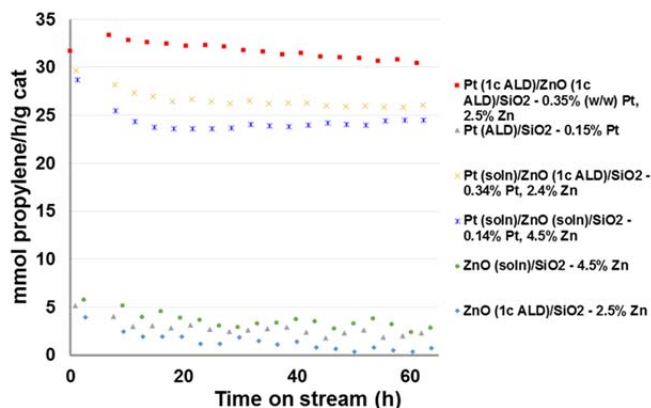


Figure 2. Comparison of propane dehydrogenation activity of a series of Pt-containing catalysts synthesized via ALD and/or solution-phase methods. Testing conditions: 50 mg catalyst, 46 mL/min 5% C₃H₈/Ar, 550 °C, 65 h.

Descriptor-Based Catalysts Design: In the past grant period, computational studies were focused on molecular understanding and predictive design of new single-site catalysts with improved efficiency for H–H and C–H bond activations. Both SiO₂ and a catechol-containing porous organic polymer (Cat-POP) were considered. DFT calculations for propylene hydrogenation on the silica supported single-site catalysts reveal that the reaction is initiated by the heterolytic dissociation of H₂ with the formation of metal-hydride and support hydroxyl intermediates. Moreover, the hydrogenation activity of a series of SiO₂-supported single-site catalysts directly correlate with the formation enthalpy of the hydride intermediate (Figure 3). Our recent results show that the SiO₂-supported single-site Ga(III) has the highest

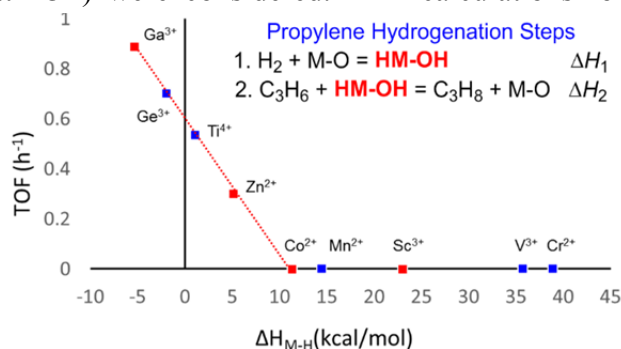


Figure 3. Linear correlation between the TOF (h⁻¹) of propylene hydrogenation and the calculated hydrogen activation using SiO₂ supported single site catalysts. (■) Experimental TOF, (■) Computed TOF.

activity for propylene hydrogenation and readily forms a Ga-H intermediate, while SiO₂-supported single-site Co^{II} has the lowest activity, and DFT calculations suggest that Co^{II} has an unfavorable reaction enthalpy for the formation of the Co-H intermediate. These results suggest that the enthalpy of metal-hydride intermediate formation can serve as a descriptor of activity for hydrogenation catalysts and can be used to screen potential new catalyst compositions. Based on this descriptor, single-site Ge supported on SiO₂ should be the more active dehydrogenation catalyst, which synthesis is currently underway.

Publications Acknowledging Exclusively this Grant in 2013-2016

- 1) Camacho-Bunquin, J.; Ferrandon, M.; Das, U.; Dogan, F.; Liu, C.; Larsen, C.; Curtiss, L. A.; Hock, A. S.; Miller, J. T.; Nguyen, S. T.; Marshall, C. L.; Stair, P. C. Supported Aluminum Catalysts for Olefin Hydrogenation. **2016**, *Submitted*.
- 2) Theodore R. Helgert, Debabrata Mukherjee, Guanghui Zhang, Fanjie Kong, James R. Gallagher, Jens Niklas, Jeff Miller, Julius Jellineka, Oleg Poluektov, and SonBinh T. Nguyen Dicopper(I) on Catecholate Porous Organic Polymer for Catalytic Oxidation of Alcohols. **2016**, *Submitted*.
- 3) Camacho-Bunquin, J.; Aich, P.; Ferrandon, M.; Getsoian, A.; Das, U.; Dogan, F.; Curtiss, L.; Miller, J. T.; Marshall, C. L.; Hock, A. S.; Stair, P. C. Single-Site Zinc on Silica Catalysts for Propylene Hydrogenation and Propane Dehydrogenation. Synthesis and Reactivity Evaluation through Integrated Atomic Layer Deposition-Catalysis Experimentation. **2016**, *Submitted*.
- 4) Stair, P. C.; Camacho-Bunquin, J.; Marshall, C. L.; Hock, A. S. Multimetallic catalysts on oxides for selective alkane dehydrogenation and synthesis thereof. **2016**, US patent pending.
- 5) Getsoian A; Hu B; Miller J.T.; Hock A.S. Supported single site Sc and Y alkyl catalysts for olefin hydrogenation. **2016**, *submitted*.
- 6) Getsoian, A.; Das, U.; Camacho-Bunquin, J.; Zhang, G.; Gallagher, J. Hu, B; Schaidle, J.; Ruddy, D. A.; Kraft, S. J.; Henley, J.; Curtiss, L. A. Miller, J. T.; Hock, A.S. Oxidation State and Ligand Field Effects in Ga K-edge XANES: Mechanistic Implications for Alkane Dehydrogenation by Ga-Zeolite Catalysts. *Catal. Sci. Technol.* **2016**, ASAP.
- 7) Das, U.; Zhang, G.; Hu, B.; Hock, A. S.; Redfern, P. C.; Miller, J. T.; Curtiss, L. A. Effect of Siloxane Ring Strain and Cation Charge Density on the Formation of Coordinately Unsaturated Metal Sites on Silica: Insights from Density Functional Theory (DFT) Studies. *ACS Catal.* **2015**, *5*, 7177-7185.
- 8) Camacho-Bunquin, J.; Shou, H.; Aich, P.; Beaulieu, D. R.; Klotzsch, H.; Bachman, S.; Marshall, C. L.; Hock, A. S.; Stair, P. C. Catalyst Synthesis and Evaluation Using A High-Throughput Atomic Layer Deposition-Catalysis Testing Tool *Rev. Sci. Instrum.* **2015**, *86*, 084103/084101-084103/084107.
- 9) Hu, B.; Schweitzer, N. M.; Zhange, G.; Kraft, S. J.; Childers, D. J; Lanci, M. P.; Miller, J. T.; Hock, A. S. Isolated Fe^{II} on Silica As a Selective Propane Dehydrogenation Catalyst. *ACS Catal.* **2015**, *5*, 3494-3503.
- 10) Camacho-Bunquin, J.; Siladke, N. A.; Zhang, G.; Niklas, J.; Poluektov, O. G.; Nguyen, S. T.; Miller, J. T.; Hock, A. S. Synthesis and Catalytic Hydrogenation

- Reactivity of a Chromium Catecholate Porous Organic Polymer. *Organometallics* **2015**, *34*, 947-952.
- 11) Hu, B.; Schweitzer, N. M.; Das, U.; Kim, H. K.; Stair, P. C.; Curtiss, L.; Hock, A. S.; Miller, J. T. Selective Propane Dehydrogenation with Single Site Co^{II} on SiO₂ by a Non-redox Mechanism. *J. Catal.* **2015**, *322*, 24-37.
 - 12) Tanabe, K. K.; Ferrandon, M. S.; Siladke, N. A.; Kraft, S. J.; Zhang, G.; Niklas, J.; Poluektov, O. G.; Lopykinski, S. J.; Bunel, E. E.; Krause, T. R.; Miller, J. T.; Hock, A. S.; Nguyen, S. T. Discovery of highly selective alkyne semi-hydrogenation catalysts based on 1st-row transition metallated porous organic polymers. *Angew. Chem. Int. Ed.* **2014**, *53*, 12055-12058.
 - 13) Kraft, S. J.; Zhang, G.; Childers, D.; Dogan, F.; Miller, J. T.; Nguyen, S. T.; Hock, A. S., Rhodium Catechol Containing Porous Organic Polymers: Defined Catalysis for Single-Site and Supported Nanoparticulate Materials. *Organometallics* **2014**, *33*, 2517-2522.
 - 14) Schweitzer, N. M.; Hu, B.; Das, U.; Kim, H.; Greeley, J.; Curtiss, L. A.; Stair, P. C.; Miller, J. T.; Hock, A. S. Propylene Hydrogenation and Propane Dehydrogenation by a Single-Site Zn²⁺ on Silica Catalyst. *ACS Catal.* **2014**, *4*, 1091-1098.
 - 15) Kraft, S. J.; Hu, B.; Zhang, G.; Miller, J. T.; Hock, A. S. In Situ X-ray Absorption Spectroscopy and Nonclassical Catalytic Hydrogenation with an Iron(II) Catecholate Immobilized on a Porous Organic Polymer. *Eur. J. Inorg. Chem.* **2013**, 3972-3977.
 - 16) Kraft, S. J.; Sánchez, R. H.; Hock, A. S., A Remarkably Active Iron Catecholate Catalyst Immobilized in a Porous Organic Polymer. *ACS Catal.* **2013**, *3*, 826-830.
 - 17) Schweitzer, N. M.; Hu, B.; Miller, J. T.; Hock, A. S. Selective Alkane Activation with Single Site Atoms on Amorphous Supports. U.S. patent pending, 2013/182.
 - 18) Tanabe, K. K.; Siladke, N. A.; Broderick, E. M.; Kobayashi, T.; Goldston, J. F.; Weston, M. H.; Farha, O. K.; Hupp, J. T.; Pruski, M.; Mader, E. A.; Johnson, M. J. A.; Nguyen, S. T. Stabilizing unstable species through single-site isolation: a catalytically active Ta^V trialkyl in a porous organic polymer. *Chem. Sci.* **2013**, *4*, 2483-2489.

Publications Acknowledging Jointly Funded by this Grant and Other Grants with Leading Intellectual Contribution from this Grant in 2013-2016

- 19) Krogman, J. P.; Gallagher, J. R.; Zhang, G.; Hock, A. S.; Miller, J. T.; Thomas C. Definitive Assignment of the Oxidation States of Zr and Co in a Highly Reactive Heterobimetallic Zr/Co Complex Using X-ray Absorption Spectroscopy (XANES). *Dalton Trans.* **2014**, 13852-13857.
- 20) Maria, S.; Poli, R.; Gallagher, K. J.; Hock, A. S.; Johnson, M. J. A. Ether Complexes Of Molybdenum(III) And (IV) Chloride. *Inorg. Synth.* **2014**, *36*, 15-19.
- 21) Broderick, E. M.; Browne, S. C.; Johnson, M. J. A.; Hitt, T. A.; Girolami, G. S. Dimolybdenum and Ditungsten Hexa(Alkoxides). *Inorg. Synth.* **2014**, *36*, 96-102.

Benchmarking Computational Approaches for Catalytic Reactions on TMO Nanoclusters

David A. Dixon,¹ Zdenek Dohnálek,² Roger Rousseau,² Bruce D. Kay²

¹ Department of Chemistry, The University of Alabama

²Fundamental and Computational Sciences Directorate and Institute for Integrated Catalysis, Pacific Northwest National Laboratory

Presentation Abstract

We report extensions of our studies of the reactions of alcohols on transition metal oxide (TMO) nanoclusters to polyols and acids and to an Al_8O_{12} cluster model of $\gamma\text{-Al}_2\text{O}_3$. A range of reactions were studied to obtain fundamental information about the basic concepts governing reactivity. Quantitative reactivity mechanism information could only be obtained at the correlated molecular orbital theory coupled cluster CCSD(T) level. Dehydration and dehydrogenation reactions probe both the Lewis/Brønsted acid/base and redox properties of the metal centers. The prediction of the heats of formation of group IV and group VI TMO nanoclusters with the coupled cluster CCSD(T) method has been improved by using Kohn-Sham density functional theory (DFT) and Brueckner orbitals for the initial wave function. The predicted heat of formation of CrO_3 using the PW91 orbitals is consistent with previous calculations including high order corrections beyond CCSD(T). The heats of formation of the $(\text{CrO}_3)_n$ cluster have been improved by 5, 10, 25 and 27 kcal/mol for $n = 1, 2, 3,$ and 4 . The improved heats of formation are due to the DFT and Brueckner orbitals being closer to the actual orbitals. Pure DFT functionals perform slightly better than the hybrid B3LYP functional due to the presence of exact exchange in the hybrid functional. 55 widely used exchange-correlation DFT functionals were benchmarked against the best CCSD(T) (including Feller-Peterson-Dixon) results for the relative energies (REs) of isomers, normalized clustering energies (NCEs), electron affinities (EAs), and fluoride affinities (FAs) of $(\text{MO}_2)_n$ ($M = \text{Ti}, \text{Zr}, \text{Hf}, n = 1 - 4$) and $(\text{MO}_3)_n$ ($M = \text{Cr}, \text{Mo}, \text{W}, n = 1 - 3$) nanoclusters. The REs provide the lowest energy structure of the catalyst, the NCEs provide the energetics of the catalyst, the EAs provide the redox capability of the catalyst, and the FAs provide a measure of the Lewis acidity of the catalyst. Hybrid functionals usually give better REs and NCEs than do pure functionals. The prediction of the EAs is more complicated than for the REs and NCEs and hybrid functionals do not give better results than do the pure functionals, with most absolute errors within 10 kcal/mol. A large fraction of DFT functionals overestimate the FAs, and, again, the hybrid functionals do not perform better than the pure functionals. The B1B95 and PBE1PBE functionals provide the most reliable energetic properties for most of the isomers for these properties.

This work is part of the PNNL FWP 47319, “Multifunctional Catalysis to Synthesize and Utilize Energy Carriers”.

Postdoctoral Fellow: Zongtang Fang (UA)

Control of Reactivity in Nanoporous Metal/Ionic Liquid Composite Catalysts

Jonah Erlebacher
Johns Hopkins University
Department of Materials Science and Engineering

Presentation Abstract

In this program, we have been exploring a new concept in nanostructured heterogeneous catalysis design – the use of a nanoporous metal, either alone or impregnated with an ionic liquid (IL) to form a composite catalyst [1,2]. The idea behind this concept is to tailor the chemical environment within and near the pores of a metallic electrocatalyst in order to enhance the aggregate composite activity and selectivity. Most recent electrocatalyst design focuses upon lowering the activation barrier for a particular synthesis reaction. While we also try to minimize this quantity, one should also recognize that significant catalytic enhancements can be made by biasing the reaction to completion via control of the environment in which the reaction occurs.

In this phase of the program, we have been working toward understanding fundamental electrocatalysis challenges in the reduction of small molecules under highly reducing condition, i.e., under conditions of hydrogen evolution and/or water reduction. The ultimate aim is to develop methods for electrochemical reduction of nitrogen to ammonia. Our strategy has been to tailor reactant and product transport to a nanostructured catalyst. A first result has been significant improvements in the oxygen reduction reaction (ORR) using nanoporous dealloyed nickel-platinum (np-NiPt) impregnated with ionic liquids that are simultaneously oxophilic and hydrophobic. As a model system, we have examined the ORR under highly reducing conditions, and found that hydrogen evolution can be completely suppressed in favor of oxygen reduction when the reaction is proton diffusion limited and occurs over a nanoporous metal catalyst that acts as a sink for reaction intermediates. Simultaneously, we have been developing nanoporous refractory metal catalysts for nitrogen reduction, and developing a novel flow-through electrochemical cell that independently controls the relative concentration of protons compared to reactants.

DE-SC0008686: Control of Reactivity in Nanoporous Metal/Ionic Liquid Composite Catalysts

Student(s): Ellen Benn, Bernard Gaskey

RECENT PROGRESS

Fundamental electrochemistry using nanoporous metal/ionic liquids composite catalysts. In this segment of the program, we have been studying the fundamental electrochemical response of nanoporous metal/ionic liquid catalysts, primarily using a dealloyed nanoporous Pt/Ni electrode impregnated with IL, and using the oxygen reduction reaction as a model system. We have been looking at a variety of ionic liquids, particularly the response of protic versus aprotic ionic liquids, with more or less hydrophobicity (water solubility). Figure 1 shows results of oxygen reduction activity

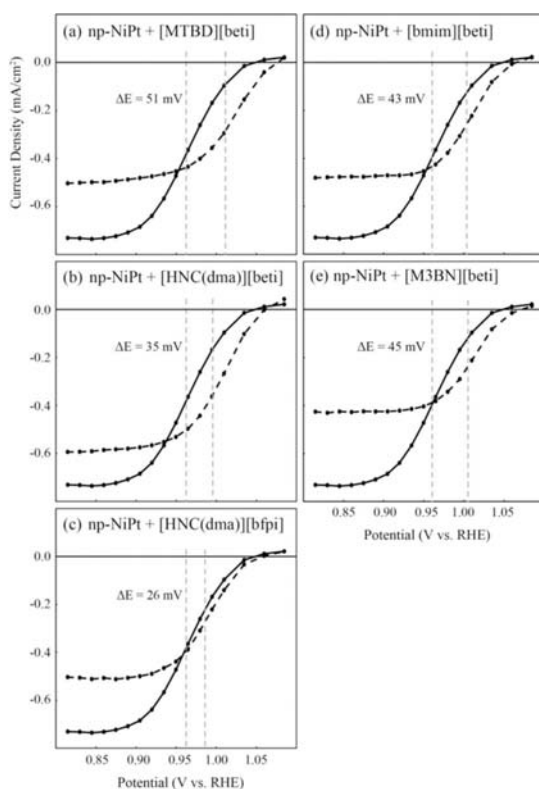


Figure 1. Potentiostatic ORR current density versus potential for np-NiPt (solid line) filled with a variety of different ionic liquids (a) np-NiPt+[MTBD][beti] (high oxygen solubility), (b) np-NiPt+[HNC(dma)][beti] (high proton conductivity and low viscosity), (c) np-NiPt+[HNC(dma)][bfpi] (relatively high hydrophobicity), (d) np-NiPt+[bmim][beti] (aprotic and high viscosity), and (e) np-NiPt+[M3BN][beti] (aprotic and low viscosity) [2].

over np-NiPt for a survey of ionic liquids exhibiting a range of properties, each of which to some extent improves the ORR activity by shifting the half-wave to higher potentials. This study concluded that the primary determinants of ORR improvement are simultaneous high oxygen solubility and high hydrophobicity [2].

An ancillary goal of this study was to see if aprotic ionic liquids in the nanoporous metal could stymie proton transport to the electrocatalyst surface. If this were possible, then reduction of other small molecules from an essentially aqueous solution could occur even at highly reducing potentials, in particular at potentials at which hydrogen evolution occurs, below 0.0 V vs. RHE. This remains a viable new strategy for CO₂ or N₂ reduction, but requires design and synthesis of ionic liquids with essentially no water solubility. In our above-mentioned survey, we found that even “very hydrophobic” ionic liquids had water solubilities of order 1 M.

The oxygen reduction reaction under proton diffusion-limited conditions.

Hydrogen evolution is a ubiquitous problem in the electroreduction of many small molecules such as carbon dioxide or nitrogen. Here we used oxygen reduction as a model system to study reduction kinetics below 0.0 V vs. RHE, when hydrogen evolution is facile. The essential idea is simple: oxygen solubility is of order 1 mM, so under mildly acidic conditions (pH 4), the flux of oxygen should overwhelm the flux of protons to the catalyst surface.

Figure 2 shows that the oxygen reduction reaction over np-NiPt at pH 4 is favored over hydrogen evolution, down to potentials where water is reduced. Planar electrodes, in contrast, continuously build up adsorbed oxygen under these conditions, eventually switching the reaction pathway from 4-electron, 4-proton reduction to water, to 4-electron reduction to hydroxide, and basifying the interface. We interpret our results to indicate that the nanoporous catalyst has a shallow electrochemically active surface area, through which adsorbed oxygen intermediates can diffuse and be gettered by the high surface area interior of the catalyst. This prevents buildup of excess surface oxygen, an effect that stymies oxygen dissociation.

Multi-electrode flow cell for nitrogen reduction. We have been designing and building a new flow-through reactor, with the goal of using it for nitrogen reduction. Figure 3 shows the schematic design. We have been using the ionic liquid N-Methyl-N-propylpiperidinium bis(trifluoromethylsulfonyl) imide ([PP13][Tf2N]), which is electrochemically stable to -3.0 V as a carrier for hydrogen and nitrogen. The idea is to use a first electrode to dissociate hydrogen to produce a carefully controlled flux of protons to the second electrode, which will be a nanoporous metal catalyst. Technical challenges we have been overcoming include (a) dehydration of the IL. We have found that electrolysis of the IL under vacuum can bring the water content below the ppm level. (b) development of a suitable nanoporous catalyst. Here, we have been using liquid metal dealloying of X-Ti alloys to make nanoporous Ta and Mo (Figure 4), that will be assayed for electroreduction activity.

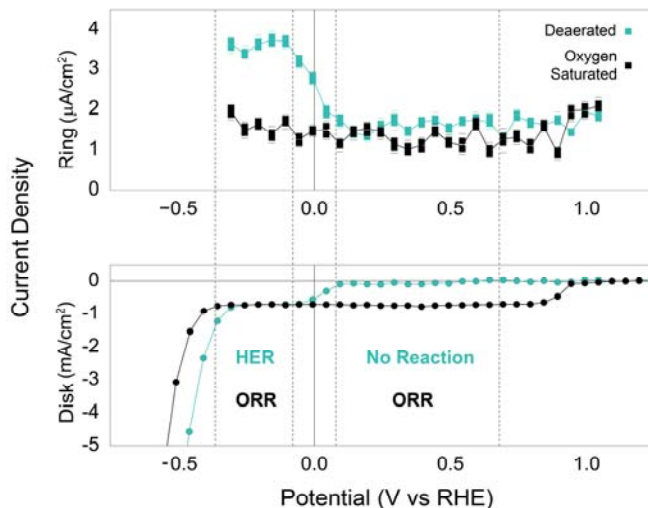


Figure 2. Potentiostatic rotating ring disk electrode measurements of current density vs potential at pH 4 in oxygen-saturated vs. deaerated solutions. Here, both HER and ORR is expected to occur under proton diffusion limited conditions. Hydrogen evolved in deaerated solutions below 0.0 V vs. RHE is detected via hydrogen oxidation at the ring. In oxygen-saturated solutions, HER is suppressed in favor of oxygen reduction, due to a combination of a higher flux of oxygen to the electrode than protons, and nanoporosity which acts to getter excess reaction intermediates [1].

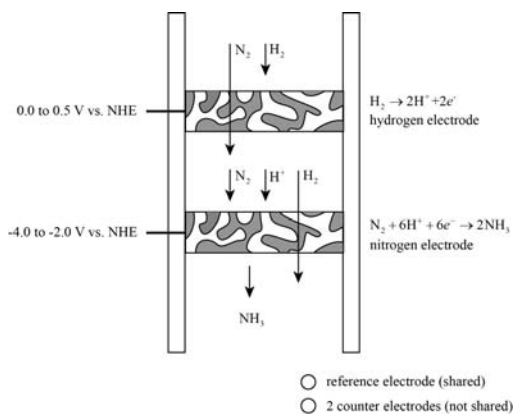


Figure 3. Electrochemical reactor for the synthesis of ammonia via electroreduction of nitrogen. Here, the nitrogen flux is controlled by the solubility of the gas in a carrier ionic liquid, and a controlled (lower) flux of protons is controlled by hydrogen decomposition at an upstream electrode.

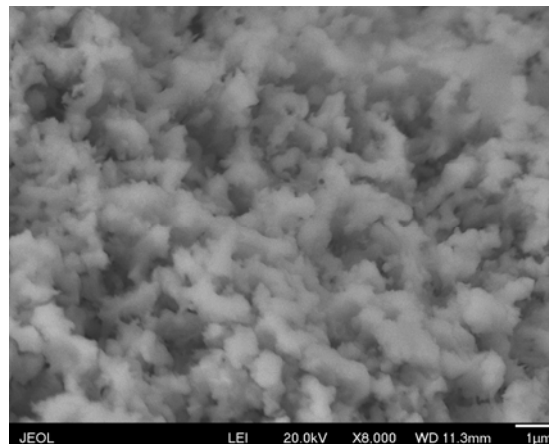


Figure 4. Nanoporous molybdenum made by liquid metal dealloying of Mo-Ti-Si alloy in molten copper, and then dissolving out the Cu phase.

Publications Acknowledging this Grant in 2013-2016

(all publication research exclusively funded by this grant)

1. E. Benn, J. Erlebacher, "Suppression of Hydrogen Evolution by Oxygen Reduction in Nanoporous Electrocatalysts," in preparation, 2016.
2. E. Benn, H. Uvegi, J. Erlebacher, "Characterization of Nanoporous Metal-Ionic Liquid Composites for the Electrochemical Oxygen Reduction Reaction," *J. Electrochem. Soc.*, **162** (2015), H759-H766.
3. J. Snyder, K. Livi, J. Erlebacher, "Oxygen Reduction Reaction Performance of [MTBD][beti]-Encapsulated Nanoporous NiPt Alloy Nanoparticles," *Adv. Func. Mat.*, **23** (2013), 5494-5501.
4. "Encapsulated Nanoporous Metal Nanoparticle Catalysts," United State Patent Application 20140113218, published 4/24/2014.

Fabrication of Nano-Structured Catalyst Supports by ALD

R. J. Gorte and T. M. Onn
Chemical & Biomolecular Engineering
University of Pennsylvania
Philadelphia, PA 19104

Interactions between a transition-metal catalyst and its support can strongly alter the stability and activity of the catalyst. Important examples include support effects with ceria and the so-called “Intelligent Catalysts” in which the metal can be redispersed by reversible ex-solution from a perovskite lattice. However, the surface areas of these functional supports are often too low or unstable; and, in the case of perovskites, the length scales for ingress and egress may be too long to take advantage of the effect. We are addressing these issues by depositing very thin films of various functional oxides, ~1 to 2 nm thick, onto high-surface-area Al₂O₃ by Atomic Layer Deposition. Early work with ZrO₂ ALD films on Pd/Al₂O₃ demonstrated that films less than 1 nm thick were able to stabilize Pd particle size. On Pd/CeO₂, dense, 0.5-nm ZrO₂ films were shown to stabilize CeO₂ crystallite size and surface area, as well as suppressed Ce(SO₄)₂ formation upon exposure to SO₂. More recent work has demonstrated the uniform deposition of dense, 1- to 2-nm films of LaFeO_x, CeO₂, and FeO_x. The films are stable and x-ray amorphous to 1073 K. The CeO₂ and FeO_x films promote the activity of supported Pd for reactions like WGS. The properties of the LaFeO_x films are still under exploration.

DE-FG02-85ER13350: Nano-Structured Catalysts for Improved Oxide-Metal Interactions

Student(s): Tzia Ming Onn, Jiayao Chen

RECENT PROGRESS

The Effect of ZrO₂ ALD Coatings on a Pd/CeO₂ Catalyst

We prepared a CeO₂ support by precipitation of aqueous Ce(NO₃)₃, impregnated it with 1-wt% Pd, and then modified the catalyst by coating it with 20 rounds of ZrO₂ ALD. This produced a catalyst with a 0.4-nm thick film of ZrO₂ (11-wt% ZrO₂), uniformly covering the surface. Calcination of the unmodified CeO₂ caused a large decrease in surface area and increase in crystallite size, as determined by XRD line broadening, between 673 and 1073 K. However, catalysts modified by 0.4-nm ZrO₂ films showed no change in either surface area or CeO₂ crystallite size upon calcination to 1073 K. Methane-oxidation rates in 0.5% CH₄ and 5% O₂ were slightly lower on the ZrO₂-covered catalyst when both materials were calcined at 673 K but the activity of the ZrO₂-modified catalyst did not decrease with catalyst calcination temperature. Both catalysts showed good activity for the water-gas-shift reaction. However, the unmodified catalyst

was irreversibly poisoned by exposure to SO₂ due to formation of cerium sulfates that were difficult to remove, while activity of the ZrO₂-modified catalyst film could be restored by simple calcination.

Improved Thermal Stability and Methane-Oxidation Activity of Pd/Al₂O₃ Catalysts by Atomic Layer Deposition of ZrO₂

The effect of modifying Pd/Al₂O₃ catalysts by Atomic Layer Deposition of 1-nm ZrO₂ films was studied. For deposition on oxidized, PdO/Al₂O₃ catalysts, TEM imaging, EDS mapping, and metal-dispersion measurements confirmed the presence of a thin ZrO₂ over both the Al₂O₃ support and the metal particles. When the Pd was reduced, the ZrO₂ film only grew on the support, as demonstrated by CO chemisorption measurements. The ZrO₂ films were surprisingly stable, only forming a well-crystallized phase observable by XRD above 1173 K. The ZrO₂ coating over the PdO particles created a semi-core-shell-like structure that stabilized the metal against sintering in air at 1073 K. Steady-state, methane-oxidation rates on unmodified PdO/Al₂O₃ decreased with increasing catalyst calcination temperature but rates on the ZrO₂-covered surfaces increased with increasing calcination temperature. Evidence for ZrO₂ playing a promotional effect on methane oxidation was demonstrated by the fact that the ZrO₂-covered catalyst that had been calcined to 1073 K was more active than any of the unmodified PdO/Al₂O₃ catalysts.

The Effect of Water on Methane Combustion Over Pd@Ceria:

The influence of water vapor on methane catalytic combustion was studied over Pd@CeO₂/Si-Al₂O₃ catalysts and compared to results on a conventional impregnated catalyst with identical chemical composition. While the nanostructured Pd@CeO₂/Si-Al₂O₃ catalyst is thermally stable, the addition of water to the reaction feed leads to a transient deactivation at low temperatures, consistent with well documented competitive adsorption of water on PdO. In addition to this, the hierarchically structured, core-shell catalyst exhibits an additional severe deactivation after methane oxidation in the presence of water vapor at 600°C that can be reversed only by heating the catalyst above 700°C. The presence of water in the reaction feed deactivates the conventional impregnated catalyst less severely and the activity largely returns upon water removal. Catalytic, FTIR, and CO-chemisorption data indicate that the severe deactivation process in the hierarchical catalyst is due to the ceria shell transforming to Ce(OH)₃. This significantly inhibits the oxygen spillover from the CeO₂ nanoparticles to Pd, preventing the efficient re-oxidation of Pd, as observed by *operando* XANES experiments in which the Pd is observed to transform from PdO to Pd under methane oxidation conditions when water is added. At the same time, the presence of the hydroxyls can limit the accessibility of Pd to gas-phase reactants, as indicated by the decrease of CO chemisorption capability. The presence of hydroxyls plays a relatively minor role in the deactivation of conventional catalysts at 600°C.

Methane Oxidation on Pd@ZrO₂:

The catalytic properties of Pd@ZrO₂ core-shell catalysts supported on Si-modified alumina were studied for application to methane oxidation and compared to the analogous Pd@CeO₂ catalysts. In the absence of water (dry conditions), both Pd@ZrO₂ and Pd@CeO₂ were highly active and showed nearly identical reaction rates and thermal stabilities. However, unlike catalysts based on Pd@CeO₂, the Pd@ZrO₂ catalysts were also very stable in the presence of high concentrations of water vapor. By means of

Coulometric titration and pulse-reactor studies, we demonstrated that ZrO_2 in contact with Pd can be reduced. Additionally, Coulometric titration showed that the Pd-PdO equilibrium at 600°C is shifted to much lower $P(\text{O}_2)$ in the Pd@ ZrO_2 catalyst compared to conventional Pd/ ZrO_2 or Pd/ Al_2O_3 catalysts. Because PdO is more active for methane oxidation, this observation provides a possible explanation for the superior performance of the Pd@ ZrO_2 catalyst.

Stabilization of Au Catalysts Through Formation of Core-Shell Structures:

A catalyst system consisting of core-shell nanostructures with Au cores and porous TiO_2 shells was synthesized and characterized for room temperature CO oxidation. The core-shell structures were prepared by colloidal methods starting from pre-formed 3-nm Au particles in solution and then adsorbed onto high-surface-area, functionalized, hydrophobic Al_2O_3 supports. The Au@ TiO_2 /Si- Al_2O_3 catalysts prepared in this way showed higher activity and thermal stability than conventional Au/ TiO_2 samples prepared by impregnation of the same Au particles onto commercial titania P25. The core-shell catalyst was able to maintain its activity and 3-nm Au particles size upon calcination up to 600°C , whereas the Au/ TiO_2 sample was found to sinter. Furthermore, it was found that the crystallization of TiO_2 was suppressed in the core-shell structure, resulting in a thin layer of small TiO_2 particles, which is favorable for the dispersion and thermal stability of Au nanoparticles.

Supported Pt-Zn and Pd-Zn Nanoparticles for Methanol Steam Reforming:

Platinum-zinc oxide (Pt@ZnO) and palladium-zinc oxide (Pd@ZnO) core-shell nanoparticles were synthesized in solution using a method based on self-assembly and deposited onto a functionalized alumina (Si- Al_2O_3) support. TEM investigations of the samples confirm the formation of core-shell structures of approximately 6 nm of diameter following calcination to remove the ligands. In-situ TEM and coulometric titration experiments suggest that Pt-Zn alloys are formed upon reduction and that these are highly tunable in size. While methanol-steam reforming (MSR) measurements on conventional Pt/ Al_2O_3 and Pd/ Al_2O_3 catalysts show poor CO_2 selectivities, a Pt(1-wt.%)@ZnO(9-wt.%) / Si- Al_2O_3 system showed comparable activity and selectivity for CO_2 as a conventional Pt/ZnO catalyst, providing further indication that Pt@ZnO forms a Pt-Zn alloy upon reduction due to the intimate contact between the two materials. The Pd@ZnO/Si- Al_2O_3 exhibited lower CO_2 selectivities than Pt@ZnO/Si- Al_2O_3 .

A Comparison of Hierarchical Pt@CeO₂/Si-Al₂O₃ and Pd@CeO₂/Si-Al₂O₃

The catalytic properties of Pt@CeO₂/Si- Al_2O_3 and Pd@CeO₂/Si- Al_2O_3 core-shell catalysts were compared. For calcination at 773 K, Pt@CeO₂/Si- Al_2O_3 exhibits Water-Gas-Shift (WGS) rates that are similar to rates found on conventional Pt/CeO₂, suggesting that there is good contact between the Pt and CeO₂ phases. While WGS rates over Pd@CeO₂/Si- Al_2O_3 declined rapidly due to reduction of CeO₂, rates over Pt@CeO₂/Si- Al_2O_3 were reasonably stable with time indicating a different interaction between metal and CeO₂ phases. Reduction of CeO₂ also greatly suppresses CO adsorption capacities on Pd@CeO₂/Si- Al_2O_3 but has minimal effect on Pt@CeO₂/Si- Al_2O_3 , suggesting that these interactions with CeO₂ are stronger with Pd than with Pt. After calcination to 1073 K, large metal particles were observed with Pt@CeO₂/Si- Al_2O_3 , but not on Pd@CeO₂/Si- Al_2O_3 . Coulometric titration measurements on these two materials also suggest stronger interactions between CeO₂ and Pd.

Publications Acknowledging this Grant in 2013-2016

Exclusively funded by this grant

1. "Phosphorus poisoning during wet oxidation of methane over Pd@CeO₂/Graphite model catalysts", M. Monai, T. Montini, M. Melchionna, T. Duchoň, P. Kúš, N. Tsud, K. Prince, V. Matolin, R. J. Gorte, P. Fornasiero, *Applied Catalysis B*, **2016**, <http://dx.doi.org/10.1016/j.apcatb.2015.10.001>.
2. "Improved Thermal Stability and Methane-Oxidation Activity of Pd/Al₂O₃ Catalysts by Atomic Layer Deposition of ZrO₂", T. M. Onn, S. Zhang, L. Arroyo-Ramirez, Y.-C. Chung, G. W. Graham, X. Pan, R. J. Gorte, *ACS Catalysis*, **2015**, *5*, 5696-5701.
3. "A Comparison of Hierarchical Pt@CeO₂/Si-Al₂O₃ and Pd@CeO₂/Si-Al₂O₃", L. Arroyo-Ramírez, C. Chen, M. Cargnello, C. B. Murray, and R. J. Gorte, *Catalysis Today*, **2015**, *253*, 137-141.
4. "Efficient Removal of Organic Ligands From Supported Nanocrystals by Fast Thermal Annealing Enables Catalytic Studies on Well Defined Active Phases", M. Cargnello, C. Chen, B. Diroll, V. Doan-Nguyen, R. J. Gorte, and C. B. Murray, *Journal of the American Chemical Society*, **2015**, *137*, 6906-11.
5. "Structure, morphology and catalytic properties of pure and alloyed Au-ZnO hierarchical nanostructures", M. Cargnello, D. Sala, C. Chen, M. D'Arienzo, R. J. Gorte, and C. B. Murray, *RSC Advances*, **2015**, *5*, 41920-33.
6. "Supported Platinum-Zinc Oxide Core-Shell Nanoparticle Catalysts for Methanol Steam Reforming", L. Arroyo-Ramírez, Chen Chen, M. Cargnello, C. B. Murray, P. Fornasiero, and R. J. Gorte, *Journal of Materials Chemistry A*, **2014**, *2*, 19509-14.
7. "Methane catalytic combustion over hierarchical Pd@CeO₂/Si-Al₂O₃: Effect of the presence of water", M. Monai, T. Montini, Chen Chen, E. Fonda, R. J. Gorte, P. Fornasiero, *ChemCatChem*, **2015**, *7*, 2038-46.
8. "Thermodynamic and catalytic properties of Pd@ZrO₂/Si-Al₂O₃ core-shell catalysts", Chen Chen, Yu-Hao Yeh, Matteo Cargnello, Christopher B. Murray, Paolo Fornasiero, Raymond. J. Gorte, *ACS Catalysis*, **2014**, *4*, 3902-09.
9. "Au@TiO₂ core-shell nanostructures with high thermal stability", Chen Chen, Mengxue Shi, Matteo Cargnello, Paolo Fornasiero, Christopher B. Murray, and Raymond. J. Gorte, *Catalysis Letters*, **2014**, *144*, 1939-45.
10. "Playing with structures at the nanoscale: designing catalysts by manipulation of the component building blocks", M. Cargnello, P. Fornasiero, and R. J. Gorte, *ChemPhysChem*, **2013**, *14*, 3869-77.
11. "High Temperature Calcination Improves the Catalytic Properties of Alumina-Supported Pd@Ceia Prepared by Self Assembly", Chen Chen, J. Cao, M. Cargnello, P. Fornasiero, and R. J. Gorte, *Journal of Catalysis*, **2013**, *306*, 109-115.
12. "Exceptional Thermal Stability of Monolayer Films of Pd@Ceia Core-Shell Catalyst Nanostructures Grafted onto an Oxide Surface", L. Adijanto, D. Bennett, C. Chen, A. S. Yu, M. Cargnello, P. Fornasiero, R. J. Gorte, John M. Vohs, *Nanoletters*, **2013**, *13*, 2252-2257.
13. "Core-Shell-Type Materials Based on Ceria", M. Cargnello, R. J. Gorte, and P. Fornasiero, in "Catalysis by Ceria and Related Materials, 2nd Edition", A. Trovarelli and P. Fornasiero, Editors, Imperial College Press, **2013**, pp 361-396, DOI: 10.1142/9781848169647_0007.

Dual Site Requirement for Efficient Hydrodeoxygenation of Model Biomass Compounds

Lars C. Grabow with Byeongjin Baek, Sashank Kasiraju, Juan Manuel Arce-Ramos
University of Houston, Chemical and Biomolecular Engineering

Presentation Abstract

Fast pyrolysis of biomass is a promising low-cost technology that produces bio-oil suitable for the production of chemicals and use as transportation fuel after hydrodeoxygenation (HDO). In the recent literature there is a growing number of bifunctional catalyst combinations that show good activity and selectivity for (HDO). Using Density Functional Theory (DFT) we have obtained insight into the role of each type of site and propose a dual site structure-performance relationship for efficient HDO catalysts. For Ru/TiO₂ and Pd/ZrO₂ the amphoteric character of the support is suggested to be paramount for selective C-O cleavage, while the metal functionality is required to activate H₂. We find that this dual site requirement extends to other catalysts systems as well. Of particular interest are Mo-oxycarbides, which have acidic sites similar to those of Mo-oxide, whereas Mo-carbide sites have metallic character. We have compared the potential energy diagram for HDO of furan on Mo-oxide with the equivalent reaction of thiophene hydrodesulfurization (HDS) on MoS₂. Our results show that H₂ activation for both HDO and HDS requires metallic sites, which are present on the brim sites of MoS₂ or are provided by Mo-carbide-like phases in Mo-oxycarbide. Once H₂ dissociates, the acid site for C-O scission can readily form.

Grant or FWP Number: Unifying principles for catalytic hydrotreating processes

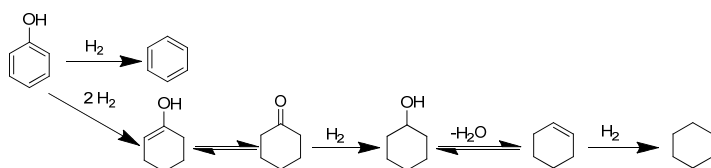
Postdoc(s): Juan Manuel Arce-Ramos, Unmesh Menon

Student(s): Byeongjin Baek, Sashank Kasiraju, Xiao Li, Samantha Bryant, Cecil Meritt

RECENT PROGRESS

Hydrodeoxygenation of phenolics over Ru/TiO₂

Phenolics are bio-oil model compounds that are well-suited for computational and experimental studies. Notably, under hydrogen atmosphere Scheme 1 shows that these compounds can undergo selective C-O bond cleavage (desired), but also aromatic ring hydrogenation (undesired). Our computational work combined



Scheme 1. HDO pathways for phenol. The direct deoxygenation (top) is desired because it requires less H₂ than the hydrogenation path (bottom).

with the experiments contributed by the teams of Profs. Rachel Narehood Austin and Steven Crossley provides evidence for the direct deoxygenation of phenol and m-cresol on Ru/TiO₂ catalysts to occur at perimeter sites at the interface between the Ru metal and the TiO₂ support. A key step in producing this active perimeter site is the heterolytic H₂ cleavage across the interface, as depicted in Fig. 1.

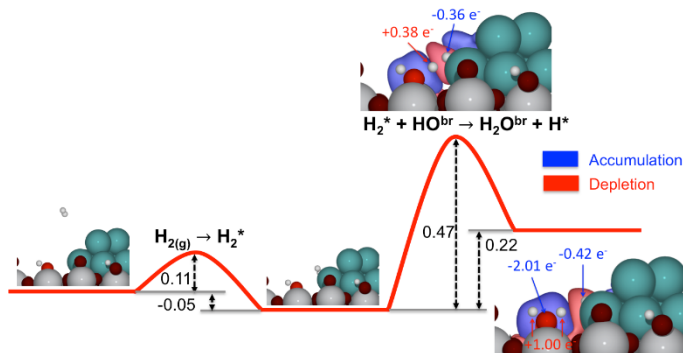


Fig. 1. Heterolytic H₂ activation at the Ru/TiO₂ interface. The proton is accommodated on the support, the hydride remains on a Ru metal site.

Electron density difference and Bader charge analysis suggests that this step forms a support site with Brønsted acid character and a metal-hydride on the metallic Ru cluster.

The following direct C-O scission in phenol or m-cresol is then assisted by the support proton, which results in a substantial reduction of the activation barrier.

During this desired reaction path TiO₂ acts both as a base (proton acceptor) and acid (proton donor). Notably, the activation barriers for both of these key processes are ideally balanced as we try to illustrate in Fig. 2. Based on this work we propose that the key property of the support is its amphoteric character, i.e., its ability to accept protons during H₂ activation and to donate protons during C-O scission, rather than its reducibility, i.e. its ability to form oxygen vacancy defects. The role of the metal sites is mainly related to hydrogen activation.

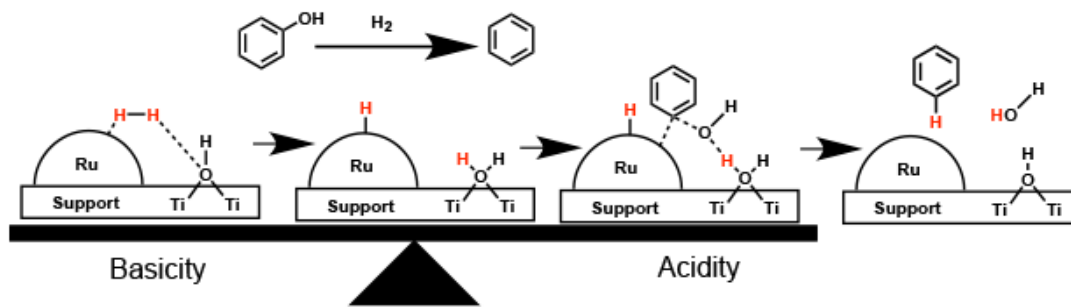


Fig. 2. Proposed hydrodeoxygenation (HDO) mechanism at the Ru/TiO₂ interface. A basic surface hydroxyl on titania abstracts a proton from hydrogen. In a subsequent step, this now acidic surface water donates the proton to the phenolic oxygen, weakening the C-O bond and facilitating bond heterolysis. A hydride from the ruthenium surface forms a C-H bond to generate the product, benzene.

Hydrodeoxygenation on Mo-oxide compared to Hydrodesulfurization on Mo-sulfide

We find that the dual site requirement as introduced for the Ru/TiO₂ system extends to other catalysts systems as well. Of particular interest are Mo-oxy-carbides, which have acidic sites similar to those of Mo-oxide, whereas Mo-carbide sites have metallic character. We show a comparison of the *d*-band density of states (DOS) for both phases in Fig. 3 and the metallic character, i.e. continuous band of *d*-states at the Fermi level, is clearly shown for Mo₂C(100). In Fig. 4 we compare the potential energy diagram for thiophene hydrodesulfurization (HDS) on the S- and Mo-edge of MoS₂ (adopted from

Moses, Hinnemann, Nørskov, *J. Catal.* **248**, 188-203, 2007) with furan hydrodeoxygenation (HDO) on MoO₃(010). One immediate observation in this comparison is the large barrier for H₂ activation on MoO₃(010), which is similar to the barrier of H₂ activation on the S-edge of MoS₂. In the case of MoS₂ metallic brim states can form along the Mo-edge or the promoted S-edge, which can alleviate the H₂ activation problem during HDS. Similarly, the formation of a Mo-oxycarbide or Mo-carbide phase can create sites with metallic character. The investigation of the Mo-carbide phase is still ongoing, but we have confirmed that the Mo₂C(100) surface can spontaneously dissociate H₂. The activated hydrogen may then form an acid site on the MoO₃ phase and drive the selective HDO reaction.

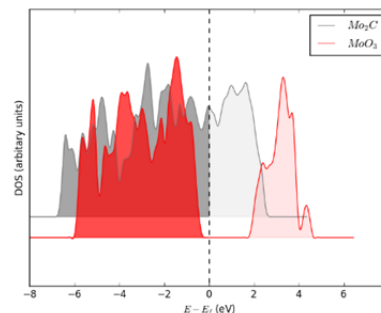


Fig. 3. The *d*-band density of states (DOS) for MoO₃(010) and Mo₂C(100).

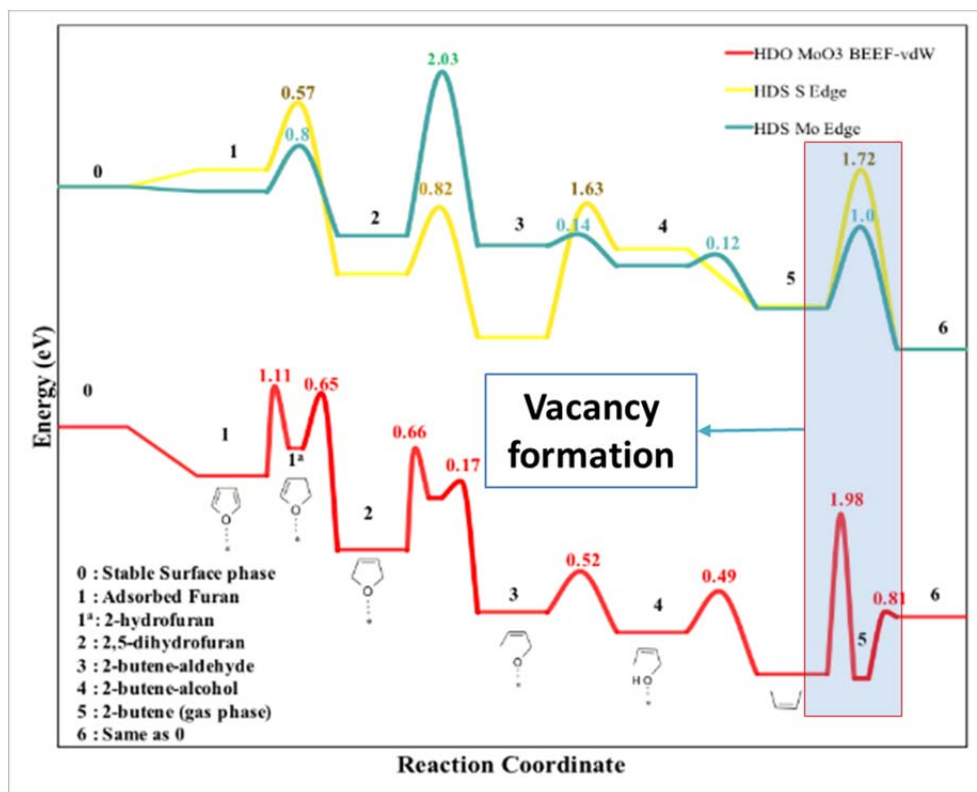


Fig. 4. Juxtaposition of the thiophene hydrodesulfurization (HDS) pathway on the S and Mo edge of MoS₂ (adopted from Moses, Hinnemann, Nørskov, *J. Catal.* **248**, 188-203, 2007) with the furan hydrodeoxygenation (HDO) pathway on MoO₃. HDO on MoO₃(010) is limited by H₂ activation, just as HDS on the S edge of MoS₂.

Overall, our DFT results for HDO of phenolics and furan on Ru/TiO₂ and MoO₃/Mo₂C along with literature knowledge of thiophene HDS on MoS₂ support the preliminary conclusion that a good HDO catalyst requires both metal and acid sites. The acid sites, however, should not be too strong such that their reprotonation is hindered. It appears that amphoteric materials that are readily protonated/deprotonated are most suitable. Our current conclusion and hypothesis is that the right balance between metal and acid

character is necessary for the design of an optimal HDO catalyst. In fact, this explanation seems capable of rationalizing the activity and selectivity of many other catalysts (e.g. Pd/ZrO₂) tested for HDO, but it has never been clearly stated before.

Publications Acknowledging this Grant in 2013-2016

- (I) *Work exclusively funded by this grant;*
- a. Baek, B. First Principle Investigations of Bio-oil Hydrodeoxygenation (HDO) over Ru/TiO₂(110). Ph.D. Thesis, **2015**, University of Houston, Houston, TX, USA.
- (II) *Work jointly funded by this grant and other grants with leading intellectual contribution from this grant;*
2. Nelson, R. C.; Baek, B.; Ruiz, P.; Goundie, B.; Brooks, A.; Wheeler, M. C.; Frederick, B. G.; Grabow, L. C.; Austin, R. N. Experimental and Theoretical Insights into the Hydrogen-Efficient Direct Hydrodeoxygenation Mechanism of Phenol over Ru/TiO₂. *ACS Catal.* **2015**, *5*, 6509–6523.
- (III) *Work jointly funded by this grant and other grants with relatively minor intellectual contribution from this grant;*
3. Goulas, K. A.; Sreekumar, S.; Song, Y.; Kharidehal, P.; Gunbas, G.; Dietrich, P. J.; Johnson, G. R.; Wang, Y. C.; Grippo, A. M.; Grabow, L. C.; Gokhale, A. A.; Toste, F. D. Synergistic Effects in Bimetallic Palladium–Copper Catalysts Improve Selectivity in Oxygenate Coupling Reactions. *J. Am. Chem. Soc.* **2016**, DOI: 10.1021/jacs.6b02247.
 4. Shuai, J.; Yoo, H. D.; Liang, Y.; Li, Y.; Yao, Y.; Grabow, L. C. Density Functional Theory Study of Li, Na, and Mg Intercalation and Diffusion in MoS₂ with Controlled Interlayer Spacing. *Mater. Res. Express* **2016**, just accepted.
 5. Ghorbanpour, A.; Gumidyala, A.; Grabow, L. C.; Crossley, S. P.; Rimer, J. D. Epitaxial Growth of ZSM-5@Silicalite-1: A Core–Shell Zeolite Designed with Passivated Surface Acidity. *ACS Nano* **2015**, *9*, 4006–4016.

Characterization of Tungsten and Zirconium Decorated Multi-walled Carbon Nanotube Catalysts by XAS and NO_x-TPD

Patrick R. Kelleher,^a Cyril Thomas,^b Gary L. Haller,^a

^aDepartment of Environmental and Chemical Engineering, Yale University, New Haven, CT, 06517, USA; ^bSorbonne Universités, UPMC Univ Paris 06, Laboratoire de Réactivité de Surface, F-75252, Paris, France

Presentation Abstract

We have previously shown that zirconia supported on MWCNT (ZrO₂/MWCNT) is hydrothermally stable and can be made a solid acid catalyst by sulfating the zirconia. Although this makes a relatively good acid catalyst, we have found that the sulfur species is not particularly stable in hot liquid water. On the other hand we have demonstrated that the tungsten-modified analogue (WO_x-ZrO₂/MWCNT) is hydrothermally stable and it is expected to have similar, but somewhat lower, acid catalytic activity. The catalyst annealing temperature and oxide loading effects on the oxide particle size were investigated. This was accomplished with XRD and TEM and there was good agreement in the ZrO₂ particle size of ~2 nm and the WO_x particle size of ~6 nm at high loadings, 30 wt%, (but immeasurable at low loading, < 10wt%) using these two techniques. X-Ray absorption near edge spectroscopy (XANES), has shown changes in the W L₃ edge and Zr K edge white line intensities of WO_x-ZrO₂/MWCNT upon annealing at different temperatures, indicating a change in the interaction and/or oxidation state of the tungsten and/or zirconium. To interpret the XANES, it is essential to estimate accessible zirconia surface as a function of WO_x loading and annealing temperature at constant ZrO₂ loading and particle size of the ZrO₂/MWCNT. This was done using NO_x-TPD [H. Y. Law, J. Blanchard, X. Carrier, C. Thomas, J. Phys. Chem. C 114 (2010) 9731-9738].

DE-FG02-01ER15183: ZrO₂/MWCNT as a Support Platform for Acid and Metal Catalysis in Water

Student(s): Patrick R. Kelleher

RECENT PROGRESS

Catalysts were prepared by functionalizing commercially available MWCNT (10-20 nm OD, 10-30 μm). Functionalization consisted of reacting 2 g of MWCNT in 500 mL of refluxing nitric acid (~ 70 wt%) for 2 hours. After functionalization the MWCNT was washed and dried at 100 $^{\circ}\text{C}$ overnight. The MWCNT was then grafted with ZrO_2 by a zirconium acetylacetonate precursor in refluxing toluene for 3 hours to obtain a final ZrO_2 loading of 8–15 wt%. The catalysts were then annealed in flowing helium (50 cc/min) at 450 $^{\circ}\text{C}$ to form ZrO_2 nanoparticles. Finally, the $\text{ZrO}_2/\text{MWCNT}$ complex was impregnated with ammonium metatungstate hydrate and annealed at varying temperatures in flowing helium (50 cc/min) to obtain WO_3 loadings of 10–30 wt%. The resulting ZrO_2 and WO_3 loadings were determined by TGA with flowing air (50 cc/min). X-Ray absorption transmission measurements were performed on pressed pellet samples at NSLS (X23A2) and at APS (9BM). The amount of sample pressed into the pellet was varied to obtain an edge step of 0.2-1. All X-ray absorption data was aligned and normalized using the Demeter software package to give an edge step of 1. The NO_x -TPD method has been described in detail in a previous article. However, one part of the procedure was altered to take account of the MWCNT support. In the original method the desorbing carrier gas was oxidizing (8% O_2 in He) but this would cause combustion of the MWCNT. It was confirmed, using a known ZrO_2 bulk sample, that using pure He as the desorbing gas did not significantly alter the measurement that was found to be in agreement with previous measurements.

The XAS results show that as the annealing temperature is increased (250-850 $^{\circ}\text{C}$) for a given WO_x loading, the white line intensity of the Zr K edge decreases. Furthermore, we have found that as the WO_x loading is increased, the white line intensity of the Zr K edge again decreases. Data collected at the W L_3 edge shows similar trends to the data collected at the Zr K edge. The decrease in the white line intensity results from increased electron density at the Fermi level. This indicates an apparent reduction and/or rehybridization of Zr/W at higher temperatures and with higher WO_x loadings. Mutual reduction of the W and Zr is chemically unlikely, and moreover, it is likely that the coverage of ZrO_2 by WO_x varies with both temperature of annealing and WO_x loading. Thus, we use NO_x -TPD to estimate the accessible zirconia surface as a function of WO_x loading and annealing temperature in order to assess the WO_x - ZrO_2 interaction at constant ZrO_2 loading and constant WO_x coverage. A selection of NO_x -TPD data is summarized in Table 1 from which it can be deduced that: 1) As synthesized, the $\text{ZrO}_2/\text{MWCNT}$ annealed in He at 450 $^{\circ}\text{C}$ retains amorphous C on the ZrO_2 that is removed by repetitive NO_x -TPD (presumably oxidized by NO_2), as indicated by the observed increase in the accessible ZrO_2 surface as the number of successive NO_x -TPD

experiments increases (see Table 1, Exp. 3-6), 2) the C free ZrO₂ particle size, deduced from NO_x-TPD, is 2.2 nm (see exp. 5,6) and consistent with that measured by XRD and TEM, and 3) this amorphous C contamination, that interferes with WO_x/ZrO₂ interaction, appears to be partially removed by interaction with WO_x (enhanced interaction by higher WO_x loading), Exp. 8-9, although this may simply be a result of the greater concentration of WO_x.

Table 1. Summary of the NO_x-TPD Data

Exp. No.	NO _x -TPD run	Sample	ZrO ₂ WO ₃		NO _x released		Accessible surface		ZrO ₂ Crystall size nm
			(wt%)	(wt%)	μmol/g	μmol/g _{ZrO₂}	m ² /g	m ² /g _{ZrO₂}	
1	1	MWCNT = C	-	-	57.9	-	-	-	-
2	1	ZrO ₂ /C	8.2	-	238.4	2259	30.9	377	2.8
3	1	ZrO ₂ /C	8.1	-	220.3	2063	27.8	344	3.0
4	2	ZrO ₂ /C	8.1	-	235.6	2252	30.4	375	2.8
5	3	ZrO ₂ /C	8.1	-	279.6	2795	37.7	466	2.2
6	4	ZrO ₂ /C	8.1	-	286.0	2874	38.8	479	2.2
7	1	ZrO ₂ -WO _x /C-450	6.9	14.8	76.2	447	5.1	75	-
8	2	ZrO ₂ -WO _x /C-450	6.9	14.8	70.2	360	4.1	60	-
9	1	ZrO ₂ -WO _x /C-450	5.8	28.4	41.6	60	0.6	10	-
10	1	ZrO ₂ -WO _x /C-850	6.9	14.8	129.8	-	-	-	-
11	1	ZrO ₂ -WO _x /C-850	5.8	28.4	98.0	-	-	-	-

Publications Acknowledging this Grant in 2013-2016

- *Exclusively funded by this grant;*
1. Wang, X.; Li, N.; Pfefferle, L. D.; Haller, G. L.; Metal nanoparticles inside multi-walled carbon nanotubes: A simple method of preparation and of microscopic image analysis, *Micro Mesoporous Mater.* **2013**, 176, 139-144.
 2. Liu, Changchang; Bolin, Trudy; Northup, Paul; Lee, Sungchul; McEnally, Charles; Kelleher, Patrick; Pfefferle, Lisa; Haller, Gary L.; Combined Zr and S XANES Analysis on S-ZrO₂/MWCNT Solid Acid Catalyst, *Topics in Catal.* **2014**, 57, 693-705.

3. Liu, Changchang; Pfefferle, Lisa D.; Haller, Gary L.; The Electronic Structure or Charge Delocalization of Sulfated Zirconia (Supported on Multi-walled Carbon Nanotubes): Acid Sites Probed by X-ray Absorption Spectroscopy, *Topics in Catal.* **2014**, 57, 774-784.
4. Zhang, Zhiteng; Pfefferle, Lisa; Haller, Gary L.; Comparing characterization of functionalized multi-walled carbon nanotubes by potentiometric proton titration, NEXAFS, and XPS, *Chin. J. Catal.* **2014**, 35, 856-863.
5. Zhang, Zhiteng; Pfefferle, Lisa; Haller, Gary L.; Characterization of functional groups on oxidized multi-wall carbon nanotubes by potentiometric titration, *Catalysis Today* **2015**, 249, 23-29.

Andreas Heyden

**Theoretical Investigation of Heterogeneous Catalysis at the Solid-Liquid Interface
for the Conversion of Lignocellulosic Biomass Model Molecules**

Andreas Heyden
University of South Carolina, Department of Chemical Engineering

Presentation Abstract

It is the objective of this research program to develop and test a hierarchy of multi-scale methods for computing activation and reaction free energies of elementary processes occurring at metal-liquid interfaces relevant for conversion of lignocellulosic biomass into transportation fuels or chemicals that are only up to two orders of magnitude slower than current conventional catalysis tools for catalytic gas-solid studies. As a result, these novel tools will permit within a decade computational metal catalysis studies at solid-liquid interfaces with similar ease to current gas-metal catalysis studies (assuming a similar growth in computing infrastructure as seen in the past couple of decades). Our hierarchy of novel multi-scale methods starts with (i) the use of implicit solvation models to approximately describe solvation effects on elementary reactions at metal surfaces, (ii) the application of our hybrid quantum mechanics (QM) and molecular mechanics (MM) solvation scheme for computing free energies of reactions at metal-liquid interfaces, and (iii) the inclusion of solvent coordinates in the reaction coordinate when computing free energies with our QM/MM approach. Considering that current implicit solvation model parameters for transition metal elements contain significant uncertainties, that molecular mechanics force fields for solvents such as water with transition metal surfaces hardly exist, and that there are also no reliable experimental data of solvent free energies on elementary metal surface processes, we are (i) developing a high dimensional neural network potential for the interaction between Ru(0001) and TIP3P water and (ii) parameterize implicit solvation parameters against our explicit solvation model and rigorously consider uncertainty in the implicit solvation parameters. As model systems for our computational study, we investigate selectivity issues in the hydro-deoxygenation (HDO) of organic alcohols, guaiacol, and propionic acid over transition metal catalysts under liquid-phase processing conditions.

DE-SC0007167: Theoretical Investigation of Heterogeneous Catalysis at the Solid-Liquid Interface for the Conversion of Lignocellulosic Biomass Model Molecules

Postdoc: Vijay Solomon

Student: Mohammad S. Saleheen

RECENT PROGRESS

Explicit Solvation for Metal Surfaces (eSMS)

We have previously reported the development of a quantum mechanics/molecular mechanics free energy perturbation (QM/MM-FEP) method for modeling chemical reactions at metal-water interfaces. This novel solvation scheme combines plane-wave density function theory (DFT), periodic electrostatic embedded cluster method (PEECM) calculations using Gaussian-type orbitals, and classical molecular dynamics (MD) simulations to obtain a free energy description of a complex metal-water system. A limitation of our approach is that its success hinges on the availability of approximate force fields for solvent-metal interactions. While such force fields exist for Pt(111)-water systems, no such force fields exist for the interaction of water with other transition metal surfaces. Hence, our aim is to construct a high dimensional neural network potential to describe the interaction between Ru(0001) and water geometry. While our approach is independent of the specific transition metal surface, we decided to initially focus on Ru due to its recent application in many HDO processes of biomass platform chemicals. We used supervised machine learning techniques where a large data set of metal-water interaction energies and forces calculated by DFT are provided to a feed forward neural network. The neural network code has been provided by Dr. Jörg Behler from Ruhr-Universität Bochum. The atomic configurations were described using symmetry functions and an extended Kalman filter (EKF) was used for optimization of the weights. The fitting procedure has been performed for varying number of cutoff radii, symmetry functions and nodes. Each of these procedures has been performed for varying random seeds ranging from 25 to 200. Our fitting procedure indicated that increasing the cutoff radius does not improve the neural network potential but increasing the number of nodes lowers the root mean square error (RMSE) for energies and forces. Finally, the RMSE for the energies and forces in the training and test set was found to be on the order of ~ 10 meV/atom and ~ 100 meV/Bohr, respectively, which suggest that there is still room for improvement for the NN potential.

Applications of our Implicit Solvation Model for Metal Surfaces: HDO of Organic Alcohols

As an application of our implicit solvation model for metal surfaces (*iSMS*) and as our test bed system for our *eSMS* method development, we are investigating the HDO of ethanol over a Ru(0001) model catalyst under vapor and aqueous phase processing conditions. Specifically, we want to understand the solvent effect on the selectivity of C-C cleavage versus C-O bond scission. Our results suggest that under both vapor and aqueous phase processing conditions, C-C cleavage is favored over C-O cleavage and C₁ products dominate. Under gas phase experimental processing conditions, the TOF calculated for CO and C₂H₆ production are 5.3×10^{-3} and 8.8×10^{-6} (1/s) which are one and two orders of magnitude lower than the experimentally reported values, respectively. For studying the reaction mechanism under aqueous processing conditions, we used our *iSMS* strategy with COSMO-RS implicit solvation model to calculate the solvent effects for all adsorbed species. Considering the uncertainty in the solvation parameters for Ru, we performed calculations with default cavity radius for Ru and with both a 10% increased and decreased cavity radius. Our microkinetic modeling results

suggest that with the default and 10% increased Ru cavity radii, C-C cleavage dominates over C-O bond cleavage; however, at a 10% reduced cavity radius, the two mechanisms become competitive which somewhat agrees with the experimental observation that Ru is sufficiently oxophilic that it prefers C-O bond cleavage over C-C bond scission during aqueous phase processing conditions.

Applications of our Implicit Solvation Model for Metal Surfaces: HDO of Propionic Acid

Finally, we investigated the HDO of propanoic acid in vapor and liquid phase reaction environments over various flat transition metal surfaces such as Rh(111), Ni(111), Pt(111), Ru(0001), Cu(111), Ag(111), and Re(0001). Our objective is to elucidate how solvent effects change the activity and selectivity of various transition metals for the HDO of organic acids. In addition, we aim at identifying scaling relations for solvent effects on elementary Gibbs' free energies of reaction and activation.

Publications Acknowledging this Grant in 2013-2016

(I) Exclusively funded by this grant;

1. Lu, J.; Behtash, S.; Mamun, O.; Heyden, A. Theoretical Investigation of the Reaction Mechanism of the Guaiacol Hydrogenation over a Pt(111) Catalyst. *ACS Catalysis* **2015**, 5, 2423-2435.
2. Lu, J.; Heyden, A. Theoretical Investigation of the Reaction Mechanism of the Hydrodeoxygenation of Guaiacol over a Ru(0001) Model Surface. *J. Catal.* **2015**, 321, 39-50.
3. Faheem, M.; Heyden, A. Hybrid Quantum Mechanics/Molecular Mechanics Solvation Scheme for Computing Free Energies of Reactions at Metal-Water Interfaces. *J. Chem. Theory Comput.* **2014**, 10, 3354-3368.

(II) Jointly funded by this grant and other grants with leading intellectual contribution from this grant;

1. Behtash, S.; Lu, J.; Mamun, O.; Williams, C. T.; Monnier, J. R.; Heyden, A. Solvation Effects in the Hydrodeoxygenation of Propanoic Acid over a Model Pd(211) Catalyst. *J. Phys. Chem. C* **2016**, 120, 2724-2736.
2. Behtash, S.; Lu, J.; Walker, E.; Heyden, A. Solvent Effects in the Liquid Phase Hydrodeoxygenation of Methyl Propionate over a Pd(111) Catalyst Model. *J. Catal.* **2016**, 333, 171-183.
3. Behtash, S.; Lu, J.; Faheem, M.; Heyden, A. Solvent Effects on the Hydrodeoxygenation of Propanoic Acid over Pd(111) Model Surfaces. *Green Chem.* **2014**, 16, 605-616.

(III) Jointly funded by this grant and other grants with relatively minor intellectual contribution from this grant;

1. Lu, J.; Faheem, M.; Behtash, S.; Heyden, A. Theoretical Investigation of the Decarboxylation and Decarbonylation Mechanism of Propanoic Acid over a Ru(0001) Model Surface. *J. Catal.* **2015**, 324, 14-24.
2. Lu, J.; Behtash, S.; Faheem, M.; Heyden, A. Microkinetic Modeling of the Decarboxylation and Decarbonylation of Propanoic Acid over Pd(111) Model Surfaces based on Parameters Obtained from First Principles. *J. Catal.* **2013**, 305, 56-66.

Thomas F. Jaramillo

Engineering surfaces and nanomaterials for H₂ and O₂ electrocatalysis

Thomas F. Jaramillo, Jakob Kibsgaard, Alaina Strickler, Pong Chakthranont, Linsey C. Seitz
Department of Chemical Engineering, Stanford University, Stanford, CA
SUNCAT Center for Interface Science and Catalysis, SLAC National Accelerator
Laboratory
E-mail: jaramillo@stanford.edu

Presentation Abstract

The development of new, renewable pathways to produce and use fuels could play a major role in reaching sustainability goals for the globe. To address technical challenges in this area, we are focusing on three reactions relevant to this objective: the hydrogen evolution reaction (HER), the oxygen reduction reaction (ORR), and the oxygen evolution reaction (OER).

First, recent research will be described in an effort to develop H₂ evolution catalysts that are active, stable, and comprised of only earth-abundant elements. We will also show results in integrating these catalysts into PEM water electrolyzers. Next, electrocatalyst development for the ORR and the OER will be discussed, with a focus on enhancing catalyst activity. In particular, a core-shell approach will be described as a means to engineer surfaces with appropriate properties to drive these reactions.

FWP SLAC-10049: SUNCAT Center for Interface Science and Catalysis

PI: Jens K. Nørskov

Postdoc(s): Jakob Kibsgaard

Student(s): Jia-Wei Desmond Ng, Alaina Strickler, Pong Chakthranont, Linsey C. Seitz

RECENT PROGRESS

The overarching goal of the experimental program within this FWP is to provide fundamental insights and understanding in catalysis related to important energy conversion reactions. The experimental efforts encompass two general areas of catalysis science: electrocatalysis and thermal heterogeneous catalysis. For electrocatalysis we have focused our attention on developing active catalyst materials for the hydrogen evolution reaction (HER), oxygen evolution reaction (OER) and oxygen reduction reaction (ORR) and for thermal heterogeneous catalysis we have focused on syngas conversion to ethanol.

Catalyst development for the HER/HOR

Hydrogen (H_2) is one of the world's most important chemicals mainly used for petroleum refining and synthesizing ammonia-based fertilizers. Catalyzing the electrochemical hydrogen evolution reaction (HER) coupled to renewable energy sources, e.g., wind or solar, is a potential sustainable source of H_2 . Platinum is the most effective HER catalyst, but high cost and scarcity may inhibit its wide spread use. We have investigated several non-precious metal HER catalysts.

Thiomolybdate $[Mo_3S_{13}]^{2-}$ clusters for HER

We synthesized catalytically active thiomolybdate $[Mo_3S_{13}]^{2-}$ nanoclusters, that bridge molecular and solid-state electrocatalysis when supported on carbonelectrode surfaces.¹⁴ The $[Mo_3S_{13}]^{2-}$ nanoclusters exhibited excellent HER activity and stability in acid and imaging at the atomic-scale with scanning tunneling microscopy (STM) allowed for direct observation (see Fig. 1) and quantification of the clusters which enabled determination of the turnover frequency (TOF).

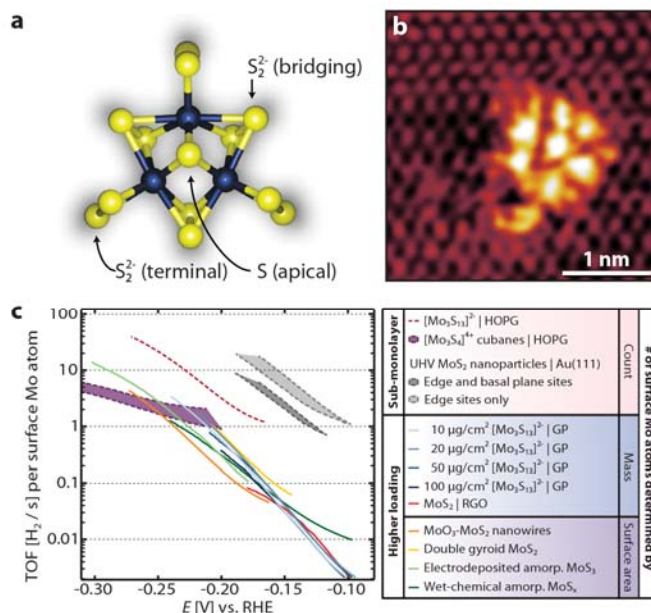


Figure 2: $[Mo_3S_{13}]^{2-}$ for HER.

(a) Model of a single $[Mo_3S_{13}]^{2-}$ cluster containing 3 different types of sulfur ligands. (b) Atom-resolved STM image of a single $[Mo_3S_{13}]^{2-}$ cluster revealing an ordered atomic-scale structure. (c) Plot displaying the turnover frequency of $[Mo_3S_{13}]^{2-}$ clusters together with several other molybdenum sulfide-based HER catalysts. The $[Mo_3S_{13}]^{2-}$ clusters exhibit the highest HER turnover frequency of any molybdenum sulfide catalyst synthesized by scalable route.^{9, 14}

Amorphous MoS_x for HER

Amorphous MoS_x has also shown great promise as a cost-effective and scalable HER catalyst.¹⁵⁻¹⁸ We have employed both *in situ* transmission electron microscopy (TEM)¹⁹ and ambient pressure X-ray photoelectron spectroscopy (AP-XPS)²⁰ in combination with density functional theory (DFT) to gain a better understanding the active phase of amorphous MoS_x. Our results suggest that the surface of the amorphous MoS_x catalyst is dynamic: the *in situ* TEM and AP-XPS reveal a consistent view that the initial catalyst activation forms the primary active surface of amorphous MoS₂, however continued transformation to the crystalline phase during electrochemical operation could contribute to catalyst deactivation due to extended basal planes.

Transition metal phosphides for HER

Recently, transition metal phosphides (TMPs) have also emerged as highly active for the HER.²¹⁻²⁵ However, trends in activity are not well understood. We have provided a new level of understanding through a combined theory-experiment approach. We synthesized different TMPs and correlated experimentally determined HER activities with the hydrogen adsorption free energies, ΔG_H , calculated using DFT, and showed that this correlation follow a volcano relationship (see Fig. 2).¹ Using our combined experimental-theoretical model, we further predicted that the mixed metal TMP, Fe_{0.5}Co_{0.5}P, should have a near-optimal ΔG_H . We synthesized and confirmed that, indeed, Fe_{0.5}Co_{0.5}P exhibits the highest HER activity of the investigated TMPs.

Molybdenum phosphosulfide (MoP|S) for HER

We have furthermore shown that in the case of molybdenum phosphide (MoP), it is possible to improve both the HER activity and stability by introducing sulfur in the surface region to form a

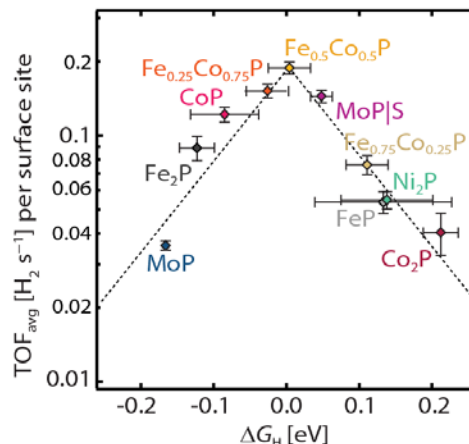


Figure 3: Activity volcano for transition metal phosphides.

Activity volcano for the HER showing the average TOF at an overpotential of 100 mV as a function of ΔG_H .¹⁻⁷

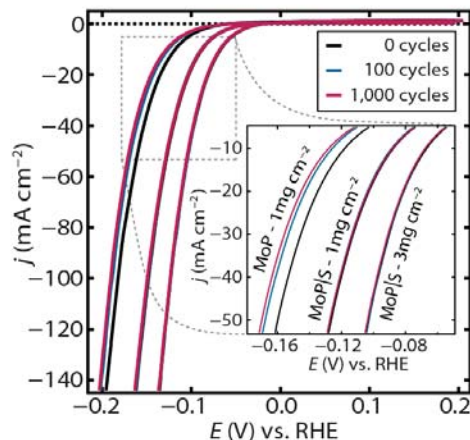


Figure 4: MoP|S for HER.

Accelerated stability test. Initial and post-potential-cycling linear sweep voltam-mograms of MoP and MoP|S. Whereas MoP experiences a slight decrease in current density upon increased potential cycling, MoP|S

molybdenum phosphosulfide (MoP|S).^{10, 26}

Metal alloy catalyst for HER and HOR

We have also investigated metal alloy catalysts that are active for both the HER and hydrogen oxidation reaction (HOR) to develop electrocatalysts for unitized regenerative fuel cells. Using electron-beam co-evaporation, we synthesized metastable NiAg bulk alloys across a range of compositions and showed that NiAg alloys are indeed more active than pure Ni for the HER and, possibly, the HOR.²⁷ DFT calculations supported our experimental findings, showing that bulk alloying of Ni and Ag creates a variety of adsorption sites, some of which have near-optimal ΔG_H .

Catalyst development for the OER

Oxygen evolution reaction (OER) is the complementary half-reaction to the HER in electrochemical water splitting, and similarly provides a source of protons for other processes such as electrochemical CO₂ reduction. To overcome the significant kinetic limitations for the OER, we have used a combination of theory and experiment to investigate and better understand catalysts function.

SrIrO₃ perovskite catalyst for OER

One example is identification of a promising SrIrO₃ perovskite catalyst.²⁸ This material was synthesized using pulsed laser deposition resulting in very flat, crystalline films for a well-controlled study of intrinsic catalyst activity.⁸ The measured activity for this catalyst was even higher than predicted by theory and was also higher than any known OER catalysts previously reported in acid or base (see Fig. 4).²⁻⁷ In addition to showing excellent stability over 30 hours of testing with no measurable degradation. Investigation of the catalyst surface after electrochemical testing revealed Sr leaching which likely leads to formation of a primarily IrO_x terminated surface.

Gold-supported, nickel cerium oxide for OER

One of the most promising catalyst systems we recently discovered for use in basic electrolyte is a gold-supported, nickel cerium oxide (NiCeO_x/Au) thin film which outperforms the best known OER catalysts reported in base, including fully precious

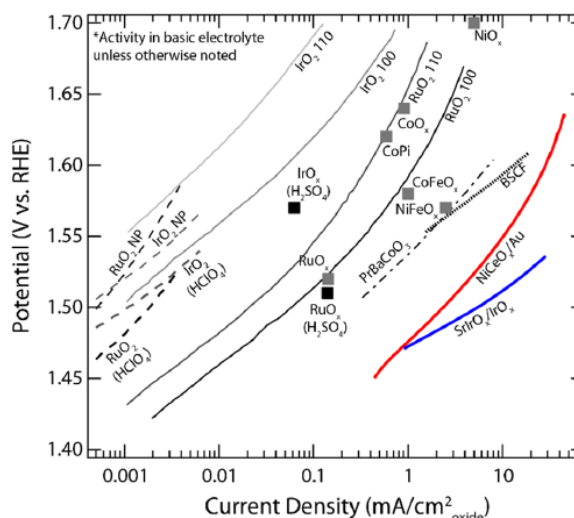


Figure 5: SrIrO_x/IrO_x and NiCeO_x/Au for OER.

OER performance of our SrIrO_x/IrO_x and NiCeO_x/Au catalysts. Specific activity normalized to actual surface area of the metal oxide catalysts.²⁻¹⁰

metal systems (see Fig. 4). Based on experimental observations and theoretical modeling, we ascribe the activity enhancement to a combination of electronic, geometric and support effects, where highly active under-coordinated sites at the oxide-support interface are modified by the local chemical binding environment and by doping the host Ni-oxide with Ce. This new high-performance catalyst is further demonstrated in a device context by pairing it with a nickel-molybdenum hydrogen evolution catalyst in a water electrolyzer, which delivers 50 mA consistently at 1.5 V over 24 hours of continuous operation.

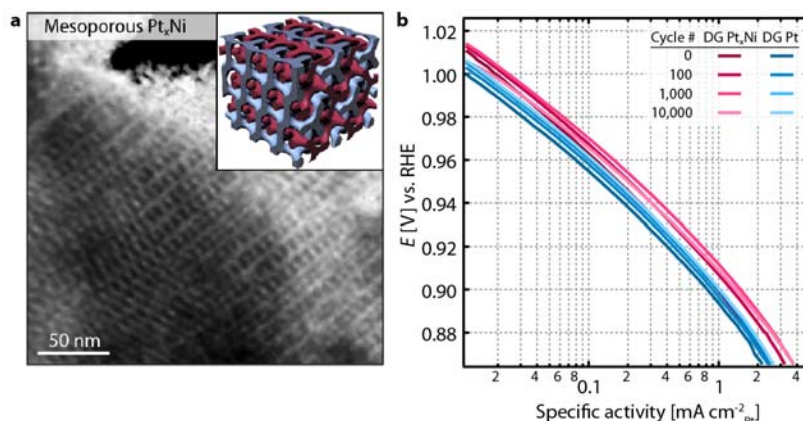


Figure 6: Double gyroid Pt_xNi for ORR.

TEM image and model of the bi-continuous mesoporous Pt_xNi with double gyroid morphology. Initial and post potential cycling Tafel plot of the kinetic current densities of DG Pt_xNi (Pt: $17 \mu g cm^{-2}$) and DG Pt (Pt: $40 \mu g cm^{-2}$).^{10, 13}

Catalyst development for the ORR

Oxygen electrochemistry also plays a key role in fuel cells; the oxygen reduction reaction (ORR) is the complementary reaction to the HOR and is a major source of efficiency limitations due to sluggish kinetics. Improving both the activity and stability of the cathode catalyst in platinum-based polymer electrolyte fuel cells is a key technical challenge for next generation sustainable-energy conversion technologies.

Double gyroid Pt_xNi for ORR

To this end we have synthesized a high surface area supported meso-structured Pt_xNi alloy thin film with double gyroid (DG) morphology that both exhibits high activity and stability for the ORR (see Fig. 5).¹³ The DG Pt_xNi

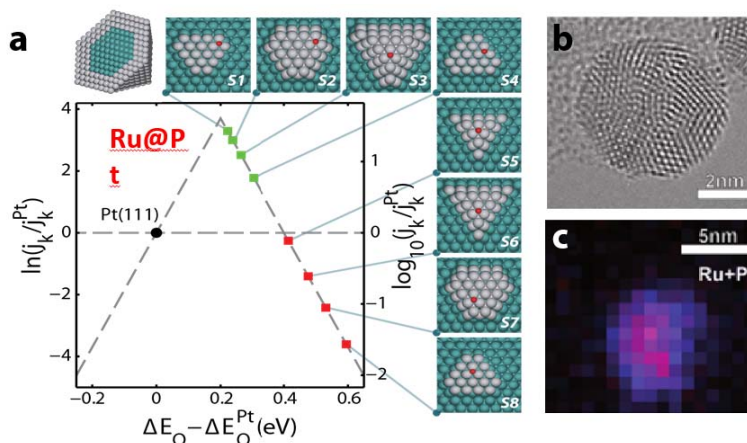


Figure 7: Core-shell $Ru@Pt$ for ORR.

Theoretical oxygen reduction reaction activity volcano plotted as a function of oxygen binding energy. The core-shell strategy allows one to take advantage of two effects: weakening oxygen binding energies by means of thin-film overlayers, and strengthening oxygen binding energies through nano-scale effects. (b) and (c), TEM image and EDS map of $Ru@Pt$ core-shell nanoparticle.

represent the first ever reported fully contiguous large area supported thin film of a highly ordered mesoporous metal alloy. Our studies of ORR catalysis on these thin films show that the DG meso-structure remains intact and maintains good activity even after intensive accelerated stability testing.

Core-shell Ru@Pt nano-particles for the ORR

Additionally, through a combined theory-experiment approach, we identified and developed highly active Ru@Pt core-shell nano-particles for the ORR.¹² Following theoretical pre-dictions of improved oxygen binding on many sites for the Ru@Pt system compared to those of Pt(111), core shell structures (see Fig. 6) were synthesized using a scalable polyol synthesis method. Experimental optimization led to the creation of a highly active and stable Ru@Pt catalyst which outperformed state-of-the-art commercial Pt/C (TKK) nanoparticles and exceeded the DOE 2017 target for mass activity.²⁹

Transition metal catalysts for syngas to ethanol

The prospect of fossil fuel shortages and the need to control carbon emissions have spurred the search for alternative paths to fuels. The production of higher alcohols from sustainably produced syngas (a mixture of CO and H₂) is an attractive route to synthetic fuels; however, there is currently no commercially viable catalyst for this reaction.

One promising reaction scheme is a thermal process utilizing heterogeneous catalysts which can be readily integrated into the existing industrial infrastructure.

Co-Cu alloy catalysts

Based on theory predictions, we have synthesized and tested bimetallic copper-cobalt catalysts for conversion of syngas to higher alcohols.³⁰ In particular, Co₃Cu surfaces were identified as a target of research. Preliminary experimental surveys across the Co-Cu composition spectrum confirmed that this cobalt-rich regime was the most selective, settling on Co_{2.5}Cu as the desired bulk composition. However, copper and cobalt are largely immiscible in the bulk, and initial catalysts prepared via traditional methods

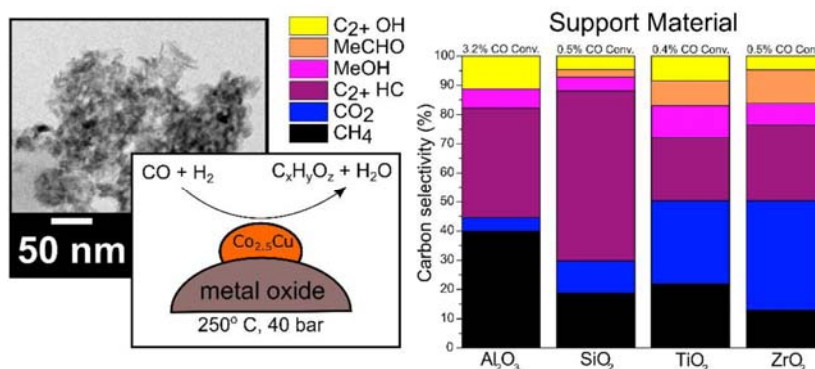


Figure 8: Co_{2.5}Cu catalysts for syngas to ethanol.

Copper-cobalt nanoparticles, prepared by a polyol synthesis and supported on various metal oxides, show selectivity for higher alcohols synthesis from syngas. Co_{2.5}Cu nanoparticles supported on alumina had a carbon selectivity of 11.3% towards higher alcohols at 3.2% CO conversion.¹¹

(incipient wetness, coprecipitation) had limited degrees of alloying. For improved control of the catalyst, we developed a polyol-based nanoparticle synthesis for preparing the desired $\text{Co}_{2.5}\text{Cu}$ catalysts in an alloy form.¹¹ These nanoparticle catalysts show increased selectivity for higher alcohols and oxygenates. Characterization using X-ray diffraction indicates that alloy formation was successful, leading to the higher alcohol activity observed.

Transition metal phosphide catalysts

Recently we have initiated studies on transition metal phosphide catalysts for syngas to alcohol. Our preliminary results show that transition metal phosphide catalysts are activity for both methanol, higher oxygenate and higher hydrocarbon products

REFERENCES:

1. J. Kibsgaard, C. Tsai, K. Chan, J. D. Benck, J. K. Nørskov, F. Abild-Pedersen and T. F. Jaramillo, *Energy and Environmental Science*, 2015, **8**, 3022-3029.
2. A. Grimaud, K. J. May, C. E. Carlton, Y.-L. Lee, M. Risch, W. T. Hong, J. Zhou and Y. Shao-Horn, *Nature Communications*, 2013, **4**.
3. Y. Lee, J. Suntivich, K. J. May, E. E. Perry and Y. Shao-Horn, *Journal of Physical Chemistry Letters*, 2012, **3**, 399-404.
4. K. J. May, C. E. Carlton, K. A. Stoerzinger, M. Risch, J. Suntivich, Y.-L. Lee, A. Grimaud and Y. Shao-Horn, *The Journal of Physical Chemistry Letters*, 2012, **3**, 3264-3270.
5. C. C. L. McCrory, S. Jung, J. C. Peters and T. F. Jaramillo, *J. Am. Chem. Soc.*, 2013, **135**, 16977-16987.
6. K. A. Stoerzinger, L. Qiao, M. D. Biegalski and Y. Shao-Horn, *Journal of Physical Chemistry Letters*, 2014, **5**, 1636-1641.
7. J. Suntivich, K. J. May, H. A. Gasteiger, J. B. Goodenough and Y. Shao-Horn, *Science*, 2011, **334**, 1383-1385.
8. L. C. Seitz, C. F. Dickens, K. Nishio, Y. Hikita, J. Montoya, A. Doyle, C. Kirk, A. Vojvodic, H. Y. Hwang, J. K. Nørskov and T. F. Jaramillo, *Submitted*, 2016.
9. J. W. D. Ng, M. García-Melchor, M. Bajdich, C. Kirk, P. Chakhranont, A. Vojvodic and T. F. Jaramillo, *Submitted*, 2015.
10. J. Kibsgaard and T. F. Jaramillo, *Angewandte Chemie International Edition*, 2014, **53**, 14433-14437.
11. L. V. P. Mendes, J. L. Sinder, S. D. Fleischman, J. Kibsgaard, D. A. G. Aranda and T. F. Jaramillo, *Submitted*, 2016.
12. A. Jackson, V. Viswanathan, A. J. Forman, A. H. Larsen, J. K. Nørskov and T. F. Jaramillo, *ChemElectroChem*, 2014, **1**, 67-71.
13. J. Kibsgaard, A. Jackson and T. F. Jaramillo, *Nano Energy*, 2016, DOI:10.1016/j.nanoen.2016.1005.1005.
14. J. Kibsgaard, T. F. Jaramillo and F. Besenbacher, *Nature Chemistry*, 2014, **6**, 248-253.
15. J. D. Benck, Z. Chen, L. Y. Kuritzky, A. J. Forman and T. F. Jaramillo, *Acs Catalysis*, 2012, **2**, 1916-1923.
16. D. Merki, S. Fierro, H. Vrubel and X. Hu, *Chemical Science*, 2011, **2**, 1262-1267.
17. X. Ge, L. Chen, L. Zhang, Y. Wen, A. Hirata and M. Chen, *Advanced Materials*, 2014, **26**, 3100-3104.

18. B. Seger, A. B. Laursen, P. C. K. Vesborg, T. Pedersen, O. Hansen, S. Dahl and I. Chorkendorff, *Angew. Chem. Int. Ed.*, 2012, **51**, 9128-9131.
19. S. C. Lee, J. D. Benck, C. Tsai, J. Park, A. L. Koh, F. Abild-Pedersen, T. F. Jaramillo and R. Sinclair, *ACS Nano*, 2016, **10**, 624–632.
20. H. G. S. Casalongue, J. D. Benck, C. Tsai, R. K. B. Karlsson, S. Kaya, M. L. Ng, L. G. M. Pettersson, F. Abild-Pedersen, J. K. Nørskov, H. Ogasawara, T. F. Jaramillo and A. Nilsson, *The Journal of Physical Chemistry C*, 2014, **118**, 29252-29259.
21. M. Caban-Acevedo, M. L. Stone, J. R. Schmidt, J. G. Thomas, Q. Ding, H.-C. Chang, M.-L. Tsai, J.-H. He and S. Jin, *Nature Materials*, 2015, **14**, 1245-1251.
22. M. Ledendecker, S. K. Calderon, C. Papp, H. P. Steinruck, M. Antonietti and M. Shalom, *Angew. Chem. Int. Ed.*, 2015, **54**, 12361-12365.
23. E. J. Popczun, J. R. McKone, C. G. Read, A. J. Biacchi, A. M. Wiltrot, N. S. Lewis and R. E. Schaak, *Journal of the American Chemical Society*, 2013, **135**, 9267-9270.
24. E. J. Popczun, C. G. Read, C. W. Roske, N. S. Lewis and R. E. Schaak, *Angew. Chem. Int. Ed.*, 2014, **53**, 5427-5430.
25. F. H. Saadi, A. I. Carim, E. Verlage, J. C. Hemminger, N. S. Lewis and M. P. Soriaga, *J. Phys. Chem. B*, 2014, **118**, 29294-29300.
26. J. W. D. Ng, T. R. Hellstern, J. Kibsgaard, A. C. Hinckley, J. D. Benck and T. F. Jaramillo, *Chemsuschem*, 2015, **8**, 3512-3519.
27. M. H. Tang, C. Hahn, A. J. Klobuchar, J. W. D. Ng, J. Wellendorff, T. Bligaard and T. F. Jaramillo, *Phys. Chem. Chem. Phys.*, 2014, **16**, 19250-19257.
28. J. H. Montoya, M. Garcia-Mota, J. K. Nørskov and A. Vojvodic, *Phys. Chem. Chem. Phys.*, 2015, **17**, 2634-2640.
29. D. Papageorgopoulos, *FY 2013 Annual Progress Report, Fuel Cells Program Overview. Program, D. H. a. F. C., Ed. 2013*.
30. A. J. Medford, A. C. Lausche, F. Abild-Pedersen, B. Temel, N. C. Schjødt, J. K. Nørskov and F. Studt, *Topics in Catalysis*, 2014, **57**, 135-142.

This abstract and progress report represents work on electrocatalysis and thermal heterogeneous catalysis for syngas conversion supervised by Thomas F. Jaramillo within the SUNCAT FWP.

Publications Acknowledging this Grant in 2013-2016:

(I) Exclusively funded by this grant

1. Kibsgaard, J.; Jaramillo, T. F.; Besenbacher, F. Building an appropriate active-site motif into a hydrogen-evolution catalyst with thiomolybdate $[\text{Mo}_3\text{S}_{13}]^{2-}$ clusters. *Nature Chemistry* **2014**, *6*, 248-253.
2. Kibsgaard, J.; Jaramillo, T.F. Molybdenum Phosphosulfide: An Active, Acid-Stable Earth-Abundant Catalyst for the Hydrogen Evolution Reaction. *Angewandte Chemie International Edition* **2014**, *53*, 14433-14437.
3. Kibsgaard, J.; Tsai, C.; Chan, K.; Benck, J.D.; Nørskov, J.K.; Abild-Pedersen, F.; Jaramillo, T.F. Designing an Improved Transition Metal Phosphide Catalyst for

- Hydrogen Evolution using Experimental and Theoretical Trends. *Energy and Environmental Science* **2015**, *8*, 3022-3029.
4. Kibsgaard, J.; Jackson, A.; Jaramillo, T.F. Mesoporous platinum nickel thin films with double gyroid morphology for the oxygen reduction reaction. *Nano Energy*, accepted **2016**. DOI:10.1016/j.nanoen.2016.05.005.
 5. Ng, J.W.D.; García-Melchor, M.; Bajdich, M.; Kirk, C.; Chakthranont, P.; Vojvodic, A.; Jaramillo, T.F. Leveraging Electronic, Geometric and Support Effects in Electrocatalyst Development: Au Supported NiCeO_x for Water Oxidation. *Nature Energy*, accepted **2016**.
 6. Mendes, L.V.P.; Snider, J.L.; Fleischman, S.D.; Kibsgaard, J.; Aranda, D.A.G.; Jaramillo, T.F. Polyol synthesis of cobalt-copper alloy catalysts for higher alcohol synthesis from syngas. Submitted **2016**.

(II) Jointly funded by this grant and other grants with leading intellectual contribution from this grant

7. Jackson, A.; Viswanathan, V.; Forman, A.J.; Larsen, A.H.; Nørskov, J.K.; Jaramillo, T.F. Climbing the Activity Volcano: Core-Shell Ru@Pt Electrocatalysts for Oxygen Reduction. *ChemElectroChem* **2014**, *1*, 67-71.
8. Seitz, L.C.; Dickens, C.F.; Nishio, K.; Hikita, Y.; Montoya, J.; Doyle, A.; Kirk, C.; Vojvodic, A.; Hwang, H.Y.; Nørskov, J.K.; Jaramillo, T.F. A Highly Active and Stable SrIrO₃/IrO_x Catalyst for the Oxygen Evolution Reaction. Submitted, **2016**.

(III) Jointly funded by this grant and other grants with relatively minor intellectual contribution from this grant

9. Tang, M.H.; Hahn, C.J.; Klobuchar, A.J.; Ng, J.W.D.; Wellendorff, J.; Bligaard, T.; Jaramillo, T.F. Nickel-silver alloy electrocatalysts for hydrogen evolution and oxidation in an alkaline electrolyte. *Physical Chemistry Chemical Physics* **2014**, *16*, 19250-19257.
10. Ng, J.W.D.; Hellstern, T.R.; Kibsgaard, J.; Hinckley, A.C.; Benck, J.D.; Jaramillo, T.F. Polymer Electrolyte Membrane Electrolyzers Utilizing Non-precious Mo-based Hydrogen Evolution Catalysts. *Chemsuschem* **2015**, *8*, 3512-3519.

Determination of Rhodium-Alkoxide Bond Strengths in $\text{Tp}'\text{Rh}(\text{PMe}_3)(\text{OR})\text{H}$

Jing Yuwen, Yunzhe Jiao, William W. Brennessel, and William D. Jones*
Department of Chemistry, University of Rochester, Rochester, NY 14627

Presentation Abstract

The active fragment $[\text{Tp}'\text{Rh}(\text{PMe}_3)]$, generated from a thermal precursor $\text{Tp}'\text{Rh}(\text{PMe}_3)(\text{CH}_3)\text{H}$, underwent oxidative addition of water and alcohols to give O-H adducts of the type $\text{Tp}'\text{Rh}(\text{PMe}_3)(\text{OR})\text{H}$ ($\text{R} = \text{H}, \text{Me}, \text{Et}, {}^n\text{Pr}, {}^n\text{Bu}, \text{CH}_2\text{Ph}, {}^i\text{Pr}, c\text{-pentyl}, \text{CH}_2\text{CF}_3, \text{CH}_2\text{CH}_2\text{OH}$) at ambient temperature. These activation products eliminate water or alcohols in benzene, which allows determination of the relative metal-oxygen bond energies by using previously established kinetic techniques. Analysis of the relationship between the relative M-O bond strengths and O-H bond strengths showed a linear correlation with $R_{\text{M-O/O-H}}$ of 1.00 for aliphatic alcohols. The two extraordinary substrates ($\text{R} = \text{CH}_2\text{CF}_3, \text{CH}_2\text{CH}_2\text{OH}$) both have stronger M-O bonds than would be predicted from this trend, suggesting the stabilization of the M-O bond when an electron-withdrawing substituent is present as previously seen in M-C bond strengths. In addition, the O-H activation products of aliphatic alcohols are thermally unstable at 80 °C, as rearrangement to form $\text{Tp}'\text{Rh}(\text{PMe}_3)\text{H}_2$ from β -elimination is observed after 1 or 2 days. Benzyl alcohol and 2,2,2-trifluoroethanol activation products were stable. For benzyl alcohol, although the O-H activation product was kinetically favored, the C-H activation products of the benzene ring were thermally stable.

We have observed C-CN cleavage in nitriles using Pd(0). We have also investigated reactions of alkyl chlorides and nitriles with $[\text{Tp}'\text{Rh}(\text{PMe}_3)]$, as well as with B-H, Si-H, and C-F containing substrates.

FG02-86ER13569:

Transition Metal Activation and Functionalization of C-H and C-C Bonds

RECENT PROGRESS FOR THE PROJECT PERIOD 2015-2016

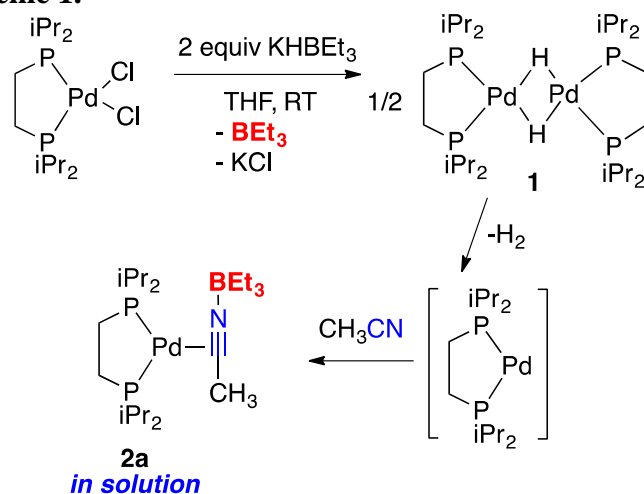
This report summarizes research that has been performed since August 15, 2015, and includes the last 4 months of the prior award and the first eight months of the current award.

1. Cleavage of C-C Bonds in Nitriles (*Coralys Torres, Lloyd Munjanja*).

We have also investigated C-CN cleavage in acetonitrile and benzonitrile using $[\text{Pd}(\text{dippe})]$. The (dippe)palladium(0) fragment generated from $[(\text{dippe})\text{Pd}(\mu\text{-H})]_2$, has been shown to form an intermediate η^2 -nitrile complex with acetonitrile $(\text{dippe})\text{Pd}(\eta^2\text{-C}, \text{N-CH}_3\text{CN-BEt}_3)$ in the presence of BEt_3 [(dippe = bis-diisopropylphosphino)ethane]. On introducing a solution of this compound to 1 equiv of BPh_3 , rapid formation of

(dippe)Pd(η^2 -C,N-CH₃CNBPh₃), is observed. Heating this material at 100°C in THF-*d*₈ results in the C-CN activation product, (dippe)Pd(CH₃)-(CNBPh₃).

Scheme 1.



Reaction of the [Pd(dippe)] precursor with benzonitrile in the presence of BEt₃ gives the C-CN activation product, (dippe)Pd(Ph)(CN-BE₃), exclusively.

2. Cleavage of RO-H Bonds in Alcohols.

One area of research we have just completed is a study of the activation of the O-H bonds of alcohols. The [Tp'¹Rh(PMe₃)] fragment, generated by methane loss from Tp'¹Rh(PMe₃)MeH, reacts with many primary and secondary alcohols to give oxidative addition products of the type Tp'¹Rh(PMe₃)(OR)H. These products are readily isolated and characterized by NMR spectroscopy, and conversion to the bromide derivative permits X-ray structure determination. Note that these products appear to result from oxidative addition, the detailed mechanism has not been determined. For example, it is possible that the alcohol first protonates the Rh^I intermediate and then coordinates alkoxide. Alternatively, it is possible that the oxygen of the alcohol first binds to the metal, and then a hydrogen migration takes place. We favor the latter, as this type of process has been seen in laser flash photolysis experiments of ROH with Cr(CO)₆. Also, it was somewhat surprising not to see C-H activation of the alcohol methyl groups competing with the O-H activation. With [Tp'¹Rh(CNneopentyl)] and alkyl chlorides and nitriles, C-H activation dominated completely.

Even water undergoes oxidative addition to give Tp'¹Rh(PMe₃)(OH)H cleanly. Conversion to the bromide Tp'¹Rh(PMe₃)(OH)Br allows X-ray structure determination. It is worth noting that these ROH studies are only possible with the PMe₃ derivative. Our earlier studies (1990-2010) were exclusively with the neopentylisocyanide derivative as a spectator ligand, but we found that this ligand is susceptible to attack by alcohols to give Fischer carbene adducts (i.e., Rh[=C(NR)(OR)]!). The PMe₃ derivative avoids this undesirable side reaction.

With these alkoxide derivatives in hand, we were then able to examine their rate of reductive elimination in C₆D₆. Our first studies were fraught with problems of reproducibility, and we discovered that any water present could wreak havoc on the kinetics. With this problem solved, we could obtain reliable rate data that provided the

kinetic barrier for RO-H reductive elimination. These barriers are very similar for most alcohols (and water), and are only slightly higher for benzyl alcohol and trifluoroethanol.

Finally, we did kinetic competition studies between each alcohol and benzene. Here, once again, very little variability was seen in the relative rates of activation of the alcohol RO-H bonds. With this $\Delta\Delta G^\ddagger$ data in hand, we were able to determine the relative Rh-OR bond strengths for this series of derivatives using equation 1 below. Equation 1 contains a correction for the statistical (entropic) effect of the number of hydrogens available for activation. A plot of the $D_{\text{Rh-OR}}$ vs. the known $D_{\text{RO-H}}$ bond strengths provides a correlation as shown in Figure 1. Here, the slope of the plot is 1.00(1), which indicates that variations in RO-H bond strengths map exactly onto Rh-OR bond strengths. This conclusion is similar to that made by Bercaw and Bryndza using far less data.

$$D_{\text{rel}}(\text{Rh-OR}) = [\Delta\text{H}(\text{Rh-OR}) - \Delta\text{H}(\text{Rh-Ph})] = \Delta G^\circ + RT \ln(6/\#H) + [\Delta\text{H}(\text{RO-H}) - \Delta\text{H}(\text{Ph-H})] \quad (1)$$

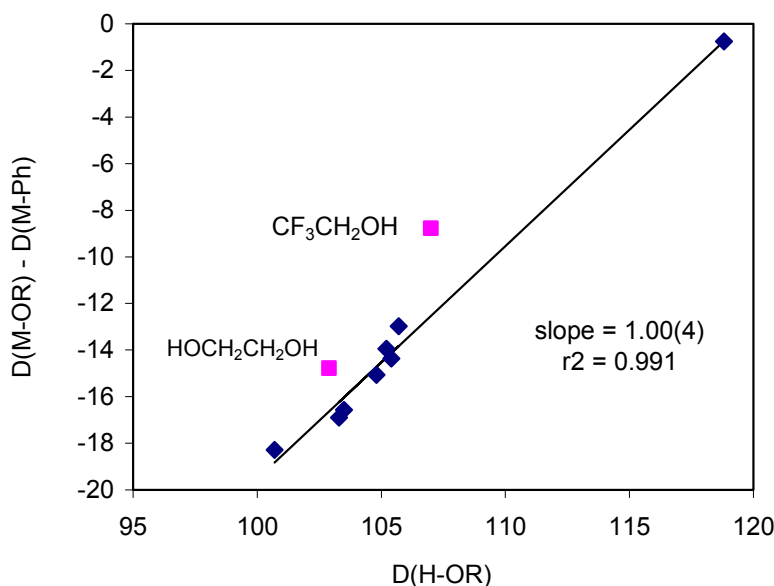


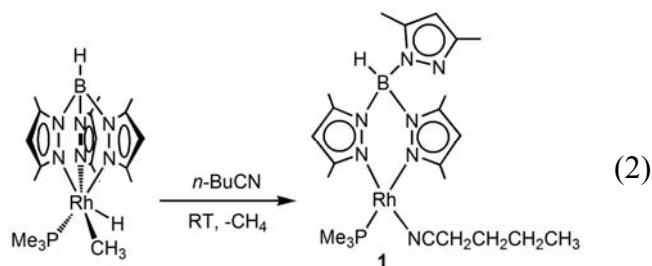
Figure 1. Relative Rh-OR and H-OR bond strengths. The pink data are not included in the fit.

3. Reactions of Alkyl Chlorides and Nitriles with $[Tp^*Rh(PMe_3)]$.

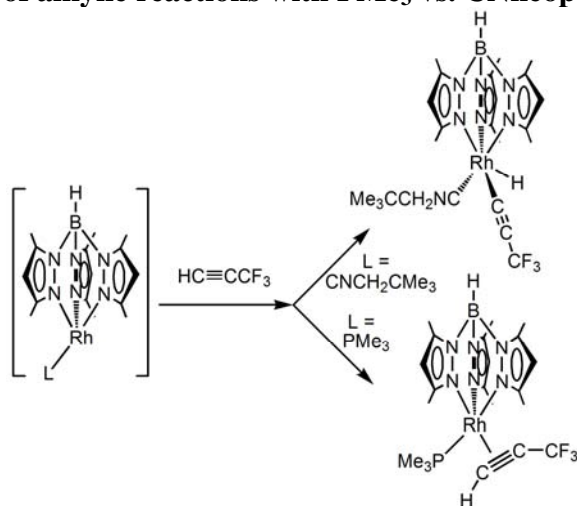
For comparison with the reactivity of $[Tp^*Rn(CNneopentyl)]$, we examined reactions of $Tp^*Rh(PMe_3)MeH$ with alkyl chlorides. Reaction with chloromethane leads to C-H activation product $Tp^*Rh(PMe_3)(CH_2Cl)H$ initially. However, over the course of a month at RT, the compound isomerizes to the C-Cl cleavage product $Tp^*Rh(PMe_3)MeCl$ in benzene solvent. This means that the rearrangement is intramolecular, and avoids free MeCl in solution. DFT calculations indicate that the rearrangement proceeds via an α -chloro elimination to make an intermediate carbene complex, that then inserts into the Rh-H bond. A pathway involving a MeCl sigma complex was found to be too high in energy.

The reaction of $Tp^*Rh(PMe_3)MeH$ with nitriles was also examined for comparison to the CNneopentyl derivative. Reaction with valeronitrile gives exclusively the N-bound terminal nitrile complex (eq 2). Apparently, the alkyl hydride product is too unstable

with PMe_3 as a spectator ligand, so the N-bound nitrile complex is now lower in energy. A similar preference for π -complexes with alkynes was also seen with the PMe_3 derivative as compared to the CNneopentyl derivative (Scheme 2).

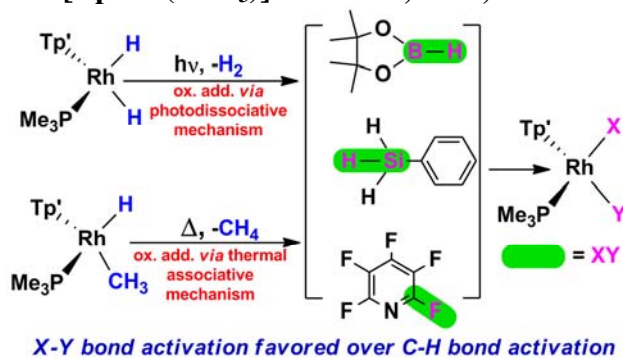


Scheme 2. Comparison of alkyne reactions with PMe_3 vs. CNneopentyl derivatives.



Reactions of $[\text{Tp}'\text{Rh}(\text{PMe}_3)]$ with B-H, Si-H, and C-F bonds. In a collaborative project with Prof. Robin N. Perutz of the University of York, we examined the reactions of several substrates containing B-H, Si-H, and C-F bonds with various precursors for the $[\text{Tp}'\text{Rh}(\text{PMe}_3)]$ fragment. We were able to determine the stabilities of these oxidative addition products, and found them to be among the most stable of all X-H activations we have studied. A summary of the observed reactivity is shown in Scheme 3.

Scheme 3. Reactions of $[\text{Tp}'\text{Rh}(\text{PMe}_3)]$ with B-H, Si-H, and C-F containing substrates.



Publications Acknowledging this Grant in 2013-2016

(I) Exclusively funded by this grant;

1. Jiao, Y.; Evans, M. E.; Morris, J.; Brennessel, W. W.; Jones, W. D. Rhodium-Carbon Bond Energies in Tp'Rh(CNneopentyl)(CH₂X)H: Quantifying Stabilization Effects in M-C Bonds. *J. Am. Chem. Soc.* **2013**, *135*, 6994–7004.
2. Jiao, Y.; Brennessel, W. W.; Jones, W. D. A Trispyrazolylboraterhodium Phosphite Complex that Undergoes an Arbusov-Like Rearrangement. *Acta Cryst. C*, **2013**, *C69*, 939-942.
3. Jiao, Y.; Morris, J.; Brennessel, W. W.; Jones, W. D. Kinetic and Thermodynamic Selectivity of Intermolecular C-H Activation at [Tp'Rh(PMe₃)]. How Does the Ancillary Ligand Affect the Metal-Carbon Bond Strength? *J. Am. Chem. Soc.* **2013**, *135*, 16198–16212.
4. Li, J.; Morris, J.; Brennessel, W. W.; Jones, W. D. Nickel(0) Addition to a Disulfide Bond. *J. Chem. Cryst.* **2013**, *44*, 15-19.
5. Jiao, Y.; Brennessel, W. W.; Jones, W. D. Synthesis and Energetics of Tp'Rh[P(OMe)₃](R)H: A Systematic Investigation of Ligand Effects on C-H Activation at Rhodium. *Chem. Sci.* **2014**, *4*, 804-812.
6. Topics in Current Chemistry, C-C Bond Activation, Guangbin Dong, Ed., "Mechanistic Studies of Transition Metal-Mediated C-C Bond Activation," William D. Jones, Springer-Verlag: Berlin, Heidelberg, **2014**, 1-32.
7. Gunay, A.; Brennessel, W. W.; Jones, W. D. Investigation of C-C Bond Activation of sp-sp³ C-C Bonds of Acetylene Derivatives via Photolysis of Pt Complexes. *Organometallics* **2015**, *34*, 2233-2239.
8. Jiao, Y.; Brennessel, W. W.; Jones, W. D. Oxidative Addition of Chlorohydrocarbons to a Rhodiumtrispyrazolylborate Complex. *Organometallics*, **2015**, *34*, 1552-1566.
9. Jones, W. D. The Effects of Ancillary Ligands on Metal-Carbon Bond Strengths. In *Topics in Organometallic Chemistry: C-H Bond Activation And Catalytic Functionalization (vol. 56)*; Doucet, H. and Dixneuf, P., Eds., Springer-Verlag: Berlin, 2016; pp. 67-89. *Top. Organomet. Chem.*, **2016**, *56*, 67-90.
10. Jiao, Y.; Brennessel, W. W.; Jones, W. D. Nitrile Coordination to Rhodium Does Not Lead to C-H Activation. *Acta Cryst. C*, **2016**, in press.

(II) Jointly funded by this grant and other grants with leading intellectual contribution from this grant:

11. Laviska, D. A.; Guan, C.; Emge, T. J.; Wilklow-Marnell, M.; Brennessel, W. W.; Jones, W. D.; Krogh-Jespersen, K.; Goldman, A. S. Addition of C-C and C-H Bonds by Pincer-Iridium Complexes: A Combined Experimental and Computational Study. *Dalton Trans.* **2014**, *43*, 16354-16365.
12. Procacci, B.; Jiao, Y.; Evans, M. E.; Jones, W. D.; Perutz, R. N.; Whitwood, A. C. Activation of B-H, Si-H, and C-F bonds with Tp'Rh(PMe₃): Kinetics, Mechanism and Selectivity. *J. Am. Chem. Soc.* **2015**, *137*, 1258–1272.
13. Bligaard, T.; Bullock, R. M.; Campbell, C. T.; Chen, J.; Gates, B. C.; Gorte, R. J.; Jones, C. W.; Jones, W. D.; Kitchin, J. R.; Scott, S. L. Towards Benchmarking in Catalysis Science: Best Practices, Opportunities and Challenges. *ACS Catalysis* **2016**, *6*, 2590-2602.
14. Munjanja, L.; Torres-López, C.; Brennessel, W. W.; Jones, W. D. C-CN Cleavage using Palladium Supported by a Dippe Ligand. *Organometallics* **2016**, *35*, in press.

Abhi Karkamkar

Multifunctional Catalysts for CO₂ Reduction

Abhi Karkamkar, Mahendra Yadav, John Linehan, Dave Heldebrant

Physical and Computational Sciences Directorate and Institute for Integrated Catalysis,
Pacific Northwest National Laboratory

Presentation Abstract

We synthesized stable homotopic, single-site catalysts supported on MCM-41 by a combination of sol-gel and surface organometallic chemistry (SOMC). These systems are ideal for the study of CO₂ and H₂ reactivity toward a metal site as a function of the environment. We synthesized several versions of MCM-41-supported ligands and characterized them by multinuclear NMR, FTIR, and MS.

We demonstrated that a variety of metal atoms (Ni, Cu, Ru and Pd) could be anchored on these ligands. In addition to incorporation of single metal sites we have been able to incorporate multi-nuclear clusters of metals. We have devised and synthesized monomeric, dimeric, trimeric and tetrameric clusters that have been incorporated in high surface area mesoporous silica with high degree of control. Structural characterization of these catalytic materials has shown desirable properties such as high surface area, high degree of porosity and high thermal stability. In tetrahydrofuran (THF), for example, catalytic reduction studies show that CO₂ conversion proceeds to formate at low temperature (60°C) with activity comparable to that of the unsupported organometallic catalyst alone.

This work was supported by the US Department of Energy, Office of Basic Energy Sciences, Division of Chemical Sciences, Geosciences & Biosciences. Pacific Northwest National Laboratory (PNNL) is a multi-program national laboratory operated for DOE by Battelle.

**DE-AC06-76RLO 1830: Multifunctional
Catalysis to Synthesize and Utilize
Energy Carriers**

Alexander Katz

Control of Supported Catalysis with Metallocalixarene Surface Complexes

Andrew Palermo,^{1,2} Nicolás A. Grosso Giordano,¹ Andrew Solovyov,¹ Daniel Erter,¹ Erin M. May,¹ Yijun Guo,¹ Bruce C. Gates,² David A. Dixon,³ Sonjong Hwang,⁴ Andriy Drapailo,⁵ Yury Matveev,⁵ Vitaly Kalchenko,⁵ Alexander Katz¹

¹Department of Chemical and Biomolecular Engineering, University of California, Berkeley, California 94720-1462

²Department of Chemical Engineering and Materials Science, University of California at Davis, One Shields Avenue, Davis, California 95616, United States

³Department of Chemistry, The University of Alabama, Tuscaloosa, Alabama 35487

⁴Division of Chemistry and Chemical Engineering, California Institute of Technology, Pasadena, CA 91125, USA

⁵Institute of Organic Chemistry, National Academy of Sciences of Ukraine, 02660, Kyiv-94, Ukraine

Presentation Abstract

Metallocalixarene complexes have been used in three different catalysis-related areas comprising: (i) P(III)-calixarene-based ligands complexed to supported tetrairidium clusters, where the calixarene plays the role of a steric blocking group that prevents metal-site aggregation and also a moiety that tunes the bonding affinity and activity of the supported active site; (ii) grafted Ti(IV) complexes on inorganic oxides, for understanding and controlling epoxidation catalysis with organic hydroperoxides; (iii) a new class of materials for immobilizing lanthanide and actinide Lewis acid sites consisting of grafted carbamoyl-phosphine-oxide-based calixarene ligands on silica.

DE-FG02-05ER15696: Control of Supported Molecular Catalysts Using Metallocalixarene Active Sites

Postdoc(s): Daniel Ertler, Alexander Okrut, Yijun Guo, Andrew Solovyov

Student(s): Andrew Palermo, Erin M. May, Nicolas Grosso Giordano, Audrey Harker

RECENT PROGRESS

P(III)-calixarene-based ligands complexed to supported tetrairidium clusters

A sterically closed tetrairidium carbonyl cluster with three tert-butyl-calix[4]-arene(OPr)₃(OCH₂PPh₂) ligands at the basal plane **1** was selectively opened at the apical site by removal of a CO ligand with trimethylamine N-oxide (TMAO) as an oxidant reacting in the presence of ethylene. The reaction led to the selective bonding of an ethyl ligand at this single Ir atomic site, whereas the reaction in the absence of ethylene removed predominantly bridging carbonyl ligands in the basal plane. The clusters with ethyl ligands on the apical sites, stably supported on silica, constitute unique single-site catalysts for ethylene hydrogenation, with all these active sites being equivalent. Reaction orders of ethylene and hydrogen in the ethylene hydrogenation reaction were nearly identical to those measured for general supported-metal catalysts for this reaction, which have been invoked to function with two different types of sites that bond hydrogen either competitively and non-competitively relative to ethylene, in classic papers spanning over 75 years. Our supported cluster catalyst thus provides a molecular analog of these types of such sites, as well as a means to dial in their respective number density on the catalyst surface.

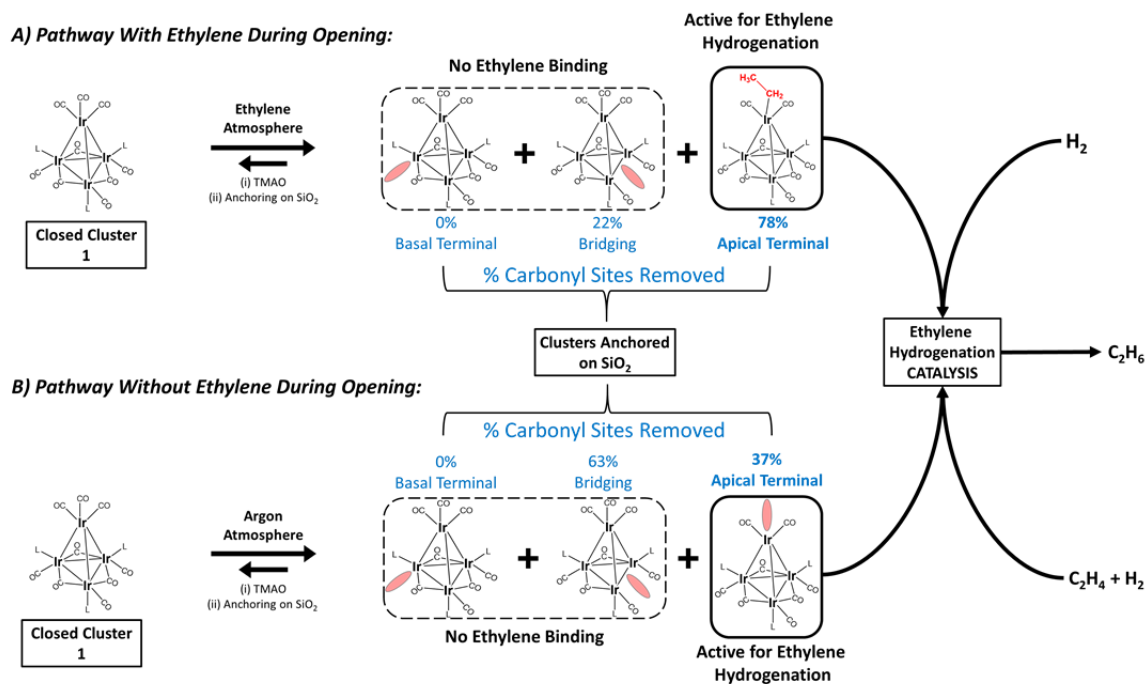


Figure 1. Schematic representation of reactive decarbonylation (vacant carbonyl sites represented by red ovals) of tetrairidium carbonyl cluster **1** (which incorporates terminal and bridging CO ligands, the latter in the basal plane) performed with or without an ethylene atmosphere, leading to a single-site catalyst for ethylene hydrogenation (in red) at the apical position.

Grafted Ti(IV) complexes on inorganic oxides, for understanding and controlling epoxidation catalysis with organic hydroperoxides

The effect of calixarene ligand symmetry, as dictated by lower-rim substitution pattern, on the coordination to a Ti(IV) cation is assessed in solution and when grafted on SiO₂, and its effect on epoxidation catalysis by Ti(IV)-calixarene grafted on SiO₂ is investigated. C_{2v} symmetric Ti-*tert*-butylcalix[4]arene complexes that are 1,3-alkyl disubstituted at the lower rim (di-R-Ti) are compared to previously reported grafted C_s symmetric complexes, which are singly substituted at the lower rim (mono-R-Ti). ¹³C MAS NMR spectra of complexes isotopically enriched at the lower-rim alkyl position indicate that di-R-Ti predominantly grafts onto silica as the conformation found in solution, exhibiting a deshielded alkyl resonance compared to the grafted mono-R-Ti complexes, which is consistent with stronger alkyl ether→Ti dative interactions that are hypothesized to result in higher electron density at the Ti center. Moreover, ¹³C MAS NMR spectroscopy detects an additional contribution from an “endo” conformer for grafted di-R-Ti sites, which is not observed in solution. Based on prior molecular modeling studies and on ¹³C MAS NMR spectroscopy chemical shifts, this “endo” conformer is proposed to have similar Ti-(alkyl ether) distances at the lower-rim and electron density at the Ti center relative to grafted mono-R-Ti complexes. Differences between grafted mono-R-Ti and di-R-Ti sites can be observed by ligand-to-metal charge transfer edge-energies, calculated from diffuse-reflectance UV-visible spectroscopy at 2.24 ± 0.02 eV and 2.16 ± 0.02 eV, respectively. However, rates of *tert*-butyl hydroperoxide consumption in the epoxidation of 1-octene are found to be largely unchanged when compared to those of the grafted mono-R-Ti complexes, with average rate constants of ~1.5 M⁻²s⁻¹ and initial TOF of ~4 ks⁻¹ at 323 K. This suggests that an “endo” conformation of grafted di-R-Ti may prevail during catalysis.

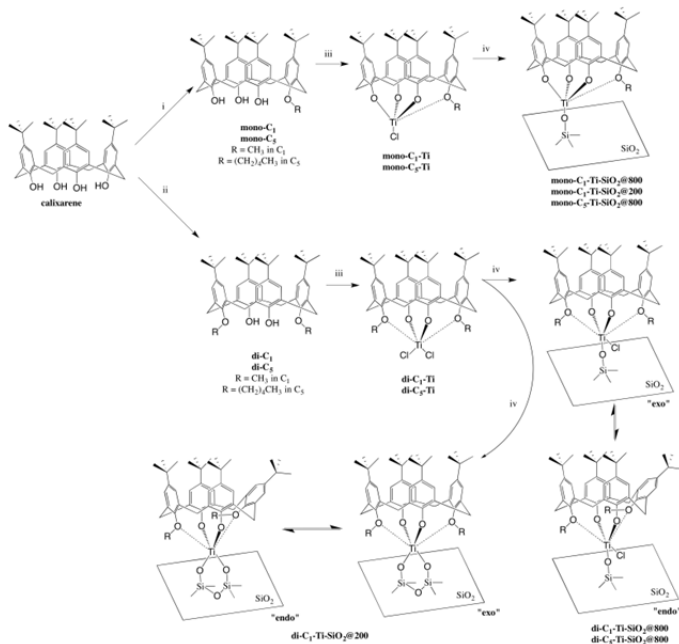
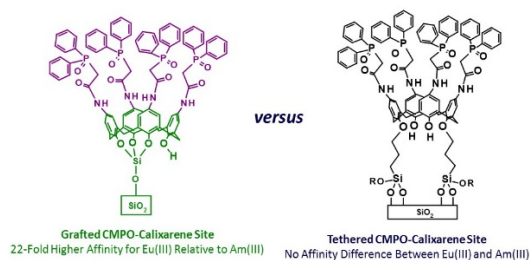


Figure 2. Synthesis of Grafted Ti(IV)-calixarene materials. O-Ti dative interactions are shown in with dashed lines. Reversible arrows indicate the two proposed conformations for the complex on the surface.

Grafted carbamoyl-phosphine-oxide-based calixarene ligands

Grafting of a carbamoylmethylphosphine oxide (CMPO) calix[4]arene ligand to the silica surface yields an anchored host site that displays an unusual 22.4-fold higher affinity (kD value) for Eu(III) relative to Am(III). This selective cation recognition is in stark contrast to a more flexible propoxy-tethered CMPO-calix[4]arene site on silica, which exhibits low selectivity.



Publications Acknowledging this Grant in 2013-2016

(I) Exclusively funded by this grant

- 1) May, E. M.; Solovyov, A.; Guo, Y.; Drapailo, A.; Matveev, Y.; Kalchenko, V.; Nitsche, H.; Katz, A. Unprecedented Affinity Increase for EuIII over AmIII via Silica Grafting of a Carbamoylmethylphosphine Oxide-Calix[4]arene Site, *submitted*.
- 2) Yabushita, M.; Li, P.; Bernales, V.; Kobayashi, H.; Fukuoka, A.; Gagliardi, L.; Farha, O. K.; Katz, A. Unprecedented selectivity in molecular recognition of carbohydrates by a metal-organic framework, *ChemComm* **2016**, 52, 7094 – 7097.
- 3) Grosso-Giordano, N. A.; Solovyov, A.; Hwang, S.; Katz, A. Effect of Coordination Environment in Grafted Single-Site Ti–SiO₂ Olefin Epoxidation Catalysis, *Topics in Catalysis* **2016**, in press.
- 4) Winner, L.; Daniloff, G.; Nichiporuk, R. V.; Solovyov, A.; Katz, A. Patterned Grafted Lewis-Acid Sites on Surfaces: Olefin Epoxidation Catalysis Using Tetrameric Ti(IV)-Calix[4]arene Complexes, *Topics in Catalysis* **2015**, 58, 441 – 450.
- 5) Nandi, P.; Solovyov, A.; Okrut, A.; Katz, A. AlIII–Calix[4]arene Catalysts for Asymmetric Meerwein–Ponndorf–Verley Reduction, *ACS Catalysis*, **2014**, 4, 2492-2495.
- 6) Nandi, P.; Tang, W.; Okrut, A.; Kong, S.; Hwang, S.-J.; Neurock, M.; Katz, A. Catalytic Consequences of Open and Closed Grafted Al(III)-Calix[4]arene Complexes for Hydride and Oxo Transfer Reactions, *Proc. Natl. Acad. Sci. USA* **2013**, 110, 2484 – 2489.

(II) Jointly funded by this grant and other grants with leading intellectual contribution from this grant

- 1) Palermo, A.; Solovyov, A.; Ertler, D.; Okrut, A.; Gates, B. C.; Katz, A. Molecular control of a supported multi-site metal cluster catalyst: dialing in single-site reactivity in tetrairidium, *submitted*.

(III) *Jointly funded by this grant and other grants with relatively minor intellectual contribution from this grant*

- 1) Charmot, A.; Solovyov, A.; Katz, A. Silica-Supported Phosphonic Acids as Thermally and Oxidatively Stable Organic Acid Sites, *submitted*.
- 2) Chung, P.-W.; Yabushita, M.; To, A. T.; Bae, Y.-J.; Jankolovits, J.; Kobayashi, H.; Fukuoka, A.; Katz, A. Long-chain glucan adsorption and depolymerization in zeolite-templated carbon catalysts, *ACS Catalysis* **2015**, *5*, 6422–6425.
- 3) To, A. T.; Chung, P.-W.; Katz, A. Weak-Acid Sites Catalyze Crystalline-Cellulose Hydrolysis to Glucose in Water: Importance of Carbon Post-Synthetic Surface Functionalization, *Angewandte Chemie International Edition in English* **2015**, *54*, 11050–11053.
- 4) Chung, P.-W.; Charmot, A.; Click, T.; Lin, Y.; Bae, Y.-J.; Chu, J.-W.; Katz, A. Importance of Internal Porosity for Glucan Adsorption in Mesoporous Carbon Materials, *Langmuir* **2015**, *31*, 7288-7295.

Michelle K. Kidder

Morphological Role of Binary Metal Oxides on Organic Catalytic Transformations

Michelle K. Kidder and Sheng Dai
Oak Ridge National Laboratory, Chemical Sciences Division

Presentation Abstract

Perovskite-structured mixed metal oxides (ABO_3) are regarded as cost effective and efficient alternatives to noble metals for various catalytic processes due to their high temperature stability, variety of metallic cations available and interesting surface properties, which allow for designing and tuning their physical and chemical properties. In catalytic applications, specific surface area and crystal structure play an important role, and can be controlled by synthetic methods for the resulting desired materials. Synthetic methods to increase surface area include soft templating, reactive grinding, sol-gel processes and nanocasting. Nanocasting is a more suitable method for obtaining higher surface area and crystal growth of a structurally and chemically more stable material. Here we employ mesoporous-templated (SBA-15 or MCM-41) perovskites that possess high surface areas while exchanging the A-cation of the perovskite which will allow us to additionally investigate the role that oxygen vacancies, oxygen mobility, cation reducibility and acid/base character have on the kinetics and product selectivity on oxygenated molecules. We examine the catalytic performance for methanol oxidation reactions over a mesoporous $LaMnO_3$ and $CeMnO_3$ (ca. $100\text{ m}^2/\text{g}$), in comparison to non-porous, lower surface area counterparts (ca. $5\text{-}10\text{ m}^2/\text{g}$) prepared by conventional methods. The structural properties of the perovskites are analyzed by XRD, TEM and BET. Initial results show much higher activity for methanol oxidation reactions using the mesoporous perovskite, compared to their non-porous counterparts, which is thought to be due to the higher specific surface area and higher amount of adsorbed oxygen species available on the surface of the nanocasted perovskites. Additionally, no changes either in the phase or structure of the nanocast materials were observed under the reaction conditions.

*This research is part of FWP ERKCC96: Fundamentals of Catalysis and Chemical Transformations.

Supported Tetrahedral Oxo-Sn Catalyst: Single Site, Two Modes of Catalysis

Evgeny V. Beletskiy^a, Xianliang Hou,^{a,e} Zhongliang Shen,^a James R. Gallagher,^c Jeffrey T. Miller,^d Yuyang Wu,^b Tiehu Li,^e Mayfair C. Kung,^{a*} and **Harold H. Kung.**^{a*}

^a Chemical and Biological Engineering and ^b Chemistry Department, Northwestern University, Evanston, IL 60208

^c Chemical Sciences Division, Argonne National Laboratory, Naperville, IL 60429

^d Chemical Engineering Department, Purdue University, West Lafayette, IN 47907

^e Northwestern Polytechnical University, Xi'an, Shaanxi 710072, P. R. China

Presentation Abstract

We have successfully synthesized a solid Lewis acid with uniform, isolated T_d Sn(IV)oxo centers on a high surface area, nonporous silica, by mild ozone calcination of an anchored precursor (POSS)-Sn-(POSS) complex (POSS = incompletely condensed polyhedral oligomeric silsesquioxane). Upon adsorption of 2-propanol, the hydrogen of the hydroxyl group was transferred to the Sn-O-Si bond to form a Brønsted acid. The precursor (POSS)-Sn-(POSS) was formed by reaction of Sn isopropoxide with POSS. The T_d coordination of Sn in this compound was confirmed by single crystal structure, Sn NMR, and EXAFS characterization. Binding of diethylamine or ethylenediamine to this precursor resulted in formation of octahedrally coordinated Sn, which was confirmed by single crystal structures and Sn NMR. Anchoring the precursor onto a silica surface by hydrosilylation followed by calcination in ozone to remove the hydrocarbon substituents resulted in a Sn(IV)oxo unit. Retention of T_d coordination in the Sn(IV)oxo centers was deduced from characterization using EXAFS, NMR, UV-vis, and DRIFT. Pyridine adsorbed stoichiometrically onto the Sn-oxo unit, and FTIR results indicated adsorption on Lewis acid sites, implying uniformity of sites. No Brønsted acids were detected. These Sn sites were active catalysts in hydride transfer reactions between an alcohol and an aldehyde as a typical solid Lewis acid. Adsorption of 2-propanol created Brønsted acidity, confirmed by pyridine adsorption, by binding the alcohol strongly as alkoxide on Sn and transferring the hydroxyl H to the neighboring Sn-O-Si bond. In the presence of a large excess of alcohol, the bound alkoxide was not displaced when a stoichiometric amount of pyridine was added. This Brønsted acidic silanol was active in epoxide ring opening and acetalization reactions, and could be quantitatively titrated and poisoned by pyridine. In contrast, the Lewis acid-catalyzed hydride transfer reaction was not affected by pyridine. The open structure of the Sn-oxo unit made it possible to be catalytically active for large molecules, such as in reactions involving cellobiose.

Understanding Catalysis of Lignin to Fuels on a Molecular Level

Johannes Lercher,^{a,b} Don Camaioni,^a Donghai Mei,^a Nigel Browning,^a Mirek Derewinski,^a Yong Wang,^a John Fulton,^a Jian Zhi Hu,^a Andreas Jentys^b

^a Pacific Northwest National Laboratory, Physical and Computational Sciences Directorate and Institute for Integrated Catalysis

^b Technical University Munich, Department of Chemistry

Presentation Abstract

The catalyzed-conversion of lignin to alkane energy carriers requires a cascade of reactions for deconstructing and reducing the polymeric, highly oxofunctionalized material. While lignin is the most intractable component of lignocellulose, its conversion to useful products is particularly important, because the carbon in lignin is the most reduced fraction of lignocellulose. Our recent work has been structured to investigate the catalysis of steps important for the deconstruction of lignin, for hydrogenation and hydrodefunctionalization of oxygenated intermediates, and for C–C bond coupling reactions to adjust the size of the product molecules. This has been complemented by focusing on understanding the state and stability of catalysts in the reaction media. We emphasize understanding of the principal chemistry, and we are gradually deepening that by studying more complex representatives of the principal monomers, as well lignin itself, in the envisioned chemistries and to synthesize new generations of catalysts, basing the directions on the physicochemical insight realized by these studies. Key insights highlighted in the poster include demonstrations that confinement in pores significantly enhances rates for acid-catalyzed dehydration and alkylation reactions, that the presence of hydronium ion also enhances rates of metal-catalyzed reactions involving H₂, and that solvents critically control the activity of catalysts.

FWP 47319: Low Temperature Catalytic Routes for Energy Carriers via Spatial and Chemical Organization

PI: Johannes Lercher

Co-PI's: Co-PI's: Don Camaioni, Donghai Mei (Subtask 1.1); Zdenek Dohnálek, David Dixon (U Alabama), Enrique Iglesia (UC Berkeley), Bruce Kay, Roger Rousseau, Yong Wang (Washington State U) (1.2); Aaron Appel, John Linehan, Eric Wiedner, Morris Bullock, Monte Helm, Wendy Shaw (2.1); Roger Rousseau, Mirek Derewinski, Zdenek Dohnálek, Vassiliki-Alexandra Glezakou, David Heldebrant, Abhi Karkamkar, Igor Lyubinetsky, János Szanyi (2.2); Michael Henderson, Zdenek Dohnálek, Roger Rousseau, Greg A. Kimmel, Igor V. Lyubinetsky (3.1); Tom Autrey, Bojana Ginovska, Abhi Karkamkar, Don Camaioni, Greg Schenter (3.2); Wendy Shaw, John Linehan, Bojana Ginovska, Garry Buchko, David Baker (U Washington) (3.3.)

RECENT PROGRESS

This program focuses on the fundamental understanding of catalytic transformations that utilize common carbon resources, such as bioderived molecules (Thrust Area 1) and CO₂ (Thrust Area 2), and access and activate H₂ (Thrust Area 3) (Figure 1). Our strategy is to explore and understand the molecular and atomistic pathways of selected reactions on catalysts spanning from single-crystal surfaces to molecular complexes. Such fundamental understanding of the elemental steps of reaction sequences enables the knowledge-based design of novel catalysts that operate at lower temperatures and with higher rates than practiced today. We believe we can make rapid progress on our research objectives using an integrated approach enabled by the synergy within our large multidisciplinary team that is created by focusing on the four crosscutting research themes that bridge our research areas (subtasks):

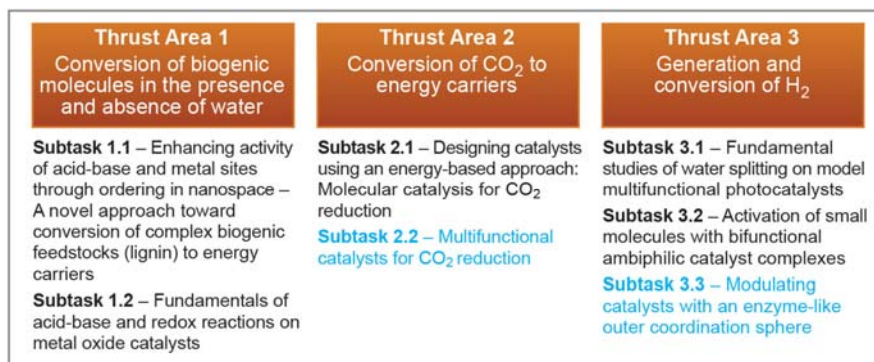


Figure 1. Program Structure showing the three thrust areas and seven subtasks; i.e., the areas of experimental testing for the four common elements of research. Subtasks in blue letters mark activities currently only partly funded and that would be key elements in our strategy

- Multifunctional catalytic sites or catalytic sites acting in concert
- Spatially constrained, chemospecific environments of active centers
- Use of condensed phase to stabilize reactants, intermediates, and products along the catalytic pathway
- Dynamics and kinetics of charge transfer and the availability of charge-carrying species.

Examples of Recent Results:

Subtask 1.1: Enhancing Activity of Acid Base and Metal Sites through an Ordering in Nanospace – A Novel Approach toward Conversion of Complex Biogenic Feedstocks to Energy Carriers

Concertedly acting catalysts containing acid and metal functions are being explored in aqueous and apolar phases to understand the elementary steps of hydrogenation and HDO of phenols. It has been shown that the rate-determining step is the dehydration of the intermediately formed cyclic alcohols. The dehydration of alcohols catalyzed by hydronium ions in zeolites with sufficiently large pores to adsorb the alcohols is faster than in the homogenous aqueous phase, whereas dehydration is slower in mesoporous solids. As an example, Figure 2 shows an Arrhenius plot of the turnover frequencies (TOFs) for dehydration of aqueous cyclohexanol. They span more than three orders of magnitude and are seen to increase with decreasing size of the zeolite pores, except chabasite for which the pores are too small for cyclohexanol to enter. The lower activation barrier in tighter confines is partly offset by a concomitantly smaller entropy gain. While the intrinsic activation barrier for dehydration by aqueous hydronium ion is very similar to the intrinsic barrier for zeolite HBEA, the entropy of activation is less. This is due

to the favorable adsorption of cyclohexanol molecules in HBEA pores leading to pore saturation with approximately 5 cyclohexanol and 20 water molecules per unit cell at reaction temperatures (160–200 °C). This effectively increases the probability for hydronium ion to associate with the alcohol in the pore compared to in the open solution.

Subtask 1.2: Fundamentals of Acid/base and Redox Reactions on Metal Oxide Catalysts

Structure/Function of Redox-Active Supported VO_x ODH Catalysts. We have been studying supported VO_x/TiO₂-Rod catalysts using ⁵¹V MAS NMR at high field using a sample spinning rate of 55 kHz. The superior spectral resolution allows for the observation of at least five vanadate species (Figure 3). The assignment of these vanadate species was carried out by quantum chemical calculations of ⁵¹V NMR chemical shifts of model V-Surface structures. Methanol oxidative dehydrogenation (ODH) was used to establish a correlation between catalytic activity and the various surface V-Sites. It is found that monomeric V-Species are predominant at low vanadium loadings with two ⁵¹V NMR peaks observed at about -502 and -529 ppm. V-Dimers with two bridged oxygens result in a peak at about -555 ppm. Vanadate dimers and polyvanadates connected by one bridged oxygen atom between two adjacent V atoms resonate at about -630 ppm. A positive correlation is found between the V-Dimers giving rise to the -555 ppm peak and the ODH rate, and an even better correlation is obtained by including V-Monomer contributions (Figure 3). This result suggests that surface V-Dimers related to the -555 ppm peak and monomers are the primary active sites for the methanol ODH reaction.

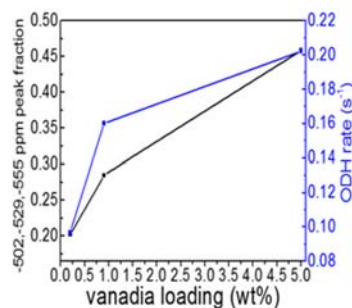
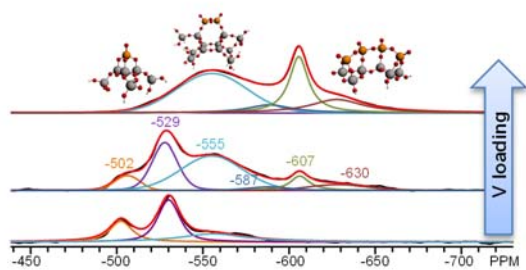


Figure 3. Quantification of V species using ⁵¹V MAS NMR assisted by quantum chemical calculations (left); A positive correlation between surface V-dimers/monomers and methanol oxidative dehydrogenation (right).

Furthermore, a portion of the V-Species is found to be invisible to NMR and the level of such invisibility increases with decreasing V-loading levels, suggesting the existence of paramagnetic V-species at the surface. These paramagnetic V-species are also found to be much less active in methanol ODH.

Cerium Oxide-induced Intercalation of Oxygen on Supported Graphene. We have investigated the growth of ceria nanoclusters and their oxygen storage/release properties on single-layer graphene (Gr) on Ru(0001) with a view towards fabricating a stable system for model catalysis studies. The ceria nanoclusters are of the CeO₂(111)-type and are anchored at the intrinsic defects of the Gr surface. To follow the cluster redox properties we examined their oxygen storage and release in an oxygen atmosphere (<10⁻⁶ Torr) at elevated temperature (550 – 700 K).

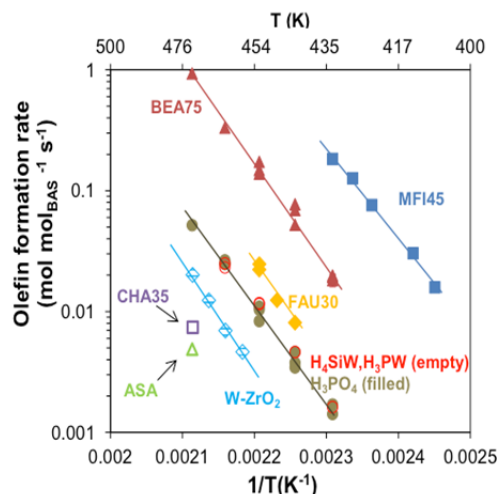


Figure 2. Temperature dependence of the TOFs for dehydration of aqueous cyclohexanol on different acid catalysts. H₃PW₁₂O₄₀ (H₃PW), H₄SiW₁₂O₄₀ (H₄SiW), amorphous silica-alumina (ASA), zeolites (BEA, CHA, FAU, MFI).

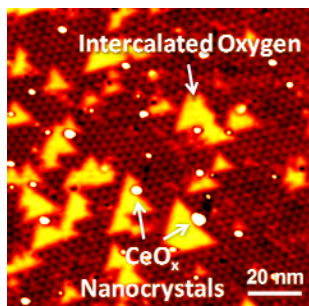


Figure 4. High resolution scanning tunneling microscopy image of ceria nanoclusters supported on Gr monolayer on Ru(0001) illustrating the oxygen intercalation underneath the Gr film in O₂ background of 2×10^{-7} Torr at 600 K.

Under oxidizing conditions, oxygen intercalation under the Gr layer is observed. Time dependent studies demonstrate that the intercalation starts in the vicinity of the CeO_x clusters (Figure 4) and extends until a completely intercalated layer is observed. Temperature dependent studies yield an apparent kinetic barrier for the intercalation of 1.2 eV. At higher temperatures, the intercalation is followed

by a slower etching of the intercalated Gr. These studies demonstrate that the easily reducible CeO_x clusters act as intercalation gateways capable of efficiently delivering oxygen underneath the Gr layer.

Subtask 2.1 Designing Catalysts Using an Energy-Based Approach: Molecular Catalysis for CO₂ Reduction

For the hydrogenation of CO₂ to formate, many molecular catalysts are known, but relatively few are based on non-precious metal complexes. We have previously reported cobalt complexes for the hydrogenation of CO₂ with catalytic activities higher than analogs based on precious metals, however, one of the limiting factors for these cobalt-containing catalysts is the low acidity of the H₂ addition product. One route to improving the acidity is to investigate the nickel analogs, but these complexes are typically hindered by inadequate hydricity for hydride transfer to CO₂. By moving from organic solvents to water, this later obstacle has been overcome.

Catalysts based on copper are of interest for CO₂ reduction, but few effective molecular systems have been designed. Copper hydride complexes have been used for stoichiometric reactions with CO₂, as well as many other catalytic transformations, but no well-defined complexes have been used for the hydrogenation of CO₂. We have now reported the hydrogenation of CO₂ using the triphosphine-copper complex shown in Figure 5. One unusual aspect of the catalytic transformation with this complex is that base coordination appears to facilitate catalysis, rather than hinder it.

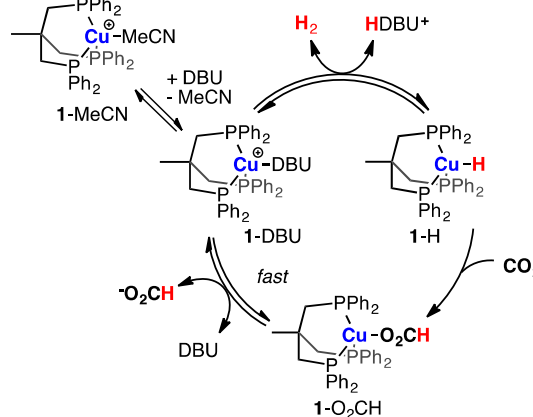


Figure 5. We reported the first well-defined copper-hydride complex that is catalytically active for the hydrogenation of CO₂. Optimal activity for the catalyst requires coordination of base to the metal-center.

Subtask 2.2: Multifunctional Catalysts for CO₂ Activation and Reduction

The catalytic reduction of CO₂ requires bifunctional catalysts as both CO₂ and H₂ need to be activated prior to their reaction. We have shown that on oxide-supported metal catalysts (Pd/ and Ru/ γ -Al₂O₃) the metal component was responsible for the activation (dissociation) of H₂, while the oxide support activated CO₂ by binding it as bicarbonate. The focus of our work has been the understanding of the mechanistic consequences of metal dispersion in the heterogeneous catalytic CO₂ reduction over Pd and Ru on γ -Al₂O₃ catalysts. To this end we have carried out detailed kinetic and transient diffuse reflectance infrared Fourier transform spectroscopy (DRIFTS) studies. Transient DRIFTS measurements showed when hydrogen was

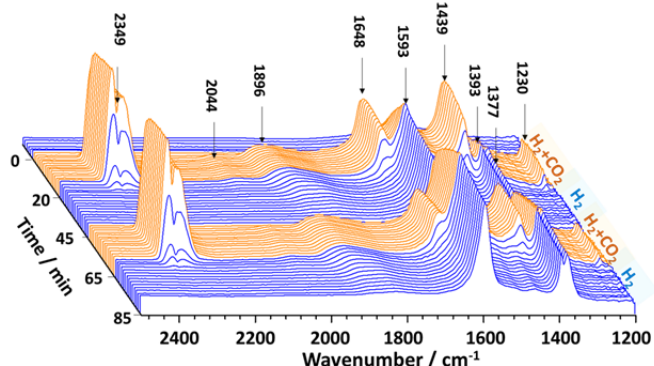


Figure 6. DRIFT spectra collected during alternate switching between H_2 and CO_2+H_2 over 0.5% Pd/ Al_2O_3 at

the amount of available activated hydrogen. At high metal dispersion the availability of hydrogen is limited, therefore the product selectivity is shifted toward CO. On the other hand, on large metal particles a large pool of active H is available, allowing further reduction of the initially formed CO to produce CH_4 with high selectivity.

Subtask 3.1: Fundamental Studies of Water Splitting on Model Multifunctional Photocatalysts

Photo-activated Desorption of H_2 from $RuO_2(110)$. Efforts have focused on fundamental studies of water, H_2 and O_2 on this surface at slightly reduced conditions (i.e., with an oxygen vacancy population of ~5-10%). In particular, we have examined the photodesorption of H_2/D_2 from a combined theoretical and experimental approach, the latter utilizing both ensemble averaged and atomically resolved studies. We find that H_2/D_2 photodesorbs in the visible via a charge redistribution in the surface brought about by a resonant O 2p to Ru 4d excitation process that results in depolarization of the Ru- H_2/D_2 Kubas-like surface complex. On-going studies included the thermal properties of hydrogen dissociation and the role of water in inducing H_2 thermal decomposition.

Subtask 3.2: Activation of Small Molecules with Bifunctional Ambiphilic Catalyst Complexes

Transfer of FLP Activated Hydrogen H^+/H to Unsaturated Substrates. Our time-resolved reaction calorimetry experiments have provided the first absolute rates of H_2 transfer from the zwitterion, PBCATH₂, to a series of p-X-tert-butylbenzaldimine, (X = CF_3 , F, H, Me, CH_3O), kPBCATH₂ ranging from 0.6 to 3.6 $M^{-1}s^{-1}$ at 298 K. The presence of electron withdrawing groups (EWG) decreases the rate while electron donating groups (EDG) increase rate of H_2 transfer. A Hammett plot (Figure 7) of the relative rates measured by both C80 and NMR experiments shows a linear relationship and yields a negative slope ($\rho = -1.8$) suggesting a build-up of (+) charge in the TS, and a ratelimiting H^+ transfer. H_2 activation and transfer under catalytic reaction conditions. We were able to obtain the rate of H_2 transfer under catalytic operating conditions; i.e., 100 mM imine, 13 bar H_2

present on the metal, adsorbed CO formed on the metal while the oxide remained saturated with bicarbonates. This was explained by the ready reaction between bicarbonates (on the oxide) and atomic H (on the metal) that initially formed formate species at the metal/oxide interface and was further reduced to CO. When H_2 was introduced into the CO_2/He gas mixture bicarbonates were rapidly converted to formates, and the formates to CO, and some of the CO to CH_4 (Figure 6). The key difference that ultimately seems to control the product selectivity is the

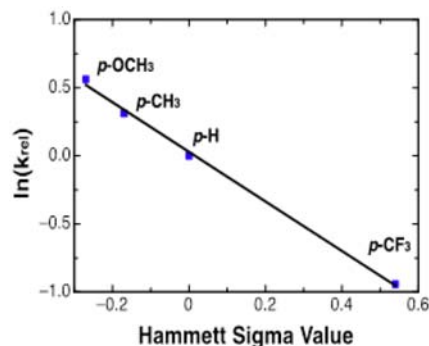


Figure 7. The effect of the X substituents on the imine on the rates of reduction by PBCATH₂, measured by C80 calorimetry experiment.

and 4 mol% PBCAT, using our kinetic modeling approach. We obtain the rate of H₂ transfer, ~2.2 M⁻¹s⁻¹, that is in excellent agreement with the rate obtained in the stoichiometric experiment, 2 M⁻¹s⁻¹, and the corresponding reaction enthalpy, ΔH = 6.7 kcal/mol as well as the rate of H₂ activation, ~1 M⁻¹s⁻¹, and overall thermodynamic driving force for the reduction of the imine to the corresponding amine, ΔH ca. 17.7 kcal/mol. Our preliminary calculations for the reduction of the imine with Me₂NC₂H₄BCl₂ show that the reaction mechanism is stepwise, with the proton transfer step occurring first, forming a stable FLPH/imineH⁺ intermediate, and an H⁺ transfer step associated with large conformational changes.

Subtask 3.3: Modulating Catalysts with an Enzyme-like Outer Coordination Sphere

Achieving room temperature reversibility for a molecular complex. The H₂ oxidation catalyst [Ni(P^{Cy}₂N^{Phe}₂)₂]²⁺ (Cy=cyclohexyl, Phe=phenylalanine) was prepared. Reminiscent of enzymes,

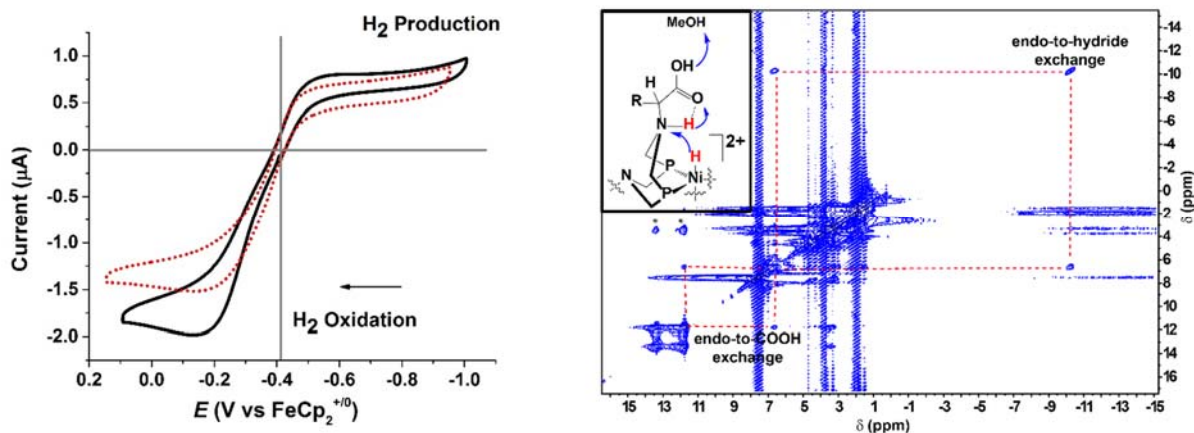


Figure 8. (Left) Electrochemical reversibility was achieved at room temperature for [Ni(P^{Cy}₂N^{Phe}₂)₂]²⁺ (Cy=cyclohexyl, Phe=phenylalanine). This behavior is seldom observed in molecular catalysts and is reminiscent of the behavior in enzymes. (Right) NMR Exchange Spectroscopy data confirm that the -COOH groups in the outer coordination sphere enabling rapid proton transfer, a critical element in achieving reversibility.

electrochemical reversibility is achieved while fast rates are maintained (Figure 8, left). The influence of the amino acids on these catalytic properties is proposed to result from directly transferring protons via the carboxylic acid groups (Figure 8, right) as well as interactions between the side chain groups such as guanidinium or aromatic groups that result in structural modifications to facilitate H₂ addition and electron transfer. These observations demonstrate that outer coordination sphere amino acids work in synergy with the active site and can play an equally important role for synthetic molecular electrocatalysts as the protein scaffold does for redox active enzymes. Moving forward, the principles learned here will be applied to CO₂ hydrogenation catalysts, with some initial results demonstrating feasibility.

Publications Acknowledging this Grant in 2013-2016

Subtask 1.1: Enhancing Activity of Acid/5.1.1 Base and Metal Sites through an Ordering in Nanospace – A Novel Approach toward Conversion of Complex Biogenic Feedstocks to Energy Carriers

Publications exclusively funded by this grant

1. Chase, Z. A.; Fulton, J. L.; Camaioni, D. M.; Mei, D.; Balasubramanian, M.; Pham, V.-T.; Zhao, C.; Weber, R. S.; Wang, Y.; Lercher, J. A., State of Supported Pd during Catalysis in Water. *J. Phys. Chem. C* **2013**, *117*, 17603-17612.
2. Vjunov, A.; Hu, M. Y.; Feng, J.; Camaioni, D. M.; Mei, D.; Hu, J. Z.; Zhao, C.; Lercher, J. A., Following Solid-Acid-Catalyzed Reactions by MAS NMR Spectroscopy in Liquid Phase—Zeolite-Catalyzed Conversion of Cyclohexanol in Water. *Angew. Chem., Int. Ed.* **2014**, *53*, 479-482.
3. Zhi, Y.; Shi, H.; Mu, L.; Liu, Y.; Mei, D.; Camaioni, D. M.; Lercher, J. A., Dehydration Pathways of 1-Propanol on HZSM-5 in the Presence and Absence of Water. *J. Am. Chem. Soc.* **2015**, *137*, 15781-15794.
4. Vjunov, A.; Fulton, J. L.; Camaioni, D. M.; Hu, J. Z.; Burton, S. D.; Arslan, I.; Lercher, J. A., Impact of Aqueous Medium on Zeolite Framework Integrity. *Chem. Mater.* **2015**, *27*, 3533-3545.
5. Kasakov, S.; Zhao, C.; Baráth, E.; Chase, Z. A.; Fulton, J. L.; Camaioni, D. M.; Vjunov, A.; Shi, H.; Lercher, J. A., Glucose- and Cellulose-Derived Ni/C-SO₃H Catalysts for Liquid Phase Phenol Hydrodeoxygenation. *Chem. Eur. J.* **2015**, *21*, 1567-1577.
6. Chase, Z. A.; Kasakov, S.; Shi, H.; Vjunov, A.; Fulton, J. L.; Camaioni, D. M.; Balasubramanian, M.; Zhao, C.; Wang, Y.; Lercher, J. A., State of Supported Nickel Nanoparticles during Catalysis in Aqueous Media. *Chem. Eur. J.* **2015**, *21*, 16541-16546.

Publications jointly funded by this grant and other grants with leading intellectual contribution from this grant

7. He, J.; Lu, L.; Zhao, C.; Mei, D.; Lercher, J. A., Mechanisms of catalytic cleavage of benzyl phenyl ether in aqueous and apolar phases. *J. Catal.* **2014**, *311*, 41-51.
8. He, J.; Zhao, C.; Mei, D.; Lercher, J. A., Mechanisms of selective cleavage of C–O bonds in di-aryl ethers in aqueous phase. *J. Catal.* **2014**, *309*, 280-290.
9. He, J.; Zhao, C.; Lercher, J. A., Impact of solvent for individual steps of phenol hydrodeoxygenation with Pd/C and HZSM-5 as catalysts. *J. Catal.* **2014**, *309*, 362-375.
10. Vjunov, A.; Fulton, J. L.; Huthwelker, T.; Pin, S.; Mei, D.; Schenter, G. K.; Govind, N.; Camaioni, D. M.; Hu, J. Z.; Lercher, J. A., Quantitatively Probing the Al Distribution in Zeolites. *J. Am. Chem. Soc.* **2014**, *136*, 8296-8306.
11. Yoon, Y.; Rousseau, R.; Weber, R. S.; Mei, D.; Lercher, J. A., First-Principles Study of Phenol Hydrogenation on Pt and Ni Catalysts in Aqueous Phase. *J. Am. Chem. Soc.* **2014**, *136*, 10287-10298.

12. Foraita, S.; Fulton, J. L.; Chase, Z. A.; Vjunov, A.; Xu, P.; Baráth, E.; Camaioni, D. M.; Zhao, C.; Lercher, J. A., Impact of the Oxygen Defects and the Hydrogen Concentration on the Surface of Tetragonal and Monoclinic ZrO₂ on the Reduction Rates of Stearic Acid on Ni/ZrO₂. *Chem. Eur. J.* **2015**, *21*, 2423-2434.
13. Hu, J. Z.; Hu, M. Y.; Zhao, Z.; Xu, S.; Vjunov, A.; Shi, H.; Camaioni, D. M.; Peden, C. H. F.; Lercher, J. A., Sealed rotors for in situ high temperature high pressure MAS NMR. *Chem. Commun.* **2015**, *51*, 13458-13461.
14. Kasakov, S.; Shi, H.; Camaioni, D.; Zhao, C.; Barath, E.; Jentys, A.; Lercher, J. A., Reductive Deconstruction of Organosolv Lignin Catalysed by Zeolite Supported Nickel Nanoparticles. *Green Chem.* **2015**, *17*, 5079-5090.
15. Shi, H.; Lercher, J. A.; Yu, X.-Y., Sailing Into Uncharted Waters: Recent Advances in the In Situ Monitoring of Catalytic Processes in Aqueous Environments. *Catalysis Science & Technology* **2015**, *5*, 3035-3060.
16. Song, W.; Liu, Y.; Barath, E.; Zhao, C.; Lercher, J. A., Synergistic effects of Ni and acid sites for hydrogenation and C-O bond cleavage of substituted phenols. *Green Chem.* **2015**, *17*, 1204-1218.
17. Vjunov, A.; Derewinski, M. A.; Fulton, J. L.; Camaioni, D. M.; Lercher, J. A., Impact of Zeolite Aging in Hot Liquid Water on Activity for Acid-Catalyzed Dehydration of Alcohols. *J. Am. Chem. Soc.* **2015**, *137*, 10374-10382.
18. Alexopoulos, K.; Lee, M.-S.; Liu, Y.; Zhi, Y.; Liu, Y.; Reyniers, M.-F.; Marin, G. B.; Glezakou, V.-A.; Rousseau, R.; Lercher, J. A., Anharmonicity and Confinement in Zeolites: Structure, Spectroscopy, and Adsorption Free Energy of Ethanol in H-ZSM-5. *J. Phys. Chem. C* **2016**, *120*, 7172-7182.
19. Prodingler, S.; Derewinski, M. A.; Vjunov, A.; Burton, S. D.; Arslan, I.; Lercher, J. A., Improving Stability of Zeolites in Aqueous Phase via Selective Removal of Structural Defects. *J. Am. Chem. Soc.* **2016**, *138*, 4408-4415.
20. Song, W.; Liu, Y.; Baráth, E.; Wang, L. L.; Zhao, C.; Mei, D.; Lercher, J. A., Dehydration of 1-Octadecanol over H-BEA: A Combined Experimental and Computational Study. *ACS Catal.* **2016**, *6*, 878-889.

Publications jointly funded by this grant and other grants with relatively minor intellectual contribution from this grant

21. Shi, H.; Gutierrez, O. Y.; Haller, G. L.; Mei, D. H.; Rousseau, R.; Lercher, J. A., Structure sensitivity of hydrogenolytic cleavage of endocyclic and exocyclic C-C bonds in methylenecyclohexane over supported iridium particles. *J. Catal.* **2013**, *297*, 70-78.

Subtask 1.2: Fundamentals of Acid/base and Redox Reactions on Metal Oxide Catalysts

Publications exclusively funded by this grant

1. Li, W.-Z.; Kovarik, L.; Mei, D.; Liu, J.; Wang, Y.; Peden, C. H. F., Stable platinum nanoparticles on specific MgAl₂O₄ spinel facets at high temperatures in oxidizing atmospheres. *Nat. Commun.* **2013**, *4*, 2481.

2. Li, Y.; Wei, Z.; Sun, J.; Gao, F.; Peden, C. H. F.; Wang, Y., Effect of Sodium on the Catalytic Properties of VO_x/CeO₂ Catalysts for Oxidative Dehydrogenation of Methanol. *J. Phys. Chem. C* **2013**, *117*, 5722-5729.
3. Li, W.-Z.; Kovarik, L.; Mei, D.; Engelhard, M. H.; Gao, F.; Liu, J.; Wang, Y.; Peden, C. H. F., A General Mechanism for Stabilizing the Small Sizes of Precious Metal Nanoparticles on Oxide Supports. *Chem. Mater.* **2014**, *26*, 5475-5481.
4. Li, Y.; Wei, Z.; Gao, F.; Kovarik, L.; Peden, C. H. F.; Wang, Y., Effects of CeO₂ support facets on VO_x/CeO₂ catalysts in oxidative dehydrogenation of methanol. *J. Catal.* **2014**, *315*, 15-24.
5. Li, Y.; Wei, Z.; Gao, F.; Kovarik, L.; Baylon, R. A. L.; Peden, C. H. F.; Wang, Y., Effect of Oxygen Defects on the Catalytic Performance of VO_x/CeO₂ Catalysts for Oxidative Dehydrogenation of Methanol. *ACS Catal.* **2015**, *5*, 3006-3012.
6. Hu, J. Z.; Xu, S.; Li, W.-Z.; Hu, M. Y.; Deng, X.; Dixon, D. A.; Vasiliu, M.; Craciun, R.; Wang, Y.; Bao, X.; Peden, C. H. F., Investigation of the Structure and Active Sites of TiO₂ Nanorod Supported VO_x Catalysts by High-Field and Fast-Spinning 51V MAS NMR. *ACS Catal.* **2015**, 3945-3952.
7. Li, W.-Z.; Gao, F.; Li, Y.; Walter, E. D.; Liu, J.; Peden, C. H. F.; Wang, Y., Nanocrystalline Anatase Titania-Supported Vanadia Catalysts: Facet-Dependent Structure of Vanadia. *J. Phys. Chem. C* **2015**, *119*, 15094-15102.
8. Kwak, J. H.; Hu, J. Z.; Kim, D. H.; Szanyi, J.; Peden, C. H. F., Penta-coordinated Al³⁺ ions as preferential nucleation sites for BaO on γ -Al₂O₃: An ultra-high-magnetic field ²⁷Al MAS NMR study. *J. Catal.* **2007**, *251*, 189-194.
9. Liu, C.; Sun, J.; Smith, C.; Wang, Y., A study of Zn_xZr_yO_z mixed oxides for direct conversion of ethanol to isobutene. *Appl. Catal. A* **2013**, *467*, 91-97.
10. Sun, J.; Mei, D.; Karim, A. M.; Datye, A. K.; Wang, Y., Minimizing the Formation of Coke and Methane on Co Nanoparticles in Steam Reforming of Biomass-Derived Oxygenates. *ChemCatChem* **2013**, *5*, 1299-1303.
11. Sun, J.; Wang, Y., Recent Advances in Catalytic Conversion of Ethanol to Chemicals. *ACS Catal.* **2014**, *4*, 1078-1090.
12. Davidson, S. D.; Sun, J. M.; Hong, Y. C.; Karim, A. M.; Datye, A. K.; Wang, Y., The effect of ZnO addition on Co/C catalyst for vapor and aqueous phase reforming of ethanol. *Catal. Today* **2014**, *233*, 38-45.
13. Liu, C.; Wang, H.; Karim, A. M.; Sun, J.; Wang, Y., Catalytic fast pyrolysis of lignocellulosic biomass. *Chem. Soc. Rev.* **2014**, *43*, 7594-7623.
14. Wei, Z.; Karim, A. M.; Li, Y.; King, D. L.; Wang, Y., Elucidation of the roles of Re in steam reforming of glycerol over Pt-Re/C catalysts. *J. Catal.* **2014**.
15. Zhang, H.; Sun, J.; Dagle, V. L.; Halevi, B.; Datye, A. K.; Wang, Y., Influence of ZnO Facets on Pd/ZnO Catalysts for Methanol Steam Reforming. *ACS Catal.* **2014**, *4*, 2379-2386.

16. Sun, J.; Karim, A. M.; Mei, D.; Engelhard, M.; Bao, X.; Wang, Y., New insights into reaction mechanisms of ethanol steam reforming on Co–ZrO₂. *Appl. Catal. B* **2015**, *162*, 141-148.
17. Kovarik, L.; Bowden, M.; Shi, D.; Washton, N. M.; Andersen, A.; Hu, J. Z.; Lee, J.; Szanyi, J.; Kwak, J.-H.; Peden, C. H. F., Unraveling the Origin of Structural Disorder in High Temperature Transition Al₂O₃: Structure of θ -Al₂O₃. *Chem. Mater.* **2015**, *27*, 7042-7049.
18. Hu, J. Z.; Xu, S.; Kwak, J. H.; Hu, M. Y.; Wan, C.; Zhao, Z.; Szanyi, J.; Bao, X.; Han, X.; Wang, Y.; Peden, C. H. F., High field 27Al MAS NMR and TPD studies of active sites in ethanol dehydration using thermally treated transitional aluminas as catalysts. *J. Catal.* **2016**, *336*, 85-93.
19. Zhao, Z.; Xu, S.; Hu, M. Y.; Bao, X.; Peden, C. H. F.; Hu, J., Investigation of Aluminum Site Changes of Dehydrated Zeolite H-Beta during a Rehydration Process by High-Field Solid-State NMR. *J. Phys. Chem. C* **2015**, *119*, 1410-1417.
20. Xu, S.; Walter, E. D.; Zhao, Z.; Hu, M. Y.; Han, X.; Hu, J. Z.; Bao, X., Dynamic Structural Changes of SiO₂ Supported Pt–Ni Bimetallic Catalysts over Redox Treatments Revealed by NMR and EPR. *J. Phys. Chem. C* **2015**, *119*, 21219-21226.
21. Zhao, Z.; Xu, S.; Hu, M. Y.; Bao, X.; Hu, J. Z., In Situ High Temperature High Pressure MAS NMR Study on the Crystallization of AlPO₄-5. *J. Phys. Chem. C* **2016**, *120*, 1701-1708.
22. Xu, S.; Zhao, Z.; Hu, M. Y.; Han, X.; Hu, J. Z.; Bao, X., Investigation of water assisted phase transformation process from AlPO₄-5 to AlPO₄-tridymite. *Microporous Mesoporous Mat.* **2016**, *223*, 241-246.
23. Li, Z.; Kay, B. D.; Dohnalek, Z., Dehydration and dehydrogenation of ethylene glycol on rutile TiO₂(110). *Phys. Chem. Chem. Phys.* **2013**, *15*, 12180-12186.
24. Acharya, D. P.; Yoon, Y.; Li, Z.; Zhang, Z.; Lin, X.; Mu, R.; Chen, L.; Kay, B. D.; Rousseau, R.; Dohnalek, Z., Site-Specific Imaging of Elemental Steps in Dehydration of Diols on TiO₂(110). *ACS Nano* **2013**, *7*, 10414-10423.
25. Li, Z.; Fang, Z.; Kelley, M. S.; Kay, B. D.; Rousseau, R.; Dohnalek, Z.; Dixon, D. A., Ethanol Conversion on Cyclic (MO₃)₃ (M = Mo, W) Clusters. *J. Phys. Chem. C* **2014**, *118*, 4869-4877.
26. Rousseau, R.; Dixon, D. A.; Kay, B. D.; Dohnalek, Z., Dehydration, dehydrogenation, and condensation of alcohols on supported oxide catalysts based on cyclic (WO₃)₃ and (MoO₃)₃ clusters. *Chem. Soc. Rev.* **2014**, *43*, 7664-7680.
27. Fang, Z.; Li, Z.; Kelley, M. S.; Kay, B. D.; Li, S.; Hennigan, J. M.; Rousseau, R.; Dohnalek, Z.; Dixon, D. A., Oxidation, Reduction, and Condensation of Alcohols over (MO₃)₃ (M = Mo, W) Nanoclusters. *J. Phys. Chem. C* **2014**, *118*, 22620-22634.
28. Chen, L.; Li, Z.; Smith, R. S.; Kay, B. D.; Dohnalek, Z., Molecular Hydrogen Formation from Proximal Glycol Pairs on TiO₂(110). *J. Am. Chem. Soc.* **2014**, *136*, 5559-5562.
29. Chen, L.; Li, Z.; Smith, R. S.; Kay, B. D.; Dohnalek, Z., Conversion of 1,2-Propylene Glycol on Rutile TiO₂(110). *J. Phys. Chem. C* **2014**, *118*, 15339-15347.

30. Chen, L.; Li, Z.; Smith, R. S.; Kay, B. D.; Dohnalek, Z., Conversion of 1,3-Propylene Glycol on Rutile TiO₂(110). *J. Phys. Chem. C* **2014**, *118*, 23181-23188.
31. Chen, L.; Smith, R. S.; Kay, B. D.; Dohnálek, Z., Adsorption of small hydrocarbons on rutile TiO₂(110). *Surf. Sci.* **2015**.
32. Knaeble, W.; Carr, R. T.; Iglesia, E., Mechanistic interpretation of the effects of acid strength on alkane isomerization turnover rates and selectivity. *J. Catal.* **2014**, *319*, 283-296.
33. Deshlahra, P.; Carr, R. T.; Iglesia, E., Ionic and Covalent Stabilization of Intermediates and Transition States in Catalysis by Solid Acids. *J. Am. Chem. Soc.* **2014**, *136*, 15229-15247.
34. Deshlahra, P.; Iglesia, E., Methanol Oxidative Dehydrogenation on Oxide Catalysts: Molecular and Dissociative Routes and Hydrogen Addition Energies as Descriptors of Reactivity. *J. Phys. Chem. C* **2014**, *118*, 26115-26129.
35. Deshlahra, P.; Carr, R. C.; Chai, S.; Iglesia, E., Mechanistic Details and Reactivity Descriptors in Oxidation and Acid Catalysis of Methanol. *ACS Catal.* **2015**, *5*, 666-682.
36. Knaeble, W.; Iglesia, E., Kinetic and Theoretical Insights into the Mechanism of Alkanol Dehydration on Solid Brønsted Acid Catalysts. *J. Phys. Chem. C* **2016**, *120*, 3371-3389.
37. Li, S.; Dixon, D. A., Structural and Electronic Properties of Group 6 Transition Metal Oxide Clusters. In *New and Future Development in Catalysis: Catalysis by Nanoparticles*, Suib, S., Ed. Elsevier: 2013; pp 21-61.
38. Fang, Z. T.; Dixon, D. A., Computational Study of H₂ and O₂ Production from Water Splitting by Small (MO₂)_n Clusters (M = Ti, Zr, Hf). *J. Phys. Chem. A* **2013**, *117*, 3539-3555.
39. Fang, Z.; Dixon, D. A., Hydrolysis of ZrCl₄ and HfCl₄: The Initial Steps in the High-Temperature Oxidation of Metal Chlorides to Produce ZrO₂ and HfO₂. *J. Phys. Chem. C* **2013**, *117*, 7459-7474.
40. Mendez, M.; Francisco, J. S.; Dixon, D. A., Thermodynamic Properties of the Isomers of HNOS, HNO₂S, and HNOS₂ and the Role of the Central Sulfur. *Chem.-Eur. J.* **2014**, *20*, 10231-10235.
41. Vasiliu, M.; Arduengo, A. J.; Dixon, D. A., Role of Electronegative Substituents on the Bond Energies in the Grubbs Metathesis Catalysts for M = Fe, Ru, Os. *J. Phys. Chem. C* **2014**, *118*, 13563-13577.
42. Fang, Z.; Wang, Y.; Dixon, D. A., Computational Study of Ethanol Conversion on Al₈O₁₂ as a Model for γ-Al₂O₃. *J. Phys. Chem. C* **2015**, *119*, 23413-23421.
43. Fang, Z.; Zetterholm, P.; Dixon, D. A., 1,2-Ethanediol and 1,3-Propanediol Conversions over (MO₃)₃ (M = Mo, W) Nanoclusters: A Computational Study. *J. Phys. Chem. A* **2016**, *120*, 1897-1907.

Publications jointly funded by this grant and other grants with leading intellectual contribution from this grant

44. Zhao, Z.; Xu, S.; Hu, M.; Bao, X.; Peden, C. H. F.; Hu, J. Z., Investigation of Aluminum Site Changes of Dehydrated Zeolite H-Beta during a Rehydration Process by High Field Solid State NMR. *J. Phys. Chem. C* **2014**, *119*, 1410-1417.
45. Halevi, B.; Lin, S.; Roy, A.; Zhang, H.; Jeroro, E.; Vohs, J.; Wang, Y.; Guo, H.; Datye, A. K., High CO₂ Selectivity of ZnO Powder Catalysts for Methanol Steam Reforming. *J. Phys. Chem. C* **2013**, *117*, 6493-6503.
46. Hensley, A. J. R.; Wang, Y.; McEwen, J.-S., Adsorption of phenol on Fe (110) and Pd (111) from first principles. *Surf. Sci.* **2014**, *630*, 244-253.
47. Hensley, A. J. R.; Wang, Y.; McEwen, J.-S., Phenol Deoxygenation Mechanisms on Fe(110) and Pd(111). *ACS Catal.* **2015**, *5*, 523-536.
48. Sun, J.; Zhang, H.; Yu, N.; Davidson, S.; Wang, Y., Effect of Cobalt Particle Size on Acetone Steam Reforming. *ChemCatChem* **2015**, *7*, 2932-2936.
49. Hensley, A. J. R.; Schneider, S.; Wang, Y.; McEwen, J.-S., Adsorption of aromatics on the (111) surface of PtM and PtM₃ (M = Fe, Ni) alloys. *RSC Advances* **2015**, *5*, 85705-85719.
50. Zhang, H.; Sun, J.; Liu, C.; Wang, Y., Distinct water activation on polar/non-polar facets of ZnO nanoparticles. *J. Catal.* **2015**, *331*, 57-62.
51. Rahman, M. M.; Davidson, S. D.; Sun, J.; Wang, Y., Effect of Water on Ethanol Conversion over ZnO. *Top. Catal.* **2015**, *59*, 37-45.
52. Wei, Z.; Karim, A.; Li, Y.; Wang, Y., Elucidation of the Roles of Re in Aqueous-Phase Reforming of Glycerol over Pt-Re/C Catalysts. *ACS Catal.* **2015**, *5*, 7312-7320.
53. Sun, J.; Baylon, R. A. L.; Liu, C.; Mei, D.; Martin, K. J.; Venkitasubramanian, P.; Wang, Y., Key Roles of Lewis Acid-Base Pairs on Zn_xZr_yO_z in Direct Ethanol/Acetone to Isobutene Conversion. *J. Am. Chem. Soc.* **2016**, *138*, 507-517.
54. Baylon, R. A. L.; Sun, J.; Martin, K. J.; Venkitasubramanian, P.; Wang, Y., Beyond ketonization: selective conversion of carboxylic acids to olefins over balanced Lewis acid-base pairs. *Chem. Commun.* **2016**, *52*, 4975-4978.
55. Baylon, R. A. L.; Sun, J.; Wang, Y., Conversion of ethanol to 1,3-butadiene over Na doped Zn_xZr_yO_z mixed metal oxides. *Catal. Today* **2016**, *259*, Part 2, 446-452.
56. Yu, N.; Zhang, H.; Davidson, S. D.; Sun, J.; Wang, Y., Effect of ZnO facet on ethanol steam reforming over Co/ZnO. *Catal. Commun.* **2016**, *73*, 93-97.
57. Davidson, S. D.; Sun, J.; Wang, Y., The effect of ZnO addition on H₂O activation over Co/ZrO₂ catalysts. *Catal. Today* **2016**, *269*, 140-147.
58. Hensley, A. J. R.; Wang, Y.; McEwen, J.-S., Adsorption of guaiacol on Fe (110) and Pd (111) from first principles. *Surf. Sci.* **2016**, *648*, 227-235.
59. Novotny, Z.; Netzer, F. R.; Dohnalek, Z., Cerium Oxide Nanoclusters on Graphene/Ru (0001): Intercalation of Oxygen via Spillover. *ACS Nano* **2015**, *9*, 8617-8626.

60. Asthagiri, A.; Dixon, D. A.; Dohnálek, Z.; Kay, B. D.; Rodriguez, J. A.; Rousseau, R.; Stacchiola, D. J.; Weaver, J. F., Catalytic Chemistry on Oxide Nanostructures. In *Oxide Materials at the Two-Dimensional Limit*, Netzer, P. F.; Fortunelli, A., Eds. Springer International Publishing: Cham, 2016; pp 251-280.
61. Novotny, Z.; Netzer, F. P.; Dohnálek, Z., Ceria nanoclusters on graphene/Ru(0001): A new model catalyst system. *Surf. Sci.* **2016**, DOI: 10.1016/j.susc.2016.03.020.
62. Jones, A. J.; Carr, R. T.; Zones, S. I.; Iglesia, E., Acid strength and solvation in catalysis by MFI zeolites and effects of the identity, concentration and location of framework heteroatoms. *J. Catal.* **2014**, *312*, 58-68.
63. Wang, Y. G.; Yoon, Y.; Glezakou, V. A.; Li, J.; Rousseau, R., The Role of Reducible Oxide-Metal Cluster Charge Transfer in Catalytic Processes: New Insights on the Catalytic Mechanism of CO Oxidation on Au/TiO₂ from ab Initio Molecular Dynamics. *J. Am. Chem. Soc.* **2013**, *135*, 10673-10683.
64. Wang, Y.-G.; Mei, D.; Li, J.; Rousseau, R., DFT+U Study on the Localized Electronic States and Their Potential Role During H₂O Dissociation and CO Oxidation Processes on CeO₂(111) Surface. *J. Phys. Chem. C* **2013**, *117*, 23082-23089.
65. Wang, Y.-G.; Mei, D.; Glezakou, V.-A.; Li, J.; Rousseau, R., Dynamic formation of single-atom catalytic active sites on ceria-supported gold nanoparticles. *Nat. Commun.* **2015**, *6*.
66. Garner, E. B.; Arduengo, A. J.; Streubel, R.; Dixon, D. A., Electronic structure predictions of the properties of non-innocent P-ligands in group 6B transition metal complexes. *Dalton. Trans.* **2014**, *43*, 2069-2078.
67. Thanthiriwatte, K. S.; Spruell, J. M.; Dixon, D. A.; Christe, K. O.; Jenkins, H. D. B., Structures, Vibrational Frequencies, and Stabilities of Halogen Cluster Anions and Cations, X_n^{+/-}, n=3, 4, and 5. *Inorg. Chem.* **2014**, *53*, 8136-8146.
68. Allayarov, S. R.; Gordon, D. A.; Henderson, P. B.; Fernandez, R. E.; Jackson, V. E.; Dixon, D. A., Photochemistry of long-lived [(CF₃)₂CF]₂C•C₂F₅ radicals. *J. Fluorine Chem.* **2015**, *180*, 240-247.
69. Thanthiriwatte, K. S.; Vasiliu, M.; Battey, S. R.; Lu, Q.; Peterson, K. A.; Andrews, L.; Dixon, D. A., Gas Phase Properties of MX₂ and MX₄ (X = F, Cl) for M = Group 4, Group 14, Cerium, and Thorium. *J. Phys. Chem. A* **2015**, *119*, 5790-5803.
70. Fang, Z.; Thanthiriwatte, K. S.; Dixon, D. A.; Andrews, L.; Wang, X., Properties of Cerium Hydroxides from Matrix Infrared Spectra and Electronic Structure Calculations. *Inorg. Chem.* **2016**, *55*, 1702-1714.
71. Finney, B.; Fang, Z.; Francisco, J. S.; Dixon, D. A., Energetic Properties and Electronic Structure of [Si,N,S] and [Si,P,S] Isomers. *J. Phys. Chem. A* **2016**, *120*, 1691-1697.

Publications jointly funded by this grant and other grants with relatively minor intellectual contribution from this grant

72. Appel, A. M.; Bercaw, J. E.; Bocarsly, A. B.; Dobbek, H.; DuBois, D. L.; Dupuis, M.; Ferry, J. G.; Fujita, E.; Hille, R.; Kenis, P. J. A.; Kerfeld, C. A.; Morris, R. H.; Peden, C.

- H. F.; Portis, A. R.; Ragsdale, S. W.; Rauchfuss, T. B.; Reek, J. N. H.; Seefeldt, L. C.; Thauer, R. K.; Waldrop, G. L., Frontiers, Opportunities, and Challenges in Biochemical and Chemical Catalysis of CO₂ Fixation. *Chem. Rev.* **2013**, *113*, 6621-6658.
73. Yang, Y.; Mims, C. A.; Mei, D. H.; Peden, C. H. F.; Campbell, C. T., Mechanistic studies of methanol synthesis over Cu from CO/CO₂/H₂/H₂O mixtures: The source of C in methanol and the role of water. *J. Catal.* **2013**, *298*, 10-17.
74. Peterson, E. J.; DeLaRiva, A. T.; Lin, S.; Johnson, R. S.; Guo, H.; Miller, J. T.; Hun Kwak, J.; Peden, C. H. F.; Kiefer, B.; Allard, L. F.; Ribeiro, F. H.; Datye, A. K., Low-temperature carbon monoxide oxidation catalysed by regenerable atomically dispersed palladium on alumina. *Nat. Commun.* **2014**, *5*.
75. Yang, Y.; Mei, D.; Peden, C. H. F.; Campbell, C. T.; Mims, C. A., Surface-Bound Intermediates in Low-Temperature Methanol Synthesis on Copper: Participants and Spectators. *ACS Catal.* **2015**, *5*, 7328-7337.
76. Pruski, M.; Sadow, A. D.; Slowing, I. I.; Marshall, C. L.; Stair, P.; Rodriguez, J.; Harris, A.; Somorjai, G. A.; Biener, J.; Matranga, C.; Wang, C.; Schaidle, J. A.; Beckham, G. T.; Ruddy, D. A.; Deutsch, T.; Alia, S. M.; Narula, C.; Overbury, S.; Toops, T.; Bullock, R. M.; Peden, C. H. F.; Wang, Y.; Allendorf, M. D.; Nørskov, J.; Bligaard, T., Virtual Special Issue on Catalysis at the U.S. Department of Energy's National Laboratories. *ACS Catal.* **2016**, *6*, 3227-3235.
77. Kwak, J. H.; Dagle, R.; Tustin, G. C.; Zoeller, J. R.; Allard, L. F.; Wang, Y., Molecular Active Sites in Heterogeneous Ir-La/C-Catalyzed Carbonylation of Methanol to Acetates. *J. Phys. Chem. Lett.* **2014**, *5*, 566-572.
78. Sun, J.; Karim, A. M.; Li, X. S.; Rainbolt, J.; Kovarik, L.; Shin, Y.; Wang, Y., Hierarchically structured catalysts for cascade and selective steam reforming/hydrodeoxygenation reactions. *Chem. Commun.* **2015**, *51*, 16617-16620.
79. Liu, C.; Sun, J.; Brown, H. M.; Marin-Flores, O. G.; Bays, J. T.; Karim, A. M.; Wang, Y., Aqueous phase hydrodeoxygenation of polyols over Pd/WO₃-ZrO₂: Role of Pd-WO₃ interaction and hydrodeoxygenation pathway. *Catal. Today* **2016**, *269*, 103-109.
80. Zhang, Z.; Tang, M.; Wang, Z.-T.; Ke, Z.; Xia, Y.; Park, K. T.; Lyubinetsky, I.; Dohnalek, Z.; Ge, Q., Imaging of Formaldehyde Adsorption and Diffusion on TiO₂(110). *Top. Catal.* **2015**, *58*, 103-113.
81. Zhu, K.; Xia, Y.; Tang, M.; Wang, Z.-T.; Jan, B.; Lyubinetsky, I.; Ge, Q.; Dohnalek, Z.; Park, K. T.; Zhang, Z., Tracking Site-Specific C-C Coupling of Formaldehyde Molecules on Rutile TiO₂(110). *J. Phys. Chem. C* **2015**, *119*, 14267-14272.
82. Zhu, K.; Xia, Y.; Tang, M.; Wang, Z.-T.; Lyubinetsky, I.; Ge, Q.; Dohnalek, Z.; Park, K. T.; Zhang, Z., Low-Temperature Reductive Coupling of Formaldehyde on Rutile TiO₂(110). *J. Phys. Chem. C* **2015**, *119*, 18452-18457.
83. Du, Y.; Li, G.; Peterson, E. W.; Zhou, J.; Zhang, X.; Mu, R.; Dohnalek, Z.; Bowden, M.; Lyubinetsky, I.; Chambers, S. A., Iso-oriented monolayer α -MoO₃(010) films epitaxially grown on SrTiO₃(001). *Nanoscale* **2016**, *8*, 3119-3124.

84. Clayton, D. A.; McPherson, T. E.; Pan, S. L.; Chen, M. Y.; Dixon, D. A.; Hu, D. H., Spatial and temporal variation of surface-enhanced Raman scattering at Ag nanowires in aqueous solution. *Phys. Chem. Chem. Phys.* **2013**, *15*, 850-859.
85. Sung, Y. M.; Vasiliu, M.; Dixon, D. A.; Bonizzoni, M.; Kim, D.; Vaid, T. P., Electronic structure and photophysics of (C=C)tetra-p-tolylporphyrin²⁺. *Photochem. Photobiol. Sci.* **2013**, *12*, 1774-1779.
86. Wang, J.; Pan, S. L.; Chen, M. Y.; Dixon, D. A., Gold Nanorod-Enhanced Light Absorption and Photoelectrochemical Performance of alpha-Fe₂O₃ Thin-Film Electrode for Solar Water Splitting. *J. Phys. Chem. C* **2013**, *117*, 22060-22068.
87. Johnson, M. S.; Kota, R.; Mattern, D. L.; Hill, C. M.; Vasiliu, M.; Dixon, D. A.; Metzger, R. M., A two-faced "Janus-like" unimolecular rectifier exhibits rectification reversal. *J. Mater. Chem. C* **2014**, *2*, 9892-9902.
88. Christe, K. O.; Dixon, D. A.; Vasiliu, M.; Wagner, R. I.; Haiges, R.; Boatz, J. A.; Ammon, t. I. H. L., Are DTTO and iso-DTTO Worthwhile Targets for Synthesis? *Propellants, Explosives, Pyrotechnics* **2015**, *40*, 463-468.
89. Haiges, R.; Skotnitzki, J.; Fang, Z.; Dixon, D. A.; Christe, K. O., The First Molybdenum(VI) and Tungsten(VI) Oxoazides MO₂(N₃)₂, MO₂(N₃)₂·2 CH₃CN, (bipy)MO₂(N₃)₂, and [MO₂(N₃)₄]²⁻ (M=Mo, W). *Angew. Chem., Int. Ed.* **2015**, *54*, 9581-9585.
90. Haiges, R.; Skotnitzki, J.; Fang, Z.; Dixon, D. A.; Christe, K. O., The Molybdenum(V) and Tungsten(VI) Oxoazides [MoO(N₃)₃], [MoO(N₃)₃·2 CH₃CN], [(bipy)MoO(N₃)₃], [MoO(N₃)₅]²⁻, [WO(N₃)₄], and [WO(N₃)₄·CH₃CN]. *Angew. Chem., Int. Ed.* **2015**, *54*, 15550-15555.
91. Haiges, R.; Vasiliu, M.; Dixon, D. A.; Christe, K. O., The Vanadium(V) Oxoazides [VO(N₃)₃], [(bipy)VO(N₃)₃], and [VO(N₃)₅]²⁻. *Angew. Chem., Int. Ed.* **2015**, *54*, 9101-9105.
92. Leclerc, M. C.; Bayne, J. M.; Lee, G. M.; Gorelsky, S. I.; Vasiliu, M.; Korobkov, I.; Harrison, D. J.; Dixon, D. A.; Baker, R. T., Perfluoroalkyl Cobalt(III) Fluoride and Bis(perfluoroalkyl) Complexes: Catalytic Fluorination and Selective Difluorocarbene Formation. *J. Am. Chem. Soc.* **2015**, *137*, 16064-16073.
93. Feller, D.; Peterson, K. A.; Dixon, D. A., The Impact of Larger Basis Sets and Explicitly Correlated Coupled Cluster Theory on the Feller-Peterson-Dixon Composite Method. In *Annual Reports in Computational Chemistry*, Dixon, D. A., Ed. Elsevier: Amsterdam, 2016; Vol. 12.
94. Kaneza, N.; Zhang, J.; Liu, H.; Archana, P. S.; Shan, Z.; Vasiliu, M.; Polansky, S. H.; Dixon, D. A.; Adams, R. E.; Schmehl, R. H.; Gupta, A.; Pan, S., Electrochemical and Spectroscopic Properties of Boron Dipyrromethene–Thiophene–Triphenylamine-Based Dyes for Dye-Sensitized Solar Cells. *J. Phys. Chem. C* **2016**, *120*, 9068-9080.
95. Laminack, W.; Gole, J. L.; White, M. G.; Ozdemir, S.; Ogden, A. G.; Martin, H. J.; Fang, Z.; Wang, T.-H.; Dixon, D. A., Synthesis of nanoscale silicon oxide oxidation state distributions: The transformation from hydrophilicity to hydrophobicity. *Chem. Phys. Lett.* **2016**, *653*, 137-143.

96. Matthiesen, J. E.; Carraher, J. M.; Vasiliu, M.; Dixon, D. A.; Tessonnier, J.-P., Electrochemical Conversion of Muconic Acid to Biobased Diacid Monomers. *ACS Sustain. Chem. Eng.* **2016**, DOI: 10.1021/acssuschemeng.6b00679.
97. Haiges, R.; Vasiliu, M.; Dixon, D. A.; Christe, K., The Niobium Oxoazides [NbO(N₃)₃], [NbO(N₃)₃·2CH₃CN], [(bipy)NbO(N₃)₃], Cs₂[NbO(N₃)₅] and [PPh₄]₂[NbO(N₃)₅]. *Dalton. Trans.* **2016**, DOI: 10.1039/C6DT01479H.

Subtask 2.1: Designing Catalysts Using an Energy-Based Approach

Publications exclusively funded by this grant

1. van der Eide, E. F.; Yang, P.; Bullock, R. M., Isolation of Two Agostic Isomers of an Organometallic Cation: Different Structures and Colors. *Angew. Chem., Int. Ed.* **2013**, *52*, 10190-10194.
2. Jeletic, M. S.; Mock, M. T.; Appel, A. M.; Linehan, J. C., A Cobalt-Based Catalyst for the Hydrogenation of CO₂ under Ambient Conditions. *J. Am. Chem. Soc.* **2013**, *135*, 11533-11536.
3. Appel, A. M., Carbon-Fuelled Future. *Journal Name: Chemistry and Industry*, 78(4):36-39 **2014**, Medium: X.
4. Appel, A. M., Electrochemistry: Catalysis at the boundaries. *Nature* **2014**, *508*, 460-461.
5. Wiedner, E. S.; Appel, A. M., Thermochemical Insight into the Reduction of CO to CH₃OH with [Re(CO)]⁺ and [Mn(CO)]⁺ Complexes. *J. Am. Chem. Soc.* **2014**, *136*, 8661-8668.
6. Zall, C. M.; Linehan, J. C.; Appel, A. M., A Molecular Copper Catalyst for Hydrogenation of CO₂ to Formate. *ACS Catal.* **2015**, *5*, 5301-5305.
7. Zhang, S.; Bullock, R. M., Molybdenum Hydride and Dihydride Complexes Bearing Diphosphine Ligands with a Pendant Amine: Formation of Complexes with Bound Amines. *Inorg. Chem.* **2015**, *54*, 6397-6409.
8. Miller, D. L.; Boro, B. J.; Grubel, K.; Helm, M. L.; Appel, A. M., Synthesis and Characterization of a Triphos Ligand Derivative and the Corresponding PdII Complexes. *Eur. J. Inorg. Chem.* **2015**, *2015*, 5781-5785.
9. Connelly, S. J.; Wiedner, E. S.; Appel, A. M., Predicting the reactivity of hydride donors in water: thermodynamic constants for hydrogen. *Dalton. Trans.* **2015**, *44*, 5933-5938.
10. Priyadarshani, N.; Ginovska, B.; Bays, J. T.; Linehan, J. C.; Shaw, W. J., Photoswitching a molecular catalyst to regulate CO₂ hydrogenation. *Dalton. Trans.* **2015**, *44*, 14854-14864.
11. Connelly Robinson, S. J.; Zall, C. M.; Miller, D. L.; Linehan, J. C.; Appel, A. M., Solvent influence on the thermodynamics for hydride transfer from bis(diphosphine) complexes of nickel. *Dalton. Trans.* **2016**, DOI: 10.1039/C6DT00309E.

Publications jointly funded by this grant and other grants with leading intellectual contribution from this grant

12. Galan, B. R.; Reback, M. L.; Jain, A.; Appel, A. M.; Shaw, W. J., Electrocatalytic Oxidation of Formate with Nickel Diphosphine Dipeptide Complexes: Effect of Ligands Modified with Amino Acids. *Eur. J. Inorg. Chem.* **2013**, 2013, 5366-5371.
13. Eide, E. F. v. d.; Hou, G.-L.; Deng, S. H. M.; Wen, H.; Yang, P.; Bullock, R. M.; Wang, X.-B., Metal-Centered 17-Electron Radicals CpM(CO)₃• (M = Cr, Mo, W): A Combined Negative Ion Photoelectron Spectroscopic and Theoretical Study. *Organometallics* **2013**, 32, 2084-2091.
14. van der Eide, E. F.; Helm, M. L.; Walter, E. D.; Bullock, R. M., Structural and Spectroscopic Characterization of 17- and 18-Electron Piano-Stool Complexes of Chromium. Thermochemical Analyses of Weak Cr–H Bonds. *Inorg. Chem.* **2013**, 52, 1591-1603.
15. Kumar, N.; Camaioni, D. M.; Dupuis, M.; Raugei, S.; Appel, A. M., Mechanistic insights into hydride transfer for catalytic hydrogenation of CO₂ with cobalt complexes. *Dalton. Trans.* **2014**, 43, 11803-11806.
16. Galan, B. R.; Wiedner, E. S.; Helm, M. L.; Linehan, J. C.; Appel, A. M., Effects of Phosphine–Carbene Substitutions on the Electrochemical and Thermodynamic Properties of Nickel Complexes. *Organometallics* **2014**, 33, 2287-2294.
17. Bays, J. T.; Priyadarshani, N.; Jeletic, M. S.; Hulley, E. B.; Miller, D. L.; Linehan, J. C.; Shaw, W. J., The Influence of the Second and Outer Coordination Spheres on Rh(diphosphine)₂ CO₂ Hydrogenation Catalysts. *ACS Catal.* **2014**, 4, 3663-3670.
18. Weiss, C. J.; Das, P.; Miller, D. L.; Helm, M. L.; Appel, A. M., Catalytic Oxidation of Alcohol via Nickel Phosphine Complexes with Pendant Amines. *ACS Catal.* **2014**, 4, 2951-2958.
19. Jeletic, M. S.; Helm, M. L.; Hulley, E. B.; Mock, M. T.; Appel, A. M.; Linehan, J. C., A Cobalt Hydride Catalyst for the Hydrogenation of CO₂: Pathways for Catalysis and Deactivation. *ACS Catal.* **2014**, 4, 3755-3762.
20. Weiss, C. J.; Wiedner, E. S.; Roberts, J. A. S.; Appel, A. M., Nickel phosphine catalysts with pendant amines for electrocatalytic oxidation of alcohols. *Chem. Commun.* **2015**, 51, 6172-6174.

Publications jointly funded by this grant and other grants with relatively minor intellectual contribution from this grant

21. Liu, T.; DuBois, D. L.; Bullock, R. M., An iron complex with pendent amines as a molecular electrocatalyst for oxidation of hydrogen. *Nat Chem* **2013**, 5, 228-233.
22. Appel, A. M.; Bercaw, J. E.; Bocarsly, A. B.; Dobbek, H.; DuBois, D. L.; Dupuis, M.; Ferry, J. G.; Fujita, E.; Hille, R.; Kenis, P. J. A.; Kerfeld, C. A.; Morris, R. H.; Peden, C. H. F.; Portis, A. R.; Ragsdale, S. W.; Rauchfuss, T. B.; Reek, J. N. H.; Seefeldt, L. C.; Thauer, R. K.; Waldrop, G. L., Frontiers, Opportunities, and Challenges in Biochemical and Chemical Catalysis of CO₂ Fixation. *Chem. Rev.* **2013**, 113, 6621-6658.

23. Hulley, E. B.; Welch, K. D.; Appel, A. M.; DuBois, D. L.; Bullock, R. M., Rapid, Reversible Heterolytic Cleavage of Bound H₂. *J. Am. Chem. Soc.* **2013**, *135*, 11736-11739.
24. Wiedner, E. S.; Roberts, J. A. S.; Dougherty, W. G.; Kassel, W. S.; DuBois, D. L.; Bullock, R. M., Synthesis and Electrochemical Studies of Cobalt(III) Monohydride Complexes Containing Pendant Amines. *Inorg. Chem.* **2013**, *52*, 9975-9988.
25. Franz, J. A.; O'Hagan, M.; Ho, M.-H.; Liu, T.; Helm, M. L.; Lense, S.; DuBois, D. L.; Shaw, W. J.; Appel, A. M.; Raugai, S.; Bullock, R. M., Conformational Dynamics and Proton Relay Positioning in Nickel Catalysts for Hydrogen Production and Oxidation. *Organometallics* **2013**, *32*, 7034-7042.
26. DuBois, D. L., Development of Molecular Electrocatalysts for Energy Storage. *Inorg. Chem.* **2014**, *53*, 3935-3960.
27. Lewandowska-Andralojc, A.; Grills, D. C.; Zhang, J.; Bullock, R. M.; Miyazawa, A.; Kawanishi, Y.; Fujita, E., Kinetic and Mechanistic Studies of Carbon-to-Metal Hydrogen Atom Transfer Involving Os-Centered Radicals: Evidence for Tunneling. *J. Am. Chem. Soc.* **2014**, *136*, 3572-3578.
28. Laws, D. R.; Bullock, R. M.; Lee, R.; Huang, K.-W.; Geiger, W. E., Comparison of the One-Electron Oxidations of CO-Bridged vs Unbridged Bimetallic Complexes: Electron-Transfer Chemistry of Os₂Cp₂(CO)₄ and Os₂Cp*₂(μ-CO)₂(CO)₂ (Cp = η⁵-C₅H₅, Cp* = η⁵-C₅Me₅). *Organometallics* **2014**, *33*, 4716-4728.
29. Liu, T.; DuBois, M. R.; DuBois, D. L.; Bullock, R. M., Electrochemical oxidation of H₂ catalyzed by ruthenium hydride complexes bearing P₂N₂ ligands with pendant amines as proton relays. *Energy Environ. Sci.* **2014**, *7*, 3630-3639.
30. Bayram, E.; Linehan, J. C.; Fulton, J. L.; Szymczak, N. K.; Finke, R. G., Determination of the Dominant Catalyst Derived from the Classic [RhCp*Cl₂]₂ Precatalyst System: Is it Single-Metal Rh₁Cp*-Based, Subnanometer Rh₄ Cluster-Based, or Rh(0)_n Nanoparticle-Based Cyclohexene Hydrogenation Catalysis at Room Temperature and Mild Pressures? *ACS Catal.* **2015**, *5*, 3876-3886.
31. Bligaard, T.; Bullock, R. M.; Campbell, C. T.; Chen, J. G.; Gates, B. C.; Gorte, R. J.; Jones, C. W.; Jones, W. D.; Kitchin, J. R.; Scott, S. L., Toward Benchmarking in Catalysis Science: Best Practices, Challenges, and Opportunities. *ACS Catal.* **2016**, *6*, 2590-2602.
32. Pruski, M.; Sadow, A. D.; Slowing, I. I.; Marshall, C. L.; Stair, P.; Rodriguez, J.; Harris, A.; Somorjai, G. A.; Biener, J.; Matranga, C.; Wang, C.; Schaidle, J. A.; Beckham, G. T.; Ruddy, D. A.; Deutsch, T.; Alia, S. M.; Narula, C.; Overbury, S.; Toops, T.; Bullock, R. M.; Peden, C. H. F.; Wang, Y.; Allendorf, M. D.; Nørskov, J.; Bligaard, T., Virtual Special Issue on Catalysis at the U.S. Department of Energy's National Laboratories. *ACS Catal.* **2016**, *6*, 3227-3235.

Subtask 2.2: Multifunctional Catalysts for CO₂ Activation and Reduction

Publications exclusively funded by this grant

1. Lin, X.; Wang, Z.-T.; Lyubinetsky, I.; Kay, B. D.; Dohnalek, Z., Interaction of CO₂ with oxygen adatoms on rutile TiO₂(110). *Phys. Chem. Chem. Phys.* **2013**, *15*, 6190-6195.
2. Yoon, Y.; Wang, Y.-G.; Rousseau, R.; Glezakou, V.-A., Impact of Nonadiabatic Charge Transfer on the Rate of Redox Chemistry of Carbon Oxides on Rutile TiO₂(110) Surface. *ACS Catal.* **2015**, *5*, 1764-1771.
3. Szanyi, J.; Yi, C.; Mudiyansele, K.; Kwak, J., Understanding Automotive Exhaust Catalysts Using a Surface Science Approach: Model NO_x Storage Materials. *Top. Catal.* **2013**, *56*, 1420-1440.
4. Kovarik, L.; Bowden, M.; Genc, A.; Szanyi, J.; Peden, C. H. F.; Kwak, J. H., Structure of δ -Alumina: Toward the Atomic Level Understanding of Transition Alumina Phases. *J. Phys. Chem. C* **2014**, *118*, 18051-18058.
5. Szanyi, J.; Kwak, J. H., Dissecting the steps of CO₂ reduction: 1. The interaction of CO and CO₂ with γ -Al₂O₃: an in situ FTIR study. *Phys. Chem. Chem. Phys.* **2014**, *16*, 15117-15125.
6. Szanyi, J.; Kwak, J. H., Dissecting the steps of CO₂ reduction: 2. The interaction of CO and CO₂ with Pd/ γ -Al₂O₃: an in situ FTIR study. *Phys. Chem. Chem. Phys.* **2014**, *16*, 15126-15138.
7. Yi, C.-W.; Szanyi, J., The thermal behavior of Pd on graphene/Ru(0001). *Surf. Sci.* **2015**, *641*, 154-158.
8. Wang, X.; Shi, H.; Kwak, J. H.; Szanyi, J., Mechanism of CO₂ Hydrogenation on Pd/Al₂O₃ Catalysts: Kinetics and Transient DRIFTS-MS Studies. *ACS Catal.* **2015**, *5*, 6337-6349.
9. Wang, X.; Hong, Y.; Shi, H.; Szanyi, J., Kinetic modeling and transient DRIFTS-MS studies of CO₂ methanation over Ru/Al₂O₃ catalysts. *J. Catal.*, DOI: 10.1016/j.jcat.2016.02.001.
10. Kwak, J. H.; Lee, J.; Szanyi, J.; Peden, C. H. F., Modification of the acid/base properties of γ -Al₂O₃ by oxide additives: An ethanol TPD investigation. *Catal. Today* **2016**, *265*, 240-244.

Publications jointly funded by this grant and other grants with leading intellectual contribution from this grant

11. Lee, M.-S.; Peter McGrail, B.; Rousseau, R.; Glezakou, V.-A., Structure, dynamics and stability of water/scCO₂/mineral interfaces from ab initio molecular dynamics simulations. *Scientific Reports* **2015**, *5*, 14857.
12. Kwak, J. H.; Kovarik, L.; Szanyi, J., CO₂ Reduction on Supported Ru/Al₂O₃ Catalysts: Cluster Size Dependence of Product Selectivity. *ACS Catal.* **2013**, *3*, 2449-2455.
13. Kwak, J. H.; Kovarik, L.; Szanyi, J., Heterogeneous Catalysis on Atomically Dispersed Supported Metals: CO₂ Reduction on Multifunctional Pd Catalysts. *ACS Catal.* **2013**, *3*, 2094-2100.

14. Kovarik, L.; Genc, A.; Wang, C. M.; Qiu, A. N.; Peden, C. H. F.; Szanyi, J.; Kwak, J. H., Tomography and High-Resolution Electron Microscopy Study of Surfaces and Porosity in a Plate-like γ -Al₂O₃. *J. Phys. Chem. C* **2013**, *117*, 179-186.
15. Yadav, M.; Linehan, J. C.; Karkamkar, A. J.; van der Eide, E.; Heldebrant, D. J., Homogeneous Hydrogenation of CO₂ to Methyl Formate Utilizing Switchable Ionic Liquids. *Inorg. Chem.* **2014**, *53*, 9849-9854.

Publications jointly funded by this grant and other grants with relatively minor intellectual contribution from this grant

16. Schwenzler, B.; Cosimbescu, L.; Glezakou, V.-A.; Karkamkar, A. J.; Wang, Z.; Weber, R. S., Use of Solvatochromism to Assay Preferential Solvation of a Prototypic Catalytic Site. *Top. Catal.* **2015**, *58*, 258-270.
17. Lee, J.; Jeon, H.; Oh, D. G.; Szanyi, J.; Kwak, J. H., Morphology-dependent phase transformation of γ -Al₂O₃. *Appl. Catal. A* **2015**, *500*, 58-68.
18. Miranda, B. C.; Chimentão, R. J.; Szanyi, J.; Braga, A. H.; Santos, J. B. O.; Gispert-Guirado, F.; Llorca, J.; Medina, F., Influence of copper on nickel-based catalysts in the conversion of glycerol. *Appl. Catal. B* **2015**, *166-167*, 166-180.

Subtask 3.1: Fundamental Studies of Water Splitting on Model Multifunctional Photocatalysts

Publications exclusively funded by this grant

1. Henderson, M. A., Photooxidation and Photodesorption in the Photochemistry of Isobutene on TiO₂(110). *J. Phys. Chem. C* **2013**, *117*, 14113-14124.
2. Henderson, M. A., Comparison of the Photodesorption Activities of cis-Butene, trans-Butene, and Isobutene on the Rutile TiO₂(110) Surface. *J. Phys. Chem. C* **2013**, *117*, 23840-23847.
3. Henderson, M. A.; Shen, M.; Wang, Z.-T.; Lyubinetsky, I., Characterization of the Active Surface Species Responsible for UV-Induced Desorption of O₂ from the Rutile TiO₂(110) Surface. *J. Phys. Chem. C* **2013**, *117*, 5774-5784.
4. Herman, G. S.; Zehr, R. T.; Henderson, M. A., Characterization of oxygen and titanium diffusion at the anatase TiO₂(001) surface. *Surf. Sci.* **2013**, *612*, L5-L8.
5. Mu, R.; Cantu, D. C.; Lin, X.; Glezakou, V.-A.; Wang, Z.; Lyubinetsky, I.; Rousseau, R.; Dohnalek, Z., Dimerization Induced Deprotonation of Water on RuO₂(110). *J. Phys. Chem. Lett.* **2014**, *5*, 3445-3450.
6. Mu, R.; Cantu, D. C.; Glezakou, V.-A.; Lyubinetsky, I.; Rousseau, R.; Dohnalek, Z., Deprotonated Water Dimers: The Building Blocks of Segmented Water Chains on Rutile RuO₂(110). *J. Phys. Chem. C* **2015**, *119*, 23552-23558.
7. Wang, Z.-T.; Henderson, M. A.; Lyubinetsky, I., Origin of Coverage Dependence in Photoreactivity of Carboxylate on TiO₂(110): Hindering by Charged Coadsorbed Hydroxyls. *ACS Catal.* **2015**, *5*, 6463-6467.

8. Petrik, N. G.; Kimmel, G. A.; Shen, M.; Henderson, M. A., Quenching of electron transfer reactions through coadsorption: A study of oxygen photodesorption from TiO₂(110). *Surf. Sci.* **2016**, DOI: 10.1016/j.susc.2015.12.038.

Publications jointly funded by this grant and other grants with leading intellectual contribution from this grant

9. Henderson, M. A.; Lyubinetsky, I., Molecular-Level Insights into Photocatalysis from Scanning Probe Microscopy Studies on TiO₂(110). *Chem. Rev.* **2013**, *113*, 4428-4455.
10. Petrik, N. G.; Kimmel, G. A., Probing the photochemistry of chemisorbed oxygen on TiO₂(110) with Kr and other co-adsorbates. *Phys. Chem. Chem. Phys.* **2014**, *16*, 2338-2346.
11. Nandasiri, M. I.; Shutthanandan, V.; Manandhar, S.; Schwarz, A. M.; Oxenford, L.; Kennedy, J. V.; Thevuthasan, S.; Henderson, M. A., Instability of Hydrogenated TiO₂. *J. Phys. Chem. Lett.* **2015**, *6*, 4627-4632.
12. Petrik, N. G.; Henderson, M. A.; Kimmel, G. A., Insights into Acetone Photochemistry on Rutile TiO₂(110). 1. Off-Normal CH₃ Ejection from Acetone Diolate. *J. Phys. Chem. C* **2015**, *119*, 12262-12272.
13. Petrik, N. G.; Henderson, M. A.; Kimmel, G. A., Insights into Acetone Photochemistry on Rutile TiO₂(110). 2. New Photodesorption Channel with CH₃ Ejection along the Surface Normal. *J. Phys. Chem. C* **2015**, *119*, 12273-12282.
14. Szanyi, J.; Kwak, J. H., Photo-catalytic oxidation of acetone on a TiO₂ powder: An in situ FTIR investigation. *Journal of Molecular Catalysis A: Chemical* **2015**, *406*, 213-223.
15. Wang, Z.-T.; Garcia, J. C.; Deskins, N. A.; Lyubinetsky, I., Ability of TiO₂(110) surface to be fully hydroxylated and fully reduced. *Phys. Rev. B* **2015**, *92*, 081402.
16. Yoon, Y.; Du, Y.; Garcia, J. C.; Zhu, Z.; Wang, Z.-T.; Petrik, N. G.; Kimmel, G. A.; Dohnalek, Z.; Henderson, M. A.; Rousseau, R.; Deskins, N. A.; Lyubinetsky, I., Anticorrelation between Surface and Subsurface Point Defects and the Impact on the Redox Chemistry of TiO₂(110). *ChemPhysChem* **2015**, *16*, 313-321.

Publications jointly funded by this grant and other grants with relatively minor intellectual contribution from this grant

17. Kim, B.; Li, Z.; Kay, B. D.; Dohnalek, Z.; Kim, Y. K., Low-Temperature Desorption of N₂O from NO on Rutile TiO₂(110)-1 x 1. *J. Phys. Chem. C* **2014**, *118*, 9544-9550.
18. Kim, B.; Kay, B. D.; Dohnalek, Z.; Kim, Y. K., Ammonia Formation from NO Reaction with Surface Hydroxyls on Rutile TiO₂(110)-1 x 1. *J. Phys. Chem. C* **2015**, *119*, 1130-1135.
19. Kim, B.; Dohnalek, Z.; Szanyi, J.; Kay, B. D.; Kim, Y. K., Temperature-programmed desorption study of NO reactions on rutile TiO₂(110)-1×1. *Surf. Sci.* **2016**, DOI: 10.1016/j.susc.2016.01.032.

Subtask 3.2: Activation of Small Molecules with Bifunctional Ambiphilic Catalyst Complexes

Publications exclusively funded by this grant

1. Karkamkar, A.; Parab, K.; Camaioni, D. M.; Neiner, D.; Cho, H.; Nielsen, T. K.; Autrey, T., A thermodynamic and kinetic study of the heterolytic activation of hydrogen by frustrated borane-amine Lewis pairs. *Dalton. Trans.* **2013**, *42*, 615-619.
2. Nielsen, T. K.; Karkamkar, A.; Bowden, M.; Besenbacher, F.; Jensen, T. R.; Autrey, T., Methods to stabilize and destabilize ammonium borohydride. *Dalton. Trans.* **2013**, *42*, 680-687.
3. Kathmann, S. M.; Cho, H.; Chang, T.-M.; Schenter, G. K.; Parab, K.; Autrey, T., Experimental and Theoretical Study of Molecular Response of Amine Bases in Organic Solvents. *J. Phys. Chem. B* **2014**, *118*, 4883-4888.
4. Whittemore, S. M.; Edverson, G.; Camaioni, D. M.; Karkamkar, A.; Neiner, D.; Parab, K.; Autrey, T., Catalytic reduction of polar substrates without metals: A thermodynamic and kinetic study of heterolytic activation of hydrogen by vacancies in frustrated Lewis pairs. *Catal. Today* **2015**, *251*, 28-33.
5. Whittemore, S. M.; Autrey, T., Kinetic and Thermodynamic Study of the Reduction of 1,1-Diphenylethylene by a Thermally Frustrated Diethyl Ether-BCF Lewis Pair. *Isr. J. Chem.* **2015**, *55*, 196-201.
6. Ginovska, B.; Autrey, T.; Parab, K.; Bowden, M. E.; Potter, R. G.; Camaioni, D. M., Heterolysis of H₂ Across a Classical Lewis Pair, 2,6-Lutidine·BCl₃: Synthesis, Characterization, and Mechanism. *Chem. Eur. J.* **2015**, *21*, 15713-15719.

Publications jointly funded by this grant and other grants with leading intellectual contribution from this grant

7. Cantelli, R.; Paolone, A.; Palumbo, O.; Leardini, F.; Autrey, T.; Karkamkar, A.; Luedtke, A. T., Rotational dynamics in ammonia borane: Evidence of strong isotope effects. *J. Alloys Compd.* **2013**, *580*, Supplement 1, S63-S66.

Publications jointly funded by this grant and other grants with relatively minor intellectual contribution from this grant

8. Norton, J. R.; Spataru, T.; Camaioni, D. M.; Lee, S.-J.; Li, G.; Choi, J.; Franz, J. A., Kinetics and Mechanism of the Hydrogenation of the CpCr(CO)₃•/[CpCr(CO)₃]₂ Equilibrium to CpCr(CO)₃H. *Organometallics* **2014**, *33*, 2496-2502.

Subtask 3.3: Modulating Catalysts with an Enzyme-like Outer Coordination Sphere

Publications exclusively funded by this grant

1. Buchko, G. W.; Jain, A.; Reback, M. L.; Shaw, W. J., Structural characterization of the model amphipathic peptide Ac-LKKLLKLLKLLKLL-NH₂ in aqueous solution and with 2,2,2-trifluoroethanol and 1,1,1,3,3,3-hexafluoroisopropanol. *Can. J. Chem.* **2013**, *91*, 406-413.

- Priyadarshani, N.; Ginovska, B.; Bays, J. T.; Linehan, J. C.; Shaw, W. J., Photoswitching a molecular catalyst to regulate CO₂ hydrogenation. *Dalton. Trans.* **2015**, *44*, 14854-14864.

Publications jointly funded by this grant and other grants with leading intellectual contribution from this grant

- Dutta, A.; Lense, S.; Hou, J.; Engelhard, M. H.; Roberts, J. A. S.; Shaw, W. J., Minimal Proton Channel Enables H₂ Oxidation and Production with a Water-Soluble Nickel-Based Catalyst. *J. Am. Chem. Soc.* **2013**, *135*, 18490-18496.
- Galan, B. R.; Reback, M. L.; Jain, A.; Appel, A. M.; Shaw, W. J., Electrocatalytic Oxidation of Formate with Nickel Diphosphine Dipeptide Complexes: Effect of Ligands Modified with Amino Acids. *Eur. J. Inorg. Chem.* **2013**, *2013*, 5366-5371.
- Reback, M. L.; Ginovska-Pangovska, B.; Ho, M.-H.; Jain, A.; Squier, T. C.; Raugei, S.; Roberts, J. A. S.; Shaw, W. J., The Role of a Dipeptide Outer-Coordination Sphere on H₂-Production Catalysts: Influence on Catalytic Rates and Electron Transfer. *Chem. Eur. J.* **2013**, *19*, 1928-1941.
- Shaw, W. J.; Helm, M. L.; DuBois, D. L., A modular, energy-based approach to the development of nickel containing molecular electrocatalysts for hydrogen production and oxidation. *Biochimica et Biophysica Acta (BBA) - Bioenergetics* **2013**, *1827*, 1123-1139.
- Ginovska-Pangovska, B.; Ho, M.-H.; Linehan, J. C.; Cheng, Y.; Dupuis, M.; Raugei, S.; Shaw, W. J., Molecular dynamics study of the proposed proton transport pathways in [FeFe]-hydrogenase. *Biochimica et Biophysica Acta (BBA) - Bioenergetics* **2014**, *1837*, 131-138.
- Lense, S.; Dutta, A.; Roberts, J. A. S.; Shaw, W. J., A proton channel allows a hydrogen oxidation catalyst to operate at a moderate overpotential with water acting as a base. *Chem. Commun.* **2014**, *50*, 792-795.
- Reback, M. L.; Buchko, G. W.; Kier, B. L.; Ginovska-Pangovska, B.; Xiong, Y.; Lense, S.; Hou, J.; Roberts, J. A. S.; Sorensen, C. M.; Raugei, S.; Squier, T. C.; Shaw, W. J., Enzyme Design from the Bottom Up: An Active Nickel Electrocatalyst with a Structured Peptide Outer Coordination Sphere. *Chem. Eur. J.* **2014**, *20*, 1510-1514.
- Bays, J. T.; Priyadarshani, N.; Jeletic, M. S.; Hulley, E. B.; Miller, D. L.; Linehan, J. C.; Shaw, W. J., The Influence of the Second and Outer Coordination Spheres on Rh(diphosphine)₂ CO₂ Hydrogenation Catalysts. *ACS Catal.* **2014**, *4*, 3663-3670.
- Dutta, A.; Roberts, J. A. S.; Shaw, W. J., Arginine-Containing Ligands Enhance H₂ Oxidation Catalyst Performance. *Angew. Chem., Int. Ed.* **2014**, *53*, 6487-6491.
- Ginovska-Pangovska, B.; Dutta, A.; Reback, M. L.; Linehan, J. C.; Shaw, W. J., Beyond the Active Site: The Impact of the Outer Coordination Sphere on Electrocatalysts for Hydrogen Production and Oxidation. *Acc. Chem. Res.* **2014**, *47*, 2621-2630.
- Dutta, A.; DuBois, D. L.; Roberts, J. A. S.; Shaw, W. J., Amino acid modified Ni catalyst exhibits reversible H₂ oxidation/production over a broad pH range at elevated temperatures. *Proc. Natl. Acad. Sci. U. S. A.* **2014**, *111*, 16286-16291.

14. Rodriguez-Maciá, P.; Dutta, A.; Lubitz, W.; Shaw, W. J.; Rüdiger, O., Direct Comparison of the Performance of a Bio-inspired Synthetic Nickel Catalyst and a [NiFe]-Hydrogenase, Both Covalently Attached to Electrodes. *Angew. Chem., Int. Ed.* **2015**, *54*, 12303-12307.
15. Dutta, A.; Lense, S.; Roberts, J. A. S.; Helm, M. L.; Shaw, W. J., The Role of Solvent and the Outer Coordination Sphere on H₂ Oxidation Using [Ni(P^{Cy2}N^{Pyz2})₂]²⁺. *Eur. J. Inorg. Chem.* **2015**, *2015*, 5218-5225.
16. Dutta, A.; Ginovska, B.; Raugei, S.; Roberts, J. A. S.; Shaw, W. J., Optimizing conditions for utilization of an H₂ oxidation catalyst with outer coordination sphere functionalities. *Dalton. Trans.* **2016**, DOI: 10.1039/C6DT00280C.

Publications jointly funded by this grant and other grants with relatively minor intellectual contribution from this grant

17. Franz, J. A.; O'Hagan, M.; Ho, M.-H.; Liu, T.; Helm, M. L.; Lense, S.; DuBois, D. L.; Shaw, W. J.; Appel, A. M.; Raugei, S.; Bullock, R. M., Conformational Dynamics and Proton Relay Positioning in Nickel Catalysts for Hydrogen Production and Oxidation. *Organometallics* **2013**, *32*, 7034-7042.
18. Hou, J.; Fang, M.; Cardenas, A. J. P.; Shaw, W. J.; Helm, M. L.; Bullock, R. M.; Roberts, J. A. S.; O'Hagan, M., Electrocatalytic H₂ production with a turnover frequency >10⁷ s⁻¹: the medium provides an increase in rate but not overpotential. *Energy Environ. Sci.* **2014**, *7*, 4013-4017.
19. Ho, M.-H.; O'Hagan, M.; Dupuis, M.; DuBois, D. L.; Bullock, R. M.; Shaw, W. J.; Raugei, S., Water-assisted proton delivery and removal in bio-inspired hydrogen production catalysts. *Dalton. Trans.* **2015**, *44*, 10969-10979.

Toward Modeling Practical Catalytic Environments from first principles

Ping Liu, Jose A. Rodriguez, and Mike G. White
Brookhaven National Laboratory

Presentation Abstract

A significant change in fundamental research is driven by the need to move from consideration of idealized, model catalyst system under UHV conditions to practical powder catalysts under relatively high pressures. Working toward bridging the pressure gap, using density functional theory (DFT) we identified a $\text{Fe}_3\text{O}_4/\text{Au}$ as a stable and active phase during CO oxidation on FeO/Au catalyst, being able to facilitate the reaction via interfacial sites.¹ Along bridging the material gap, the nanostructures in the size and shape synthesized experimentally was considered in DFT calculations. Such realistic model allowed us to describe well the experimentally observed trend in specific and mass activity for the oxygen reduction reaction (ORR) on various $\text{Au}_x\text{Pd}_y@\text{Pt}_{\text{ML}}$ core-shell nanowires.² It also opened a new possibility, enabling the design of a novel $\text{Ni}_{201}@\text{Au}_{84}\text{Pt}_{120}$ ORR catalysts to fulfill challenges in durability, activity and cost.³ Finally, our DFT-based calculations were able to reproduce the scanning tunneling microscope (STM) pattern for the complex potassium-modified 44 structure of $\text{Cu}_x\text{O}/\text{Cu}(111)$.⁴ The identified tuning effect of potassium in electronic structures and the selectivity of surface binding properties opened new opportunity to catalyst design for the complex reactions.

References

1. Yu, L.; Liu, Y.; Yang, F.; Evans, J.; Rodriguez, J. A.; Liu, P., *J. Phys. Chem. C* **2015**, *119*, 16614-16622.
2. Liu, H.; An, W.; Li, Y.; Frenkel, A. I.; Sasaki, K.; Koenigsmann, C.; Su, D.; Anderson, R. M.; Crooks, R. M.; Adzic, R. R.; Liu, P.; Wong, S. S., *J. Am. Chem. Soc.* **2015**, *137*, 12597-12609.
3. An, W.; Liu, P., *ACS Catal.* **2015**, *5*, 6328-6336.
4. An, W.; Xu, F.; Stacchiola, D.; Liu, P., *ChemCatChem* **2015**, *7*, 3865-3872.

Dehydration and dehydrogenation of isopropanol on metal oxide catalysts

Daniel A. Lutterman,[#] Michael Quintero,[€] Michelle K. Kidder,[#] Felipe G. Polo,[#] Benjamin Doughty,[#] Luke Daemen,[¥] and Yongqiang Cheng[¥]

Oak Ridge National Laboratory, [#]Chemical Sciences and [¥]Chemical and Engineering Materials Divisions

[€]Johns Hopkins University, Department of Chemistry

Presentation Abstract

The overarching goal of this project is to understand how to control reaction selectivity through tuning cooperativity in multi-functional catalysts and to understand the role that atomic surface structure plays in controlling selectivity at catalytic oxide surfaces. Adsorption and reactivity of oxygenates can be controlled not only by the surface structure of oxides such as CeO₂ with different facets, but also by the surface composition of oxides such as binary oxides including perovskites and mixed oxides. Here, we focused our investigation on the reactivity and selectivity with respect to the dehydration and dehydrogenation of isopropyl alcohol (IPA) to yield acetone and propylene, respectively. While CeO₂ shows selectivity towards dehydrogenation, cobalt oxide (Co₃O₄) and LaCoO₃ highly favor the dehydration reaction pathway, providing two catalytic pathways to investigate the selectivity of IPA reactions. Two spectroscopic techniques have been developed to investigate the interaction of IPA with the surfaces of these oxide catalysts as a function of temperature and surface coverage.

In the first approach, we have initiated our research using highly ordered CeO₂ surfaces with (100), (110), and (111) orientations to contrast the absolute surface orientations of isopropanol on the different surfaces at room temperature using sum frequency generation (SFG) spectroscopy. Currently, we are expanding this approach to include other catalytic materials at elevated temperatures and pressures so that reactivity and energies can be followed simultaneously and correlated to surface orientation and speciation observed.

In another approach, because of its great sensitivity to hydrogen, neutron scattering (NS) can be a valuable approach in the study of catalytic reactions, particularly those involving hydrogen-rich organic molecules like isopropanol, acetone, propylene and intermediates. This is especially useful when it comes to optically opaque materials that traditional optical spectroscopy has difficulty to deal with. Changes in NS spectral features reflect the adsorbate-adsorbent interactions. Chemisorption and reaction products can similarly be observed through their spectral signature. Here, we will discuss how neutron vibrational spectroscopy provides us a means to follow the reactant intermediates, and products on the surface of catalysts, such as Co₃O₄ and LaCoO₃ and our future work to follow reactions *in situ* by neutron vibrational spectroscopy.

Elucidating the Function of Each Metal in Pd/Fe Bimetallic Catalysts for Hydrodeoxygenation Reactions

Alyssa J. R. Hensley^a, Breanna Wong^a, Kushal Ghale^b, Yongchun Hong^a, Carolin Rieg^a, Thanh Dang^b, Emily Anderst^a, Felix Studt^c, Ye Xu^b, Charles T. Campbell^d, Pierre Gaspard^e, Yong Wang^a, Jean-Sabin McEwen^{a*}

^aWashington State University (WSU), Pullman, WA 99164

^bLouisiana State University, Baton Rouge, LA 70803

^cKarlsruhe Institute of Technology, Baden-Württemberg 76131, Germany

^dUniversity of Washington, Box 351700, Seattle, WA 98195-1700, USA

^eUniversité Libre de Bruxelles, B-1050 Brussels, Belgium

Presentation Abstract

One aspect crucial to the design of effective catalysts is knowledge of the elementary reaction mechanism, which is difficult to divine from experiment alone. However, first principle modeling techniques can be used to address this knowledge gap. An area currently in need of such fundamental insight is the hydrodeoxygenation (HDO) of bio-oil to create useable biofuels. Here we present our recent progress on this work in collaboration with several experimental groups. Firstly, we present a new method for accurately predicting both molecular and dissociative adsorption energies based on DFT calculations with periodic boundary conditions, which properly captures the adsorption energetics across the spectrum from strongly chemisorbed to strongly van der Waals bonded systems. This method is benchmarked against a set of 39 experimental adsorption reactions with corresponding accurate calorimetric measurements. Secondly, we identify the different synergetic effects of two bimetallic catalysts (Pd/Fe and Sn/Pt), since such catalysts have demonstrated synergistic behavior that contributes to a more cost-effective and longer-lasting catalyst. In particular, we present our modeling results for the benzene-benzene lateral interactions on Pt (111) and PtSn (111) surfaces, so as to be able to compare our modeling results with the temperature programmed desorption (TPD) results that are available in the literature. Thirdly, we study the initial reducibility of the clean and Pd doped Fe₂O₃ (0001) surface using the DFT+U method proposed by Meredig, et al. as well as the hybrid HSE06 functional to further examine the role of Pd in a bimetallic catalyst composed of Pd and Fe. The most significant effect of Pd doping on the initial reduction of the Fe₂O₃ (0001) surface is in the creation of the first surface oxygen vacancy which becomes exothermic due to the Pd-O interactions. As creating the first oxygen vacancy in the Fe₂O₃ (0001) surface is the most energy intensive step examined here, the addition of Pd is likely to significantly enhance the reducibility of the Fe₂O₃ (0001) surface.

DE-SC0014560: Developing Multi-Scale Models for the Effective Design of Bimetallic Catalysts for the Targeted Refinement of Bio-oil to Usable Biofuels

Students: Alyssa Hensley, Breanna Wong, Ian de Joode

Affiliations: Washington State University (WSU), Voiland School of Chemical Engineering and Bioengineering, Pullman, WA 99164

RECENT PROGRESS

Specific Aim 1: Determining the chemical nature of the synergetic properties between the two metals of a bimetallic catalyst and the lateral interactions between the phenolic compounds

In the proposed work, the optB88 functional was thought to be the most accurate functional that could properly capture the lateral interaction between the aromatic adspecies on a metal surface. To verify this assertion, we benchmarked this functional and the optB86b functional against a database of 39 experimentally measured, highly accurate adsorptive reaction energies as obtained in the group of Charles T. Campbell (University of Washington) [1] in collaboration with Ye Xu (Louisiana State University). Our benchmarking work shows that the optB-vdW functionals perform exceptionally well for adsorption systems with significantly large vdW contributions. However, they perform poorly for those systems that are dominated by chemisorption. To address this shortcoming, we propose a simple method of combining the results of the optB-vdW and RPBE functionals to generate more accurate predictions for the adsorption energies for both chemisorption and vdW-dominated systems. As such, this method accurately predicts adsorption energies for processes dominated by both charge transfer and dispersion forces to produce superior accuracy to any current standard DFT functional alone.

Specific Aim 2: Predict the cooperative effects and concerted behavior on several facets at the surface of a single catalytic grain under hydrodeoxygenation conditions

One crucial part in developing experimentally accurate kinetic models of catalysts is validating that the particular method correctly captures the chemical interactions between the adspecies. This is made difficult on our catalysts of interest, bimetallic Fe surfaces, due to the instability of single crystal Fe surfaces. Therefore, we have begun our elucidation of the lateral interactions between the adspecies present during the HDO of phenolics by modeling the temperature programmed desorption of benzene on Pt(111). The reason for choosing such a system is that experimental information is available for comparison, thereby allowing us to validate our model of the lateral interactions between adsorbed benzene. The work by Koel, et al. [2] shows that benzene desorption occurs in a temperature range of 230 K to 500 K at high coverage. This broad temperature range for desorption was proposed to be due to the adsorption of benzene on two different sites; one that binds benzene strongly and another that binds benzene weakly. Figure 1 shows our preliminary modeling results for this system, from which we draw two major conclusions. First, by studying the change in benzene's adsorption energy with surface coverage, we determined that a mean field model accurately describes the benzene-benzene lateral interactions. The coverage dependence of the adsorption energy of benzene was determined for several different adsorption sites for benzene and all showed a similar, linear trend. Second, after modeling the TPD of benzene using the mean field models developed for different benzene adsorption sites, we determined that the broad temperature range seen experimentally for benzene desorption from Pt(111) was due to a coverage effect and not to two different adsorption sites (Figure 1). However, as can be seen in Figure 1b, the temperature range of the simulated TPD spectra when using the mean field interaction as deduced from the DFT calculations is smaller than the experimental results. On the other hand, if one uses the coverage

dependence of the heat of adsorption as measured by Campbell and coworkers [3] to model the TPD spectra we get a larger temperature range for the simulated TPD spectra (Figure 1a). As such, this work represents a significant step forward in our ability to kinetically model the adsorption behavior of large aromatic compounds on surfaces and also provides a benchmark for our future studies on this system and on bimetallic Fe surfaces.

Specific Aim 3: Determining the dominant mechanism for the deoxygenation of phenol on low Miller indexed Fe surfaces in the presence of Pd, Pt, Rh, Ni and Cu promoters in the presence of water

We have examined the role of a noble metal dopant during the hydrodeoxygenation (HDO) reaction by studying the adsorption of both H and O on Pd/Fe surfaces and the reduction of Pd doped Fe₂O₃. The adsorption studies were done in preparation for building a microkinetic model of the formation of H₂O on said surfaces. This, along with the Pd/Fe₂O₃ reduction studies, suggests that Pd's major role during the HDO reaction is to weaken the adsorption of O, thereby protecting the Fe surface from oxidation and deactivation.

Our initial investigations into this system used the DFT+U method in order to correctly model the semiconductor nature of the Fe₂O₃ surface. In this method, a correction term is applied to the DFT energy which is proportional to the chosen value of U. The major difficulty with this method is therefore the choice of the U parameter. In our work, we examined the stability of the (0001) Fe₂O₃ surface at five different states of reduction at 8 different U values (Figure 2a), i.e. complete (no O vacancies), one surface O vacancy, one subsurface O vacancy, two surface O vacancies, and one surface and one subsurface O vacancies. Such a scan of U values was shown to be necessary by the work of Meredig, et al. [4] as the absence of such a scan in U values, i.e. applying a single U value, makes it possible to potentially converge the given calculation to a local minimum energy as opposed to the global minimum energy. Our results show that as the U value changes, the relative stability of the five studied surfaces change significantly. Most importantly, different U values produce different trends in the stability of the different surfaces. What these results show is that no conclusions can be made as to the structure or reduction mechanism of the clean or doped Fe₂O₃ surface using the traditional DFT+U method. Therefore, we have decided to continue our studies with the more computationally expensive, yet rigorous, hybrid HSE06 functional. Our preliminary results with the HSE06 functional, see Figure 2b,

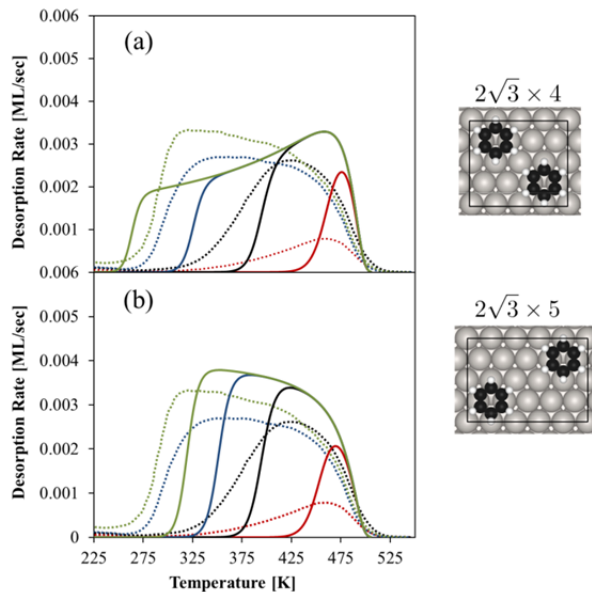


Figure 1. (a) Modeled temperature programmed desorption (TPD) spectra for benzene on Pt(111) using the coverage dependence of the adsorption energy as deduced by Campbell and coworkers (solid lines) at initial coverages of 0.01, 0.05, 0.09 and 0.14 ML (red, black, blue and green curves, respectively). The corresponding experimental TPD spectra are shown as dotted lines. (b) Modeled TPD spectra using the mean field interaction term as obtained from the DFT calculations (solid lines) as compared to the experimental results (dashed lines). The structures on the right show two of the experimentally observed ordered structures, placed in the most favorable bridge 30° site, used to develop the model.

show that the addition of a Pd dopant to the surface of the (0001) Fe_2O_3 surface significantly decreases the O vacancy formation energy, which is consistent with our experimental work.

References

- Wellendorff, J.; Silbaugh, T.L.; Garcia-Pintos D.; Nørskov, J.K.; Bligaard, T.; Studt, F.; Campbell, C.T. A Benchmark Database for Adsorption Bond Energies to Transition Metal Surfaces and Comparison to Selected DFT Functionals, *Surf. Sci.*, **2015**, 648, 36-44.
- Xu, C.; Tsai, Y. L.; Koel, B. E. Adsorption of Cyclohexane and Benzene on Ordered Sn/Pt(111) Surface Alloys, *J. Phys. Chem.*, **1994**, 98, 585-593.
- Ihm, H.; Ajo, H. M.; Gottfried, J. M.; Bera, P.; Campbell, C.T. Calorimetric Measurement of the Heat of Adsorption of Benzene on Pt(111), *J. Phys. Chem. B*, **2004**, 108, 14627.
- Meredig, B.; Thompson, A.; Hansen, H. A.; Wolverton, C.; van de Walle, A. Method for Locating Low-Energy Solutions within DFT+U, *Phys. Rev. B*, **2010**, 82, 195128.

Publications Acknowledging this Grant in 2013-2016

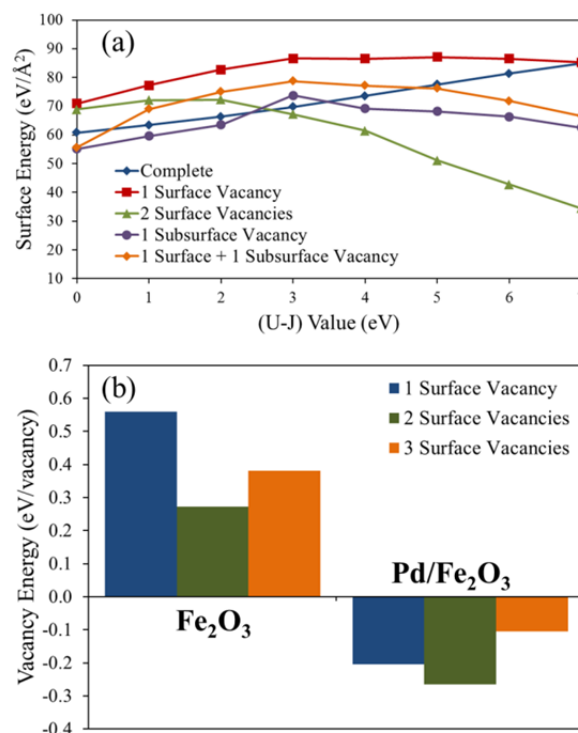
(I) Exclusively funded by this grant: None.

(II) Jointly funded by this grant and other grants with leading intellectual contribution from this grant:

- Hongchun, H.; Hensley, A. J. R.; McEwen, J.-S.; Wang, Y. Perspective on Catalytic Hydrodeoxygenation of Biomass Pyrolysis Oils: Essential Roles of Fe-based Catalysts, *Catal. Lett.* **2016**, in press.
- Hensley, A. J. R.; Wang, Y.; McEwen, J.-S. Adsorption of Guaiacol on Fe(110) and Pd(111) from First Principles, *Surf. Sci.* **2016**, 648, 74-83.
- Hensley, A. J. R.; Schneider, S.; Wang, Y.; McEwen, J.-S. Adsorption of Aromatics on the (111) Surface of PtM and PtM₃ (M = Fe, Ni) Alloys, *RSC Adv.* **2015**, 5, 85705-85719.

(III) Jointly funded by this grant and other grants with relatively minor intellectual contribution from this grant: None.

Figure 2. The variation in the surface energy with the U value using the DFT+U method for the Fe_2O_3 (0001) surface under five different conditions (a) and the oxygen vacancy formation energy for three different systems on the undoped and Pd doped Fe_2O_3 (0001) surface (b).



Tuning the dehydration activity of alcohols using phosphonic acid self-assembled monolayers

J. Will Medlin, Lucas D. Ellis, Daniel K. Schwartz
University of Colorado

Presentation Abstract

Over the last decade use of capping ligands and self-assembled monolayers (SAMs) have been developed as a means to control the selectivity of reactions on supported metal catalysts. We sought to utilize a similar approach for metal oxide catalysts. We developed a simple and rapid approach to functionalize anatase titania and other metal oxides with phosphonic acid SAMs. These SAMs are exceptionally robust, resisting thermal degradation up to 400°C. We investigated the selectivity of these catalysts for reactions of alcohols on titania. When 1-propanol was reacted over titania three main pathways were observed: dehydration, dehydrogenation, and condensation. At low temperatures (~250°C), dehydrogenation is favored on the native catalyst, closely followed by condensation. However, upon functionalization of titania with phosphonic acids having various alkyl tails (methyl, octadecyl, benzyl, etc), dehydration becomes the dominant pathway. More surprisingly, depending on the functionality of the alkyl tail function (e.g. 4-aminobenzylphosphonic vs 3-fluorobenzylphosphonic acid), the activity of dehydration can be tuned over a wide range, allowing far higher dehydration activities than on the uncoated catalysts. Our reactor studies and surface characterization results have suggested that this effect is due to tuning of electronic character of the surface via the organic ligand.

DE-SC0005239: Selectivity Control Through Modification of Metal Catalysts with Organic Monolayers

Students: Lucas D. Ellis and Pengxiao Hao

RECENT PROGRESS

Modification of metal oxide catalysts and supports with silanes and phosphonates

We have recently investigated the modification of metal oxide catalysts and supports with organic monolayers. In particular, we used phosphonic acid and silane groups to tether organic functions onto a variety of oxides including Al₂O₃, WO₃, TiO₂, and ZrO₂. We developed reproducible self-limiting deposition procedures to coat these metal oxides with well-organized phosphonate monolayers. An attractive feature of these SAMs is that they are stable to relatively high temperatures of at least 400 °C, as demonstrated by DRIFTS studies (Figure 5). In

preliminary studies using octadecyl (C18) phosphonate-coated oxide catalysts for selective dehydration of 1,2-propanediol, we found that the coating resulted in a moderate decrease in activity with no change in selectivity, suggesting that the coating was merely blocking access to surface sites. However, we have very recently observed much more interesting effects for phosphonate modification of the TiO₂ and Pt/Al₂O₃ catalysts, as will be partly discussed in the poster presentation.

In contrast to the phosphonate-coated catalysts, catalysts coated with trimethylsilane were found to strongly increase the activity of WO₃ and Al₂O₃ catalysts for 1,2-propanediol dehydration (Al₂O₃ results in Fig. 1). DRIFT and X-ray photoelectron spectra collected after exposure to reaction conditions indicated that the active form of the coating involved partial oxidation of the central Si atom, so that only a single methyl group was retained on the ligand. The higher activity was observed despite a significant decrease in the number of acid and base sites on the catalysts as measured by probe molecule adsorption. Interestingly, the coated catalysts were less reactive for dehydration of the simple alcohols 1-propanol and 2-propanol. Extensive temperature programmed desorption studies utilizing the reactants and dehydration products suggested that the coating increased the rate of diol dehydration by preventing bidentate adsorption; since there are no analogous bidentate forms of simple alcohols, the coating was ineffective for promoting their dehydration. This result is reminiscent of our recent work with thiolate-modified Pd catalysts, where the coating increased reactivity by preventing strong adsorption on active sites.

Selective alcohol oxidation

Most of our work with thiolate-modified catalysts has focused on hydrogenation reactions, but recently we have extended the technique to selective oxidation. We found that thiolates actually lead to a significantly increased activity for Pd/Al₂O₃ catalysts during liquid phase aerobic oxidation of trans-2-hexen-1-ol. While the uncoated supported Pd catalyst suffered from rapid deactivation (Fig. 2), thiol-modified catalysts exhibited lower initial rates but limited deactivation, and maintained excellent selectivity to the unsaturated aldehyde product; the catalyst was also stable over

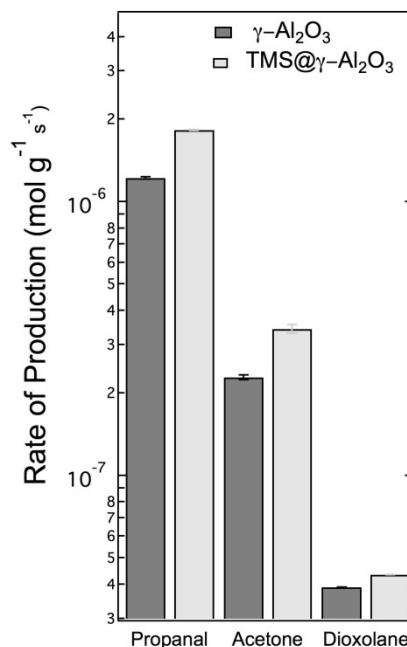


Figure 1: Promoting effect of trimethylsilane on 1,2-propanediol dehydration. The TMS coating improved the reaction rates for all products, despite decreasing the acid site density by 50%.

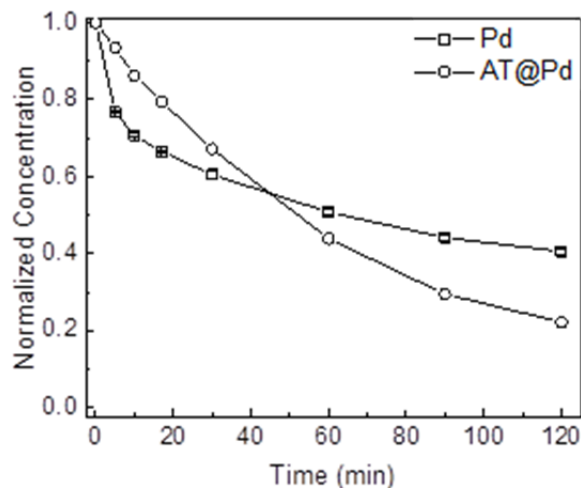


Figure 2: Batch kinetic data of 1-hexenal concentration as a function of reaction time for equal loadings of uncoated and adamantanethiol-coated Pd/Al₂O₃ catalysts.

multiple recycles. Kinetic studies combined with temperature programmed desorption (TPD) and DRIFTS experiments revealed that the thiolate SAMs weakened the adsorption of strongly adsorbed intermediates generated from the reaction product trans-2-hexenal. Somewhat more surprisingly, XPS studies of spent catalysts clearly demonstrated that the thiol remained in a reduced form after reaction, and did not form appreciable coverage of sulfates.

Publications Acknowledging this Grant in 2013-2016

(I) Exclusively funded by this grant;

1. Kahsar, K.R.; Schwartz, D.K.; Medlin, J.W. Control of Metal Catalyst Selectivity through Specific Non-Covalent Molecular Interactions. *J. Am. Chem. Soc.*, **2014**, *136*, 520-526.
2. Kahsar, K. R.; Schwartz, D. K.; Medlin, J. W. Selective Hydrogenation of Unsaturated Fatty Acids on Pd/Al₂O₃ Catalysts Modified with Self-Assembled Monolayers. *ACS Catal.* **2013**, *3*, 2041
3. Kahsar, K.R.; Schwartz, D.K.; Medlin, J.W. Stability of Self-Assembled Monolayer Coated Pt/Al₂O₃ Catalysts for Liquid Phase Hydrogenation. *Journal of Molecular Catalysis A: Chemical*, **2015**, *396*,188-195.
4. Kahsar, K.R.; Johnson, S.; Schwartz, D.K.; Medlin, J.W. Hydrogenation of cinnamaldehyde over Pd/Al₂O₃ catalysts modified with thiol monolayers. *Topics in Catalysis*, **2014**, *57*, 1505-1511.
5. Ellis, L.D.; Pylypenko, S.; Ayotte, S.R.; Schwartz, D.K.; Medlin, J.W. Trimethylsilyl functionalization of alumina increases activity for 1,2-propanediol dehydration. *Catalysis Science and Engineering*, **2016**, advance article, DOI: 10.1039/C6CY00574H

(II) Jointly funded by this grant and other grants with leading intellectual contribution from this grant;

6. Pang, S. H.; Schoenbaum, C. A.; Schwartz, D. K.; Medlin, J. W. Directing Reaction Pathways by Catalyst Active-Site Selection Using Self-Assembled Monolayers. *Nat. Commun.* **2013**, *4*, 1–6.
7. Schoenbaum, C. A.; Schwartz, D. K.; Medlin, J. W. Controlling Surface Crowding on a Pd Catalyst with Thiolate Self-Assembled Monolayers. *J. Catal.* **2013**, *303*, 92–99.
8. Pang, S.H.; Schoenbaum, C.A.; Schwartz, D.K.; Medlin, J.W. Effects of Thiol Modifiers on the Kinetics of Furfural Hydrogenation over Pd Catalysts. *ACS Catal.* **2014**, *4*, 3123-3131.
9. Schoenbaum, C.A.; Schwartz, D.K.; Medlin, J.W. Controlling the Surface Environment of Heterogeneous Catalysts Using Self-Assembled Monolayers. *Accounts of Chemical Research* **2014**, *47*, 1438-1445.
10. Corpuz, A.R.; Pang, S.H; Schoenbaum, C.A.; Medlin, J.W. Hydrogen Exposure Effects on Pt/Al₂O₃ Catalysts Coated with Thiolate Monolayers. *Langmuir*, **2014**, *30*, 4104-41110.

(III) Jointly funded by this grant and other grants with relatively minor intellectual contribution from this grant;

11. Pang, S.H; Lien, C.-H.; Medlin, J.W. Control of surface alkyl catalysis with thiolate monolayers. *Catal. Sci. Eng.*, **2016**, *6*, 2413-2418.
12. Pang, S. H.; Medlin, J. W. Controlling Catalytic Selectivity via Adsorbate Orientation on the Surface: From Furfural Deoxygenation to Reactions of Epoxides. *J. Phys. Chem. Lett.* **2015**, *6*, 1348–1356.

Donghai Mei

Chemistry of the Metal Catalyzed C-O Bond Cleavage of Lignin in the Condensed Phase

Johannes Lercher,^{a,b} Don Camaioni,^a Donghai Mei,^a Nigel Browning,^a Mirek Derewinski,^a Yong Wang,^a John Fulton,^a Jian Zhi Hu,^a Andreas Jentys^b

^a Pacific Northwest National Laboratory, Physical and Computational Sciences Directorate and Institute for Integrated Catalysis

^b Technical University Munich, Department of Chemistry

Presentation Abstract

As one of most abundant lignocellulosic biomass resources, lignin has been considered as the potential feedstock for the production of transportation fuels and other value-added fine chemicals. Although its molecular structure is still not fully clarified, lignin is generally characterized as a three dimensional biopolymer network of aromatic units that are linked by either C-C or C-O bonds. Due to the high bond energy of the C-C bond, effectively cleaving the C-O bond of linkages such as aryl ether model compounds becomes the important step in the depolymerization of lignin. To develop stable, most importantly, highly selective catalysts for this catalytic process, understanding the chemistry of the C-O bond scission in aryl ethers over various potential metal catalysts is the key. Our recent work focuses on the selective C-O bond cleavage of three model diaryl ether compounds in condensed phases over a series of supported transition metal catalysts using combined experimental kinetics measurements and computational modeling. The selectivity of ether conversion can be tuned and controlled by using different transition metal catalysts as well as the physicochemical properties of condensed phases. This is demonstrated in this poster that the dominant C-O bond cleavage reaction route (hydrogenolysis and hydrolysis) varies over four (Pt, Pd, Rh and Ru) metals in aqueous phase. In particular, the heterogeneously catalyzed hydrolysis of diaryl ethers in the presence of hydrogen has been highlighted.

Grant or FWP Number: FWP 47319: Low Temperature Catalytic Routes for Energy Carriers via Spatial and Chemical Organization

PI: Johannes Lercher

Molecular Titanium Nitrides. Nucleophiles Unleashed

Daniel J. Mindiola,¹ Lauren N. Grant,¹ Maria E. Carroll,¹ Balazs Pinter,² Gang Wu,³ and Patrick J. Carroll¹

¹Department of Chemistry, University of Pennsylvania, 231 South 34th Street, Philadelphia, Pennsylvania 19104, United States

²Eenheid Algemene Chemie (ALGC), Vrije Universiteit Brussel (VUB), Pleinlaan 2, 1050, Brussels (Belgium).

³Department of Chemistry, Queen's University, Kingston, Ontario, Canada K7L 3N6.

Presentation Abstract

The nitride anion reagent, $[\mu_2\text{-K}(\text{OEt}_2)]_2[(\text{PN})_2\text{Ti}\equiv\text{N}]$ (**1**) ($\text{PN}^- = (\text{N}-(2\text{-diisopropylphosphino})-4\text{-methylphenyl})-2,4,6\text{-trimethylanilide}$), prepared from reduction of the azide precursor $(\text{PN})_2\text{Ti}(\text{N}_3)$, has been reacted with various electrophiles and demonstrated to be a powerful nucleophile as well as N-atom transfer reagent. The role of the alkali metal in the $\text{Ti}\equiv\text{N}$ bonding has been explored by preparing mononuclear as well as discrete salt of the nitride. Using this nitride reagent, we have been able to prepare functional groups (in some case rather unusual) having the moiety $\text{Ti}=\text{N}-\text{X}$, where X represents a phosphonyl, boryl, H, silyl, and alkyl. The nucleophilic nature of the titanium nitride has also allowed us to probe N-atom transfer reactions where acid chlorides are converted to nitriles, as well as redox reactions where transient nitridyl species are formed. We report herein the chemistry of the titanium nitride ligand.

Grant or FWP Number: DE-FG02-07ER15893. Synthesis and Exploratory Catalysis of 3d Metals: Atom and Group-Transfer Reactions and the Activation and Functionalization of Small Molecules Including Greenhouse Gases.

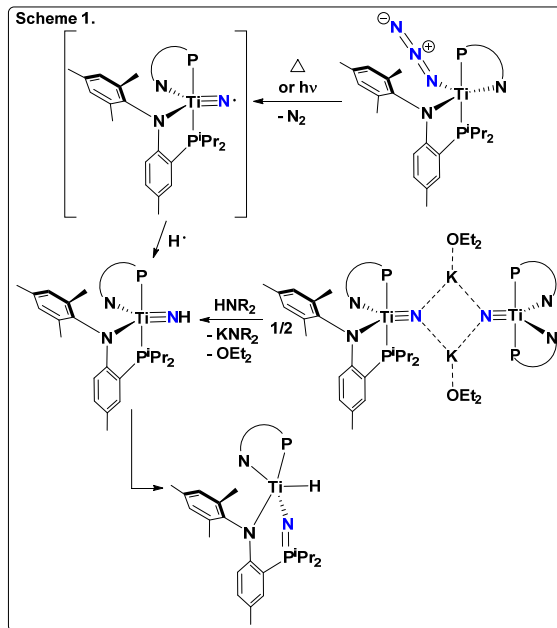
PI: Daniel J. Mindiola

Postdoc(s): Maria E. Carroll, Jaime E. Flores

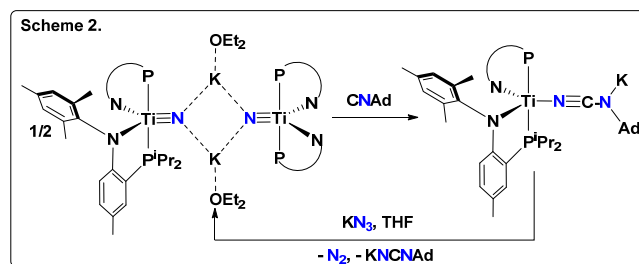
Student(s): Lauren L. Grant, Ba L. Tran, Rick Thompson

RECENT PROGRESS

Spectroscopic Identification of Titanium Nitridyls and Reactivity of Parent Imides of Titanium. Photolysis or thermolysis of $(\text{PN})_2\text{Ti}(\text{N}_3)$ results in extrusion of N_2 and formation of a transient titanium nitridyl, $(\text{PN})_2\text{Ti}=\text{N}\cdot$, which then abstracts $\text{H}\cdot$ (not from solvent medium) to form the parent imide $(\text{PN})_2\text{Ti}=\text{NH}$. We have spectroscopically identified the Ti(III) azide as well as the $(\text{PN})_2\text{Ti}=\text{N}\cdot$, using frozen conditions. In addition, the pK_a of the parent imide $(\text{PN})_2\text{Ti}=\text{NH}$ has been estimated to be within 26-36 based on these set of control experiments using various amines HNR_2 with the nitride salt $[\mu_2\text{-K}(\text{OEt}_2)]_2[(\text{PN})_2\text{Ti}=\text{N}]_2$. Given these pK_a ranges for the nitride, we are able to estimate the pK_b of **1** on the order of -20, in accord with such a moiety being a strong base and nucleophile as demonstrated through our reactivity. We have also found the parent imide $(\text{PN})_2\text{Ti}=\text{NH}$ to be a reactive (under photolytic conditions) via insertion of the N-H into the Ti-P bond of the chelating ligand to form the phosphinimide-hydride $(\text{PN})(\text{N}'\text{PN})\text{Ti}(\text{H})$. A summary of these set of reactions is depicted in Scheme 1. Interestingly, it was found that the nitride salt $[\mu_2\text{-K}(\text{OEt}_2)]_2[(\text{PN})_2\text{Ti}=\text{N}]_2$ cannot be prepared from reductive splitting of N_2 via the complex $(\text{PN})_2\text{Ti}=\text{N}=\text{N}=\text{Ti}(\text{PN})_2$ (**2**), a species prepared in 48% yield from KC_8 reduction of $(\text{PN})_2\text{TiCl}$ under N_2 . Lastly, the covalent and ionic nature of the nitride titanium linkage has been probed theoretically and also with the aid of solid state ^{15}N NMR (MAS) spectroscopy.

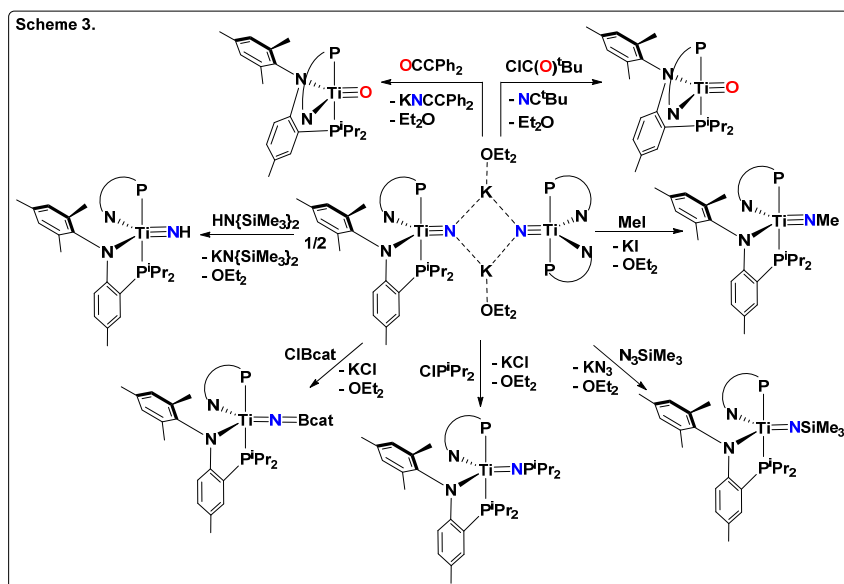


Nitrogen Atom Transfer to Produce Carbodiimides and Dialkylamino Nitrile Using Ti(II) Species. Compound $[\mu_2\text{-K}(\text{OEt}_2)]_2[(\text{PN})_2\text{Ti}=\text{N}]_2$ can deliver the nitride atom to unsaturated small molecules such as CNR and CO . In the case of CNAd ($\text{Ad} = 1\text{-adamantyl}$), we observe formation of the carbodiimide salt $[(\text{PN})_2\text{Ti}-\text{N}=\text{C}-\text{N}(\text{K})\text{Ad}]$, in nearly quantitative yield and as a paramagnetic d^2 species (Scheme 2). Treatment of the latter species with Me_3SiCl results in formation of the carbodiimide complex $[(\text{PN})\text{Ti}(\eta^2\text{-Me}_3\text{SiNCNAd})]$ whereas addition of smaller nucleophiles, produce the dialkylaminonitrile species $[(\text{PN})_2\text{Ti}(\eta^2\text{-NCN}(\text{Me})\text{Ad})]$. The full identity of these Ti(II) species having carbodiimide and dialkylaminonitriles are presently being investigated. Present studies have examined the use of CO to produce Ti(II) isocyanate salts, as well as



the possibility to perform catalytic N-atom transfer to these substrates (CO and CNR) using excess KN_3 reagent.

Reactivity Studies of Titanium Nitrides. The reactivity of $[\mu_2\text{-K}(\text{OEt}_2)]_2[(\text{PN})_2\text{Ti}\equiv\text{N}]_2$ has been explored with a variety of electrophiles as well as oxidants. For example, we have prepared the first terminally bound methylimide species, $(\text{PN})_2\text{Ti}=\text{NMe}$, by virtue of MeI addition to $[\mu_2\text{-K}(\text{OEt}_2)]_2[(\text{PN})_2\text{Ti}\equiv\text{N}]_2$. Me_3SiCl or Me_3SiN_3 addition to the nitride also results in salt elimination concurrent with formation of the imide $(\text{PN})_2\text{Ti}=\text{NSiMe}_3$. The borylimido complex $(\text{PN})_2\text{Ti}=\text{NBcatechol}$, a type of species extremely rare in early transition metals, can be readily produced upon treatment of $[\mu_2\text{-K}(\text{OEt}_2)]_2[(\text{PN})_2\text{Ti}\equiv\text{N}]_2$ with two equiv of ClBcatechol. Likewise, the phosphanylimido, $(\text{PN})_2\text{Ti}=\text{NP}^i\text{Pr}_2$, can be also prepared in good



yield by addition of ClP^iPr_2 to the nitride salt. Complex N-atom transfer can be accomplished when $[\mu_2\text{-K}(\text{OEt}_2)]_2[(\text{PN})_2\text{Ti}\equiv\text{N}]_2$ is treated with $\text{ClC}(\text{O})\text{tBu}$ or the ketene OCCPh_2 to form the titanium oxo, $(\text{PN})_2\text{Ti}\equiv\text{O}$, along with the organic products NC^tBu and KNCCPh_2 . Scheme 3 summarizes these set of reactions. Lastly, redox reactions involving the nitride and various oxidants such as

$[\text{FeCp}_2][\text{OTf}]$, I_2 , ClCPh_3 can produce transient nitridyl species that engage in P oxidation of the PN ligand to form phosphinimides-anilide scaffolds.

Publications Acknowledging this Grant in 2013-2016

(I) Exclusively funded by this grant;

1. Tran, B. L.; Krzystek, J.; Ozarowski, A.; Chen, C.-H.; Pink, M.; Karty, J. A.; Telser, J.; Meyer, K.; Mindiola, D. J. *Eur. J. Inorg. Chem.* (Special issue on small molecule activation) **2013**, 3916-3929.
2. Searles, K.; Tran, B. L.; Pink, M.; Chen, C.-H.; Mindiola, D. J. *Inorg. Chem.* **2013**, 52, 11126-11135.
3. Thompson, R.; Tran, B. L.; Ghosh, S.; Gao, X.; Chen, C.-H.; Baik, M.-H.; Mindiola, D. J. *Chem. Commun.* **2013**, 49, 2768-2770.
4. Thompson, R.; Wu, G.; Chen, C.-H.; Pink, M.; Mindiola, D. J. *J. Am. Chem. Soc.* **2014**, 136, 8197-8200.

5. Hounjet, L. J.; Adhikari, D.; Pink, M.; Carroll, P. J.; Mindiola, D. J. *Zeitschrift für Anorganische und Allgemeine Chemie (Special issue on Reactive Nitrogen-Containing Species: Generation, Characterization and Functionalization)* **2015**, *641*, 45-48.
6. Fortier, S.; Jackson, T. A.; Wijeratne, G. B.; Chen, C.-H.; Carroll, P. J.; Zolnhofer, E. M.; Grant, L. N.; Meyer, K.; Krzystek, J.; Ozarowski, A.; Mindiola, D. J.; Telser, J. *Inorg. Chem.* **2015**, *54*, 10380-10397.
7. Thompson, R.; Tran, B. L.; Ghosh, S.; Chen, C.-H.; Pink, M.; Gao, X.; Carroll, P. J.; Baik, M.-H.; Mindiola, D. J. *Inorg. Chem.* **2015**, *54*, 3068-3077.
8. Carroll, M. E.; Pinter, B.; Carroll, P. J.; Mindiola, D. J. *J. Am. Chem. Soc.* **2015**, *137*, 8884-8887.
9. Pinter, B.; Smith, K. T.; Kamitani, M.; Zolnhofer, E. M.; Tran, B. L.; Fortier, S.; Pink, M.; Wu, G.; Manor, B. C.; Meyer, K.; Baik, M.-H.; Mindiola, D. J. *J. Am. Chem. Soc.* **2015**, *137*, 15247-15261.
10. Grant, L. N.; Carroll, M. E.; Carroll, P. J.; Mindiola, D. J. *Manuscript accepted to Inorg. Chem.*

(II) *Jointly funded by this grant and other grants with leading intellectual contribution from this grant;*

1. Nobuyuki, K.; Flores, J. A.; Pal, K.; Caulton, K. G.; Mindiola, D. J. *Organometallics* **2013**, *32*, 3185-3191.
2. Franke, S. M.; Tran, B. L.; Heinemann, F. W.; Hieringer, W.; Mindiola, D. J.; Meyer, K. *Inorg. Chem.* **2013**, *52*, 10552-10558.

David R. Mullins

**Adsorption and Reaction of Methanol and Ethanol on
La_{0.7}Sr_{0.3}MnO₃(100) Perovskite by Ambient Pressure XPS***

David R. Mullins¹, Thomas Z. Ward² and Steven H. Overbury¹
Oak Ridge National Laboratory

¹Chemical Sciences Division, ²Material Science and Technology Division

Presentation Abstract

Perovskites which have the common compositional formula of ABO₃ can have a wide variety of catalytic behavior depending on their cationic constituents. Our goal is to understand and control this behavior at a fundamental level. Methanol and ethanol oxidation are being used as probe reactions to characterize the chemistry on these materials. Alcohol oxidation on a doped La_{0.7}Sr_{0.3}MnO₃(001) perovskite thin film has been studied using ambient pressure x-ray photoelectron spectroscopy (APXPS). In order to investigate the “pressure gap” that may occur between reactions studied under vacuum conditions and at pressure approaching atmospheric pressure, experiments were conducted at nominally 10⁻⁵ torr and at 0.1 torr between 250 °C and 350 °C.

Methanol forms methoxy when adsorbed on the perovskite surface at 250 °C. The surface coverage was four times greater at 0.1 torr compared to 10⁻⁵ torr. Methoxy was the only C-containing surface species observed at 10⁻⁵ torr with or without O₂. Methoxy was also the dominant surface species at 0.1 torr in the absence of O₂. However, small amounts of formate and atomic C were also evident. At the higher pressure, the Mn 2p spectra indicated that the alcohol partially reduced Mn³⁺ to Mn²⁺. There was also an indication in the O 1s spectra that O was removed from the surface.

In contrast to what was observed at 10⁻⁵ torr, when O₂ was present at 0.1 torr, formate became the dominant surface species with only trace amounts of methoxy and C evident. Gas phase CO₂ and H₂O products were also detected in the C 1s and O 1s spectra.

Results using ethanol rather than methanol as the reactant were generally the same, i.e., only ethoxy on the surface at lower pressures, a mixture of ethoxy and acetate at higher pressure in the absence of O₂, and exclusively acetate on the surface at high pressure when O₂ was present. The only significant difference between methanol and ethanol was a greater tendency for ethanol to form the carboxylate in the absence of O₂.

These experiments demonstrate that the surface coverage of the active molecular species depends strongly on the reactant pressure, and that the O₂ pressure can alter the nature of the adsorbed species.

*This research is part of FWP ERKCC96: **Fundamentals of Catalysis and Chemical Transformations**. For a full description of recent progress see the Abstract submitted by Zili Wu.

Dually functionalized MOF-NP Catalysts: Understanding and Controlling Oxidant generation-Epoxidation Catalysis in Solution Phase

Rungmai Limvorapitux,^a Lien-Yang Chou,^b Chia-Kuang Tsung,^{*b} and SonBinh T. Nguyen^{*a}

^aDepartment of Chemistry and the Institute for Catalysis in Energy Processes, Northwestern University, 2145 Sheridan Road, Evanston, Illinois 60208-3113. ^b Department of Chemistry, Boston College, 2609 Beacon St., Chestnut Hill, MA 02467

Presentation Abstract

In synthesis, the catalyzed epoxidation of alkene often involves two separate steps: a separate generation of high-energy oxidant such as peracids or hydrogen peroxide, and then the oxidation itself, which can require the use of excess oxidants, leading to waste. To this end, our research aims to couple the direct synthesis of H₂O₂ from hydrogen and oxygen together with the alkene oxidation in one step using a metal-organic framework (MOF) support that can encapsulate a peroxide-generating nanoparticle (NP) catalyst inside and be decorated with molecular epoxidation catalyst moieties on the outside. Owing to their well-defined cage-like porous structure and high tunability, MOF crystals can serve as a molecularly selective “window” that only pass hydrogen and oxygen into the inside of the MOF crystal to interact with the NP to generate H₂O₂, which migrates to MOF-solution interface and react with the epoxidation catalyst and the alkene. As the epoxidation catalyst is localized at the exterior of the MOF particles, H₂O₂ turnover and alkene epoxidation should be the most efficient. In addition, the alkene substrate can be designed to not pass into the interior of the MOF crystals to interact with the NP, thus preventing alkene hydrogenation. This presentation will describe our work in incorporating palladium and gold NPs H₂O₂-generation catalysts into the UiO-66-NH₂ MOF platform. The free amino ligands of the resulting MOFs can then be modified to incorporate Schiff-base(Mo^{VI}) alkene oxidation catalyst on the outside. Catalytic studies of the individual catalyst components show that the Au- and Pd-NP-incorporated MOFs are active in catalytic H₂O₂ generation, and that Schiff-base(Mo^{VI})-modified MOF are active in cyclooctene oxidation. Gratifyingly, the dually functionalized catalyst systems, [Pd-NP + Schiff-base(Mo^{VI})] and [Au-NP + Schiff-base(Mo^{VI})] MOFs both exhibit tandem catalytic behavior for the solution-phase epoxidation of cyclooctene with good selectivity.

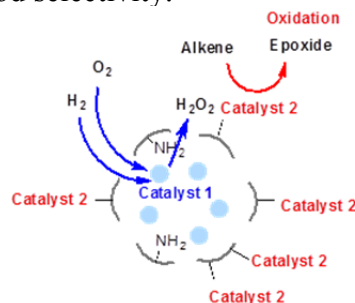


Figure 1. Dually functionalized MOFs

Dynamic Restructuring of Working Catalysts Revealed by Correlating Multiple (Optical, X-ray and Electron) Probes and First Principle Simulations

S. Zhao,¹ U. Jung,¹ A. Elsen,¹ D. Liu,¹ R. G. Nuzzo,¹ Y. Li,² A. I. Frenkel,² A. Gamalski,³ E. A. Stach,³ J. Kas,⁴ F. Vila,⁴ J. J. Rehr⁴

¹Department of Chemistry, University of Illinois, Urbana-Champaign, ²Department of Physics, Yeshiva University, ³Center for Functional Nanomaterials, Brookhaven National Laboratory ⁴Department of Physics, University of Washington

Presentation Abstract

A major goal of our work is to better understand the mechanisms of catalytic reactions. This interest is being addressed foremost through efforts that seek to provide and exploit new multi-modal means of characterization—ones that will make it possible to explore catalytic materials with multiple techniques, with the hope of using this combined data to elucidate the complex structure-property-rate relationships of catalysis with unprecedented clarity. The current work exploits a microfabricated catalytic reactor designed for correlated use with synchrotron x-ray absorption spectroscopy, scanning transmission electron microscopy, micro-IR and Raman spectroscopies. The power of the method, fully supported by first principle simulations, is illustrated in its ability to capture dynamic transformations that are revealed in an ensemble of monometallic (Pt, Pd and Au), as well as bimetallic (PtNi) clusters during exemplary catalytic reactions—the hydrogenation of ethylene, CO oxidation and reverse water gas shift (RWGS). We uncovered a complex co-dependency between multiple components of catalytic system (catalyst-support-surface species) that span sizes ranging from single atoms to large agglomerates, throughout changing reaction conditions. These impacts are highly responsive to the reactant atmosphere composition and conversion regimes of the reaction. This method is generalizable to quantitative *operando* studies of complex systems using a wide variety of x-ray and electron based experimental probes.

Grant Number: DE FG02-03ER15476

Grant Title: The Reactivity and Structural Dynamics of Supported Metal Nanoclusters Using Electron Microscopy, *in situ* X-Ray Spectroscopy, Electronic Structure Theories, and Molecular Dynamics Simulations.

PIs: Ralph G. Nuzzo, Anatoly I. Frenkel, John J. Rehr

Postdoc(s): A. Elsen, D. Liu, U. Jung, S. Zhao, J. Kas, Y. Li, F. Vila

RECENT PROGRESS

Mechanism of Deactivation of Pd Catalysts in Ethylene Hydrogenation Reaction

Understanding how heterogeneous catalysts change size, shape and structure during chemical reactions is limited by the paucity of methods for studying catalytic ensembles in working state, i.e., in *operando* conditions. Here, by a correlated use of synchrotron x-ray absorption spectroscopy, scanning transmission electron microscopy (STEM) and micro-IR spectroscopy in the same *operando* conditions, we quantitatively describe the complex structural dynamics of SiO₂ supported Pd catalysts exhibited during an exemplary catalytic reaction—ethylene hydrogenation. This work exploits a microfabricated catalytic reactor compatible with the three probes. A series of different feed gas atmospheres of hydrogen/ethylene mixture were applied in *operando* conditions in order to reveal the structure-property-performance relationship. Pronounced changes in the electronic structures of Pd-SiO₂ catalysts such as transitions between hydrogen and hydrocarbon covered surfaces were found to occur during the reaction. Combined use of *operando* XAS, IR and GC-MS results revealed selectivity of gas phase and surface-bound oligomer formation and reaction-driven restructuring between different states of Pd catalysts (the hydride and the carbide).

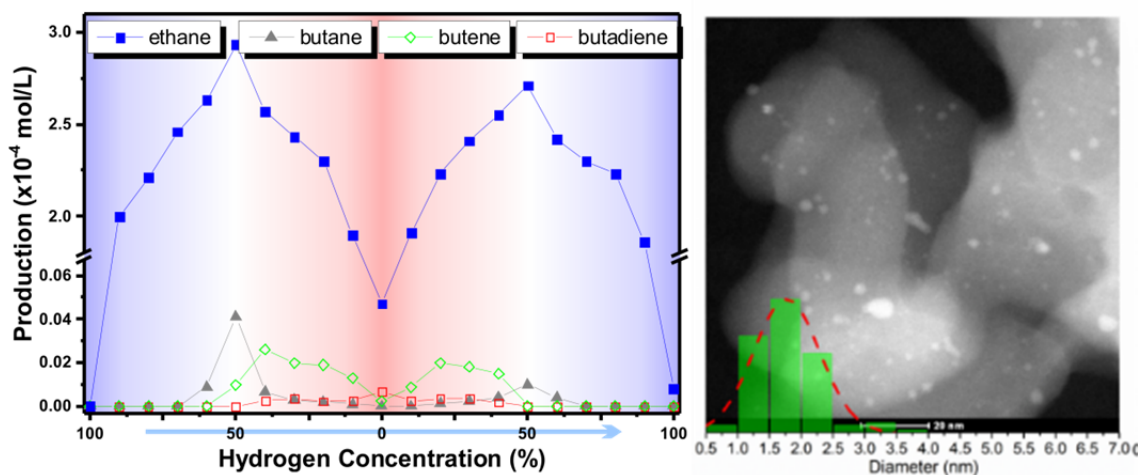


Figure 1. Left: Hydrocarbon production of ethylene hydrogenation as the function of feed gas (H₂ and C₂H₄) composition over Pd-SiO₂ catalyst: main product (ethane) and by-products (oligomers). Feed gas composition gradually switched from pure H₂ to pure C₂H₄ (forward) at a 10% step and then reversed to pure H₂ (backward) with the same step size. Right: *Operando* STEM data and particle size distributions (insets) measured in Pd NPs supported on SiO₂ under different reaction stages at 1 atm (the data shown are under pure H₂).

Restructuring of PtNi Catalysts in Reverse Water Gas Shift (RWGS) Reaction

Bimetallic catalysts have attracted much attention, in part, because they may display better catalytic properties compared to their monometallic counterparts. Driven by external environments, the distribution of elements in bimetallic catalysts can change, which in turn can affect the catalytic properties. To correlate structural changes of bimetallic catalysts with their properties it is vital to monitor their structure and dynamics in *operando* conditions. We study Pt-Ni catalysts supported on silica SBA-15 during the RWGS reaction at 400°C by combined experimental techniques (XAS and STEM) and theoretical methods to investigate correlations between the reactivity and structure of the catalysts. In April 2016 the *operando* XAS

measurements were carried out at the microXAS beamline at the Swiss Light Source. The setup of the experiment shown in Figure 3A. The Ni and Pt edge EXAFS spectra are shown in Figures 3B and 3C. For both edges, the spectra collected in the reaction condition are closer to those in H₂ condition, indicating predominantly reducing effects of the RWGS reaction mixture. Figures 3B,C demonstrate that the RWGS reaction causes additional and unique structural change to the catalyst compared to either reducing or oxidizing atmospheres. STEM measurements are planned in near future using the new Talos electron microscope at the CFN in BNL, in the same micro-reactor and the same reaction conditions as those at the MicroXAS beamline experiments.

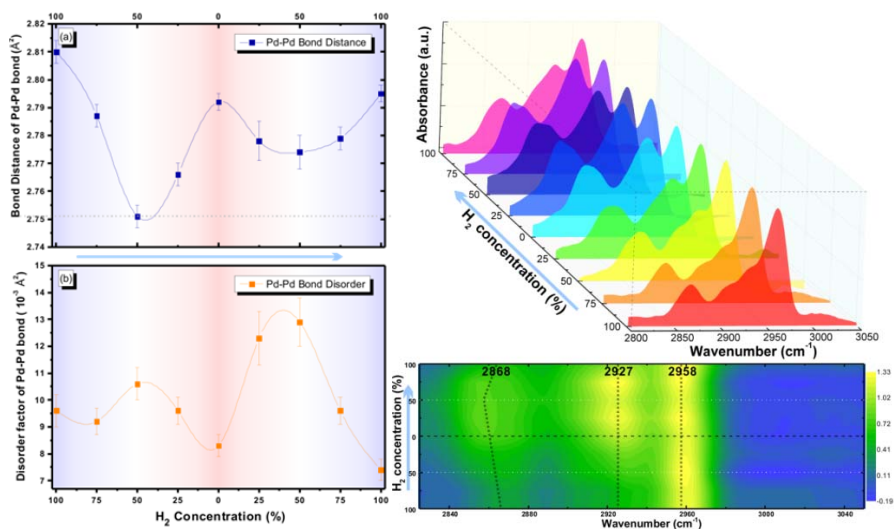


Figure 2. Left: EXAFS analysis results of (a) the interatomic distances r and (b) bond length distribution (disorder factor) for Pd-SiO₂ catalyst (Pd-Pd scattering path) under different feed gas composition regimes of H₂ and C₂H₄ (from pure H₂ to pure C₂H₄ and then back to pure H₂). The dashed line in (a) indicates the bond length of bulk Pd (foil) as a benchmark. Right: Operando IR spectra collected under different regimes of feed gas concentration for room temperature ethylene hydrogenation over Pd-SiO₂ catalysts. Top waterfall figure show individual spectra acquired under different regimes, the lower contour map highlights the maxima of hydrocarbon fingerprint bands.

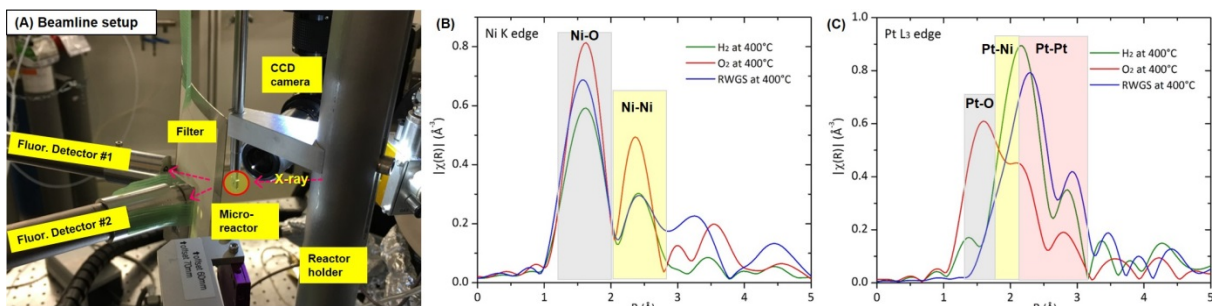


Figure 3. (A) Experimental setup at the MicroXAS beamline; Fourier transformed (B) Ni K edge and (C) Pt L₃ edge EXAFS spectra of PtNi/SBA-15 catalyst under different conditions

A combination of ab initio density functional theory molecular dynamics (DFT/MD) and X-ray absorption spectroscopy data analysis provides additional crucial information on the relationship between dynamical structural fluctuations and properties of supported catalysts. In our previous simulation of an analogous bimetallic system (Pt_nSn_m/γ-Al₂O₃) we obtained new information

structural, dynamic and physicochemical properties of catalysts and their interactions with adsorbates: 1) Sn atoms tend to reside on the surface of the cluster and are very mobile. They effectively shield the Pt atoms from the support, increasing the average number of Pt-O bonds from 2 in Pt₁₀Sn₁₀ to 7 in Pt₁₅Sn₅. 2) This O-interaction change affects the average Pt charge which varies from -0.5e in Pt₁₀Sn₁₀ to -0.1e in Pt₁₅Sn₅, and hence its catalytic properties. The striking effects of both structural and electronic inhomogeneity on reactivity can be seen in Figure 4. Major rearrangements of the structure of the nanoparticle and its interaction with the adsorbate disorder change the chemical nature of the reactants, transition states and products, resulting in large energy changes, such as the shift from endothermic behavior in path 3, to exothermic in path 2.

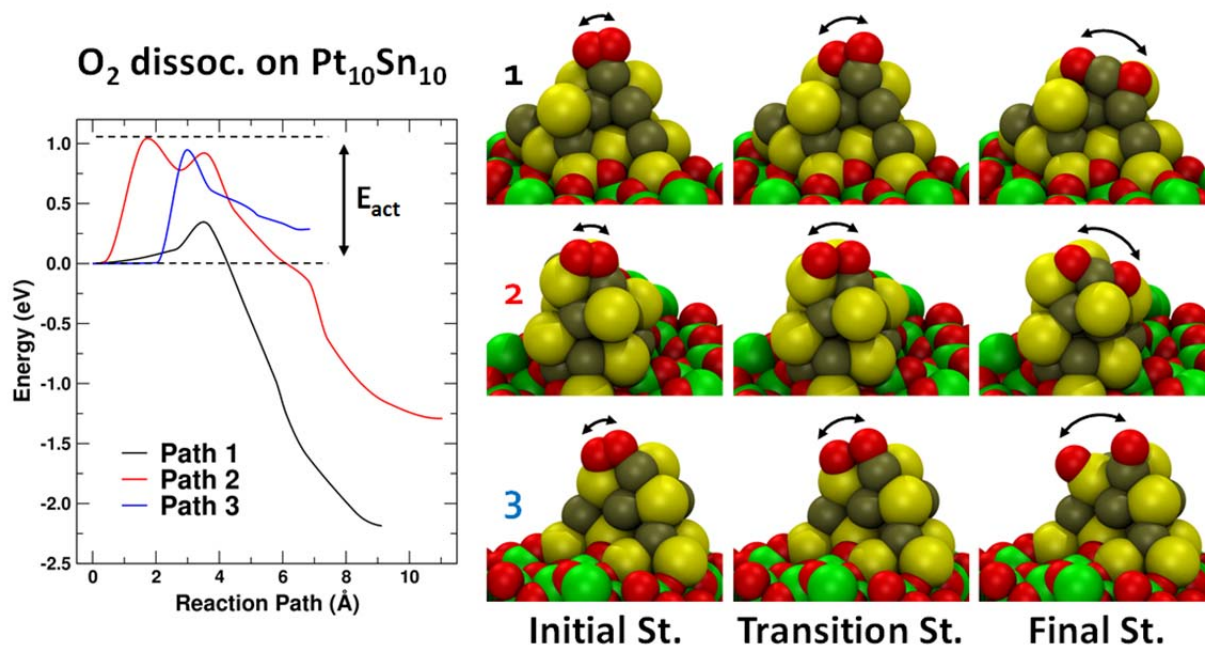


Figure 4. Left: Reactions paths for the dissociation of O₂ on three different disorder states of a Pt₁₀Sn₁₀ nanoparticle on γ -Al₂O₃. Right: Structures for the initial, transition and final states for each path.

Based on the past success in theoretical calculations and experimental results (XAFS and STEM) on Pt and PtNi catalysts, we are currently developing models that will help both interpret and guide experimental data analysis. On the basis of initial characterizations of the catalyst, we started building realistic models of the catalysts (Figure 5, left) to estimate the complexity of the simulations and then investigated the types of acceptable simplifications. We proposed to simplify initial complex models by replacing the curved surface of the SBA-15 channel by a flat slab (Figure 5, right). This model will be used to investigate the structural and electronic disorder in the nanoparticles under different coverage conditions using MD simulations: 1) No adsorbates, 2) “reactant” conditions (NPs covered with CO₂ and H₂), and 3) “product” conditions (NPs covered with CO and H₂O). The aim of these simulations is twofold: First, provide detailed information of changes in the catalyst induced by environments. These simulations will inform and tune up the EXAFS models that are used to analyze experimental data. This correlative analysis is essential to alleviate the average nature of spectroscopy probes. Second, the trajectories calculated for reactants and products along different reaction paths will provide us with reactivity information using the nudged elastic band (NEB) approach (Figure 4).

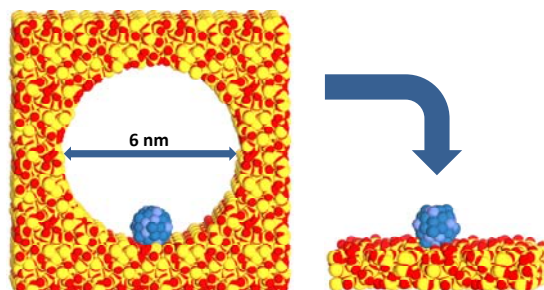


Figure 5. Full (left) and simplified (right) models of a PtNi nanoparticle in a channel in mesoporous silica SBA-15.

Publications Acknowledging this Grant in 2013-2016

(I) Exclusively funded by this grant:

1. Li, Y.; Frenkel, A., Chapter 8.9 Clusters in: X-ray absorption spectroscopy and related techniques. *International Tables for Crystallography, V. 1, IUCR Publisher Submitted*.
2. Li, Y.; Frenkel, A., Metal nanocatalysts in: XAFS techniques for catalysis, nanomaterials, and surfaces, Eds: Y. Iwasawa, K. Asakura, M. Tada. *World Scientific Publishing In press*.
3. Li, Y.; Kraynis, O.; Kas, J.; Weng, T.-C.; Sokaras, D.; Zacharowicz, R.; Lubomirsky, I.; Frenkel, A. I., Geometry of electromechanically active structures in Gadolinium - doped Cerium oxides. *AIP Advances* **2016**, *6* (5), 055320.
4. Frenkel, A., Two views at strained nanocrystals from the opposite sides of spatial resolution limit. (Invited) *Physica Scripta* **2015**, *90* (9), 098004.
5. Frenkel, A. I.; van Bokhoven, J. A., X-ray spectroscopy for chemical and energy sciences: the case of heterogeneous catalysis. (Invited) *J. Synchrotron Rad.* **2014**, *21* (5), 1084-1089.
6. Frenkel, A. I.; Cason, M. W.; Elsen, A.; Jung, U.; Small, M. W.; Nuzzo, R. G.; Vila, F. D.; Rehr, J. J.; Stach, E. A.; Yang, J. C., Critical review: Effects of complex interactions on structure and dynamics of supported metal catalysts. (Invited) *J. Vac. Sci. Technol. A* **2014**, *32* (2), 020801. (Top 10 Cited Article in JVST in 2014)
7. Rehr, J. J.; Vila, F. D., Dynamic structural disorder in supported nanoscale catalysts. *J. Chem. Phys.* **2014**, *140* (13), 134701.
8. Zhang, Z.; Li, L.; Yang, J. C., Adhesion of Pt Nanoparticles Supported on γ -Al₂O₃ Single Crystal. *J. Phys. Chem. C* **2013**, *117* (41), 21407-21412.
9. Zhao, S.; Li, Y.; Stavitski, E.; Tappero, R.; Crowley, S.; Castaldi, M. J.; Zakharov, D. N.; Nuzzo, R. G.; Frenkel, A. I.; Stach, E. A., Operando Characterization of Catalysts through use of a Portable Microreactor. (Invited) *ChemCatChem* **2015**, *7* (22), 3683-3691.
10. Elsen, A.; Jung, U.; Vila, F.; Li, Y.; Safonova, O. V.; Thomas, R.; Tromp, M.; Rehr, J. J.; Nuzzo, R. G.; Frenkel, A. I., Intracluster Atomic and Electronic Structural Heterogeneities in Supported Nanoscale Metal Catalysts. *J. Phys. Chem. C* **2015**, *119* (45), 25615-25627.
11. Stach, E. A.; Li, Y.; Zhao, S.; Gamalski, A.; Zakharov, D.; Tappero, R.; Chen-Weigart, K.; Thieme, J.; Jung, U.; Elsen, A.; Wu, Q.; Orlov, A.; Chen, J.; Nuzzo, R. G.; Frenkel, A., Characterizing Working Catalysts with Correlated Electron and Photon Probes. *Microsc. Microanal.* **2015**, *21* (SupplementS3), 563-564.
12. Li, Y.; Zakharov, D.; Zhao, S.; Tappero, R.; Jung, U.; Elsen, A.; Baumann, P.; Nuzzo, R. G.; Stach, E. A.; Frenkel, A. I., Complex structural dynamics of nanocatalysts revealed in Operando conditions by correlated imaging and spectroscopy probes. *Nat. Commun.* **2015**, *6*, 7583.
13. Jung, U.; Elsen, A.; Li, Y.; Smith, J. G.; Small, M. W.; Stach, E. A.; Frenkel, A. I.; Nuzzo, R. G., Comparative in Operando Studies in Heterogeneous Catalysis: Atomic and Electronic Structural Features in the Hydrogenation of Ethylene over Supported Pd and Pt Catalysts. *ACS Catalysis (Perspective)* **2015**, *5* (3), 1539-1551.
14. Wu, L.-b.; Wu, L.-h.; Yang, W.-m.; Frenkel, A. I., Study of the local structure and oxidation state of iron in complex oxide catalysts for propylene ammoxidation. (Invited) *Catal. Sci. Technol.* **2014**, *4* (8), 2512-2519.

15. Small, M. W.; Kas, J. J.; Kvashnina, K. O.; Rehr, J. J.; Nuzzo, R. G.; Tromp, M.; Frenkel, A. I., Effects of Adsorbate Coverage and Bond-Length Disorder on the d-Band Center of Carbon-Supported Pt Catalysts. *ChemPhysChem* **2014**, *15* (8), 1569-1572.
16. Frenkel, A. I.; Small, M. W.; Smith, J. G.; Nuzzo, R. G.; Kvashnina, K. O.; Tromp, M., An in Situ Study of Bond Strains in 1 nm Pt Catalysts and Their Sensitivities to Cluster–Support and Cluster–Adsorbate Interactions. *J. Phys. Chem. C* **2013**, *117* (44), 23286-23294.
17. Li, L.; Wang, L.-L.; Johnson, D. D.; Zhang, Z.; Sanchez, S. I.; Kang, J. H.; Nuzzo, R. G.; Wang, Q.; Frenkel, A. I.; Li, J.; Ciston, J.; Stach, E. A.; Yang, J. C., Noncrystalline-to-Crystalline Transformations in Pt Nanoparticles. *J. Am. Chem. Soc.* **2013**, *135* (35), 13062-13072. (The Nanoparticle Transformers, a “Science Editor’s Choice” review by M. Lavine)
18. Frenkel, A. I.; Khalid, S.; Hanson, J. C.; Nachttegaal, M., QEXAFS in Catalysis Research: Principles, Data Analysis, and Applications. In *In-situ Characterization of Heterogeneous Catalysts*, John Wiley & Sons, Inc.: 2013; pp 23-47.
19. Frenkel, A. I.; Wang, Q.; Sanchez, S. I.; Small, M. W.; Nuzzo, R. G., Short range order in bimetallic nanoalloys: An extended X-ray absorption fine structure study. *J. Chem. Phys.* **2013**, *138* (6), 064202.

(II) Jointly funded by this grant and other grants with leading intellectual contribution from this grant:

20. Nguyen, L.; Zhang, S.; Wang, L.; Li, Y.; Yoshida, H.; Patlolla, A.; Takeda, S.; Frenkel, A. I.; Tao, F., Reduction of nitric oxide with hydrogen on catalysts of singly dispersed bimetallic sites Pt₁Co_m and Pd₁Co_n. *ACS Catalysis* **2016**, *6* (2), 840-850.
21. Vila, F. D.; Hayashi, S. T.; Moore, J. M.; Rehr, J. J., Molecular dynamics simulations of supported Pt nanoparticles with a hybrid Sutton–Chen potential. **Submitted**.
22. Wang, J.; Wang, Q.; Jiang, X.; Liu, Z.; Yang, W.; Frenkel, A. I., Determination of Nanoparticle Size by Measuring the Metal–Metal Bond Length: The Case of Palladium Hydride. *J. Phys. Chem. C* **2015**, *119* (1), 854-861.
23. Spanjers, C. S.; Senftle, T. P.; van Duin, A. C. T.; Janik, M. J.; Frenkel, A. I.; Rioux, R. M., Illuminating surface atoms in nanoclusters by differential X-ray absorption spectroscopy. (Invited) *Phys. Chem. Chem. Phys.* **2014**, *16* (48), 26528-26538.
24. Anderson, R. M.; Zhang, L.; Loussaert, J. A.; Frenkel, A. I.; Henkelman, G.; Crooks, R. M., An Experimental and Theoretical Investigation of the Inversion of Pd@Pt Core@Shell Dendrimer-Encapsulated Nanoparticles. *ACS Nano* **2013**, *7* (10), 9345-9353.
25. Amit, Y.; Eshet, H.; Faust, A.; Patlolla, A.; Rabani, E.; Banin, U.; Frenkel, A. I., Unraveling the Impurity Location and Binding in Heavily Doped Semiconductor Nanocrystals: The Case of Cu in InAs Nanocrystals. *J. Phys. Chem. C* **2013**, *117* (26), 13688-13696.
26. Patlolla, A.; Baumann, P.; Xu, W.; Senanayake, S. D.; Rodriguez, J. A.; Frenkel, A. I., Characterization of Metal-Oxide Catalysts in Operando Conditions by Combining X-ray Absorption and Raman Spectroscopies in the Same Experiment. *Topics in Catalysis* **2013**, *56* (11), 896-904.
27. Yancey, D. F.; Chill, S. T.; Zhang, L.; Frenkel, A. I.; Henkelman, G.; Crooks, R. M., A theoretical and experimental examination of systematic ligand-induced disorder in Au dendrimer-encapsulated nanoparticles. (Edge Article) *Chem. Sci.* **2013**, *4* (7), 2912-2921.
28. Stach, E. A.; Baumann, P.; Li, Y.; Zakharov, D.; Frenkel, A., Using Operando Methods to Characterize Working Catalysts with TEM, XAS, EXAFS and Raman Spectroscopy. *Microsc. Microanal.* **2013**, *19* (SupplementS2), 1674-1675.
29. Sanchez, S. I.; Small, M. W.; Bozin, E. S.; Wen, J.-G.; Zuo, J.-M.; Nuzzo, R. G., Metastability and Structural Polymorphism in Noble Metals: The Role of Composition and Metal Atom Coordination in Mono- and Bimetallic Nanoclusters. *ACS Nano* **2013**, *7* (2), 1542-1557.
30. Frenkel, A. I.; Hanson, J. C., Combined X-ray Diffraction and Absorption Spectroscopy in Catalysis Research: Techniques and Applications. In *In-situ Characterization of Heterogeneous Catalysts*, John Wiley & Sons, Inc.: 2013; pp 345-367.
31. Merrill, N. A.; McKee, E. M.; Merino, K. C.; Drummy, L. F.; Lee, S.; Reinhart, B.; Ren, Y.; Frenkel, A. I.; Naik, R. R.; Bedford, N. M.; Knecht, M. R., Identifying the Atomic-Level Effects of Metal Composition on the Structure and Catalytic Activity of Peptide-Templated Materials. *ACS Nano* **2015**, *9* (12), 11968-11979.

32. Briggs, B. D.; Bedford, N. M.; Seifert, S.; Koerner, H.; Ramezani-Dakhel, H.; Heinz, H.; Naik, R. R.; Frenkel, A. I.; Knecht, M. R., Atomic-scale identification of Pd leaching in nanoparticle catalyzed C-C coupling: effects of particle surface disorder. Edge article, *Chem. Sci.* **2015**, *6* (11), 6413-6419.
33. Korobko, R.; Lerner, A.; Li, Y.; Wachtel, E.; Frenkel, A. I.; Lubomirsky, I., In-situ extended X-ray absorption fine structure study of electrostriction in Gd doped ceria. *Appl. Phys. Lett.* **2015**, *106* (4), 042904.
34. Amit, Y.; Fasut, A.; Milo, O.; Rabani, E.; Frenkel, A.; Banin, U., (Invited) How to Dope a Semiconductor Nanocrystal. (Invited) *ECS Transactions* **2013**, *58* (7), 127-133.
35. Kossoy, A.; Wang, Q.; Korobko, R.; Grover, V.; Feldman, Y.; Wachtel, E.; Tyagi, A. K.; Frenkel, A. I.; Lubomirsky, I., Evolution of the local structure at the phase transition in CeO₂-Gd₂O₃ solid solutions. *Phys. Rev. B* **2013**, *87* (5), 054101.
36. Bonifacio, C. S.; Carenco, S.; Wu, C. H.; House, S. D.; Bluhm, H.; Yang, J. C., Thermal Stability of Core-Shell Nanoparticles: A Combined in Situ Study by XPS and TEM. *Chem. Mater.* **2015**, *27* (20), 6960-6968.

(III) Jointly funded by this grant and other grants with relatively minor intellectual contribution from this grant:

37. Tao, F.; Nguyen, L.; Zhang, S.; Li, Y.; Tang, Y.; Zhang, L.; Frenkel, A.; Xia, Y.; Salmeron, M., Formation of second-generation nanoclusters on metal nanoparticles driven by reactant gas. **Submitted**.
38. Oezaslan, M.; Herrmann, A.-K.; Werheid, M.; Frenkel, A. I.; Nachtegaal, M.; Bonnaud, C.; Yilmaz, H. C.; Kuhn, L.; Rhiel, E.; Gaponik, N.; Eychmuller, A.; Schmidt, T.-J., Structural analysis and electrochemical properties of bimetallic Pd-Pt aerogels prepared by a two-step gelation process. **Submitted**.
39. Oezaslan, M.; Liu, W.; Nachtegaal, M.; Frenkel, A. I.; Rutkowski, B.; Werheid, M.; Herrmann, A.-K.; Bonnaud, C. L.; Yilmaz, H.-C.; Gaponik, N.; Czyrska-Filemonowicz, A.; Eychmuller, A.; Schmidt, T.-J., Homogeneity and elemental distribution in self-assembled bimetallic Pd-Pt aerogels prepared by a spontaneous one-step gelation process. **Submitted**.
40. Keturakis, C. J.; Zhu, M.; Gibson, E.; Daturi, M.; Tao, F.; Frenkel, A. I.; Wachs, I. E., The dynamics of CrO₃ - Fe₂O₃ catalysts during the high temperature Water-Gas Shift reaction: Molecular structure and reactivity. **Submitted**.
41. Senanayake, S. D.; Pappoe, N. A.; Nguyen-Phan, T.-D.; Luo, S.; Li, Y.; Xu, W.; Liu, Z.; Mudiyansele, K.; Johnston-Peck, A. C.; Frenkel, A. I.; Heckler, I.; Stacchiola, D.; Rodriguez, J. A., Interfacial Cu⁺ promoted surface reactivity: Carbon monoxide oxidation reaction over polycrystalline copper-titania catalysts. *Surface Science* **In press**.
42. Ganzler, A. M.; Lichtenberg, H.; Frenkel, A. I.; Casapu, M.; Boubnov, A.; Wang, D.; Grunwaldt, J.-D., Using combined XAS/DRIFTS to study CO/NO oxidation over Pt/Al₂O₃ catalysts. *J. Phys.: Conf. Series* **In press**.
43. Lwin, S.; Li, Y.; Frenkel, A. I.; Wachs, I. E., Nature of WO_x sites on SiO₂ and their molecular structure-reactivity/selectivity relationships for propylene metathesis. *ACS Catalysis* **2016**, *6* (5), 3061-3071.
44. Liu, H.; An, W.; Li, Y.; Frenkel, A. I.; Sasaki, K.; Koenigsmann, C.; Su, D.; Anderson, R. M.; Crooks, R. M.; Adzic, R. R.; Liu, P.; Wong, S. S., In Situ Probing of the Active Site Geometry of Ultrathin Nanowires for the Oxygen Reduction Reaction. *J. Am. Chem. Soc.* **2015**, *137* (39), 12597-12609.
45. Zhang, S.; Nguyen, L.; Liang, J.-X.; Shan, J.; Liu, J.; Frenkel, A. I.; Patlolla, A.; Huang, W.; Li, J.; Tao, F., Catalysis on singly dispersed bimetallic sites. *Nat. Commun.* **2015**, *6*, 7938.
46. Bedford, N. M.; Ramezani-Dakhel, H.; Slocik, J. M.; Briggs, B. D.; Ren, Y.; Frenkel, A. I.; Petkov, V.; Heinz, H.; Naik, R. R.; Knecht, M. R., Elucidation of Peptide-Directed Palladium Surface Structure for Biologically Tunable Nanocatalysts. (February 2015 Issue Cover) *ACS Nano* **2015**, *9* (5), 5082-5092.
47. Lwin, S.; Keturakis, C.; Handzlik, J.; Sautet, P.; Li, Y.; Frenkel, A. I.; Wachs, I. E., Surface ReO_x Sites on Al₂O₃ and Their Molecular Structure-Reactivity Relationships for Olefin Metathesis. *ACS Catalysis* **2015**, *5* (3), 1432-1444.
48. Patete, J. M.; Han, J.; Tian, A. L.; Liu, H.; Han, M.-G.; Simonson, J. W.; Li, Y.; Santulli, A. C.; Aronson, M. C.; Frenkel, A. I.; Zhu, Y.; Wong, S. S., Observation of Ferroelectricity and Structure-Dependent Magnetic Behavior in Novel One-Dimensional Motifs of Pure, Crystalline Yttrium Manganese Oxides. *J. Phys. Chem. C* **2014**, *118* (37), 21695-21705.
49. Shan, J.; Huang, W.; Nguyen, L.; Yu, Y.; Zhang, S.; Li, Y.; Frenkel, A. I.; Tao, F., Conversion of Methane to Methanol with a Bent Mono(μ-oxo)nickel Anchored on the Internal Surfaces of Micropores. *Langmuir* **2014**, *30* (28), 8558-8569.

50. Zhang, L.; Yang, C.; Frenkel, A. I.; Wang, S.; Xiao, G.; Brinkman, K.; Chen, F., Co-generation of electricity and chemicals from propane fuel in solid oxide fuel cells with anode containing nano-bimetallic catalyst. *Journal of Power Sources* **2014**, *262*, 421-428.
51. Zhang, S.; Shan, J.-j.; Zhu, Y.; Frenkel, A. I.; Patlolla, A.; Huang, W.; Yoon, S. J.; Wang, L.; Yoshida, H.; Takeda, S.; Tao, F., WGS Catalysis and In Situ Studies of CoO_{1-x} , $\text{PtCo}_n/\text{Co}_3\text{O}_4$, and $\text{Pt}_m\text{Co}_m/\text{CoO}_{1-x}$ Nanorod Catalysts. *J. Am. Chem. Soc.* **2013**, *135* (22), 8283-8293.
52. Wang, L.; Zhang, S.; Zhu, Y.; Patlolla, A.; Shan, J.; Yoshida, H.; Takeda, S.; Frenkel, A. I.; Tao, F., Catalysis and In Situ Studies of $\text{Rh}_1/\text{Co}_3\text{O}_4$ Nanorods in Reduction of NO with H_2 . *ACS Catalysis* **2013**, *3* (5), 1011-1019.
53. Perelshtein, I.; Ruderman, E.; Perkas, N.; Tzanov, T.; Beddow, J.; Joyce, E.; Mason, T. J.; Blanes, M.; Molla, K.; Patlolla, A.; Frenkel, A. I.; Gedanken, A., Chitosan and chitosan-ZnO-based complex nanoparticles: formation, characterization, and antibacterial activity. *J. Mater. Chem. B* **2013**, *1* (14), 1968-1976.
54. Zhu, Q.; Saidi, W. A.; Yang, J. C., Step-Induced Oxygen Upward Diffusion on Stepped Cu(100) Surface. *J. Phys. Chem. C* **2015**, *119* (1), 251-261.
55. He, L.; Liu, F.; Hautier, G.; Oliveira, M. J. T.; Marques, M. A. L.; Vila, F. D.; Rehr, J. J.; Rignanesi, G. M.; Zhou, A., Accuracy of generalized gradient approximation functionals for density-functional perturbation theory calculations. *Phys. Rev. B* **2014**, *89* (6), 064305.
56. Zhu, Q.; Fleck, C.; Saidi, W. A.; McGaughey, A.; Yang, J. C., TFOx: A versatile kinetic Monte Carlo program for simulations of island growth in three dimensions. *Comput. Mater. Sci.* **2014**, *91*, 292-302.
57. Merte, L. R.; Ahmadi, M.; Behafarid, F.; Ono, L. K.; Lira, E.; Matos, J.; Li, L.; Yang, J. C.; Roldan Cuenya, B., Correlating Catalytic Methanol Oxidation with the Structure and Oxidation State of Size-Selected Pt Nanoparticles. *ACS Catalysis* **2013**, *3* (7), 1460-1468.
58. Lwin, S.; Li, Y.; Frenkel, A. I.; Wachs, I. E., Activation of Surface ReO_x Sites on Al_2O_3 Catalysts for Olefin Metathesis. *ACS Catalysis* **2015**, *5* (11), 6807-6814.
59. Erickson, E. M.; Oruc, M. E.; Wetzel, D. J.; Cason, M. W.; Hoang, T. T. H.; Small, M. W.; Li, D.; Frenkel, A. I.; Gewirth, A. A.; Nuzzo, R. G., A Comparison of Atomistic and Continuum Approaches to the Study of Bonding Dynamics in Electrocatalysis: Microcantilever Stress and in Situ EXAFS Observations of Platinum Bond Expansion Due to Oxygen Adsorption during the Oxygen Reduction Reaction. *Anal. Chem.* **2014**, *86* (16), 8368-8375.
60. Stach, E. A.; Zakharov, D.; Akatay, M. C.; Baumann, P.; Ribeiro, F.; Zvenich, Y.; Li, Y.; Frenkel, A., Developments in environmental transmission electron microscopy for catalysis research. *Microsc. Microanal.* **2013**, *19* (SupplementS2), 1174-1175.
61. Crooks, A. B.; Yih, K.-H.; Li, L.; Yang, J. C.; Özkar, S.; Finke, R. G., Unintuitive Inverse Dependence of the Apparent Turnover Frequency on Precatalyst Concentration: A Quantitative Explanation in the Case of Ziegler-Type Nanoparticle Catalysts Made from $[(1,5\text{-COD})\text{Ir}(\mu\text{-O}_2\text{C}_8\text{H}_{15})]_2$ and AlEt_3 . *ACS Catalysis* **2015**, *5* (6), 3342-3353.
62. Merte, L. R.; Ahmadi, M.; Behafarid, F.; Ono, L. K.; Lira, E.; Matos, J.; Li, L.; Yang, J. C.; Roldan Cuenya, B., Correlating Catalytic Methanol Oxidation with the Structure and Oxidation State of Size-Selected Pt Nanoparticles. *ACS Catalysis* **2013**, *3* (7), 1460-1468.

Support and Artificial SMSI Effects on Selective Hydrogenation by Noble Metal Nanoparticles

Kenneth R. Poeppelmeier, Robert M. Kennedy, James A. Enterkin, Lawrence Crosby, Laurence D. Marks, Christopher L. Marshall, Peter C. Stair
Department of Chemistry, Northwestern University
Department of Materials Science & Engineering, Northwestern University
Chemical Sciences and Engineering Division, Argonne National Laboratory

Presentation Abstract

The selective hydrogenation of aldehydes to alcohols is a critical step in the efficient conversion of biomass to hydrocarbon energy carriers thereby increasing the energy density of the fuel. Selective hydrogenation is needed to preserve olefin groups for later functionalization and to efficiently use hydrogen. Highly active metal catalysts, like platinum, are non-selective for the hydrogenation of aldehydes. Our focus has been on understanding how metal/oxides interfaces can modify the selectivity of metal catalysts for hydrogenation. Two different oxide interfaces have been examined: 1) metal/support interfaces on oxide supports with designed facets, and 2) artificial strong metal support interaction (SMSI) from thin atomic layer deposition (ALD) overcoats of oxides on top of supported metal nanoparticles. Platinum nanoparticles were grown by ALD on the surface of hydrothermally synthesized $\text{Ba}_x\text{Sr}_{1-x}\text{TiO}_3$ nanocuboids. Lattice matching was used to stabilize the platinum nanoparticles, with the most stabilization observed for SrTiO_3 . Selectivity for aldehyde hydrogenation increased with stabilization, as a result of changes in the shape of the supported platinum nanoparticles. Titania- and alumina-ALD coats were deposited on Pt/SrTiO_3 nanocuboids. For the two artificial SMSI catalysts, only the reducible oxide, titania, had an effect on selectivity. The increase in aldehyde selectivity of titania-ALD/ Pt/SrTiO_3 is predicted to be a result of reduced titanium centers at TiO_x/Pt interfaces, similar to high temperature reduced (HTR) Pt/TiO_2 catalysts. These experiments are examples of how rational catalyst design can be used to study the effects of specific interfaces on catalyst performance.

Characterization of Catalytic Materials by DNP-Enhanced Solid-State NMR

Takeshi Kobayashi, Frederic A. Perras, Aaron D. Sadow, Igor I. Slowing, Marek Pruski
Ames Laboratory, U.S. DOE, Iowa State University, Ames, IA 50011-3111

Presentation Abstract

This work is part of Ames Laboratory research on “Homogeneous and Interfacial Catalysis in 3D Controlled Environments” (AL-03-380-011), described in detail elsewhere.

Recent advances in high-field dynamic nuclear polarization (DNP) boosted the sensitivity of solid-state nuclear magnetic resonance (SSNMR) spectroscopy, offering signal enhancements of 2 orders of magnitude and savings in experimental time of up to *4-5 orders of magnitude*. Additionally, DNP is uniquely suited for the studies of catalytic surfaces and interfaces because they can be most efficiently or even selectively sensitized by this technique, enabling measurements that are off-limits to conventional SSNMR.¹ We will report several novel applications of this technique to the studies of catalytic materials in our laboratory, enabled by the recently installed 400 MHz DNP NMR spectrometer funded by DOE Basic Energy Sciences.

(1) Systematic studies were conducted to precisely determine the DNP sensitivity enhancement (per unit time) in ¹³C and ²⁹Si cross-polarization magic angle spinning (CPMAS) NMR of functionalized mesoporous silica nanoparticles (MSNs).² The most recently developed biradical polarizing agents (AMUPol, TEKPol) afforded enhancements exceeding 200 in our laboratory. (2) We demonstrated that DNP can be used to enhance NMR signals of ¹³C, ¹⁵N and ²⁹Si nuclei located several hundreds of nanometers from the polarizing radicals, using MSNs functionalized with 3-(N-phenylureido)propyl (PUP) groups filled with the surfactant (CTAB).³ We employed the same approach to study the host-guest interaction between metal ions (Pt²⁺ and Cu²⁺) and a zirconium metal-organic framework (MOF, UiO-66-NH₂) using DNP-enhanced ¹⁵N{¹H} CPMAS NMR⁴ and DNP-enhanced ¹H{¹⁹⁵Pt} wideline NMR.⁵ (3) New DNP-based measurements enabled routine use of natural abundance ¹⁷O SSNMR, including the facile measurement of undistorted lineshapes, two-dimensional ¹H-¹⁷O heteronuclear correlation spectra, as well as accurate internuclear distances.^{6,7} These techniques were applied for distinguishing hydrogen-bonded and non-hydrogen-bonded ¹⁷O sites on the surface of silica.⁸ (4) DNP-enhanced SSNMR enabled studies of other challenging systems, including natural abundance ¹⁵N spectra of a new silica-supported zirconium Zr(NMe₂)_n@MSN catalyst for hydroboration of aldehydes and ketones developed in our catalysis program,⁹ isolated (-AlO)₃Si(OH) sites deposited on the γ-Al₂O₃ surface via atomic layer deposition (with T.J. Marks and P.C. Stair, from Northwestern University),¹⁰ and organic molecules adsorbed on alumina-supported metal nanoparticle catalysts (with J. Dumesic and T. Schwartz, from UW-Madison, and B. Shanks from Iowa State University).

References

1. Kobayashi, T.; Perras, F. A.; Slowing, I. I.; Sadow, A. D.; Pruski, M. Dynamic Nuclear Polarization Solid-State NMR in Heterogeneous Catalysis Research. *ACS Catal.*, **2015**, *5*, 7055-7062.

- Kobayashi, T.; Lafon, O.; Lilly Thankamony, A. S.; Slowing, I. I.; Kandel, K.; Carnavale, D.; Vitzthum, V.; Vezin, H.; Amoureux, J.-P.; Bodenhausen G.; Pruski M. Analysis of sensitivity enhancement by dynamic nuclear polarization in solid-state NMR: a case study of functionalized mesoporous materials. *Phys. Chem. Chem. Phys.*, **2013**, *15*, 5553-5562.
- Lafon, O.; Lilly Thankamony, A. S.; Kobayashi, T.; Carnavale, D.; Vitzthum, V.; Slowing, I. I.; Kandel, K.; Vezin, H.; Amoureux, J.-P.; Bodenhausen G.; Pruski M. Mesoporous silica nanoparticles loaded with surfactant: low temperature magic angle spinning ^{13}C and ^{29}Si NMR enhanced by dynamic nuclear polarization. *J. Phys. Chem. C*, **2013**, *117*, 1375-1382.
- Guo, Z.; Kobayashi, T.; Wang, L.-L.; Goh, T. W.; Xiao, C.; Caporini, M. A.; Rosay, M.; Johnson, D. D.; Pruski, M.; Huang W. Selective host-guest interaction between metal ions and metal organic framework using dynamic nuclear polarization enhanced solid-state NMR spectroscopy. *Chem-Eur. J.*, **2014**, *20*, 16308-16313.
- Kobayashi, T.; Perras, F.A.; Goh, T.W.; Metz, T.L.; Huang W.; Pruski, M. DNP-Enhanced Ultra-Wideline Solid-State NMR Spectroscopy: Studies of Platinum in Metal-Organic Frameworks. *J. Phys. Chem. Lett.*, submitted.
- Perras, F. A.; Kobayashi, T.; Pruski, M. Natural Abundance ^{17}O DNP Two-Dimensional and Surface-Enhanced NMR Spectroscopy. *J. Am. Chem. Soc.*, **2015**, *137*, 8336-8339.
- Perras, F. A.; Kobayashi, T.; Pruski, M. PRESTO Polarization Transfer to Quadrupolar Nuclei: Implications for Dynamic Nuclear Polarization. *Phys. Chem. Chem. Phys.*, **2015**, *17*, 22616-22622.
- Perras, F.A.; Chaudhary, U.; Slowing I.I.; Pruski, M. Probing Surface Hydrogen Bonding and Dynamics by Natural Abundance, Multidimensional, ^{17}O DNP-NMR Spectroscopy. *J. Phys. Chem. C*, DOI: 10.1021/acs.jpcc.6b02579 (**2016**).
- Eedugurala, N.; Wang, Z.; Chaudhary, U.; Nelson, N.; Kandel, K.; Kobayashi, T.; Slowing, I. I.; Pruski, M.; Sadow, A. D. Mesoporous Silica-Supported Amidozirconium-Catalyzed Carbonyl Hydroboration. *ACS Catal.*, **2015**, *5*, 7399-7414.
- Mouat, A. R.; George, C.; Kobayashi, T.; Pruski, M.; van Duyne, R. P.; Marks, T. J.; Stair, P. C. Highly Dispersed $\text{SiO}_x/\text{Al}_2\text{O}_3$ Catalysts Illuminate the Reactivity of Isolated Silanol Sites. *Angew. Chem. Int. Ed.*, **2015**, *54*, 13346-13351.
- Johnson, R.L.; Perras, F.A.; Kobayashi, T.; Schwartz, T.J.; Dumesic, J.A.; Shanks, B.H.; Pruski, M. Identifying Low-Coverage Surface Species on Supported Noble Metal Nanoparticle Catalysts by DNP-NMR. *Chem. Commun.*, **2016**, *52*, 1859-1862.

Ashwin Ramasubramaniam

Thermodynamics of Methanol Decomposition on Graphene–Pt₁₃ Nanocomposites

Ashwin Ramasubramaniam
Department of Mechanical & Industrial Engineering
University of Massachusetts Amherst

Presentation Abstract

Defective graphene has been shown experimentally to be an excellent support for transition-metal electrocatalysts in direct methanol fuel cells. Computational modeling reveals that the improved catalytic activity of graphene-supported metal clusters is in part due to increased resistance to catalyst sintering and to CO poisoning, but the increased reaction rate for the methanol decomposition reaction (MDR) is not yet fully explained. Using density functional theory, we investigated the adsorption and reaction thermodynamics of MDR intermediates on defective graphene-supported Pt₁₃ nanoclusters with realistic, low-symmetry morphologies. We found that the support-induced shifts in catalyst electronic structure correlate well with an overall change in adsorption behavior of MDR intermediates and that the reaction thermodynamics are modified in a way that suggests the potential of greater catalytic activity. We also found that adsorption energy predictors established for traditional heterogeneous catalysis studies of MDR on macroscopic crystalline facets are equally valid on catalyst nanoclusters (supported or otherwise) with irregular, low-symmetry surface morphologies. Our studies provide theoretical insights into experimental observations of enhanced catalytic activity of graphene-supported Pt nanoclusters for MDR and suggest promising avenues for further tuning of catalytic activity through engineering of catalyst–support interactions.

DE-SC0010610: Computational Design of Graphene–Nanoparticle Catalysts

PI: Dr. Ashwin Ramasubramaniam

Students: Mr. Raymond Gasper, Mr. Hongbo Shi

RECENT PROGRESS

Thermodynamics of Methanol Decomposition on Graphene-Supported Pt₁₃ Nanoclusters (Research Assistant – Raymond Gasper): Having demonstrated the improved CO tolerance and reduced reaction barriers for CO oxidation on graphene-supported Pt₁₃ clusters [1], we have turned our attention to the more complex, yet ultimately most relevant, issue of the methanol decomposition reaction (MDR). [2] Using optimized, low-energy Pt₁₃ clusters (unsupported and graphene-supported) as model catalysts, we have examined in extensive detail the potential MDR pathways while sampling multiple inequivalent binding sites on the cluster surface to generate adequate statistics. While this process is computationally expensive (200-300 DFT structural relaxation calculations), such detailed calculations are essential for extending our understanding of reactions on realistic catalyst surfaces rather than relying on studies performed on idealized crystalline facets.

Figure 1(a) displays the adsorption energies of MDR intermediates on unsupported and graphene-supported Pt₁₃ clusters along with baseline calculations for the Pt(111) surface. We find that unsupported clusters bind the reaction intermediates much more strongly than Pt (111) surfaces due to significant undercoordination of surface Pt atoms. The introduction of the graphene support, significantly reduces the binding of adsorbates, with support defects leading to further reduction of the binding energies. The latter effect can be attributed to lowering of cluster *d*-band centers due to strong cluster–support interaction. [1,3] Indeed, in several cases, binding of MDR intermediates on clusters anchored at divacancy defects is comparable with that on Pt (111) surfaces. This is a *particularly significant result* as it suggests that the simple approach of defect-engineering of an otherwise inert carbon support can appreciably improve the activity of Pt nanoclusters, rendering them competitive with Pt(111), one of the best MDR catalysts.

As ultra-small nanoclusters have no well-defined surface structure (e.g., facets, edges, corners) each surface site is, in principle, distinct from the point of catalytic activity. Nevertheless, it is imperative to seek macroscopic descriptors that can provide insight into the *average* behavior of the surface active sites. Figure 1(b) displays the adsorption energies of MDR intermediates on unsupported as well as graphene-supported Pt₁₃ clusters as a function of the adsorption energy on Pt(111) surfaces, from which is immediately apparent that these two adsorption energies are correlated. Furthermore, not only are the adsorption energies on clusters and Pt(111) correlated, but the linear relationship is, to within an excellent approximation, given by a *simple vertical shift* of the dashed parity line in Fig. 1(b). In keeping with the trends in Fig. 1(a), the unsupported Pt₁₃ cluster displays the largest downward shift from the parity due to strongest binding of MDR intermediates; as the binding weakens in going from pristine-graphene-supported clusters to defective-graphene-supported clusters, the linear correlation approaches the Pt(111) parity line. Most interestingly, the vertical offsets of the linear fits are *inversely correlated with the average d-band position* of the Pt₁₃ cluster as seen from the inset in Fig. 1(b). This is *the key finding* of our studies, which is both a new result and of immediate practical relevance for cluster catalysis: in a nutshell, knowing the adsorption energy of an intermediate on Pt(111) and the average *d*-band position of the nanocluster—both trivial calculations within DFT—allows us to obtain from scaling relationships the average adsorption energy of an intermediate on the cluster. Figure 1(c) shows the comparison between predicted adsorption energies from our scaling relationships (fit to a handful of DFT calculations) versus the calculated DFT binding energies for our entire dataset (averaged over multiple surface sites) of MDR intermediates. The data essentially lie exactly along the parity line and confirm the

validity of our approach. Thus, we now have for the first time a set of scaling relationships for graphene-supported Pt₁₃ nanoclusters, which obviates the need for exhaustive statistical sampling of distinct surface sites.

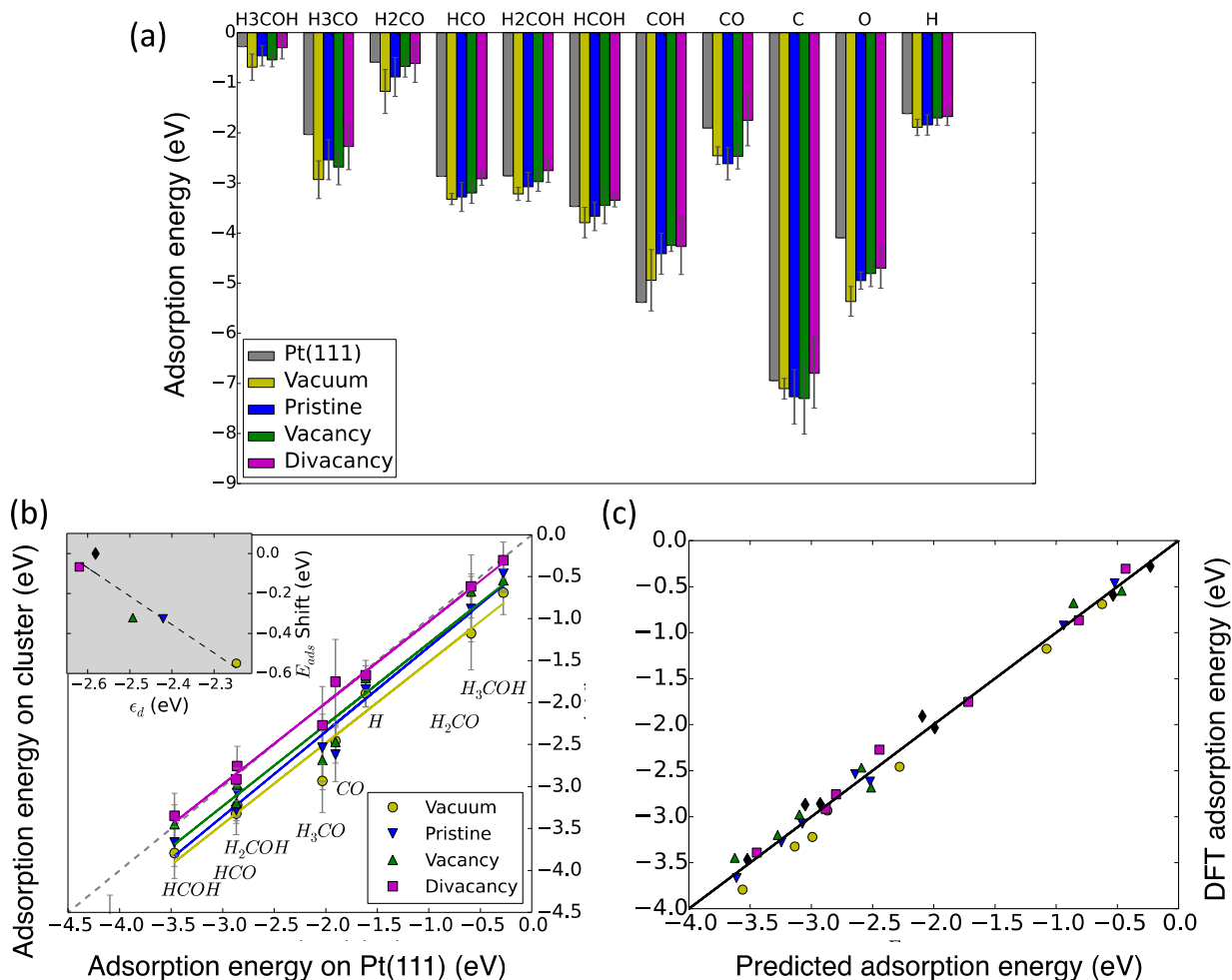


Figure 1: (a) Adsorption energies of MDR intermediates on unsupported and graphene-supported Pt₁₃ clusters, as well as Pt(111) surfaces. In general, clusters anchored at support defects bind adsorbates more weakly than unsupported clusters, reactions beyond MDR (to the extent that adsorbates bind at individual similar functional groups). These questions will be examined next. Also, the final step in this study of MDR decomposition is the connection between reaction thermodynamics and kinetics via Brønsted-Evans-Polyani relationships (to enable microkinetic modeling); calculations are underway to uncover these structure–property–function relationships.

References:

- [1] Fampiou, I.; Ramasubramaniam, A. The Influence of Support Effects on CO Oxidation Kinetics on Graphene-Supported Pt₁₃ Nanoclusters, *J. Phys. Chem. C* **2015**, 119 (16), 8703-8710.
- [2] Gasper, R.; Ramasubramaniam, A. The Role of Support Effects in Methanol Decomposition on Graphene-Supported Pt₁₃ Clusters, submitted to *J. Phys. Chem. C* **2016**.
- [3] Fampiou, I.; Ramasubramaniam, A. CO Adsorption on Defective Graphene-Supported Pt₁₃ Nanoclusters, *J. Phys. Chem. C* **2013**, 117 (39), 19927-19933.

Publications Acknowledging this Grant in 2013-2016

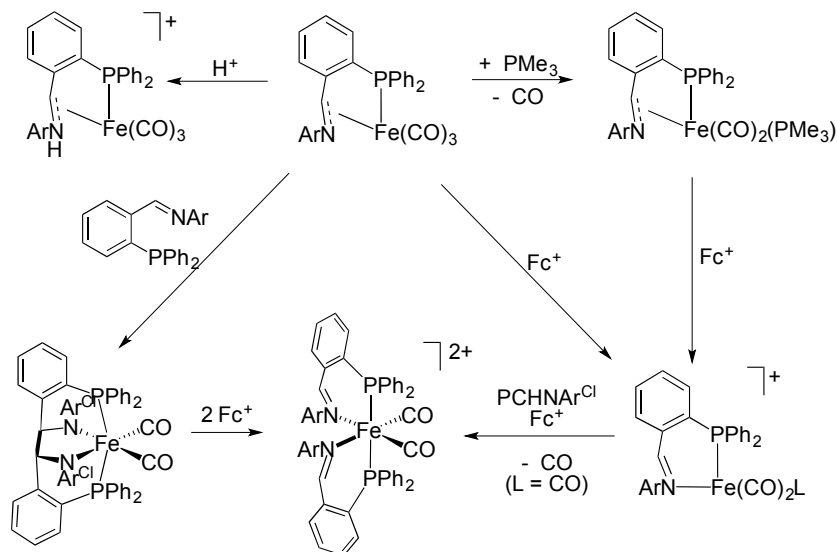
1. Fampiou, I.; Ramasubramaniam, A. CO Adsorption on Defective Graphene-Supported Pt₁₃ Nanoclusters, *J. Phys. Chem. C* **2013**, 117, 19927.
2. Fampiou, I.; Ramasubramaniam, A. The Influence of Support Effects on CO Oxidation Kinetics on Graphene-Supported Pt₁₃ Nanoclusters, *J. Phys. Chem. C* **2015**, 119 (16), 8703-8710.
3. Shi, H.; Auerbach, S. M.; Ramasubramaniam, A. First-Principles Predictions of Structure-Function Relationships of Graphene-Supported Platinum Nanoclusters, *J. Phys. Chem. C* **2016** (in press). <http://dx.doi.org/10.1021/acs.jpcc.6b01288>

Redox Reactions of Redox-Innocent Imine Ligands on Fe

Thomas B. Rauchfuss
University of Illinois at Urbana-Champaign

Presentation Abstract

Given the increased interest in imine ligands in catalysis (see work of Chirik, Caulton, Morris, Fujita, and others), this project is aimed at developing imine ligands linked to phosphine anchors. This particular poster will give an overview of efforts to elucidate reactivity of imino-phosphine ligands on the simple $\text{Fe}(\text{CO})_x^{n+}$ platform. Studies focused on $\text{Ph}_2\text{PC}_6\text{H}_4\text{CH}=\text{NC}_6\text{H}_4\text{-4-Cl}$ ($\text{PCHNAr}^{\text{Cl}}$) complexes of iron(0), iron(I), and iron(II). Even $\text{Fe}(\text{PCHNAr}^{\text{Cl}})(\text{CO})_3$ exhibits unusual properties, indicated by evidence for both η^2 - and N-bonded imine forms. Protonation of by $\text{HBF}_4 \cdot \text{Et}_2\text{O}$ occurs, not at Fe, but at the imine giving $[\text{1H}]\text{BF}_4$. The related diphosphine complex $\text{Fe}(\text{PCHNAr}^{\text{Cl}})(\text{PMe}_3)(\text{CO})_2$ (**2**) was also prepared and shown to undergo N-protonation. Oxidation of the Fe(0) complexes with FcBF_4 gave the Fe(I) compounds induced change in hapticity of the imine from η^2 to κ^1 . Attempted substitution of the parent tricarbonyl with $\text{PCHNAr}^{\text{Cl}}$ gave the complex $\text{Fe}[\text{P}_2(\text{NAr}^{\text{Cl}})_2](\text{CO})_2$, containing the tetradentate diamidodiphosphine. C-C coupling is reversed by Fc^+ . Oxidative C-C scission proceeds via an Fe(I) intermediate.



Grant Number: DEFG02-90ER14146

Title: Supramolecular Ensembles in Catalysis

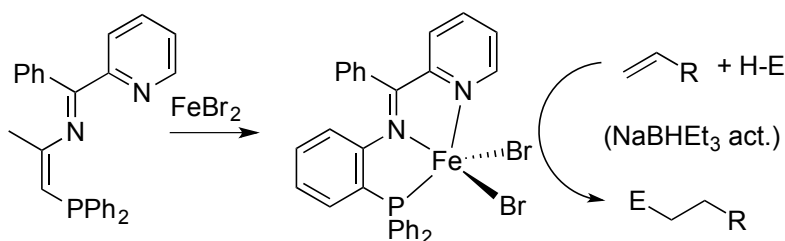
Postdocs: Noemie Lalaoui, Casseday Richers

Student: Wan-Yi "Amy" Chu

RECENT PROGRESS

Ligand-Centered Reactions of Phosphine-Imines on Iron

Condensation of $\text{Ph}_2\text{PC}_6\text{H}_4\text{NH}_2$ with benzoylpyridine yielded the $\text{Ph}_2\text{P}(\text{C}_6\text{H}_4)\text{N}=\text{C}(\text{Ph})(\text{C}_5\text{H}_4\text{N})$, which, upon treatment with ferrous halides gave the adduct $\text{FeX}_2(\text{PN}^{\text{Ph}}\text{py})$ ($\text{X} = \text{Cl}, \text{Br}$). Cyclic voltammetric studies show that this complex and its derivatives are redox active. Reduction of $\text{Fe}(\text{PN}^{\text{Ph}}\text{py})\text{X}_2$ with NaBHET_3H gave active catalysts for the hydroboration of 1-octene with pinacolborane. Similarly, these catalysts proved active for the addition of diphenylsilane, but not $\text{HSiMe}(\text{OSiMe}_3)_2$, to 1-octene and vinylsilanes.



Forced Ni-Ni Bonding in 36 Dinickel Complexes

In this study, we investigate the possibility that unusual electronic structures could be achieved by forcing together pairs of 18e metal center. The force was applied by chelating dithiolates. Nickelocene (Cp_2Ni) react with simple thiols to give "boring" diamagnetic $\text{Cp}_2\text{Ni}_2(\text{SR})_2$ species with planar Ni_2S_2 cores and long $\text{Ni}\cdots\text{Ni}$ distances. Propanedithiol (pdtH_2) behaves similarly, ostensibly, affording the $36e^-$ $\text{Cp}_2\text{Ni}_2(\text{pdt})$, which adopts a symmetrical butterfly Ni_2S_2 structure. Variable temperature NMR spectra indicate that this species possesses a thermally accessible triplet state ($\Delta G = 2.65 \pm 0.05$ kcal/mol) in equilibrium with a diamagnetic ground state. DFT calculations indicate that the singlet-triplet gap is highly sensitive to the nonplanarity of the Ni_2S_2 core. The calculations further reveal that only the high-spin form of features Ni-Ni bonding, which is unprecedented. Oxidation gives cations described as delocalized mixed valence $\text{Ni}(\text{II})\text{-Ni}(\text{III})$ species.

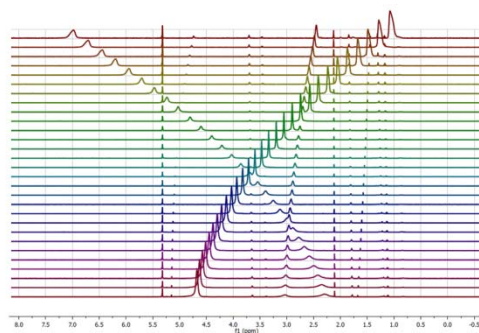


Figure. Variable temperature ^1H -NMR spectra of the $36e$ dimer $\text{Cp}_2\text{Ni}_2(\text{pdt})$.

Publications Acknowledging this Grant in 2013-2016

(I) Exclusively funded by this grant;

- [1] Chu, W-Y; Kahle, E.; Rauchfuss, T. B.; Arrigonim F.; Zampella, G. Redox-Induced Reactions of the Imine Ligands in Imino-Phosphine Complexes of Iron" *Organometallics*, **2016**, in press.
- [2] Chambers, G. M.; Rauchfuss, T. B.; Arrigoni, F.; Zampella, G., "Effect of Pyramidalization of the $\text{M}_2(\text{SR})_2$ Center: The Case of $(\text{C}_5\text{H}_5)_2\text{Ni}_2(\text{SR})_2$ ", *Organometallics* **2016**, *35*, 836-846.

- [3] Chu, W.-Y.; Zhou, X.; Rauchfuss, T. B., "Cooperative Metal–Ligand Reactivity and Catalysis in Low-Spin Ferrous Alkoxides", *Organometallics* **2015**, *34*, 1619-1626.
- [4] Wang, W.; Rauchfuss, T. B.; Zhu, L.; Zampella, G., "New Reactions of Terminal Hydrides on a Diiron Dithiolate", *Journal of the American Chemical Society* **2014**, *136*, 5773-5782.
- [5] Chambers, G. M.; Mitra, J.; Rauchfuss, T. B.; Stein, M., "NiI/RuII Model for the Ni-L State of the [NiFe]Hydrogenases: Synthesis, Spectroscopy, and Reactivity", *Inorganic Chemistry* **2014**, *53*, 4243–4249.
- [6] Chambers, G. M.; Angamuthu, R.; Gray, D. L.; Rauchfuss, T. B., "Organo Ruthenium-Nickel Dithiolates with Redox-Responsive Nickel Sites", *Organometallics* **2013**, *32*, 6324-6329.

(II) *Jointly funded by this grant and other grants with leading intellectual contribution from this grant;*

- [1] Chu, W.-Y.; Gilbert-Wilson, R.; Rauchfuss, T. B., van Gastal, M.; Neese, F. "Cobalt Phosphino- α -Iminopyridine-Catalyzed Hydrofunctionalization of Alkenes: Catalyst Development and Mechanistic Analysis" submitted for publication.
- [2] Gilbert-Wilson, R.; Chu, W.-Y.; Rauchfuss, T. B., "Phosphine-Iminopyridines as Platforms for Catalytic Hydrofunctionalization of Alkenes", *Inorganic Chemistry* **2015**, *54*, 5596-5603.
- [3] Richers, C. P.; Burtke, J.; Rauchfuss, T. B., "Insights into the Hydrolytic Polymerization of Trimethoxy-methylsilane. Crystal Structure of (MeO)₂MeSiONa", *Inorganic Chemistry* **2016**, in press.
- [4] Ogata, H., et al., "Hydride bridge in [NiFe]-hydrogenase observed by nuclear resonance vibrational spectroscopy", *Nature Communications* **2015**, *6*, 7890.
- [5] Mitra, J.; Zhou, X.; Rauchfuss, T., "Pd/C-catalyzed reactions of HMF: decarbonylation, hydrogenation, and hydrogenolysis", *Green Chemistry* **2015**, *17*, 307-313.
- [6] Zhou, X.; Mitra, J.; Rauchfuss, T. B., "Lignol Cleavage by Pd/C Under Mild Conditions and Without Hydrogen: A Role for Benzylic C-H Activation?", *ChemSusChem* **2014**, *7*, 1623-1626.
- [7] Zhou, X.; Rauchfuss, T. B., "Production of Hybrid Diesel Fuel Precursors from Carbohydrates and Petrochemicals Using Formic Acid as a Reactive Solvent", *ChemSusChem* **2013**, *6*, 383-388.

(III) *Jointly funded by this grant and other grants with relatively minor intellectual contribution from this grant;*

- [1] Li, Y.; Rauchfuss, T. B., "Synthesis of Diiron(I) Dithiolato Carbonyl Complexes", *Chemical Reviews* **2016**, in revision,

Fundamental Studies of Oxidation Reactions on Model Catalysts
Gradient Check a Tool to Check Heat and Mass Transfer Gradients in a Catalyst

Fabio H. Ribeiro and W. Nicholas Delgass
School of Chemical Engineering, 480 Stadium Mall Drive, West Lafayette, IN 47907

Presentation Abstract

We continued to focus on (i) further understanding the *site requirements* for the PO reaction (H₂O₂ production) via kinetic studies including isotopic switch experiments, titration experiments, periodic Density Functional Theory calculations, and using specially designed materials combined with various characterization techniques, (ii) studying the *origin of the catalyst deactivation* in the Au/TS-1 system via *operando* IR experiments, (iii) further exploring the higher *H₂ selectivity* observed in the Au/Uncalcined-TS-1 system, and (iv) participating in the *development of the new technique* of X-ray emission spectroscopy. We have also developed a tool for estimating internal and external temperature and concentration gradients for porous heterogeneous catalysts. This tool achieves this by combining established correlations from the literature for mixture properties, external heat and mass transfer, and internal transport effects. The tool itself is programmed into an easy-to-use website (www.gradientcheck.com) that uses standard web programming languages and is compatible with modern web browsers.

Grant title: Fundamental Studies of Oxidation Reactions on Model Catalysts

Grant number: DE-FG02-03ER15408

PI: Fabio H. Ribeiro and W. Nicholas Delgass

Student(s): Viktor J. Cybulskis, James Harris, Garrett Mitchell

RECENT PROGRESS

We do not have new results on the epoxidation reaction. With the no-cost extension for this grant, we are training new students. In collaboration with Dow Chemical, we have developed a tool for estimating internal and external temperature and concentration gradients for porous heterogeneous catalysts. This tool achieves this by combining established correlations from the literature for mixture properties, external heat and mass transfer, and internal transport effects. The tool itself is programmed into an easy-to-use website (www.gradientcheck.com) that uses standard web programming languages and is compatible with modern web browsers. A screenshot of the tool is shown below.

There have been many examples of reported heterogeneous catalyst rate data in the literature in which the rate of reaction is affected or even controlled by the rate of heat or mass transfer. This issue affects scientific researchers in both academia and industry due to the common desire to measure and catalog accurate and intrinsic rate data. Researchers in industry often desire to use this data to design pilot or larger scale reactors, and/or forecast the economics of such a process. This is hampered by lack of confidence in the accuracy and applicability of the rate data that is measured in e.g. lab-scale reactors to their larger counterparts. Both academic and industrial researchers may desire to discover catalysts with enhanced performance, and thus desire rate data that represent the intrinsic performance of the catalyst – free from the disguises of heat and mass transfer.

There are several experimental methodologies that have been recommended in the past for determining if these effects are significant. Another complementary approach is to predict the presence of concentration or temperature gradients from knowledge of the physical properties of the reactants, operating conditions, and catalyst properties. This approach allows one to estimate these effects without the need for multiple experimental data points – that may be costly or otherwise difficult to obtain.

We are working now to publish this tool with a summary of all assumptions made in the calculations.




- Home
- GradientCheck
- History
- How to Use
- License
- News and Outreach
- Members
- Prospective Students
- Seminars
- Publications
- Contact Us
- Links

Gradient✓ (GradientCheck) for Heterogeneous Catalysis:

By using this tool you agree to the terms of the license.

Inputs Section

Open JSON Input File No file chosen

Reaction Phase: / default: Gas Phase

Temperature (T_0 & T_w): / K

Pressure (P): / bar

Reactor Radius (R_r): / m – [Accepts scientific notation e.g. 1e-3]

Bed Length (L_b): / m

Catalyst Particle Shape:

Particle Radius (R_p): / m

Observed Reaction Rate (r_{obs}): / moles of A \times kg-cat $^{-1}$ \times s $^{-1}$

Enthalpy of Reaction (ΔH_{rxn}): / J \times mole $^{-1}$

Reaction Order (n):

Activation Energy (E_{app}): / J \times mole $^{-1}$

Conversion (X_d): / unitless (0 to 1)

Catalyst Bulk Density (ρ_{bulk}): / kg \times m $^{-3}$ [usually 500-1500]

Catalyst Void Fraction (ϵ): / (0 to 1) [often 0.35-0.45 (default 0.4)]

Catalyst Thermal Conductivity (k_p): / W \times m $^{-1}$ \times K $^{-1}$ [often 0.13-0.25]

Catalyst Surface Area (S_{int}): / m 2 \times g $^{-1}$

Catalyst Pore Volume (V_{pore}): / m 3 \times g $^{-1}$

Catalyst Pore Tortuosity (τ): / unitless [often 3-7 for porous catalysts]

Number of Reactants: Number of Products:

	Main Reactant A	Product B	Diluent C	
Inlet Mole Fractions:	<input type="text"/>	<input type="text"/>	<input type="text"/>	/ must add to 1
Fluid Viscosity (μ_f):	<input type="text"/>	<input type="text"/>	<input type="text"/>	/ kg \times m $^{-1}$ \times s $^{-1}$
Heat Capacity (C_p):	<input type="text"/>	<input type="text"/>	<input type="text"/>	/ J \times kg $^{-1}$ \times K $^{-1}$
Thermal Conductivity (k_f):	<input type="text"/>	<input type="text"/>	<input type="text"/>	/ W \times m $^{-1}$ \times K $^{-1}$
Diffusion Volume ($Z_{v,i}$):	<input type="text"/>	<input type="text"/>	<input type="text"/>	<input type="button" value="Estimate <math>Z_{v,i}</math>"/>
Molecular Weight (MW):	<input type="text"/>	<input type="text"/>	<input type="text"/>	/ g \times mol $^{-1}$

Notes:

+ Advanced Option

Output Filename: .json

+ Calculated Properties

Publications Acknowledging this Grant in 2012-2016

- Lee, W.-S.; Akatay, M. C.; Stach, E. A.; Ribeiro, F. H.; Delgass, W. N. Reproducible Preparation of Au/TS-1 with High Reaction Rate for Gas Phase Epoxidation of Propylene. *J. Catal.* **2012**, 287, 178-189.
- Lee, W.-S.; Lai, L.-C.; Akatay, M. C.; Stach, E. A.; Ribeiro, F. H.; Delgass, W. N. Probing the Gold Active Sites in Au/TS-1 for Gas Phase Epoxidation of Propylene in the Presence of Hydrogen and Oxygen. *J. Catal.* **2012**, 296, 31-42.
- Lee, W.-S.; Akatay, M. C.; Stach, E. A.; Ribeiro, F. H.; Delgass, W. N. Enhanced Reaction Rate for Gas Phase Epoxidation of Propylene using H₂ and O₂ by Cs Promotion of Au/TS-1. *J. Catal.* **2013**, 308, 98-113.
- Zemlyanov, D.; Klötzer, B.; Gabasch, H.; Smeltz, A.; Ribeiro, F. H.; Zafeiratos, S.; Teschner, D.; Schnörrch, P.; Vass, E.; Hävecker, M.; Knop-Gericke, A.; Schlögl, R. Kinetics of Palladium Oxidation in the mbar Pressure Range: Ambient Pressure XPS Study. *Top. Catal.* **2013**, 56, 885-895.
- Lee, W.-S.; Akatay, M. C.; Stach, E. A.; Ribeiro, F. H.; Delgass, W. N. Gas Phase Epoxidation of Propylene in the Presence of H₂ and O₂ over Small Gold Ensembles in Uncalcined TS-1. *J. Catal.* **2014**, 313, 104-112.

227

Jeffrey D. Rimer

Structure-Performance Relationships in Zeolite Catalysis: Impact of Crystal Size and Morphology in MTH

Yufeng Shen and Jeffrey D. Rimer
University of Houston, Department of Chemical and Biomolecular Engineering

Presentation Abstract

Critical challenges in zeolite catalyst design stem from an inability to *a priori* tune crystal properties and limited, often phenomenological, understandings of fundamental mechanisms of crystal growth and the relationships between crystal structure and catalytic performance. Here we will discuss efforts to develop a versatile platform for tailoring the physicochemical properties of zeolites. Given the future outlook of shale gas in U.S. energy markets, there is renewed interest in the production of fuels and chemicals from C₁ chemistry, notably methanol-to-hydrocarbon (MTH) reactions. Research thrusts in our group seek to develop optimal MTH catalysts via concerted initiatives in synthesis, characterization, testing, and modeling. We have developed techniques to control properties of zeolites, such as size, morphology, and composition (i.e., Si/Al ratio), for a variety of framework types with disparate pore topology. Here we will present recent findings regarding the impact of crystal size on MTH selectivity and on stream lifetime. Using organic molecules, termed zeolite growth modifiers (ZGMs), we have prepared a set of ZSM-5 and ZSM-11 catalysts with comparable crystal sizes and Si/Al ratios. MTH catalytic tests reveal that the latter exhibit much longer lifetime with trends that increase with decreasing crystal size. The results of these experiments will be discussed along with progress made in the rational design of zeolites with limited mass transport (e.g., small-pore and 1-dimensional zeolites).

DE-SC0014468:

Tailoring Zeolite Catalysts for the Conversion of Methanol to Hydrocarbons

Lead PI: Jeffrey D. Rimer

Student(s): Yufeng Shen, Thuy Le, Rui Li

RECENT PROGRESS

Synthesis of ZSM-11 (MEL framework type) Catalysts. We systematically investigated synthesis conditions leading to the formation of MEL crystals with varying size (0.1 – 1.0 μm) and identical composition (i.e., Si/Al = 20). Scanning electron micrographs of these samples (Figure 1) reveal distinct rod-like shape of MEL crystals. It is challenging to tune the dimensions of MEL crystals with precise control. The width of the crystal determines the length of straight channels in the MEL framework structure. As such, reductions in the width significantly reduce the diffusion path length along the microporous channels. To the best of our knowledge, the 150nm sample is the smallest isolated aluminosilicate MEL crystal reported. Moreover, these MEL crystals share almost identical physicochemical properties (i.e., uniform shape, similar SAR, and smooth surfaces), which renders these samples ideal for studying the effects of crystal size on catalyst performance. The size of MEL crystals was further refined using zeolite growth modifiers (ZGMs), which are organic additives used to tailor the crystal morphology. ZGMs bind to specific crystal faces and alter the anisotropic rate(s) of crystal growth. We have identified modifiers with specificity for binding to MEL {100} and {001} surfaces, leading to reductions in crystal width and length, respectively.

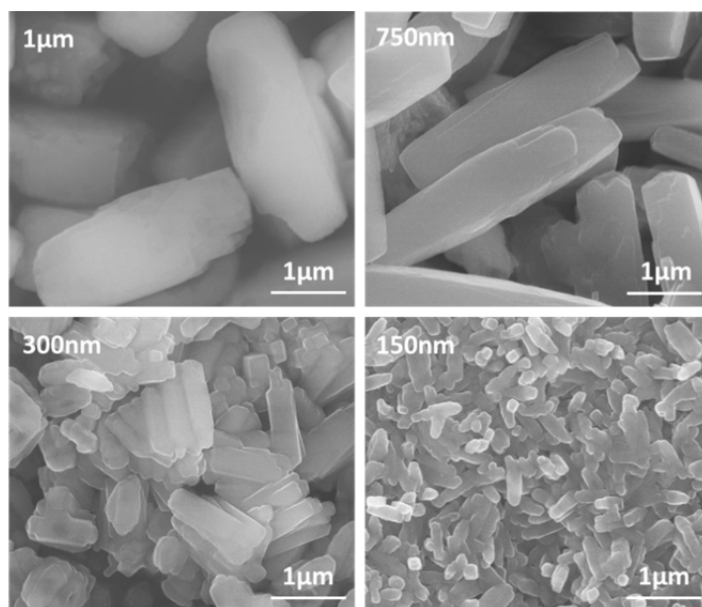


Figure 1. Scanning electron micrographs of ZSM-11 zeolite crystals prepared with different sizes: 1 μm , 750 nm, 300 nm, 150 nm.

Testing ZSM-11 Catalysts in MTH Reactions. We analyzed three H-ZSM-11 samples with varying size (150, 300, and 750 nm) in methanol to hydrocarbon (MTH) reactions. Catalytic testing was performed on a fixed bed reactor using a temperature of 350°C and space velocity $\text{WHSV} = 9\text{h}^{-1}$. Comparison of the on stream lifetime indicates a progressive shift towards longer time with decreased particle size. For instance, the lifetime at conversion $\geq 95\%$ for 150 nm particles is approximately 7-times longer than the 750 nm particles. The MTH product

distribution also varied with crystal size. As shown in Figure 2, the selectivity of light olefins (C2 and C3) increased with increasing crystal size, while the selectivity of heavy aromatic products decreased with increasing crystal size.

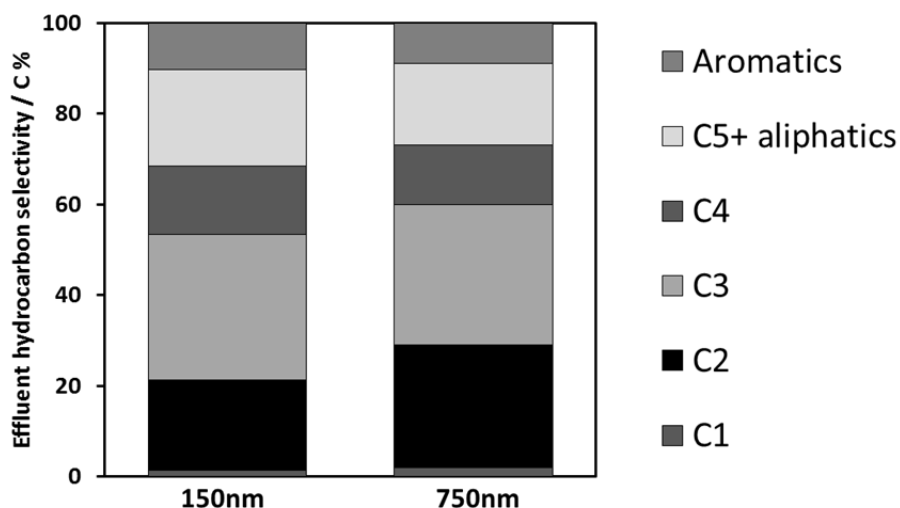


Figure 2. Comparison of MTH product selectivity for small (150 nm) and large (750 nm) H-ZSM-11 catalysts at 50% conversion.

Publications Acknowledging this Grant in 2013-2016

Jointly funded by this grant and other grants with leading intellectual contribution from this grant

1. Rimer, J.D. and Tsapatsis, M.. Nucleation of Open Framework Materials: Navigating the Voids, *MRS Bulletin* **2016**, 41, 393-398.
2. Ghorbanpour, A.; Rimer, J.D.; Grabow, L.C.. Computational Assessment of the Dominant Factors Governing the Mechanism of Methanol Dehydration over H-ZSM-5 with Heterogeneous Al Distribution, *ACS Catalysis* **2016**, 6, 2287-2298.

**Mechanistic Studies on the Water-gas Shift and CO₂ Hydrogenation:
Importance of the Metal-Oxide Interface**

José A. Rodriguez, Ping Liu, Sanjaya Senanayake, Dario Stacchiola, Michael G. White,
and Jan Hrbek, Chemistry Department, Brookhaven National Laboratory

Presentation Abstract

Fundamental studies have been performed to investigate the chemistry associated with the water-gas shift (WGS) and CO₂ hydrogenation (CH) reactions on a series of model and powder metal/oxide catalysts. A combination of *in-situ* techniques {X-ray diffraction (XRD), pair-distribution function analysis (PDF), X-ray absorption spectroscopy (XAS), environmental scanning tunneling spectroscopy (ESTM), infrared spectroscopy (IR) and ambient-pressure X-ray photoelectron spectroscopy (AP-XPS)} and theoretical calculations {Density Functional Theory and kinetic Monte Carlo} were used to characterize the properties of the active phase in the catalysts and the reaction mechanism. Under reaction conditions most WGS and CH metal/oxide catalysts undergo chemical transformations that drastically affect the reaction mechanism. The active phase of catalysts which combine Cu, Au or Pt with oxides such as ZnO, CeO₂, and TiO₂ essentially involves nanoparticles of the reduced metals and partially reduced oxide supports. Both components of each catalyst participate in the bonding of the reactants and intermediates for the WGS and CH reactions. Starting with single crystals of metals {Cu(111) and Au(111)}, we have performed detailed mechanistic studies that illustrate the importance of the metal-oxide interface. Extremely high catalytic activity was found after depositing nanoparticles of CeO_x on the metal surfaces. IR and AP-XPS indicate that this enhancement in catalytic activity is the result of opening new reaction paths that lead to the formation of a HOCO intermediate at the metal-oxide interface. Data of IR spectroscopy and DFT calculations indicate that this species plays a key role in the water-gas shift and CO₂ hydrogenation reactions.

FWP-BNL-CO040: Catalysis for Advanced Fuel Synthesis and Energy

Co-PIs: Ping Liu, Sanjaya Senanayake, Dario Stacchiola, Michael G. White

Postdoc(s): Wenqian Xu (partly), Huanru Wang, Robert Palomino(partly), David Grinter

Student(s): Si Luo, Zongyuan Liu, Fang Xu, Dimitriy Vovchok, Zhijun Zuo.

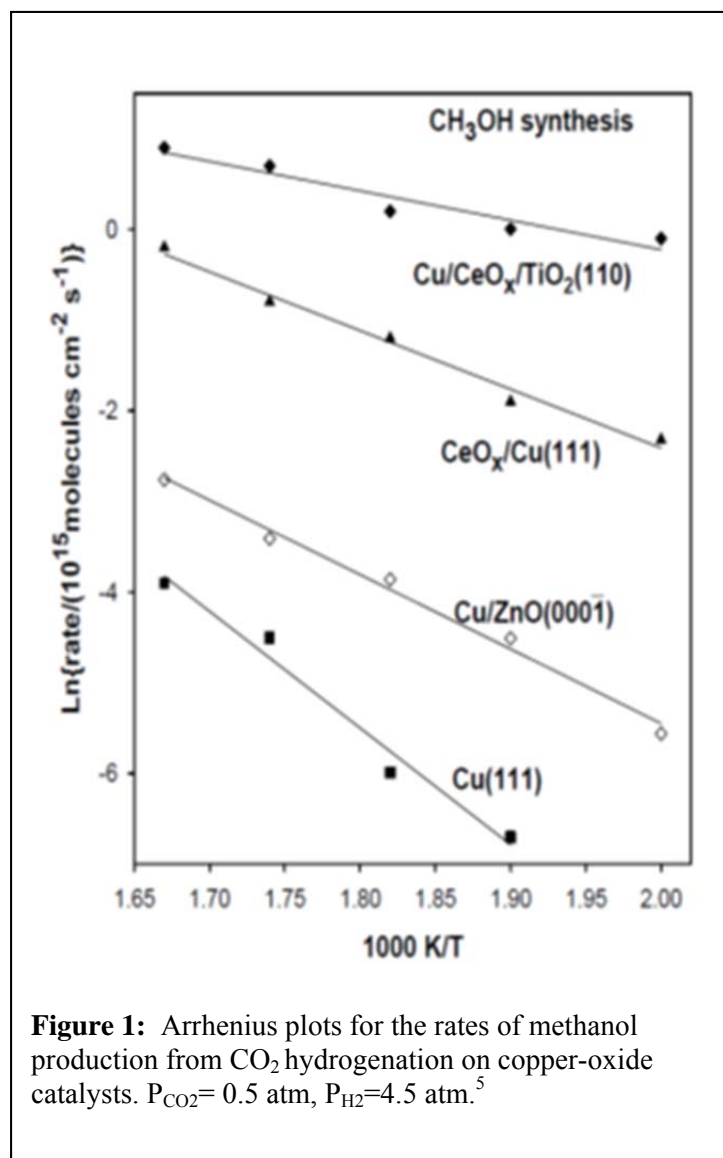
Affiliations(s): all students are from SUNY Stony Brook, Department of Chemistry

RECENT PROGRESS

Catalysis, Structure and Reactivity

1. Conversion of CO₂ on metal/oxide catalysts. Methanol is a key commodity used to produce acetic acid, formaldehyde, and a number of key chemical intermediates.ⁱ It is synthesized industrially from mixtures of H₂, CO₂, and CO at elevated pressures (50 to 100 atm) and temperatures (450 to 600K) with a Cu/ZnO/Al₂O₃ catalyst.^{ii,iii} Of particular interest is the synthesis of methanol from CO₂ not only as a way to mitigate this greenhouse gas but also because of the potential use of CO₂ as an alternative and economical feedstock.^{iv}

The activity for methanol synthesis of a series of catalysts which contain copper is compared in Fig 1.^v Extended surfaces

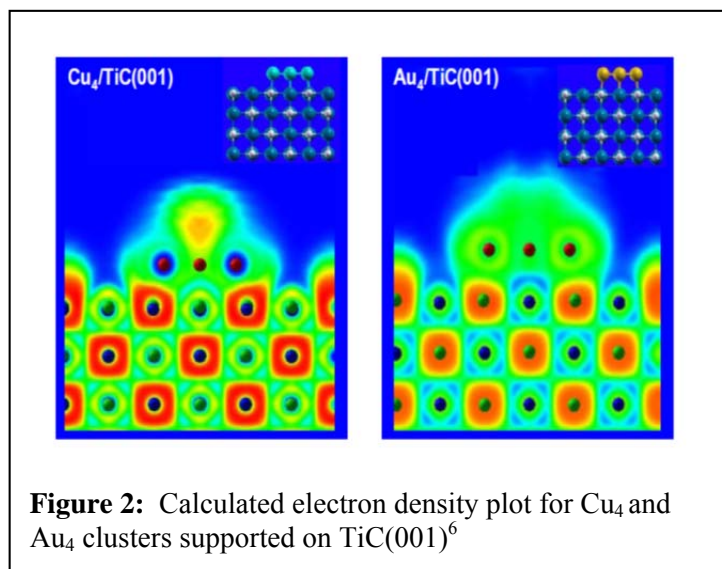


of pure copper, like Cu(111), bind the CO₂ molecular poorly and exhibit a very low activity for the hydrogenation of CO₂ to methanol. A drastic increase in the catalytic activity is observed in Figure 1 after depositing nanoparticles of ceria on Cu(111) or after co-depositing nanoparticles of Cu and ceria on TiO₂(110).⁵ The combination of metal and oxide sites in the copper-ceria interface gives complementary chemical properties that lead to special reaction pathways for the CO₂→CH₃OH conversion.⁵ Thus, the rate of methanol production on CeO_x/Cu(111) is ~ 200 times faster than on Cu(111). Furthermore, the rate of methanol production on Cu/CeO_x/TiO₂(110), where Cu and ceria nanoparticles are present, is ~ 1280 times faster than on Cu(111). CeO_x/Cu(111) and Cu/CeO_x/TiO₂(110) are also much much better catalysts than Cu/ZnO(0001).⁵ The results of ambient-pressure X-ray photoelectron and infrared spectroscopies, plus density-function calculations, point to a reaction mechanism that involves the initial formation of a OCOH species which can yield CO or HCO (formyl), H₂CO

(formaldehyde), H₃CO (methoxy) and methanol upon hydrogenation.⁵ The calculated energy barriers for these processes were all lower than 14 kcal/mol and the reaction intermediates were simultaneously bonded to Cu and ceria sites at the metal-oxide interface.⁵

2. Conversion of CO₂ on metal/carbide catalysts. There is a growing interest to use metal carbides for conversion of CO₂.^{vi} Using MoC(001) and Mo₂C(001) surfaces, we have investigated the effects of the metal-to-carbon ratio in the carbide on the hydrogenation of CO₂.⁶ The molecule chemisorbs molecularly on MoC(001) and there is no dissociation of C-O bonds. The breaking of one of these bonds can be achieved by hydrogen to form a HOCO intermediate.⁶ On the other hand, there is spontaneous dissociation of CO₂ on Mo₂C(001).⁶ This different patterns for the reactivity towards CO₂ mark the trends seen for the hydrogenation of the molecule. On a surface with a metal-to-carbon ratio of 1:1, MoC(001), only CO and methanol are seen as reaction products for CO₂ hydrogenation.^{6,vii} On the other hand, on a surface with a metal-to-carbon ratio of 2:1, Mo₂C(001), methane and other alkanes are also seen as reaction products.^{6,7} The metal-to-carbon ratio has a strong effect on the activity, selectivity and stability of the carbide catalyst.

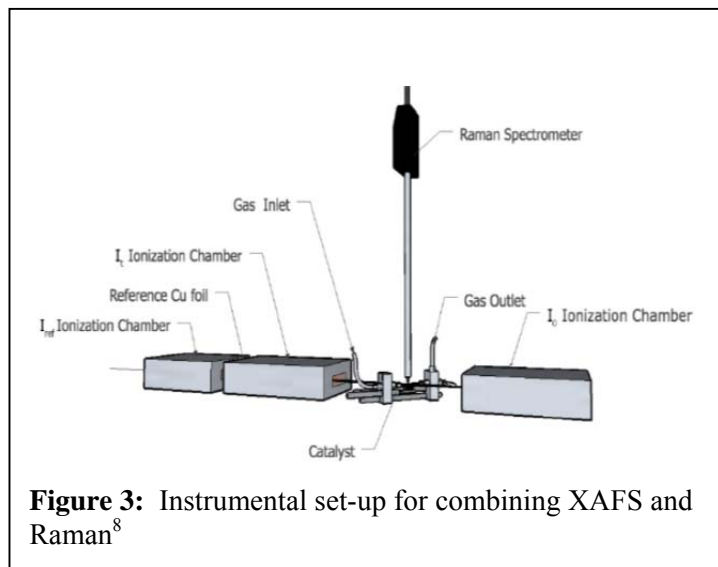
Two-dimensional Cu and Au clusters in contact with TiC(001) and molybdenum carbides undergo a significant polarization of electrons (Figure 2) that enhances their reactivity towards CO₂.^{viii,9} Cu(111) and Au(111) do not bind the CO₂ molecule at all. Adsorption of CO₂ on these surfaces can be achieved in the presence of H atoms and yields a formate intermediate, which is very difficult to transform into methanol.^{8,9} In contrast, the Au₄/TiC(001) and Cu₄/TiC(001) systems bind the CO₂ molecule well.⁸ On Cu₄/TiC(001), CO₂ is bound in a η³ configuration with a large elongation of the C-O bonds. The metal/carbide systems bind and dissociate the H₂ molecule very well, yielding a reservoir of hydrogen atoms that can be used for the hydrogenation of CO₂ all the way to methanol.



Indeed, excellent performance for the CO₂→CH₃OH reaction was observed after depositing Cu or Au on TiC(001) and MoC surfaces.^{8,9} The results of DFT calculations indicate that a OCOH species is again a key intermediate in the production of CH₃OH.⁹ The turnover frequencies for methanol production on Cu/TiC(001) are 170-500 times much larger than on Cu(111).⁸ High catalytic performance was also observed after depositing Cu on MoC.⁹ A comparison of the performance of Cu/MoC and Cu/Mo₂C showed that the metal/carbon ratio in the carbide plays an important role defining the activity, selectivity and stability of the catalysts for the conversion of CO₂ to methanol. The Cu/Mo₂C surface was extremely reactive towards CO₂ completely dissociating the molecule. On Cu/Mo₂C, the hydrogenation of CO₂ produced methane as a side product and the catalyst was not stable with time due to the formation of oxycarbides.^{ix}

3. Development of techniques for in-situ characterization of powder catalysts: Time-resolved PDF, XAFS/XRD, XAFS/IR and XAFS/Raman. The development of techniques for characterizing the structural properties of catalysts under the high-pressure conditions of industrial processes is widely recognized as a top priority in the area of heterogeneous catalysis. In the last years, the Catalysis Group at BNL has been very active in developing instrumentation for the characterization of catalysts with pair-distribution function (PDF) analysis and the integration of XAFS and XRD or XAFS and IR or Raman.^x The integration of IR or Raman with

XAFS (Figure 3) allows a simultaneous determination of the reaction intermediates on the surface and the chemical state and structure of the catalyst.⁸ Raman spectroscopy adds sensitivity to crystallographic phase and long range order that both XANES and EXAFS are lacking. *In-situ* PDF has been used to study the structure of amorphous metal and metal oxide nanoparticles under reaction.^{xi} Using a XAFS/IR combination, we have studied reaction mechanisms and correlations between structure/reactivity for CO oxidation and CO₂ hydrogenation.^{xii}



Fundamental Studies on the Water-gas Shift

Current industrial catalysts for the water-gas shift reaction (WGS, $\text{CO} + \text{H}_2\text{O} \rightarrow \text{H}_2 + \text{CO}_2$) are commonly mixtures of Fe-Cr and Zn-Al-Cu oxides, used at temperatures between 350-500 C and 180-250 C, respectively. These oxide catalysts are pyrophoric and normally require lengthy and complex activation steps before usage. Improved catalysts are being sought, particularly for lower temperature (e.g., at $T < 150\text{C}$, equilibrium lowers the product CO concentration into ranges for direct fuel cell use without further purification.). Ceria (Au, Cu or Pt on CeO₂), titania (Au, Pd or Pt on TiO₂) and molybdena (Ni, Cu and Au on MoO₂) based nanostructured catalysts are very promising new candidates for high activity, lower temperature operation in WGS systems. However, the design and optimization of these and other metal/oxide WGS nanocatalysts are hindered by controversy about basic questions regarding the nature of the active sites and the reaction mechanism.

A series of model catalysts {CeO_x/Cu(111), CeO_x/Au(111), Pt/CeO₂(111), Ni/CeO₂(111), Pt/TiO₂(110), Pt/CeO_x/TiO₂(110)} was used to study fundamental aspects of the water-gas shift reaction.^{xiii,xiv} These studies revealed that the oxide component of the catalyst can affect the reaction process in two different ways. First, the presence of O vacancies in the oxide greatly facilitates the dissociation of water.¹⁴ And second, the electronic properties of the metal can be affected by interactions with the oxide producing special chemical properties.^{13,14} This is the case in the Ni/CeO₂(111), Pt/CeO₂(111) and Pt/CeO_x/TiO₂(110) systems.^{13,14} The results of valence photoemission point to a new type of metal-support interaction which produces large electronic perturbations for small Ni and Pt particles in contact with ceria.¹⁴ The Ni/CeO₂(111) Pt/CeO₂(111) and Pt/CeO_x/TiO₂(110) systems exhibited a density of metal d states near the Fermi level that was much smaller than that expected for bulk metallic Ni or Pt.^{13,14} The electronic perturbations induced by ceria on Ni made this metal a very poor catalyst for CO methanation, but transformed Ni into an excellent catalyst for the production of hydrogen through the water-gas shift.¹⁴ Furthermore, the large electronic perturbations seen for small Pt and Ni particles in contact with ceria significantly enhanced the ability of the admetal to adsorb and dissociate water made it a highly active catalyst for the water-gas shift.¹⁴ The behavior seen for Ni/CeO₂(111), Pt/CeO₂(111) and Pt/CeO_x/TiO₂(110) systems illustrates the positive effects

derived from electronic metal-support interactions and points to a promising approach for improving or optimizing the performance of metal/oxide catalysts.^{13,14}

Nanostructured materials for catalysis

This subtask of the FWP provides nanostructured materials that are currently used in experiments for CO₂ hydrogenation and the water-gas shift.^{13,xv,xvi,xvii} Inverse oxide/metal catalysts can be very powerful tools to study the mechanism of surface reactions.^{15,16,17} A combination of theory and experiment was used to investigate electron transfer at Cu-metal oxide interfaces and its potential role in determining reactivity.^{xviii,xix} Bonding interactions leading to Cu→oxide electron transfer are expected to stabilize the formation of oxygen vacancies which can enhance the WGS activity of Cu catalysts by acting as active sites for water dissociation.^{18,19} In this study, we have examined how electron transfer varies with the size, atomic structure and state of reduction for a number of different inverse model catalysts composed of size-selected metal oxide nanoclusters (MO_x; M = Mo, W, Ti, Nb) deposited on Cu(111) and Cu₂O/Cu(111) surfaces. A major advantage of mass-selected deposition is the ability to control stoichiometry of the clusters, i.e., metal-to-oxygen ratio, thereby allowing studies of “reduced” clusters without post annealing treatment of the surface. Novel two-photon photoemission (2PPE) measurements were used to extract surface dipoles as a probe of interfacial electron transfer and temperature programmed reaction (TPR) was used to assess activity for water dissociation.^{18,19} All the oxide clusters on Cu(111) exhibit negative surface dipoles, indicative of Cu → cluster charge transfer, with the dipoles for sub-stoichiometric and reducible oxides (i.e., Ti_xO_y and Nb_xO_y) being smaller. The observed trends are generally consistent with Bader charge analyses from DFT calculations, but in some cases, the calculations suggest that the intrinsic dipole of the deposited cluster (structure dependent) is more important than charge transfer. TPR experiments show that the Ti_xO_y and Nb_xO_y clusters promote water dissociation, with the ‘reduced’ Ti_xO_y clusters (x/y = 3/5, 4/7) more active than their stoichiometric counterparts (x/y = 3/6, 4/8). The Nb_xO_y clusters behave differently, with both stoichiometric (x/y = 3/7, 4/10) and reduced clusters (x/y = 3/5, 4/8) able to dissociate water on Cu(111) (see Figure 4).¹⁹ Moreover, only the reduced Nb_xO_y clusters show activity for water dissociation on the Cu₂O/Cu(111) oxide thin film surface. Overall, we find that the magnitude of electron transfer (surface dipole) and oxide cluster stoichiometry are correlated, and these influence the ability of the cluster to promote water dissociation by modifying the coordination and oxidation state of the cation active site.

We made great efforts toward bridging the pressure gap and the material gap between theoretical modeling using DFT and experimental conditions. It enhances the comparability between theory and experiment, enabling theory to provide more meaningful insight into the reaction mechanism and active sites. In this aspect, new approaches were used to investigate the oxidation of CO on supported iron oxide nanoparticles¹⁷ and the

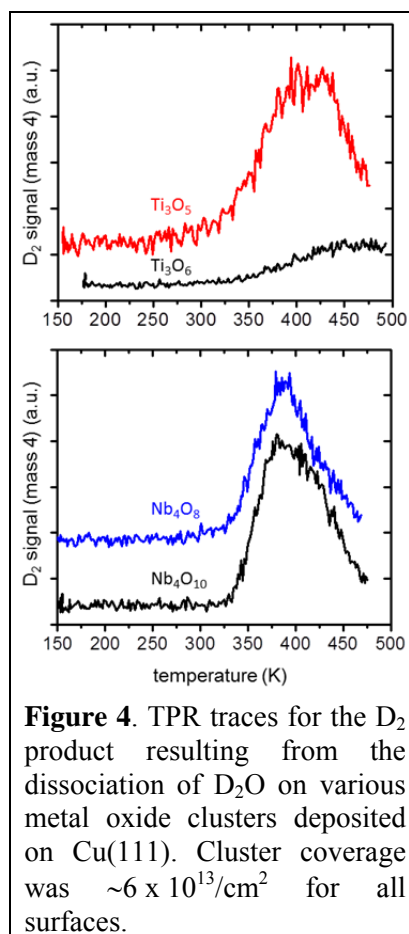


Figure 4. TPR traces for the D₂ product resulting from the dissociation of D₂O on various metal oxide clusters deposited on Cu(111). Cluster coverage was $\sim 6 \times 10^{13}/\text{cm}^2$ for all surfaces.

oxygen reduction reaction (ORR) on various Au_xPd_y@Pt_{ML} core-shell nanowires.^{xx}

References

- i. Olah, G.A., Goeppert, A., and Surya Prakash, G.K. *Beyond Oil and Gas: The Methanol Economy*. Wiley-VCH, Weinheim, Germany, 2011.
- ii. Behrens M. *et al*, *Science*, **2012**, 336, 893 .
- iii. Spenser, M.S. *Top. Catal.* **1999**, 8, 259 .
- iv. Aresta, M. (editor), *Carbon Dioxide as Chemical Feedstock*. Wiley, New York, 2010.
- v. Graciani, J. *et al*, *Science*, **2014**, 345, 546.
- vi. Posada-Perez, S. *et al*, *Phys. Chem. Chem. Physics*. **2014**, 16, 14912.
- vii. Xu, W. *et al*, *Catal. Lett.* **2014**, 144, 1418.
- viii. Vidal, A.B. *et al*, *J. Phys. Chem. Lett.* **2012**, 3, 2275
- ix. Posada-Perez, S. *et al*, *Catal. Sci. & Eng.* **2016**, DOI: 10.1039/C5CY02143J.
- x. Platolla, A., *et al.*, *Topics in Catalysis*, **2013**, 56, 896.
- xi. Hanson, J.C. *et al*, *Catalysis Today*, **2014**, 229, 64.
- xii. Yao, S.Y. *et al.*, *ACS Catalysis*, **2014**, 4, 1650.
- xiii. Rodriguez, J. A. *et al*, *Acc. Chem. Res.*, **2014**, 47, 773.
- xiv. Carrasco, J. *et al*, *Angew. Chem. Int. ed.* **2015**, 54, 3917.
- xv. Mudiyansele, K., *et al.*, *Angewandte Chemie Int. Ed.*, **2013**, 52, 5101.
- xvi. Senenayake, S.D. *et al*. *Accounts of Chemical Research*, **2013**, 46, 1702.
- xvii. Yu, L. *et al*, *Journal of Physical Chemistry C* **2015**, 119, 16614.
- xviii. Yang, Y. X. *et al*, *J. Phys. Chem. C* **2014**, 118, 13697.
- xix. Nakayama, M. *et al*. *Journal of Physical Chemistry C* **2015**, 119, 14756.
- xx. Liu, H. *et al*, *Journal of the American Chemical Society* **2015**, 137, 12597.

Publications acknowledging this grant in 2013-2016

1. Stacchiola, D.J., *et al.*, *Chemical Reviews*, **2013**, 113, 4373-4390.
2. Mudiyansele, K., *et al.*, *Angewandte Chemie Int. Ed.*, **2013**, 52, 5101-5105.
3. Dos Santos Politi, J.A., *et al*, *Phys. Chem. Chem. Phys.*, **2013**, 15, 12617-12625.
4. Carrasco, J., *et al.*, *Journal of Physical Chemistry C*, **2013**, 117, 8241-8250.
5. Xu, W., *et al.*, *ACS Catalysis*, **2013**, 3, 975-984.
6. Wang, H., *et al.*, *Journal of the American Chemical Society*, **2013**, 135, 4149-4158.

-
7. Rodriguez, J.A.; Hanson, J.C.; Chupas, P. *Goals and Challenges for the In-situ Characterization of Heterogeneous Catalysts*, in *In-situ Characterization of Heterogeneous Catalysts*, J.A. Rodriguez, J.C. Hanson, and P. Chupas, Editors. 2013, Wiley: New York.
 8. Platolla, A., et al., *Topics in Catalysis*, **2013**, *56*, 896-904.
 9. Senenayake, S.D.; Stacchiola, D.; Rodriguez, J.A. *Accounts of Chemical Research*, **2013**, *46*, 1702-1711.
 10. Johnston-Peck, A., et al., *Journal of Physical Chemistry C*, **2013**, *117*, 14463-14471.
 11. Senenayake, S.D.; Rodriguez, J.A.; Stacchiola, D., *Topics in Catalysis*, **2013**, *56*, 1488-1498.
 12. Rodriguez, J.A., et al., *Physical Chemistry Chemical Physics*, **2013**, *15*, 12004-12025.
 13. Rodriguez, J.A. et al., *Journal of Catalysis*, **2013**, *307*, 162-169.
 14. Wang, H. et al, *Angew. Chem. Int. Ed.* **2013**, *52*, 9210-9214
 15. Graciani, J., et al. *Science*, **2014**, *345*, 546-550.
 16. Zhao, F., et al., *J. Phys. Chem. C*, **2014**, *118*, 2528–2538.
 17. Rodriguez, J., et al. *Angew. Chem. Int. Ed.* **2014**, *53*, 11270-11274.
 18. Xu, W.; Ramirez, P.J.; Stacchiola, D.; Rodriguez, J.A.. *Catal. Lett.* **2014**, *144*, 1418-1424.
 19. Asara, G., et al., *Journal of Physical Chemistry C*, **2014**, *118*, 19224-19231.
 20. Posada-Perez, S.; Vines, F.; Ramirez, P.J.; Vidal, A.; Rodriguez, J.A. Illas, F. *Phys. Chem. Chem. Physics*. **2014**, *16*, 14912-14921
 21. Rodriguez, J. A.; Senenayake, S. D.; Stacchiola, D.; Liu, P.; Hrbek, J., *Acc. Chem. Res.*, **2014**, *47*, 773–782.
 22. Yao, S.Y. et al., *ACS Catalysis*, **2014**, *4*, 1650-1661.
 23. Hanson, J.C. et al, *Catalysis Today*, **2014**, *229*, 64-71
 24. Guzman-Blas, R. et al, *Electrocatalysis*, **2014**, *5*, 50-61.
 25. Baber, A.E. et al, *Angew. Chem. Int. Ed.* **2014**, *53*, 5336-5340.
 26. Yao, S.Y., et al. *Physical Chemistry Chemical Physics*, **2014**, *16*, 17183-17195.
 27. Yang, Y. X.; Zhou, J.; Nakayama, M.; Nie, L. Z.; Liu, P.; White, M. G. *J. Phys. Chem. C* **2014**, *118*, 13697.
 28. Nakayama, M.; Xue, M.; An, W.; Liu, P.; White, M. G. *The Journal of Physical Chemistry C* **2015**, *119* 14756.
 29. Yu, L.; Liu, Y.; Yang, F.; Evans, J.; Rodriguez, J. A.; Liu, P. *The Journal of Physical Chemistry C* **2015**, *119*, 16614.
 30. Liu, H.; An, W.; Li, Y.; Frenkel, A. I.; Sasaki, K.; Koenigsmann, C.; Su, D.; Anderson, R. M.; Crooks, R. M.; Adzic, R. R.; Liu, P.; Wong, S. S. *Journal of the American Chemical Society* **2015**, *137*, 12597
 31. An, W.; Liu, P. *ACS Catalysis* **2015**, *5*, 6328.
 32. Mudiyansele, K., et al., *Topics in Catal.* **2015**, *58*, 271-280.
 33. An, W.; Xu, F.; Stacchiola, D.; Liu, P. *ChemCatChem* **2015**, *7*, 3865.

-
34. Zhao, F. et al., *Catal. Lett.* **2015**, *145*, 808-815.
 35. Carrasco, J. et al, *Angew. Chem. Int. ed.* **2015**, *54*, 3917-3921.
 36. Posada-Perez, S. et al, *J. Chem. Phys.* **2015**, *143*, 1114704-1,5
 37. Yang, X. et al, *J. Am. Chem. Soc.* **2015**, *137*, 10104-10107.
 38. Graciani et al, *Phys. Chem. Chem. Phys.* **2015**, *17*, 26813-26818.
 39. Xu, W. et al, *Catal. Lett.* **2015**, *145*, 1365-1373.
 40. Asara, G.G.; Ricart, J.M.; Rodriguez, J.A.; Illas, *Surf. Sci.* **2015**, *640*, 141-149.
 41. Lei, W. et al, *ACS Catalysis*, **2015**, *5*, 4385-4393.
 42. Liu, Z. et al, *J. Catal.* **2015**, *321*, 90-99
 43. Rodriguez, J.A. et al. *ACS Catal.* **2015**, *5*, 6696-6706.
 44. Liu, Z., et al. *J. Phys. Chem. C*, **2015**, *119*, 18248-18256.
 45. Guzman, H. et al, *J. Catal.* **2015**, *332*, 83-94.
 46. Senanayake, S; et al, *J. Phys. Chem. C*, **2016**, *120*, 1778-1784
 47. Posada-Perez, S. et al, *Catal. Sci. & Eng.* **2016**, DOI: 10.1039/C5CY02143J

Aaron D. Sadow

Interfacial catalysts for reactions of oxygenates: characterization, catalytic activity and reaction mechanisms

Aaron D. Sadow, Igor I. Slowing, Takeshi Kobayashi, Marek Pruski
Ames Laboratory, U.S. DOE, Iowa State University, Ames, IA 50011-3111

Presentation Abstract

The overarching goal of this collaborative research project is to develop new catalytic principles for bringing together the best features of homogeneous and heterogeneous catalysis and ultimately enable the design of efficient catalysts with molecular-scale control of chemical conversions, particularly those relevant to reduction of highly oxygenated compounds. The substantial challenges for rational design of catalysts for selective conversions require understanding and control of the catalytic environment and reaction mechanisms. These requirements are addressed through the design of 3D, mesoporous interfacial catalysts. Doing so provides advantages in catalyst recovery, reaction control, sensitivity and efficiency. Our efforts combine expertise in mesoporous catalyst synthesis, transition metal chemistry, mechanisms of catalytic reactions, and solid-state (SS)NMR. Here, we specifically highlight catalytic reductions mediated by earth-abundant metals in 3D mesoporous catalytic materials, and catalytic systems that enhance the activity and selectivity of precious metal catalysts. Our development of single-site grafted zirconium catalysts for reductions of oxygenates are presented. In addition, we have advanced SSNMR characterization methodology utilizing ultrafast MAS. Studies of our developments of new 3D materials for catalytic applications, as well as spectroscopic studies utilizing the emerging SSNMR methodologies that employ dynamic nuclear polarization (DNP), are shown in separate presentations.

AL-03-380-011: Homogeneous and Interfacial Catalysis in 3D Controlled Environment

Postdoc(s): Naftali Opembe

Student(s): Dilini Singappuli-Arachchige, Jennifer F. Goldston, Kapil Kandel, Nicholas C. Nelson, Naresh Eedugurala, Bosky Parikh, Zachary Weinstein, Zhuoran Wang

RECENT PROGRESS

(1) *Selective reduction of fatty acids to fatty alcohols by synergistic Copper-Iron oxides.* One of the specific goals of our program is to design catalytic systems for selectively reducing oxygenated species under milder conditions than conventional catalysts. Because fatty alcohols are an important chemical commodity (>2.5 million Ton/yr market) and the process involves high temperatures and H₂ pressures (300 °C, 200 – 300 bar), developing more efficient catalysts that lower the energy input of the process is of significant interest. Our previous research within this FWP identified iron/iron oxide nanoparticles supported on mesoporous silica nanoparticles (MSN) as an efficient catalyst for hydrodeoxygenation of fatty acids to hydrocarbons under relatively mild conditions (290 °C, 30 bar H₂), and provided evidence that fatty alcohols were intermediates in the reaction.¹¹ Because iron oxide is able to dehydrate alcohols at temperatures higher than 200 °C, the resulting alkenes are quickly hydrogenated to alkanes under the reaction conditions. Thus, we considered that lowering the reaction temperature to 200 °C or less should prevent alcohol dehydration and give the desired product. However, TPR studies of iron oxide catalyst on MSN suggested that metallic iron (required for H₂ activation) does not form in significant amounts below 250 °C, which limits the number of H₂ activation sites and gives poor fatty acid conversion at 200 °C. Because copper oxide nanoparticles are easier to reduce than iron oxide (TPR_{max} at 170 °C), we considered forming a complex catalyst supporting both metal oxides on MSN and testing the activity at temperatures where Cu⁰ would be expected to form. The composite catalyst was much more active than the corresponding single metal oxides under moderate conditions, giving >95% yield of fatty alcohols at 180 °C and 30 bar H₂. Under those conditions, mono-metal oxide catalysts gave only <3% conversion of fatty acids and

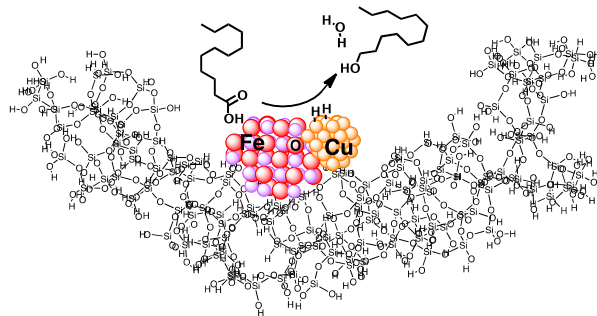


Figure 2. Proposed mechanism of the synergistic selective reduction of fatty acid to its alcohol.

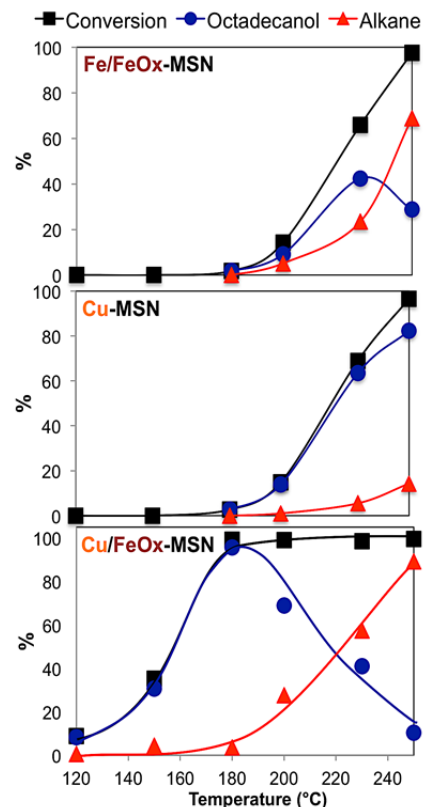


Figure 1. Hydrogenation of stearic acid using metal/metal oxide nanoparticles supported on mesoporous silica nanoparticles (MSN), batch mode, 30 bar H₂, 3 h, 10 μmol substrate, 10 μmol cat.

poorer selectivity. The activity of the co-supported oxides was also significantly higher than that of a physical mixture of individually supported metal oxides, which suggested a synergistic behavior of the composite. Dispersion, XRD, TPR and acetic acid TPD experiments showed that the original material was a mixed copper-iron oxide, that segregates into metallic copper and iron oxide at 150 °C. Our data suggest that *in situ* reduction of copper oxide to its metallic form provides sites for H₂

activation, and that the activated hydrogen spills over to iron oxide where fatty acids bind and are selectively reduced to the alcohol.⁸

(2) Transfer hydrogenation of phenol in aqueous media catalyzed by Pd/Na-doped ceria. Our previous research showed that ceria is a robust and active support for the Pd-catalyzed reduction of phenol, providing quantitative conversions at room temperature and only 1 bar H₂. Since the activity of ceria seems to be related to its defect sites, we decided to enhance the number of defects by doping the oxide with metals that would disrupt the lattice. Using a combustion synthesis approach we discovered that addition of Na produced a material with increased number of defects, as indicated by Raman spectroscopy and oxygen storage capacity (OSC) measurements. The increased number of defects translated into enhanced redox activity, as evaluated by comparing the rates of aerobic 2-propanol oxidation between the undoped and the Na-containing ceria. Sodium doping increased acetone formation rate twofold. Based on these results we attempted to couple ceria catalyzed 2-propanol oxidation with Pd catalyzed reduction of phenol. It was expected that Pd could promote hydrogen transfer between the two substrates. The reaction was performed in flow mode, and high (80%) and stable (over 7 days continuous flow) conversions were obtained using Pd supported on Na containing ceria. Consistent with the behavior observed for the 2-propanol oxidation, the rate was around 4 times higher using the Na doped material than the undoped ceria (Fig. 3), with apparent activation energies of 11.8 ± 0.4 and 27.4 ± 0.7 kcal/mol respectively.

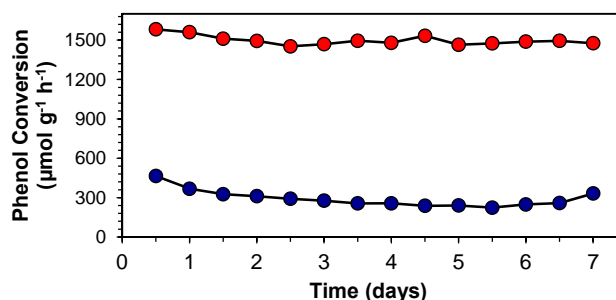


Figure 3. Transfer hydrogenation of phenol catalyzed by Pd on ceria (blue) and Pd on Na-doped ceria (red). Conditions: 0.15 M PhOH, 90 v/v % *i*-PrOH_(aq), 0.5 g cat., 0.1 mL min⁻¹, T = 140 °C, V_{bed} = 0.4 mL.

(3) Catalytic hydroboration of carbonyls with an oxophilic surface-supported zirconium catalyst. The hydroboration of aldehydes and ketones using a silica-supported zirconium catalyst is reported.⁷ Reaction of Zr(NMe₂)₄ and Mesoporous Silica Nanoparticles (MSN) provides the catalytic material Zr(NMe₂)_n@MSN. Characterization of Zr(NMe₂)_n@MSN with solid-state NMR and infrared spectroscopy, elemental analysis, powder X-ray diffraction, electron microscopy, and reactivity studies suggests that its surface structure is primarily the monopodal ≡SiO–Zr(NMe₂)₃ (data detailed in Table 1).

Table 1. Characterization data for Zr(NMe₂)_n@MSN.

Experiment	Observation	Interpretation
Electron microscopy/EDX	well-dispersed Zr	no Zr or ZrO ₂ clusters formed
Reaction stoichiometry	1.2 mmol HNMe ₂ detected/g MSN 1.0 mmol Zr(NMe ₂) ₄ consumed/g MSN	
ICP-OES	0.91 mmol Zr/g	zirconium loading established
C, N combustion analysis	4.9 mmol C/g, 2.5 mmol N/g	Zr:NMe ₂ ~ 1:2.7 suggests a 3:7 mixture of Zr(NMe ₂) ₂ and Zr(NMe ₂) ₃ groups
¹³ C DPMAS/spin counting	2.7 mmol NMe ₂ /g	Zr:NMe ₂ ~ 1:3 suggests primarily three NMe ₂ -containing

		ligands/Zr
IR	new ν_{CH} bands at $\sim 2900 \text{ cm}^{-1}$ ν_{OH} band at 3747 cm^{-1} not detected	NMe ₂ groups present on surface isolated silanols have reacted
¹⁵ N SSNMR:	strong signal at -355 ppm polarized by Me groups, weakly by H	nitrogen is primarily present as dimethylamide groups
Reaction with HBpin (below)	2.5 mmol Me ₂ NBpin formed/g Zr(NMe ₂) _n @MSN	ca. 2.7 reactive NMe ₂ groups per Zr center

Excitingly, the ¹⁵N NMR spectra of Zr(NMe₂)_n@MSN under natural isotopic abundance obtained under DNP-enhanced conditions matched the conventional CPMAS spectrum acquired using an ¹⁵N-enriched sample (Fig. 4). Thus, we show for the first time that the DNP experimental conditions, employing tetrachloroethane and the nitroxide-based TEKPol biradical, are compatible with a reducing, early-metal amide surface species. For comparison, the nitroxide TEMPO and (solution-phase) Zr(NMe₂)₄ react in benzene rapidly, and Zr(NMe₂)₄ also reacts with tetrachloroethane. In addition, the CP build-up curves indicate that the nitrogen is polarized by methyl groups, not NH, indicating that the primary surface species is a zirconium amide, rather than amine.

This material reacts with pinacolborane (HBpin) to provide Me₂N-Bpin and a surface bonded zirconium hydride, which was characterized by solid-state NMR spectroscopy and infrared spectroscopy and through its reactivity with D₂ (summarized in Table 2).

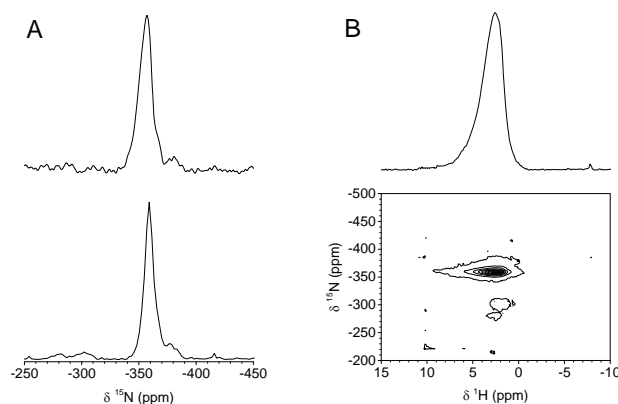


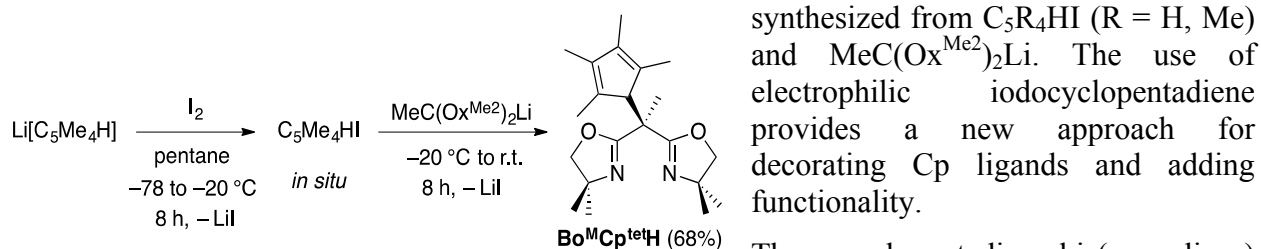
Figure 4. (A) Top spectrum: DNP-enhanced ¹⁵N CPMAS spectrum of Zr(NMe₂)_n@MSN under natural ¹⁵N abundance. Lower spectrum: skyline ¹⁵N projection of the 2D ¹⁵N-¹H idHetcor spectrum in figure (B). (B) 2D ¹⁵N-¹H idHetcor spectrum of ¹⁵N-enriched Zr(¹⁵NMe₂)_n@MSN.

Table 2. Characterization of ZrH/Bpin@MSN.

Experiments	Observations	Interpretations
Reaction stoichiometry: Zr(NMe ₂) _n @MSN + HBpin	2.5 mmol Me ₂ NBpin formed/g Zr(NMe ₂) _n @MSN	all but ca. 0.2 mmol NMe ₂ /g are desorbed from the material
ICP-OES: Zr(NMe ₂) _n @MSN + HBpin	0.89 mmol Zr/g material 0.86 mmol B/g material	the Zr:B ratio is $\sim 1:1$, and Zr does not leach from MSN
IR:	ν_{ZrH} observed at 1592 cm^{-1}	ZrH formed using HBpin is distinct from $(\text{=SiO})_3\text{ZrH}$
Reaction with D ₂ , then H ₂	band at 1592 cm^{-1} disappears upon D ₂ addition, then reappears upon H ₂ addition	exchangeable zirconium hydride
¹ H SSNMR: treatment with D ₂	δ_{ZrH} at 6.9 ppm, 0.5 mmol H/g Signal disappears upon D ₂ addition	the zirconium hydride surface species is distinct from $(\text{=SiO})_3\text{ZrH}$

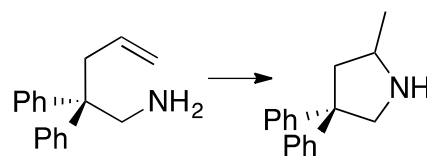
The zirconium hydride material or the zirconium amide precursor $\text{Zr}(\text{NMe}_2)_n@ \text{MSN}$ catalyze the hydroboration of aldehydes and ketones with HBpin. This catalytic material may be recycled without loss of activity at least eight times, and air-exposed materials are catalytically active, showing that these single-site zirconium centers are robust catalytic sites for carbonyl reduction. Note that the Zr center is bonded to the surface by Zr-O interactions, and these are not disrupted by the HBpin reagent. In contrast, the $[\text{Zr}]\text{-OCHR}_2$ catalytic intermediate reacts rapidly with HBpin to give the product and catalytic turnover.

(4) New ligands for early metal catalysts. A new class of cyclopentadiene-bis(oxazoline) compounds and their piano-stool-type organometallic compounds have been prepared as catalysts for hydroamination of aminoalkenes.² The two compounds $\text{MeC}(\text{Ox}^{\text{Me}_2})_2\text{C}_5\text{H}_5$ ($\text{Bo}^{\text{M}}\text{Cp}^{\text{H}}$; $\text{Ox}^{\text{Me}_2} = 4,4\text{-dimethyl-2-oxazoline}$) and $\text{MeC}(\text{Ox}^{\text{Me}_2})_2\text{C}_5\text{Me}_4\text{H}$ ($\text{Bo}^{\text{M}}\text{Cp}^{\text{tet}}\text{H}$) are



synthesized from $\text{C}_5\text{R}_4\text{HI}$ ($\text{R} = \text{H}, \text{Me}$) and $\text{MeC}(\text{Ox}^{\text{Me}_2})_2\text{Li}$. The use of electrophilic iodocyclopentadiene provides a new approach for decorating Cp ligands and adding functionality.

These cyclopentadiene-bis(oxazolines) are converted into ligands that support a variety of metal centers in piano-stool-type geometries, and here we report the preparation of Mg, Tl, Ti, and Zr compounds. $\text{Bo}^{\text{M}}\text{Cp}^{\text{H}}$ or $\text{Bo}^{\text{M}}\text{Cp}^{\text{tet}}\text{H}$ react with $\text{MgMe}_2(\text{dioxane})_2$ to give the magnesium methyl complexes $\{\text{Bo}^{\text{M}}\text{Cp}\}\text{MgMe}$ and $\{\text{Bo}^{\text{M}}\text{Cp}^{\text{tet}}\}\text{MgMe}$. $\text{Bo}^{\text{M}}\text{Cp}^{\text{H}}$ or $\text{Bo}^{\text{M}}\text{Cp}^{\text{tet}}\text{H}$ are converted to $\text{Bo}^{\text{M}}\text{CpTl}$ and $\text{Bo}^{\text{M}}\text{Cp}^{\text{tet}}\text{Tl}$ by reaction with TIOEt. The thallium derivatives react with $\text{TiCl}_3(\text{THF})_3$ to provide $\{\text{Bo}^{\text{M}}\text{Cp}\}\text{TiCl}_2$ and $\{\text{Bo}^{\text{M}}\text{Cp}^{\text{tet}}\}\text{TiCl}_2$, the former of which is crystallographically characterized as a dimeric species. $\text{Bo}^{\text{M}}\text{Cp}^{\text{H}}$ and $\text{Zr}(\text{NMe}_2)_4$ react to eliminate dimethylamine and afford $\{\text{Bo}^{\text{M}}\text{Cp}\}\text{Zr}(\text{NMe}_2)_3$, which is crystallographically characterized as a monomeric four-legged piano-stool compound. $\{\text{Bo}^{\text{M}}\text{Cp}\}\text{Zr}(\text{NMe}_2)_3$, $\{\text{Bo}^{\text{M}}\text{Cp}\}\text{MgMe}$, and $\{\text{Bo}^{\text{M}}\text{Cp}^{\text{tet}}\}\text{MgMe}$ are efficient catalysts for the hydroamination/cyclization of aminoalkenes under mild conditions. A trend in activity of oxazoline-substituted cyclopentadienyl ligands follows: $\{\text{PhB}(\text{Ox}^{\text{Me}_2})_2\text{Cp}\}\text{Zr}(\text{NMe}_2)_2 > \{\text{Bo}^{\text{M}}\text{Cp}\}\text{Zr}(\text{NMe}_2)_3 > \text{CpZr}(\text{NMe}_2)_3$. Remarkably, the parent piano-stool complex catalyzes some conversion of the typical aminoalkene to 2-methyl-pyrrolidine under mild, room temperature conditions (ca. 60 °C for full conversion). It is also interesting to note that the combination of the bis(oxazoline) and cyclopentadienyl ligands on zirconium gives more reactive catalytic species than the oxazoline-free $\text{CpZr}(\text{NMe}_2)_3$ catalyst precursor.



(5) Solid-state (SS)NMR spectroscopy. SSNMR is our spectroscopic tool of choice for atomic-scale characterization of the surfaces and interfaces of crystallographically disordered catalytic materials. These studies use state-of-the-art ‘conventional’ SSNMR methods based on direct excitation of nuclear spins, as well as “hyper-polarization” of ^1H and/or other nuclei via dynamic nuclear polarization (DNP). DNP provides game-changing boost to SSNMR’s sensitivity through excitation of the unpaired electrons at their electron paramagnetic resonance (EPR) frequency and subsequent transfer of polarization to the material’s nuclei of interest. The capabilities and applications offered by DNP SSNMR are described separately in our

presentation entitled “Characterization of Catalytic Materials by DNP-enhanced Solid-State NMR”.

Conventional SSNMR. Previously, our program has benefitted from characterizations by two-dimensional (2D) correlation methods under fast magic angle spinning (MAS) at rates of ~40+ kHz, some of which we developed. A most recent area of inquiry for SSNMR methodology involved 2D heteronuclear correlation (HETCOR) spectroscopy under ultrafast MAS, at rates exceeding 100 kHz. Our experiments, carried out in collaboration with JEOL Resonance Inc., demonstrated that this technology affords surprisingly high efficiency of heteronuclear polarization transfer (e.g. ^1H - ^{13}C) and endows SSNMR with spectral editing capabilities hitherto limited to solution NMR, essentially instituting the convergence of solid-state and solution NMR. For example, highly resolved 2D HMQC- and HSQC-type spectra of surface species can be acquired on natural abundance samples. These experiments will provide new insights about intra- and intermolecular correlations, which in turn are needed to unravel the conformations of surface species, characterize the distributions of multiple functionalities, and understand the cooperative catalytic phenomena.

A 2D HETCOR $^1\text{H}\{^{13}\text{C}\}$ (HSQC-type) spectrum of natural abundance mercaptopropyl functional groups (MP) on MSN surface prepared by the Slowing group is shown in Fig. 5.¹⁷ In spite of the minuscule sample volume (290 nL) and the low concentration of surface-bound groups (comprising *less than 20 nanomoles* of ^{13}C - ^1H pairs), we obtained the spectrum within hours. The experiment was very easy to optimize and yielded excellent resolution in ^1H dimension without resorting to ^1H - ^1H homonuclear RF decoupling. The HMQC spectra of surface-bound species can be also acquired under 100 kHz MAS, although the decoherence of transverse ^1H magnetization of strongly coupled spins has significant influence on the transfer efficiency. These methods offer an attractive strategy for probing surface species in mass-limited samples that are not amenable to DNP conditions.

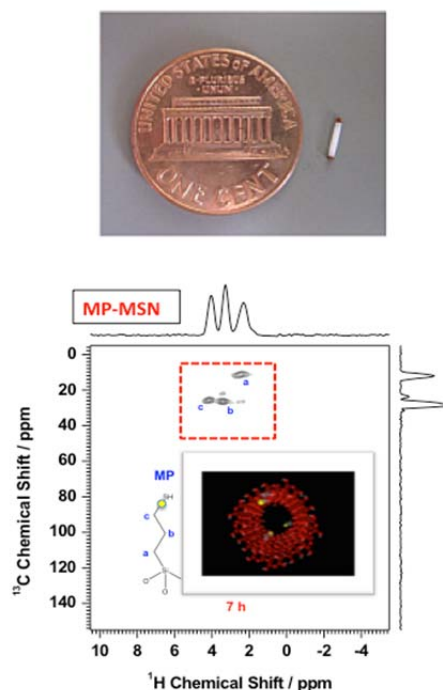


Figure 5. Top: the MAS rotor capable of MAS at 100+ kHz in a prototype JEOL Resonance Inc. probe. Bottom: ^1H - ^{13}C HSQC spectrum of MP-MSN taken at 14.1 T under MAS at 100 kHz.

Publications Acknowledging this Grant in 2013-2016

(I) Exclusively funded by this grant

1. Manna, K.; Eedugurala, N.; Sadow, A. D., Zirconium-Catalyzed Desymmetrization of Aminodialkenes and Aminodialkynes through Enantioselective Hydroamination. *Journal of the American Chemical Society* **2015**, *137*, 425-435. <http://dx.doi.org/10.1021/ja511250m>
2. Eedugurala, N.; Hovey, M.; Ho, H.-A.; Jana, B.; Lampland, N. L.; Ellern, A.; Sadow, A. D., Cyclopentadienyl-bis(oxazoline) Magnesium and Zirconium Complexes in Aminoalkene Hydroaminations. *Organometallics* **2015**, *34*, 5566-5575. <http://dx.doi.org/10.1021/acs.organomet.5b00771>
3. Althaus, S. M.; Mao, K.; Stringer, J. A.; Kobayashi, T.; Pruski, M., Indirectly Detected Heteronuclear Correlation Solid-state NMR Spectroscopy of Naturally Abundant N-15 Nuclei. *Solid State Nuclear Magnetic Resonance* **2014**, *57-58*, 17-21. <http://dx.doi.org/10.1016/j.ssnmr.2013.11.001>
4. Wang, J.; Ackerman, D. M.; Lin, V. S. Y.; Pruski, M.; Evans, J. W., Controlling Reactivity of Nanoporous Catalyst Materials by Tuning Reaction Product-Pore Interior Interactions: Statistical Mechanical Modeling. *Journal of Chemical Physics* **2013**, *138*. <http://dx.doi.org/10.1063/1.4798463>
5. Kandel, K.; Althaus, S. M.; Peeraphatdit, C.; Kobayashi, T.; Trewyn, B. G.; Pruski, M.; Slowing, I. I., Solvent-Induced Reversal of Activities between Two Closely Related Heterogeneous Catalysts in the Aldol Reaction. *ACS Catalysis* **2013**, *3*, 265-271. <http://dx.doi.org/10.1021/cs300748g>
6. Bataineh, H.; Pestovsky, O.; Bakac, A., Iron(II) Catalysis in Oxidation of Hydrocarbons with Ozone in Acetonitrile. *ACS Catalysis* **2015**, *5*, 1629-1637. <http://dx.doi.org/10.1021/cs501962m>
7. Eedugurala, N.; Wang, Z.; Chaudhary, U.; Nelson, N.; Kandel, K.; Kobayashi, T.; Slowing, I. I.; Pruski, M.; Sadow, A. D., Mesoporous Silica-Supported Amidozirconium-Catalyzed Carbonyl Hydroboration. *ACS Catalysis* **2015**, *5*, 7399-7414. <http://dx.doi.org/10.1021/acscatal.5b01671>
8. Kandel, K.; Chaudhary, U.; Nelson, N. C.; Slowing, I. I., Synergistic Interaction between Oxides of Copper and Iron for Production of Fatty Alcohols from Fatty Acids. *ACS Catalysis* **2015**, *5*, 6719-6723. <http://dx.doi.org/10.1021/acscatal.5b01664>
9. Nelson, N.; Chaudhary, U.; Kandel, K.; Slowing, I. I., Heterogeneous Multicatalytic System for Single-Pot Oxidation and C-C Coupling Reaction Sequences. *Topics in Catalysis* **2014**, *57*, 1000-1006. <http://dx.doi.org/10.1007/s11244-014-0263-y>
10. Carraher, J. M.; Bakac, A., Generation of Free Oxygen Atoms O(P-3) in Solution by Photolysis of 4-benzoylpyridine N-oxide. *Physical Chemistry Chemical Physics* **2014**, *16*, 19429-19436. <http://dx.doi.org/10.1039/c4cp02751e>
11. Kandel, K.; Anderegg, J. W.; Nelson, N. C.; Chaudhary, U.; Slowing, I. I., Supported Iron Nanoparticles for the Hydrodeoxygenation of Microalgal Oil to Green Diesel. *Journal of Catalysis* **2014**, *314*, 142-148. <http://dx.doi.org/10.1016/j.jcat.2014.04.009>
12. Carraher, J. M.; Ellern, A.; Bakac, A., Preparation and Reactivity of Macrocyclic Rhodium(III) Alkyl Complexes. *Inorganica Chimica Acta* **2014**, *409*, 254-258. <http://dx.doi.org/10.1016/j.ica.2013.09.022>
13. Xu, S.; Manna, K.; Ellern, A.; Sadow, A. D., Mixed N-Heterocyclic Carbene-Bis(oxazolanyl)borato Rhodium and Iridium Complexes in Photochemical and Thermal Oxidative Addition Reactions. *Organometallics* **2014**, *33*, 6840-6860. <http://dx.doi.org/10.1021/om500891h>
14. Carraher, J. M.; Bakac, A., Alkyl Group versus Hydrogen Atom Transfer from Metal Alkyls to Macrocyclic Rhodium Complexes. *Chemical Communications* **2013**, *49*, 6099-6101. <http://dx.doi.org/10.1039/c3cc43472a>
15. Kandel, K.; Althaus, S. M.; Pruski, M.; Slowing, I. I., Supported Hybrid Enzyme-Organocatalysts for Upgrading the Carbon Content of Alcohols. In *Novel Materials for Catalysis and Fuels*

- Processing*, American Chemical Society: **2013**; Vol. 1132, pp 261-271. <http://dx.doi.org/10.1021/bk-2013-1132.ch011>
16. Xu, S.; Magoon, Y.; Reinig, R. R.; Schmidt, B. M.; Ellern, A.; Sadow, A. D., Organometallic Complexes of Bulky, Optically Active, C₃-Symmetric Tris(4S-isopropyl-5,5-dimethyl-2-oxazolinyl)phenylborate (To^{P*}). *Organometallics* **2015**, *34*, 3508-3519. <http://dx.doi.org/10.1021/acs.organomet.5b00225>
 17. Nishiyama, Y.; Kobayashi, T.; Malon, M.; Singappuli-Arachchige, D.; Slowing, I. I.; Pruski, M., Studies of Minute Quantities of Natural Abundance Molecules using 2D Heteronuclear Correlation Spectroscopy under 100 kHz MAS. *Solid State Nuclear Magnetic Resonance* **2015**, *66-67*, 56-61. <http://dx.doi.org/10.1016/j.ssnmr.2015.02.001>
 18. Wang, C. J.; Ackerman, D. M.; Slowing, I. I.; Evans, J. W., Langevin and Fokker-Planck Analyses of Inhibited Molecular Passing Processes Controlling Transport and Reactivity in Nanoporous Materials. *Physical Review Letters* **2014**, *113*, 038301. <http://dx.doi.org/10.1103/PhysRevLett.113.038301>
 19. Wang, J.; Garcia, D. M.; Ackerman, D. M.; Gordon, M. S.; Slowing, I. I.; Kobayashi, T.; Pruski, M.; Evans, J. W., Multi-functionalization of Nanoporous Catalytic Materials to Enhance Reaction Yield: Statistical Mechanical Modeling for Conversion Reactions with Restricted Diffusive Transport. *Materials Research Society Symposium Proceedings Series* **2014**, *1641*, mrsf13-1641-aa08-02. <http://dx.doi.org/10.1557/opl.2014.321>
 20. Kandel, K.; Frederickson, C.; Smith, E. A.; Lee, Y.-J.; Slowing, I. I., Bifunctional Adsorbent-Catalytic Nanoparticles for the Refining of Renewable Feedstocks. *ACS Catalysis* **2013**, *3*, 2750-2758. <http://dx.doi.org/10.1021/cs4008039>

(II) Jointly funded by this grant and other grants with leading intellectual contribution from this grant;

21. Webb, J. D.; Seki, T.; Goldston, J. F.; Pruski, M.; Crudden, C. M., Selective Functionalization of the Mesopores of SBA-15. *Microporous and Mesoporous Materials* **2015**, *203*, 123-131. <http://dx.doi.org/10.1016/j.micromeso.2014.10.032>
22. Kobayashi, T.; Lafon, O.; Thankamony, A. S. L.; Slowing, I. I.; Kandel, K.; Carnevale, D.; Vitzthum, V.; Vezin, H.; Amoureux, J.-P.; Bodenhausen, G.; Pruski, M., Analysis of Sensitivity Enhancement by Dynamic Nuclear Polarization in Solid-state NMR: A Case Study of Functionalized Mesoporous Materials. *Physical Chemistry Chemical Physics* **2013**, *15*, 5553-5562. <http://dx.doi.org/10.1039/c3cp00039g>
23. Kobayashi, T.; Mao, K.; Paluch, P.; Nowak-Krol, A.; Sniechowska, J.; Nishiyama, Y.; Gryko, D. T.; Potrzebowski, M. J.; Pruski, M., Study of Intermolecular Interactions in the Corrole Matrix by Solid-State NMR under 100 kHz MAS and Theoretical Calculations. *Angewandte Chemie-International Edition* **2013**, *52*, 14108-14111. <http://dx.doi.org/10.1002/anie.201305475>
24. Lafon, O.; Thankamony, A. S. L.; Kobayashi, T.; Carnevale, D.; Vitzthum, V.; Slowing, I. I.; Kandel, K.; Vezin, H.; Amoureux, J.-P.; Bodenhausen, G.; Pruski, M., Mesoporous Silica Nanoparticles Loaded with Surfactant: Low Temperature Magic Angle Spinning C-13 and Si-29 NMR Enhanced by Dynamic Nuclear Polarization. *Journal of Physical Chemistry C* **2013**, *117*, 1375-1382. <http://dx.doi.org/10.1021/jp310109s>
25. Perras, F. A.; Kobayashi, T.; Pruski, M., Magnetic Resonance Imaging of DNP Enhancements in a Rotor Spinning at the Magic Angle. *Journal of Magnetic Resonance* **2016**, in press. <http://dx.doi.org/10.1016/j.jmr.2016.01.004>
26. Perras, F. A.; Kobayashi, T.; Pruski, M., Natural Abundance ¹⁷O DNP Two-Dimensional and Surface-Enhanced NMR Spectroscopy. *Journal of the American Chemical Society* **2015**, *137*, 8336-8339. <http://dx.doi.org/10.1021/jacs.5b03905>

27. Perras, F. A.; Kobayashi, T.; Pruski, M., PRESTO Polarization Transfer to Quadrupolar Nuclei: Implications for Dynamic Nuclear Polarization. *Physical Chemistry Chemical Physics* **2015**, *17*, 22616-22622. <http://dx.doi.org/10.1039/c5cp04145g>
28. Perras, F. A.; Chaudhary, U.; Slowing, I. I.; Pruski, M., Probing Surface Hydrogen Bonding and Dynamics by Natural Abundance, Multidimensional, 17O DNP-NMR Spectroscopy. *The Journal of Physical Chemistry C* **2016**. <http://dx.doi.org/10.1021/acs.jpcc.6b02579>
29. Kobayashi, T.; Perras, F. A.; Slowing, I. I.; Sadow, A. D.; Pruski, M., Dynamic Nuclear Polarization Solid-State NMR in Heterogeneous Catalysis Research. *ACS Catalysis* **2015**, *5*, 7055-7062. <http://dx.doi.org/10.1021/acscatal.5b02039>
30. Manna, K.; Everett, W. C.; Schoendorff, G.; Ellern, A.; Windus, T. L.; Sadow, A. D., Highly Enantioselective Zirconium-Catalyzed Cyclization of Aminoalkenes. *Journal of the American Chemical Society* **2013**, *135*, 7235-7250. <http://dx.doi.org/10.1021/ja4000189>
31. Hull, E. A.; West, A. C.; Pestovsky, O.; Kristian, K. E.; Ellern, A.; Dunne, J. F.; Carraher, J. M.; Bakac, A.; Windus, T. L., UV-visible Spectroscopy of Macrocyclic Alkyl, Nitrosyl and Halide Complexes of Cobalt and Rhodium. Experiment and Calculation. *Dalton Transactions* **2015**, *44*, 3811-3816. <http://dx.doi.org/10.1039/C4DT03143A>
32. Xu, S.; Boschen, J. S.; Biswas, A.; Kobayashi, T.; Pruski, M.; Windus, T. L.; Sadow, A. D., Mild Partial Deoxygenation of Esters Catalyzed by an Oxazolinyborate-coordinated Rhodium Silylene. *Dalton Transactions* **2015**, *44*, 15897-15904. <http://dx.doi.org/10.1039/c5dt02844b>
33. Reichert, M. D.; Lin, C. C.; Vela, J., How Robust are Semiconductor Nanorods? Investigating the Stability and Chemical Decomposition Pathways of Photoactive Nanocrystals. *Chemistry of Materials* **2014**, *26*, 3900-3908. <http://dx.doi.org/10.1021/cm500896n>
34. Alvarado, S. R.; Guo, Y. J.; Ruberu, T. P. A.; Tavasoli, E.; Vela, J., Inorganic Chemistry Solutions to Semiconductor Nanocrystal Problems. *Coordination Chemistry Reviews* **2014**, *263*, 182-196. <http://dx.doi.org/10.1016/j.ccr.2013.09.001>
35. Xu, S.; Everett, W. C.; Ellern, A.; Windus, T. L.; Sadow, A. D., Oxygen Insertion Reactions of Mixed N-Heterocyclic Carbene-oxazolinyborato Zinc Alkyl Complexes. *Dalton Transactions* **2014**, *43*, 14368-14376. <http://dx.doi.org/10.1039/C4DT01011F>
36. Bakac, A.; Pestovsky, O.; Durfey, B. L.; Kristian, K. E., Kinetics and thermodynamics of nitric oxide binding to transition metal complexes. Relationship to dioxygen binding. *Chemical Science* **2013**, *4*, 2185-2192. <http://dx.doi.org/10.1039/c3sc50157d>
37. Vela, J., Molecular Chemistry to the Fore: New Insights into the Fascinating World of Photoactive Colloidal Semiconductor Nanocrystals. *Journal of Physical Chemistry Letters* **2013**, *4*, 653-668. <http://dx.doi.org/10.1021/jz302100r>
38. Reinig, R. R.; Mukherjee, D.; Weinstein, Z. B.; Xie, W.; Albright, T.; Baird, B.; Gray, T. S.; Ellern, A.; Miller, G. J.; Winter, A. H.; Bud'ko, S. L.; Sadow, A. D., Synthesis and Oxidation Catalysis of [Tris(oxazoliny)borato]cobalt(II) Scorpionates. *European Journal of Inorganic Chemistry* **2016**. doi: <http://dx.doi.org/10.1002/ejic.201600237>
39. Johnson, R. L.; Perras, F. A.; Kobayashi, T.; Schwartz, T. J.; Dumesic, J. A.; Shanks, B. H.; Pruski, M., Identifying low-coverage surface species on supported noble metal nanoparticle catalysts by DNP-NMR. *Chemical Communications* **2016**, *52*, 1859-1862. <http://dx.doi.org/10.1039/C5CC06788J>
40. Mao, K.; Kennedy, G. J.; Althaus, S. M.; Pruski, M., Determination of the Average Aromatic Cluster Size of Fossil Fuels by Solid-State NMR at High Magnetic Field. *Energy & Fuels* **2013**, *27*, 760-763. <http://dx.doi.org/10.1021/ef301804p>

(III) Jointly funded by this grant and other grants with relatively minor intellectual contribution from this grant

41. Guo, Z.; Kobayashi, T.; Wang, L.-L.; Goh, T. W.; Xiao, C.; Caporini, M. A.; Rosay, M.; Johnson, D. D.; Pruski, M.; Huang, W., Selective Host-Guest Interaction between Metal Ions and Metal-Organic Frameworks Using Dynamic Nuclear Polarization Enhanced Solid-State NMR

- Spectroscopy. *Chemistry-A European Journal* **2014**, *20*, 16308-16313. <http://dx.doi.org/10.1002/chem.201403884>
42. de Lima Batista, A. P.; Zahariev, F.; Slowing, I. I.; Braga, A. A. C.; Ornellas, F. R.; Gordon, M. S., Silanol-Assisted Carbinolamine Formation in an Amine-Functionalized Mesoporous Silica Surface: Theoretical Investigation by Fragmentation Methods. *Journal of Physical Chemistry B* **2016**, in press. <http://dx.doi.org/10.1021/acs.jpcc.5b08446>.
43. Gu, W.; Stalzer, M. M.; Nicholas, C. P.; Bhattacharyya, A.; Motta, A.; Gallagher, J. R.; Zhang, G.; Miller, J. T.; Kobayashi, T.; Pruski, M.; Delferro, M.; Marks, T. J., Benzene Selectivity in Competitive Arene Hydrogenation: Effects of Single-Site Catalyst···Acidic Oxide Surface Binding Geometry. *Journal of the American Chemical Society* **2015**, *137*, 6770-6780. <http://dx.doi.org/10.1021/jacs.5b03254>
44. Mouat, A. R.; George, C.; Kobayashi, T.; Pruski, M.; van Duyne, R. P.; Marks, T. J.; Stair, P. C., Highly Dispersed SiO_x/Al₂O₃ Catalysts Illuminate the Reactivity of Isolated Silanol Sites. *Angewandte Chemie-International Edition* **2015**, *54*, 13346-13351. <http://dx.doi.org/10.1002/anie.201505452>
45. Hara, K.; Kobayashi, H.; Komanoya, T.; Huang, S.-J.; Pruski, M.; Fukuoka, A., Supported Metal Catalysts for Green Reactions. In *RSC Green Chemistry*, Clark, J. H.; Kraus, G.; Stankiewicz, A.; Seidl, P.; Hu, C., Eds. Royal Society of Chemistry: **2015**; Vol. 33, pp 61-76. <http://dx.doi.org/10.1039/9781849737494-00061>
46. Tanabe, K. K.; Siladke, N. A.; Broderick, E. M.; Kobayashi, T.; Goldston, J. F.; Weston, M. H.; Farha, O. K.; Hupp, J. T.; Pruski, M.; Mader, E. A.; Johnson, M. J. A.; Nguyen, S. T., Stabilizing Unstable Species through Single-Site Isolation: A Catalytically Active Ta-V Trialkyl in a Porous Organic Polymer. *Chemical Science* **2013**, *4*, 2483-2489. <http://dx.doi.org/10.1039/c3sc22268c>
47. Fang, X. K.; Hansen, L.; Haso, F.; Yin, P. C.; Pandey, A.; Engelhardt, L.; Slowing, I.; Li, T.; Liu, T. B.; Luban, M.; Johnston, D. C., {Mo₂₄Fe₁₂} Macrocycles: Anion Templatation with Large Polyoxometalate Guests. *Angewandte Chemie-International Edition* **2013**, *52*, 10500-10504. <http://dx.doi.org/10.1002/anie.201304887>
48. Opembe, N. N.; Guild, C.; King'onde, C.; Nelson, N. C.; Slowing, I. I.; Suib, S. L., Vapor-Phase Oxidation of Benzyl Alcohol Using Manganese Oxide Octahedral Molecular Sieves (OMS-2). *Industrial & Engineering Chemistry Research* **2014**, *53*, 19044-19051. <http://dx.doi.org/10.1021/ie5024639>

Neil M. Schweitzer

The CleanCat Core Facility – a Facilitator and Educator in Catalysis Research

Neil M. Schweitzer, Randall Q. Snurr, Peter C. Stair

Northwestern University, Center for Catalysis and Surface Science

Presentation Abstract

The Clean Catalysis (CleanCat) Core Facility at Northwestern University is dedicated to aiding investigators and students in the advancement of understanding the catalytic function of materials for environmental and energy processes. Supported by the Center for Catalysis and Surface Science (CCSS) and perhaps the first of its kind in the United States, the CleanCat lab has been instrumental in the cross cutting efforts of ICEP. It serves as a centralized location where students with vastly different expertise can both learn about experimental techniques used in catalysis research and also get hands-on experience performing such experiments. **We not only train students to use equipment, we teach students how to collect data that answers their research questions.** This poster demonstrates CleanCat's dual role in ICEP as both facilitator and educator in catalysis research.

As a facilitator, CleanCat provides lab space, equipment, and expertise required to perform both standard and difficult experiments. For example, we helped ICEP researchers construct a reactor to study vapor phase cyclohexene epoxidation on a mesoporous TS-1 using vapor phase hydrogen peroxide. Extensive kinetic studies yielded valuable insight into the epoxidation mechanism, suggesting that competitive co-adsorption between hydrogen peroxide and water on the titania site control the observed kinetic parameters. The true kinetic parameters for these reactions can only be determined under specific experimental conditions.

As educator, CleanCat staff has organized a seminar series entitled: "Modern Techniques in Heterogeneous Catalysis." The seminar discusses some fundamental concepts, but focuses more on practical aspects of experimentation that comes with experience: how experiments are performed, why they are performed certain ways, what are the limitations of certain techniques, and the limits of data analysis and interpretation. The underlying goal is to give students 1) a better understanding of instrumentation they typically run as a "black box" and 2) to help students critically evaluate data presented in literature.

**Unraveling Reforming Reactions over Ni-CeO_x Catalysts:
Importance of Metal-Oxide Interactions in Chemical Conversion**

Sanjaya D. Senanayake, Zongyuan Liu, Si Luo, Iradwikanari Waluyo, David C. Grinter, Dario J. Stacchiola, Jose A. Rodriguez
Chemistry Department, Brookhaven National Laboratory
Upton, NY 11973 (USA)

Presentation Abstract

We have studied several conversion reactions including Steam Reforming (SR: $C_2H_5OH+3H_2O\rightarrow 2CO_2+6H_2$) and Dry Reforming (DRM: $CH_4+CO_2\rightarrow 2CO+2H_2$) over Ni-CeO_x powder and model catalysts to elucidate the active species and reaction mechanism utilizing *in situ* experimental methods including hard X-ray spectroscopy/scattering (XRD/EXAFS) and soft X-ray and infrared spectroscopy (AP-XPS/RAIRS). We have identified strong interactions between small Ni nanoparticles (Ni⁰/Ni^{δ+}) and reduced CeO_x surfaces (Ce⁴⁺/Ce³⁺) particularly under heavily reducing catalytic environments. The chemical state of Ni and the electronic effects that result are especially important for catalytic chemistry. This metal-oxide interaction is also important for the activation of C-C, C-H, O-C-O and O-H bonds towards the dissociation of challenging reactants. Properties typical for bulk Ni can be mitigated by sustaining the interaction between Ni and the Ceria support, including methanation, particle sintering, coke formation and encapsulation. Strategies to improve stability of Ni-CeO_x catalysts have been successfully tested including the synthesis of solid solutions (Ni_xCe_yO_z) where Ni is protected as a dopant inside CeO_x lattice or with the incorporation of interfacial agents such as W, Ti that stabilize metal-oxide interactions.

1. Zhou et al. *Angewandte Chemie* 122 (50), (2010) 9874-9878.
2. Senanayake et al. *Topics in Catalysis* 54 (1-4), (2011) 34-41.
3. Xu et al. *ACS Catalysis* 3 (5), (2013) 975-984.
4. Carrasco et al. *Angewandte Chemie* 54 (13), (2015) 3917-3921.
5. Liu et al. *The Journal of Physical Chemistry C* 119 (32), (2015) 18248-18256.
6. Liu et al. *Physical Chemistry Chemical Physics* (2016) 10.1039/C6CP01212D.
7. Liu et al. *Angewandte Chemie* (2016) 10.1002/ange.201602489.

Achieving enzyme-like behavior with amino acids and peptides in the outer coordination sphere of hydrogenase mimics

Wendy J. Shaw, Nilusha Borolugodage, Arnab Dutta, John Roberts
Pacific Northwest National Laboratory

Presentation Abstract and Recent Progress

Hydrogenases interconvert H_2 and protons at high rates and with high energy efficiencies, providing inspiration for the development of molecular catalysts. Studies designed to determine how the protein scaffold can influence a catalytically active site have led to the synthesis of amino acid derivatives of $[Ni(P^R_2N^{R'}_2)_2]^{2+}$ complexes, $[Ni(P^{Cy}_2N^{Amino\ acid}_2)_2]^{2+}$ (for H_2 oxidation) and $[Ni(P^{Ph}_2N^{Ph-Amino\ acid}_2)_2]^{2+}$ (for H_2 production). For H_2 oxidation catalysts, the amino acids render the complexes water soluble, and the resulting catalysts have faster rates and significantly lower overpotentials than the unmodified complexes. Reminiscent of enzymes, electrochemical reversibility is achieved while fast rates are maintained (Figure 1, left). The influence of the amino acids on these catalytic properties is proposed to result from directly transferring protons via the carboxylic acid groups (Figure 1, right) as well as interactions between the side chain groups such as guanidinium or aromatic groups that result in structural modifications to facilitate H_2 addition and electron transfer. These observations demonstrate that outer coordination sphere amino acids work in synergy with the active site and can play an equally important role for synthetic molecular electrocatalysts as the protein scaffold does for redox active enzymes. Moving forward, the principles learned here will be applied to CO_2 hydrogenation catalysts, with some initial results demonstrating feasibility.

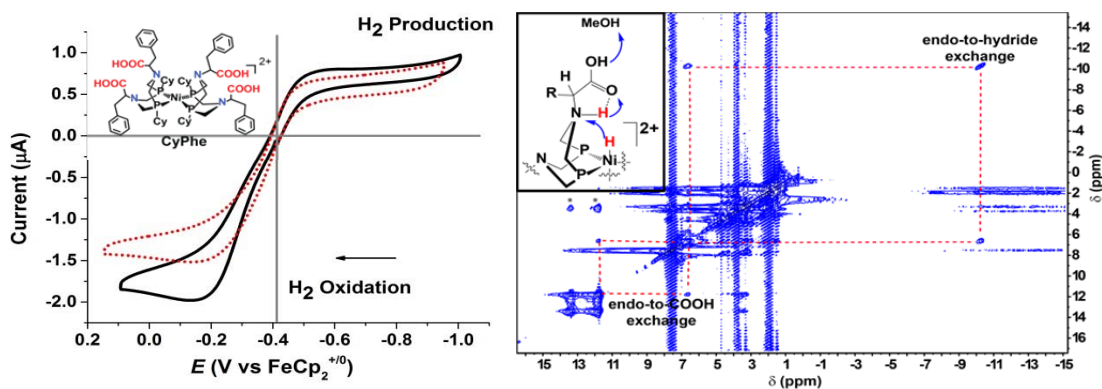


Figure 1. (Left) Electrochemical reversibility was achieved at room temperature for $[Ni(P^{Cy}_2N^{Phe}_2)_2]^{2+}$ (Cy=cyclohexyl, Phe=phenylalanine). This behavior is seldom observed in molecular catalysts and is reminiscent of the behavior in enzymes. (Right) NMR EXSY data confirm that the $-COOH$ groups in the outer

Grant or FWP Number: Low-Temperature Catalytic Routes for Energy Carriers via Spatial and Chemical Organization, 47319

PI: Johannes Lercher

Postdoc(s): Nilusha Boralugodage

Student(s): NA

Publications Acknowledging this Grant in 2013-2016

(I) *Exclusively funded by this grant:*

1. Nilusha Priyadarshani, Bojana Ginovska, J. Timothy Bays, John C. Linehan, **Wendy J. Shaw**. "Photoswitching a molecular catalyst to regulate CO₂ hydrogenation", *Dalton Transactions*, **2015**, 44, 14854-14864. DOI: 10.1039/C5DT01649E
2. Garry W. Buchko, Avijita Jain, Matthew L. Reback, **Wendy J. Shaw**. "Structural Characterization of the Model Amphipathic Peptide Ac-LKKLLKLLKLLKLL-NH₂ in Aqueous Solution and with 2,2,2-trifluoroethanol and 1,1,1,3,3,3-hexafluoroisopropanol." *Canadian Journal of Chemistry*, **2013**, 91,406-413.

(II) *Jointly funded by this grant and other grants with leading intellectual contribution from this grant:*

1. Nilusha Priyadarshani, Arnab Dutta, Bojana Ginovska, Garry W. Buchko, Molly O'Hagan, Simone Raugei, and **Wendy J. Shaw**. "Room temperature reversible electrocatalytic H₂ oxidation/production achieved with molecular complexes containing aromatic amino acids in the outer coordination sphere", *ACS Catalysis*, **2016**, Submitted.
2. (Invited) Matthew L. Reback, Bojana Ginovska, Garry W. Buchko, Arnab Dutta, Nilusha Priyadarshani, Brandon L. Kier, Monte L. Helm, Simone Raugei, and **Wendy J. Shaw**. "Room temperature reversible electrocatalytic H₂ oxidation/production achieved with molecular complexes containing aromatic amino acids in the outer coordination sphere", *Journal of Coordination Chemistry*, **2016**, Accepted.
3. Adam J. Cornish, Bojana Ginovska, Adam Thelen, Julio C. S. da Silva, Thereza A. Soares, Simone Raugei, Michel Dupuis, **Wendy J. Shaw***, Eric L. Hegg*, "Single amino Acid modifications reveal additional controls on the proton pathway of [FeFe]-hydrogenase", *Biochemistry*, **2016**, Accepted.
4. (Invited-Book Chapter) Bojana Ginovska, Simone Raugei, and **Wendy J. Shaw**. "Assessing proton transport and correlation with electron transport in hydrogenases," *Methods in Enzymology Computational Approaches for studying Enzyme Mechanism*, **2016**, Accepted
5. (Invited) Arnab Dutta, John A. S. Roberts, Simone Raugei, and **Wendy J. Shaw**. "Optimizing conditions for utilization of an H₂ oxidation catalyst with outer coordination sphere functionalities", *Dalton Transactions (Special Issue: New Talent America)*, **2016**, Published on line. DOI:10.1039/C6DT00280C
6. Arnab Dutta, Sheri Lense, John A. S. Roberts, Monte L. Helm, and **Wendy J. Shaw**. "The role of solvent and an outer coordination sphere on H₂ oxidation using

$[\text{Ni}(\text{P}^{\text{Cy}}_2\text{N}^{\text{Pyz}}_2)_2]^{2+}$ ”, *European Journal of Inorganic Chemistry*, **2015**, 31, 5218-5225.
DOI:10.1002/ejic.201500732

7. Rodriguez-Macia, Arnab Dutta, Wolfgang Lubitz, **Wendy J. Shaw**, Olaf Rudiger, “Direct comparison of the performance of a bio-inspired synthetic Ni-catalyst and a [NiFe]-hydrogenase covalently attached to electrodes.” *Angewandte Chemie International Edition*, **2015**, 54, 12303-12307. DOI: 10.1002/anie.201502364
8. Arnab Dutta, Daniel L. DuBois, John A. S. Roberts*[†], and **Wendy J. Shaw***, “Amino acid modified Ni catalyst exhibits reversible H₂ oxidation/production over a broad pH range at elevated temperatures.” *Proceedings of the National Academy of Sciences*, **2014**, 111, 16286-16291. DOI:10.1073/pnas.1416381111
9. (Invited) Bojana Ginovska-Pangovska, Arnab Dutta, Matthew L. Reback, John C. Linehan, **Wendy J. Shaw**, “Beyond the active site: the impact of the outer coordination sphere on electrocatalysts for hydrogen production and oxidation,” *Accounts of Chemical Research*, **2014**, 47, 2621-2630. DOI:10.1021/ar5001742
10. Arnab Dutta, Sheri Lense, John A. S. Roberts, **Wendy J. Shaw**, “Learning from Nature:Equation Chapter 1 Section 1 Arg-Arg pairing enhances H₂ oxidation catalyst,” *Angewandte Chemie*, **2014**, 53, 6487-6491.
11. J. Tim Bays, Nilusha Priyadarshani, Matthew S. Jeletic, Elliott B. Hulley, Deanna L. Miller, John C. Linehan, **Wendy J. Shaw**. “The influence of the second and outer coordination spheres on Rh(diphosphine)₂ CO₂ hydrogenation catalysts.” *ACS Catalysis* **2014**;4:3663-70. DOI:10.1021/cs5009199
12. Matthew L. Reback, Garry W. Buchko, Brandon L. Kier, Bojana Ginovska-Pangovska, Yijia Xiong, John A.S. Roberts, Christina M. Sorensen, Simone Raugei, Thomas C. Squier, **Wendy J. Shaw**, “Enzyme design from the bottom-up: an active nickel electrocatalyst with a peptide outer coordination sphere.”, *Chemistry a European Journal*, **2014**, 20,1510-1514. DOI:10.1002/chem.201303976
13. Sheri Lense, Arnab Dutta, John A. S. Roberts, **Wendy J. Shaw**, “A proton channel allows a hydrogen oxidation catalyst to operate at a moderate overpotential with water acting as a base.” *Chemical Communications*, **2014**, 50 (7), 792-795.
DOI:10.1039/C3CC46829A
14. Bojana Ginovska-Pangovska, Ming-Hsun Ho, Yuhui Cheng, Michel Dupuis, Simone Raugei, **Wendy J. Shaw**. “Molecular dynamics study of the proposed proton transport channels in [FeFe]-Hydrogenase.” *Biochimica Et Biophysica Acta:Bioenergetics*, **2014**, 1837, 131-138. DOI:10.1016/j.bbatio.2013.08.004
15. **Wendy J. Shaw**, Monte L. Helm, Daniel L. DuBois. “A modular, energy-based approach to the development of nickel containing molecular electrocatalysts for hydrogen production and oxidation.” *Biochimica et Biophysica Acta*, **2013**, 1827, 1123-1139.
16. (Selected as VIP and for cover) Matthew L. Reback, Bojana Ginovska-Pangovska, Ming-Hsun Ho, Avijita Jain, Thomas C. Squier, Simone Raugei, John A. S. Roberts, **Wendy J. Shaw**. “The Role of a Dipeptide Outer-Coordination Sphere on H₂ Production Catalysts: Influence on Catalytic Rates and Electron Transfer.” *Chemistry: A European Journal*. **2013**, 19, 1928-1941.

17. Brandon R. Galan, Matthew L. Reback, Avijita Jain, Aaron M. Appel, **Wendy J. Shaw**. “Electrocatalytic Oxidation of Formate Using $[\text{Ni}(\text{PR}_2\text{NR}'_2)_2]^{2+}$ Complexes: Effect of Ligands Modified with Amino Acids.”, *European Journal of Inorganic Chemistry*, **2013**, 5366-5371.
18. Arnab Dutta, Sheri Lense, Jianbo Hou, Mark H. Engelhard, John A. S. Roberts, **Wendy J. Shaw**, “Proton Channel Enables H_2 oxidation and production for a Water-Soluble Ni Catalyst,” *Journal of the American Chemical Society*, **2013**, 135, 18490-18496.

(III) *Jointly funded by this grant and other grants with relatively minor intellectual contribution from this grant:*

1. Ming-Hsun Ho, Molly O’Hagan, Michel Dupuis, Daniel L. DuBois, R. Morris Bullock, **Wendy J. Shaw**, and Simone Raugei, “Water-assisted proton delivery and removal in bio-inspired hydrogen production catalysts”, *Dalton Transactions*, **2015**, 44, 10969-10979. DOI:10.1039/C5DT00782H
2. Jianbo Hou, Ming Fang, Allan J.P. Cardenas, **Wendy J. Shaw**, Monte L. Helm, R. Morris Bullock, John A.S. Roberts, Molly O’Hagan, “Electrocatalytic H_2 production with a turnover frequency $>10^7 \text{ s}^{-1}$: medium provides increase in rate but not overpotential,” *Energy and Environmental Science*, **2014**, 7, 4013-4017. DOI:10.1039/c4ee01899k
3. James A. Franz, Molly O’Hagan, Ming-Hsun Ho, Tianbio Liu, Monte Helm, Sheri Lense, Daniel L. DuBois, **Wendy J. Shaw**, Aaron M. Appel, Simone Raugei, R. Morris Bullock, “Conformational Dynamics of $[\text{Ni}(\text{P}^{\text{R}}_2\text{N}^{\text{R}'_2})]^{n+}$ Hydrogen Production and Oxidation Catalysts.”, *Organometallics*, **2013**, 32, 7034-7042.

Understanding and Controlling the Effects of Surface Species on Catalytic Processes within Mesoporous Silica Supports

Takeshi Kobayashi, Marek Pruski, Aaron D. Sadow, Igor I. Slowing,
Mark S. Gordon, Dilini Singappuli-Arachchige, J. Sebastian Manzano, Ana P. Lima
US DOE Ames Laboratory/Iowa State University, Ames, IA 50011-3111

This work is part of FWP AL-03-380-011: “Homogeneous and Interfacial Catalysis in 3D Controlled Environments”. For more details please see abstract by Aaron D. Sadow.

Presentation Abstract

The effects of surface chemistry of organofunctionalized mesoporous silica on the performance of catalytic reactions were investigated using computational and experimental methods.

Experimental studies by us and other groups have shown that surface silanols play an active role in the aldol and related condensations catalyzed by amines on mesoporous silica. Kinetic and spectroscopic evidence suggested that surface Si-OH groups activate substrates and act as proton shuttles between reaction intermediates. These hypotheses were further evaluated via computational modeling. The initial step of the aldol condensation catalyzed by amines on silica was modeled using a large molecular cluster (1718 atoms, $\text{Si}_{1392}\text{O}_{958}\text{C}_6\text{NH}_{361}$) with surface integrated molecular orbital/molecular mechanics (SIMOMM) and fragment molecular orbital (FMO) methods. Comparison of the reaction pathways with and without silanol participation showed that silanols induce a large drop in activation barriers (around 20 kcal/mol calculated by MP2//DFT/M06-2X), and suggested the mechanism involves the silanol groups forming and breaking covalent bonds in the carbinolamine step of the reaction. Further work is in progress to model the entire reaction mechanism.

Modification of the surface of mesoporous silica with organic moieties can be used to control local environments and induce solvent-like effects on supported catalysts. To better understand these pseudo-solvent effects, we explored structure-property relationships between surface organic modifiers and Stokes shifts of a solvatochromic dye. Comparing the shifts of the dye in the materials and in protic solvents allowed producing a local polarity scale for functionalized pores. The measurements were performed in aqueous suspensions of mesoporous particles, demonstrating that the dielectric properties within the functionalized pores were different than those of the bulk solvent. The importance of controlling pore polarity was evidenced by fine-tuning the catalytic activity of TEMPO in the aerobic oxidation of furfuryl alcohol to furfural in water. An inverse relationship was found between pore polarity and catalytic activity of TEMPO impregnated in the functionalized pores. This observation was explained based on the differences in stabilization of the oxoammonium intermediate and the activated complex of the rate limiting step by the local environment. These findings provide fundamental tools for the rational design of catalysts with controlled local environments and tunable activity.

**Highly Dispersed SiO_x/Al₂O₃ Materials Illuminate
the Reactivity of Isolated Silanol Sites**

Aidan R. Mouat¹, Cassandra George¹, Takeshi Kobayashi², Marek Pruski², Richard P. Van Dwyne¹, Tobin J. Marks¹, **Peter C. Stair**¹

¹Department of Chemistry, Northwestern University, Evanston, IL 60208

²Ames Laboratory & Department of Chemistry, Iowa State University, Ames, IA 50011

Presentation Abstract

By reacting γ -Al₂O₃ substrates with tetraethylorthosilicate (TEOS) vapor at low temperatures, the alumina surface can be selectively modified with isolated SiO_x sites. Surface saturation of these silicon species is reached at a density of 2.7 Si/nm². The self-limiting nature of the deposition reaction suggests it occurs preferentially at a single reactive site on the surface, leading to the formation of isolated $\equiv\text{Si}(\text{OH})$ sites. These materials were characterized by PXRD, XPS, DRIFTS of adsorbed NH₃, CO, and pyridine, and ²⁹Si and ²⁷Al DNP-enhanced solid-state NMR spectroscopy. NMR indicates that isolated Brønsted acid sites of the form (-AlO)₃Si(OH) are produced on calcination. DNP-enhanced ²⁹Si-²⁹Si double quantum/single quantum (DQ/SQ) correlation NMR spectroscopy confirmed that the silanols are, indeed, isolated. In-situ DRIFTS measurements indicate that the TEOS reacts preferentially at strong Lewis acid sites on the alumina surface. The catalytic competence of the silanol Brønsted acid sites was evaluated using the liquid-phase dehydration of cyclohexanol to cyclohexene as a diagnostic reaction. The isolated silanol sites exhibit up to 3.5-fold higher specific activity than the parent γ -Al₂O₃ substrate with identical selectivity.

Institute for Catalysis in Energy Processes (ICEP)

Additional PIs: M. Bedzyk, L. Broadbelt, O. Farha, F. Geiger, J. Hupp, H. Kung, M. Kung, L. Marks, T. Marks, S. Nguyen, J. Notestein, K. Poepelmeier, G. Schatz, N. Schweitzer, R. Snurr, R. Van Duyne, E. Weitz

Contact: Peter C. Stair, Department of Chemistry, Northwestern University, 2145 Sheridan Road, Evanston, IL 60208-3113, pstair@northwestern.edu

Background

Most commercial catalysts are inhomogeneous, containing numerous different possible active sites. Some of these are spectators, playing no role; some are active for desirable reactions, others lead to undesirable side products. Since direct interrogation of individual active sites in an inhomogeneous system is rarely possible, in almost all cases only indirect evidence about the key sites and steps can be gleaned from experimental and theoretical models. However, more than this will be required to achieve truly disruptive advances in our understanding of important catalytic processes. An overarching ICEP goal is targeted research to address *the inhomogeneity challenge in heterogeneous catalysis*. The ICEP vision is to *create catalysts with unique types of active sites in an atomistically controlled fashion* so that we can move beyond indirect evidence to definitive, control-oriented science. We do not target optimization of specific commercial reactions, rather focus on how the different types of active sites we create can alter catalytic activity and selectivity for the C-C, C-H, and C-O transformations of interest in energy applications. Specific probe reactions have been selected to provide a detailed chemical view of catalyst uniformity.

ICEP Organization

The ICEP team is organized into three complementary and interacting thrusts, each of which focuses on different classes of materials systems.

Thrust I. *Understanding and Control of Catalyst Performance by Metal-Oxide Nanoparticle System Design.* The focus is on creation and control of supported metal nanoparticles using new strategies for designing the interaction of nanoparticles with oxide supports. We borrow from well-developed concepts in the fields of epitaxy and nanoscale engineering as well as new strategies for controlling the active sites on nanoparticles using advanced fabrication methods such as Atomic Layer Deposition (ALD).

ICEP Thrusts and Sub-Thrusts

I. Supported Nanoparticles	II. Oxide-Oxide Interfaces	III. Catalytic Environments
Nanoparticle control by the substrate (I.1)	Tuning nanocrystalline supports (II.1)	Creating new electrophiles (III.1)
Extended control of active sites (I.2)	Precursor design & deposition strategies (II.2)	Organometallic complexes supported on MOFs (III.2)
	Nanocavity Structures (II.3)	Cage-like environments (III.3)
		Metal-siloxane complexes (III.4)

Thrust II. *Atom-Scale Control of Critical Oxide-Oxide Interfaces* makes use of three strategies: A) Lattice and electronic tuning of nanocrystalline supports, B) Novel precursor

design and implementation, and C) Novel oxide nanocavity structures. These three complementary approaches seek to impart control at the length scales appropriate for oxide catalysis: atomic scale control of the support and the active oxide in approaches A and B, and nm-scale control in approach C.

Thrust III. Understanding-Based Manipulation of Catalytic Environments draws inspiration from homogeneous organometallic and enzyme catalysis and uses soft matter ligand concepts analogous to the effects of inner or outer sphere ligands in coordination chemistry.

Examples of Recent Results:

Thrust I: Understanding and Control of Catalyst Performance by Metal-Oxide Nanoparticle System Design.

Key to the ICEP effort is achieving suitable quantities of different shape-controlled oxide supports. The groups of **Bedzyk**, **L. Marks** and **Poepelmeier** have made significant steps forward. Strontium titanate nano-rhombic dodecahedra have been grown using a glycerol-mediated hydrothermal synthesis. These are dominated by $\{110\}$ planes which are TiO_2 rich with a surface reconstruction that involves tetrahedrally-coordinated TiO_4 units, **Figure 1**. These contrast to existing nanocuboid strontium titanate nanoparticles that are dominated by $\{001\}$ surfaces which are also TiO_2 rich but with octahedral TiO_5 units. We now have two fundamentally different surface structures in supports which are readily fabricated for catalytic testing. The group is now moving forward with ALD deposition of Pd and Pt nanoparticles (NP) and catalytic testing, with **Stair**, and the ICEP team.

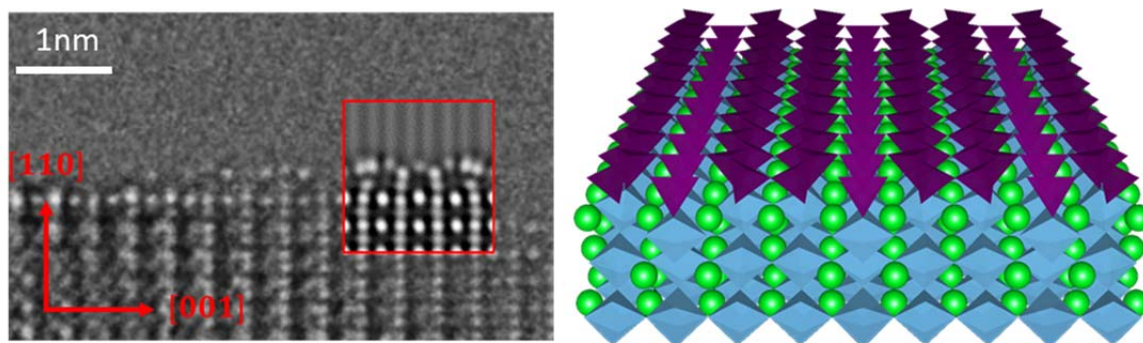


Figure 1. Surface of $\{110\}$ faceted nanoparticles along the $[1\bar{1}0]$ zone axis, inset with an image simulation of the (3×1) reconstruction. The polyhedral atomic model on the right shows the tetrahedral coordination of the TiO_2 -rich surface.

A second set of research achievements focused on what we call “artificial SMSI”, i.e., developing new approaches to oxide/metal-NP structures that mimic conventional SMSI effects, but with more control so we can test in detail models for effects that are most important. One project involved **L. Marks**, **Poepelmeier** and **Stair** in ALD growth of both Al_2O_3 and TiO_2 onto conventional SrTiO_3 supports; we find significant promotion of selective acrolein hydrogenation to the unsaturated alcohol with a TiO_2 overcoat whereas Al_2O_3 has no effect. In parallel work, **Kung** demonstrated that decorating 1-2 nm Au nanoparticles with TiO_x clusters significantly changes the activity and selectivity of 2-propanol decomposition. As shown in **Table 1**, the individual components of Au NPs on a SiO_2 support and a SiO_2 support decorated

with TiO_x clusters ($\text{TiO}_x/\text{SiO}_2$) show low activities. When Au NPs are decorated with TiO_x clusters ($\text{TiO}_x/[\text{Au}/\text{SiO}_2]$ in **Table 1**), activities were high and acetone is the major product, with propene selectivity increasing with increasing TiO_x coverage ($3\text{TiO}_x/[\text{Au}/\text{SiO}_2]$ in **Table 1**).

Table 1. 2-Propanol decomposition at 180°C.

Catalyst	i-PrOH Conv. %	Selectivity %	
		Acetone	C_3H_6
$\text{TiO}_x/\text{SiO}_2$	6.6	0	100
Au/SiO_2	2.7	45	55
$\text{TiO}_x/[\text{Au}/\text{SiO}_2]$	45.5	86	14
$3\text{TiO}_x/[\text{Au}/\text{SiO}_2]$	34.7	34	66

A third area where the team has made significant progress is in creating/transforming single atom catalysts to ones containing a very limited number of metal atoms. In several papers involving **Delferro, L. Marks, T. Marks, Schweitzer, and Stair** we successfully combined sophisticated organometallic synthesis with detailed catalytic testing, chemical spectroscopies such as high-resolution solid state NMR and IR spectroscopy that are sensitive to precursor ligation and metal atom cluster size, with aberration-corrected TEM. The first significant result was for Pt catalysts and involved combining IR spectroscopy with aberration-corrected microscopy to demonstrate that the spectroscopy was exquisitely sensitive to whether there were large numbers of single atoms. Armed with these data, we unequivocally showed that single Pt atoms are not important for CO oxidation, only nanoparticles. More recently the group has taken this further and is now using combined aberration-corrected microscopy and IR spectroscopies as a tool to guide synthetic strategies for stabilizing single atoms and in the future, clusters with only a few atoms created in high yields. As an example, **Figure 2** shows that ALD-ZnO overcoats significantly reduce sintering. These first steps are opening doors to new ways of determining in detail how cluster size and environment effect catalytic performance, unravelling the key science that can lead to better catalysts in the future *by design*.

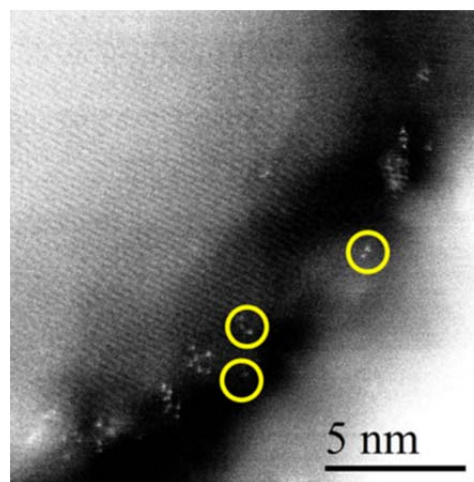


Figure 2. High angle annular dark field image of Pt single atoms on an Al_2O_3 support with 20 cycles of ZnO ALD.

Thrust II: Atom-Scale Control of Critical Oxide-Oxide Interfaces

In parallel with Thrust I activities, ICEP researchers have focused on understanding and controlling speciation of oxides grafted onto nanocrystalline supports. The inability to directly assess the size of supported MO_x domains is a long standing challenge in supported oxide catalysis. This arises in part from the difficulty in directly visualizing many important supported oxide catalysts. A collaboration between **Notestein** and **L. Marks** utilizes TiO_2 (anatase) nanosheets with lateral dimensions of order 100 nm, but thickness of <10 nm as supports. The very thin, regular structure, allows aberration-corrected TEM to image atomic distributions of suitably chosen supported oxides. Ta was deposited using two different precursors (Ta-

calixarene and Ta ethoxide) and imaged after ligand removal by ozone. Some materials were also overcoated with Al₂O₃ by ALD prior to removal of the Ta precursor ligands, thus generating nanocavities in the alumina layer. Ta was chosen for contrast between Ta and Ti. Image (**Figure 3**) analysis enables a direct comparison of TaOx dispersion arising from different precursors and demonstrates that Al₂O₃ deposition does not alter the underlying TaOx dispersion. Ta atoms act as markers for nanocavities that cannot be imaged directly.

A second research area is the development of new precursors to control metal oxide structure in supported oxide catalysts. One example is the developing new oxo precursors for Mo(VI) and W(VI) ALD by **T. Marks** and **Stair**. The Mo amidate precursor in **Figure 4** contains metal-oxo functionalities not previously available for ALD. Films or isolated domains can be synthesized by choice of deposition conditions.

These supported Mo and W oxides are acid and redox catalysts with very strong structure sensitivity, and the precursors will help understand and control their structure, paralleling similar advances made possible by ALD synthesis of supported VOx by this group.

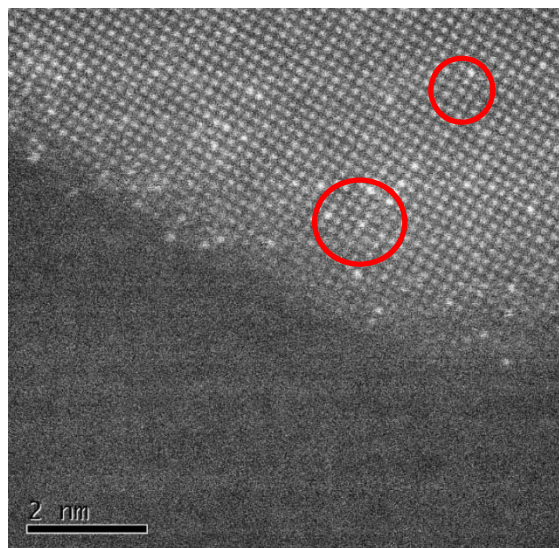


Figure 3. HAADF of Ta on a TiO₂ (anatase) nanosheet. Ta was deposited at an average surface density of 0.3 Ta.nm⁻². Note that the entire sheet can be imaged. Surface includes isolated Ta as well as small clusters (examples circled).

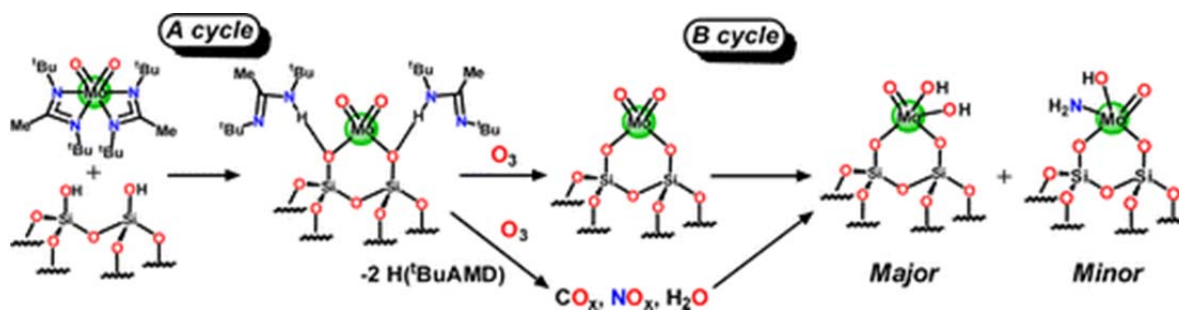


Figure 4. Molybdenum amidate as the first dioxo precursor optimized for atomic layer deposition. As shown here, using O₃ in the B cycle of deposition leads to growth of oxide and oxynitride films.

ICEP researchers are also developing new materials based on a ‘nanocavity’ platform. These materials are proposed to consist of <2 nm diameter cavities in <2 nm thick oxide layers, supported on a carrier oxide. Cavities are generated using an organic template, and the oxide film can be generated by ALD, or as now shown by **Notestein**, controlled deposition of siloxane precursors to grow silica shells. **Figure 5** shows ~2 nm SiO₂ shells conformally grown on Al₂O₃ from tetraethoxy orthosilicate (TEOS). Unexpectedly, these materials are strong acids, capable of cracking alkyl benzenes, and will thus serve as very well-defined models of amorphous aluminosilicates, as well as supports for subsequent cation exchange. Likewise, we have shown that similar materials can be synthesized using TiO₂ as the core material, and the resulting nano-

cavity materials stabilize both Ag nanoparticles grown by photoreduction, and Pt nanoparticles deposited by incipient wetness impregnation.

Thrust III: Understanding-Based Manipulation of Catalytic Environments

Single-site, molecule-derived supported catalysts offer molecular level control of catalyst–substrate interactions by tuning the chemical properties of the support surface (**T. Marks**). For example, **Figure 6** portrays a highly electrophilic organozirconium catalyst weakly bound to the conjugate base of a strongly Brønsted acidic oxide (characterized by XAS, high-resolution solid state NMR, and IR spectroscopy, and DFT computation). In contrast, chemisorption of the same molecular precursors on weakly acidic surfaces, such as Al₂O₃ or SiO₂, results in condensation with surface hydroxyls and formation of covalently bound, poorly electrophilic/-catalytically

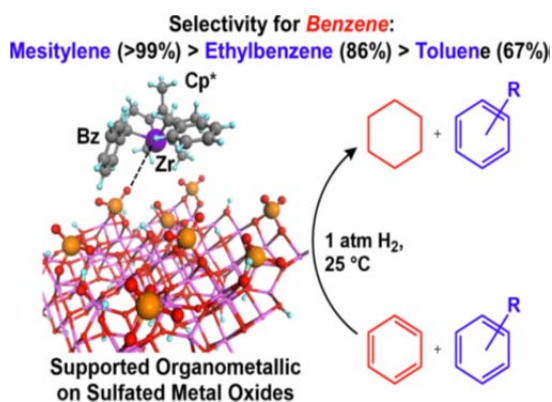


Figure 6. Proposed structure of supported organo-metallic catalysts for selective benzene hydrogenation.

ethylbenzene, 86% > toluene, 67%. Structural investigation of the surface complex with XAS, solid state NMR, and DFT suggests that the bulky catalyst benzyl groups expand the “cationic” metal center–anionic sulfated oxide surface distances, weaken the ion-pairing and enable the activation/insertion of more sterically encumbered arenes, thereby influencing hydrogenation rates and selectivity patterns. Arene hydrogenation on the acidic oxide-supported organozirconium complexes Cp*ZrBz₂/ZrS proceeds exclusively via a single-face/all-cis mechanism, **Figure 7**. Thus, hydrogenation of poly-alkylbenzenes and other fused arenes produce stereopure substituted cyclohexanes, and the reaction proceeds with kinetic parameters of $\Delta H^\ddagger = 4.8 \pm 0.5 \text{ kcal mol}^{-1}$, $\Delta S^\ddagger = -58.7 \pm 1.9 \text{ eu}$, and $E_a = 5.3 \pm 0.6 \text{ kcal mol}^{-1}$, suggesting a highly organized transition state.

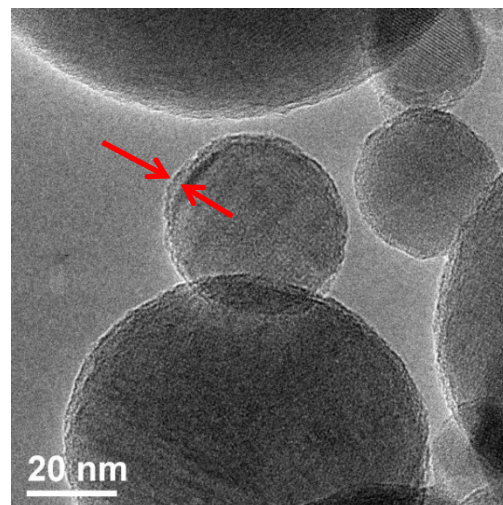


Figure 5. Conformal ~2 nm silica shell around spherical alumina grown by TEOS deposition (indicated) is strongly acidic.

inert species. **T. Marks** finds that Cp*ZrR₂⁺, formed by chemisorption of Cp*ZrMe₃, Cp*ZrBz₃, or Cp*ZrPh₃ on acidic sulfated oxides, are highly active arene hydrogenation catalysts. On sulfated ZrO₂ (ZrS), sulfated Al₂O₃ (AlS), and ZrO₂–WO₃ (ZrW), the activity for benzene hydrogenation increases with increasing Brønsted acidity, AlS ≈ ZrW ≪ ZrS, by forming stronger surface organometallic electrophiles. For benzene/toluene mixtures, the selectivities for benzene hydrogenation vary with catalyst: ZrBz₃⁺/ZrS[−], 83% > Cp*ZrMe₂⁺/ZrS[−], 80% > Cp*ZrBz₂⁺/ZrS[−], 67% > Cp*ZrPh₂⁺/ZrS[−], 57%. For Cp*ZrBz₂⁺/ZrS[−], the benzene selectivity in benzene/arene mixtures vary with arene: mesitylene, 99%, >

Single-site metal oxide clusters have the advantages of more uniform kinetics and product distributions than heterogeneous samples and are more straightforward to understand. However, their synthesis has been limited by precursor availability. **Kung** explored using incompletely

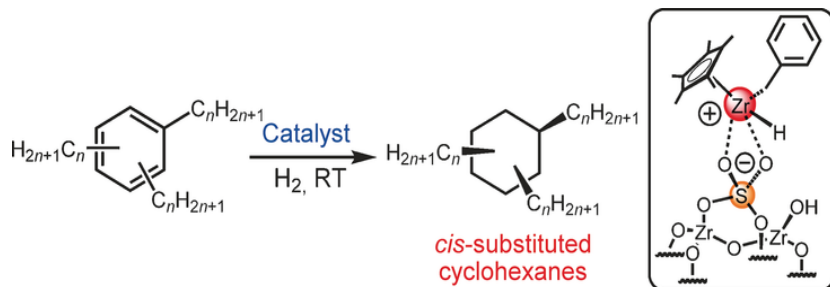


Figure 7. Face-selective arene hydrogenation.

condensed polyhedral oligomeric silsesquioxanes (POSSs) as ligands to generate tetrahedrally coordinated Sn oxo clusters on SiO₂ supports, **Figure 8**. The complex POSS-Sn-POSS was grafted successfully onto silica, and the tetrahedral coordination is retained after mild calcination in ozone to remove all organic fragments, as confirmed by EXAFS, NMR, UV-vis, and DRIFT characterization. The

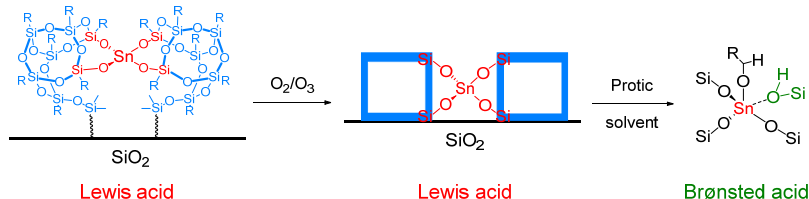


Figure 8. Single-site POSS catalysts

supported Sn oxo cluster possess Lewis acidity, and site homogeneity is demonstrated by quantitative stoichiometric pyridine adsorption. Interestingly, adsorption of 2-propanol results in quantitative enhancement of Brønsted acidity. Thus, in addition to exhibiting catalytic activity typical for Lewis acids, such as hydride transfer between an alcohol and an aldehyde, these oxo clusters also catalyze Brønsted acid catalyzed reactions, such as epoxide ring opening with alcohol and acetal formation. Furthermore, whereas pyridine has little effect on the hydride transfer reaction, it quantitatively poisons epoxide ring opening and acetal formation.

Stair and **T. Marks** also investigated the generation of isolated (-AlO)₃SiOH species on γ -Al₂O₃ by reaction of tetraethylorthosilicate (TEOS) vapor at low temperatures (**Figure 9**). Characterized by PXRD, XPS, DRIFTS of adsorbed NH₃, CO, and pyridine, and ²⁹Si and ²⁷Al DNP-enhanced solid-state NMR data demonstrate formation of isolated (-AlO)₃Si(OH) sites. Their mild Brønsted acidity provides activity for liquid-phase catalytic cyclohexanol dehydration, with up to 3.5-fold greater specific activity than the parent alumina.

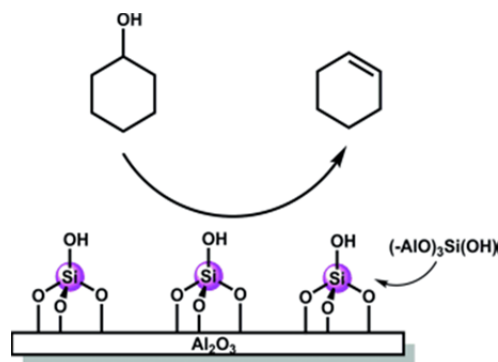


Figure 9. Single site siloxane acids.

ICEP Publications 2013-2016

Thrust 1 – Metal-Oxide Interactions, Laurence D. Marks

1. Bachrach, M.; Marks, T. J.; Notestein, J. M., Understanding the Hydrodenitrogenation of Heteroaromatics on a Molecular Level. *Acs Catalysis* **2016**, *6* (3), 1455-1476.
2. Bachrach, M.; Morlanes-Sanchez, N.; Canlas, C. P.; Miller, J. T.; Marks, T. J.; Notestein, J. M., Increasing the Aromatic Selectivity of Quinoline Hydrogenolysis Using Pd/MOx-Al₂O₃. *Catalysis Letters* **2014**, *144* (11), 1832-1838.
3. Bachrach, M.; Marks, T. J.; Notestein, J. M., C-N bond hydrogenolysis of aniline and cyclohexylamine over TaOx-Al₂O₃. *New Journal of Chemistry* **2016 in press**.
4. Chen, B. R.; George, C.; Lin, Y. Y.; Hu, L. H.; Crosby, L.; Hu, X. Y.; Stair, P. C.; Marks, L. D.; Poepelmeier, K. R.; Van Duyne, R. P.; Bedzyk, M. J., Morphology and oxidation state of ALD-grown Pd nanoparticles on TiO₂- and SrO-terminated SrTiO₃ nanocuboids. *Surface Science* **2016**, *648*, 291-298.
5. Ding, K.; Gulec, A.; Johnson, A. M.; Schweitzer, N. M.; Stucky, G. D.; Marks, L. D.; Stair, P. C., Identification of active sites in CO oxidation and water-gas shift over supported Pt catalysts. *Science* **2015**, *350* (6257), 189-192.
6. Eaton, T. R.; Boston, A. M.; Thompson, A. B.; Gray, K. A.; Notestein, J. M., Counting Active Sites on Titanium Oxide-Silica Catalysts for Hydrogen Peroxide Activation through In Situ Poisoning with Phenylphosphonic Acid. *Chemcatchem* **2014**, *6* (11), 3215-3222.
7. Eaton, T. R.; Campos, M. P.; Gray, K. A.; Notestein, J. M., Quantifying accessible sites and reactivity on titania-silica (photo) catalysts: Refining TOF calculations. *Journal of Catalysis* **2014**, *309*, 156-165.
8. Enterkin, J. A.; Kennedy, R. M.; Lu, J. L.; Elam, J. W.; Cook, R. E.; Marks, L. D.; Stair, P. C.; Marshall, C. L.; Poepelmeier, K. R., Epitaxial Stabilization of Face Selective Catalysts. *Topics in Catalysis* **2013**, *56* (18-20), 1829-1834.
9. Fu, B. S.; Lu, J. L.; Stair, P. C.; Xiao, G. M.; Kung, M. C.; Kung, H. H., Oxidative dehydrogenation of ethane over alumina-supported Pd catalysts. Effect of alumina overlayer. *Journal of Catalysis* **2013**, *297*, 289-295.
10. Haag, D.; Kung, H. H., Metal Free Graphene Based Catalysts: A Review. *Topics in Catalysis* **2014**, *57* (6-9), 762-773.
11. Lin, Y. Y.; Wu, Z. L.; Wen, J. G.; Ding, K. L.; Yang, X. Y.; Poepelmeier, K. R.; Marks, L. D., Adhesion and Atomic Structures of Gold on Ceria Nanostructures: The Role of Surface Structure and Oxidation State of Ceria Supports. *Nano Letters* **2015**, *15* (8), 5375-5381.
12. Liu, B. H.; McBriarty, M. E.; Bedzyk, M. J.; Shaikhutdinov, S.; Freund, H. J., Structural Transformations of Zinc Oxide Layers on Pt(111). *Journal of Physical Chemistry C* **2014**, *118* (49), 28725-28729.
13. Marks, L. D.; Chiamonti, A. N.; Rahman, S. U.; Castell, M. R., Transition from Order to Configurational Disorder for Surface Reconstructions on SrTiO₃(111). *Physical Review Letters* **2015**, *114* (22), 6.
14. Masango, S. S.; Peng, L. X.; Marks, L. D.; Van Duyne, R. P.; Stair, P. C., Nucleation and Growth of Silver Nanoparticles by AB and ABC-Type Atomic Layer Deposition. *Journal of Physical Chemistry C* **2014**, *118* (31), 17655-17661.
15. Mashayekhi, N. A.; Kung, M. C.; Kung, H. H., Selective oxidation of hydrocarbons on supported Au catalysts. *Catalysis Today* **2014**, *238*, 74-79.

16. Pan, Q.; Liu, B. H.; McBriarty, M. E.; Martynova, Y.; Groot, I. M. N.; Wang, S.; Bedzyk, M. J.; Shaikhutdinov, S.; Freund, H. J., Reactivity of Ultra-Thin ZnO Films Supported by Ag(111) and Cu(111): A Comparison to ZnO/Pt(111). *Catalysis Letters* **2014**, *144* (4), 648-655.
17. Stoltz, S. E.; Ellis, D. E.; Bedzyk, M. J., Structure and reactivity of zero-, two- and three-dimensional Pd supported on SrTiO₃(001). *Surface Science* **2014**, *630*, 46-63.
18. Stoltz, S. E.; Ellis, D. E.; Bedzyk, M. J., Interface of Pt with SrTiO₃(001); A combined theoretical and experimental study. *Surface Science* **2015**, *633*, 8-16.
19. Williams, L. A.; Guo, N.; Motta, A.; Delferro, M.; Fragala, I. L.; Miller, J. T.; Marks, T. J., Surface structural-chemical characterization of a single-site d(0) heterogeneous arene hydrogenation catalyst having 100% active sites. *Proceedings of the National Academy of Sciences of the United States of America* **2013**, *110* (2), 413-418.
20. Wu, Y. Y.; Mashayekhi, N. A.; Kung, H. H., Au-metal oxide support interface as catalytic active sites. *Catalysis Science & Technology* **2013**, *3* (11), 2881-2891.
21. Yacob, S.; Park, S.; Kilos, B. A.; Barton, D. G.; Notestein, J. M., Vapor-phase ethanol carbonylation with heteropolyacid-supported Rh. *Journal of Catalysis* **2015**, *325*, 1-8.

ICEP Publications 2013-2016

Thrust 2 – Oxide-Oxide Interactions, Justin M. Notestein

1. Beletskiy, E. V.; Hou, X. L.; Shen, Z. L.; Gallagher, J. R.; Miller, J. T.; Wu, Y. Y.; Li, T. H.; Kung, M. C.; Kung, H. H., Supported Tetrahedral Oxo-Sn Catalyst: Single Site, Two Modes of Catalysis. *Journal of the American Chemical Society* 2016, *138* (13), 4294-4297.
2. Beletskiy, E. V.; Shen, Z. L.; Riofski, M. V.; Hou, X. L.; Gallagher, J. R.; Miller, J. T.; Wu, Y.; Kung, H. H.; Kung, M. C., Tetrahedral Sn-silsesquioxane: synthesis, characterization and catalysis. *Chemical Communications* 2014, *50* (99), 15699-15701.
3. Beletskiy, E. V.; Wu, Y. Y.; Kung, M. C.; Kung, H. H., Addition of Sn-O'Pr across a C=C Bond: Unusual Insertion of an Alkene into a Main-Group-Metal-Alkoxide Bond. *Organometallics* 2016, *35* (3), 301-302.
4. Bhattacharyya, K.; Danon, A.; Vijayan, B. K.; Gray, K. A.; Stair, P. C.; Weitz, E., Role of the Surface Lewis Acid and Base Sites in the Adsorption of CO₂ on Titania Nanotubes and Platinized Titania Nanotubes: An in Situ FT-IR Study. *Journal of Physical Chemistry C* 2013, *117* (24), 12661-12678.
5. Bhattacharyya, K.; Wu, W. Q.; Weitz, E.; Vijayan, B. K.; Gray, K. A., Probing Water and CO₂ Interactions at the Surface of Collapsed Titania Nanotubes Using IR Spectroscopy. *Molecules* 2015, *20* (9), 15469-15487.
6. Bo, Z. Y.; Eaton, T. R.; Gallagher, J. R.; Canlas, C. P.; Miller, J. T.; Notestein, J. M., Size-Selective Synthesis and Stabilization of Small Silver Nanoparticles on TiO₂ Partially Masked by SiO₂. *Chemistry of Materials* 2015, *27* (4), 1269-1277.
7. Feng, Z.; Ma, Q.; Lu, J.; Feng, H.; Elam, J. W.; Stair, P. C.; Bedzyk, M. J., Atomic-scale cation dynamics in a monolayer VOX/□-Fe₂O₃ catalyst. *Rsc Advances* 2015, *5* (126), 103834-103840.
8. Feng, Z.; McBriarty, M. E.; Mane, A. U.; Lu, J.; Stair, P. C.; Elam, J. W.; Bedzyk, M. J., Redox-driven atomic-scale changes in mixed catalysts: VOX/WOX/□-TiO₂ (110). *Rsc Advances* 2014, *4* (110), 64608-64616.

9. Feng, Z. X.; Lu, J. L.; Feng, H.; Stair, P. C.; Elam, J. W.; Bedzyk, M. J., Catalysts Transform While Molecules React: An Atomic-Scale View. *Journal of Physical Chemistry Letters* 2013, 4 (2), 285-291.
10. Finkelstein-Shapiro, D.; Petrosko, S. H.; Dimitrijevic, N. M.; Gosztola, D.; Gray, K. A.; Rajh, T.; Tarakeshwar, P.; Mujica, V., CO₂ Preactivation in Photoinduced Reduction via Surface Functionalization of TiO₂ Nanoparticles. *Journal of Physical Chemistry Letters* 2013, 4 (3), 475-479.
11. Johnson, A. M.; Quezada, B. R.; Marks, L. D.; Stair, P. C., Influence of the Metal Oxide Substrate Structure on Vanadium Oxide Monomer Formation. *Topics in Catalysis* 2014, 57 (1-4), 177-187.
12. Kleinman, S. L.; Frontiera, R. R.; Henry, A. I.; Dieringer, J. A.; Van Duyne, R. P., Creating, characterizing, and controlling chemistry with SERS hot spots. *Physical Chemistry Chemical Physics* 2013, 15 (1), 21-36.
13. Kwon, S.; Schweitzer, N. M.; Park, S.; Stair, P. C.; Snurr, R. Q., A kinetic study of vapor-phase cyclohexene epoxidation by H₂O₂ over mesoporous TS-1. *Journal of Catalysis* 2015, 326, 107-115.
14. Masango, S. S.; Hackler, R. A.; Henry, A. I.; McAnally, M. O.; Schatz, G. C.; Stair, P. C.; Van Duyne, R. P., Probing the Chemistry of Alumina Atomic Layer Deposition Using Operando Surface-Enhanced Raman Spectroscopy. *Journal of Physical Chemistry C* 2016, 120 (7), 3822-3833.
15. Masango, S. S.; Hackler, R. A.; Large, N.; Henry, A. I.; McAnally, M. O.; Schatz, G. C.; Stair, P. C.; Van Duyne, R. P., High-Resolution Distance Dependence Study of Surface-Enhanced Raman Scattering Enabled by Atomic Layer Deposition. *Nano Letters* 2016 Submitted.
16. McBriarty, M. E.; Ellis, D. E., Cation synergies affect ammonia adsorption over VOX and (V,W)OX dispersed on α -Al₂O₃ (0001) and α -Fe₂O₃ (0001). *Surface Science* 2016, 651, 41-50.
17. Mouat, A. R.; George, C.; Kobayashi, T.; Pruski, M.; van Duyne, R. P.; Marks, T. J.; Stair, P. C., Highly Dispersed SiO_x/Al₂O₃ Catalysts Illuminate the Reactivity of Isolated Silanol Sites. *Angewandte Chemie-International Edition* 2015, 54 (45), 13346-13351.
18. Mouat, A. R.; Mane, A. U.; Elam, J. W.; Delferro, M.; Marks, T. J.; Stair, P. C., Volatile Hexavalent Oxo-amidinate Complexes: Molybdenum and Tungsten Precursors for Atomic Layer Deposition. *Chemistry of Materials* 2016, 28 (6), 1907-1919.
19. Peroff, A. G.; Weitz, E.; Van Duyne, R. P., Mechanistic studies of pyridinium electrochemistry: alternative chemical pathways in the presence of CO₂. *Physical Chemistry Chemical Physics* 2016, 18 (3), 1578-1586.
20. Savara, A.; Weitz, E., Elucidation of Intermediates and Mechanisms in Heterogeneous Catalysis Using Infrared Spectroscopy. *Annu Rev Phys Chem* 2014, 65, 249-273.
21. Wu, W. Q.; Bhattacharyya, K.; Gray, K.; Weitz, E., Photoinduced Reactions of Surface-Bound Species on Titania Nanotubes and Platinized Titania Nanotubes: An in Situ FTIR Study. *Journal of Physical Chemistry C* 2013, 117 (40), 20643-20655.
22. Wu, W. Q.; Weitz, E., Modification of acid sites in ZSM-5 by ion-exchange: An in-situ FTIR study. *Applied Surface Science* 2014, 316, 405-415.

ICEP Publications 2013-2016

Thrusters 1 and 2

1. Crosby, L.; Enterkin, J.; Rabuffetti, F.; Poeppelmeier, K.; Marks, L., Wulff shape of strontium titanate nanocuboids. *Surface Science* **2015**, *632*, L22-L25.
2. Hu, L. H.; Wang, C. D.; Kennedy, R. M.; Marks, L. D.; Poeppelmeier, K. R., The Role of Oleic Acid: From Synthesis to Assembly of Perovskite Nanocuboid Two-Dimensional Arrays. *Inorganic Chemistry* **2015**, *54* (3), 740-745.
3. Hu, L. H.; Wang, C. D.; Lee, S.; Winans, R. E.; Marks, L. D.; Poeppelmeier, K. R., SrTiO₃ Nanocuboids from a Lamellar Microemulsion. *Chemistry of Materials* **2013**, *25* (3), 378-384.
4. Lin, Y. Y.; Wen, J. G.; Hu, L. H.; Kennedy, R. M.; Stair, P. C.; Poeppelmeier, K. R.; Marks, L. D., Synthesis-Dependent Atomic Surface Structures of Oxide Nanoparticles. *Physical Review Letters* **2013**, *111* (15), 5.
5. Lin, Y. Y.; Wen, J. G.; Hu, L. H.; McCarthy, J. A.; Wang, S. C.; Poeppelmeier, K. R.; Marks, L. D., Electron-induced Ti-rich surface segregation on SrTiO₃ nanoparticles. *Micron* **2015**, *68*, 152-157.
6. Lin, Y. Y.; Wu, Z. L.; Wen, J. G.; Poeppelmeier, K. R.; Marks, L. D., Imaging the Atomic Surface Structures of CeO₂ Nanoparticles. *Nano Letters* **2014**, *14* (1), 191-196.
7. McBriarty, M. E.; Campbell, G. P.; Drake, T. L.; Elam, J. W.; Stair, P. C.; Ellis, D. E.; Bedzyk, M. J., Atomic-Scale View of VO_x-WO_x Coreduction on the alpha-Al₂O₃ (0001) Surface. *Journal of Physical Chemistry C* **2015**, *119* (28), 16179-16187.
8. Wang, S. C.; Xie, H.; Lin, Y. Y.; Poeppelmeier, K. R.; Li, T.; Winans, R. E.; Cui, Y. R.; Ribeiro, F. H.; Canlas, C. P.; Elam, J. W.; Zhang, H. B.; Marshall, C. L., High Thermal Stability of La₂O₃- and CeO₂-Stabilized Tetragonal ZrO₂. *Inorganic Chemistry* **2016**, *55* (5), 2413-2420.

ICEP Publications 2013-2016

Thrust 3 – Molecule-Metal-Environment Interactions, Harold H. Kung

1. Adhikari, D.; Miller, A. W.; Baik, M. H.; Nguyen, S. T., Intramolecular ring-opening from a CO₂-derived nucleophile as the origin of selectivity for 5-substituted oxazolidinone from the (salen)Cr-catalyzed aziridine + CO₂ coupling. *Chemical Science* **2015**, *6* (2), 1293-1300.
2. Bae, Y. S.; Liu, J.; Wilmer, C. E.; Sun, H.; Dickey, A. N.; Kim, M. B.; Benin, A. I.; Willis, R. R.; Barpaga, D.; LeVan, M. D.; Snurr, R. Q., The effect of pyridine modification of Ni-DOBDC on CO₂ capture under humid conditions. *Chemical Communications* **2014**, *50* (25), 3296-3298.
3. Galloway, J. M.; Kung, M.; Kung, H. H., Synthesis and characterization of bifunctional surfaces with tunable functional group pairs. *Surface Science* **2016**, *648*, 284-290.
4. Grosso-Giordano, N. A.; Eaton, T. R.; Bo, Z.; Yacob, S.; Yang, C.-C.; Notestein, J. M., Silica support modifications to enhance Pd-catalyzed deoxygenation of stearic acid. *Applied Catalysis B: Environmental* **2016**, *192*, 93-100.
5. Karagiari, O.; Vermeulen, N. A.; Klet, R. C.; Wang, T. C.; Moghadam, P. Z.; Al-Juaid, S. S.; Stoddart, J. F.; Hupp, J. T.; Farha, O. K., Functionalized Defects through Solvent-Assisted Linker Exchange: Synthesis, Characterization, and Partial Postsynthesis Elaboration of a Metal-Organic Framework Containing Free Carboxylic Acid Moieties. *Inorganic Chemistry* **2015**, *54* (4), 1785-1790.
6. Klet, R. C.; Tussupbayev, S.; Borycz, J.; Gallagher, J. R.; Stalzer, M. M.; Miller, J. T.; Gagliardi, L.; Hupp, J. T.; Marks, T. J.; Cramer, C. J.; Delferro, M.; Farha, O. K., Single-Site

Organozirconium Catalyst Embedded in a Metal-Organic Framework. *Journal of the American Chemical Society* 2015, 137 (50), 15680-15683.

7. Kung, H. H.; Kung, M. C., Inspiration from Nature for Heterogeneous Catalysis. *Catalysis Letters* 2014, 144 (10), 1643-1652.

8. Kung, M. C.; Riofski, M. V.; Missaghi, M. N.; Kung, H. H., Organosilicon platforms: bridging homogeneous, heterogeneous, and bioinspired catalysis. *Chemical Communications* 2014, 50 (25), 3262-3276.

9. Lalonde, M.; Bury, W.; Karagiari, O.; Brown, Z.; Hupp, J. T.; Farha, O. K., Transmetalation: routes to metal exchange within metal-organic frameworks. *Journal of Materials Chemistry A* 2013, 1 (18), 5453-5468.

10. Mondloch, J. E.; Bury, W.; Fairen-Jimenez, D.; Kwon, S.; DeMarco, E. J.; Weston, M. H.; Sarjeant, A. A.; Nguyen, S. T.; Stair, P. C.; Snurr, R. Q.; Farha, O. K.; Hupp, J. T., Vapor-Phase Metalation by Atomic Layer Deposition in a Metal-Organic Framework. *Journal of the American Chemical Society* 2013, 135 (28), 10294-10297.

11. Nguyen, H. G. T.; Mao, L.; Peters, A. W.; Audu, C. O.; Brown, Z. J.; Farha, O. K.; Hupp, J. T.; Nguyen, S. T., Comparative study of titanium-functionalized UiO-66: support effect on the oxidation of cyclohexene using hydrogen peroxide. *Catalysis Science & Technology* 2015, 5 (9), 4444-4451.

12. Nguyen, H. G. T.; Schweitzer, N. M.; Chang, C. Y.; Drake, T. L.; So, M. C.; Stair, P. C.; Farha, O. K.; Hupp, J. T.; Nguyen, S. T., Vanadium-Node-Functionalized UiO-66: A Thermally Stable MOF-Supported Catalyst for the Gas-Phase Oxidative Dehydrogenation of Cyclohexene. *ACS Catalysis* 2014, 4 (8), 2496-2500.

13. Nguyen, H. G. T.; Weston, M. H.; Sarjeant, A. A.; Gardner, D. M.; An, Z.; Carmieli, R.; Wasielewski, M. R.; Farha, O. K.; Hupp, J. T.; Nguyen, S. T., Design, Synthesis, Characterization, and Catalytic Properties of a Large-Pore Metal-Organic Framework Possessing Single-Site Vanadyl(monocatecholate) Moieties. *Crystal Growth & Design* 2013, 13 (8), 3528-3534.

14. Paddock, R. L.; Adhikari, D.; Lord, R. L.; Baik, M. H.; Nguyen, S. T., [(Salcen)Cr-III + Lewis base]-catalyzed synthesis of N-aryl-substituted oxazolidinones from epoxides and aryl isocyanates. *Chemical Communications* 2014, 50 (96), 15187-15190.

15. Planas, N.; Mondloch, J. E.; Tussupbayev, S.; Borycz, J.; Gagliardi, L.; Hupp, J. T.; Farha, O. K.; Cramer, C. J., Defining the Proton Topology of the Zr-6-Based Metal-Organic Framework NU-1000. *Journal of Physical Chemistry Letters* 2014, 5 (21), 3716-3723.

ICEP Publications 2013-2016

Other DOE Catalysis Acknowledgements

1. Childers, D. J.; Schweitzer, N. M.; Shahari, S. M. K.; Rioux, R. M.; Miller, J. T.; Meyer, R. J., Modifying structure-sensitive reactions by addition of Zn to Pd. *Journal of Catalysis* **2014**, 318, 75-84.

2. Childers, D. J.; Schweitzer, N. M.; Shahri, S. M. K.; Rioux, R. M.; Miller, J. T.; Meyer, R. J., Evidence for geometric effects in neopentane conversion on PdAu catalysts. *Catalysis Science & Technology* **2014**, 4 (12), 4366-4377.

3. Fredin, L. A.; Li, Z.; Lanagan, M. T.; Ratner, M. A.; Marks, T. J., Substantial Recoverable Energy Storage in Percolative Metallic Aluminum-Polypropylene Nanocomposites. *Advanced Functional Materials* **2013**, 23 (28), 3560-3569.

4. Fredin, L. A.; Li, Z.; Lanagan, M. T.; Ratner, M. A.; Marks, T. J., Sustainable High Capacitance at High Frequencies: Metallic Aluminum - Polypropylene Nanocomposites. *Acs Nano* **2013**, 7 (1), 396-407.
5. Gu, W. X.; Stalzer, M. M.; Nicholas, C. P.; Bhattacharyya, A.; Motta, A.; Gallagher, J. R.; Zhang, G. H.; Miller, J. T.; Kobayashi, T.; Pruski, M.; Delferro, M.; Marks, T. J., Benzene Selectivity in Competitive Arene Hydrogenation: Effects of Single-Site Catalyst ... Acidic Oxide Surface Binding Geometry. *Journal of the American Chemical Society* **2015**, 137 (21), 6770-6780.
6. Liu, S.; Motta, A.; Mouat, A. R.; Delferro, M.; Marks, T. J., Very Large Cooperative Effects in Heterobimetallic Titanium-Chromium Catalysts for Ethylene Polymerization/Copolymerization. *Journal of the American Chemical Society* **2014**, 136, 10460-10469.
7. McInnis, J. P.; Delferro, M.; Marks, T. J., Multinuclear Group 4 Catalysis: Olefin Polymerization Pathways Modified by Strong Metal-Metal Cooperative Effects. *Accounts of Chemical Research* **2014**, 47 (8), 2545-2557.
8. Motta, A.; Fragala, I. L.; Marks, T. J., Insight into Group 4 Metallocenium-Mediated Olefin Polymerization Reaction Coordinates Using a Metadynamics Approach. *Journal of Chemical Theory and Computation* **2013**, 9 (8), 3491-3497.
9. Stalzer, M. M.; Delferro, M.; Marks, T. J., Supported Single-Site Organometallic Catalysts for the Synthesis of Valuable Polyolefins. *Catalysis Letters* **2014**, 145, 3-14.
10. Stalzer, M. M.; Nicholas, C. P.; Bhattacharyya, A.; Motta, A.; Delferro, M.; Marks, T. J., Single-Face/All-cis Arene Hydrogenation by Supported Single-Site d⁰ Organozirconium Catalyst. *Angew. Chem. Int. Ed* **2016**, 55, 5263-5267.

Graphite-Conjugated Catalysis

Yogesh Surendranath
Massachusetts Institute of Technology, Department of Chemistry

Presentation Abstract

The interconversion of electrical and chemical energy requires the coupling of electron transfer with substrate bond rearrangement. This can be achieved at surface exposed active sites of heterogeneous electrocatalysts or via redox mediation facilitated by a homogeneous molecular electrocatalyst. Molecular electrocatalysts yield readily to synthetic alteration of their redox properties permitting systematic tuning of catalyst activity and selectivity. Similar control is difficult to achieve with heterogeneous electrocatalysts because they typically exhibit a distribution of active site geometries and local electronic structures, which are recalcitrant to molecular-level synthetic modification. However, heterogeneous electrocatalysts typically exhibit greater durability and are more readily integrated into functional energy conversion devices such as fuel cells and electrolyzers. We have developed a simple synthetic strategy for conjugating well-defined molecular catalyst active sites with the extended states of graphitic solids. We have used these graphite-conjugated catalysts to mediated efficient oxygen reduction and carbon dioxide reduction catalysis. Our latest efforts to expand the scope of this new class of heterogeneous catalysts will be discussed.

DE-SC0014176: Tunable Oxygen Reduction Electrocatalysis by Phenazine-Modified Carbons

PI: Yogesh Surendranath

Postdoc(s): Tomohiro Fukushima

Student(s): Megan Jackson, Seokjoon Oh, Corey Kaminsky, Travis Marshall-Roth

Affiliations(s): Massachusetts Institute of Technology

RECENT PROGRESS

Graphite-Conjugated Pyrazines as Molecularly Tunable Heterogeneous Electrocatalysts.

Condensation of ortho-phenylenediamine derivatives with ortho-quinone moieties at edge planes of graphitic carbon generates graphite-conjugated pyrazines (GCPs) that are active for oxygen reduction electrocatalysis in alkaline aqueous electrolyte. Catalytic rates of oxygen reduction are positively correlated with the electrophilicity of the active site pyrazine unit and can be tuned by over 70-fold by appending electron-withdrawing substituents to the phenylenediamine

precursors. Discrete molecular analogs containing pyrazine moieties display no activity above background under identical conditions. This simple bottom up method for constructing molecularly well-defined active sites on ubiquitous graphitic solids enables the rational design of tunable heterogeneous catalysts.

Graphite-Conjugated Rhenium Catalysts for Carbon Dioxide Reduction

Condensation of *fac*-Re(5,6-diamino-1,10-phenanthroline)(CO)₃Cl to o-quinone edge defects on graphitic carbon surfaces generates graphite-conjugated rhenium (GCC-Re) catalysts that are highly active for CO₂ reduction to CO in acetonitrile electrolyte. X-ray photoelectron and X-ray absorption

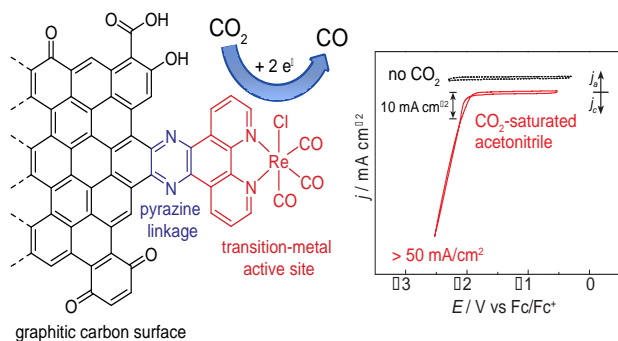


Figure 4 – Conjugated Re(phen)(CO)₃Cl to graphitic carbon surfaces generate a highly active

indicative of a catalytic mechanism involving rate-limiting one-electron transfer. This work establishes graphite conjugation as a powerful strategy for generating well-defined, tunable, heterogeneous electrocatalysts on ubiquitous graphitic carbon surfaces.

Publications Acknowledging this Grant in 2013-2016

- (I) Exclusively funded by this grant;
None
- (II) Jointly funded by this grant and other grants with leading intellectual contribution from this grant;

- Oh, S.; Gallagher, J. R.; Miller, J. T.; Surendranath, Y. Graphite-Conjugated Rhenium Catalysts for Carbon Dioxide Reduction. *J. Am. Chem. Soc.* **2016**, *138*, 1820–1823.
- Fukushima, T; Drisdell, W.; Yano, J.; Surendranath, Y. Graphite-Conjugated Pyrazines as Molecularly Tunable Heterogeneous Electrocatalysts. *J. Am. Chem. Soc.* **2015**, *137*, 10926–10929.

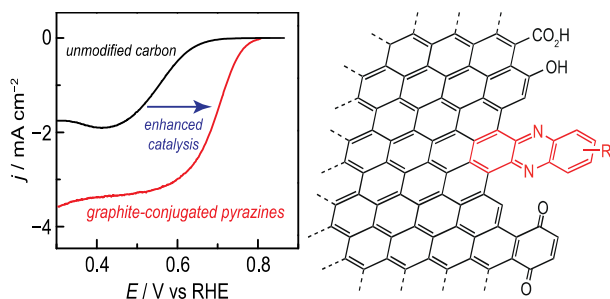
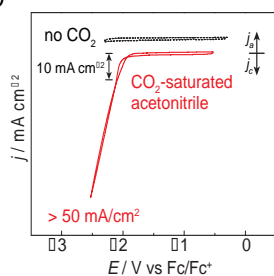


Figure 3 – Installation of pyrazine units on graphitic carbon surfaces enhances oxygen reduction catalysis in a tunable fashion.

spectroscopies establish the formation of surface-bound Re centers with well-defined coordination environments. GCC-Re species on glassy carbon surfaces display catalytic currents greater than 50 mA cm⁻² with 96 ± 3% Faradaic efficiency for CO production. Normalized for the number of Re active sites, GCC-Re catalysts exhibit higher turnover frequencies than that of a soluble molecular analogue, *fac*-Re(1,10-phenanthroline)(CO)₃Cl, and turnover numbers greater than 12,000. In contrast to the molecular analogue, GCC-Re surfaces display a Tafel slope of 150 mV/decade,



Fundamental understanding the correlation of surface of transition metal oxide and selectivity in production of ethylene through oxidative dehydrogenation of ethane

Franklin (Feng) Tao,[†] De-en Jiang,[¶] Yu Tang,[†] and Victor Fung[¶]

[†]Department of Chemical and Petroleum Engineering and Department of Chemistry,
University of Kansas, Lawrence, KS 66045

[¶]Department of Chemistry, University of California, Riverside, CA 92521

Tuning catalytic selectivity by integrating the second metal to form an alloy has been well demonstrated in literature. Here we present a method to tune catalytic selectivity of oxidative catalysis on another category of heterogeneous catalysts, transition metal oxides. By choosing oxidative dehydrogenation (ODH) of ethane to produce ethylene as a probe reaction and Co_3O_4 as a model catalyst, we demonstrated that doping nonmetallic atoms to surface lattice of a transition metal oxide could largely enhance catalytic selectivity through suppression of deep oxidation of the reactant molecules. Catalysts of Co_3O_4 with doped silicon atoms ($\text{Si}_x\text{-Co}_3\text{O}_4$) maintaining the spinel structure of pure Co_3O_4 exhibit much higher selectivity for the production of ethylene in ODH of ethane compared to pure Co_3O_4 at 600°C by 40%. The suppression of activity of surface lattice oxygen atoms was evidenced by the observation that the surface lattice oxygen atoms of $\text{Si}_x\text{-Co}_3\text{O}_4$ cannot exchange oxygen atoms with gas phase oxygen at a low temperature while pure Co_3O_4 can. The difference in releasing surface lattice oxygen atoms and dissociating molecular oxygen between pure Co_3O_4 and $\text{Si}_x\text{-Co}_3\text{O}_4$ was supported by DFT calculations. The calculated activation barriers for dissociation of molecular O_2 and energy barriers for hopping surface oxygen vacancies of $\text{Si}_x\text{-Co}_3\text{O}_4$ are obviously higher than those of pure Co_3O_4 , respectively. This study suggests an approach to increase catalytic selectivity of oxidative catalysis through suppressing activity of surface lattice oxygen atoms/vacancies via doping atoms of a non-metallic element.

U.S. Department of Energy under Grant No. DE-SC0014561 Understanding Oxidative Dehydrogenation of Ethane and Oxidative Coupling of Methane through In-situ Studies of Catalyst Surface during Catalysis and Computational Studies

Student(s): Yu Tang, Lingjuan Ma, Victor Fung

With the financial support of DOE BES catalysis program, we have performed fundamental studies of Co_3O_4 -based and NiO_{1-x} -based catalysts for chemical transformation of components of shale gas by integration of synthesis, catalytic evaluation, in-situ/operando characterization and DFT calculation with a goal of fundamental understanding of catalytic mechanism at an atomic or molecular level.

1. Fundamental understanding of the high activity of $\text{Ni}_x\text{Co}_{3-x}\text{O}_4$ in oxidation of CH_4 at a molecular level

It is critical to develop a catalyst made of earth-abundant elements highly active for a complete oxidation of methane at a relatively low temperature. NiCo_2O_4 consisting of earth-abundant elements which can completely oxidize methane in the temperature range of $350\text{--}550^\circ\text{C}$ (Figure 1). Being a cost-effective catalyst, NiCo_2O_4 exhibits activity higher than

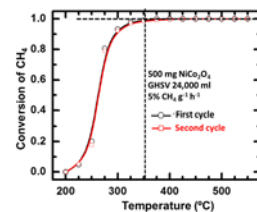


Figure 1. Catalytic performances of NiCo_2O_4 for oxidation of CH_4 .

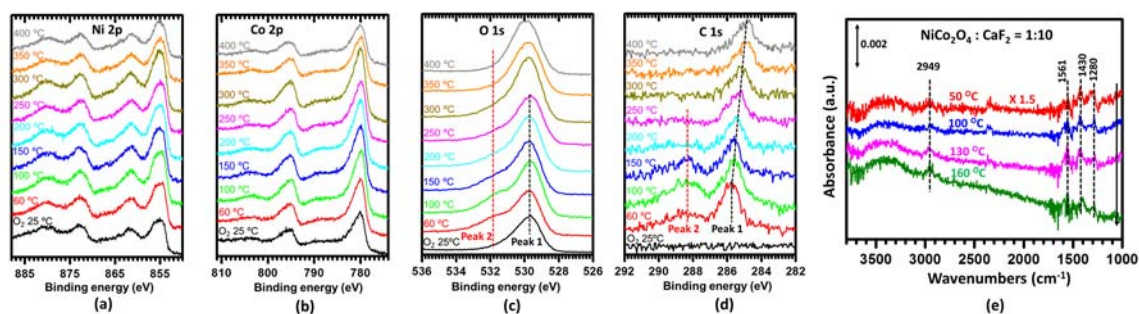


Figure 2. In situ studies using AP-XPS and infrared spectroscopy of NiCo_2O_4 during catalysis. Photoemission features of Ni 2p (a), Co 2p (b), O 1s (c), C 1s (d) and vibrational signature of NiCo_2O_4 surface at different temperatures during catalysis on NiCo_2O_4 in CH_4 and O_2 with a molar ratio of 1:5.

precious metal-based catalysts. The higher catalytic activity at a low temperature results from the integration of Ni cations, Co cations, and surface lattice oxygen atoms/oxygen vacancies at an atomic scale. In-situ studies of complete oxidation of methane on NiCo_2O_4 (Figure 2) and theoretical simulations (Figure 3) show that methane dissociates to CH_3 on Ni cations and then couple with surface lattice oxygen atoms to form $-\text{CH}_3\text{O}$ with a following dehydrogenation to form CH_2O ; a following oxidative dehydrogenation forms CHO; CHO is transformed to product molecules through two different sub-pathways including dehydrogenation of OCHO and CO oxidation.

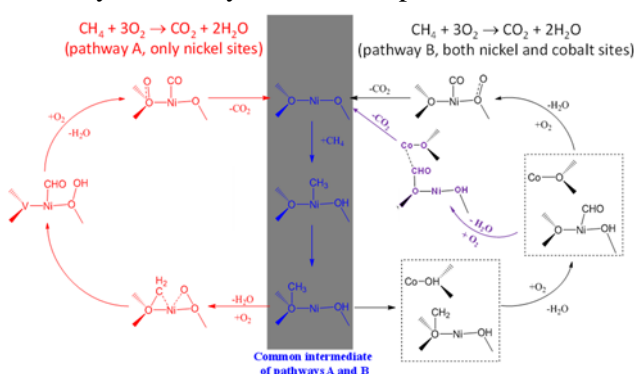


Figure 3. Two different reaction pathways of methane complete oxidation on $\text{NiCo}_2\text{O}_4(110\text{-}B)$ of type I crystal. The structures shown in blue at the middle of the schematic are the common intermediates for both pathways A and B; they are CH_3 formed through C-H dissociation and CH_3O formed through a coupling of carbon atom of CH_3 and oxygen atom of surface lattice. After CH_3O is formed, there are two different possible pathways A and B. Pathway A (shown in red) is the dehydrogenation by OH species of nickel site only, while pathway B (shown in blue) is the dehydrogenation by oxygen species of nearby cobalt site as well.

2. Tuning catalytic selectivity for production of ethylene from oxidative dehydrogenation through suppression of activity of surface lattice oxygen atoms of Co_3O_4 by doping

Our studies demonstrated that tuning of activity of surface lattice oxygen/oxygen vacancies through depositing atoms of nonmetallic elements to surface lattice of metal oxide is an efficient approach for promoting catalytic selectivity by suppression of side-reaction channels of deep oxidations such as a complete oxidation of the reactant. ODHs of ethane on silicon doped Co_3O_4 , $\text{Si}_x\text{-Co}_3\text{O}_4$ ($x = 0.1, 0.2, 0.4$) were studied toward fundamental understanding of correlation of catalytic selectivity of ODH for production of ethylene with capability of Co_3O_4 in providing active atomic oxygen. $\text{Si}_x\text{-Co}_3\text{O}_4$ exhibits a high selectivity for production of ethylene, which is twice higher than pure Co_3O_4 under the same catalytic condition (Figure 4b). This significant promotion of catalytic selectivity for production of ethylene in ODH results from the increases of both activation barriers

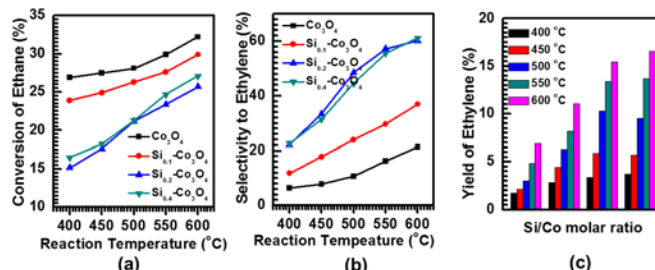


Figure 4. Catalytic activity, selectivity and yield of (a-c) $\text{Si}_x\text{-Co}_3\text{O}_4$ ($x = 0, 0.1, 0.2$ and 0.4) (400°C - 600°C).

of dissociating molecular O_2 on surface oxygen vacancies and energy barrier for hopping oxygen vacancies of catalyst surface through doping of silicon atoms to the surface lattice of Co_3O_4 (Figures 5 and 6). In addition, this method of significant promoting catalytic selectivity was supported by the observation of much higher selectivity of Ge-doped Co_3O_4 than pure Co_3O_4 .

3. Fundamental understanding of role of step sites of oxide catalysts in oxidative catalysis

More than half of catalytic reactions of chemical and energy transformations were performed on transition metal oxides. Microscopic step edge related to macroscopic surface morphology was demonstrated as key sites for many catalytic reactions on metal catalysts. Few reports on the key role of step sites of oxide catalysts are available because of the complexity of surface defects of an oxide catalyst,

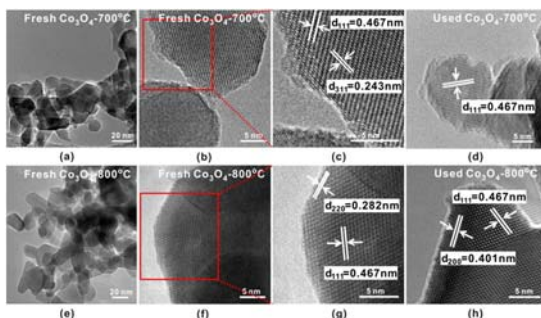


Figure 7. (a) TEM images and (b)-(c) HRTEM images of fresh Co_3O_4 -700 °C catalyst; (d) HRTEM image of used Co_3O_4 -700 °C catalyst; (e) TEM images and (f)-(g) HRTEM images of fresh Co_3O_4 -800 °C catalyst; (h) HRTEM image of used Co_3O_4 -800 °C catalyst.

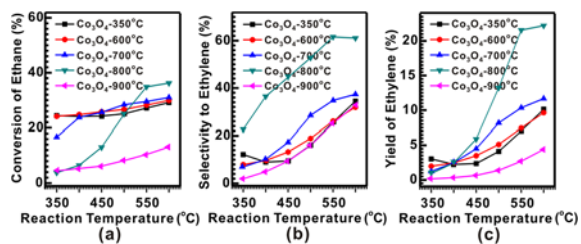


Figure 8. The catalytic performances of five catalysts Co_3O_4 -O₂-350°C, Co_3O_4 -O₂-600°C, Co_3O_4 -O₂-700°C, Co_3O_4 -O₂-800°C and Co_3O_4 -O₂-900°C in the temperature range of 350 °C to 600 °C. (a) Conversion of ethane; (b) Selectivity to ethylene; (c) Yield of ethylene.

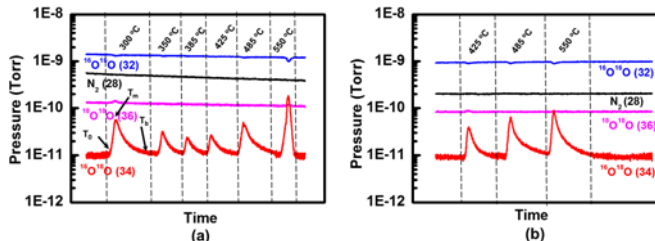


Figure 5. Mass spectra of $O^{16}O^{18}$ on $Co_3O^{16}_{4-x}O^{18}_x$ or $Si_{0.2}-Co_3O^{16}_{4-x}O^{18}_x$ in the temperature range of 30°C-600°C recorded during the exchange of surface oxygen atoms of catalysts with flowing O_{16}^2 . (a) $Co_3O^{16}_{4-x}O^{18}_x$. (b) $Si_{0.2}Co_3O^{16}_{4-x}O^{18}_x$.

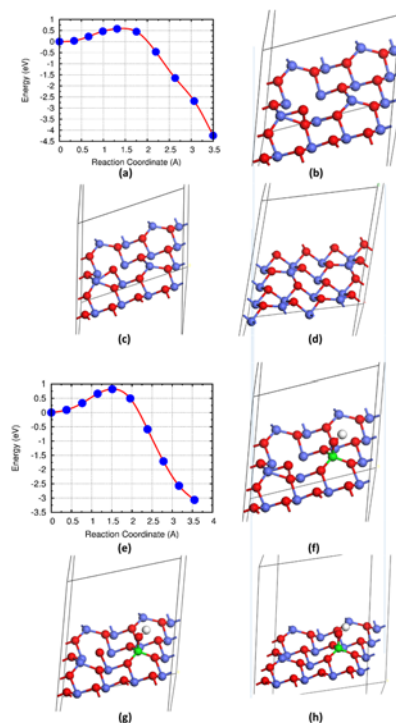


Figure 6. Energy profile for dissociation of molecular O_2 on surface oxygen vacancies on pure Co_3O_4 and Si-doped Co_3O_4 . (a) Evolution of energy in dissociation of molecular oxygen on pure Co_3O_4 along reaction coordination; (b), (c), and (d) are initial structure, transition state, and final structure of pure Co_3O_4 for dissociation of O_2 , respectively; (e) Evolution of energy in dissociation of molecular oxygen on Si-doped Co_3O_4 along reaction coordination; (f), (g), and (h) are initial structure, transition state, and final structure of Si-doped Co_3O_4 for dissociation of O_2 , respectively.

probably one order of magnitude higher than on metals due to the presence of anions and cations with multiple valence states and various coordination environments. Compared to the extensively fundamental studies of the roles of step sites of metal catalysts started in 1970s, clearly there is lack of fundamental studies of the role of step edges of oxide catalysts in catalysis.

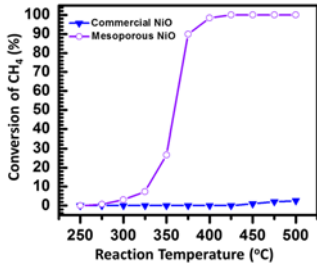


Figure 9. Catalytic performance of the synthesized NiO_{1-x} and commercial NiO .

We uncovered Co_3O_4 nanorods prepared at different temperatures exhibit quite different catalytic selectivity in production of ethylene through ODH of ethane. Co_3O_4 pretreated at $800^\circ C$ in air ($Co_3O_4-800^\circ C$) (Figures 7a-7d) exhibit higher selectivity (Figure 8) than those pretreated at $350-700^\circ C$ (Figures 7e-7h). Detailed characterizations show that the selectivity to ethylene is related to the faceting of rough, high Miller index surface of Co_3O_4 which determines the catalyst activity in dissociating molecular oxygen and releasing surface lattice oxygen atoms. The faceting performed at $700^\circ C-800^\circ C$ transforms high Miller index surface of Co_3O_4 to low Miller index one. The lack of highly under-coordinated cation sites on low Miller index surface of Co_3O_4 makes the reaction channel leading to complete oxidation to CO_2 unfavorable, thus increasing selectivity

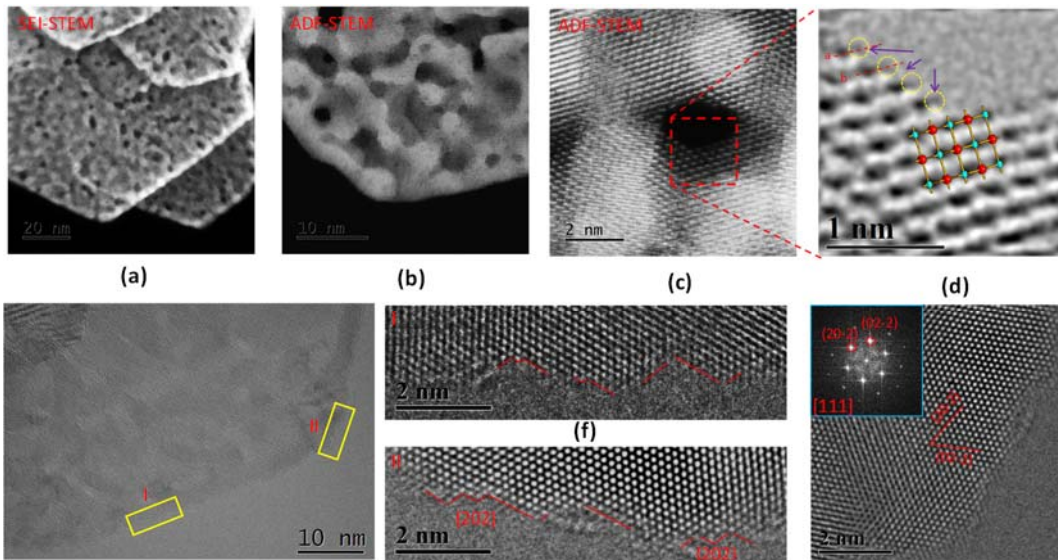


Figure 10. STEM studies of step at the step of mesopores and external edge of NiO_{1-x} mesoporous nanoparticles. (a, b) large scale STEM images. (c, d) atom-resolved step of internal edge of mesopore. (e) Edge of NiO_{1-x} mesoporous nanoparticles. (f-h) atom-resolved images of external edge of NiO_{1-x} mesoporous nanoparticles.

for production of ethylene. This study illustrated that studies of step edge of oxide in terms of under-coordinated cationic or/and anionic sites are significant for understanding catalytic performance of oxide catalysts and development of catalysts with higher selectivity.

The key role of step sites of transition metal oxide has been demonstrated in the distinctly different catalytic performance in mesoporous NiO_{1-x} and commercial NiO . As shown in Figure 9, mesoporous NiO_{1-x} with high density of step edge (Figure 10) exhibits high catalytic activity in complete oxidation of methane at temperature of $275^\circ C-425^\circ C$ but inert on commercial NiO in this temperature range. In-situ studies suggested that the under-coordinated cation sites at step edge play a key role in this catalysis. The high activity of step edge sites compared to terrace sites was confirmed by isotope-exchange experiments (Figure 11).

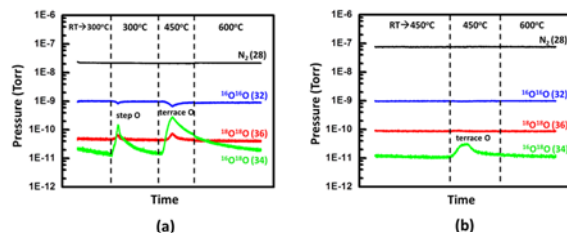


Figure 11. Evolution of partial pressures of N_2 , O_2 , O_2 , O_2 , and O_2 in a UHV chamber which received gases from reaction cell of AP-XPS where complete oxidation of methane is performed on (a) mesoporous $NiO_{0.81-x}O_x$, and (b) commercial $NiO_{1-x}O_x$.

Publications Acknowledging this Grant in 2015-2016

(I) Exclusively funded by this grant;

1. Tao, F.*; Shan, J.; Nguyen, L.; Wang, Z. Y.; Zhang, S. R.; Zhang, L.; Wu, Z. L.; Huang, W. X.; Zeng, S.; Hu, P. "Understanding Complete Oxidation of Methane on Spinel Oxides at a Molecular Level", *Nat. Commun.*, **2015**, 7798. DOI: 10.1038/ncomms8798
2. Liu, J.; Zhang, S.; Zhou, Y.; Fung, V.; Nguyen, L.; Jiang, D.; Shen, W.; Fan, J.; Tao, F.* "Tuning Catalytic Selectivity of Oxidative Catalysis through Deposition of Nonmetallic Atoms in Surface Lattice of Metal Oxide", *ACS Catal.* **2016**, DOI: 10.1021/acscatal.5b02900 (in press)
3. Fung, V.; Tao, F.; Jiang, D. "Understanding oxidative dehydrogenation of ethane on Co₃O₄ nanorods from density functional theory", *Catal. Sci. Technol.* **2016**, DOI: c6cy00749j (in press)
4. Zhang, S.; Shan, J.; Nie, L.; Nguyen, L.; Wu, Z.; Tao, F.* "In situ studies of surface of NiFe₂O₄ catalyst during complete oxidation of methane", *Surf. Sci.* **2016**, 648, 156-162.
5. Nguyen, L.; Zhang, S.; Yoo, S. J.; Tao, F.* "Preferential Oxidation of CO in H₂ on Pure Co₃O_{4-x} and Pt/Co₃O_{4-x}", *ChemCatChem* **2015**, 7, 2346-2353.
6. Shan, J.; Nguyen, L.; Zhang, S.; Tao, F.* "Water-Gas Shift on Pd/a-MnO₂ and Pt/a-MnO₂", *Catal. Lett.* **2015**, 145, 1571-1580.

(II) Jointly funded by this grant and other grants with leading intellectual contribution from this grant;

1. Tao, F.*, Crozier, P. "Atomic-Scale Observations of Catalyst Structures under Reaction Conditions and during Catalysis", *Chem. Rev.* **2016**, 116, 3487-3539.
2. Nguyen, L.; Tao, F.* "Development of a reaction cell for in-situ/operando studies of surface of a catalyst under a reaction condition and during catalysis", *Rev. Sci. Instrument* **2016**, (<http://dx.doi.org/10.1063/1.4946877>) (in press)
3. Cao, S.; Tao, F.*, Tang, Y. Li, Y.; Yu, J. "Size-and shape-dependent catalytic performances of oxidation and reduction reactions on nanocatalysts", *Chem. Soc. Rev.* **2016**, DOI: 10.1039/c6cs00094k (in press).
4. Nie, L.; Yu, J.; Jaroniec, M.; Tao, F.* "Room-temperature catalytic oxidation of formaldehyde on catalysts", *Catal. Sci. Technol.* **2016**, DOI: 10.1039/C6CY00062b. (in press)

Multimetallic Centers in Oxidation Chemistry. Mechanism for Oxygen Evolution and Development of Mixed Manganese-Cobalt Oxido Cubanes

Andy I. Nguyen and T. Don Tilley
Chemical Sciences Division, Lawrence Berkeley National Laboratory

Presentation Abstract

Multinuclear transition metal complexes are of great interest for their ability to mediate multi-step redox reactions. For example, water oxidation catalysts as markedly different as the Photosystem II Oxygen-Evolving Complex (OEC) and inorganic “cobalt-phosphate” electrocatalysts contain multinuclear metal-oxo active sites that cooperate in mediating the four-electron oxidation of water. In addition, enzymes that catalyze the oxidations of methane and molecular hydrogen incorporate bimetallic (dicopper and diiron, respectively) cores in which two metals cooperate to activate small molecules.

Investigations of the chemical and electrochemical behavior of the tetracobalt cubane cluster $\text{Co}_4(\mu\text{-O})_4(\text{OAc})_4(\text{pyr})_4$ presented an opportunity to investigate the mechanism of water oxidation by this molecular model for cobalt oxide. Kinetic and mechanistic studies were made possible by the discovery of a *stoichiometric* oxygen evolution reaction starting from the oxidized cobalt cluster (formally $\text{Co}^{\text{III}}_3\text{Co}^{\text{IV}}$), and established the requirement of a formal Co^{V} oxidation state and involvement of terminal oxygen ligands (oxo, hydroxyl, aquo) in O_2 formation. The characterization of this reaction system, along with systematic synthetic modifications of the oxide cluster, provides a viable pathway for catalyst optimization. Along these lines, it is of interest to establish reliable methods for incorporation of hetero-metals into a well-defined oxide cluster. In fact, oxide catalysts for water oxidation can be promoted by doping with other metals. The advantage of heterometallic oxide OER catalysts extends to nature: the OEC in photosystem II is a mixed calcium-manganese oxido cluster. These observations suggest that there are cooperative mechanisms unique to heterometallic systems. Efforts toward development of relevant, heterometallic oxide clusters have produced a new MnCo_3 oxido cubane complex, which is readily post-modified to obtain a range of ligand-substituted products. Addition of a fifth transition metal produces a “dangler”, pentametallal complex analogous to that found in photosystem II. The spectroscopic, magnetic, and electrochemical behaviors of these new clusters will be described.

New Fluoroalkylation Methods Employing Earth Abundant Metals

David A. Vicić
Lehigh University

Presentation Abstract

The DOE has had a long standing interest in the fundamental chemistry of fluorine ever since it was discovered that uranium hexafluoride exhibits a high vapor pressure and could be used to purify isotopically enriched uranium. Fluorination has become popular for other important reasons, like its known ability to increase the oxidative and thermal stability of new materials and its role in supporting new energy technologies is expected to grow. Tailored ligands and counter-ions that allow metals to operate under harsh oxidative conditions often feature fluoroalkyl substituents due to the chemical inertness of the [CF₃] and [CF₂] functional groups. Such harsh conditions are often required for important reactions like hydrocarbon oxidations. This report will detail our efforts to understand how to manipulate difluoromethyl and difluoromethylene groups with catalytic amounts of base metals so they can be incorporated into common organic building blocks.

DE-FG02-13ER16369:

Development of Catalytic Alkylation and Fluoroalkylation Methods

Postdoc: Huan Wang

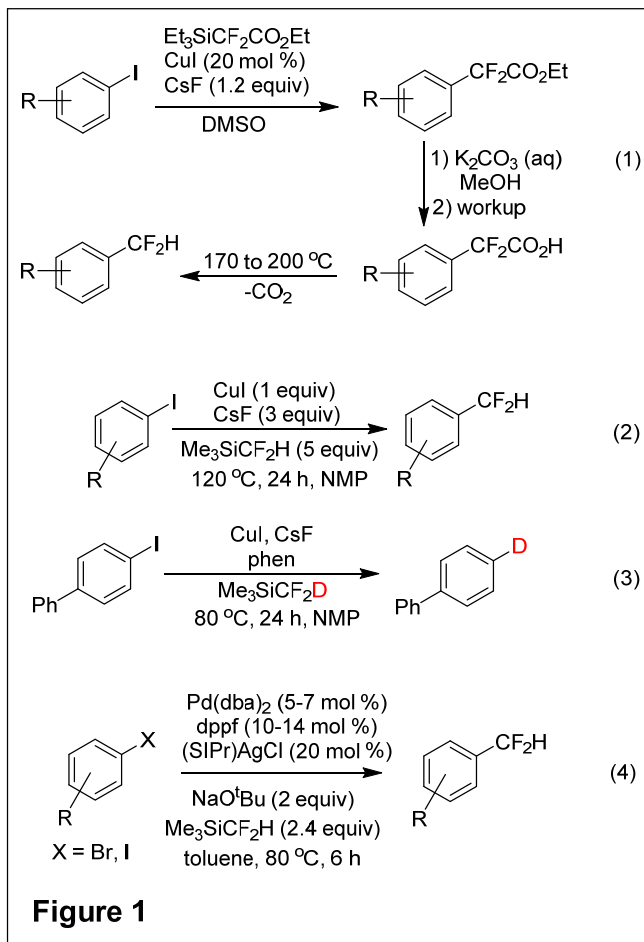
Students: Peter T. Kaplan, Long Xu, Siqi Yu

RECENT PROGRESS

Advances in metal-catalyzed direct difluoromethylation reactions:

The use of transition metals to mediate difluoromethylation reactions has been problematic. It was only in 2011 that Amii reported the difluoromethylation of aryl iodides using a metal-mediated method.¹ The route was complicated however, involving an initial coupling of α -silyldifluoroacetates with aryl iodides to afford aryldifluoroacetates in moderate to good yields (Figure 1, eq 1). Then, under forcing conditions, these difluoroacetates were hydrolyzed and decarboxylated to generate difluoromethyl arene products (eq 1). Hartwig later reported an example of direct difluoromethylations using Me₃SiCF₂H as the difluoromethyl source and a stoichiometric amount of copper catalyst at temperatures greater than 100 °C (eq 2). This reaction was not tolerant to substrates containing aldehydes, ketones, or electron withdrawing

groups. Studies showed that there was also a competing reduction pathway that shut down reactivity for substrates containing electron withdrawing groups, even mildly withdrawing groups like phenyl (eq 3). Before our most recent results of this Progress Period, there had been only one report of a method that was catalytic in metal for directly incorporating a difluoromethyl group into aryl halide substrates.³ As shown in eq 4, this method involved the use of expensive palladium and silver co-catalysts that each required their own supporting ligand. Moreover, the method used $\text{Me}_3\text{SiCF}_2\text{H}$ as the difluoromethyl source in combination with the exogenous base sodium *tert*-butoxide as the activator. Such conditions made the palladium-catalyzed method in eq 4 also incompatible with aldehyde and ketone functionalities. Considering all of the inherent aforementioned issues for the reactions outlined in eqs 1-4 (Figure 1), we focused on obtaining key initial results that improved the substrate scope and used base metals to directly install a difluoromethyl group.



We recently communicated in *JACS* the preparation of a new difluoromethyl nucleophile $[(\text{DMPU})_2\text{Zn}(\text{CF}_2\text{H})_2]$ that can be used in combination with nickel to directly and catalytically difluoromethylate aryl iodides, bromides, and triflates (Figure 2).⁴ The substrate scope was unprecedented, and successful couplings were observed with aryl halide substrates bearing electron withdrawing groups, aldehydes, ketones, and esters. The ability of the new difluoromethylzinc reagent to react in the presence of aldehydes and ketones deserves special mention. Before our studies, most cross-coupling studies focused on using $\text{Me}_3\text{Si-CF}_2\text{H}$ as the difluoromethyl delivery agent. This was undoubtedly influenced by the success of the $\text{Me}_3\text{Si-CF}_3$ in stoichiometric trifluoromethylation reactions. $\text{Me}_3\text{Si-CF}_2\text{H}$ is more electron rich than $\text{Me}_3\text{Si-CF}_3$, which has a number of important implications. First, the CF_2H anion is a poorer leaving group than the CF_3 anion, so more forcing conditions are required to release it in order to perform nucleophilic difluoromethylation chemistry. Secondly, the CF_2H anion that is generated from $\text{Me}_3\text{Si-CF}_2\text{H}$ is a much “hotter” than the CF_3 anion, and consequently a severe limitation of the $\text{Me}_3\text{Si-CF}_2\text{H}$ reagent in cross-coupling chemistry is that aldehyde and ketone functionalities are not tolerated. Ketones and aldehydes in the Hartwig and Shen examples (eqs 2 and 4, Figure 1), for instance, had to be protected in order for the cross-couplings to occur. The ability of our difluoromethylzinc reagent to tolerate carbonyl-containing functionalities bodes extremely well for its continued use in emerging difluoromethylation methodologies.

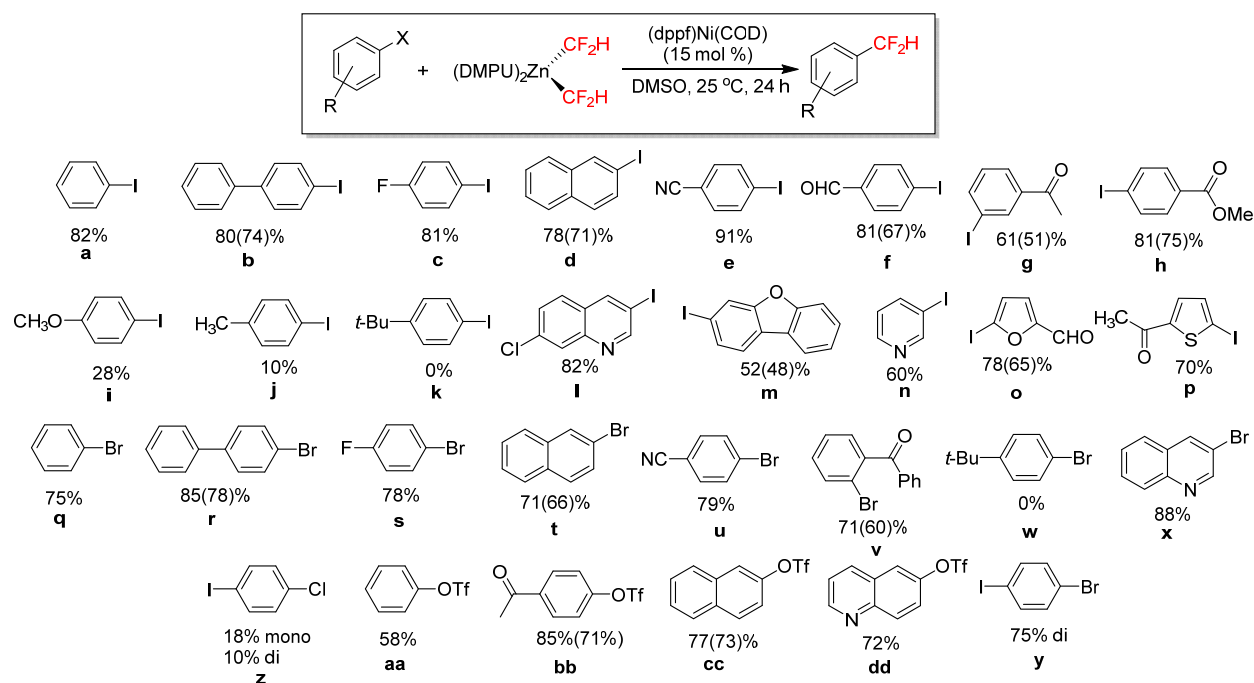
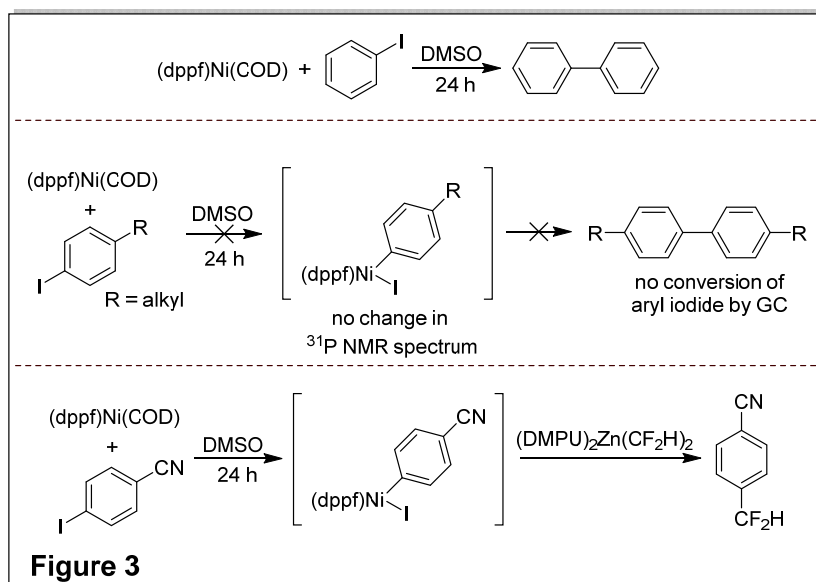


Figure 2. Nickel-catalyzed difluoromethylation of aryl iodides, bromides, and triflates.

One of the limitations of our method is the low reactivity observed for sp^3 -hybridized electron-rich substrates (Figure 2, entries **i**, **j**, **k**, **w**). Stoichiometric studies indicate that the problem with these substrates lies in the aryl halide activation step. In a control experiment, we found that addition of [(dppf)Ni(COD)] to iodobenzene in the absence of [(DMPU)₂Zn(CF₂H)₂] produced biphenyl in near quantitative theoretical yields (Figure 3, top). This indicated that [(dppf)Ni(Ph)(I)] is likely formed, but then redistributes to [(dppf)Ni(Ph)₂] and [(dppf)Ni(I)₂]. In contrast, there is no conversion of 4-*t*-butyl-iodobenzene under similar conditions (Figure 3, middle), indicating that the oxidative addition product is never formed. Finally, reaction of [(dppf)Ni(COD)] with 4-cyano-iodobenzene produces an intermediate, which upon reaction with [(DMPU)₂Zn(CF₂H)₂] leads to product formation (Figure 3, bottom). It is clear from the above studies that ligand modifications are needed in order to obtain a nickel species that is more apt at activating aryl halides bearing pendant alkyl and electron donating groups. Such studies are ongoing in our labs.



We also intend to use DFT calculations to guide the ligand design and also tell us if there are steric effects at play when the aryl halide substrates possess pendant alkyl groups. Understanding these effects may be especially critical for expanding the substrate scope, considering that prior calculations on a related system indicate that the formation of η^2 -arene intermediates precede oxidative additions of aryl halides with [(dppf)Ni].⁵ Therefore, we would like to do an in-depth computational study to profile different mechanistic pathways and determine the lowest energy route from starting materials to products. Once the lowest energy pathway with bromobenzene as a model substrate has been identified, we will then see how the energy profiles trend when: 1) alkylated aryl halide substrates are used; and 2) ligand modifications are performed. Computations may also shed light into the unique role of DMSO for promoting the difluoromethylation reactions. Schoenebeck has used calculations to parse out the beneficial role of acetonitrile additive in [(dppf)Ni] catalyzed trifluoromethylthiolations of aryl chlorides in toluene solvent.⁵ She found that the beneficial acetonitrile effect was due to the *in situ* formation of [(dppf)Ni(MeCN)] (which underwent more facile oxidative additions) and the change of the turnover limiting intermediate from nickel(0) to nickel(II) (leading to a decreased energetic span of the catalytic cycle). We are interested in knowing whether such intimately bound DMSO-nickel species affect free energy barriers in a constructive fashion, and if so, whether they may be further tuned.

References:

- 1) Fujikawa, K.; Fujioka, Y.; Kobayashi, A.; Amii, H. *Org. Lett.* **2011**, *13*, 5560.
- 2) Fier, P. S.; Hartwig, J. F. *J. Am. Chem. Soc.* **2012**, *134*, 5524.
- 3) Gu, Y.; Leng, X.; Shen, Q. *Nat. Commun.* **2014**, *5*, 5405.
- 4) Xu, L.; Vivic, D. A. *J. Amer. Chem. Soc.* **2016**, *138*, 2536.
- 5) Yin, G.; Kalvet, I.; Englert, U.; Schoenebeck, F. *J. Am. Chem. Soc.* **2015**, *137*, 4164.

Publications Acknowledging this Grant in 2013-2016

Exclusively funded by this grant:

- 1) "A Versatile Route to Arylated Fluoroalkyl Bromide Building Blocks" Kaplan, P. T.; Vivic, D. A. *Org. Lett.* **2016**, *18*, 884-886.
- 2) "Direct Difluoromethylation of Aryl Halides via Base Metal Catalysis at Room Temperature" Xu, L.; Vivic, D. A. *J. Am. Chem. Soc.* **2016**, *138*, 2536-2539.
- 3) "An Unusual Example of Halogen Bonding to Potassium t-Butoxide" Xu, L.; Cramer, R. E.; Vivic, D. A. *J. Fluorine Chem.* **2015**, *179*, 53-55.
- 4) "Stepwise Conversion of a Platinum Dimethyl Complex to a Perfluorometallacyclobutane Derivative" Xu, L.; Solowey, D. P.; Vivic, D. A. *Organometallics* **2015**, *34*, 3474-3479.
- 5) "Synthetic Utility of Dizinc Reagents Derived from 1,4-Diiodo- and 1,4-Dibromo-octafluorobutane" Kaplan, P. T.; Chen, B.; Vivic, D. A. *J. Fluorine Chem.* **2014**, *168*, 158-162.
- 6) "Improved Synthesis, Structure, and Reactivity of 1,4-Bis(trimethylsilyl)octafluorobutane" Chen, B.; Vivic, D. A. *J. Fluorine Chem.* **2014**, *167*, 139-142.

- 7) "Mild, Safe, and Versatile Reagents for (CF₂)_n Transfer and the Construction of Fluoroalkyl-Containing Rings" Kaplan, P. T.; Xu, L.; Chen, B.; McGarry, K. R.; Yu, S.; Wang, H.; Vivic, D. A. *Organometallics* **2013**, *32*, 7552-7558.
- 8) "Lithium Bromide-Induced Structural Changes in a Nickel Bis-Alkoxide Complex" Ichioka, H. and Vivic, D. A. *Acta Chim. Slov.* **2013**, *60*, 190-192.

Jointly funded by this grant and other grants with leading intellectual contribution from this grant:

- 1) "Triphenylphosphine-Mediated Deoxygenative Reduction of CF₃SO₂Na and its Application for Trifluoromethylthiolation of Aryl Iodides" Yang, Y.; Xu, L.; Yu, S.; Liu, X.; Zhang, Y.; Vivic, D. A. *Chem. Eur. J.* **2016**, *22*, 858-863.
- 2) "Accessing Perfluoroalkyl Nickel(II), (III), and (IV) Complexes Bearing a Readily Attached [C₄F₈] Ligand" Yu, S.; Dudkina, Y.; Wang, H.; Kholin, K. V.; Kadirov, M. K.; Budnikova, Y.; Vivic, D. A. *Dalton Trans.* **2015**, *44*, 19443-19446.
- 3) "Manganese-Catalyzed Aerobic Oxytrifluoromethylation of Styrene Derivatives Using CF₃SO₂Na as the Trifluoromethyl Source" Yang, Y.; Liu, Yingle; Jiang, Y.; Zhang, Y.; Vivic, D. A. *J. Org. Chem.* **2015**, *80*, 6639-6648.
- 4) "Iron-Catalyzed Electrochemical C-H Perfluoroalkylation of Arenes" Khrizanforov, M.; Strekalova, S.; Khrizanforova, V.; Grinenko, V.; Kholin, K.; Gryaznova, T.; Sinyashin, O.; Xu, L.; Vivic, D. A.; Budnikova, Y. *Dalton Trans.* **2015**, *44*, 19674-19681.
- 5) "Synthesis and Reactivity of New Aminophenolate Complexes of Nickel" Yu, S.; Wang, H.; Sledziewski, J. E.; Madhira, V. N.; Takahashi, C. G.; Leon, M. K.; Budnikova, Y. H.; Vivic, D. A. *Molecules* **2014**, *19*, 13603-13613.
- 6) "Organometallic Aspects of Fluoroalkylation Reactions with Copper and Nickel" Wang, H.; Vivic, D. A. *Synlett* **2013**, *24*, 1887-1898.
- 7) "A Five-Coordinate Nickel(II) Fluoroalkyl Complex as a Precursor to a Spectroscopically Detectable Ni(III) Species" Zhang, C. P.; Wang, H.; Klein, A.; Biewer, C.; Stirnat, K.; Yamaguchi, Y.; Xu, L.; Gomez-Benitez, V.; Vivic, D. A. *J. Am. Chem. Soc.* **2013**, *135*, 8141-8144.

Jointly funded by this grant and other grants with relatively minor intellectual contribution from this grant:

- 1) "Pyridine-directed and Palladium-Catalyzed Electrochemical Phosphonation of a C(sp²)-H Bond" Dudkina, Y. B.; Gryaznova, T. V.; Islamov, D. R.; Kataeva, O. N.; Sinyashin, O. G.; Vivic, D. A.; Budnikova, Y. H. *J. Organomet. Chem.* **2015**, *785*, 68-71.
- 2) "Nanoheterogeneous Catalysis in Electrochemically Induced Olefin Perfluoroalkylation" Dudkina, Y. B.; Gryaznova, T. V.; Davydov, N. A.; Mustafina, A. R.; Vivic, D. A.; Budnikova, Y. B. *Dalton Trans.* **2015**, *44*, 8833-8838.
- 3) "Electrochemical *Ortho*-Functionalization of Phenylpyridine with Perfluorocarboxylic Acids Catalyzed by Palladium in Higher Oxidation States" Dudkina, Y. B.; Mikhaylov, D. Y.; Gryaznova, T. V.; Tufatullin, A. I.; Kataeva, O. N.; Vivic, D. A.; Budnikova, Y. H. *Organometallics* **2013**, *32*, 4785-4792.

**Molecular Level Foundation for Olefin Metathesis by
Heterogeneous Supported Molybdena Catalysts**

Israel E. Wachs
Lehigh University, Department of Chemical and Biomolecular Engineering

Presentation Abstract

Despite being discovered 50 years ago and its industrial importance, there is very little literature concerning the fundamental details of the supported $\text{MoO}_x/\text{Al}_2\text{O}_3$ catalyst for olefin metathesis and the few reported details are sometimes even contradictory. This lack of clarity derives from the absence of spectroscopic methods that are capable of *directly* probing the catalyst surface during the catalytic reaction. It is, thus, crucial to determine the fundamental molecular level details of these catalysts so they may be rationally designed to further help meet the rising propylene demand.

To address the molecular details of olefin metathesis by supported $\text{MoO}_x/\text{Al}_2\text{O}_3$ catalysts, modern *in situ* molecular spectroscopic techniques were applied before and during reaction conditions. The initial oxidized supported $\text{MoO}_x/\text{Al}_2\text{O}_3$ catalysts were found to contain a combination of isolated and polymeric sites, dependent on molybdena concentration; at low loadings of molybdena (<9%, 2.1 Mo atoms/nm²), only isolated dioxo ($(\text{O}=\text{O})_2\text{MoO}_4$) sites are present, but as molybdena loading is increased, isolated ($\text{O}=\text{MoO}_4$) and polymeric (Mo-O-Mo) mono-oxo sites co-exist with the isolated dioxo site. *In situ* Raman spectroscopy during olefin metathesis revealed that the isolated dioxo surface sites may still be present at high molybdena coverage since they are present after the bands due to the mono-oxo sites reduce. It was also observed during propylene metathesis that both the isolated and polymeric mono-oxo sites are active for olefin metathesis, while the dioxo site is only a spectator site. The C_3H_6 -TPSR experiments corroborated these results since the activity of propylene metathesis to 2-butene was observed to increase with oligomerization of the surface MoO_x sites. These studies are beginning to establish the molecular structure-activity relationships for olefin metathesis by supported $\text{MoO}_x/\text{Al}_2\text{O}_3$ catalysts.

**Grant FG02-93ER14350: Molecular Level Foundation for Olefin Metathesis by
Heterogeneous Supported Molybdena Catalysts**

Student(s): Anisha Chakrabarti

Affiliations(s): *Operando* Molecular Spectroscopy & Catalysis Laboratory

RECENT PROGRESS

C₃H₆-TPSR Spectroscopy

TPSR spectroscopy experiments were performed to determine the relative activations of the series of catalysts. Using an online MS to monitor the gaseous products of 2-butene (m/z 56), H₂O (m/z 18), CO₂ (m/z 44), ethylene (m/z 27), and propylene (m/z 42), it was determined that the peak temperature (T_p) *decreases* with *increasing* MoO_x loading. This indicates that the activity of the catalysts for propylene metathesis to 2-butene increases with the oligomerization of the surface MoO_x sites (the presence of increasing amounts of oligomer sites is confirmed by Raman spectroscopy). Additionally, two T_p 's were detected for each catalyst, reflecting the presence of two types surface MoO_x sites with reaction intermediates – one more reactive than the other. The results of the TPSR experiments are summarized in Table 1.

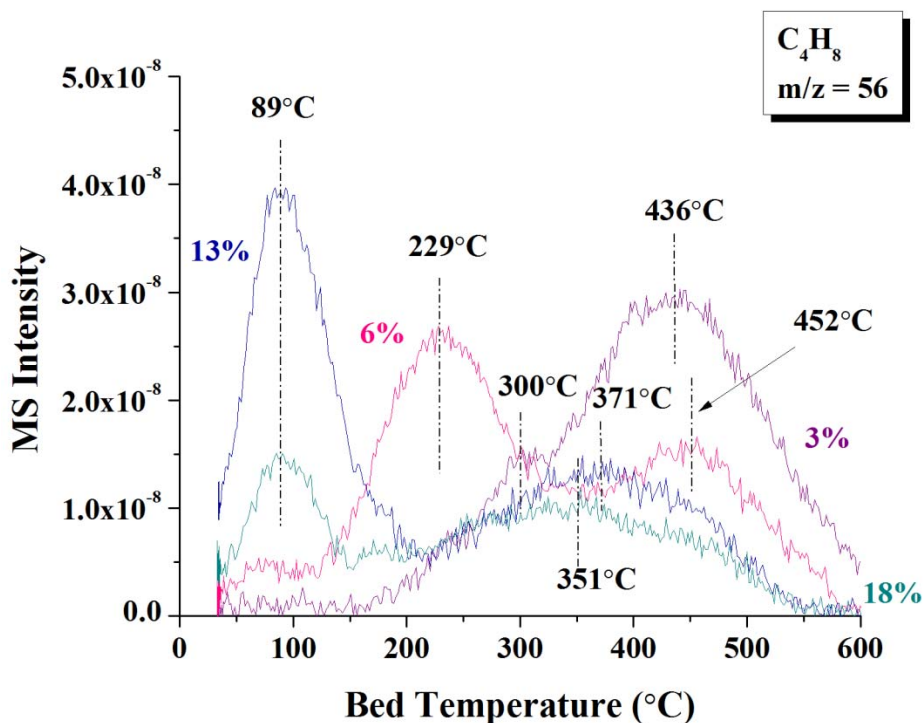


Figure 1. Production of 2-butene (m/z = 56) for supported MoO_x/Al₂O₃ catalysts (percent represents MoO_x weight loading). The experimental procedure consisted of dehydrating at 400°C for 1 h under 10% O₂/Ar, cooling to 35°C in UHP Ar and holding for 30 min (MS turned on), flowing 5% C₃H₆/Ar for 45 min, and heating at a rate of 10°C/min to 600°C under flowing 5% C₃H₆/Ar.

Table 1. TPSR Peak Temperatures (T_p)		
wt% MoO _x /Al ₂ O ₃	T_p 1 (°C)	T_p 2 (°C)
3	300	436
6	229	452
13	89	371
18	89	351

The consumption of propylene is minor below 400°C as the metathesis reaction proceeds. Above 400°C, however, the propylene is extensively combusted with oxygen from the surface MoO_x sites and reveals that high temperatures open up a new reaction pathway that is undesirable. Thus, temperatures less than 400°C represent the best metathesis performance with supported MoO_x/Al₂O₃ catalysts.

The consumption of C₃H₆ (m/z = 42) and production of the oxygenated products (CO₂ (m/z 44) and H₂O (m/z 18)) is presented in Figure 2. The consumption of propylene is minor below 400°C as the metathesis reaction proceeds. Above 400°C, however, the propylene is extensively combusted with oxygen from the surface MoO_x sites and reveals that high temperatures open up a new reaction pathway that is undesirable. Thus, temperatures less than 400°C represent the best metathesis performance with supported MoO_x/Al₂O₃ catalysts.

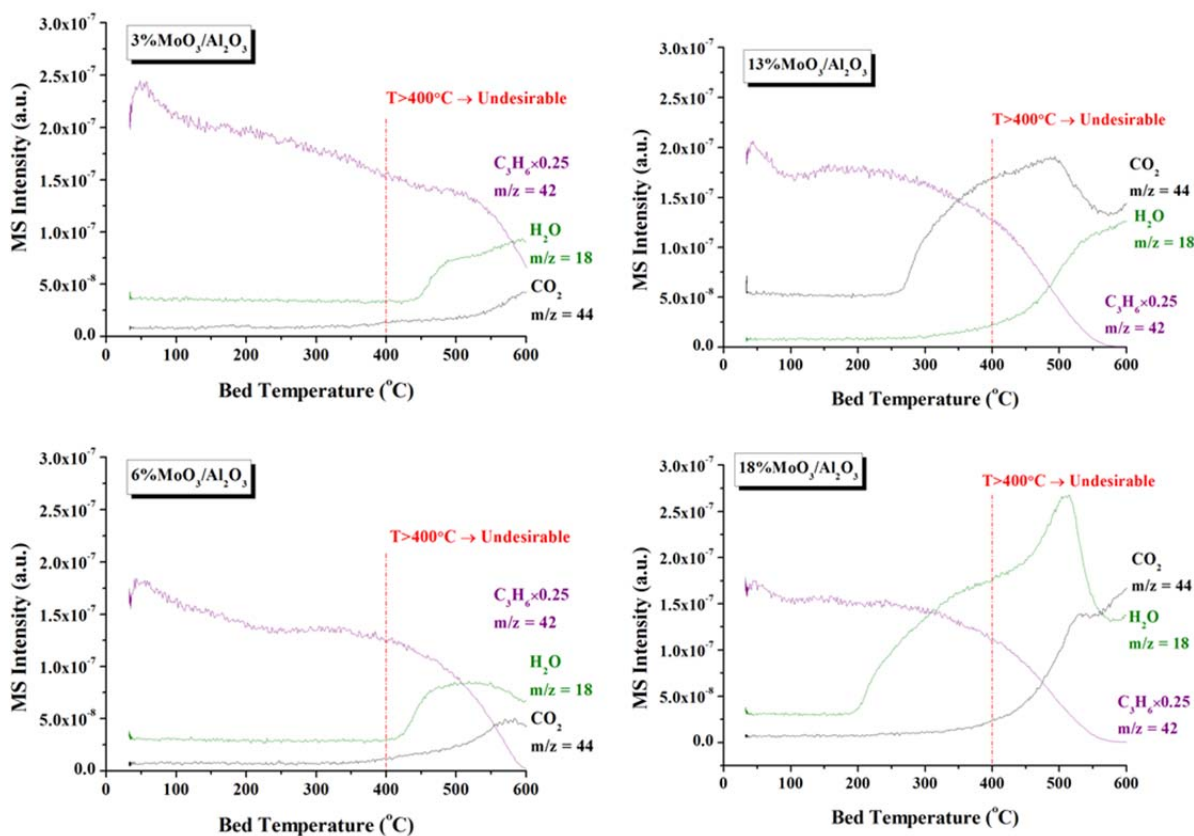


Figure 2. Consumption of propylene (m/z = 42) and production of oxygenated products (CO₂ m/z = 44 and H₂O m/z = 18) as detected with an online MS during the TPSR experiments.

Publications Acknowledging this Grant in 2013-2016

This project is in its first year and no publications or presentations have been submitted to date.

Fundamentals of Acid/base and Redox Reactions on Metal Oxide Catalysts

Yong Wang^{1,2}, Chuck Peden¹, Feng Gao², Jianzhi Hu¹, Junming Sun², Yan Li², Huamin Wang¹, Donghai Mei¹, Lu Zhang¹, Yuan Chen¹, David Dixon³, Rebecca Baylon², Berlin Sudduth²

¹Institute for Integrated Catalysis, Pacific Northwest National Laboratory

²School of Chemical Engineering and Bioengineering, Washington State University

³Department of Chemistry, The University of Alabama

Presentation Abstract

Catalysts for the full and complex range of chemical transformations required for upgrading biomass-derived molecules to fuels and chemicals include metals dispersed on oxide and carbon supports and oxides, including zeolites. Among these catalysts, metal oxides are structurally and chemically complex, making it difficult to describe them with atomic-level precision. To reduce the complexity of this class of catalyst materials to levels addressable and controllable at the atomic level—structurally and mechanistically, high surface area CeO₂, TiO₂, ZrO₂ with specifically exposed facets were synthesized. They provide direct and unambiguous characterization of the redox active metal oxide nanocluster (e.g., VO_x) and allow better understanding of the influence of both the structure and composition of the underlying oxide support on the reactivity of supported metal oxide catalysts. Key insight highlighted in this poster include identification/quantification of V species using ⁵¹V MAS NMR assisted by quantum chemical calculations to correlate surface V-dimers/monomers with methanol oxidative dehydrogenation, manipulation of Lewis acid-base pairs of ZrO₂ to enable highly selective and stable conversion of ethanol to isobutene via cascade hydrogenation/ketonization/aldolization.

FWP-47319: Low-Temperature Catalytic Routes for Energy Carriers via Spatial and Chemical Organization

PI: Johannes Lercher

Mechanistic Studies of Oxidation Reactions on Supported Vanadia Catalysts

Eric Weitz, Weiqiang Wu, Kunlun Ding, Tasha Drake, Stephanie Kwon[#], James A. McCarthy, Kenneth R. Poepelmeier and Peter C. Stair
Department of Chemistry, Northwestern University
Chemical and Biochemical Engineering, Northwestern University[#]
and Institute for Catalysis in Energy Processes, Northwestern University

Presentation Abstract

Catalysts that can selectively oxidize a reactant to the desired product(s) and also avoid over-oxidation are highly desirable and hold out the promise of more energy and cost efficient catalytic processes. A focus of our research has been on the elucidation of molecular level mechanistic information for selected catalytic oxidation reactions employing highly dispersed VO_x catalysts supported on metal oxides that are prepared by atomic layer deposition (ALD). These experiments have been carried out using transmission infrared spectroscopy as a primary probe, which, in some cases, has been supplemented by DRIFT experiments and analysis of the products under steady state reaction conditions. The effect of the support and the nature of oxidizer on product distributions, and thus reaction pathways, provide direct insights into how these factors influence pathways that a system accesses in a complex reaction mechanism. This information can then be directed toward a goal of enabling the use of mechanistic information in the development of ALD catalysts that are engineered at the atomic scale to optimize selectivity toward desired products. We propose a molecular level mechanism for methanol oxidation in the absence of added oxygen, where the vanadyl moieties supply the needed oxygen. The methoxy species, formed on adsorption of methanol, is mobile and our mechanism also invokes a mobile intermediate with carbon in the zero oxidation state, which facilitates access to and reduction of a second vanadium atom to affect the four electron oxidation of methanol. The final vanadium oxidation state can be interrogated with a CO probe molecule in the absence of added oxygen. Cyclohexene oxidation has been also investigated with oxygen and nitrous oxide oxidizers, and under anerobic conditions, on ALD prepared VO_x catalysts supported on titania and alumina with some studies using ceria supports. A primary product we observe is cyclohexene-1-one, but other species, including CO₂, are present and will be discussed.

PARTICIPANT LIST

2016 Catalysis Research PI Meeting

June 21-23, 2016

Participant List

Frank Abild-Pedersen
SLAC National Accelerator Laboratory
abild@slac.stanford.edu

Radoslav Adzic
Brookhaven National Laboratory
adzic@bnl.gov

Eric Altman
Yale University
eric.altman@yale.edu

Aaron Appel
Pacific Northwest National Laboratory
Aaron.Appel@pnnl.gov

Perla Balbuena
Texas A&M University
balbuena@tamu.edu

Simon Bare
SLAC National Accelerator Laboratory
srbare@slac.stanford.edu

Ludwig Bartels
University of California, Riverside
bartels@ucr.edu

Ali Belkacem
Lawrence Berkeley National Laboratory
abelkacem@lbl.gov

Stacey Bent
Stanford University
sbent@stanford.edu

Thomas Bligaard
SLAC National Accelerator Laboratory
bligaard@stanford.edu

Phillip Britt
Oak Ridge National Laboratory
brittpf@ornl.gov

Emilio Bunel
Argonne National Laboratory
ebunel@anl.gov

Michelle Chang
University of California, Berkeley
mcchang@berkeley.edu

Paul Chirik
Princeton University
pchirik@princeton.edu

Abhaya Datye
University of New Mexico
datye@unm.edu

Robert Davis
University of Virginia
rjd4f@virginia.edu

Massimiliano Delferro
Argonne National Laboratory
delferro@anl.gov

David Dixon
University of Alabama
dadixon@ua.edu

Jonah Erlebacher
Johns Hopkins University
Jonah.Erlebacher@jhu.edu

Chris Fecko
U.S. Department of Energy/BES
Christopher.Fecko@science.doe.gov

2016 Catalysis Research PI Meeting

June 21-23, 2016

Participant List

Maria Flytzani-Stephanopoulos
Tufts University
mflytzan@tufts.edu

Anatoly Frenkel
Yeshiva University
anatoly.frenkel@yu.edu

Michel Gagne
University of North Carolina, Chapel Hill
mgagne@unc.edu

Bruce Garrett
Pacific Northwest National Laboratory
bruce.garrett@pnnl.gov

Alan Goldman
Rutgers University
alansgoldman@yahoo.com

Raymond Gorte
University of Pennsylvania
gorte@seas.upenn.edu

Lars Grabow
University of Houston
grabow@uh.edu

Gary Haller
Yale University
gary.haller@yale.edu

Alexander Harris
Brookhaven National Laboratory
alexh@bnl.gov

Andreas Heyden
University of South Carolina
heyden@cec.sc.edu

Adam Hock
Illinois Institute of Technology
ahock@iit.edu

Enrique Iglesia
University of California, Berkeley
iglesia@berkeley.edu

Thomas Jaramillo
SLAC National Accelerator Laboratory
jaramillo@stanford.edu

William Jones
University of Rochester
jones@chem.rochester.edu

Abhijeet Karkamkar
Pacific Northwest National Laboratory
Abhi.Karkamkar@pnnl.gov

Alexander Katz
University of California, Berkeley
askatz@berkeley.edu

Michelle Kidder
Oak Ridge National Laboratory
kidderm@ornl.gov

Harold Kung
Northwestern University
hkung@northwestern.edu

Johannes Lercher
Pacific Northwest National Laboratory
Johanneslercher@hotmail.com

Suljo Linic
University of Michigan
linic@umich.edu

Ping Liu
Brookhaven National Laboratory
pingliu3@bnl.gov

Daniel Lutterman
Oak Ridge National Laboratory
luttermanda@ornl.gov

2016 Catalysis Research PI Meeting

June 21-23, 2016

Participant List

Diane Marceau
U.S. Department of Energy/BES
Diane.Marceau@science.doe.gov

Jean-Sabin McEwen
Washington State University
js.mcewen@wsu.edu

Eric McFarland
University of California
ewmcfar@engineering.ucsb.edu

Gail McLean
U.S. Department of Energy/BES
Gail.McLean@science.doe.gov

James Medlin
University of Colorado
medlin@colorado.edu

Donghai Mei
Pacific Northwest National Laboratory
donghai.mei@pnl.gov

Daniel Mindiola
University of Pennsylvania
mindiola@sas.upenn.edu

Raul Miranda
U.S. Department of Energy/BES
raul.miranda@science.doe.gov

Liviu Mirica
Washington University, St. Louis
mirica@wustl.edu

David Mullins
Oak Ridge National Laboratory
drmullins@ornl.gov

Matthew Neurock
University of Minnesota
mneurock@umn.edu

SonBinh Nguyen
Northwestern University
stn@northwestern.edu

Ralph Nuzzo
University of Illinois, Urbana-Champaign
r-nuzzo@illinois.edu

Gerard Parkin
Columbia University
parkin@columbia.edu

Charles Peden
U.S. Department of Energy/BES
charles.peden@science.doe.gov

Kenneth Poeppelmeier
Northwestern University
krp@northwestern.edu

Marek Pruski
Ames Laboratory
mpruski@iastate.edu

Talat Rahman
University of Central Florida
talat.rahman@ucf.edu

Ashwin Ramasubramaniam
University of Massachusetts, Amherst
ashwin@engin.umass.edu

Thomas Rauchfuss
University of Illinois, Urbana-Champaign
rauchfuz@illinois.edu

Fabio Ribeiro
Purdue University
fabio@purdue.edu

Jeffrey Rimer
University of Houston
jrimer@central.uh.edu

2016 Catalysis Research PI Meeting

June 21-23, 2016

Participant List

Jose Rodriguez
Brookhaven National Laboratory
rodriguez@bnl.gov

Roger Rousseau
Pacific Northwest National Laboratory
Roger.Rousseau@pnnl.gov

Aaron Sadow
Ames Laboratory
sadow@iastate.edu

Richard Schrock
Massachusetts Institute of Technology
rrs@mit.edu

Viviane Schwartz
U.S. Department of Energy/BES
viviane.schwartz@science.doe.gov

Neil Schweitzer
Northwestern University
neil.schweitzer@northwestern.edu

Sanjaya Senanayake
Brookhaven National Laboratory
ssenanay@bnl.gov

Wendy Shaw
Pacific Northwest National Laboratory
wendy.shaw@pnnl.gov

Igor Slowing
Ames Laboratory
islowing@iastate.edu

Peter Stair
Northwestern University
pstair@northwestern.edu

Yogesh Surendranath
Massachusetts Institute of Technology
yogi@mit.edu

Franklin (Feng) Tao
University of Kansas
franklin.feng.tao@ku.edu

Terry Don Tilley
Lawrence Berkeley National Laboratory
tdtilley@berkeley.edu

Wilfred Tysoe
University of Wisconsin, Milwaukee
wtt@uwm.edu

David Vivic
Lehigh University
vivic@lehigh.edu

Aleksandra Vojvodic
SLAC National Accelerator Laboratory
alevoj@stanford.edu

Israel Wachs
Lehigh University
iew0@lehigh.edu

Yong Wang
Pacific Northwest National Laboratory
yong.wang@pnnl.gov

Jason Weaver
University of Florida
weaver@che.ufl.edu

Eric Weitz
Northwestern University
weitz@northwestern.edu

Zili Wu
Oak Ridge National Laboratory
wuz1@ornl.gov

BREAKOUT SESSION SUMMARIES

H-H bonds

Fabio Ribeiro and Wendy Shaw

Attendees Day 1:

Ludwig Bartels
Tom Rauchfuss
Thomas Bligaard
Maria Flytzani-Stephanopoulos
Johannes Lercher
Ken Poepelmeier
Zili Wu
Chuck Peden

Attendees Day 2:

Ludwig Bartels
Tom Rauchfuss
Maria Flytzani-Stephanopoulos
Zili Wu
Ken Poepelmeier
Chuck Peden
Peter Stair

Questions for Discussion (suggested for first day)

- For homogeneously and heterogeneously catalyzed processes, what are the inherent similarities and differences in reaction mechanisms?
 - What are some currently proposed/accepted mechanisms for the specific bond breaking/bond making processes in each case?
 - What class(es) of catalyst(s) are responsible for carrying out these elementary bond breaking/bond making processes, and what are the properties of the catalysts that give rise to this chemistry?
 - Are there overall reactions involving these bond breaking/making steps that are uniquely catalyzed homogeneously or heterogeneously?
- Are there examples of major recent advances in understanding mechanisms of these elementary processes?
- What are some of the significant outstanding questions regarding the mechanisms of these bond making and bond breaking reactions?

Current State

Heterogeneous Catalysis

- Classes of catalysts
 - Non-metal: zeolites, silicates
 - Metals and alloys
 - With some metals, $H_2 + H\cdot$ are at quasi equilibrium
 - Metal oxides, nitrides, carbides, sulfides
 - Dopant modification

Homogeneous (and Bio) Catalysis

- Classes of catalysts/properties
 - Non-metal (FLP: BR_3 etc)
 - Precious and non-precious metals
- Ancillary factors
 - 2nd, 3rd, etc Coordination spheres
 - ET

Both hetero and homogeneous can cleave by the same mechanism

- homo vs heterolytic
- Dihydrogen complex vs end-on (or atop)
- Dihydride vs. proton-hydride
- Mono vs bifunctional (functional group or second metal)
 - hetero vs homobimetallic

Mechanistic Features

Homogeneous Catalysis

For HER and H_2 Oxidation

- Rate and overpotential
 - Inverse correlation between rate and overpotential
- Rate limiting steps for H_2 oxidation
 - Most often H_2 addition
- Rate limiting steps for H_2 production
 - Most often proton transfer

For non-fuel cell applications

- largely governed by the follow-on reaction, however, hydricities and pKa's needed to split H_2 can be problematic

Heterogeneous Catalysis

- For Group 8 metals, quasi-equilibrium, very efficient.
- Single metal atom activation/dissociation of H_2 and spillover effects; e.g. (Pt,Pd)Cu single atom alloys or supported single-atom Pd, Au for selective hydrogenation and dehydrogenation reactions
- Rate and overpotential both need to be optimized
- Is the activation on a defect? Not the whole story
- Role of the dopant
- Phase of the catalyst is not necessarily the same

Recent Advances

Homogeneous Catalysis for

- Understanding and incorporating second/outer sphere features from enzymes
- Room temperature reversibility has been achieved (fast rates/low overpotential)
 - Controlling proton movement
 - Structural contribution to stabilizing active site
- Overpotential and rate for H₂ production have been decoupled by controlling catalyst dynamics
- Using FLP's as catalysts

Heterogeneous Catalysis

- Engineered surfaces
 - Designing catalytically active sites on an atomic scale specific for H₂ activation.
 - Specifically not referring to immobilized homogeneous catalysts (different issues)
- The structure may change during catalysis
 - Not necessarily the defects you started with

Significant Outstanding Questions

Homogeneous Catalysis

- Decoupling rate and overpotential consistently
- Catalyst stability
- H₂ addition
- Bimetallic
 - what is the role of the second metal

Heterogeneous Catalysis

- Bifunctionality in single metal alloys (need theory)
- Decoupling rate and overpotential consistently
 - oxides
- Catalyst stability and regenerability
 - High temperatures
 - Due to reaction even at low T
- H₂ addition
- In situ analysis and characterization

**Cluster chemistry to reproduce surfaces challenging
Synthesis? Different ligands?**

Questions for Discussion (suggested for 2nd day)

- How do we go about determining these mechanisms for homogeneously and heterogeneously catalyzed processes?
 - What can we learn from each other by comparing/contrasting these approaches to mechanistic studies?
- What is limiting our abilities to address the significant outstanding questions?
 - While there are lots of great experimental tools available now, what is still needed to advance the field (to address these current limitations)?
 - Since theory is an essential element of mechanistic studies, what advances here are needed?
 - Are there critical elements of benchmarking that are needed?
- More generally, how do these elementary bond breaking/bond making reactions relate to current challenges for developing sustainable processes?

What Can We Learn From Each Other

- The gap is narrowing
- Heterogeneous has learned from homogeneous
 - Single site engineered surfaces
 - Think of surface as a ligand
 - Metal oxides, sulfides, carbides, etc can locally exhibit a “homogeneous-like” ligand structure
- Big differences:
 - The temperature
 - Heterogeneous community aware of engineering principles that inform their work more than homogeneous
- Theory:
 - Theory is leading the connection; they serve as the glue
 - Differences: many techniques are different (periodic boundary conditions, models that are not based on atomic orbitals).
 - Commonalities: micro-kinetic models; the heterogeneous community is starting to provide information from which you can use chemical intuition (learning from homogenous)

Limitations to Determining Outstanding Questions

- Experimental Tools
 - Direct observation of proton movement in aqueous solvents
 - More broad use of:
 - In situ characterization (high pressure XPS, high pressure/high temperature NMR, Inelastic Neutron Scattering, STM, etc)
 - More opportunities for high cost equipment (small centers; i.e. NSF MIP program)
 - More formal mechanism to establish collaborations with user facilities
 - Suggest Catalysis topics for the DOE graduate students (SCGSR)

Limitations to Determining Outstanding Questions (cont.)

- Theory
 - Higher accuracy ($<1-2$ kcal/mol, $<pK_a=1$)
 - Including both thermo and kinetics
 - Providing guidance for how to prepare materials (heterogeneous)
 - Balance transformative first-principles based predictions with experimental feasibility
 - Cross-field sharing (e.g. stability and meta-stability are better understood for heterogeneous)
- Benchmarking
 - TON (i.e. stability; for homogeneous catalysis)
 - Comparisons between heterogeneous and homogeneous are useful
 - “The same” conditions would need to be identified for each system
 - Immobilizing homogeneous catalysts would be one way to compare

How do these reactions relate to challenges for developing sustainable processes

- Understanding H₂ activation and production is essential for understanding all higher order multi-proton, multi-electron reactions (storing energy in chemical bonds)
- Can be an important step for C-O, O-O, and N-N reactivity, hydrotreating, dehydrogenating

C-H Bond Activation – Day 1

Bill Jones and Matt Neurock
22 participants

For homogeneously and heterogeneously catalyzed processes, what are the inherent similarities and differences in reaction mechanisms?

Many C-H activation reactions are carried out by essentially the same mechanisms.

Differences are due to differences in the reaction environments which dictate the sites present under working catalytic condition.

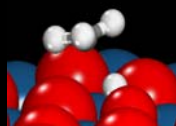
There are some reactions which may occur via different mechanisms (or controlling steps). (e.g. C-C metathesis.)

C-H Bond Activation Mechanisms

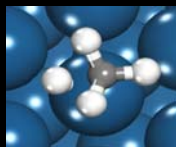
What are some currently proposed/accepted mechanisms for the specific bond breaking/bond making processes in each case?

Oxidative Addition
Hydrogen Atom Abstraction
Deprotonation
 σ -bond metathesis
Electrophilic Activation
Heterolytic Activation
Oxidative Hydrogen Migration
Metalloradical Activation
1,2 – Addition
Electrochemical C-H Activation
Enzymatic

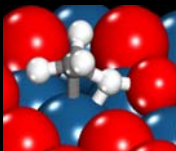
Mechanisms of C-H Activation



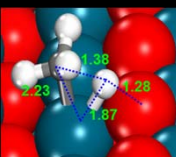
Hydrogen Abstraction



Oxidative Addition

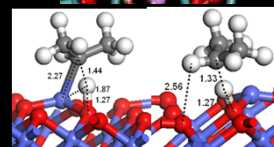
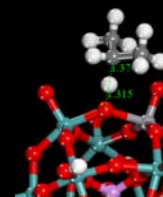


Ligand-Assisted Oxidative Addition

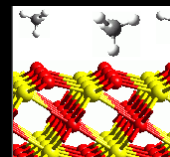


Sigma Bond Metathesis

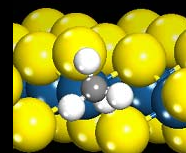
Reductive Hydrogen Abstraction



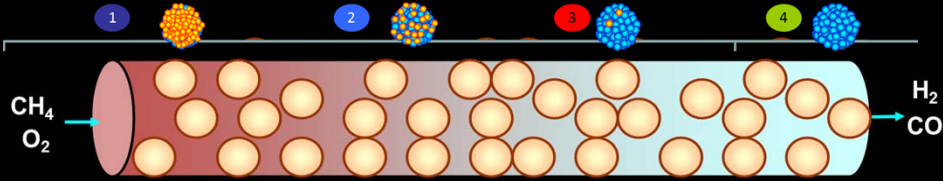
Non-Reducible H-Abstraction



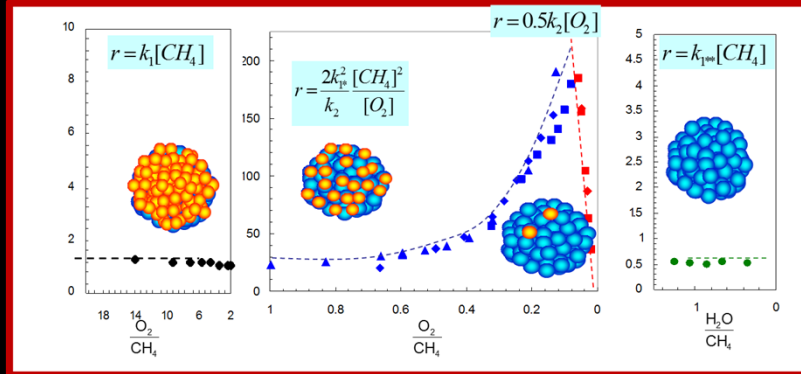
Softer Oxidants Hydrogen Abstraction



C-H Activation Kinetics Depend on Reaction Environment

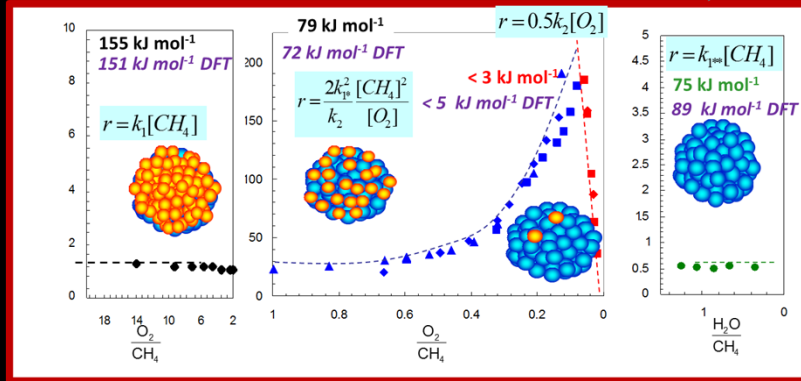
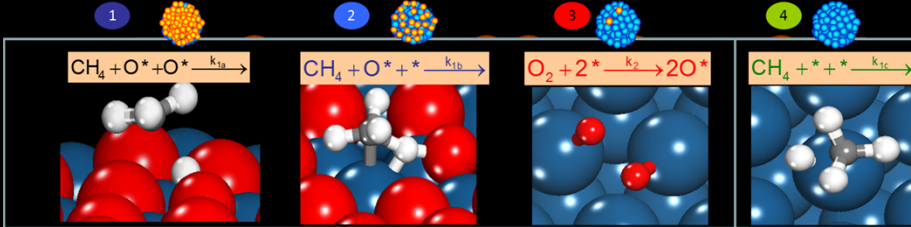


4 Different Kinetic Regimes



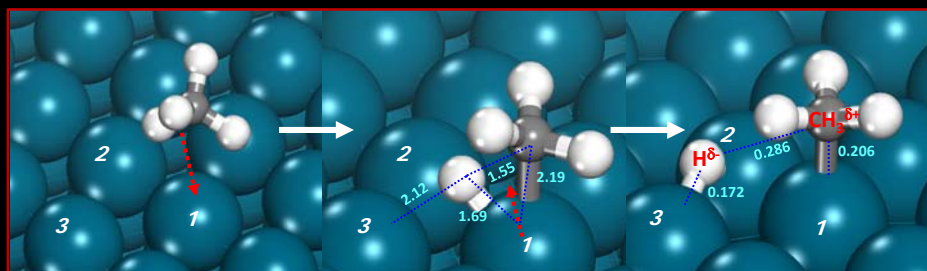
Chin, Y., C. Buda, M. Li, M. Neurock, and E. Iglesia, *J. Am. Chem. Soc.*, 133, 40, 15958-15978, 2011.

C-H Activation Kinetics Depend on Reaction Environment



Chin, Y., C. Buda, M. Li, M. Neurock, and E. Iglesia, *J. Am. Chem. Soc.*, 133, 40, 15958-15978, 2011.

Methane Activation over Pd (111) Terraces



η_1 -binding of CH₄

$\Delta E_{\text{C-H,Pd}} = 73 \text{ kJ mol}^{-1}$

$\Delta E_{\text{rxn}} = 29 \text{ kJ mol}^{-1}$

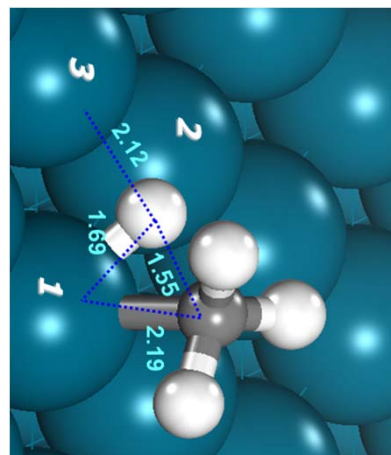
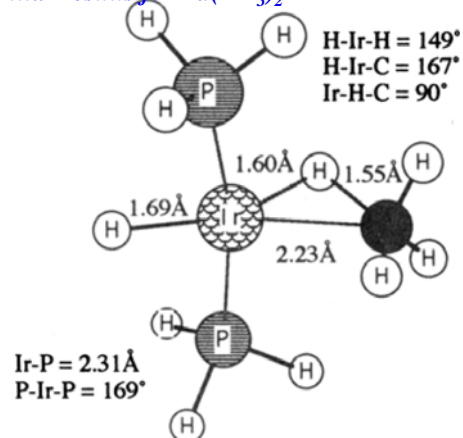
Donation from C-H to Pd₁
Pd acts an electrophile

Back-donation from Pd₁ to C-H σ^*
Pd acts as a nucleophile

Chin, Y.H., C. Buda, M. Neurock, and E. Iglesia,
J. Am. Chem. Soc., 135 (41), 15425–15442, 2013.

Comparison of Oxidative Addition over Homogeneous Ir(PH₃)₂H Complexes and Heterogeneous Pd Surface

Similar results for Pd(PH₃)₂

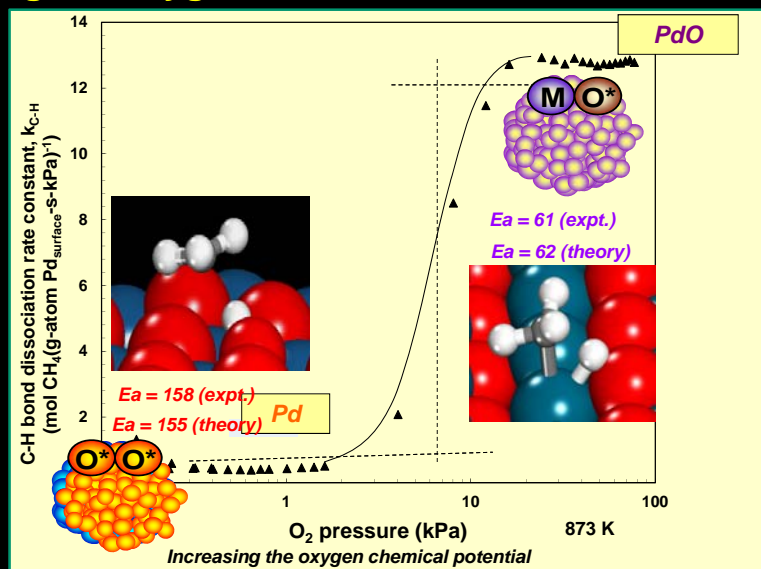


T. Cundari, *J. Am. Chem. Soc.* 1994, 116, 340-347

Electrons are delocalized in the metal so there is only small change in oxidation state of Pd

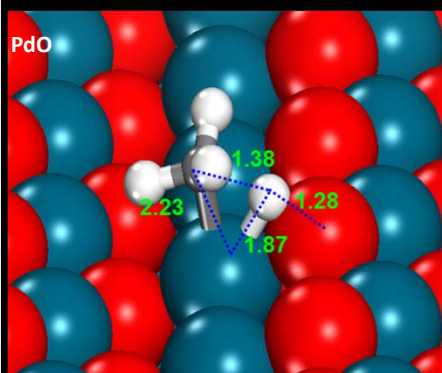
Chin, Y.H., C. Buda, M. Neurock, and E. Iglesia,
J. Am. Chem. Soc., 135 (41), 15425–15442, 2013.

Significantly Enhanced Rates on Pd at Higher Oxygen Pressures – PdO Formation



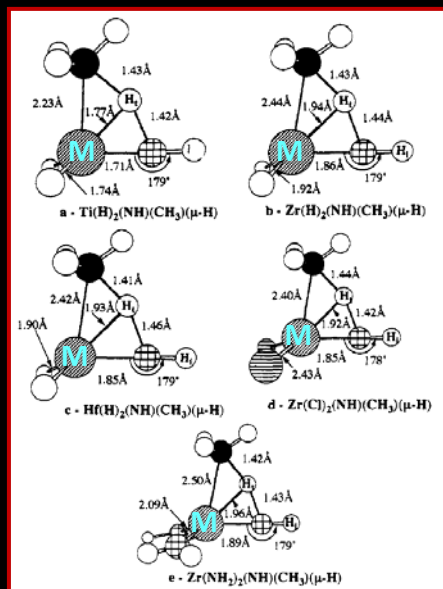
Chin, Y.H., C. Buda, M. Neurock, and E. Iglesia, *J. Am. Chem. Soc.*, 135 (41), 15425–15442, 2013.

Comparison of Oxidative Addition over Homogeneous Ir(Ph₃)₂H Complexes and Heterogeneous PdO Surfaces



Simultaneous: Oxidative Addition
Reductive Deprotonation

Chin, Y.H., C. Buda, M. Neurock, and E. Iglesia, *J. Am. Chem. Soc.*, 135 (41), 15425–15442, 2013.



T. Cundari, *J. Am. Chem. Soc.* 1992, 114, 10557-10563

What class(es) of catalyst(s) are responsible for carrying out these elementary bond breaking/bond making processes, and what are the properties of the catalysts that give rise to this chemistry?

- The presence of species (atoms) on the surface can change the kinetics of the reaction.
- Metals on metal oxides can be used for bifunctional catalysis.
- Terminology does not distinguish between two distinct catalytic sites vs. one site doing two reactions.
- Supported metals typically carry out reforming; supported metals/oxides - oxidative dehydrogenation, non-reducible & reducible metal oxides -oxidative coupling, Mo/zeolites and Fe/SiO₂ – non-oxidative dehydrogenation.

Are there overall reactions involving these bond breaking/making steps that are uniquely catalyzed homogeneously or heterogeneously?

- Non-reducible H-abstraction does not exist homogeneously.
- Are the mechanisms in heterogeneous catalysis and homogeneous catalysis the same under the same conditions? Rate determining steps might be different. e.g. metathesis at 700 C might not go through metallacyclobutane. Side-by-side comparisons are needed.
- What controls competitive vs non-competitive binding.

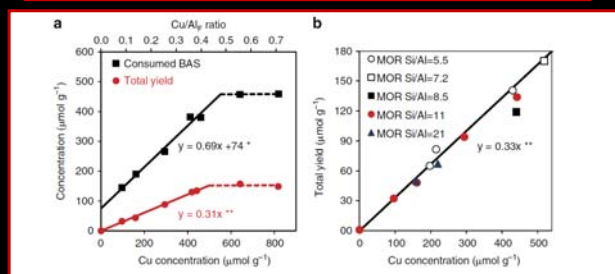
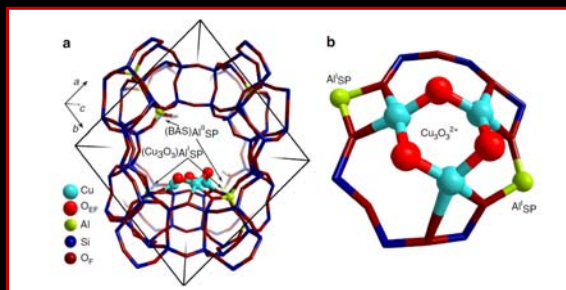
Are there examples of major recent advances in understanding mechanisms of these elementary processes?

- Spectroscopy has allowed for direct observation of reactions under catalysis: XPS, Raman, UVvis, soft X-ray
- SSITKA-steady state isotopic transient kinetic analysis – perturbation effects (also pressure, T jump) provides information about specific steps.
- Improvements with fast detectors has allowed this to be done faster (IR on ns; Raman in 1 sec; UVvis in ms).
- In-situ spectroscopy for reactions in solution (ATR, etc.)
- Synthetic techniques have improved as well. e.g. nanostructures on surfaces.
- STM, TEM improvements.
- Coupling spectroscopy and theory

What are some of the significant outstanding questions regarding the mechanisms of these bond making and bond breaking reactions?

- How do you stop further reaction in any of the mechanisms, to prevent overoxidation/coking, etc?
- Are any of these mechanisms more controllable?
- How can we control selectivity via controlling environment? E.g. zeolite confinement, control contact and hydrophobicity.
- Spillover from the metal to support can be important yet it is not widely understood. e.g., where do the elementary steps occur? Is the catalytic site needed? What are the atomistic steps of spillover? Hydrogenation may occur on the metal, metal support or support alone.
- C-H activation can be very easy at a highly activated surface – turnover is the problem.

Selective Activation of Methane to Methanol Over Single Site Trinuclear Cu-Oxo Complexes in Mordenite



S. Grunder, M. Markovits, G. Li, M. Tramp, E. Pidko, E. Hensen, A. Jentys, M. Sanchez, and J. Lercher, Nat. Comm. 2015,

What are some of the significant outstanding questions regarding the mechanisms of these bond making and bond breaking reactions?

- Heterogeneous rates are usually measured at steady state. Homogeneous rates are usually measured with stoichiometric rates. Site counting important and makes comparisons difficult.
- Mechanism is determined by the nature/polarity of the transition state polarity, where the electrons reside when the bond is broken and the role of the sites that carry out activation and the influence of dopants and promoters on the electronic structure.
- C-H activation of oxygenates – distinct from hydrocarbons – multiple types of bonds present special challenges.
- Reaction engineering strategies may be of great importance in aiding and controlling C-H activation processes. E.g. membrane reactors and the specific control local concentrations, use of molten salts.
- Catalytic behavior sensitive to what is present under working conditions and specific structure and composition of the surface (particles can have significantly different behavior than ideal surfaces)

What are some of the significant outstanding questions regarding the mechanisms of these bond making and bond breaking reactions? (cont'd)

- Bridging oxygens sites may be active in bioinorganic systems as well as heterogeneous catalytic systems.
- Difficult to mimic the 3D spatial positioning special positioning of sites and hydrophobic environments that drive enzyme reactions (Caronic Anhydraz).
Anhydraz).
- Homogeneous catalyst/Ligand stability at higher temperatures.
- Elucidating the active sites for homogeneous and heterogeneous catalysts difficult under operating conditions as a result of changes that occur in activating the materials.

C-H Bond Activation – Day 2

Bill Jones and Matt Neurock
25 participants

Questions for Discussion (suggested for 2nd day)

Questions for Discussion (suggested for 2nd day)

How do we go about determining these mechanisms for homogeneously and heterogeneously catalyzed processes?

In-situ spectroscopy and detailed isotopic kinetic studies provide important insights into the sites and mechanisms responsible. Selective probe reactions and poisoning of sites can aid in elucidating mechanism.

What can we learn from each other by comparing/contrasting these approaches to mechanistic studies?

Theory can play an important role in comparing and contrasting homogeneous & heterogeneous systems (requires reliable models of active sites).

Create teams that examine the same catalytic reaction with both homogeneous and heterogeneous catalysts and compare and contrast results and mechanisms.

What is limiting our abilities to address the significant outstanding questions?

- ❑ **Ability to determine the nature and the number of active sites which might only exist during catalysis and may change during reactions.**

Need to obtain the structure of active sites and monitor it during the reaction in situ/operando.

Experiment and theory should be combined, to identify and quantify the number of active sites.

Characteristics of active sites: space, energy.

Enhanced spatio-temporal and energy resolution methods along with theory.

Advanced synchrotron methods: modulation-excitation, HERFD/RIXS, single particle spectroscopy, combination of multiple techniques (XAFS, XRD/PDF, STEM, IR, Raman)

- ❑ **Approaches to follow the kinetics of active intermediates under working conditions?**

Spectrokinetics (SSITKA + operando spectroscopy):

MS-kinetics, IR-surface intermediate, XAS, Raman – active sites

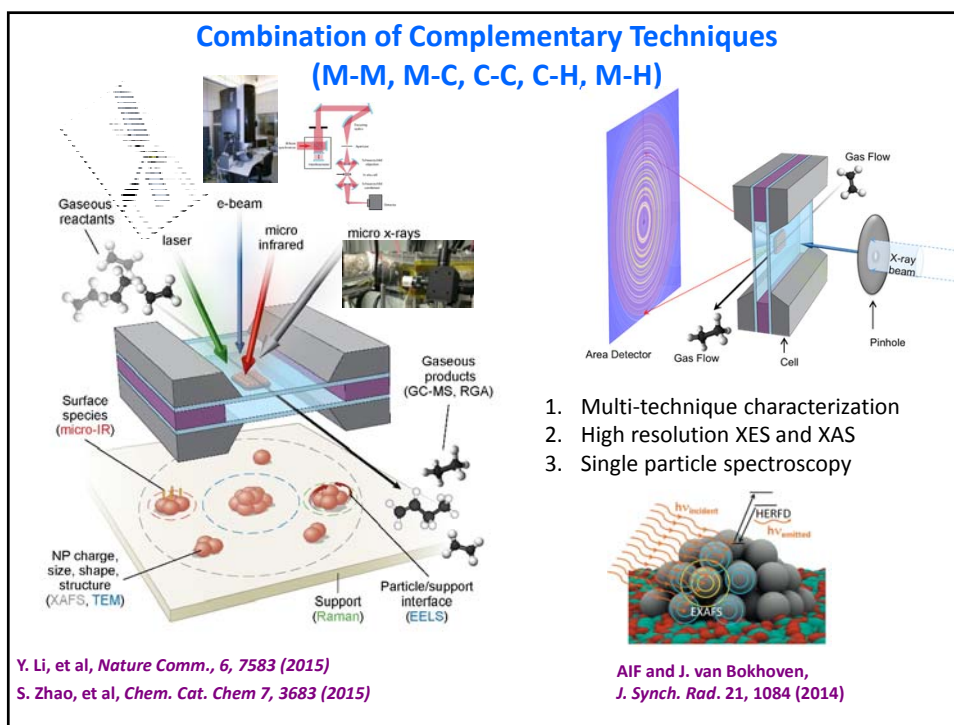
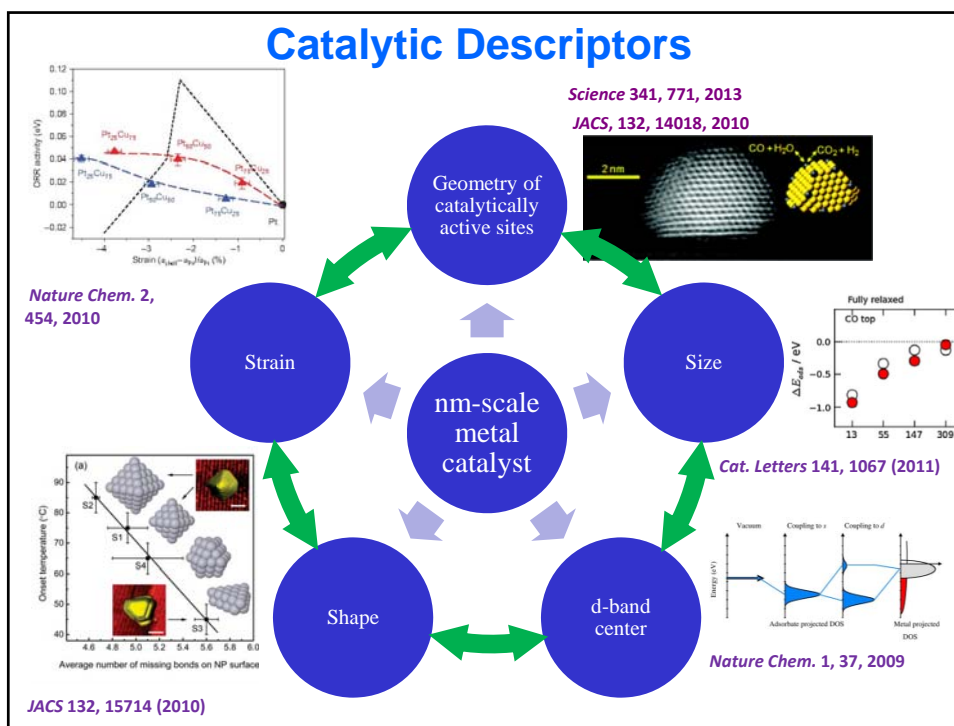
- ❑ **Determination of catalyst properties and descriptors that connect to catalytic reactivity?**

Descriptors can correlate with each other

It is critical to measure them under the same conditions.

New methods are needed, for obtaining and correlating data taken in the same conditions, e.g., spectrokinetics

A. Frenkel, R. Nuzzo, I. Wachs



What is limiting our abilities to address the significant outstanding questions?

❑ We can readily activate C-H bonds. How do we control selectivity?

Improve the intrinsic selectivity of other bond activation/formation steps or limit C-H activation cascades.

Development of bifunctional or tandem catalysts.

Electrocatalytic or photocatalytic steps to assist
Use of photo- or electro- chemical triggers.

Reaction engineering approaches (membrane reactors, specific control of local concentration, use of molten salts).

Questions for Discussion (suggested for 2nd day)

- Since theory is an essential element of mechanistic studies, what advances here are needed?
 - We need to know the active surface terminations, sites and environments under working conditions. This is a challenge.
 - Ability to simulate larger systems and longer time scales.
Ab initio simulations currently limited 100s to 1000s of atoms and femtosecond time scales.
 - Need to simulate phase changes that can also occur with changes in conditions (T and P).
 - Development of accurate reactive force fields but this is a significant challenge.
 - Simulations of relevant spectroscopic properties from X-ray, neutron scattering, NMR, optical absorption and excitations.
 - Identification of the best functionals for specific properties
 - Development of more accurate functionals that more accurately capture electron correlation, exchange and multireference character.

Questions for Discussion (suggested for 2nd day)

- Are there critical elements of benchmarking that are needed?
 - Site counting methods are important for establishing benchmarks. Methods were discussed in last year's meeting on benchmarking.
 - Need to count sites under working conditions.
 - Use of poisons to block sites. They may kill more than one site.
 - The best way is to monitor the reaction itself, e.g. using SSITKA.
 - Measuring rates and isotopes are important.
 - Dynamic counting can be done with the introduction of isotopes.
 - Dilution studies can help identify # of sites.
 - Single turnover measurements can be used to compare to steady-state measurements.

Questions for Discussion (suggested for 2nd day)

- More generally, how do these elementary bond breaking/bond making reactions relate to current challenges for developing sustainable processes?

If you know the intimate aspects of bond activation, this will aid with catalyst design for selectivity.

Can lower energy C-H cleavage processes be found?

Sustainable processes will require a balance with other bond breaking/making steps (C-O activation, C-C formation...). Bi- and multi-functional catalytic materials.

Can electrochemical methods be used?

Can processes be made to produce products that are easier to separate?

Can we utilize biological paths in concert?

Need to provide a full systems analysis of the process.

Can intermediate temperature fuel cells be made?

Four Breakout Sessions Focused on Specific Bond Activation and Formation

- C-H Bonds – Matt Neurock and Bill Jones
- H-H Bonds – Fabio Ribiero and Wendy Shaw
- **C-O Bonds – Aaron Appel and Lars Grabow**
- N-N Bonds – Dan Mindiola and Tom Jaramillo

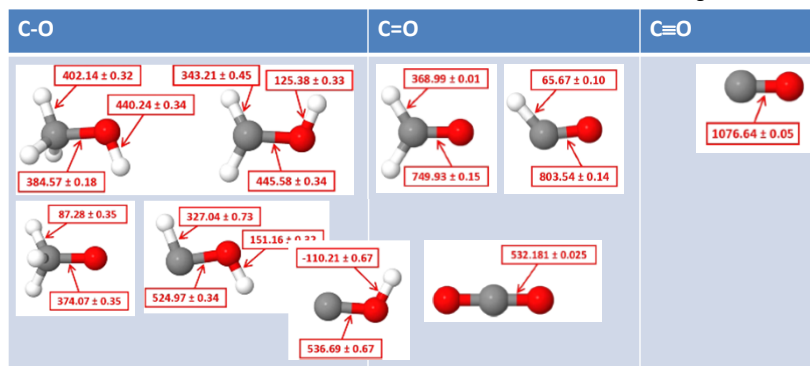
Questions for Discussion (suggested for first day)

- For homogeneously and heterogeneously catalyzed processes, what are the inherent similarities and differences in reaction mechanisms?
 - What are some currently proposed/accepted mechanisms for the specific bond breaking/bond making processes in each case?
 - What class(es) of catalyst(s) are responsible for carrying out these elementary bond breaking/bond making processes, and what are the properties of the catalysts that give rise to this chemistry?
 - Are there overall reactions involving these bond breaking/making steps that are uniquely catalyzed homogeneously or heterogeneously?
- Are there examples of major recent advances in understanding mechanisms of these elementary processes?
- What are some of the significant outstanding questions regarding the mechanisms of these bond making and bond breaking reactions?

Properties of C-O bonds

Type	Strength / $\text{kJ}\cdot\text{mol}^{-1}$	Length / pm
C-O	358	143
C=O	799	120
C \equiv O	1072	113

"Common bond energies"



Ruscic, B. Active Thermochemical Tables: Sequential Bond Dissociation Enthalpies of Methane, Ethane, and Methanol and the Related Thermochemistry. *J. Phys. Chem. A* **119**, 7810–7837 (2015).

Summary Day 1

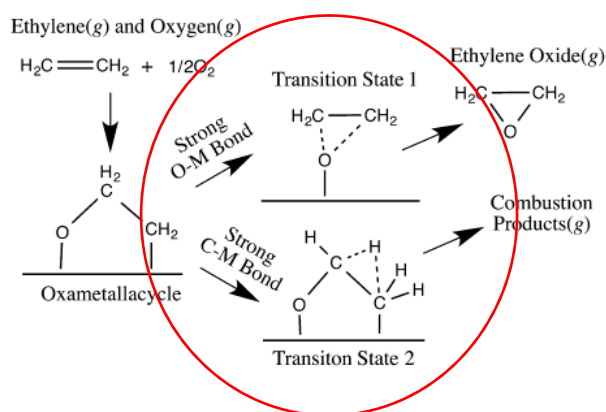
- For homogeneously and heterogeneously catalyzed processes, what are the inherent similarities and differences in reaction mechanisms?
 - The many different types of C-O bonds (single, double, triple) makes it a challenge to compare mechanisms for all C-O bonds. **Too much complexity!**
 - C-O bonds are strongly polar in contrast to N-N, H-H, C-H bonds.
 - We focused predominantly on alcohols. Even within this category many topics were discussed.
 - Should oxophilicity be a quantified (thermodynamic) parameter, similar to Lewis acidity, which has been quantified using a fluoride affinity scale? However, even if quantified, it is not clear that oxophilicity would provide consistent insight into mechanisms of C-O bond cleavage.
 - For alcohols, the reactivity is likely to be distinct based on R-group (alkyl vs aryl) and conditions, especially due to the presence or absence of a liquid phase (solvent).

Summary Day 1

- For homogeneously and heterogeneously catalyzed processes, what are the inherent similarities and differences in reaction mechanisms?
 - Dual sites or bifunctional catalysts, metal-oxide interfaces, solvents...
 - Homogeneous concepts may apply to some single site heterogeneous catalysts.
 - Single elementary steps may be common in heterogeneous and homogeneous catalysis, but not necessarily mechanisms.
 - It was generally agreed that metallic catalysts are expected to have distinct mechanisms from catalysts based on metal oxides or homogeneous complexes. One possible route toward distinction is the separation of homolytic pathways, which are more likely to occur on metallic catalysts, from heterolytic pathways, which are more likely to occur on metal oxide catalysts.

Mechanistic Trends in Heterogeneous Catalysis?

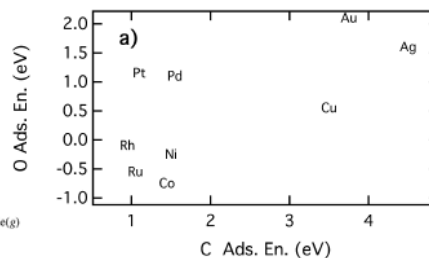
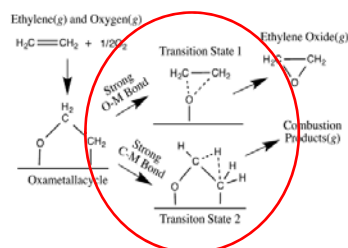
- Look at the transition state!
 - Reaction pathways are often determined by the strength of O-M vs. C-M bonds



Montemore, M. M. & Medlin, J. W. Predicting and comparing C-M and O-M bond strengths for adsorption on transition metal surfaces. *J. Phys. Chem. C* 118, 2666–2672 (2014).

Mechanistic Trends in Heterogeneous Catalysis?

- Look at the transition state!
 - Reaction pathways are often determined by the strength of O-M vs. C-M bonds



Montemore, M. M. & Medlin, J. W. Predicting and comparing C-M and O-M bond strengths for adsorption on transition metal surfaces. *J. Phys. Chem. C* 118, 2666–2672 (2014).

Summary Day 1

- Are there overall reactions involving these bond breaking/making steps that are (nearly) uniquely catalyzed homogeneously or heterogeneously?

Homogeneous:

- Free radical reactions are mostly homogeneous (auto-oxidation).
- Most enantioselective reactions are homogeneously catalyzed.

Heterogeneous:

- CO_2 to MeOH
- Electrocatalytic formation of C-C bonds.
- Steam reforming

Summary Day 1

- Are there examples of major recent advances in understanding mechanisms of these elementary processes?
 - Spectroscopies
 - Availabilities and capabilities of light sources
 - Experimentally validated models
 - A recent area of catalysis that has enable new mechanisms is photoredox catalysis, which allows access to excited states, and enables odd electron pathways instead of typically even electron pathways.
- What are some of the significant outstanding questions regarding the mechanisms of these bond making and bond breaking reactions?
 - Where to begin...
 - Nature of active site
 - ...

Questions for Discussion (suggested for 2nd day)

- How do we go about determining these mechanisms for homogeneously and heterogeneously catalyzed processes?
 - What can we learn from each other by comparing/contrasting these approaches to mechanistic studies?
- What is limiting our abilities to address the significant outstanding questions?
 - While there are lots of great experimental tools available now, what is still needed to advance the field (to address these current limitations)?
 - Since theory is an essential element of mechanistic studies, what advances here are needed?
 - Are there critical elements of benchmarking that are needed?
- More generally, how do these elementary bond breaking/bond making reactions relate to current challenges for developing sustainable processes?

Questions for Discussion (suggested for 2nd day)

How do we go about determining these mechanisms for homogeneously and heterogeneously catalyzed processes?

- There is no proof for a mechanism. Proposed mechanisms can only agree with data or must be rejected (“proof by elimination”)
- Useful data is obtained by
 - T⁵ = Tools, talent, time to think.
 - **Careful reaction kinetics** (rates/TOF, orders, temperature dependences, etc.)
 - Isotopic labeling (even for C¹²/C¹³)
 - In-situ/operando observation of intermediates (spectroscopy, microscopy)
 - Energetics (measured or calculated)
 - binding energies, bond strengths, activation barriers

Questions for Discussion (suggested for 2nd day)

How do we go about determining these mechanisms for homogeneously and heterogeneously catalyzed processes?

- A great amount of insight can be gained by examining a well-defined system such as on (i) a single crystal surface (ii) a single catalytic grain (iii) model metal/oxide interfaces
- Liquid phase is challenging (“can of worms”), but careful kinetics measurements (rates) can be done and should be done
 - Often not an emphasis in homogeneous catalysis
 - Systems with pore condensation are a good starting point
- Collecting mechanisms and consistent rate data into a single location using a common language would be an improvement (so that not everyone has to be an expert in each area)

Questions for Discussion (suggested for 2nd day)

What is limiting our abilities to address the significant outstanding questions?

Experimental tools

- More beam time, access to advanced light sources
- XANES, but limited to heavy elements for liquid phase
- 3D atomic probe field ion microscopy
 - Allows to construct a 3D atom map of any given material
 - Currently lacks dynamic information, but temporal information could be revolutionary
- GC-NMR (commercially available, but not common)

Questions for Discussion (suggested for 2nd day)

What is limiting our abilities to address the significant outstanding questions?

Experimental tools

- Careful studies of kinetics: important, but not sexy!
 - Study as many of the elementary steps as possible
 - Determine equilibria / free energies
 - Determine reverse rates
- More time
 - Access to facilities / equipment
 - Less administrative activities?



Questions for Discussion (suggested for 2nd day)

What is limiting our abilities to address the significant outstanding questions?

Theory & benchmarking

- More CPU time for capacity computing
- Theory can eliminate the obviously wrong. Quantitative agreement between theory and experiment is not needed.
- Importance of metal and metal oxide interfaces is a challenge that needs to be addressed both experimentally and computationally
- The length and the time scales involved in the simulations and those involved experimentally

Questions for Discussion (suggested for 2nd day)

What is limiting our abilities to address the significant outstanding questions?

Theory & benchmarking

- Ability to study dopant levels ($< 0.1\%$, i.e. $> 1,000$ atoms)
- *Ab initio* calculations either accurately capture systems dominated by chemisorption or those that are van der Waals dominated. Must be able to do both.
- Functionals for oxides and solvents
- Need to work towards chemical accuracy

Advances in theory for catalysis

Advances in Correlated Molecular Orbital Theory Methods

- Spin Orbit
- Improved orbitals for CCSD(T) - DFT GGA and Brueckner
- Solid State Approaches
- General Derivative Methods up to 2nd Derivatives for CCSD(T)
- F12 calculations for all catalytically interesting elements (basis set issue)
- Improved MRCI methods where needed.
- Quantum Monte Carlo? Is it here yet? Improved nodes from CCSD(T)?

Advances in DFT

- Spin Orbit
- Improved general purpose functionals
- Improved usability of solid state codes – put energies on a computational chemistry basis
- Improved spectroscopic prediction capability

Solvation

- Improved treatments for implicit solvent – accurate solvation energies
- Improved sampling techniques
- Improved and generalized approaches to predicting barrier heights and rate constants in solution
- How many explicit solvent molecules are needed?
- Enthalpy and entropy of solvation
- Temperature effects

Data Management Approaches and Sharing

- Common data needs – Example: free energy of solvation of a proton
- Benchmarking
- Structures

Questions for Discussion (suggested for 2nd day)

What is limiting our abilities to address the significant outstanding questions?

Theory & benchmarking

- While better functionals are desirable, more realistic (less ignorant) and reliable models of the **active site and reaction environment** are needed and need to be tested:
 - Metal/oxide interface
 - Solvent
 - Lateral adsorbate interactions
(can be benchmarked to coverage dependent TPD)
 - Error estimation/propagation on computational results
- More emphasis on **capacity** computing vs. **capability** computing

Questions for Discussion (suggested for 2nd day)

More generally, how do these elementary bond breaking/bond making reactions relate to current challenges for developing sustainable processes?

- Obvious: Good catalysts for any process lower energy requirements, improve selectivity, increase efficiency and are therefore related to sustainability
- Selectivity has a huge impact due to the extensive diversity in possible CO bonds to form and cleave
- For any carbon-based processes, the formation and cleavage of CO bonds will always be critical
 - CO₂ conversion
 - biomass utilization
 - selective oxidations

Questions for Discussion (suggested for 2nd day)

More generally, how do these elementary bond breaking/bond making reactions relate to current challenges for developing sustainable processes?

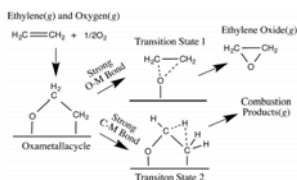
- C-O bond cleavage is important for HDO, but elementary steps for C-C, C-H, and O-H bonds are equally critical
 - Mechanistic understanding in liquid phase is critical
- Syngas production/Fischer-Tropsch/Higher alcohols
 - Many different C-O, C-C, C-H, O-H bond reactions
- The development of mechanistic understanding will be critical to design catalysts based on
 - Abundant metals
 - Abundant non-metals

Back to mechanisms

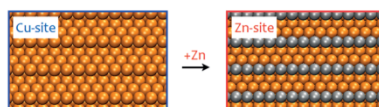
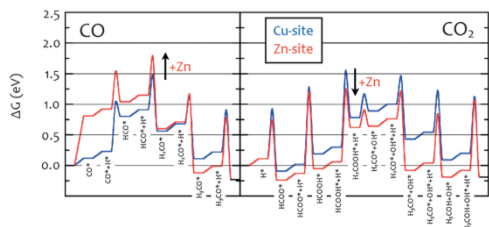
Oxophilicity, nucleophilicity, electrophilicity...

“There are two principal routes for utilizing carbon monoxide catalytically. One is insertion of the coordinated CO into a M-L bond. The other is external attack of a nucleophile on the CO ligand coordinated to a transition metal complex. Besides nucleophiles that attack the electrophilic carbon atom on the coordinated carbonyl ligand, electrophiles such as oxophilic silyl compounds can attach the oxygen atom in the carbonyl ligand.”

Adapted from “Fundamentals of Molecular Catalysis” Vol. 3 of Current Methods in Inorganic Chemistry by Hideo Kurosawa, Akio Yamamoto, Elsevier, 2003.



Montemore & Medlin *J. Phys. Chem. C* **118**, 2666–2672 (2014)
 Linc, Jankowiak, Barteau *J. Catal.* **224**, 489–493 (2004)



Studt et al. *ChemCatChem* **7**, 1105–1111 (2015)



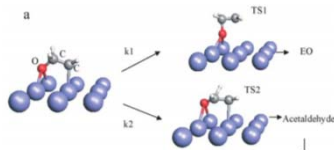
Hensley, Wang, McEwen, *ACS Catal.* **5**, 523–536 (2015)

Back to mechanisms

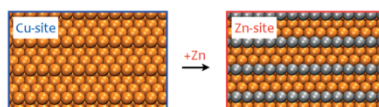
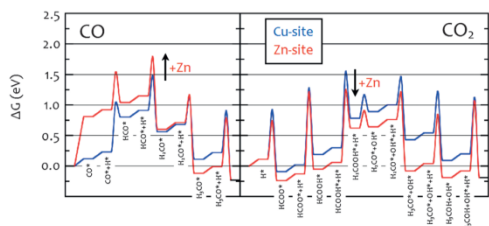
Oxophilicity, nucleophilicity, electrophilicity...

“There are two principal routes for utilizing carbon monoxide catalytically. One is insertion of the coordinated CO into a M-L bond. The other is external attack of a nucleophile on the CO ligand coordinated to a transition metal complex. Besides nucleophiles that attack the electrophilic carbon atom on the coordinated carbonyl ligand, electrophiles such as oxophilic silyl compounds can attach the oxygen atom in the carbonyl ligand.”

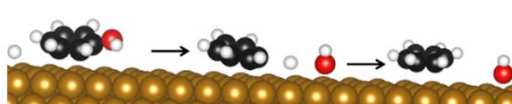
Adapted from “Fundamentals of Molecular Catalysis” Vol. 3 of Current Methods in Inorganic Chemistry by Hideo Kurosawa, Akio Yamamoto, Elsevier, 2003.



Montemore & Medlin *J. Phys. Chem. C* **118**, 2666–2672 (2014)
 Linc, Jankowiak, Barteau *J. Catal.* **224**, 489–493 (2004)



Studt et al. *ChemCatChem* **7**, 1105–1111 (2015)



Hensley, Wang, McEwen, *ACS Catal.* **5**, 523–536 (2015)

Questions for Discussion (suggested for first day)

- For homogeneously and heterogeneously catalyzed processes, what are the inherent similarities and differences in reaction mechanisms?
 - What are some currently proposed/accepted mechanisms for the specific bond breaking/bond making processes in each case?
 - What class(es) of catalyst(s) are responsible for carrying out these elementary bond breaking/bond making processes, and what are the properties of the catalysts that give rise to this chemistry?
 - Are there overall reactions involving these bond breaking/making steps that are uniquely catalyzed homogeneously or heterogeneously?
- Are there examples of major recent advances in understanding mechanisms of these elementary processes?
- What are some of the significant outstanding questions regarding the mechanisms of these bond making and bond breaking reactions?

Questions for Discussion on N-N Activation (N_2)

- For homogeneously and heterogeneously catalyzed processes, what are the inherent similarities and differences in reaction mechanisms?
 - What are some currently proposed/accepted mechanisms for the specific bond breaking/bond making processes in each case?

Similarity: In N_2 activation it is generally accepted that this molecule must bind to a metal and its π^* orbitals be reduced by electron rich metal centers.

Difference: In the homogeneous catalyzed process the binding mode of N_2 is important. This is not the case in the heterogeneous catalyzed process.

Difference: In homogeneous catalyzed reactions protons and electrons must be decoupled while in heterogeneous catalyzed reactions H_2 is directly used.

Difference: The pressure of H_2 is a huge factor in heterogeneous catalyzed reactions since it can hydrogenate the surface and poison/inhibit the catalyst.

Difference: In the homogeneous community, splitting the N-N bond with metal radicals must traverse through a distortion to allow for the mixing of different spin states.

Questions for Discussion on N-N Activation (N₂)

- For homogeneously and heterogeneously catalyzed processes, what are the inherent similarities and differences in reaction mechanisms?
 - What class(es) of catalyst(s) are responsible for carrying out these elementary bond breaking/bond making processes, and what are the properties of the catalysts that give rise to this chemistry?

Similarities: V, Mo, Fe/Co(?), U, Zr, Nb, Ta, and Cr catalysts have been reported. Properties: Lewis acidity, electron rich, low-coordination numbers or unsaturation? Ideal electronic structure?

Difference: In the heterogeneous process Ru is ideal since it greatly lowers the pressure needed for hydrogenolysis.

Questions for Discussion on N-N Activation

- Are there overall reactions involving these bond breaking/making steps that are uniquely catalyzed homogeneously or heterogeneously?

Similarities: Making NH₃ catalytically from N₂ is possible in both homogeneous and heterogeneous systems. However, in homogeneous systems H⁺ and e⁻ are usually decoupled which is not economically viable.

Differences: In homogeneous reactions lower temperatures work but there are lower TON

Similarities: Making NH₃ catalytically using M-H sites is not practical and the source of H to make NH₃ still represents an economic/energy challenge.

Questions for Discussion on N-N Activation

Are there examples of major recent advances in understanding mechanisms of these elementary processes?

Schrock: One Mo center can catalytically convert N_2 to NH_3 with H^+ and e^-

Peters: A mononuclear Fe complex can do similar catalysis at very low temperatures

Nishibayashi: A bridging N_2 complex can catalytically convert N_2 to NH_3 (or mononuclear?), up to 60 TON

Chirik: Catalytic hydrogenolysis of $LnM-NH_2$ (using Rh hydride complexes formed from H_2) bonds to form NH_3 and stoichiometric hydrogenation of N_2 to NH_3

King: Bio and Inorganic inspired catalysis using light-driven dinitrogen reduction catalyzed by a CdS:nitrogenase MoFe protein biohybrid

Kanatzidis: Bioinspired catalysis (with photons) with FeMoS-Chalcogels

Questions for Discussion on N-N Activation

What are some of the significant outstanding questions regarding the mechanisms of these bond making and bond breaking reactions?

Is 1 metal site better than 2, or 3 sites?

There are plenty of compounds that activate N_2 , but few can break the triple bond, why? (Mo and W metal can do it, so not as important)

Can we convert N_2 to NH_3 using visible light (Kanatzidis and King) and understand this process? Replace ATP, H_2 and expensive H^+/e^- source with light driven processes using non- CO_2 emitting H-sources

There are plenty of efficient (heterogeneous Ru based catalysts) that convert NH_3 to N_2 and H_2 . Could understanding this reaction (at the surface) help us understand the microscopic reverse reaction and prepare more efficient catalysts to convert N_2 to NH_3 ? (Are these systems stable enough to help us understand some of the elementary steps?).

Can H_2 (and CO_2 formation) be avoided by carrying out reactions such as $3CH_4 + 2N_2 \rightarrow 4NH_3 + 3C$?

N-N Activation: Breakout Session II

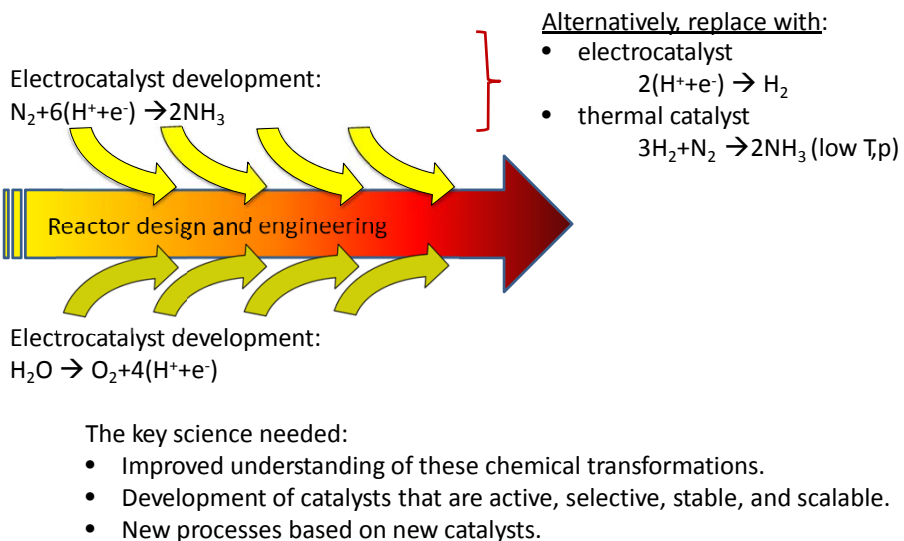
Daniel Mindiola & Thomas Jaramillo

- ***Generally, how do these elementary bond breaking/bond making reactions relate to current challenges for developing sustainable processes?***
- ***How do we go about determining these mechanisms for homogeneously and heterogeneously catalyzed processes?***
- ***What is limiting our abilities to address the significant outstanding questions? While there are lots of great experimental tools available now, what is still needed to advance the field (to address these current limitations)?***

N-N Activation

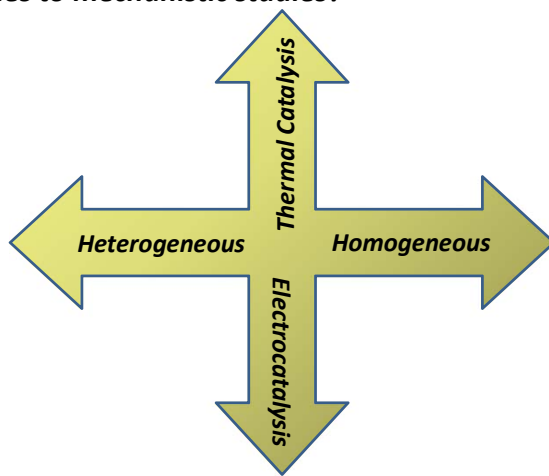
- ***Generally, how do these elementary bond breaking/bond making reactions relate to current challenges for developing sustainable processes?***
 - A broad range of important products:
nitrates, ammonia,
cyanides, N₂O,
hydrazine, proteins....
- Important aspects to consider:***
- Selectivity is at the core, e.g. competition from H₂ production.
 - C-free H₂ itself could be just as impactful, e.g. for Haber-Bosch.
 - Scalability, can the new process output the product at scale?
 - Purity of the product, needs to meet expected specs.
 - Many steps in the reaction, tandem catalysis?

The general scheme

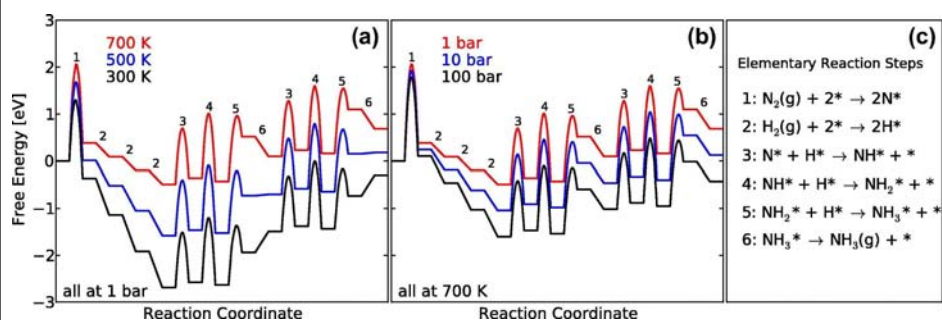


N-N Activation

- *How do we go about determining these mechanisms for homogeneously and heterogeneously catalyzed processes? What can we learn from each other by comparing/contrasting these approaches to mechanistic studies?*

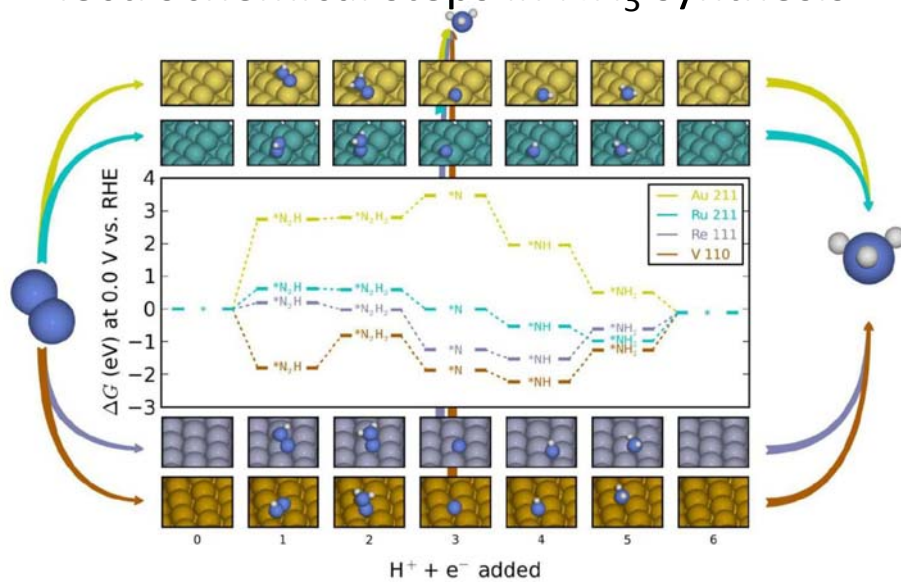


Thermochemical steps in NH₃ synthesis



A. Vojvodic, A.J. Medford, F. Studt, F. Abild-Pedersen, T. Khan, T. Bligaard, J.K. Nørskov, *Chemical Physics Letters*, v. 598, **2014**, 108–112.

Electrochemical steps in NH₃ synthesis



J.H. Montoya, C. Tsai, A. Vojvodic, J.K. Nørskov, *ChemSusChem*, v.8, **2015**, 2180-2186.

N-N Activation

- **How do we go about determining these mechanisms for homogeneously and heterogeneously catalyzed processes? What can we learn from each other by comparing/contrasting these approaches to mechanistic studies?**
 - Examine the reverse process, e.g. NH_3 decomposition (both homogeneous and heterogeneous) to understand N_2 activation/conversion. Microscopic reversibility. If you understand the elementary steps, you can apply that understanding to the reaction in the other direction.
 - Theory. For instance, applied to hydrogenolysis of N_2 . Learning about elementary steps.
 - Homogeneous systems seem to be more selective to NH_3 over H_2 vs. electrochemical materials/surfaces. What can we learn from homogeneous studies along those lines? e.g. controlling local concentration of protons vs. N_2 .
 - Understand elementary steps for competing pathways.
 - Recall that there are many possible outcomes from N-N activation, learning from one can help to understand the others. e.g. N_2 oxidation vs. N_2 reduction, C-N bond formation, N-F bond formation.

N-N Activation

- **What is limiting our abilities to address significant outstanding questions?**
 - (A) While there are lots of great experimental tools available now, what is still needed to advance the field (to address these current limitations)?**
 - Operando tools/methods, boost in P & T, improved detection sensitivity.
 - Advanced NMR methods, e.g. DNP solid-state NMR.
 - Cheaper $^{15}\text{N}_2$.
 - At this stage, more about imagination and creativity, less about the tools available.
 - (B) Since theory is an essential element of mechanistic studies, what advances are needed?**
 - We need more complete descriptors.
 - Improved methods for treating the electrolyte (e.g. strong electrolytes) and interfaces.
 - Methods for establishing uncertainty in theoretical predictions.
 - Methods for solving the kinetics of complex reaction networks.
 - Methods for self-consistent methods to study the materials surface chemistry coupled to reaction kinetics.
 - Better methods for searching for novel materials, especially outside 'conventional' materials classes.
 - Simplifications of models to accelerate throughput of calculations.
 - Nevertheless, with the current state of theory methods they can be applied as-is, again it's about creativity and imagination.

N-N Activation

- ***What is limiting our abilities to address significant outstanding questions?***

(C) Are there critical elements of benchmarking that are needed?

- Experimental: Standardization of methods/protocols, particularly with product detection.
- A common set of catalyst systems that can be used as benchmarks for theory and for experiment.